2001

An evaluation of the environmental fate of reactive dyes

Malcolm John Hetheridge

PHD

An evaluation of the environmental fate of reactive dyes

Hetheridge, Malcolm John

Award date:
2001

Awarding institution:
University of Plymouth

AN EVALUATION OF THE ENVIRONMENTAL FATE OF REACTIVE DYES

by

MALCOLM JOHN HETHERIDGE

A thesis submitted to the University of Plymouth
in partial fulfilment for the degree of

DOCTOR OF PHILOSOPHY

Department of Environmental Sciences
Faculty of Science
Drake Circus
Plymouth PL4 8AA

In collaboration with
AstraZeneca
Brixham Environmental Laboratory
Freshwater Quarry
Brixham
Devon. TQ5 8BA

March 2001

This thesis is dedicated to my wife Leigh and children Gareth and Charlotte

Thank you!

AN EVALUATION OF THE ENVIRONMENTAL FATE OF REACTIVE DYES

by

Malcolm John Hetheridge

ABSTRACT

Dyestuffs are widely used industrial chemicals, yet surprisingly little is known about their fate in the environment. The potential modes of transformation and removal of reactive dyes in treatment and in the environment are principally through anaerobic and aerobic biodegradation and photodegradation. The research herein describes the use of LC-MS analysis with laboratory simulations to develop a better understanding of the occurrence and fate of reactive dyes and their degradation products in the aquatic environment.

One reason for the lack of information on the environmental fate of reactive dyes has been the paucity of robust analytical methods suitable for the determination of dyes in aqueous samples. Robust analytical methods were optimised to provide LC-MS and MSMS identification of degradation products. Additionally, interpretation of the MSMS spectra of known reactive dyes provided novel characteristic fragment ions indicative of the triazine reactive group of reactive dyes .

Fibre reactive dyes are designed to have a degree of photostability and therefore their photodegradation behaviour has not been widely investigated. Little is known of their stability to daylight over prolonged periods of irradiation in dilute aqueous solutions and in the presence of humic substances. The kinetics of photodegradation of an anthraquinone dye (Reactive Blue H4R) and azo dye (Reactive Yellow P5G) were evaluated. The former underwent rapid and extensive degradation ($t_{1/2}$ 1.5 h). The major products formed were identified using LC-MSMS and a photodegradation pathway proposed. By comparison, the photodegradation of the azo dye was significantly slower, ($t_{1/2}$ 30 h). The addition of humic substances appeared to have little effect on the rate of photodegradation under the conditions used.

The reduction of azo dyes under anaerobic treatment has been extensively studied, but the subsequent fate of the initial reduction products when exposed to air are not understood. Three relatively simple azo dyes, Amaranth, Sunset Yellow and Naphthol Blue-Black, were reduced and their autoxidation products identified by LC-MS. These were subsequently used to predict the autoxidation products of a more complex azo reactive dye: Reactive Red 3.1. Additionally, a persistent degradation product from the anaerobic-aerobic treatment of Reactive Red 3.1 was identified from LC-MS data.

Azo reactive dyes are generally regarded as being resistant to aerobic degradation and there are few published data regarding degradation pathways for reactive anthraquinone dyes. Pure cultures of *Pseudomonas docunhae*, *P. 9046* and *P. texaco* and mixed bacterial consortia (semi-continuous activated sludge, SCAS) aerobic degradation of azo and anthraquinone reactive dyes was studied. Two azo dyes were degraded by pure cultures of *P. docunhae and P. 9046*, suggesting that azo dyes can be aerobically degraded given favourable conditions. The antraquinone dye was extensively degraded by SCAS and pure culture biodegradation. Metabolites were identified by LC-MS and a degradation pathway proposed.

The data from two parts of this study have been published to date:

M. Kudlich, M. Hetheridge, H-J Knackmuss and A Stolz (1999). Autoxidation reactions of different aromatic *ortho*-aminohydroxynaphthalenes which are formed during the anaerobic reduction of sulfonated azo dyes. ***Environ. Sci. & Technol.***, 33, 896-901.

K C A Bromley-Challenor, J S Knapp, Z Zhang, N C C Gray, M J Hetheridge and M R Evans (2000). Decolourisation of an azo dye by unacclimated activated sludge under anaerobic conditions ***Wat. Res.*** Vol.. 34, 18, 4410-4418.

TABLE OF CONTENTS

LIST OF TABLES

LIST OF FIGURES

AUTHOR'S DECLARATION

At no time during the registration for the degree of Doctor of Philosophy has the author been registered for any other University award.

This study was financed by AstraZeneca plc.

Relevant scientific seminars and conferences were regularly attended at which work was often presented:

Publications:

M. Kudlich, M. Hetheridge, H-J Knackmuss and A Stolz (1999). Autoxidation reactions of different aromatic *ortho*-aminohydroxynaphthalenes which are formed during the anaerobic reduction of sulfonated azo dyes. ***Environ. Sci. & Technol.***, 33, 896-901.

K C A Bromley-Challenor, J S Knapp, Z Zhang, N C C Gray, M J Hetheridge and M R Evans (2000). Decolourisation of an azo dye by unacclimated activated sludge under anaerobic conditions ***Wat. Res.*** Vol.. 34, 18, 4410-4418.

Presentation and Conferences Attended:

Hetheridge MJ, Comber MHI and Long KJW. Comparison of mass spectrometer interfaces for the determination of chemicals in the environment. Analytical Conference on Separation Science, Zeneca Alderley Park, April 1994

Hetheridge MJ, Comber MHI and Rowland S. Comparison of mass spectrometer interfaces for the determination of Reactive Dyes and surfactants. International Liquid Chromatography meeting, Brighton. 1995

Hetheridge MJ, Harland BJ and Rowland S. A study of the environmental fate of three reactive dyes. SETAC Bordeaux, April 1998

Signed .....Hetheridge.....

Date .....March 2001.....

ACKNOWLEDGMENTS

My deepest thanks to my director of studies, Professor Steve Rowland for his unfailing enthusiasm, inspiration and encouragement during this study.

I would also like to thank the following individuals for their help along the way:

Brian Harland, my industrial supervisor, for his guidance and encouragement, particularly during the early part of the study.

John Tapp and Prof. David Taylor of Brixham Environmental Laboratory, for providing the necessary time and funding for my study.

Dr John Easton (Avecia) for the selection and provision of reactive dyes.

Dr M Hayes (University of Birmingham) for the provision of River Trent and River Dodder humic, fulvic and hydrophilic acids.

Tim Fileman (Plymouth Marine Laboratory) and Dr Lulwa Ali (Kuwait Institute for Scientific Research) for guidance with the practicalities of photochemical experiments.

Julie Stabb for helping with thesis formatting and layout.

Finally, a special thank you to Leigh and my family for their endless support, patience and understanding through some very difficult times.

LIST OF COMMON ABBREVIATIONS

API	Atmospheric pressure ionisation
CE	Capillary electrophoresis
CID	Collision induced dissociation
COFF	Collision offset voltage
EI	Electron impact
EPA	Environmental protection agency
ESI	Electrospray ionisation
FAB	Fast atom bombardment
FIA	Flow injection analysis
HRT	Hydraulic retention time
k_p	Photodegradation rate constant
LC	Liquid chromatography, synonymous with high performance liquid chromatography
LCMS	Liquid chromatography-mass spectrometry, synonymous with high performance liquid chromatography-mass spectrometry
LOD	Limit of detection
MS	Mass spectrometry
MSMS	Tandem mass spectrometry
MWT	Molecular weight, synonymous with molecular mass
m/z	Mass to charge ratio
P.	Pseudomonas
PDA	Photodiode array
RIC	Reconstructed ion current
RSD	Relative standard deviation
s/n	Signal to noise ratio
SCAS	Semi-continuous activated sludge
SIM	Selected ion monitoring synonymous with SIR selected ion recording
SRT	Sludge residence time
STW	Sewage treatment works
TBAOH	Tetrabutylammonium hydroxide
TSP	Thermospray
UV	Ultra violet

CHAPTER 1

INTRODUCTION

1.0 DYESTUFF PRODUCTION

Historically, the main producers of dyestuffs were found in the countries of Western Europe and in America, but the last decade has seen increases in production in China, India, Japan, Taiwan and central America, as these countries have striven to become self sufficient in their dyestuff needs. For instance, China has changed from an importer, to a net exporter of dyes in the last 10 years, and now produces in excess of 180,000 tonnes per annum (www.chinaeco, 2000). India increased production from 16 tonnes / annum to 28,000 tonnes between 1951 and 1984 (Khanna, 1991). Accurate figures for the current world-wide production of dyes are not available, but world production figures based on 1993 estimates (Howe, 1993), are shown in Table 1.1

Table 1.1 World production of dyestuffs expressed as thousands of tonnes per annum (Howe, 1993)

Year	W. Europe	USA	China	USSR	Japan	Others	Total
1978	250	109	57	147	51	26	640
1993	300	138	200		68	44	750
2000 (predicted)	300	170	180	Not available	84	54	>780

1.1 DYE CLASSIFICATION

Dyes can be classified according to their usage and method of application or by their chemical nature. The former tends to be used by dye users and terms such as 'fibre reactive' dyes for cotton and 'disperse' dyes for polyester are employed. Users may additionally describe dyes by chemical nature using descriptors such as 'azo', 'anthraquinone' or 'phthalocyanine' dyes. The two methods of classification are often mixed. For instance, an 'azo reactive' dye could be used for cotton and an 'azo direct' dye for dying polyester. At >40%, textile dyes account for the biggest sector of world dye production (Colour Chemistry, 1992). Reactive dyes are becoming increasingly important and account for approximately 20% of textile dye production (at least 60,000 tonnes per annum, ICI internal com, 1994). The present study is concerned only with fibre reactive dyes of the chemical classes azo and anthraquinone, but a brief overview of all major dyestuffs follows for completeness.

Reactive dyes

The concept of binding a dye to cellulose through chemical reaction is attributed to Cross and Bevan (1895), who esterified cellulose with benzoyl chloride and then nitrated and diazotised the resultant benzene ring. The first wool reactive dye was an acid dye introduced in 1930, although it was not realised at the time that the observed fastness to washing was due to chemical bonding (Encyclopedia of Chemical Technology, 1993). The first commercial reactive dyes were introduced in 1956 (Rattee and Stephen, 1956) and were characterised by the presence of a reactive group which formed a covalent bond with fibres to become an integral part of the fibre polymer. Such dyes are particularly suited to the dying of cotton, but also are used to die wool, silk and to a lesser extent, nylon. The dye is applied in neutral solution and chemical reaction is initiated by addition of alkali. Reactive dyes

(eg I) are characterised by three functional parts; the chromophore, the fibre reactive system and a water-solublising sulphonate group:

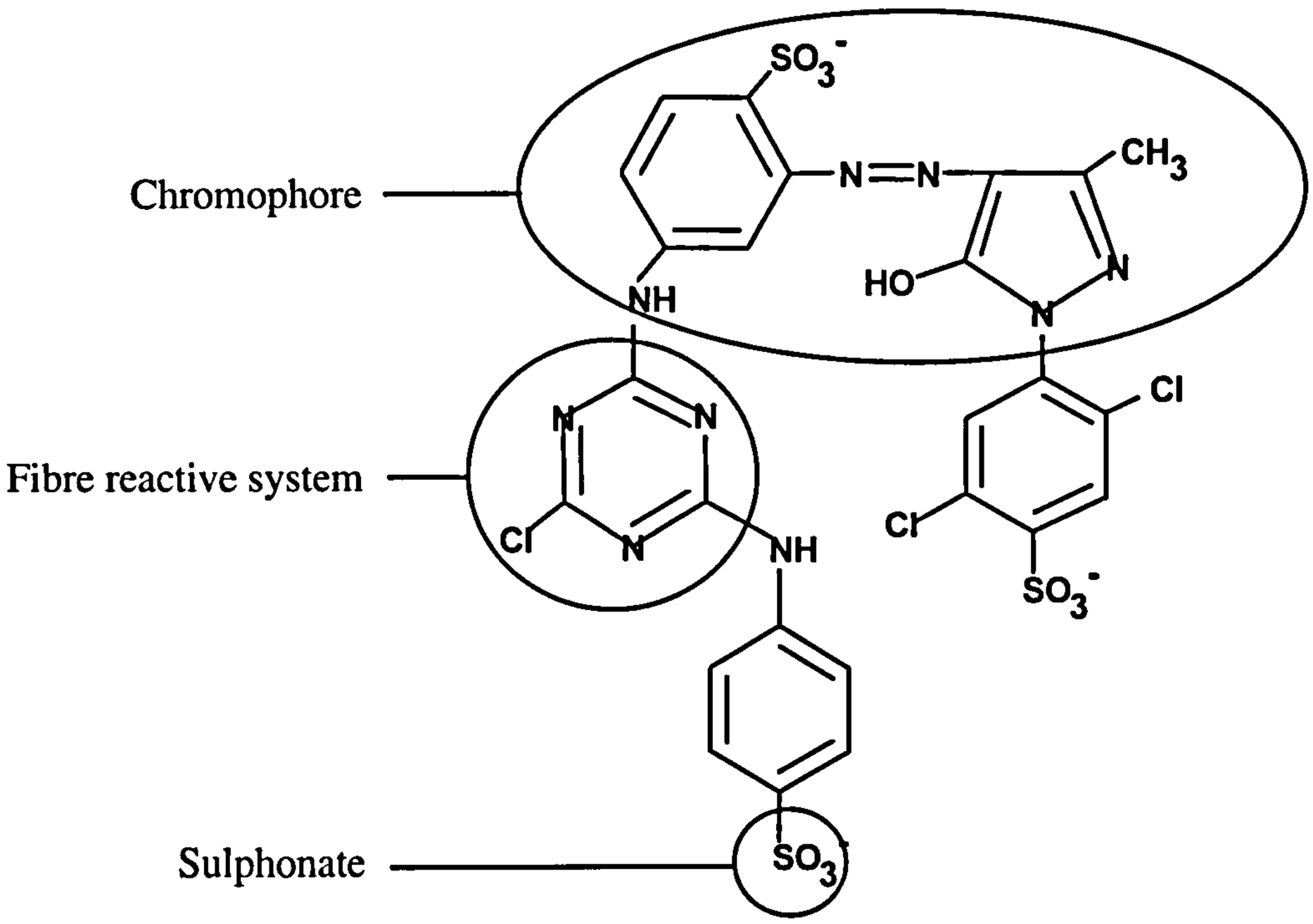

(I) Reactive Yellow P5G

(i) *Chromophore*. Interaction of light with this part of the molecule produces the colour. These groups are most commonly azo and anthraquinone moieties, or a phthalocyanine group. Reactive dyes produce a wide range of bright colours.

(ii) *Fibre reactive group*. This part of the dye molecule reacts with the target fibre material to permanently bind the dye to the fibre.

Cotton is made up of almost pure cellulose which consists of chains of glucose units joined in a 1-4 β linkage:

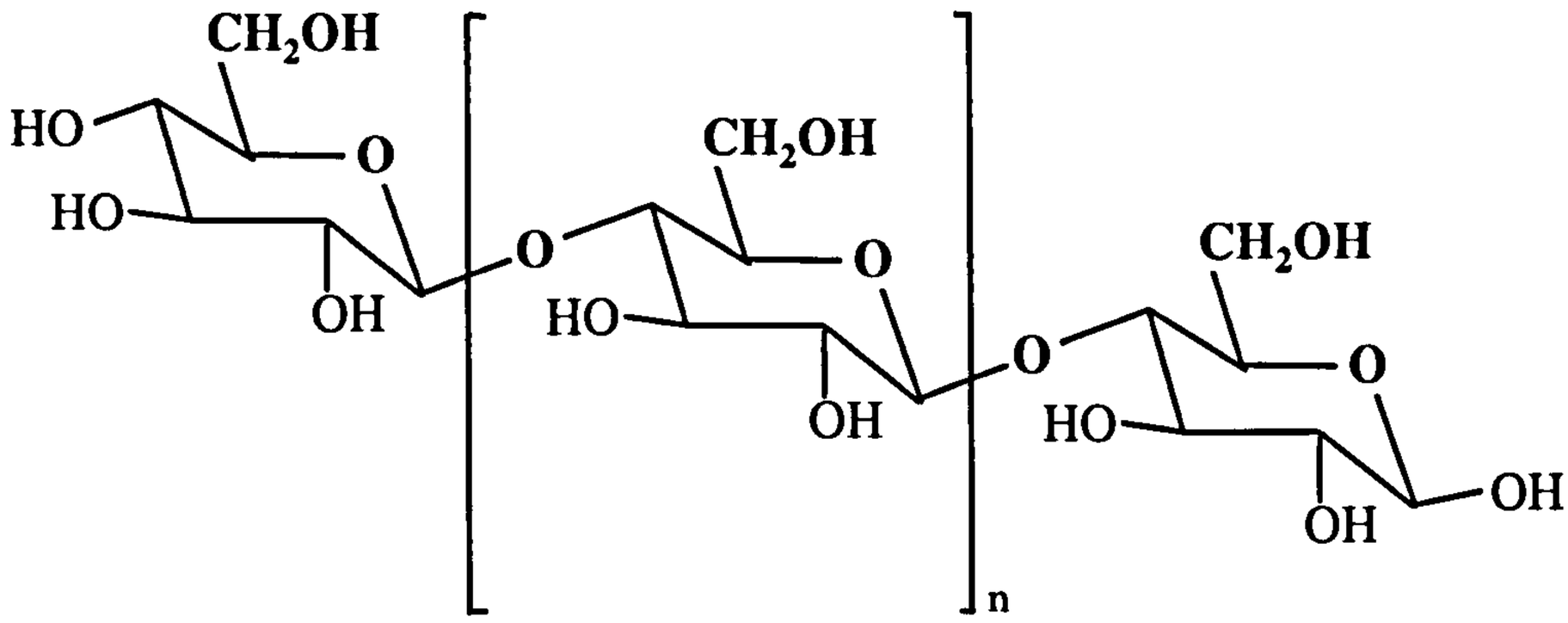

These chains lie side-by-side in bundles held together by hydrogen bonding. The bundles are twisted together to form rope-like structures, which in turn are also twisted together to give fibre strands that contain a large number of hydroxyl groups, rendering the fibre hydrophilic. The fibre readily absorbs water and therefore can be dyed by water soluble dyes.

Several mechanisms are used to bond the dye to the cellulose fibres. The main ones use either a mono- or dichlorotriazine group which reacts with the hydroxyl group of cellulose by nucleophilic substitution to form a covalent cellulose-O-dye bond with the elimination of HCl:

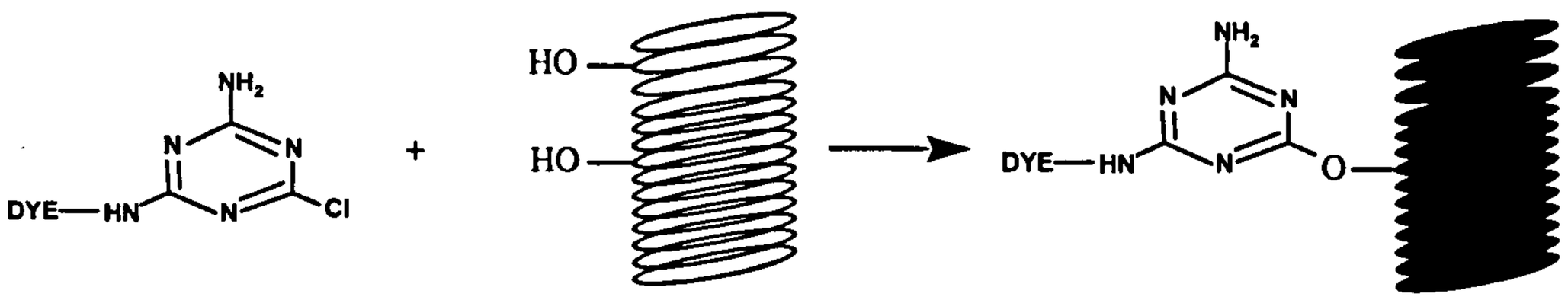

or addition to the double bond of a vinyl sulphone reactive group for example:

$$\text{Dye-SO}_2\text{CH}_2\text{=CH}_2 + \text{HO-Cellulose} \rightarrow \text{Dye-SO}_2\text{CH}_2\text{CH}_2\text{-O-Cellulose}$$

Although these are the most common forms of reactive group used today, many alternatives have been developed. These include: dichloroquinoxalines, dichloropyridazones, difluorochloropyrimidine and fluorotriazine groups. Because of the covalent chemical bonding, reactive dyes show extremely good fixation with cotton and they are well retained even after washing.

(iii) *Water-solubilising sulphonic acid* groups. Reactive dyes are also characterised by the presence of sulphonic acid groups which make the dye molecule highly polar and therefore water soluble, allowing penetration of dyes into the cellulose fibres during the dyeing process. Generally, the bigger the dye molecule, the more sulphonic acid groups that are required to achieve the desired solubility.

Reactive dyes are relatively simple to apply, and have extremely good wash fastness. Other advantages over direct dyes are increased brightness and better penetration into substrate fibres.

Direct dyes

Direct dyes (e.g. Direct Red 2, II) get their name from their ability to dye fibres directly from an aqueous solution without the need to chemically pre-treat the cellulose fibre. These dyes contain several sulphonic acid groups to make them highly water soluble and they tend to have long linear structures which align along the cellulose fibres. The dye can be attached to the fibre by hydrogen bonding or can hydrogen bond to other dye molecules to form a large aggregate which is then physically trapped within the fibre. They are most commonly used for cotton, paper and leather but they do not have the same degree of wash fastness as reactive dyes and often require additional treatments to improve this property. Most dyes in this class are azo dyes.

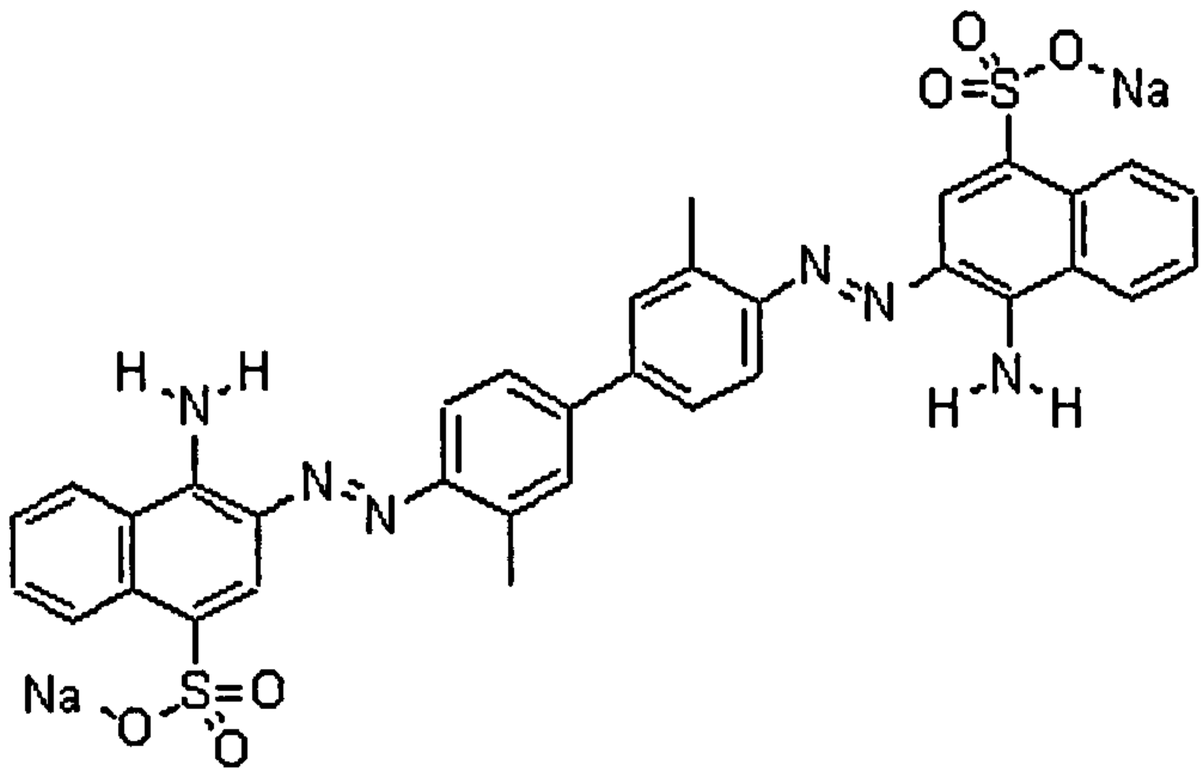

(II) Direct Red 2

Sulphur dyes

Sulphur dyes are largely of unknown and variable chemical compositions. They are applied in solution in their reduced form and an insoluble colour is produced within the fibre following chemical oxidation. Sulphur dyes have good wash fastness properties and are important because they are very low cost high bulk dyes. Therefore, in terms of tonnage production they make a significant contribution to overall world-wide dye stuff production figures. Sulphur dyes have a very limited colour range, usually blue or black.

Vat Dyes

These are water-insoluble dyes which have to be reduced to a water-soluble form using a reducing agent such as sodium dithionite in alkaline solution. This is usually achieved in a vat. The material to be dyed, usually cellulose fibres, is then dipped into the vat and the dye is regenerated in insoluble form within the fibres by chemical oxidation. Thereafter it is trapped within the fibres and because it is insoluble in water it is not readily washed out during subsequent washing. The principal chemical classes used as vat dyes are anthraquinone and indigo-based dyes. The latter is commonly used as the dye for blue denim, for example:

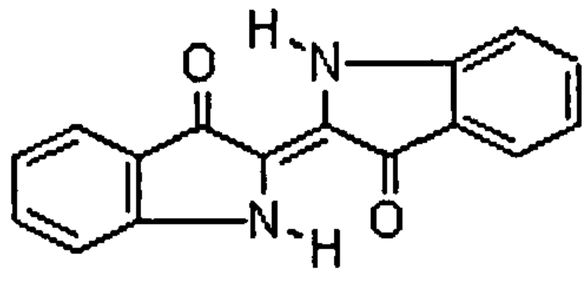

(III) Indigo

Disperse dyes

These are non-polar water-insoluble dyes (e.g. IV) used for application to hydrophobic fibres such as polyester, which are impermeable to water and therefore cannot be dyed with water-soluble dyes. The dye forms a suspension or dispersion in water, where it is adsorbed onto the fibre as a solid solution. These dyes also have niche markets for thermal transfer printing (where disperse dye is printed onto paper then transferred to fibre using a dry heat process) and in dye diffusion thermal transfer, as used in electronic photography.

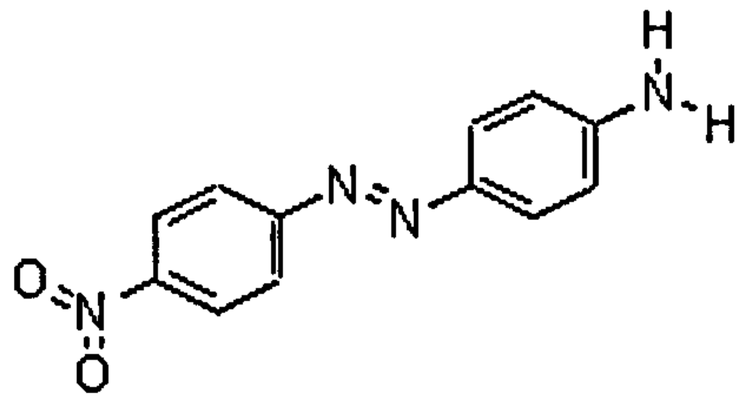

(IV) Disperse orange 3

Basic dyes

These are water-soluble, cationic dyes used predominantly for dying paper and acrylonitrile (e.g. Dralon). The latter contains many carboxylic and sulphonic acid groups and basic dyes containing an amino or other cationic function can readily form ionic bonds with these:

$$\text{Fibre-}CO_2H + \text{Dye-}NH_3^+\,Cl^- \rightarrow \text{Fibre-}CO_2^-\,.\,\text{Dye-}\,NH_3^+$$

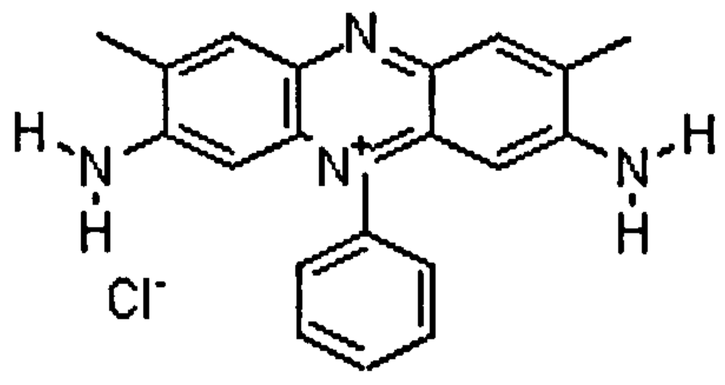

(V) Safranine

Acid dyes

These are water-soluble, anionic dyes which can react with fibres which contain a large number of amino groups such as nylon, wool and silk. The original members of this class all contained at least one sulphonic or carboxylic acid group which gave the class its name. In addition to making the dye highly soluble, the acid groups can form ionic bonds with the amine groups of the fibre:

$$\text{Fibre-}NH_2 + \text{Dye-}SO_3H \rightarrow \text{Fibre-}NH_3^+\,.\;\text{Dye-}SO_3^-$$

Azo and anthraquinone dyes are the main chemical classes in this group.

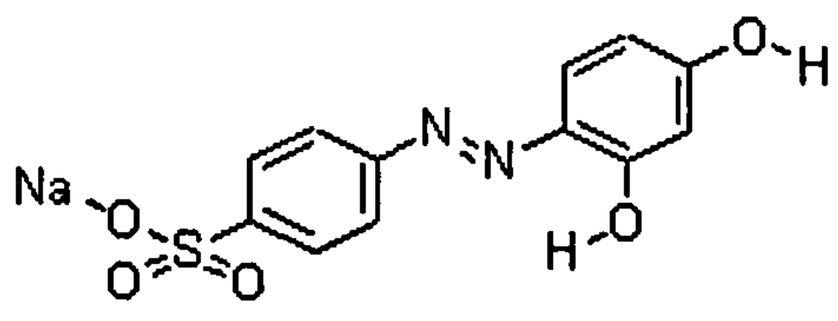

(VI) Acid Orange 6

Solvent dyes

These are totally water-insoluble dyes used for colouring plastics, petrol and waxes. Again the predominant chemical classes are azo and anthaquinone dyes.

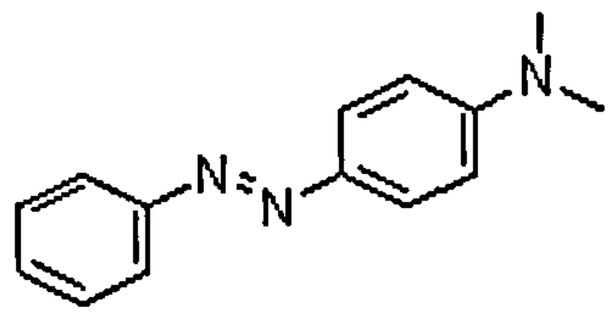

(VII) Solvent Yellow 2

Chemical classifications of dyes

Azo dyes are by far the most important and most studied class of dye and account for more than 50% of all commercial dye production. As the name suggests, these dyes contain at least one -N=N- group, and often two (diazo), three (triazo) or sometimes four or more azo groups, although this is less common. Mono azo dyes are most important. The azo bond is attached to two different groups both of which are usually aromatic and arranged in a *trans* configuration. One aromatic ring always contains an electron donating group(s), typically hydroxyl or amino and the other, electron withdrawing group(s). For example, 4-alkylphenylazo-1-naphthol (VIII).

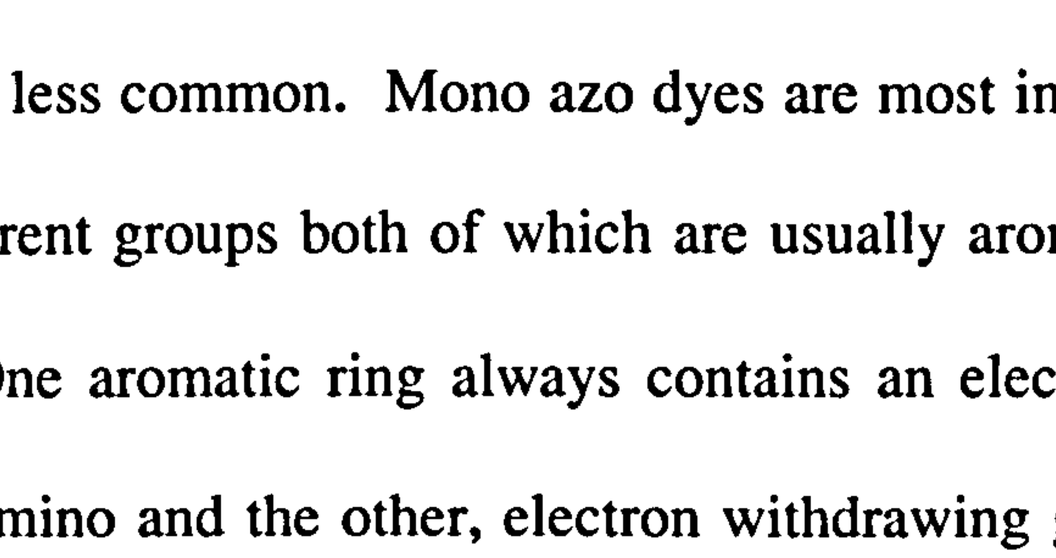

(VIII)

A most important feature of azo dyes is their ability to tautomerise. This has an effect not only on the colour of the dye, but also on its properties in terms of light fastness and its tinctorial strength (i.e. the intensity of colour produced). The value of a dye is based on the latter and so is of great importance to the manufacturing industry. The azo tautomer of 4'-phenylazo-1-naphthol dye (VIII) is yellow (λmax 410 nm), whilst the hydrazone tautomer (IX) produces a stronger orange colour (λmax 480 nm).

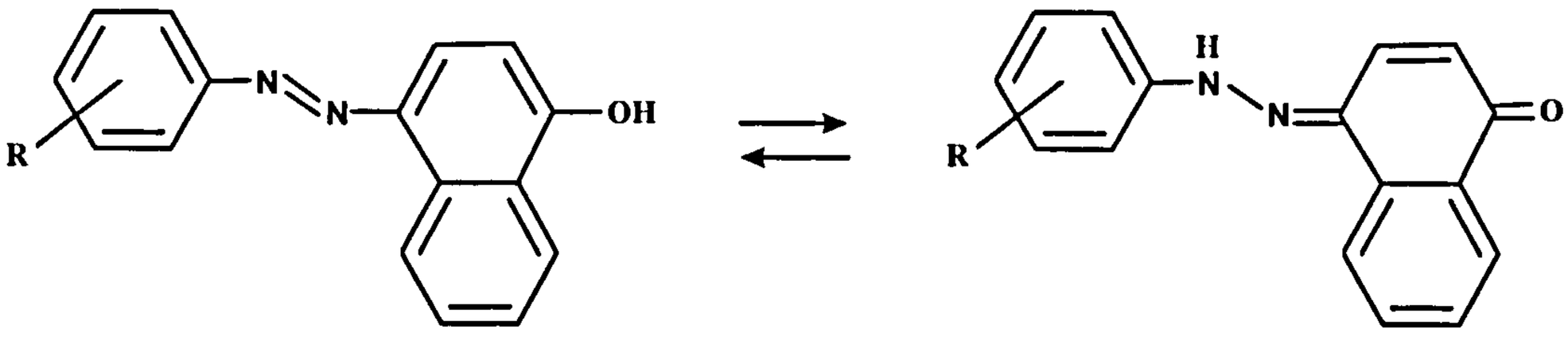

(VIII) Yellow (Azo) (IX) Orange (Hydrazone)

Individual hydroxy azo dyes vary in the proportion of each tautomer present, but generally the hydrazone tautomer produces the strongest colour and is therefore most desirable. Hence some important classes of dye contain predominantly hydrazones. Examples of these are azopyridones and azopyrazolones (X). Reactive Yellow P5G, is an example of the latter.

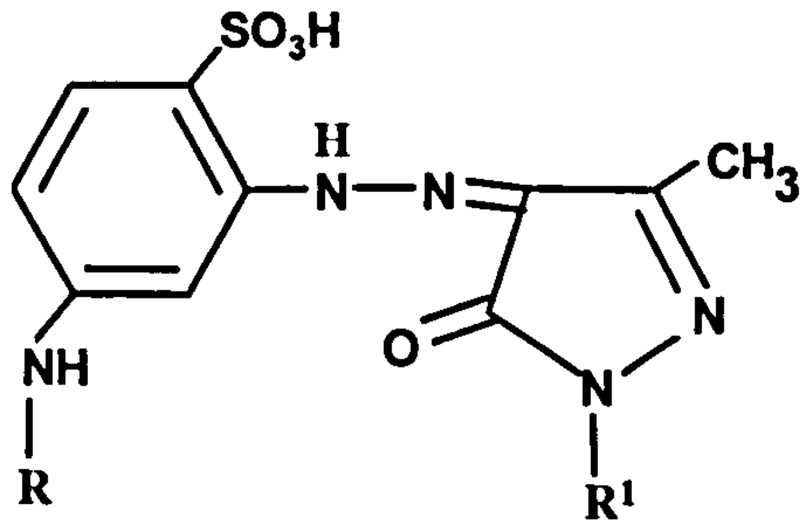

(X)

Amino-substituted mono azo dyes exist in the azo form only. The imino tautomer is believed to be unstable (Howe, 1993). In general terms of colour production, yellow dyes

are usually monoazo and most are azopyridones and azopyrazolones. Orange dyes are typically monoazo coupled to a pyrazolone, substituted phenyl or naphthyl. Red dyes are predominantly based on H-acid (XI), but substituted phenyl and naphthyl groups may also be used. Black and brown dyes are generally diazo.

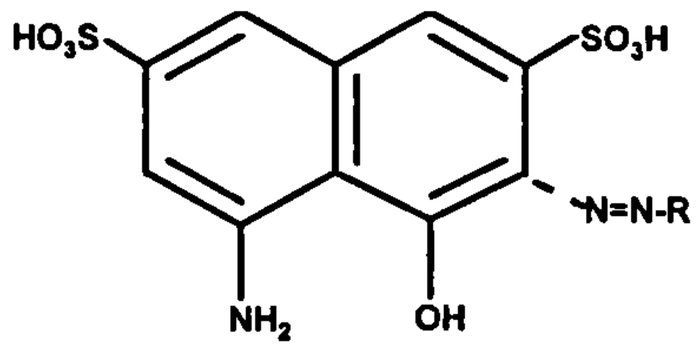

(XI) H-Acid (---N=N-R indicates typical position of azo substitution)

Anthraquinone (AQ) dyes are the second most important group of dyes. They tend to be tinctorially weaker and more expensive to produce than azo dyes, but they have brightness and colour fastness properties that still make them desirable for many applications. Antraquinone itself shows very weak absorption in the visible range and so is almost colourless. However, a wide range of colours can be produced, depending on the nature of the electron donating groups substituted at the 1, 4, 5 and 8 positions (XII).

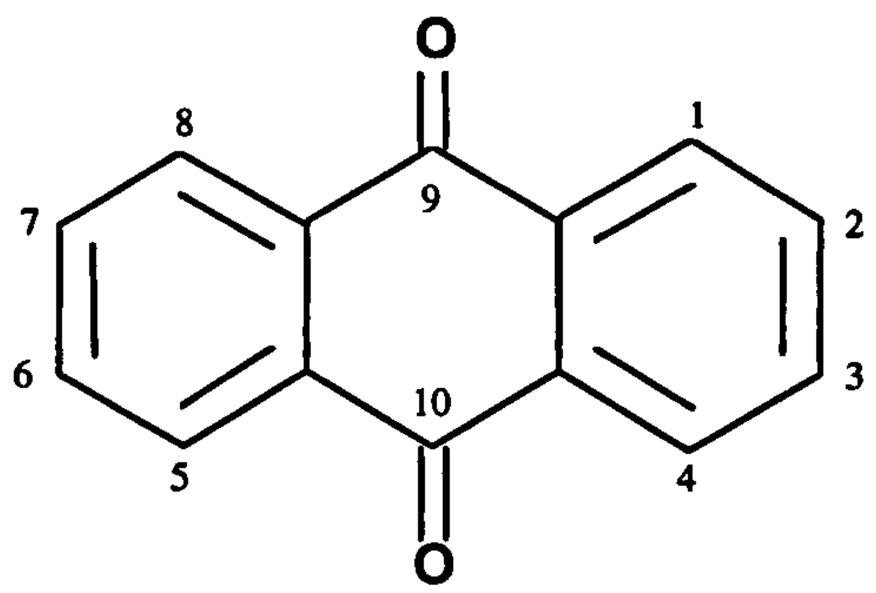

(XII)

As for azo dyes, primary and secondary amino and hydroxyl groups are most often used. These enhance intramolecular hydrogen bonding with the minimum of steric hindrance (XIII):

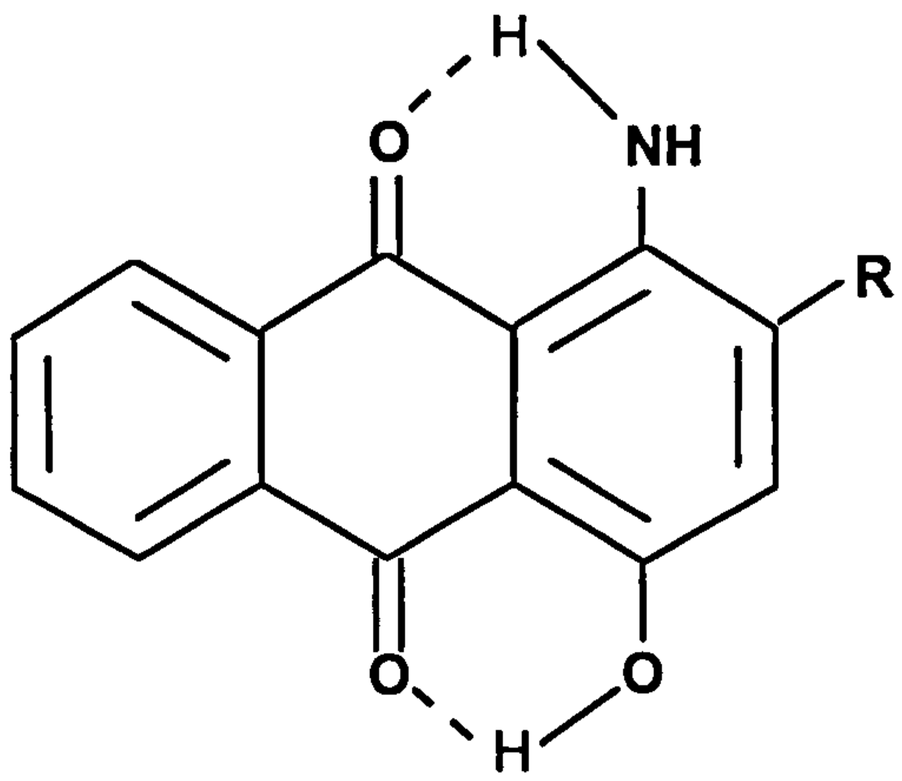

(XIII)

The strength of electron donor groups increases in the order ArNH > RNH > NH2 > OH. Addition of an hydroxyl group at C-1 produces a shift from 323 nm for anthraquinone to 402 nm. A second hydroxyl in the 5 or 8 positions produces a further shift to 425 or 470 nm respectively. Similarly substitution of an amino group in the 1 position produces a shift to 475 nm. Addition of a second in the 5 or 8 positions produce shifts to 487 and 507 nm respectively. Addition of a sulphonic acid group at the 2 position of 1,4-diaminoanthraquinone, produces absorption maxima at 562 and 603 nm. 1,4-diaminoanthraquinone is violet, 1-amino-4-methylaminoanthraquinone is blue, 1,4-diamino-2-phenoxymethylanthraquinone is orange and 1,4-di(methyl-4-phenylamino)anthraquinone is green (Shakra, 1992). Clearly a range of colours can be produced by varying the type and number of substituents.

1.2 FATE OF DYES IN THE ENVIRONMENT

The potential for dyes to enter the environment is derived mainly from two sources: discharges of manufacturing and processing (dye house) wastes to rivers.

Early studies suggested dyestuffs were unimportant pollutants. Thus, Brown (1987) calculated potential UK sewage treatment works (STW) influent concentrations of dyes as less than 10 mg l^{-1}, with expected riverine concentrations of 1-10 μg l^{-1}. These figures were based on hypothetical production quantities and average river flow rates and volumes and aimed to give an indication of environmental concentrations for use in risk assessment. A more refined approach was adopted by Hobbs (1989), who used actual values for river water flow and STW discharge flows to estimate normal and worst case scenarios for both acid and reactive dyes. These suggested that, in general, concentrations in river water would be 1-30 μg l^{-1}, but under exceptional circumstances, ie maximum release of dye waste to STW and low river flow, could reach 0.3 mg l^{-1} for acid dyes and 1.5-2 mg l^{-1} for reactive dyes. Both studies also indicated that for all but the most intensely coloured dyes, a concentration of 1-2 mg l^{-1} was needed for a visible effect on river water to be produced. Additionally, Brown (1987) reported results of an 8 week fish bioaccumulation study of 42 soluble and disperse dyes which demonstrated no bioaccumulation or observable detrimental effect on Japanese carp, for dye concentrations of 100 mg l^{-1}, and the same study indicated that 75% of ICI dyestuffs were not toxic to fish at 100 mg l^{-1}, with only 3.5% showing any toxicity below 1 mg l^{-1}. This was in agreement with the findings of Anliker (1980, 1988), who reported tests of 3000 dyestuffs for toxicity to fish. 98% showed no toxicity based on simple LC_{50} tests, at concentrations greater than 1 mg l^{-1}. The remaining 2% were almost entirely due to triphenylmethane dyes. The same authors indicated that generally dyestuffs show no inhibition of the activities of sewage sludge bacteria at concentrations below 100 mg l^{-1} and were not toxic to algae above 1 mg l^{-1}.

Additionally, Clarke (1980) demonstrated that numerous dyes were of low acute toxicity to mammals. Of more than 4000 dyestuffs tested (including replicates), less than 1% showed LD_{50} values for concentrations below 250 mg l^{-1}. The conclusion from the findings of these early studies (i.e. low predicted environmental concentrations, effectively no toxicity to fish, algae or mammals), was that dyestuffs did not constitute an environmental problem.

However, it seems these publications tended to over simplify the environmental situation. In particular, the estimated environmental concentrations based on calculated dye releases and STW concentrations were not reinforced by actual measurements. Contrary to the above early predictions ENDS (1992) indicated that 10 rivers in the UK Seven Trent region had problems with discoloration of water and at least another four rivers nationally had similar problems. These problems were attributed to the increasing popularity of the use of reactive dyes, which were poorly degraded in conventional sewage treatment works.

The same and additional articles (Cooper, 1993) highlighted the difficulties faced by textile processors, who were unable to treat their effluent on-site because treatment would not only be prohibitively expensive, but many processing works were in city centres where space for such plant was not available.

ENDS (1993), suggested little improvement from the previous year. A survey by the National Rivers Authority (NRA, now The Environment Agency, EA) found that 470 km of UK rivers had been affected by dye discoloration, producing over 500 public complaints. Once again the blame was attributed mainly to increasing popularity of reactive dyes.

These articles (ENDS, 1992, 1993) demonstrate that the discharge of reactive dyes to river waters at concentrations capable of causing significant discoloration is a regular occurrence.

One problem is the large quantities of dye in the waste effluent from textile processing plants, despite attempts of dyers to minimise dye wastage for economic reasons through the careful and sophisticated control of the dying process. Reactive dye processes which require an excess of dye (high dye ratio), generally result in about 50% of dye not being fixed to the textile. Much of this is, therefore, lost as waste material (Hobbs, 1988). The waste, which is a mixture of reactive dye and hydrolysed dye, is spent and cannot be recycled. Reactive dyes provide the least effective fixation (50 - 80%), compared to sulphur (60 - 70%), disperse, vat and direct dyes (all 80 - 90+).

Furthermore, conventional STW show poor removal of reactive dyes and some acid dyes. Holme and Thornton, (1994), outlined example calculations to demonstrate how low concentrations of some reactive dyes in river water were predictable. The authors indicated that the problem associated with this decolouration of rivers was one of aesthetics rather than potential health hazards, but neither commented on the possible fate of reactive dyes and the impact that degradation products may have on the environment.

The problem of effluent treatment has become an important consideration in discoloration of rivers (Cooper, 1993). Dyes are complex organic molecules which are designed to have a high degree of stability and fastness. It is not surprising, therefore, that they tend to show little sign of degradation in the relatively short retention times of many biological wastewater treatment systems. The effectiveness of different conventional treatment systems has been investigated (Clarke 1980; Cooper 1993) and a summary is shown in Table 1.2. Primary settlement adequately removes insoluble vat, disperse and sulphur dyes

and activated sludge treatment can remove soluble basic and direct dyes, mainly by adsorption rather than biodegradation (Hitz, 1978). However, under the same regime only one of 17 reactive dyes was removed to any extent (*ca* 35%), the others being less than 10% adsorbed. Adsorption of acid dyes also tended to be very variable. A further study (Holme and Thornton, 1994), suggested that removal of reactive dyes in conventional STWs was between 0 and 25% efficient, supporting the findings of Hitz (1978).

Table 1.2 Summary of effectiveness of different treatment processes for colour removal of different dyestuffs (Clarke, 1980; Cooper, 1993). - no data, • poor, o good and + particularly suitable

	Treatment				
Dyestuff	Coagulation	Activated Carbon	Biological	Ozone	Sludge Adsorption
Reactive	•	o	•	+	•
Acid	•	o	•	o	•
Basic	•	+	o	o	o
Disperse	o	•	•	•	•
Vat	o	•	•	o	-
Sulphur	o	•	•	o	-
Direct	-	-	-	o	o

A review by Clarke (1980) estimated that overall, 1 - 2% of dye was lost to waste in a typical manufacturing process and a further 6 - 10% in the processing operations. Based on estimated global annual production figures of *ca* 800,000 tonnes (Table 1.1), this could produce 96,000 tonnes of manufacturing and processing dyestuffs discharged into effluent streams per annum. A more recent assessment (Hobbs, 1988) broadly agreed with these estimates for discharges, but added that for certain dyes (ie reactive and acid dyes) the proportion of waste could be even higher. Approximately 6% of annual world dyestuffs production is reactive dyes (*ca* 48,000 tonnes). Considering that around 50% of reactive

dye is lost to waste in textile processing and only 10% of this is likely to be removed in treatment, this suggests a figure of 20,000 tonnes of reactive dyes alone could be released into the aquatic environment per year world wide.

As discussed earlier, most azo dyes are relatively non-toxic. However, reduction of azo dyes produces aromatic amines which may be toxic, carcinogenic or teratogenic (Chung, 1992; Brown and De Vito, 1993). Thus the release of azo dyes into the environment, in which they may be reduced, is a cause for concern. Likewise there is evidence to suggest that substituted diaminonaphthalenes produced from the degradation of some anthraquinone dyes, may have carcinogenic properties (Chung, 1992). These highlight the need for a better understanding of the environmental fate of both azo and antraquinone reactive dyes.

A summary of newer, more effective treatment processes for dye removal is presented in Table 1.3 (Cooper, 1993). Although this suggests that dyes, including reactive dyes, can be readily degraded under appropriate conditions, the implementation of such systems is far from straightforward, (Howe, 1993; Byrom, 1995; Cooper, 1993).

Table 1.3 Summary of recent improved treatment technologies for colour removal (Cooper, 1993)

Method	Colour Removal	Volume Capability	Speed	Cost
Activated Charcoal	Very good	Small	Slow	High
Membrane	Good	Large	Fast	High
Ozone treatments	Good	Large	Medium	Medium
Coagulation / flocculation	Good	Large	Fast	Medium / high

Activated carbon is very good at removing low concentrations of water soluble chemicals including dyes, but has a limited capacity and is best suited to dilute solutions. Also, the viability of such technology is based on the ability to regenerate the carbon through desorption of the trapped materials. This is very difficult for dyes, leading to increased costs in terms of disposal and replacement of the carbon. Activated carbon is therefore not viable for the large volumes involved in dye effluent treatment.

Membrane filtration is an alternative procedure and can be divided into three main types: ultrafiltration is ineffective for dye removal because of the relatively large pore sizes which allow dyes to pass through; nanofiltration and reverse osmosis membranes are both effective for dye removal. Dye molecules are concentrated on one side of the membrane, while water can pass through. The main disadvantages are high initial set-up costs and the high cost of disposal of the concentrated 'used' dye collected in the process, which generally requires incineration.

Ozone treatments in the presence of UV are very quick and effective for the degradation of dyes, but they are expensive to set-up and are also relatively small scale. This method may also produce degradation products which are more toxic than the original dyes. For example, some cases of ozone treatment may form diamino aromatic compounds from azo dyes, some of which have been shown to be carcinogenic (Brown and DeVito, 1993).

Chemical treatment by coagulation and flocculation has been shown to be one of the most robust methods for removal of colour. Usually coagulating and flocculation agents such as lime, Fe(III) or Al(III) salts are added, followed by sedimentation or dissolved air flotation to aid the process. These produce a floc that can be removed by filtration, sedimentation or can simply be scraped off. However this approach produces a large amount of sludge waste and is not effective for all dye types.

In conclusion, it is clear that reactive dyes in particular, and acid dyes to a lesser extent, can enter UK river waters at concentrations significantly greater than 1 mg l^{-1}. Few of the textile dye houses have the ability to effectively treat waste prior to discharge into rivers or sewers. Reactive dyes are not removed in conventional STW and are possibly of most concern in terms of environmental pollution. New technologies exist to remove colour, but they are either too expensive or may produce effluents which, although less coloured, are more toxic than the original dye waste.

Little is known about the fate of reactive dyes once they enter the aquatic environment. One reason for this lack of information is the paucity of analytical methods suitable for the determination of dyes in aqueous samples.

1.3 ANALYTICAL METHODS FOR THE DETERMINATION OF DYES IN AQUEOUS SAMPLES

Many intact dyes can be easily measured by spectrophotometry because they contain strong chromophores. However, process and environmental decomposition of dyes may lead to formation of complex mixtures of products, not all of them containing a chromophore. Chromatographic separations and sensitive spectroscopic techniques are desirable, especially for samples derived from complex environmental matrices such as waste effluent.

GC-MS, although applicable to the analysis of semi-volatile dye compounds and their intermediates such as disperse dyes, (Maguire, 1991, 1992), is not suited to the analysis of polar, involatile or thermally labile dyes. Several approaches have been adopted for the chromatographic separation of mixtures of sulphonated materials including dyes. The most efficient have involved use of high performance liquid chromatography (HPLC or LC). A combination of LC and mass spectrometry (MS) is needed to separate and detect or

identify dye related materials. From an historical viewpoint, several approaches were taken to overcome the incompatibility of a typical reverse phase LC mobile phase at a flow of 1 ml min^{-1} and the high vacuum (typically 10^{-5} - 10^{-6} Torr) of a mass spectrometer. Two of the first commercial approaches to overcome this incompatibility problem were the direct liquid introduction (DLI) and moving belt interfaces. Both have been widely reported (including Vestel, 1986; Cairns and Siegmund, 1990) and are not discussed in detail here. For DLI the liquid eluent was directed along a central probe into the mass spectrometer source. A 3 - 10 μm pinhole was placed in a diaphragm at the end of the probe, such that a small amount of eluent, typically 5 - 15 μl, was sprayed into the MS source. In the case of the moving belt interface, LC eluent was spray deposited onto a slowly moving polyimide belt. Analyte containing solvent was removed in two stages: first by evaporation under an infra red heater, followed by removal of residual solvent in a two stage vacuum lock. The deposited analytes were removed from the belt by flash vapourisation within the MS ion source. Neither technique was particularly robust. DLI had a tendency to block and was not particularly sensitive. The moving belt suffered from non-uniform deposition of mobile phase on the belt, particularly for highly aqueous mobile phases, leading to poor reproducibility. An inability to vapourise highly polar materials from the belt and the memory effects of analytes not wholly removed from the belt on the first pass were also commonplace. Although both DLI and moving belt provided workable interfaces for certain LC-MS applications, neither interface was particularly suited to non-volatile and thermally labile compounds and they are not now widely used.

Two further LC-MS interfaces have been used for the analysis of dyes. Particle beam was used to obtain electron impact (EI) type mass spectra for a range of low molecular weight pure non-polar disperse and solvent dyes (Yinon, 1989). A requirement of this technique is volatilisation of analytes in the interface prior to entry into the mass spectrometer source and so is not applicable to reactive dyes. Monaghan, (1982, 1983) described MSMS spectra of a

range of highly polar sulphonated and phosphonated azo dyes using fast atom bombardment-MS (FAB-MS).

However the first LC-MS interface to experience widespread usage and application for the analysis of dyes was so called thermospray MS.

1.3.1 Thermospray - Mass Spectrometry

The first robust and widely accepted LC-MS interface capable of accepting normal eluent flow rates (1 ml min^{-1}) and the highly aqueous mobile phases associated with reverse phase separations, was thermospray-MS (TSP-MS) (Blackley and Vestel 1983; Garteiz and Vestel 1985; Vestel 1986; Betowski, 1996).

In this technique, LC eluent passes through a heated capillary tube into the mass spectrometer source. A combination of flow rate through, and direct heating of, the capillary produces a supersonic jet of fine droplets at or near the capillary tip. Evaporation of solvent molecules associated with the droplets continues until the electrostatic charge on the evaporating droplet becomes large enough to expel ions associated with a few solvent molecules. Finally, these clusters equilibrate with the vapour in the ion source to give molecular ions or adduct ions which may be sampled and analysed by a mass spectrometer. Primary ions observed in this process are the same as those present in solution. NH_4^+, $CH_3CO_2^-$ and clusters of these ions with neutral species such as ammonia, acetic acid (from an ammonium acetate buffer) water and methanol (from the mobile phase), are observed after vaporisation, suggesting ion evaporation may be applicable to any analyte that is present as an ion in solution. These ions are produced without any other external means of ionisation and the process is, therefore, called thermospray or ion evaporation ionisation.

The second mode of ionisation in thermospray LC-MS is termed buffer ionisation and is effectively a gas phase chemical ionisation process where the mobile phase acts as the reagent gas. During vaporisation nearly all of a buffer, such as ammonium acetate, is converted to ammonia and acetic acid in the gas phase. The following gas phase equilibria are obtained in the ion source:

$$NH_4^+.H_2O + NH_3 \rightleftharpoons NH_4^+.NH_3 + H_2O$$

$$NH_4^+(H_2O)_2 + NH_3 \rightleftharpoons NH_4^+.H_2O.NH_3 + H_2O$$

Vaporised analyte molecules can then interact with the ammonium ions in a gas phase chemical ionisation process, where, depending on the proton affinity of the analyte compared to ammonia, either $[B.H]^+$ or $[B.NH4]^+$ ions may be formed, where B is a Lewis base. Similarly in negative ionisation mode, the gas phase ionisation process can yield A^- or $HA.CH_3CO_2^-$ ions. Mechanisms for ion formation in thermospray have been widely studied (Vestel, 1983; Alexander and Kebarle, 1986; Voyksner, 1987).

The use of thermospray for the analysis of dyestuffs has been reported (Yinon *et al.*, 1989, 1990; McLean *et al.*, 1989; Straub *et al.*, 1992). The optimisation and application of thermospray is discussed in more detail in Chapter 2.

Promising though thermospray ionisation MS has been, the advent of modern day electrospray ionisation has seen an increasing use of this method.

1.3.2 Electrospray - MS

A schematic diagram of an electrospray ionisation (ESI) interface is shown in Figure 1.1. HPLC eluent is introduced through a sample tube consisting of a short length (20 cm) of 0.1 mm id deactivated fused silica within a stainless steel syringe needle. A sheath gas (nitrogen) is passed through the needle which acts as a nebuliser to aid solvent removal. The capillary and needle are held within the ESI probe which has an applied voltage, typically 3 - 5 kV. Nitrogen auxiliary gas helps to focus the aerosol into the heated capillary region of the source and also sweeps the chamber of solvent.

The ESI process transfers ions present in solution into the gas phase making it particularly suitable for the analysis of highly polar compounds including reactive dyes. The ionisation process can be described in terms of a series of events (Dole, 1968; Irbarne and Thompson, 1976, 1979; Fenn, 1990; Kebarle and Tang, 1993; Kebarle, 1999; Voyksner,1994).

First, as the solvent and solute exit the tip of the electrospray needle, the sheath gas and high voltage gradient (between the electrospray needle and heated capillary), produce a fine mist of charged droplets. The electrical charge density at the surface of the droplets increases as the droplets become smaller through solvent evaporation, until a critical point, the Rayleigh

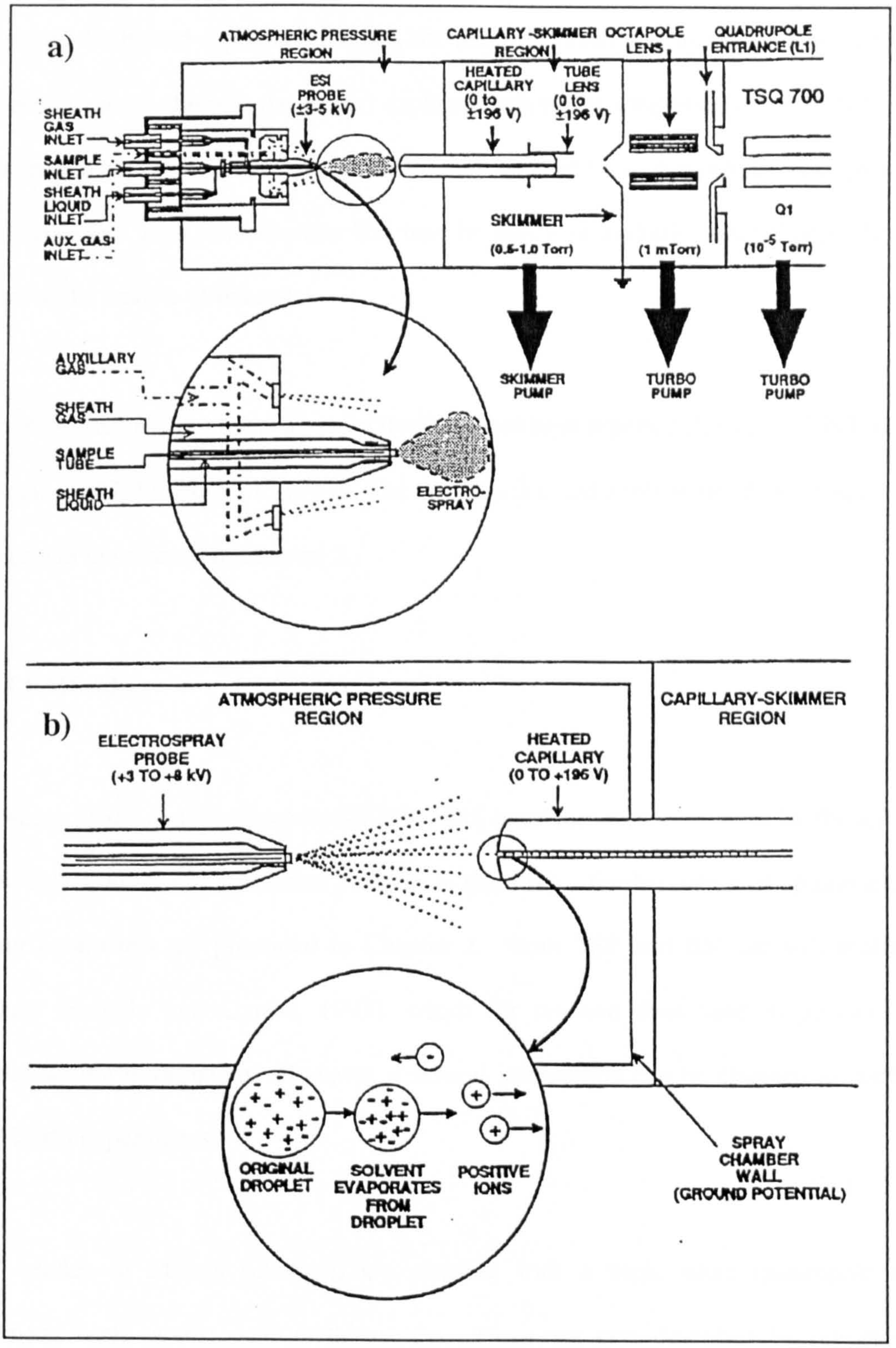

Figure 1.1 Schematic representation of an electrospray ionisation (ESI) mass spectrometer interface (APCI systems Operators manual, 1993)

stability limit, is reached, at which it divides into smaller droplets due to electrostatic repulsion. This process is repeated until droplets become very small and highly charged, when they can expel ions. As the droplets disperse, the electric field and sheath gas drive them towards the heated capillary. Finally, the aerosol containing sample ions and ambient gas molecules passes through the heated capillary, where the droplets are desolvated. The ions that remain pass into the mass spectrometer, are focused by an octapole lens and pass into the mass analyser. Ions formed under ESI may be singly or multiply charged depending on the nature of the analyte of interest.

The use of electrospray for the analysis of dyestuffs has been reported (Lin *et al.*, 1993; Rafols and Barcelo, 1997; Straub *et al.*, 1992). The optimisation and application of electrospray-MS is discussed in more detail in Chapter 2.

1.3.3 LCMS-MS

Thermospray (TSP) and Electrospray (ESI) LC-MS interfaces were both used for the analysis of reactive dyes and their degradation products in this study. Further details of optimisation of operating parameters are presented in Chapter 2. Both TSP and ESI are soft ionisation techniques (Barcelo and Garcia, 1993), which for reactive dyes tend to provide only molecular weight information. However structural information can be obtained through the use of MSMS experiments.

Several modes of MSMS operation are possible with a triple stage quadrupole mass spectrometer such as that used in this study. These are best described by reference to Figure 1.2:

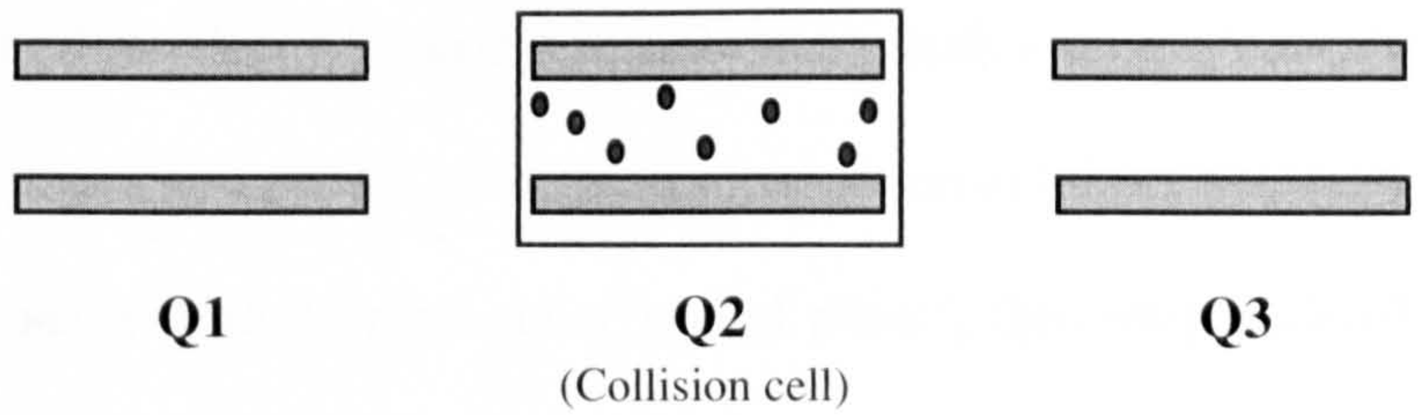

Figure 1.2 Schematic view of triple quadrupole mass spectrometer

Q1 and Q3 are mass analysers. These can be used to either transmit a single mass or can be scanned to transmit ions over a mass range. Q2 is the collision cell where an inert gas (usually argon or nitrogen) may be introduced to create a region of relatively high pressure. Ions transmitted from Q1 collide with the gas in Q2 and fragment in a process known as collision induced dissociation.

In a typical MSMS experiment conducted herein, a single mass (the parent ion, usually the molecular ion) was selected using Q1, fragmented in Q2 and Q3 was used to obtain a 'daughter ion' mass spectrum derived from the selected parent ion. This daughter ion spectrum may then be used to obtain structural information when little or no fragmentation is obtained in the normal LC-MS scanning mode.

Other modes of MSMS not applied in the present study include so-called parent ion scans, in which Q1 is scanned over a chosen mass range and each ion is fragmented in Q2. Q3 is set to monitor a selected fragment ion. This mode is useful for detecting related compounds that dissociate to a common fragment ion. For instance if *m/z* 80 (SO_3^-) was observed for a series of sulphonated compounds, and *m/z* 80 was selected using Q3, then only those molecular ions scanned using Q1 which fragmented to give an ion *m/z* 80, would be observed. This mode can sometimes be used to observe related metabolites in degradation studies.

In so-called neutral loss MSMS mode, Q1 and Q3 are both scanned 'out of phase', such that only parent ions that lose a certain group by fragmentation in Q2 are observed. For instance if Q1 and Q3 are set to scan 80 mass units 'out of phase', then only molecular ions scanned through Q1 which fragmented by loss of SO_3 (80), would pass through Q3 and be observed. This mode is often used in metabolite studies to screen for related compounds that have a common functional group such as $-SO_3$, -CO or $-CO_2H$.

1.4 THE PRESENT STUDY

Chapter 1 presented an overview of the present knowledge regarding the fate of fibre reactive dyes in the environment. Many of the highly polar reactive dyes present in trade effluent from dyestuff producers and users are not removed to any great extent by typical sewage treatment systems and therefore have a pathway into the aquatic environment. The potential modes of transformation and removal of reactive dyes in treatment and in the environment are principally through anaerobic and aerobic biodegradation and adsorption onto suspended solids. Additionally, photodegradation may also play a part in governing environmental fate.

One reason for this lack of information on the environmental fate of reactive dyes is the paucity of robust analytical methods suitable for the determination of dyes in aqueous samples. Robust analytical methods are required to characterise and identify reactive dyes and their degradation products in order to predict their transport and transformation in aqueous environmental samples. **Chapter 2**, describes the development of an LC method suitable for the separation of reactive dyes possessing up to four sulphonic acid groups. The subsequent use of this method with MS and the optimisation of LC-MS and MSMS conditions necessary for the characterisation of azo and anthraquinone reactive dyes are discussed.

Fibre reactive dyes are designed to have a degree of stability to degradation in daylight and for this reason they have not been widely investigated. However, little is known of their stability to daylight over prolonged periods of irradiation in dilute aqueous solutions and in the presence of humic substances. In **Chapter 3**, details of laboratory photodegradation studies of azo and anthraquinone reactive dyes, together with the LC-MS(MS) identification of degradation products, are discussed.

The reduction of azo dyes under anaerobic treatment has been extensively studied, but most studies have made use of relatively simple model compounds rather than real dyes. Additionally, the subsequent fate of the initial reduction products in the presence of air is not understood. Studies of the effects of autoxidation on the reduction products of both simple and more complex azo reactive dyes are discussed in **Chapter 4**, together with the LC-MS analysis of samples taken from anaerobic-aerobic treatment systems.

Reactive dyes are generally regarded as being resistant to oxidative attack by most bacteria under aerobic conditions. However, some cleavage of the azo bond of simple azo dyes has been reported under aerobic conditions and this required further investigation. Also, there are few published data regarding aerobic degradation pathways for reactive anthraquinone dyes. In **Chapter 5**, studies of single culture and mixed consortia aerobic biodegradation of azo and anthraquinone reactive dyes are discussed.

1.5 AIMS OF PRESENT STUDY

Specifically the aims of the present study were, therefore:

- To develop and optimise analytical conditions for the isolation, separation and identification of reactive dyes and their degradation products.
- To determine the potential for azo and anthraquinone dyes to photodegrade and to determine the effects of humic substances on these processes.
- To study the effects of autoxidation on the reduction products of simple azo reactive dyes and to use these as a predictive tool for the identification of autoxidation products of more complex dyes.
- To examine the role of aerobic degradation on the fate of reactive dyes.

1.6 REACTIVE DYES USED IN DEGRADATION EXPERIMENTS IN THE PRESENT STUDY

The dyes used in degradation studies are listed below and additionally as a pull-out section in Appendix 1.

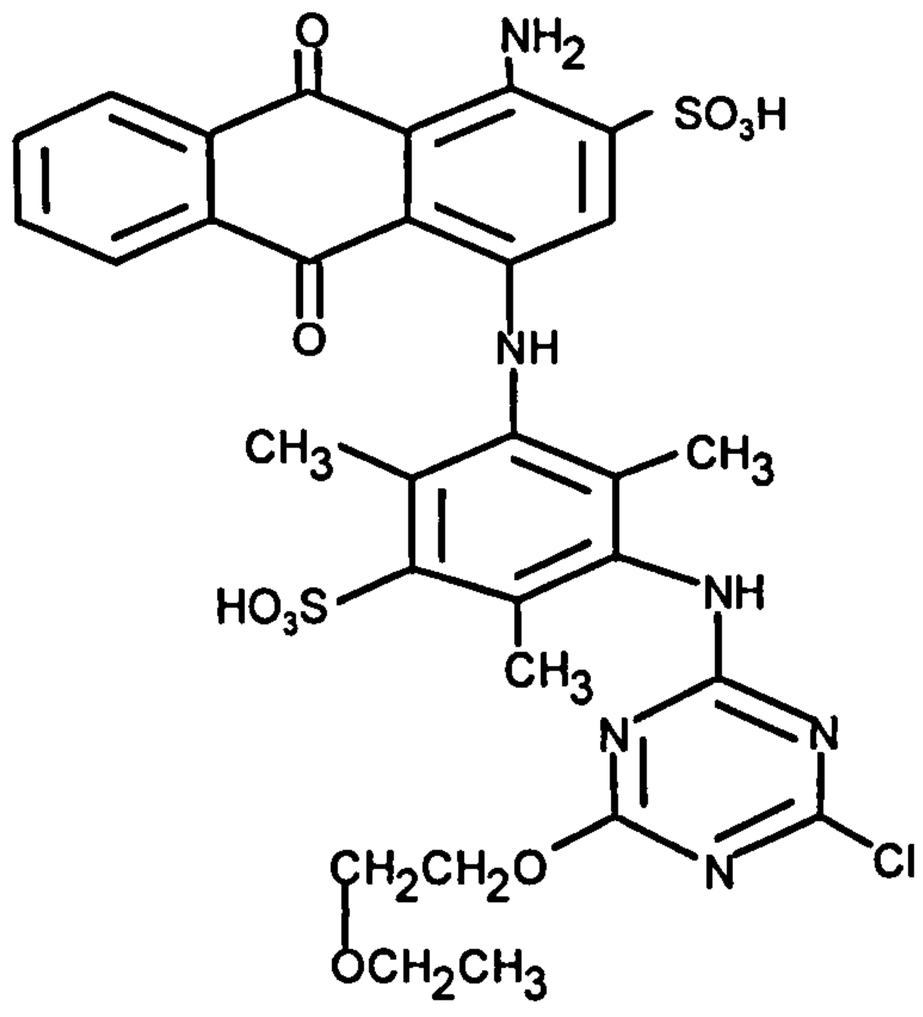

W435, Reactive Blue H4R

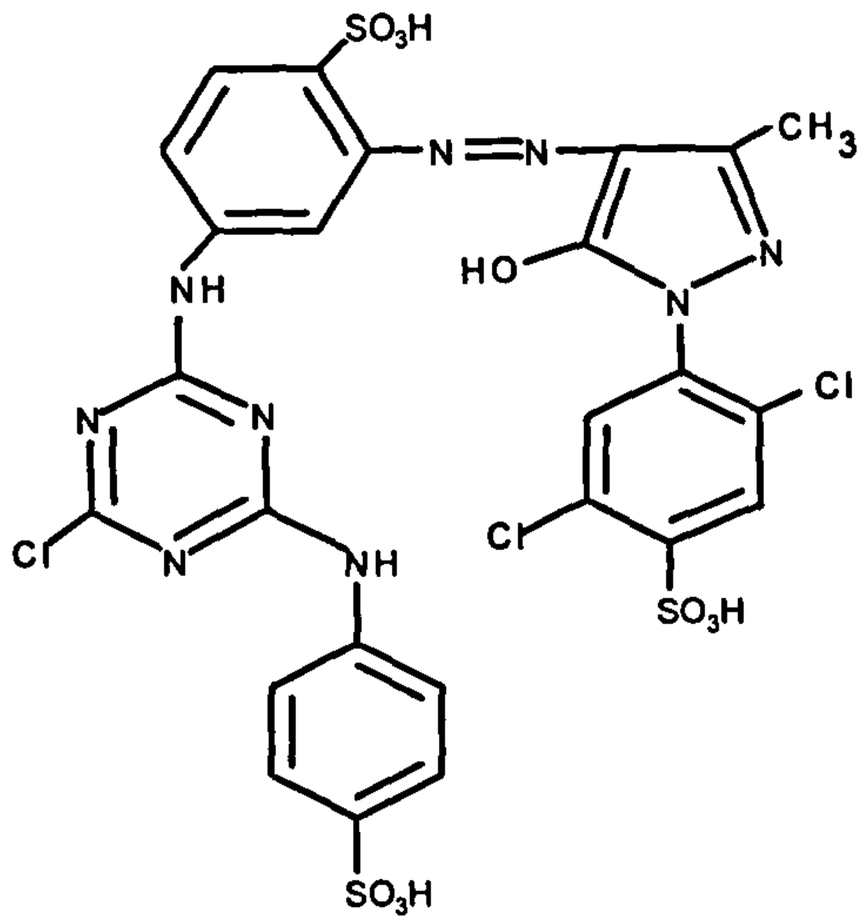

W433, Reactive Yellow 2

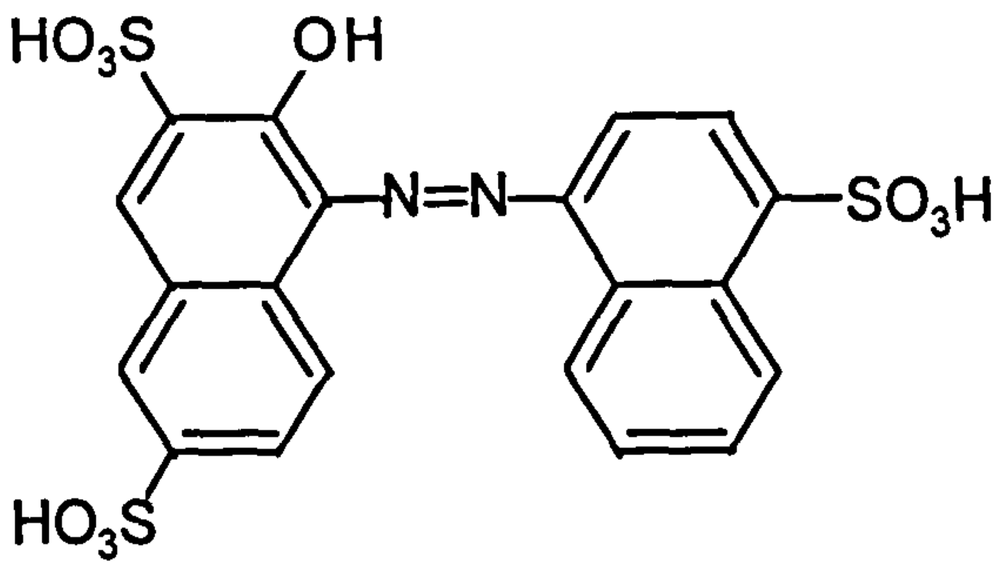

Amaranth

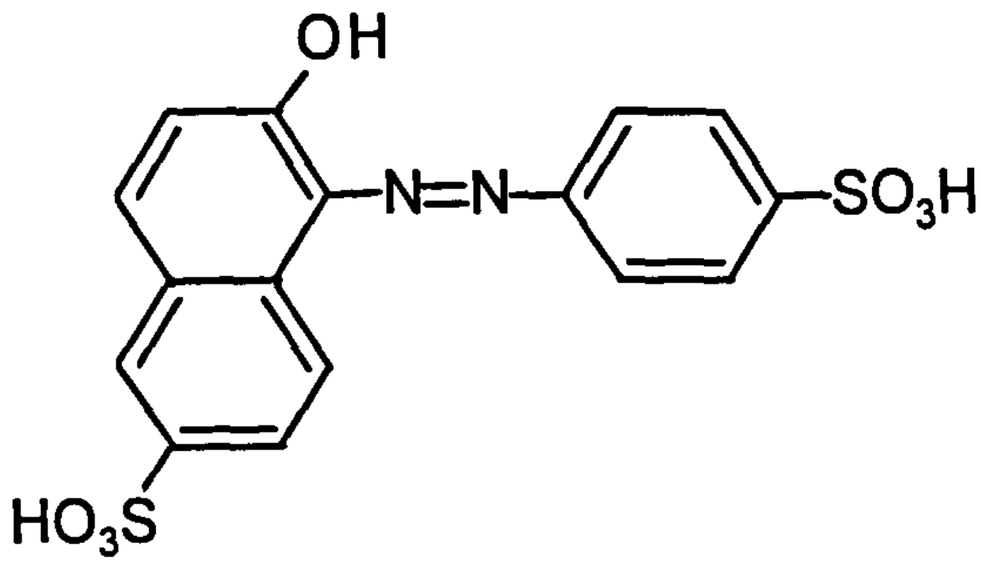

Sunset Yellow

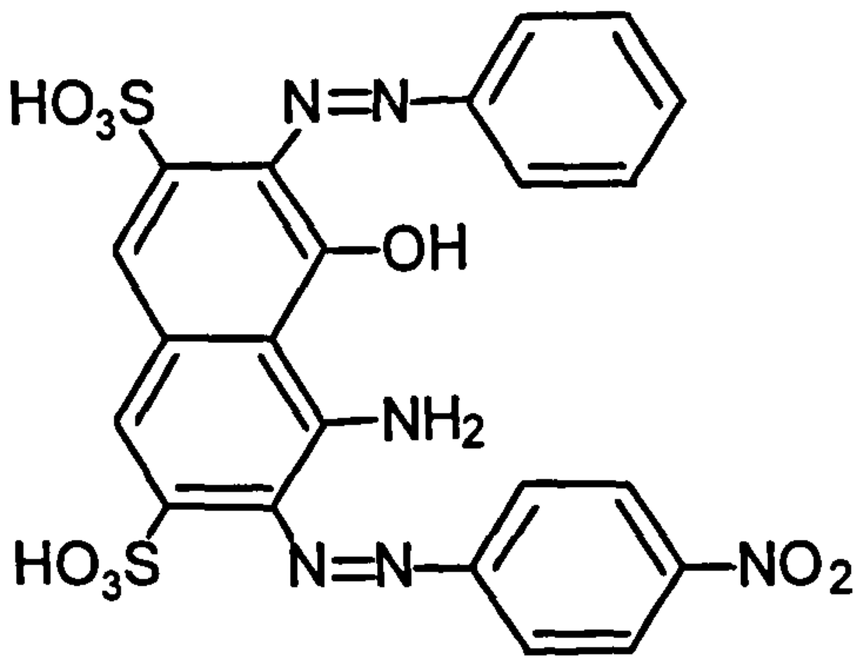

Naphthol Blue-Black

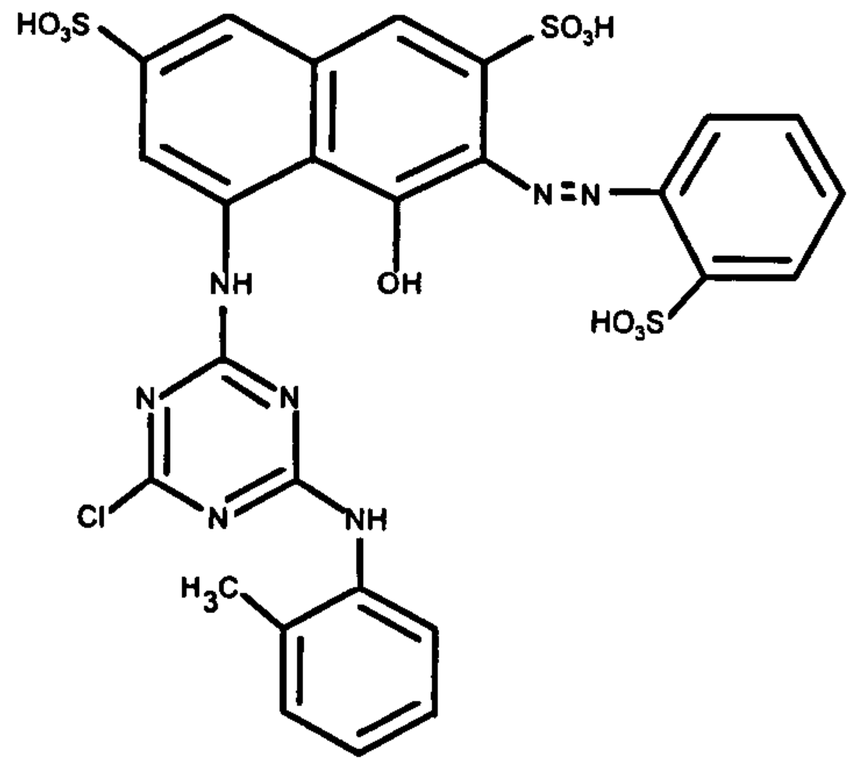

RR3.1, Reactive Red 3.1

CHAPTER 2

ANALYTICAL METHOD DEVELOPMENT

2.1 LC OPTIMISATION

2.1.1 Introduction

Several different approaches have been adopted for the LC separation of dyestuffs. Berzas-Nevado (1997) used an ion pair separation with tetrabutyl ammonium as the counter ion in a methanol / tetrabutylammonium phosphate mobile phase to study the chromatography of six acid dyes. Reverse phase LC systems have also been reported which used either sulphuric acid to adjust the pH of the mobile phase to 2.5 for the separation of acid dyes, (Speers, 1994) or included phosphate buffers (Truslove, 1992). Another method used a C8/anion exchange mixed mode column for the separation of a range of acid dyes (Weatherall, 1991), but once again phosphate buffer was used. None of these approaches are compatible with LC-MS interfaces such as those used in this study because inorganic buffers such as phosphates deposit in both thermospray and electrospray interfaces on desolvation, causing blockages and system failure. Also, reactive dyes can be detected best in negative ionisation mode whereas protonation of the sulphonic acid groups in the dyes at low pH require monitoring in positive ion mode with a reduction in sensitivity. The method developed in this study was therefore based on a reverse phase separation using tetrabutyl ammonium hydroxide as an ion pairing reagent (Truslove 1990), but used ammonium acetate in the mobile phase as buffer.

Eight reactive dyes were chosen for the initial evaluation of LC separation. The structures of the dyes are shown in Figure 2.1. Each dye was assigned a unique codename which is used as reference in the subsequent text:

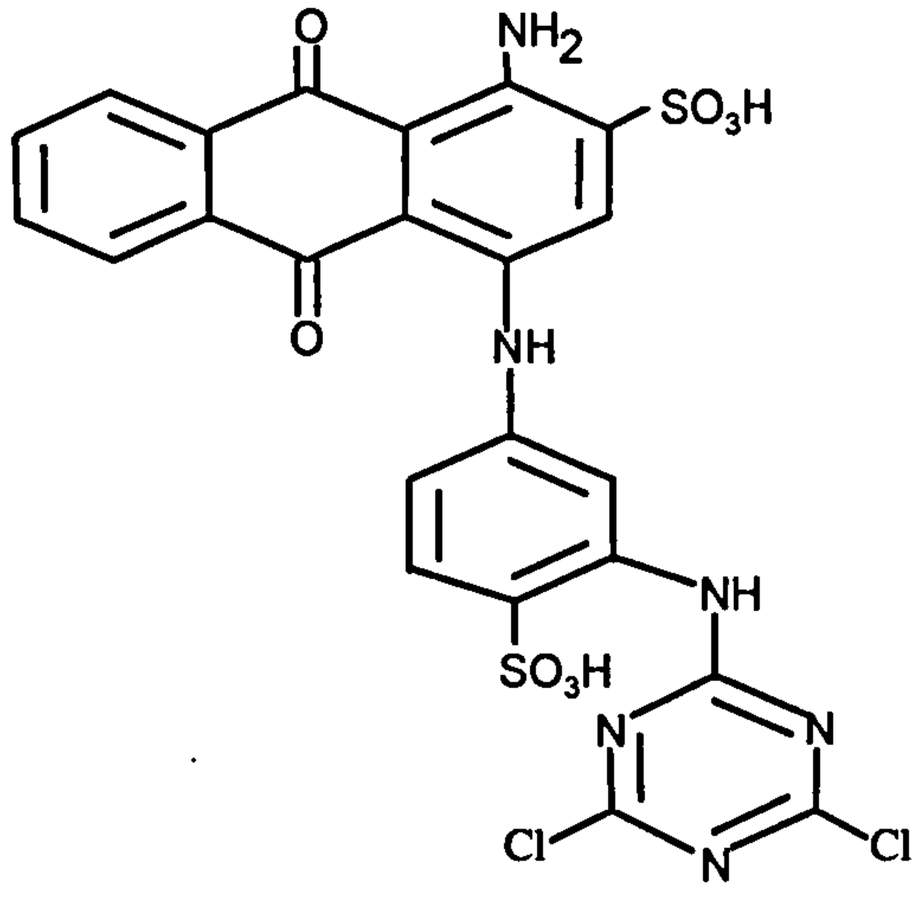

W428 Reactive Blue 4 or Blue MX-R

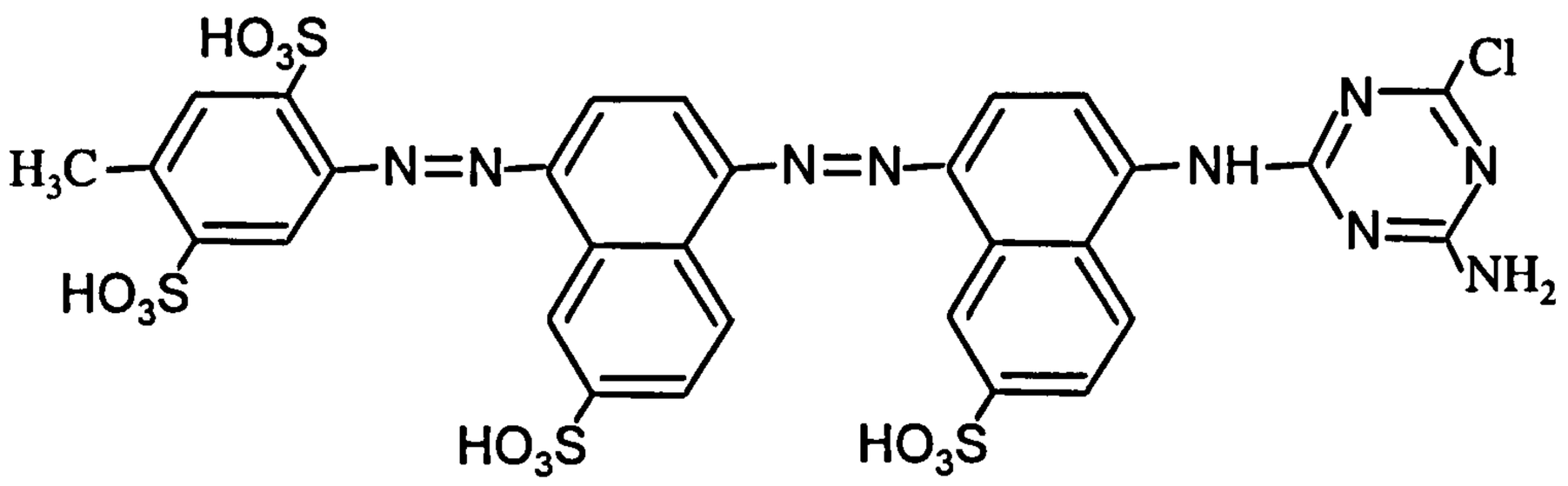

W429 Reactive Red-Brown HEXL

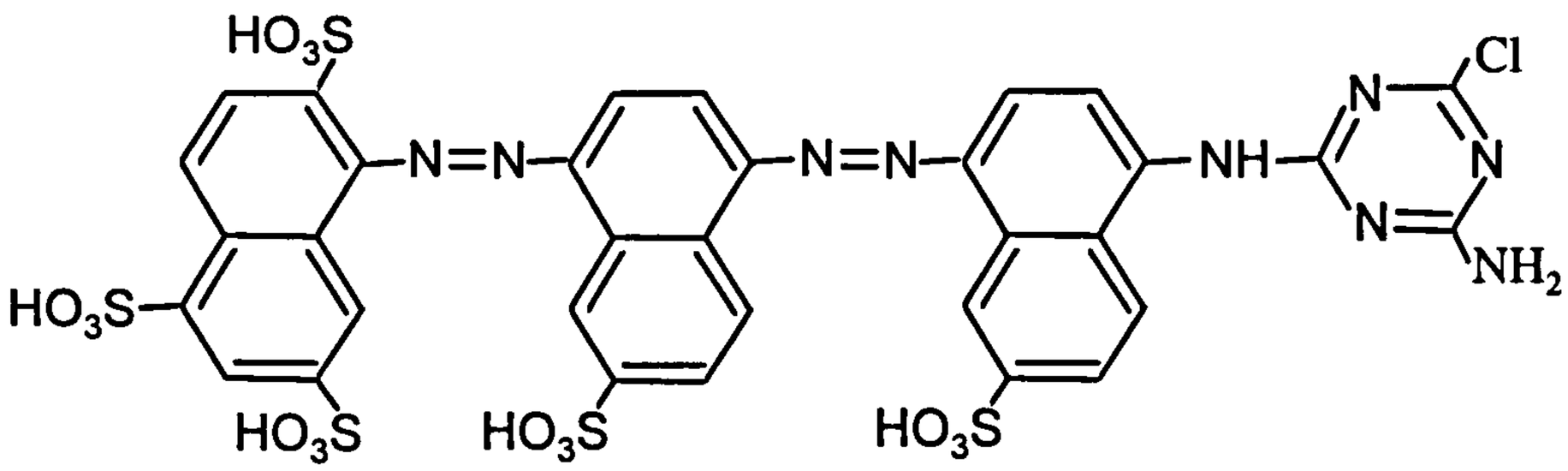

W430 Reactive Brown 7 or Brown H3R

Figure 2.1. Structures for reactive dyes used in LC optimisation

W431 Reactive Red 159, Levofix Br. Red EGBA

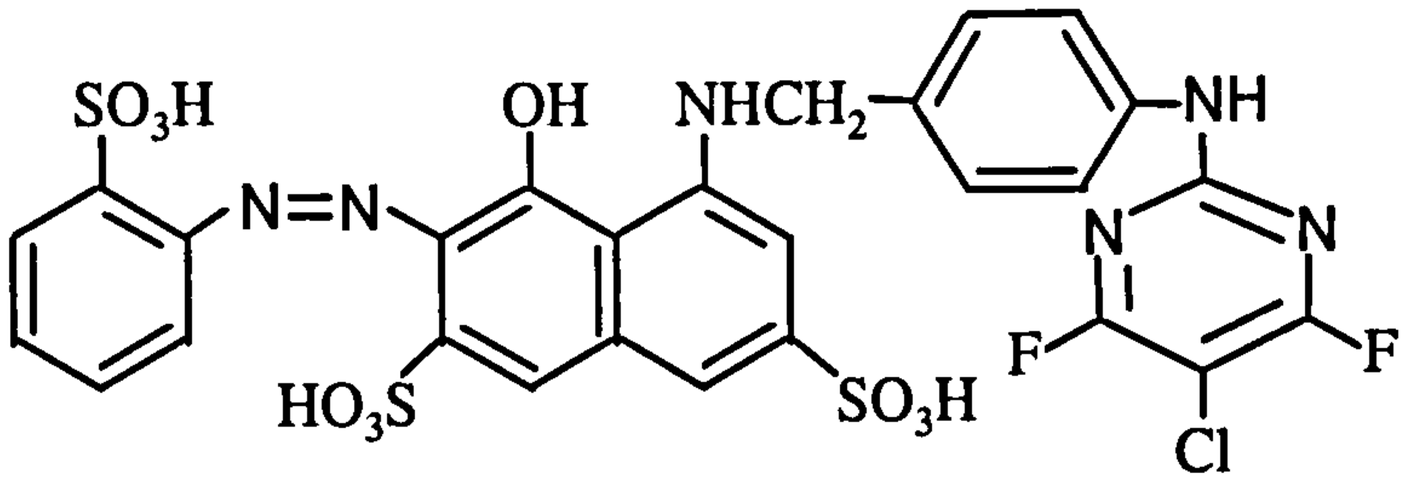

W432 Reactive Red 124, Levofix Br. Red EBA

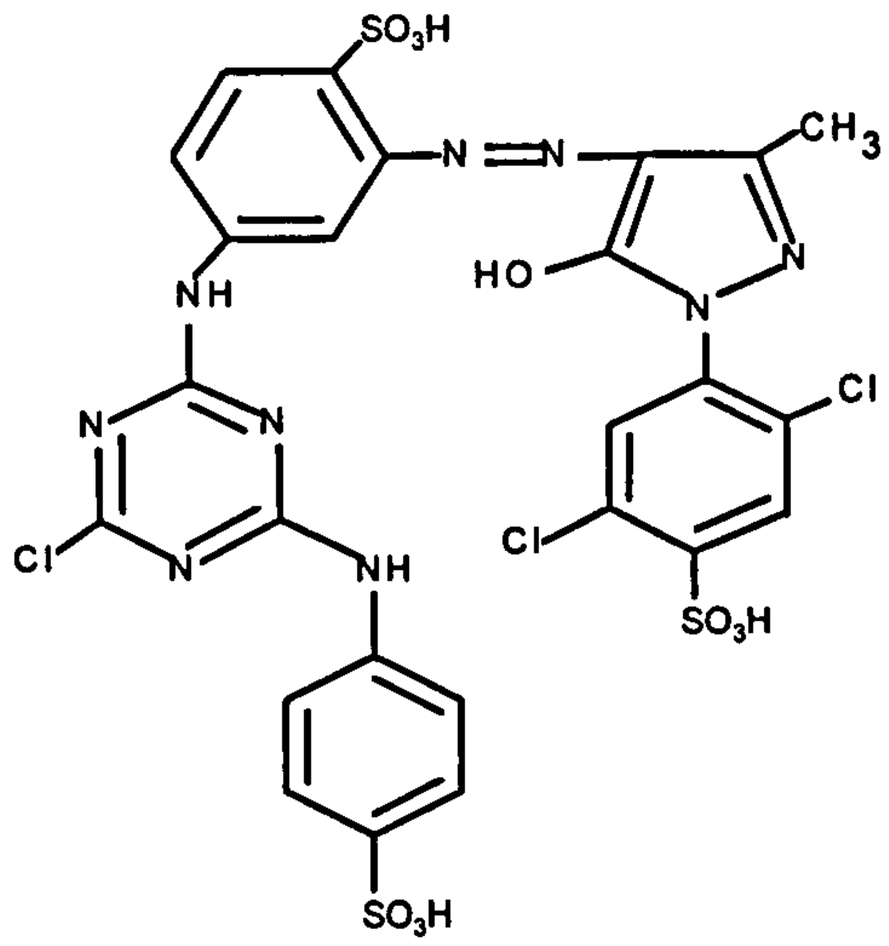

W433 Reactive Yellow 2 or Yellow P5G

Figure 2.1 contd. Structures for reactive dyes used in LC optimisation

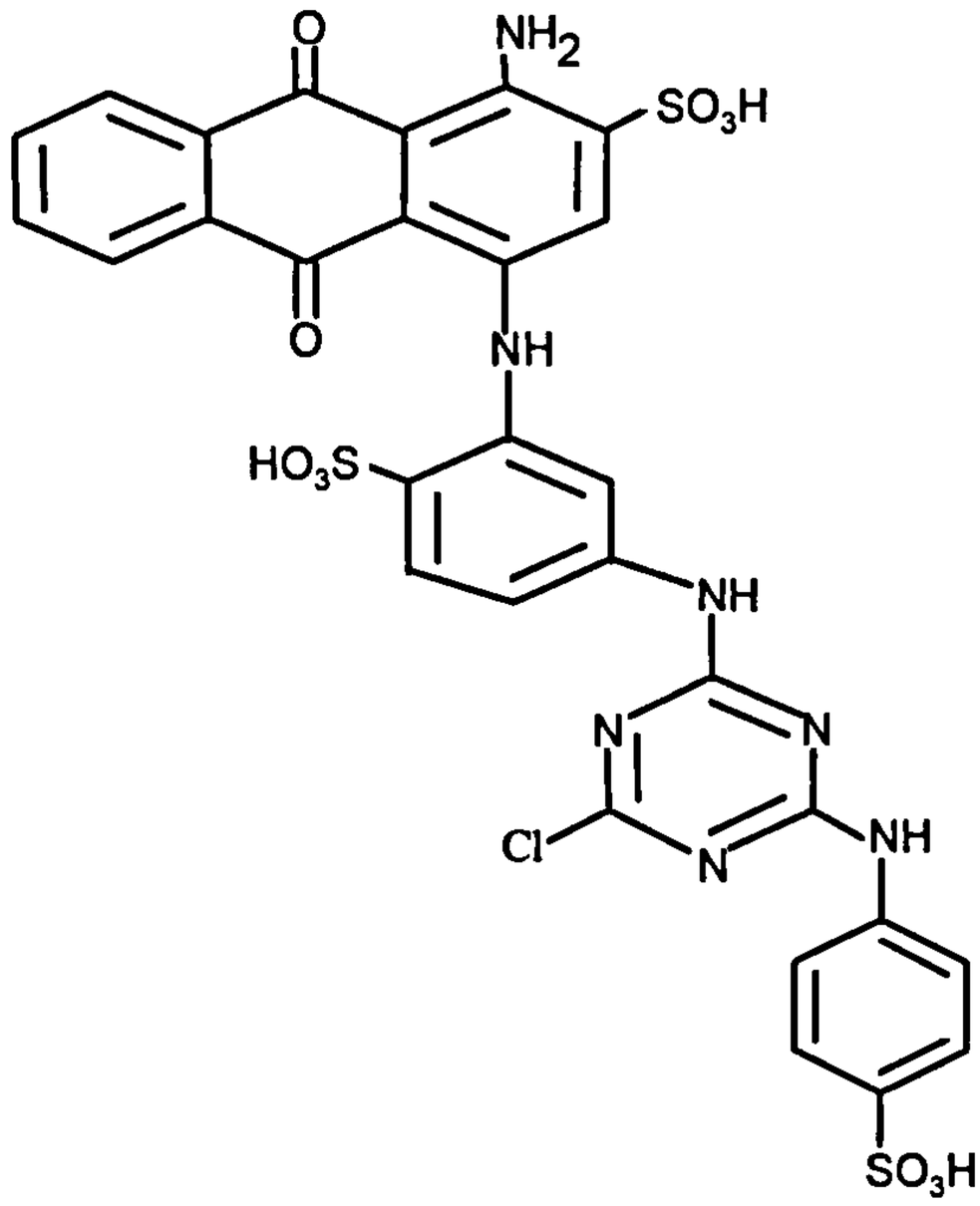

W434 Reactive Blue 5 or Blue H-GRA

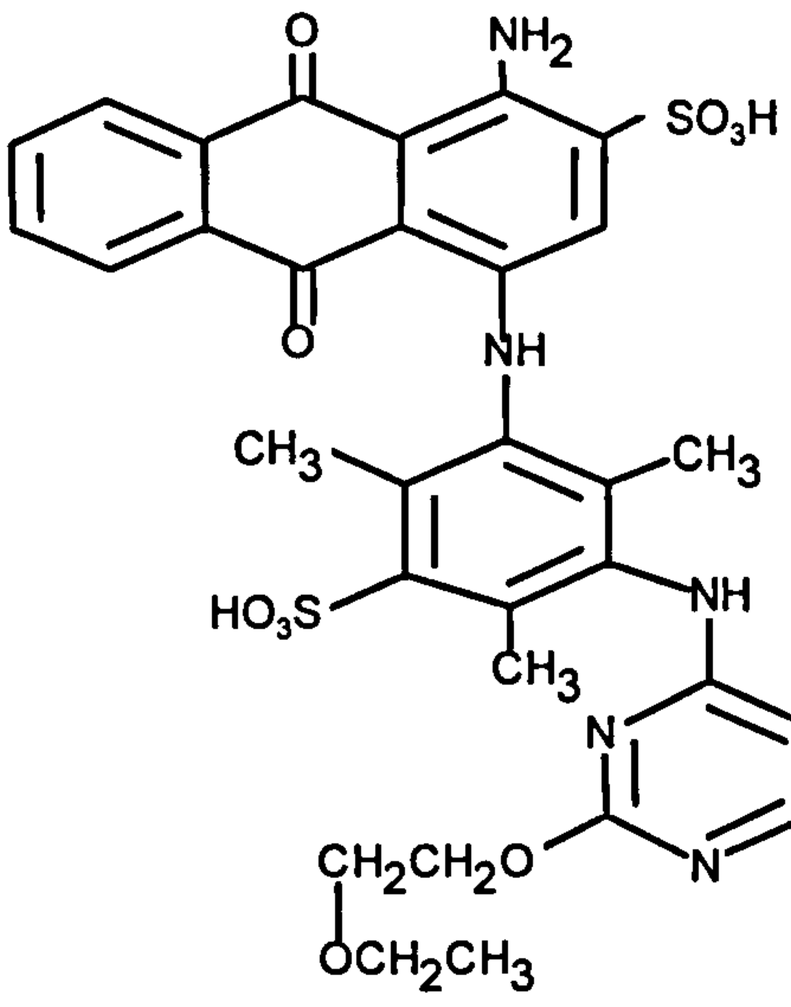

W435 Reactive Blue H4R or Blue HGR

Figure 2.1 contd. Structures for reactive dyes used in LC optimisation

The LC separation developed was based on details supplied by the dyestuffs manufacturers, Zeneca Specialties.

2.1.2 Experimental

A 25 cm x 4.6 mm id, S5ODS2 (Hichrom) LC column was used, with the mobile phase supplied by a Jasco 980 (or Waters 600e-ms) gradient elution pump. Elution was obtained using a linear gradient from 100% 0.01M ammonium acetate (10 min), to 50/50 ammonium acetate/acetonitrile (@ 30 minutes). Components were detected using a Jasco 875UV detector at 254 nm. Data were collected using an Xchrom data system (VG Ltd). Samples (50 µl) were injected either manually or *via* a Jasco 851AS autosampler.

2.1.3 Results of HPLC optimisation

Suggested conditions for HPLC separation of dyes resulting from much previous research (summarised by Truelove, 1990) used reverse phase LC with ion pairing reagents. An ion pair is required to reduce the solubilising effect of the sulphonic acid groups in the eluent, without which the dyes are unretained. However, since the sensitivity of negative ion thermospray LC-MS is impaired by the presence of buffer (Flory *et al.*, 1987; Covey *et al.*, 1988), buffer concentration has to be limited. Thus, LC conditions were re-optimised herein to give base line separation of the selected dyes at low (0.01M) buffer concentrations (Figure 2.2). The dyes were separated on the basis of decreasing polarity, ie those with four sulphonic acid groups (W430) eluted first, followed by those with three. The two dyes with two sulphonic acid groups (W435, and W428) were also resolved using this system. Analysis of four formulated dyes under these optimised conditions (Figure 2.2) suggested that several were impure (W433, 54% pure; W435, 56% pure).

2.2 PURIFICATION OF DYES BY SEMI-PREPARATIVE HPLC

2.2.1 Experimental

Semi-preparative LC separation was achieved on a 25 cm x 10 mm id ODS5 column, using a gradient of 0.01M ammonium acetate (100%) for 5 minutes, to 0.01M ammonium acetate/acetonitrile (50/50) at 40 minutes, operated at 1.5 ml min^{-1} and using a 1 ml injection loop. UV detection at 400 nm (yellow dye W433) or 630nm (blue dyes W428 and W435) was used. Fractions were collected on a Gilson model 912 fraction collector. The fractionation process was repeated several times. Fractions containing the pure dye were combined and the aqueous mobile phase removed by freeze drying.

Each purified dye was re-analysed by LC with Photo Diode Array (PDA) detection over the wavelength range 200 to 700 nm, with a Hewlett Packard 1050 system using conditions given in Section 2.1.2 and subsequently by LC-MS (conditions are described in Sections 2.3 and 2.6).

2.2.2 Results for purification of selected dyes

Given the impurity of the formulated dyes, the dyes were purified by preparative LC. This produced dyestuffs (*ca* 150 mg of each dye) of >90% purity (Table 2.1). UV spectra of each purified dye are shown in Figure 2.3. As would be expected, the two blue dyes (W435 and W428) each show an absorption maximum in the 600 nm region (λmax 590 and 630 nm) whereas W433 (yellow) shows a maximum in the 400 - 500 nm region (λmax 410 nm), under the chromatographic conditions used.

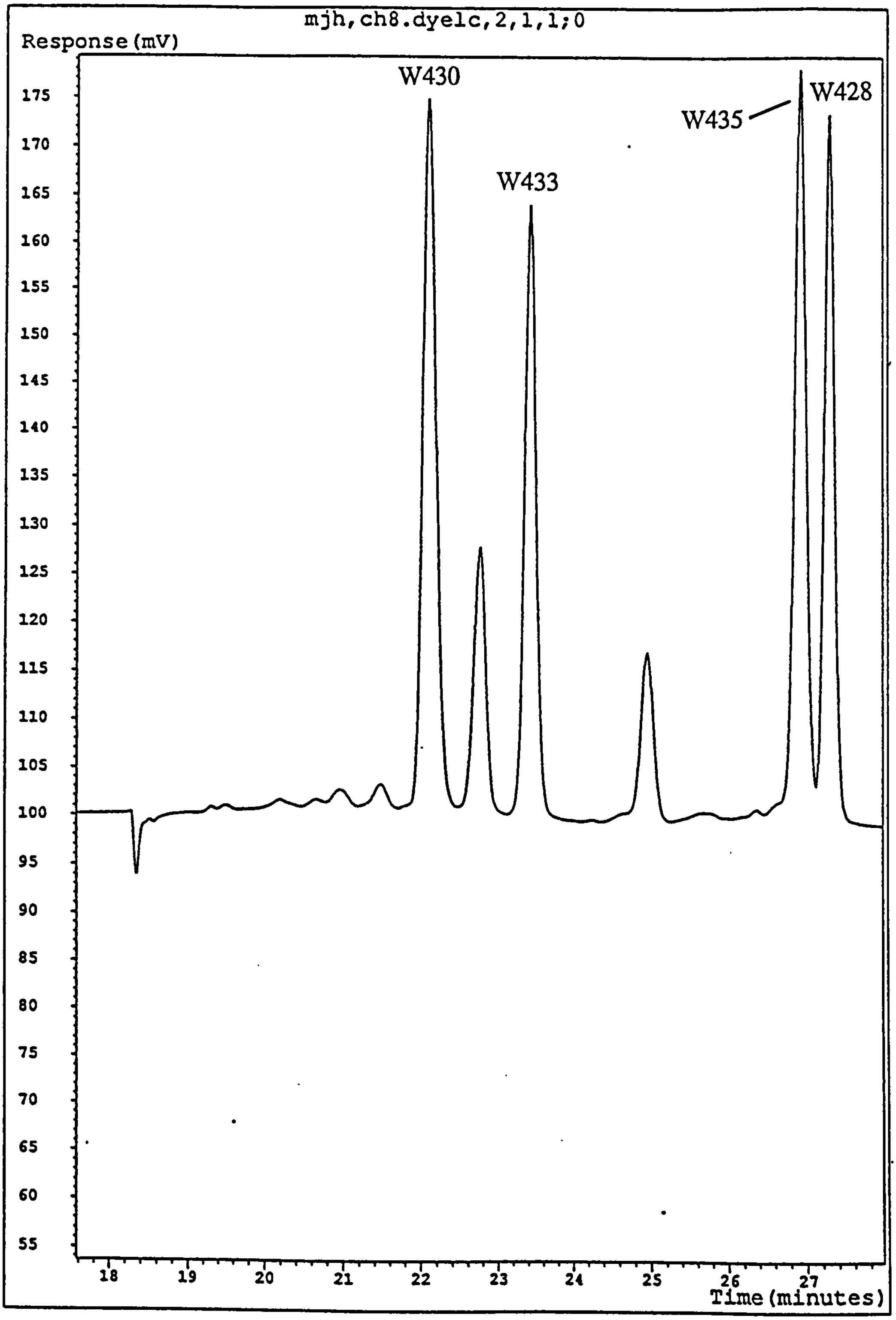

Figure 2.2 LC-UV (254 nm) separation of four reactive dyes using a gradient elution of 100% 0.01 M ammonium acetate (10 min) to 50 / 50 with acetonitrile (30 min)

Table 2.1 Purity of W428, W433 and W435 after preparative LC

W428

Peak No.	t_R (minutes)	Peak Area	%
3	**21.68**	**0.0054**	**5.1**
4	**22.01**	**0.0002**	**0.2**
5	**22.17**	**0.0006**	**0.6**
6	**23.5**	**0.0003**	**0.3**
7	**24.86**	**0.001**	**0.9**
8	**25.53**	**0.0022**	**2.1**
9	**25.88**	**0.0957**	**90.8**

W433

Peak No.	t_R (minutes)	Peak Area	%
1	**21.88**	**0.0786**	**100**

W435

Peak No.	t_R (minutes)	Peak Area	%
1	**21.72**	**0.0004**	**0.4**
2	**23.56**	**0.0047**	**4.3**
3	**24.31**	**0.0005**	**0.5**
4	**25.52**	**0.1031**	**94.6**

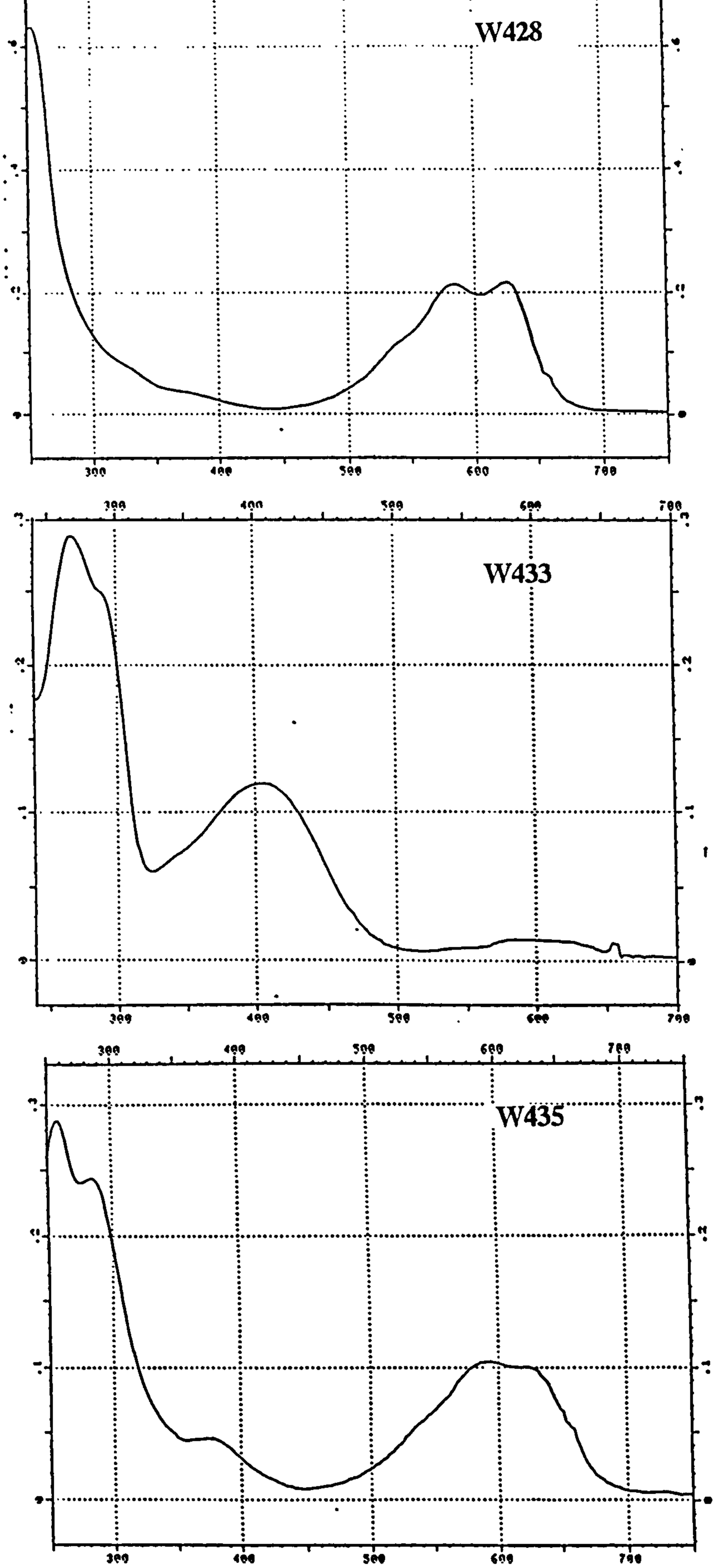

Figure 2.3 UV-Visible spectra (250-750 nm) for reactive dye W428, reactive Blue MX-R (Top), W433, reactive Yellow P5G (Middle) and W435, Reactive Blue HGR (Bottom).

2.3. THERMOSPRAY LCMS

2.3.1 Introduction

At the onset of these studies, only thermospray (TSP) was available as an interface for LC-MS analysis. TSP is both an interface for introduction of liquid samples into the mass spectrometer and an ionisation technique, (modes of ionisation were discussed in detail in Chapter 1.3). A schematic diagram showing the key elements to the interface and mass spectrometer source is shown in Figure 2.4.

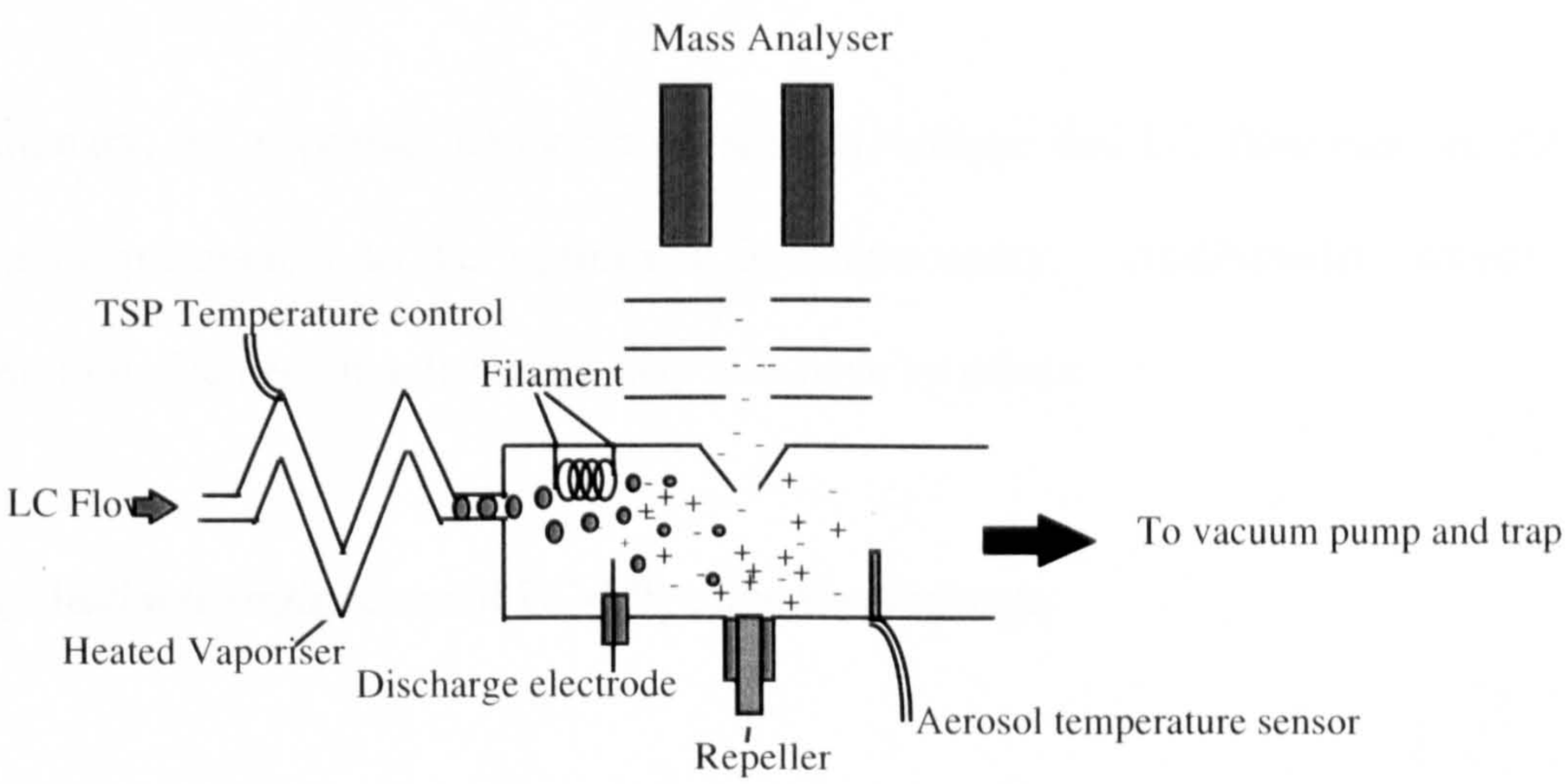

Figure 2.4. Schematic diagram of thermospray source

The flow from an LC pump passes through a heated stainless steel capillary known as the vaporiser, which has a laser drilled ruby at its tip. A combination of flow rate through the capillary and heating of the vaporiser, produces a supersonic jet of fine droplets at or near the vaporiser tip. The droplets then undergo rapid desolvation as they enter the relatively low pressure of the source, a process which is encouraged by heat supplied from the source block. Ions are formed which are focused into the sampling cone and source lenses by the repeller. The mobile phase and excess ions are removed under vacuum to a liquid nitrogen

2.3. THERMOSPRAY LCMS

2.3.1 Introduction

At the onset of these studies, only thermospray (TSP) was available as an interface for LC-MS analysis. TSP is both an interface for introduction of liquid samples into the mass spectrometer and an ionisation technique, (modes of ionisation were discussed in detail in Chapter 1.3). A schematic diagram showing the key elements to the interface and mass spectrometer source is shown in Figure 2.4.

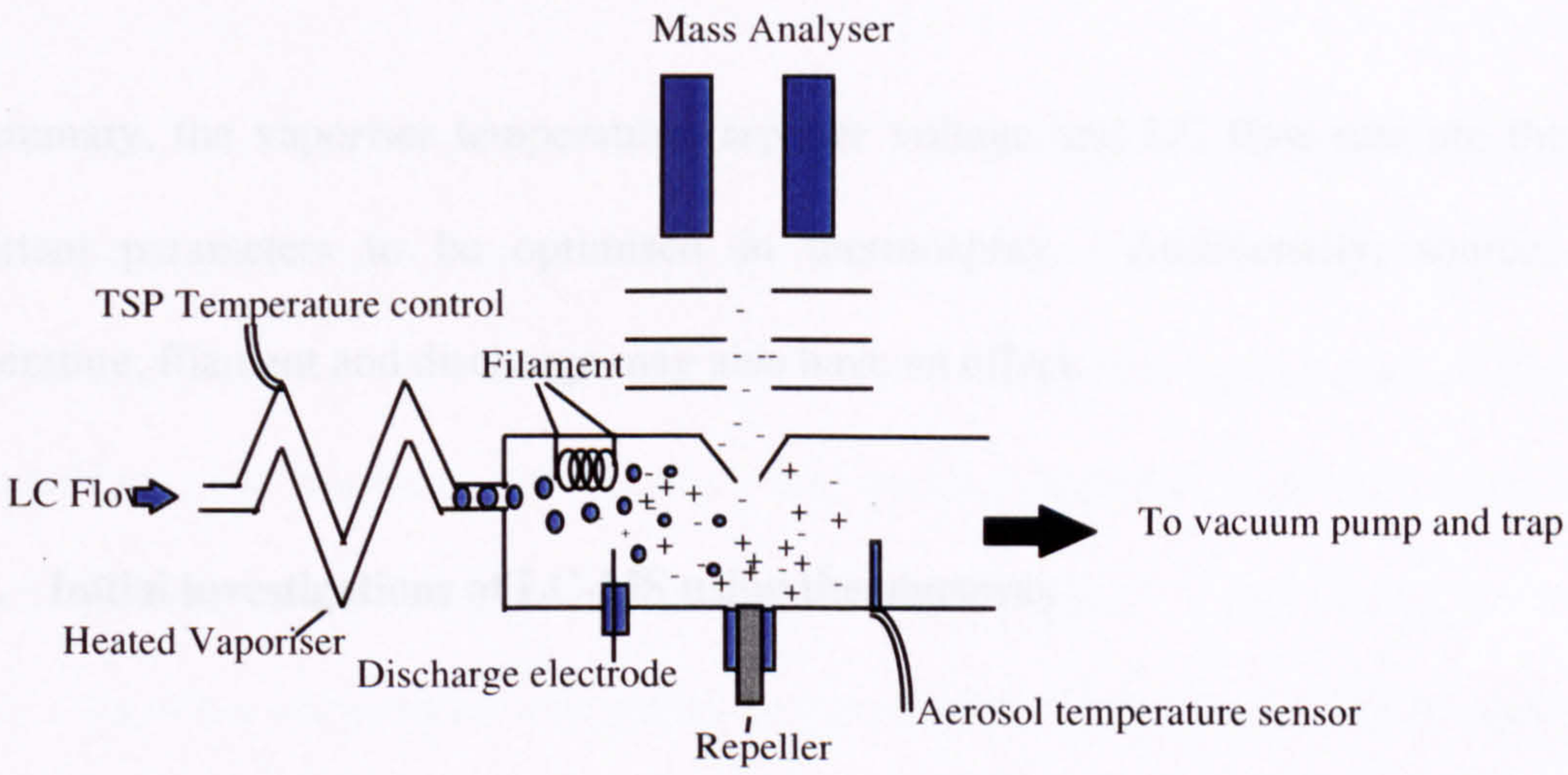

Figure 2.4. Schematic diagram of thermospray source

The flow from an LC pump passes through a heated stainless steel capillary known as the vaporiser, which has a laser drilled ruby at its tip. A combination of flow rate through the capillary and heating of the vaporiser, produces a supersonic jet of fine droplets at or near the vaporiser tip. The droplets then undergo rapid desolvation as they enter the relatively low pressure of the source, a process which is encouraged by heat supplied from the source block. Ions are formed which are focused into the sampling cone and source lenses by the repeller. The mobile phase and excess ions are removed under vacuum to a liquid nitrogen

trap. The vaporiser temperature is measured by a sensor on the heated capillary and the temperature of the eluent passing through the source is monitored by a sensor placed within the path of the aerosol through the source.

Additional to the variables described above, sensitivity can sometimes be increased through the use of a filament and/or discharge electrode. The former is an iridium filament, which ionises by means of an electron cloud. The discharge electrode is a small pin near the thermospray jet which may impart a charge on the droplets passing through. Filament and discharge can be used together or separately and their usefulness is very much compound dependent.

In summary, the vaporiser temperature, repeller voltage and LC flow rate are the most important parameters to be optimised in thermospray. Additionally, source block temperature, filament and discharge may also have an effect.

2.3.2. Initial investigations of LC-MS using thermospray

Initial work concentrated on tuning and optimisation of the TSP variables: Vaporiser heater temperature, filament, discharge and repeller voltages. For this, a test material, Reactive Blue 74 (W435), was added to the LC eluent via a 20 µl sample loop on a rheodyne valve. Replicate injections were made for each change of parameter and the optimum conditions selected.

LC eluent of 100% HPLC grade water was used, the source was set to 250°C, filament off and discharge 1200 V. The vaporiser temperature (t_{vap}) was varied between 85 and 100°C. Once optimum t_{vap} had been established, the repeller voltage was varied from -6 to -30 Volts in 2

Volt increments, to determine optimum setting. Using these optimised conditions, eight dyes were analysed by flow injection (20 µl loop), equivalent to 20 µg of each dye injected.

The LC eluent was then changed to 100% 0.01M ammonium acetate, the starting mobile phase composition for the optimised LC separation (Section 2.1). All other parameters were unchanged, but this time only those dyes giving a reasonably intense mass spectrum for the 100% water mobile phase were used, (W428, W433, W434 and W435), equivalent to 20 µg injected.

2.3.3. Initial investigation of thermospray using a needle repeller

Several authors, (Yinon, 1989a, 1989b; McLean, 1990) suggested a repeller modification which enhanced sensitivity for thermospray LC-MS. A modified needle repeller was manufactured 'in-house' for comparison with the existing flat bed repeller. The mass spectrometer was operated in negative ion mode, scanned over the mass range 200 - 900 daltons in 1 second, with a multiplier voltage of 1400 V and source temperature 250°C. Vaporiser temperature was optimised for maximum sensitivity by flow injection of W435 using an LC eluent of 100% 0.01M ammonium acetate. The repeller voltage was optimised at *m/z* 731 and 365, (singly and doubly charged W435 respectively).

Following optimisation, mixtures of dyes (100 mg l^{-1}) were analysed using the optimised LC conditions given in section 2.1.2 to obtain negative ion mass spectra.

2.3.4. Determination of limit of detection using thermospray LC-MS

The thermospray vaporiser temperature was optimised for best sensitivity and stability by flow injection of purified W435, then fine tuned under the standard gradient elution program. This gave optimum vaporiser temperatures of 87°C (100% ammonium acetate) and 83°C (50/50 ammonium acetate/acetonitrile). A small instrument control procedure was written to allow a linear decrease in temperature from 87 to 83°C over the course of the gradient elution.

Calibration standards of purified W428, W430 and W435 were prepared by serial dilution of a mixed stock solution to give concentrations in the range 25 - 500 mg l^{-1}. This was equivalent to the nominal concentration range 1 - 25 µg on column for a 50 µl injection volume. The optimised LC conditions (Section 2.1) were used. The mass spectrometer was scanned over the mass range 200 - 900 daltons in 1 second, repeller voltage ramped from -15 V (*m/z* 200) to -30 V (*m/z* 900), multiplier 1400 V and source temperature 250°C. The full scan data was collected by the data system and selected mass chromatograms for the sum of major ions of each dye plotted against concentration, to produce calibration plots.

2.3.5 Results for thermospray optimisation

2.3.5.1 Initial investigations of LC-MS using thermospray

The most critical feature for the successful and reproducible operation of TSP is the balancing of vaporiser temperature, source temperature and LC flow rate. These three are interactive. For a given LC flow rate, vaporiser and source block temperatures may be optimised to produce stable thermospray ions. Should the flow rate be increased, a higher source block and/or vaporiser temperatures are required. In practice the source block was maintained at constant temperature to avoid prolonged delays while the large mass of the

stainless steel block stabilised following a temperature change. The LC flow rate was determined by the optimised chromatographic conditions (Section 2.1) and to a lesser extent by the size of the liquid nitrogen solvent trap. The latter had a working volume of approximately 500 ml, which at LC flow rates of 1.5 ml min^{-1} provided a useful operating time of only 5 hours (including system conditioning and cleaning at the start and end of operation). This increased to 8 hours at a flow rate of 1 ml min^{-1}. Following an initial evaluation of source block temperature and using a flow rate of 1 ml min^{-1}, it was then necessary to optimise only the vaporiser temperature. At temperatures below optimum, droplets formed within the vaporiser jet are too large and do not desolvate efficiently within the source, leading to a poor response. At temperatures above optimum, the droplets can desolvate within the capillary, leading to deposition of buffers and inorganic materials within the vaporiser which change its characteristics and ultimately cause blockages. Through continued operation it was observed that the point at which the vaporiser temperature becomes too high, tended to coincide with the most intense response, but was characterised by a highly unstable signal, peaks obtained at too high temperatures being characterised by 'jagged' peak shape on flow injection. Generally a temperature about 3 - 5°C below this point was found to be most satisfactory.

Ballard and Betowski (1987) demonstrated that a range of dyes could be analysed using a thermospray interface. They had chosen positive ionisation for the majority of their analyses because most of the chosen dyes did not contain sulphonic acid groups. The exception was the azo dye Acid Orange 6, a rather simple chemical containing one sulphonic acid group. This produced mass spectra in both positive and negative ionisation modes with suggested limits of detection of 0.2 and 2 - 5 μg on-column for positive and negative ionisation respectively. Straub and Voyksner (1992) also used positive ionisation thermospray for the analysis of a range of solvent, disperse and acid dyes. However , only one of the selected dyes, Acid Orange 10, was sulphonated and this showed poor sensitivity (~35 μg on-column)

and a mass spectrum which indicated loss of the sulphonate which was probably due to thermal decomposition in the interface. Based on these data and other recommendations (Powel, personal com), which suggested that more complex reactive dyes did not produce mass spectra in positive ionisation mode, negative ionisation mode was chosen for the initial evaluation herein, using a dye concentration of 20 µg per injection.

Initial optimisation was achieved by flow injection of one of the least polar of the available dyes, (Reactive Blue 74, W435) into an LC eluent of 100% water. The mass spectrometer was operated in full scan mode and the reconstructed ion current (RIC) signal intensity plotted against vaporiser temperature (Figure 2.5). An operating temperature of 92°C was selected, 3°C below the maximum.

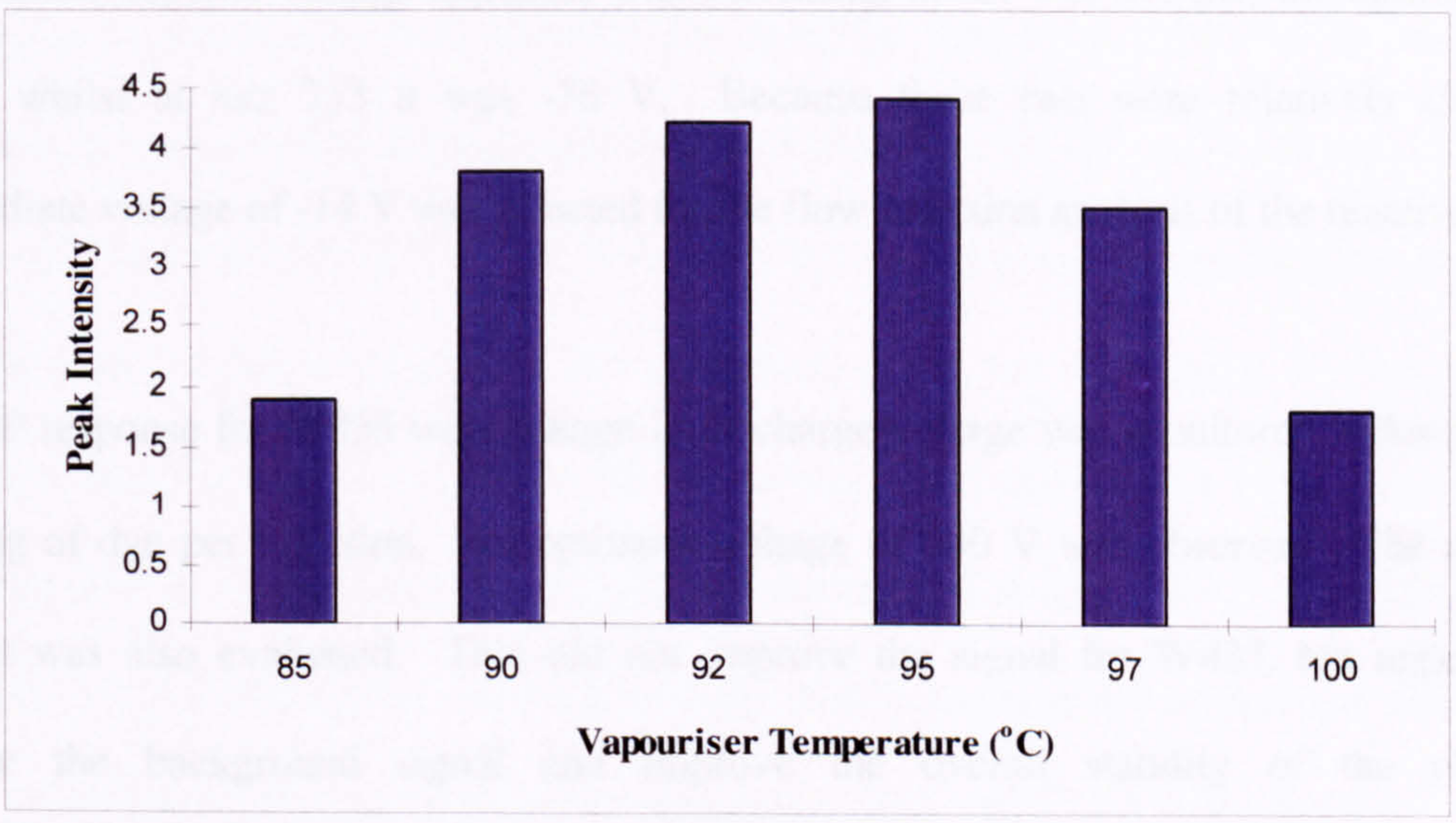

Figure 2.5. Initial TSP vapouriser optimisation for 100% water @ 1 ml min^{-1}

Having selected the vapouriser temperature, it was necessary to optimise the repeller voltage. The repeller is used to enhance the entry of ions into the sampling cone and subsequently the source lenses and mass analyser. When operated in negative ionisation mode, it had a negative charge. The repeller voltage was varied between -6 and -30 Volts and a dye concentration of 20 µg per injection was again used. The mass spectrometer was operated in full scan mode and the peak intensity of selected ion chromatograms for *m/z* 365 and 753 ($[M-2Na]^{2-}$ and $[M-Na]^{-}$ respectively) plotted against repeller voltage, (Figure 2.6).

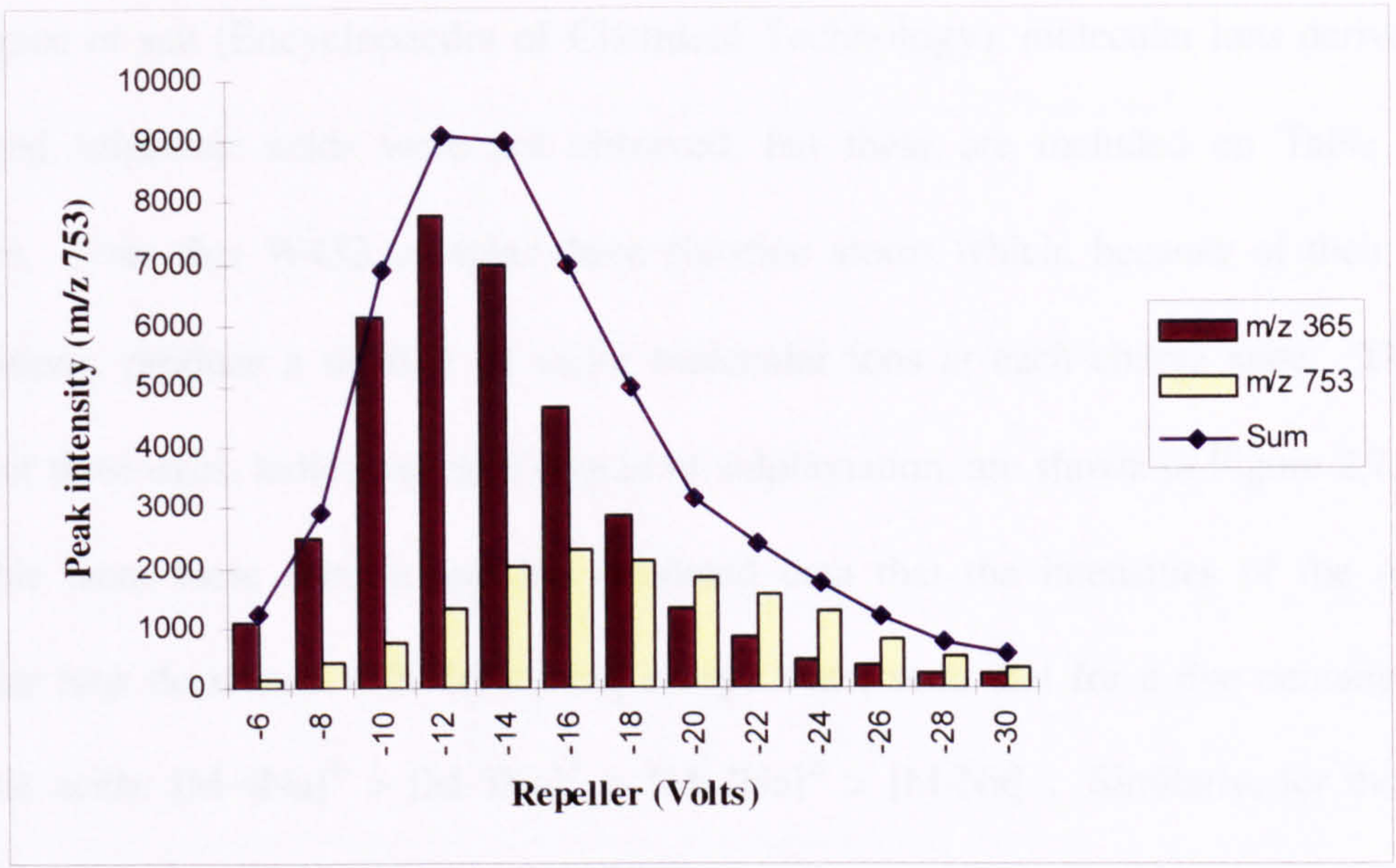

Figure 2.6 Optimisation of repeller voltage for the molecular ions of Reactive Blue 74 (W435)

The optimum repeller voltage increases with increasing mass. For *m/z* 365 the optimum was -12 V, whilst at *m/z* 753 it was -16 V. Because these two were relatively close, an intermediate voltage of -14 V was selected for the flow injection analysis of the reactive dyes.

The TSP response for W435 with change in discharge voltage was monitored following FIA of 20 µg of dye per injection. An optimum voltage of 600 V was observed. The use of a filament was also evaluated. This did not improve the signal for W435, but appeared to decrease the background signal and improve the overall stability of the observed chromatograms. A discharge voltage of 600 V and filament current of 600 µA were used for subsequent analysis.

A mass spectrum of each of the selected dyes was obtained by FIA-MS into a 100% water LC eluent. Each dye produced a series of molecular ions representing many of the possible charge states. Dyes containing four sulphonic acid groups produced four molecular ion clusters, for example. Observed ions and their relative intensities are summarised in bold in Table 2.2. Since the dye solutions were prepared from formulated material, which is known to contain a

high degree of salt (Encyclopaedia of Chemical Technology), molecular ions derived from protonated sulphonic acids were not observed, but these are included on Table 2.2 for reference. Note that W433 contains three chlorine atoms which, because of their isotope contributions, produce a doublet of major molecular ions at each charge state. The mass spectra of three dyes, indicating each degree of sulphonation, are shown in Figure 2.7. It was noticeable from these spectra and the tabulated data that the intensities of the observed molecular ions decreased with decreasing charge state, such that for a dye containing four sulphonic acids: $[M-4Na]^{4-} > [M-3Na]^{3-} > [M-2Na]^{2-} > [M-Na]^{-}$. Similarly, for those dyes containing three and two sulphonates. In most cases the singly charged molecular ion was responsible for less than 20% of the ion abundance of the base peak.

Four dyes were analysed by flow injection into an HPLC eluent containing 0.01M ammonium acetate which was to be the starting composition of the eluent for the optimised separation. Of the four dyes analysed, (W435, W434, W433 and W428), only the first produced a serviceable mass spectrum. A full evaluation of this phenomenon was not undertaken, but a qualitative assessment was made by comparison of the reconstructed ion current (RIC) intensity for W435 obtained in either a pure water or 0.01M ammonium acetate eluent. Peak intensity in pure water was 350,000 counts compared to only 10,000 counts in the presence of ammonium acetate - a 35 fold difference in observed sensitivity. This effect was also reported by Florey (1987), who indicated that ammonium acetate concentrations greater than 0.01M were detrimental to sulphonated azo dye detection in TSP, due to neutralisation reactions occurring in the ion source. From this analysis it would appear that buffers have a detrimental effect on thermospray sensitivity at even lower concentrations than previously reported. The same authors also reported the formation of $[M-2Na+H]^{-}$, the protonated form of sulphonate at higher ammonium acetate concentration, which was also observed for W435 (*m/z* 731) in this analysis.

Table 2.2. Observed (bold) and predicted molecular ions for thermospray FIA of selected dyes

Dye	MWT	[M-Na]	[M-2Na+H]	[M-3Na+2H]	[M-2Na]	[M-3Na+H]	[M-3Na]	[M-4Na+H]	[M-4Na]
W428	680	**657**	635		**317**				
(%)		25			100				
W429	951	**928**	906	884	**452.5**	441.5	**294**		**214.8**
(%)		6			30		44		100
W430	987	**964**	942	920	**470.5**	459.5	**306**	299	**223.8**
(%)		16			90		100		98
W431	900	**877**	855	833	**427**	416	**277**	270	
(%)		2			26		100		
W432	836	**813**	791	769	**395**	384	**255.7**	248	
(%)		11			42		100		
W433	871/873	**848/850**	826/828	804/806	**412.5/413.5**	401.4/402.5	**267.3/268**		
(%)		10			67		100		
W434	839	**816**	794	772	**396.5**	386	**256.7**	249	
(%)		7			58		100		
W435	776	**753**	731		**365**				
(%)		18			100				

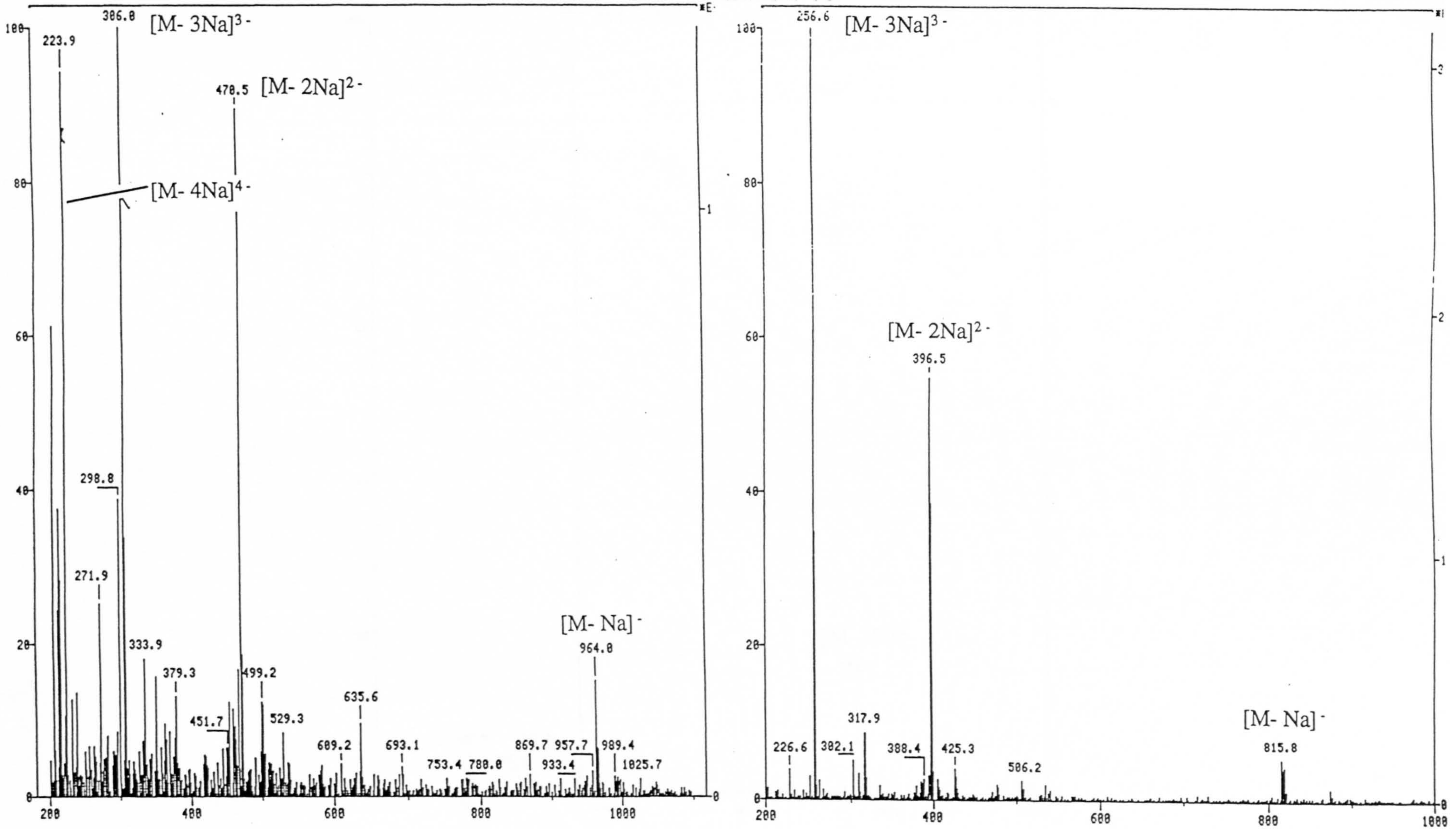

Figure 2.7 Thermospray mass spectra of W430 Reactive Brown H3R ($4*SO_3^-$) and W432 Levofix Br. Red EBA ($3*SO_3^-$)

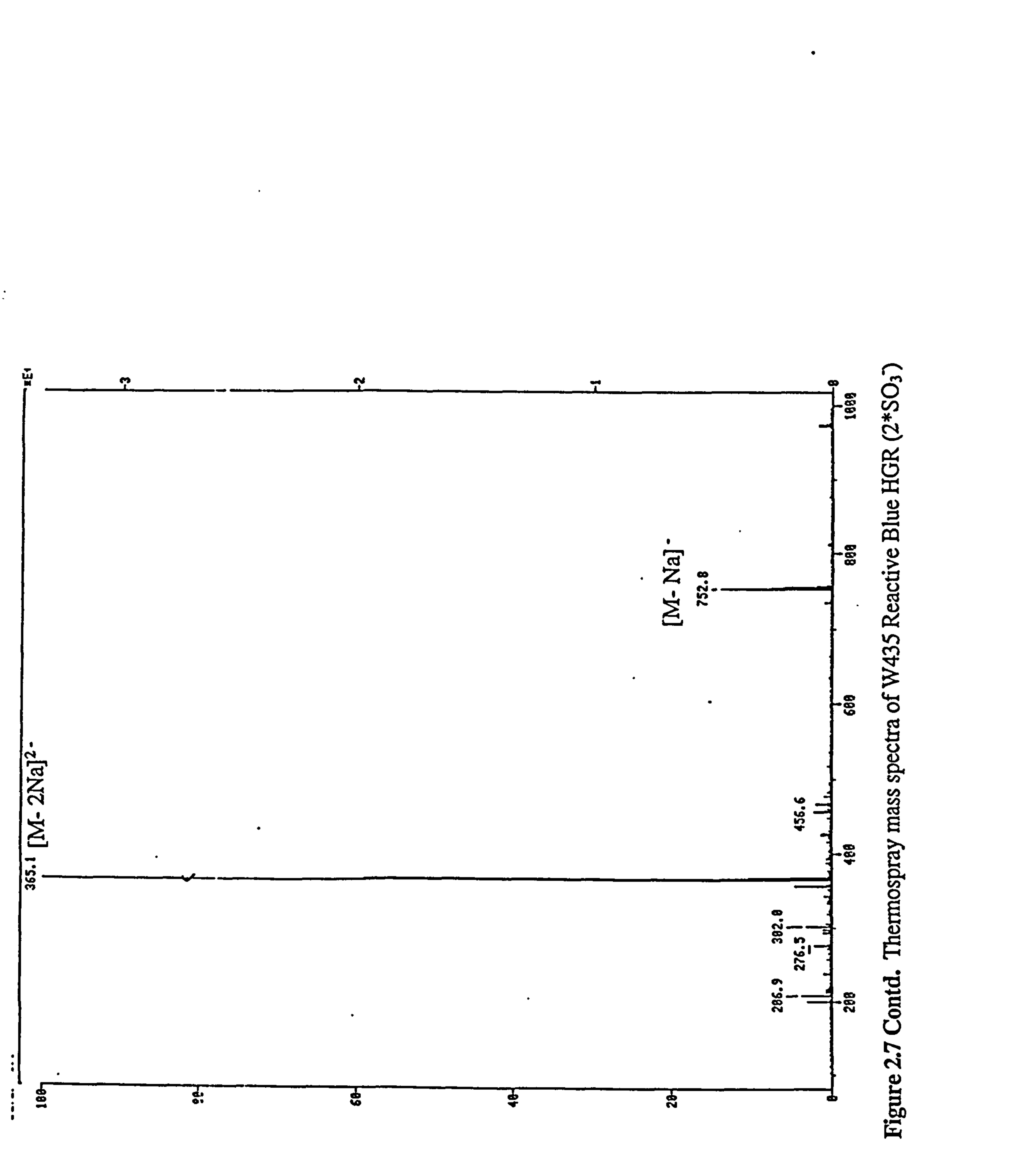

Figure 2.7 Contd. Thermospray mass spectra of W435 Reactive Blue HGR ($2*SO_3^-$)

2.3.5.2 Initial investigation of thermospray using a needle repeller

From the foregoing discussion (Section 2.3.5.1) it can be shown that the initial thermospray analysis of formulated dyes gave poor sensitivity for flow injection analysis using water as eluent and extremely poor sensitivity in the presence of buffer. However, several authors had reported increased sensitivity for dyes following modification of the repeller in the TSP source. Yinon (1989), described a wire repeller which increased the detection limit by two orders of magnitude compared to a source with no repeller, for the positive ionisation of azo dye Disperse Blue 79. McLean and Freas (1989), described in detail how modifications to both the vaporiser tip orifice and incorporation of a needle repeller made a significant impact on TSP sensitivity for sulphonated dyes. In particular, optimum flow rates of 1.4 and 0.8 ml min^{-1} were described for 100 and 50 μm orifices respectively. The commercial TSP capillary (Finnigan MAT), employed a pre-set ruby tip with an orifice diameter of 60 μm. By analogy with Mclean and Freas (1989) this would be compatible with an optimum flow rate between 0.9 to 1 ml min^{-1}, which was consistent with the LC system developed within this study (Section 2.1.2).

A modified needle repeller was manufactured (BEL engineering) which comprised a brass rod honed to a point and insulated with two ceramic spacers which were held in place with hardened ceramic paste. The basic source modification is illustrated in Figure 2.8:

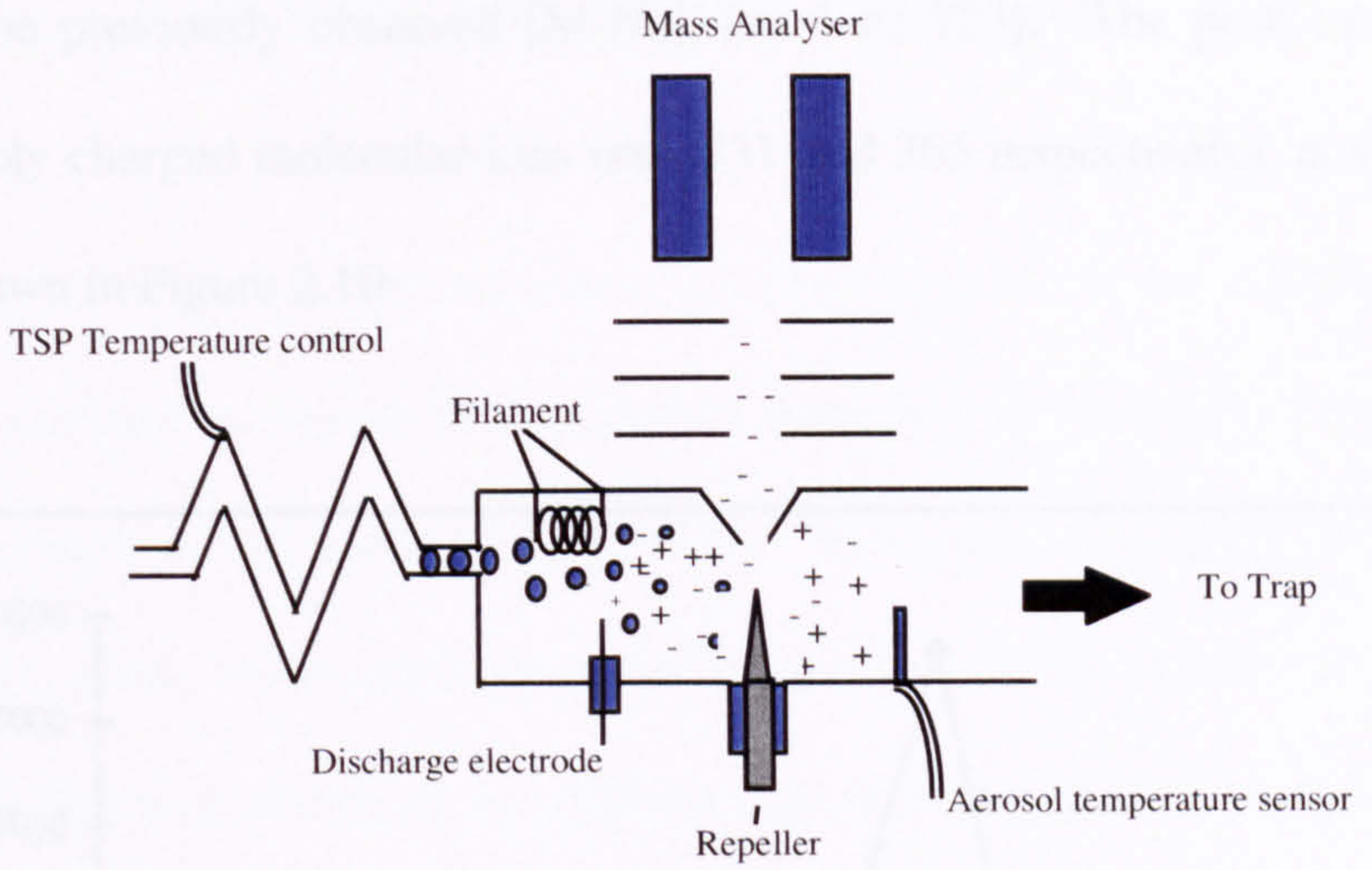

Figure 2.8 Modified TSP source

The vaporiser temperature was again optimised by FIA of W435 (equivalent to 20 µg injections), which indicated a working temperature of 95°C. Figure 2.9 shows a graphical depiction to illustrate the variability exhibited by the TSP interface at higher temperatures and in so doing confirmed the need to work below the maximum.

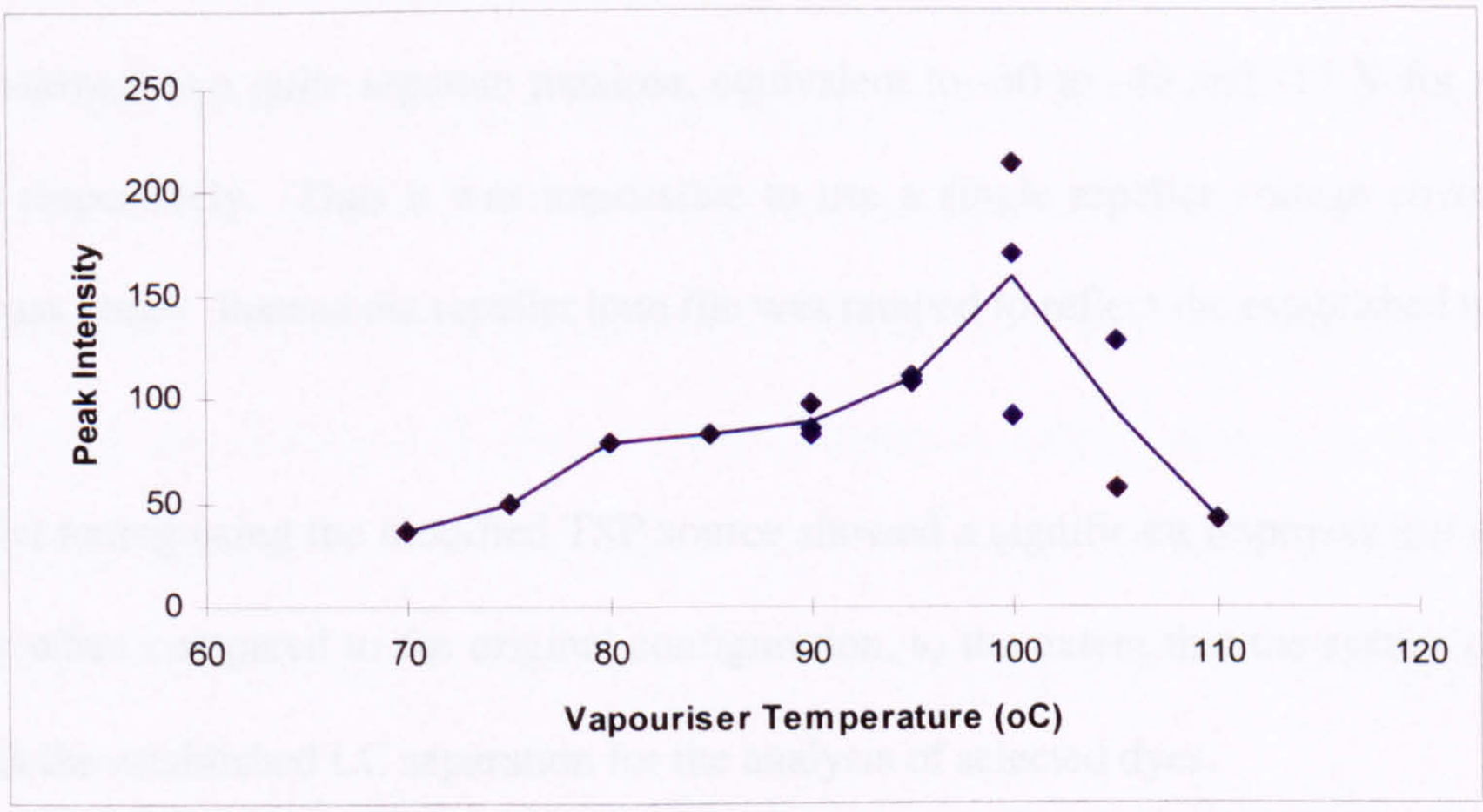

Figure 2.9 Optimisation of TSP vapouriser temperature @ 100% Aqueous eluent

The next stage in the optimisation of TSP source conditions was to determine the effect of repeller voltage on sensitivity. FIA of W435 was again used. Interestingly the LC eluent of 100% 0.01M ammonium acetate produced predominantly $[M-2Na+H]^-$ ion (*m/z* 731) in

preference to the previously observed [M-Na]$^-$ ion (*m/z* 753). The peak intensities of the singly and doubly charged molecular ions (*m/z* 731 and 365 respectively), at various repeller voltages are shown in Figure 2.10

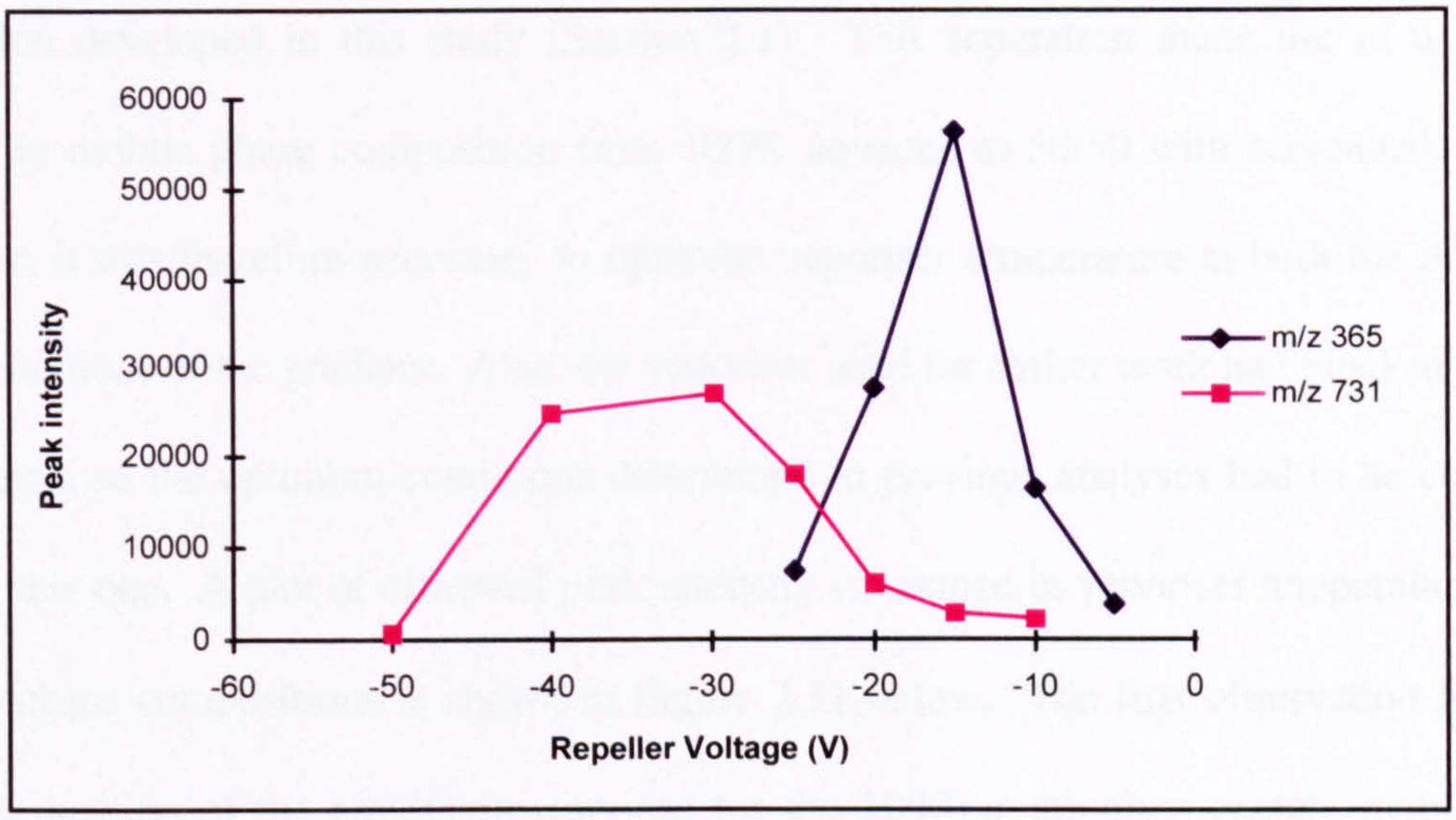

Figure 2.10 Optimisation of repeller voltage for W435

Unlike the previously described optimisation of the flat repeller (Figure 2.6), the needle repeller showed two quite separate maxima, equivalent to -30 to -40 and -15 V for *m/z* 731 and 365 respectively. Thus it was impossible to use a single repeller voltage covering the whole mass range. Instead the repeller tune file was ramped to reflect the established maxima.

The initial tuning using the modified TSP source showed a significant improvement in signal response when compared to the original configuration, to the extent that the system could be used with the established LC separation for the analysis of selected dyes.

2.3.5.3 Determination of TSP calibration and limit of detection

The thermospray interface was now capable of producing mass spectra of reactive dyes in the presence of ammonium acetate buffer. The next stage was to use the interface with the LC separation developed in this study (Section 2.1). This separation made use of a gradient change in mobile phase composition from 100% aqueous to 50/50 with acetonitrile organic modifier, it was therefore necessary to optimise vaporiser temperature at both the initial and final conditions of the gradient. Also, the vaporiser used for earlier work had blocked and was exchanged, so the optimum conditions determined in previous analyses had to be confirmed for the new one. A plot of observed peak intensity vs change in vaporiser temperature at two mobile phase compositions is shown in Figure 2.11 below. The first observation from this was the position of the maximum response for the 100% ammonium acetate mobile phase composition, (90°C), when compared to previous analysis (Figure 2.9; 100°C). This change must have been a function of the new vaporiser because all other parameters were the same. The second observation was the response for a mobile phase containing 50% acetonitrile. The optimum temperature, (85°C), was not unexpected, acetonitrile being more volatile than water. However, it was interesting to observe the associated increase in response with the presence of organic modifier. This was not pursued for TSP because of the acquisition of an electrospray interface (ESI; see Section 2.6). However, the change in signal response as a function of mobile phase composition was thought to be independent of interface type and was subsequently explored using the ESI interface. This is discussed later, (Section 2.6).

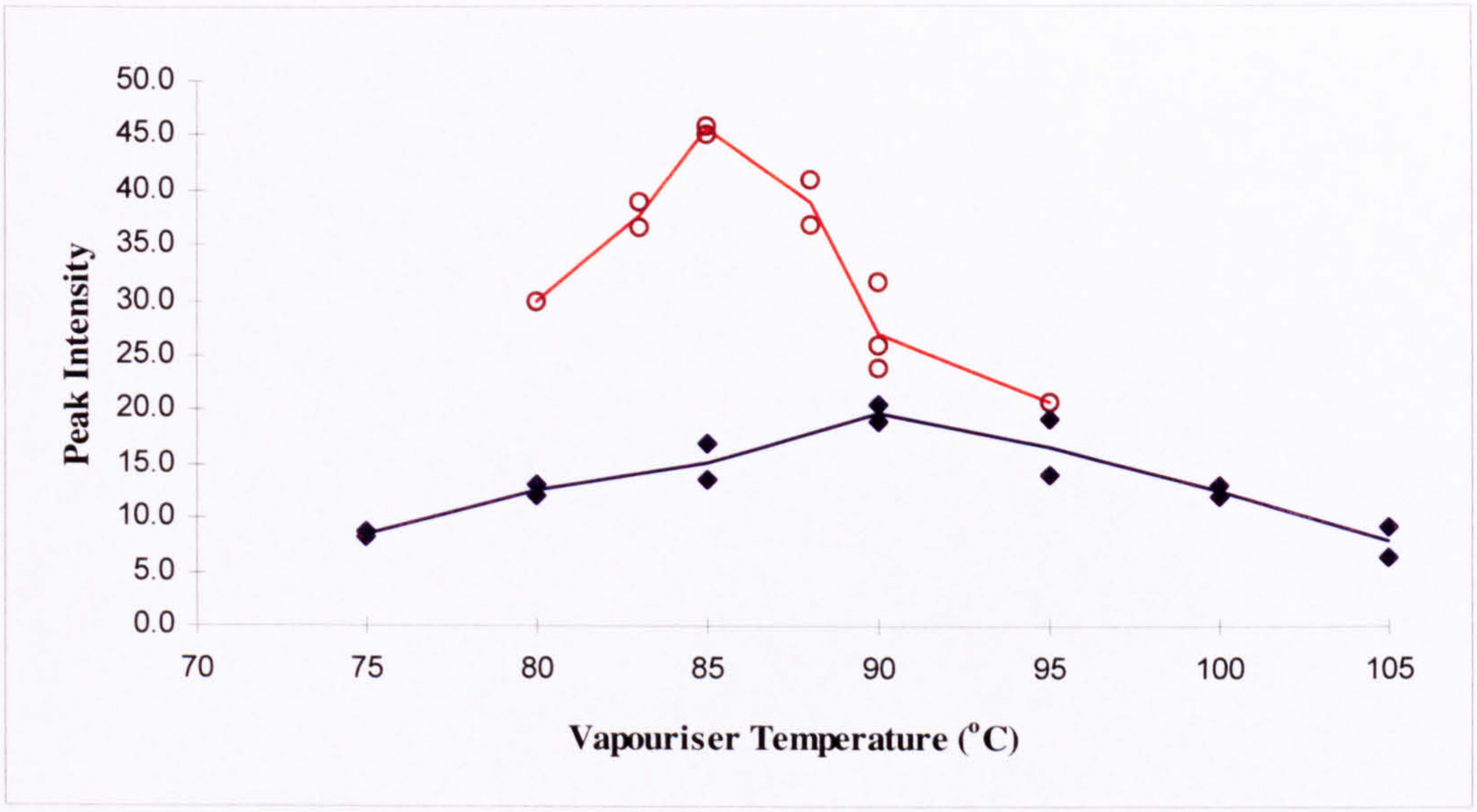

Figure 2.11. Optimisation of vapouriser temperature at mobile phase compositions of 100% 0.01M ammonium acetate (◆) and 50/50 with acetonitrile (O).

A mixture of three dyes (W433, 434 and 435) were used for the initial LC-MS analyses which was carried out using a vaporiser temperature of 87°C. However this resulted in a loss of signal for later eluting peaks, particularly W435, which was accompanied by an extremely noisy baseline, a characteristic of a high vaporiser temperature. Therefore a small mass spectrometer instrument control procedure was written to allow a linear change in vaporiser temperature (87 - 83°C), over the course of the gradient LC run:

Calibration solutions of approximately 25 - 500 mg l^{-1} W428, W433 and W435, were analysed using the optimum conditions described above. A typical chromatogram for a 25 mg l^{-1} mixed solution, equivalent to 0.88, 1.12 and 0.92 µg on column of W428, W433 and W435 respectively, is shown in Figure 2.12. The major molecular ions for each dye were summed and plotted as selected ion traces, which were then used to determine the signal to noise ratio (S/N) for each dye. These were 7:1, 20:1 and 15:1 for W428, W433 and W435 respectively. A S/N ratio of 5:1 is typically used to estimate limit of detection for analytical methods (Rafols *et al.*, 1997), suggesting concentrations of approximately 0.6 µg (W428) and 0.3 µg (W433 and W435) on column, were achievable for these three dyes. Figure 2.13 shows a

typical mass spectrum for a 25 mg l^{-1} solution of W435. All molecular ions are clearly discernible at this concentration.

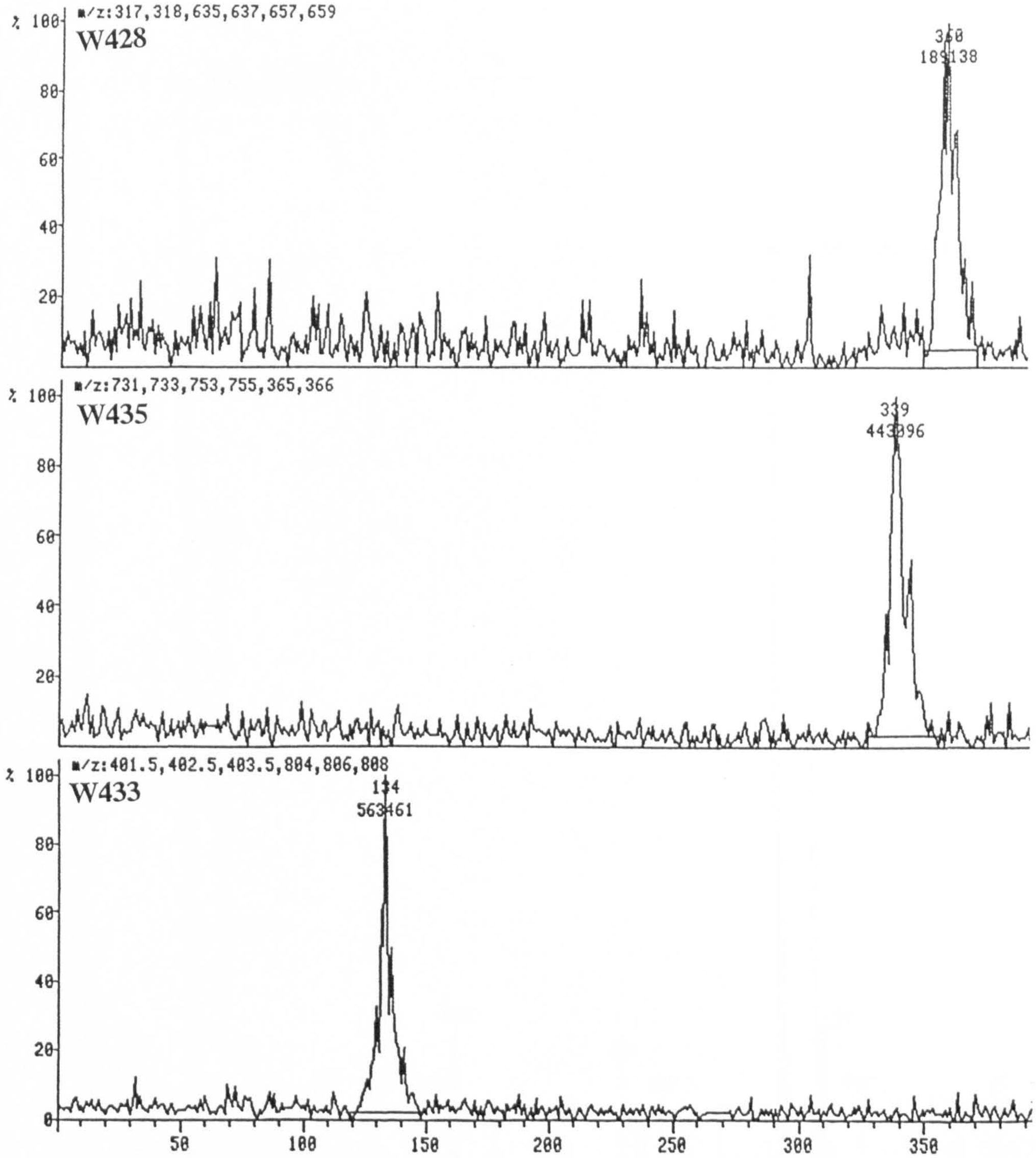

Figure 2.12 Thermospray LC-MS chromatogram showing selected mass chromatograms for molecular ions of W428 (Top), W435 (Middle) and W433 (Bottom) for 0.88, 0.92 and 1.12 μg on-column, respectively

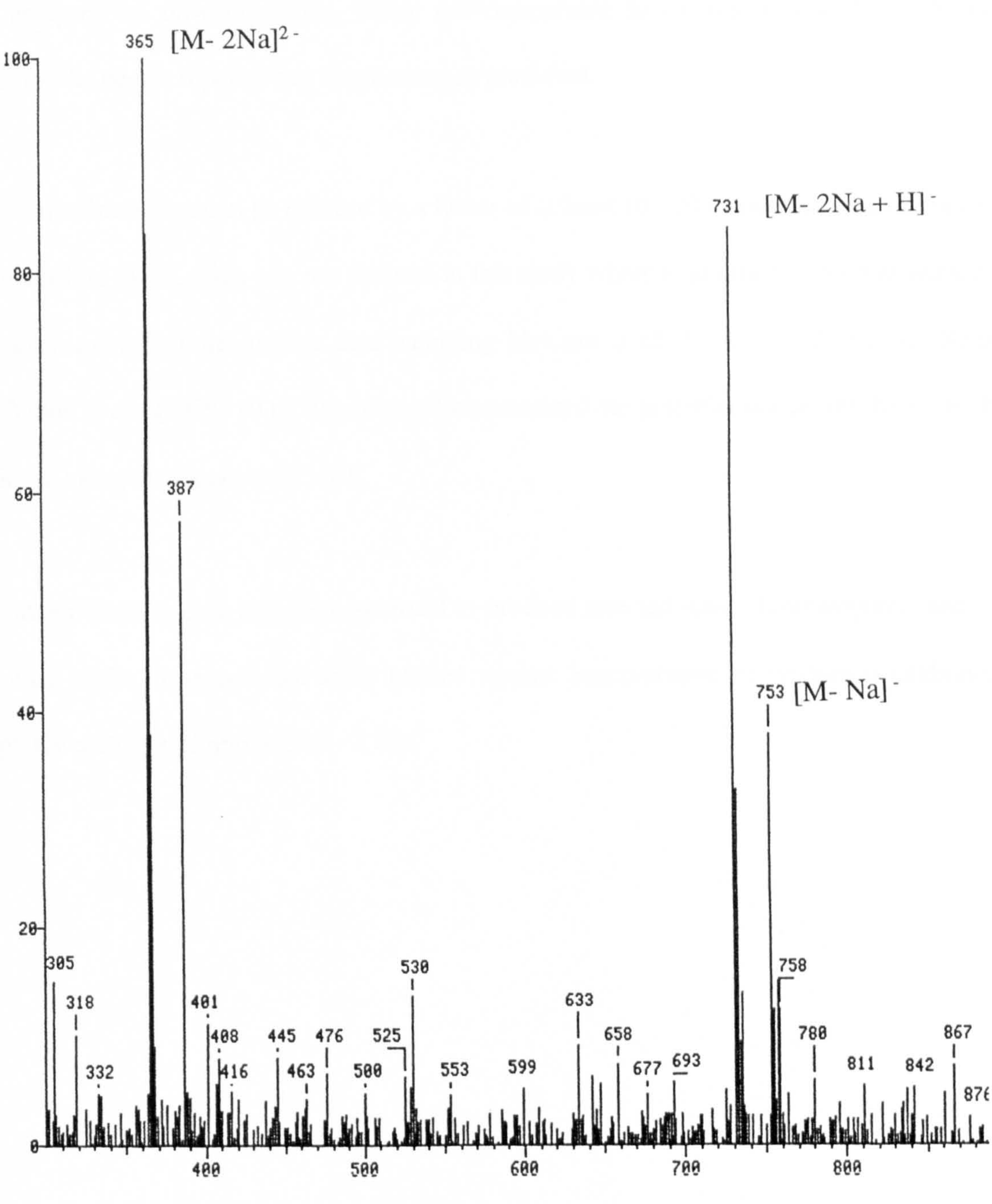

Figure 2.13 Thermospray LC-MS mass spectrum for 1.12 µg on-column of reactive dye W435

The thermospray analysis of Acid Orange 6, an azo dye with one sulphonic acid group, was reported by Ballard *et al.*, (1986). Also, Yinon *et al.*, (1989) demonstrated the analysis of a further four mono and di-sulphonated acid and direct dyes, and Rafols and Barcelo (1997), reported spectra for a further eleven acid and mordant dyes including one acid dye with three sulphonic acid groups. In all cases, full scan mass spectra could be obtained from 1 - 5 μg of dye analysed by flow injection. These are comparable to the results obtained here and confirms the needle repeller was functioning as predicted.

The limit of detection can be reduced by a factor of at least 10 - 20 through the use of selected ion recording (SIR). This was not pursued in this study where a qualitative tool was required. However, published quantitative data including McLean *et al.*, (1989) 5 - 20 ng on column and Yinon *et al.*, (1989) 10 ng on column, demonstrated the potential sensitivity that could be achieved using thermospray LC-MS.

The major ions for each dye were summed to produce selected mass chromatograms and the resulting peaks integrated and areas plotted against concentration to produce a calibration graph for each dye, (Figures 2.14 - 2.16).

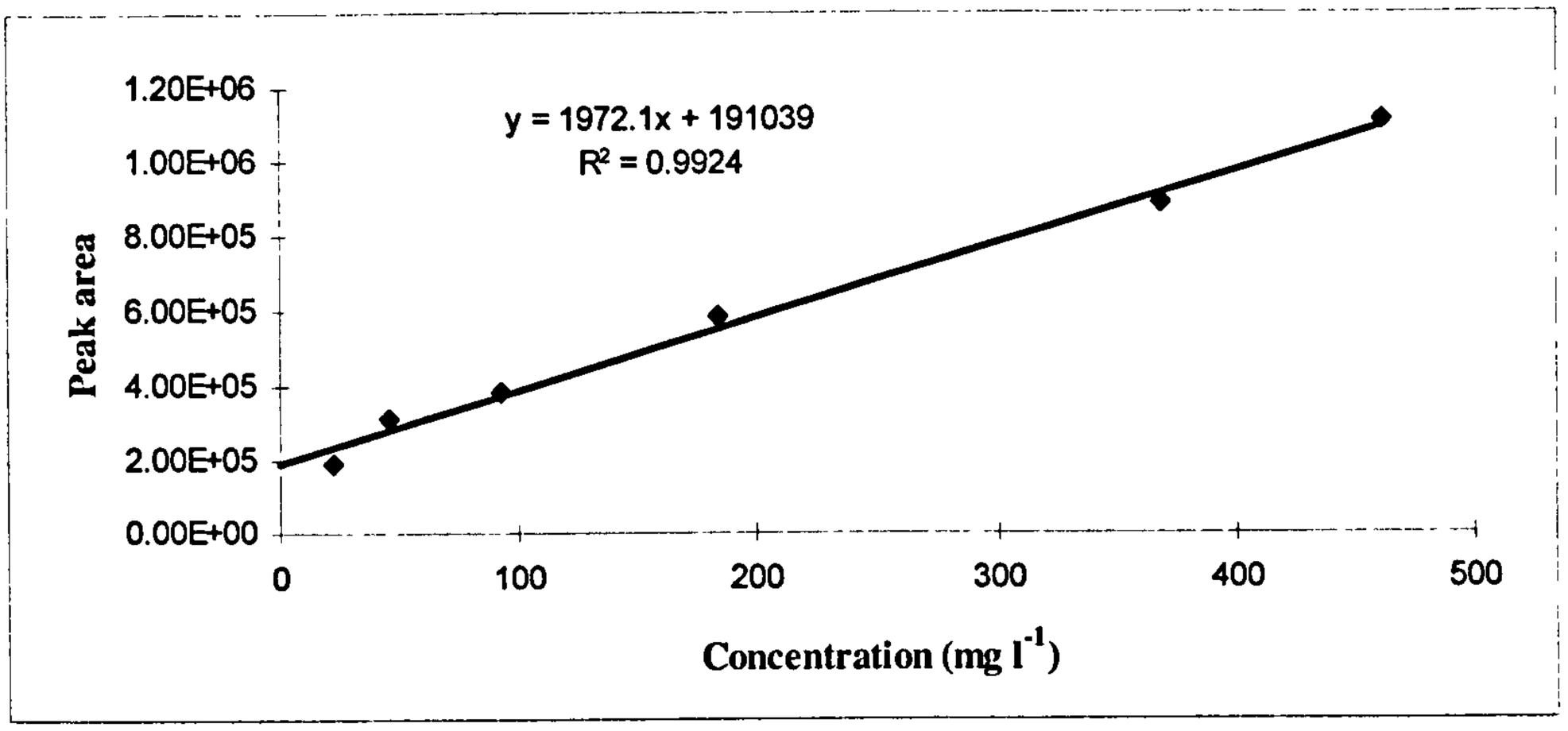

Figure 2.14. Thermospray LC-MS calibration graph for W428

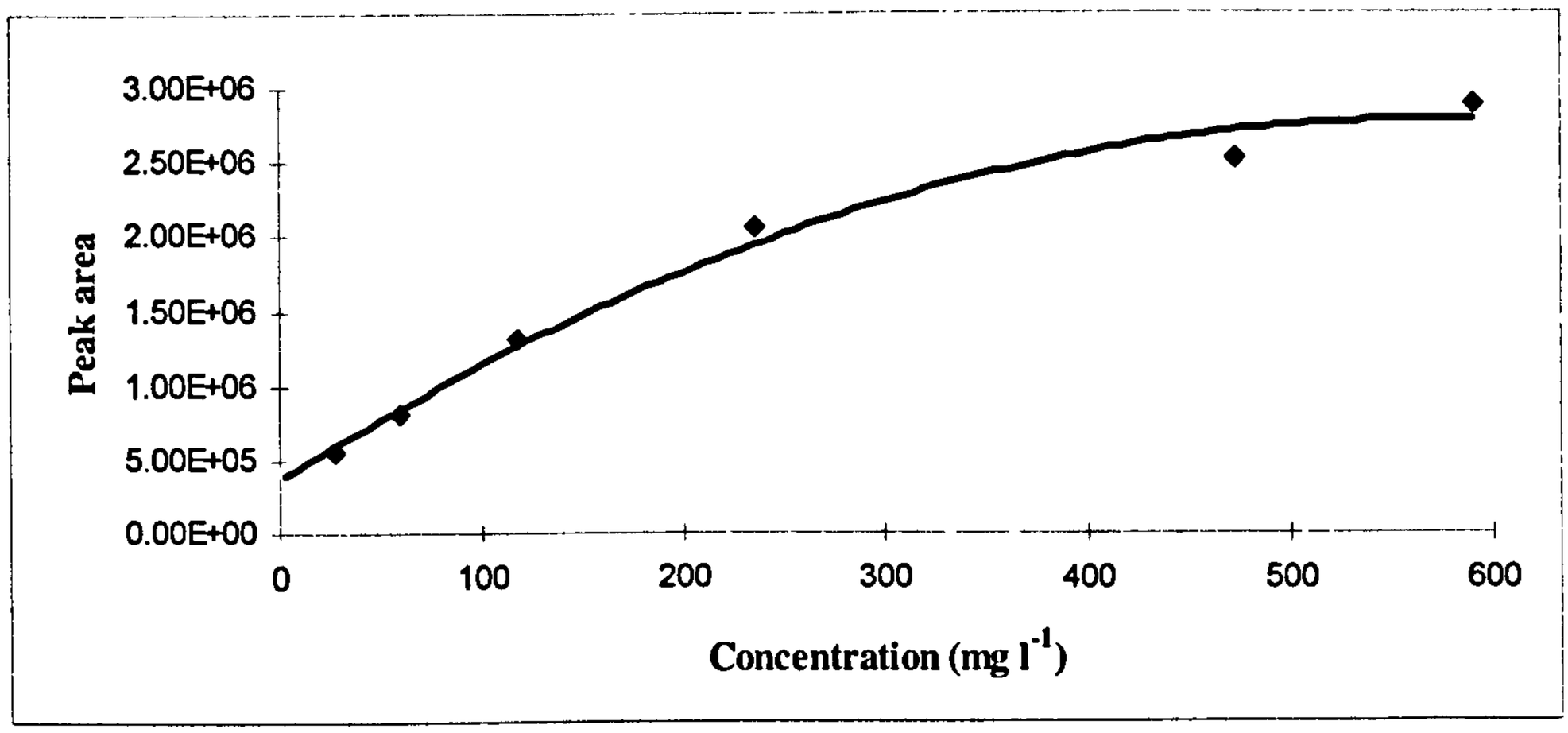

Figure 2.15a. Thermospray LC-MS calibration graph for W433

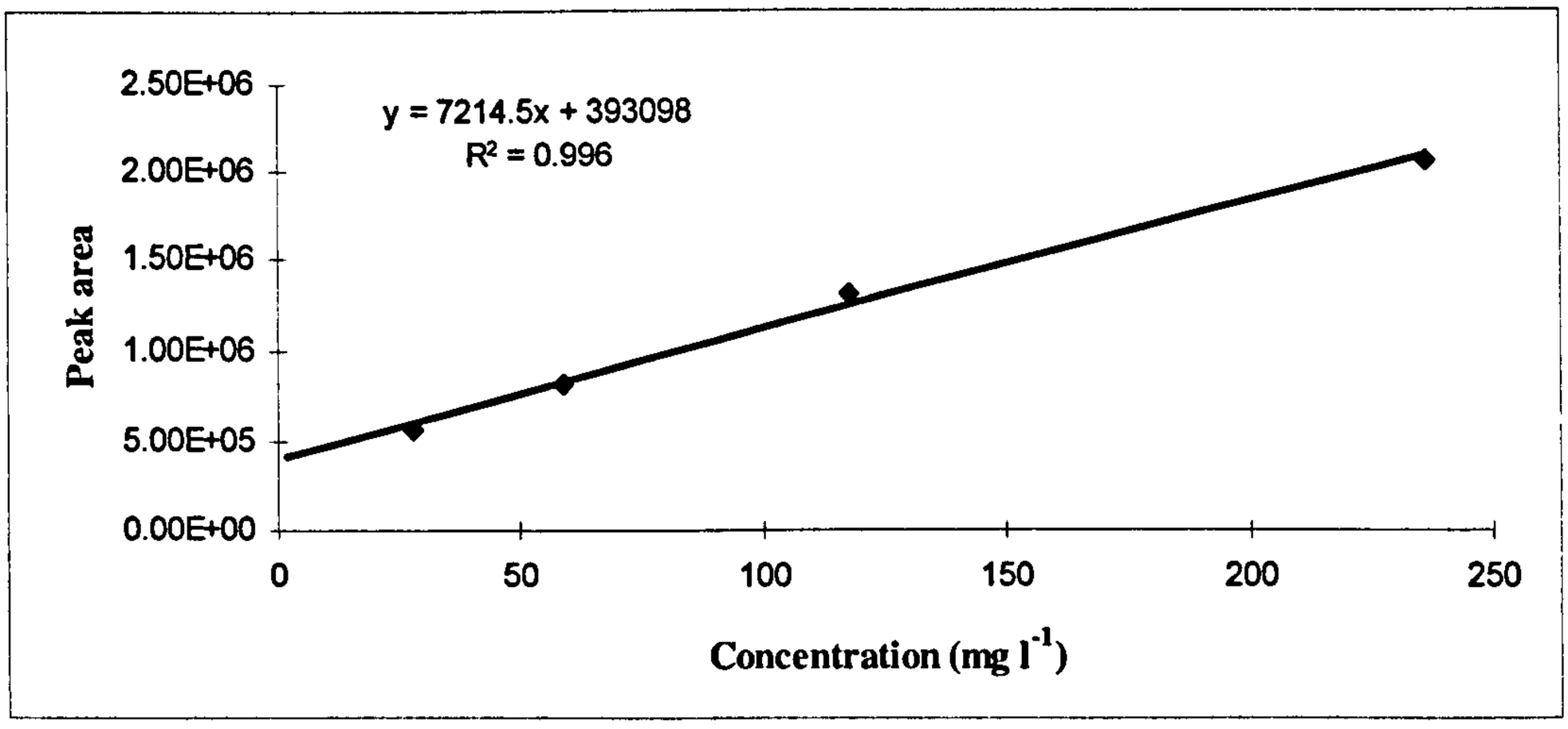

Figure 2.15b. Thermospray LC-MS calibration graph for W433 (range 25-250 mg l^{-1})

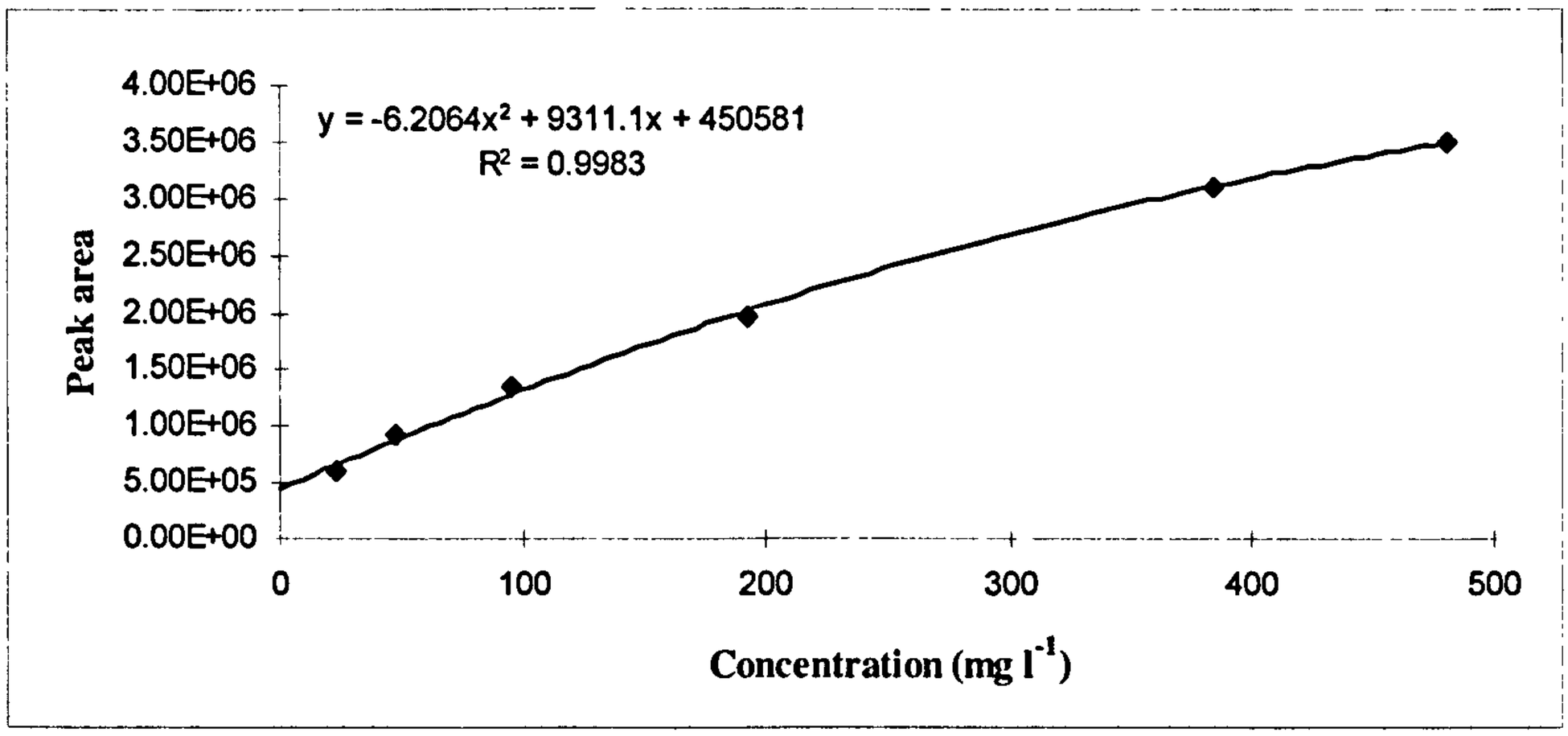

Figure 2.16. Thermospray LC-MS calibration graph for W435

It was noticeable that all calibration graphs appeared to have a large positive intercept on the y axis, yet the blank (water only), showed no background interference or carry-over. Inspection of the calibration graphs shows they are non-linear and tend to curve towards the origin at low concentrations. Therefore, it may be possible under idealised conditions to detect these dyes at lower concentrations than originally predicted from the peak height signal to noise data discussed earlier.

2.3.6 Summary of thermospray evaluation

The modification to the repeller of the TSP source made a significant improvement to the signal response of this interface for the analysis of sulphonated dyes. The detection limits observed in full scan mode (200 - 400 ng on column), were compatible with proposed dyestuff environmental fate studies, particularly if a concentration step was used and the ammonium acetate buffer required to obtain a reasonable LC separation of sulphonated dyes did not compromise the mass spectrometric determination. Considering the complete lack of suitability of the 'conventional' TSP source, this was a major advancement in the qualitative analysis of sulphonated dyes.

2.4 STABILITY OF W428

2.4.1 Experimental

A solution of purified 428 in water (100 mg l^{-1}) was prepared, divided into three test tubes and stored; a) under laboratory lighting at ambient temperature (approximately 21°C), b) in light proof flasks at ambient temperature and c) refrigerated at 4°C in the dark. Samples were taken from each tube following storage for 0, 30 and 48 h and analysed using the optimised HPLC conditions (Section 2.1). A sample taken from tube (a) post 48 h storage was subsequently analysed by LC-MS using conditions described in Section 6.1.

2.4.2 Results for the stability of W428

Given the rather low purity of even HPLC purified dye W428 (ie 90%; Table 2.1) an experiment was designed to investigate the stability of the purified dye under laboratory conditions. Some of the observed impurities had significantly different retention times to the purified dye itself, (Figure 2.17), suggesting they were not simply co-extracted during preparative LC, but instead were produced by decomposition of the dye at some stage after the isolation process.

The peak area of W428 was determined for solutions stored in the light at ambient temperature (21°C), in a darkened container at ambient temperature and in the dark below 4°C, over a 30 hour period. A summary of this data, (Table 2.3), suggests that dye W428 does indeed degrade on storage and this degradation occurs under each of the storage conditions, although it occurs at a faster rate at ambient temperature in the light.

Table 2.3. Stability of W428 following storage in daylight, in the dark and in the dark under refrigerated conditions

Time (hours)	W428		
	Fridge	Dark	Bench
0	100%	100%	100%
30	93%	93%	79%
48	90%	85%	75%

The bench stored material was subsequently analysed by thermospray LC-MS with in-line UV detection. If one considers the structure of W428 then degradation products formed on storage may be predicted based on simple hydrolysis of the chlorine(s) on the reactive group, and/or dimerisation as outlined below:

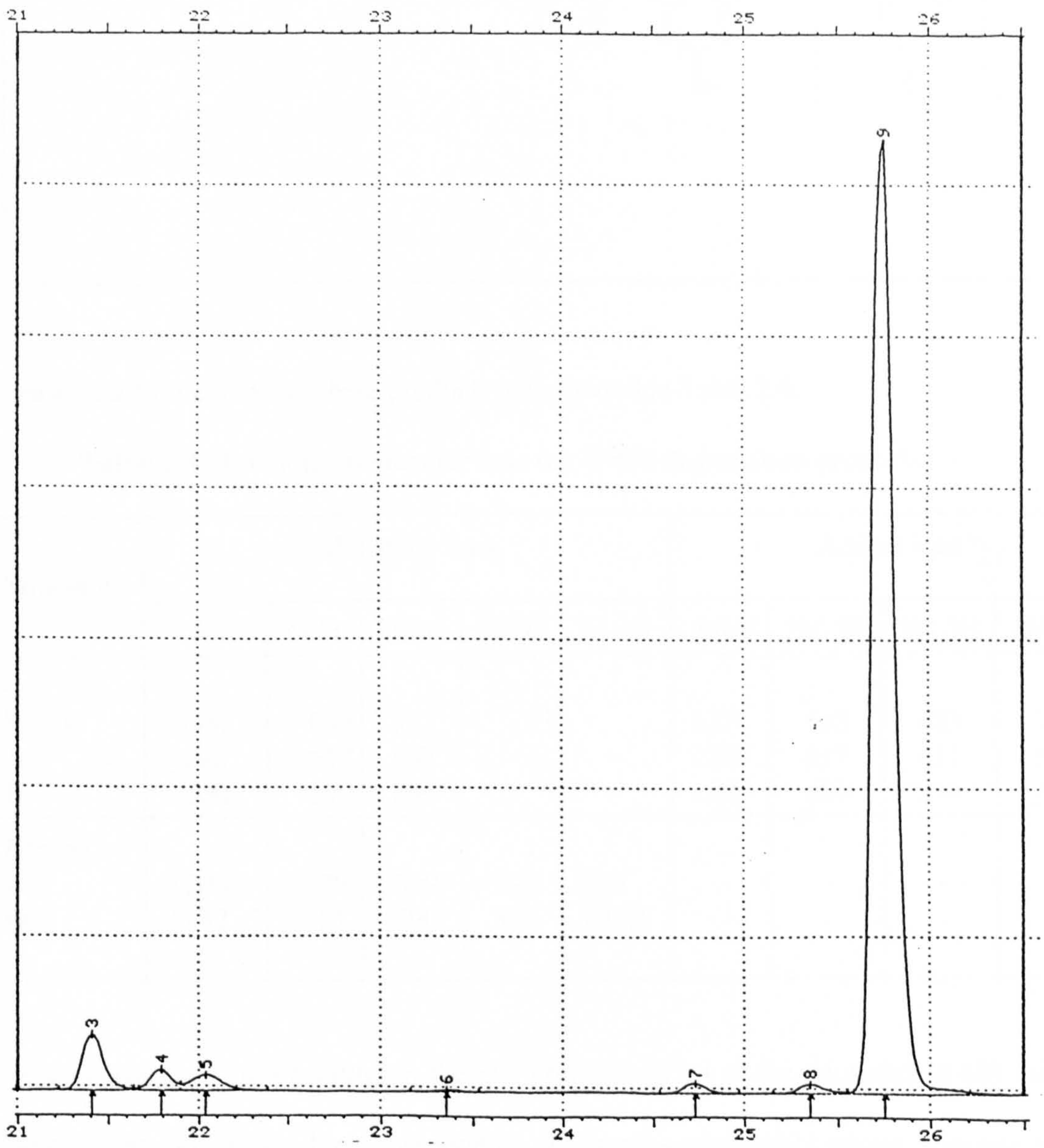

Figure 2.17. LC-UV (254 nm) chromatograms for a sample of W428 purified by semi-preparative LC.

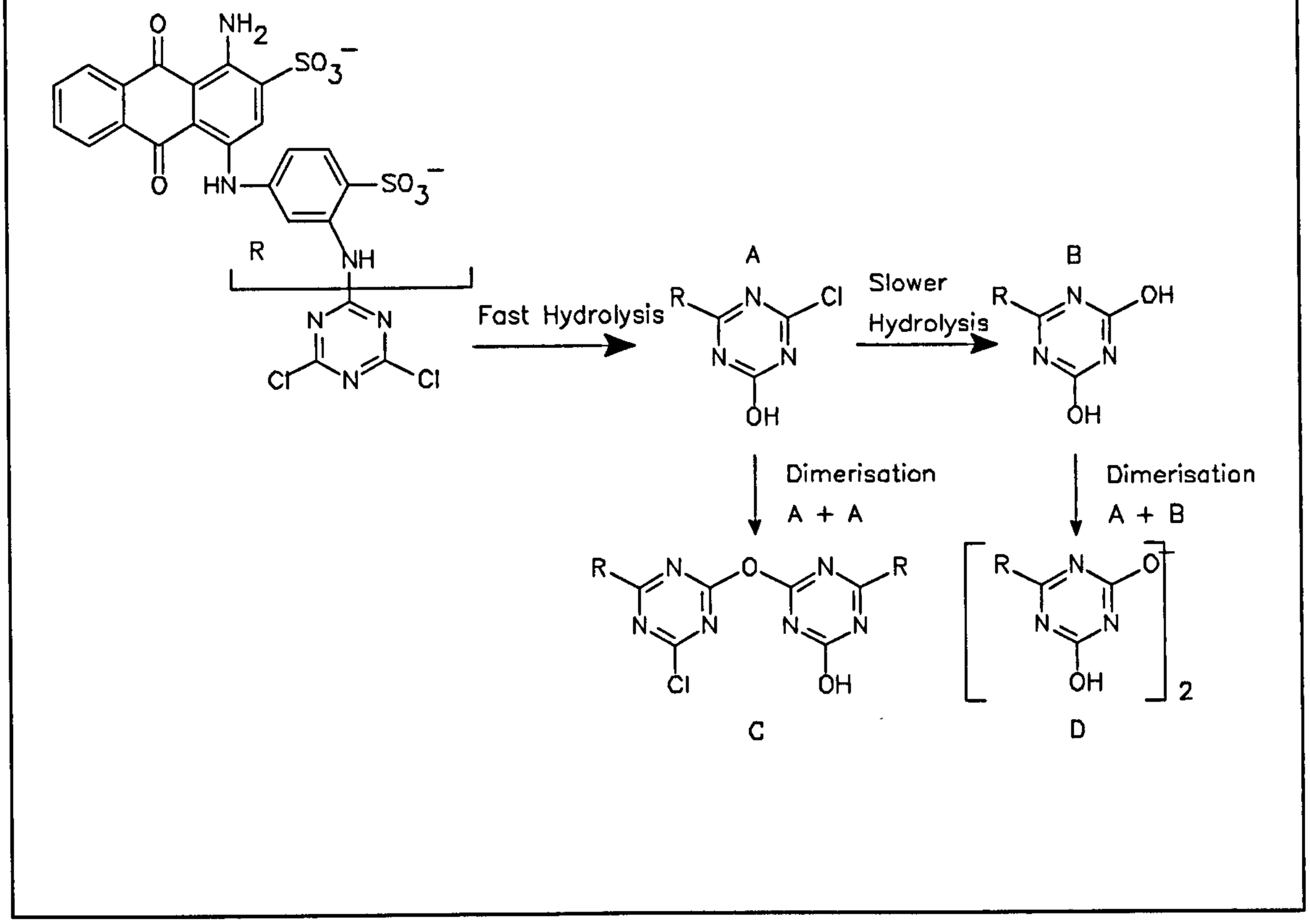

Predicted molecular ions for these products are reported in Table 2.4.

Table 2.4. Predicted molecular ions for W428 degradation products.

Structure	Molecular ions					Adduct ions			
	M	M-H	M-2H	M-3H	M-4H	2M-H	2M-2H	2M-3H	2M-4H
W428	636	635	317	-	-	1271	635	423	317
A	618	617	308	-	-	1235	617	411	308
B	600	599	299	-	-	1199	599	399	299
Dimers									
C	1200	1199	599	399	299	-	-	-	-
D	1182	1181	590	393	294.5	-	-	-	-

Five components were observed in the UV chromatogram of the degraded W428 sample, (Figure 2.18). Of these, three components produced a reasonably strong response in the reconstructed ion current chromatogram. The mass spectra derived from these peaks are shown in Figure 2.19.

Peak II showed molecular ions consistent with proposed product (D), the dihydroxy dimer. Peak III, shows ions which could be derived from either structure B or C, both of which can produce the same ions (Table 2.4). The intensity of the ion of *m/z* 399 is important. This ion can be derived from either an adduct ion $[2M-3H]^{3-}$ for structure B, or a molecular ion $[M-3H]^{3-}$ for structure C. Since adduct ions are usually weak and in this spectrum the *m/z* 399 ion is the second most abundant, this suggests peak III is most likely to be that of the chloro-, hydroxy-dimer, proposed structure C.

The *m/z* 399 ion is very weak in the mass spectrum derived from Peak V, suggesting it is an adduct ion and therefore this mass spectrum corresponds to the dihydroxy monomer, structure B.

Further experiments, including the accurate determination of molecular ion isotope contributions, would be required to confirm these observations.

The instability of W428, the tendency for standard solutions to dimerise and possibly degrade under normal laboratory storage conditions, indicated dyes containing the dichloro triazine group were not suitable reference materials for controlled laboratory degradation studies. W428 was, therefore, not used in subsequent studies.

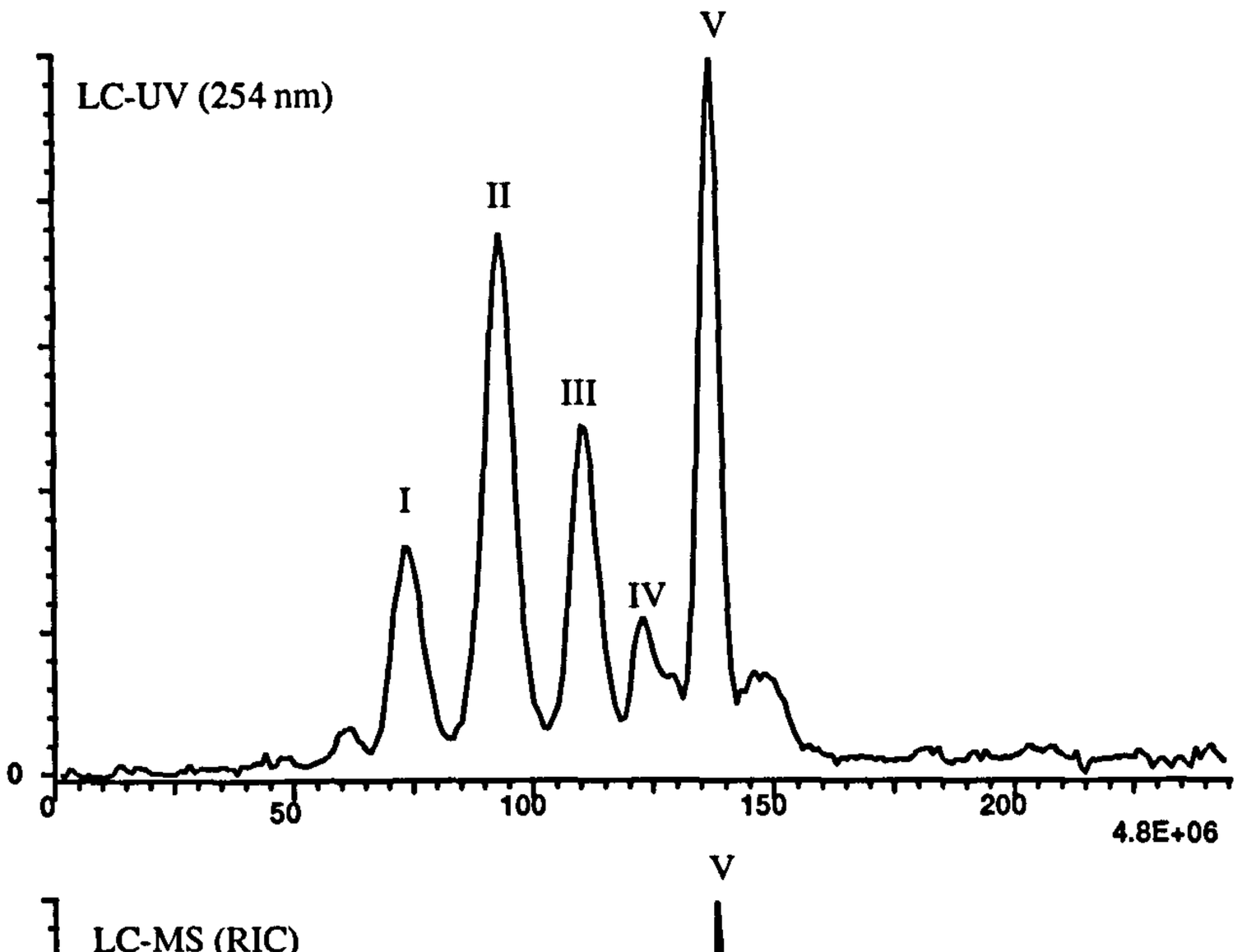

Figure 2.18. Comparison of LC-UV and LC-MS chromatograms for W428 following bench storage for 48 h

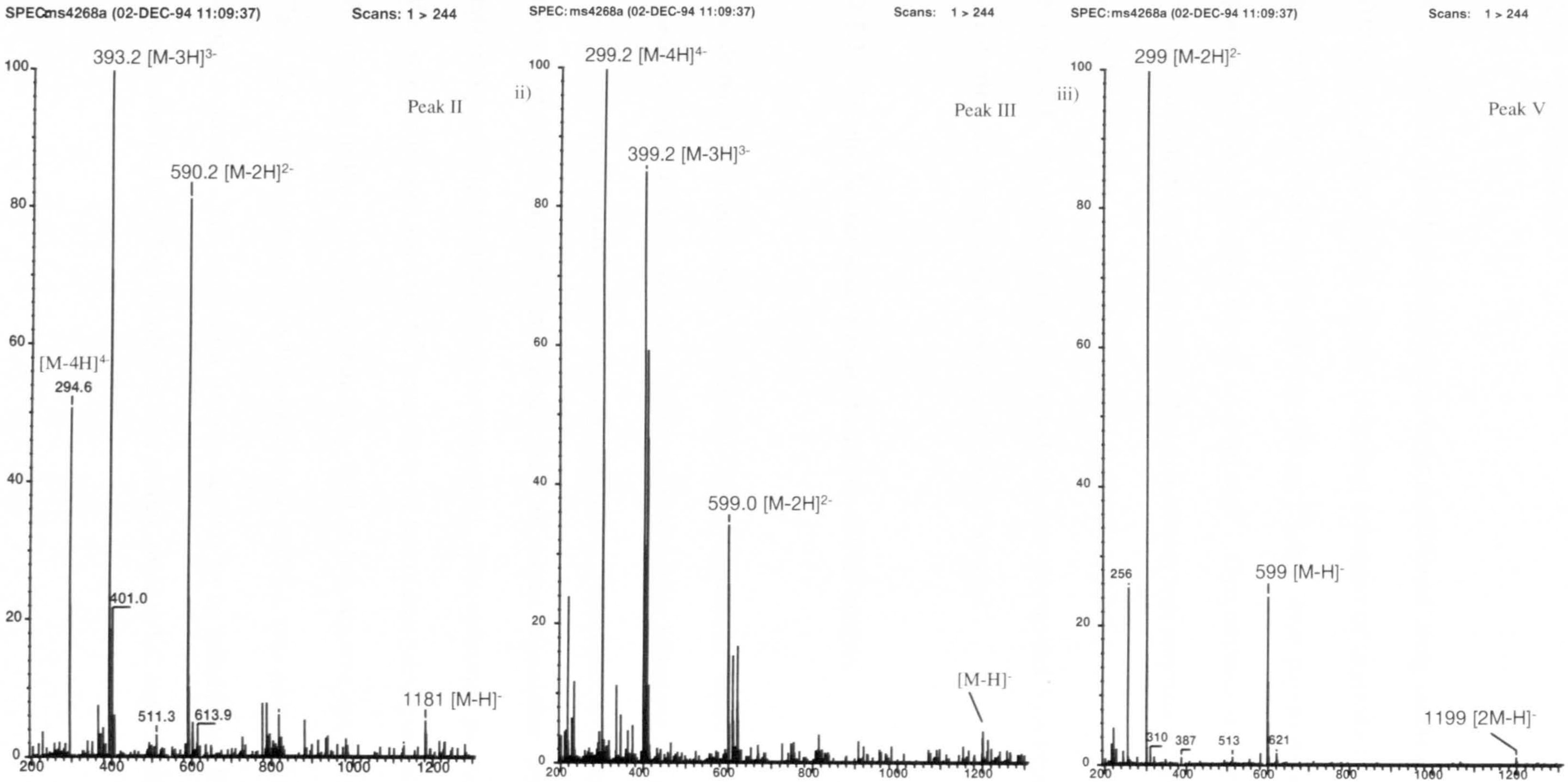

Figure 2.19 Mass spectra derived from peaks II, III and IV in Figure 2.18

2.5 SOLID PHASE EXTRACTION OF REACTIVE DYES

2.5.1 Experimental

C_{18} extraction cartridges (Bond Elute) were conditioned using methanol (5 ml) followed by 0.01M ammonium acetate (5 ml). Standard solutions of unpurified (10 ml; 5 mg l^{-1}) or purified (100 ml; 500 µg l^{-1}; 500 ml; 100 µg l^{-1}) dye, were passed through the columns by positive pressure, at a flow rate of 1 - 3 ml min^{-1}. Dye mixtures were eluted with methanol (5 ml) and collected in Reacti-vials. Residual solvent was removed with a stream of nitrogen at 50°C. Residues were re-dissolved in water (1 ml) before analysis by LC as detailed in Section 2.1. Dye concentration in the extracts was determined by comparison to calibration standards in the concentration range 5, 10, 25 and 50 mg l^{-1}.

2.5.2 Results for the solid phase extraction (SPE) of dyes

As demonstrated previously in Section 2.4, thermospray liquid chromatography mass spectrometry (LC-MS) was not a particularly sensitive technique for reactive dyes, with LODs of approximately 300 ng on column. Therefore, a concentration/extraction procedure was required before identification of minor degradation products produced in laboratory and field studies could be attempted. The extraction process chosen followed the same philosophy used for LC separation *viz* use of ion pairing and a C18 reverse phase. A summary of the recoveries obtained by SPE of five reactive dyes in water are shown in Table 2.5. An excellent extraction efficiency (≥77%), was observed for each dye at all sample volumes. The extraction process appears to be suitable for the concentration of dyes possessing up to four sulphonic acid groups, prior to LC and LC-MS analysis.

Table 2.5. Recovery data of dyes from standard mixtures containing up to four reactive dyes giving a sample loading of 50 µg of each dye

DYE (SO_3H groups)	x10 Concentration (10 ml; 5 mg l^{-1})		x100 Concentration (100 ml; 0.5 mg l^{-1})		x500 Concentration (500 ml; 0.1 mg l^{-1})	
	Recovery (%)	% SD (n=4)	Recovery (%)	% SD (n=4)	Recovery (%)	% SD (n=4)
W428(2)	-	-	77	5	88	3
W430(4)	95	7	86	9		
W433(3)	96	6	100	2	105	3
W434(3)	90	8				
W435(2)	79	8	87	4	94	1

It is interesting to compare these results to a different approach adopted by Rafols (1997), who used C18 Empore disks to extract a range of mono and di-sulphonated acid dyes spiked into drinking water at 600 ng l^{-1}. Rafols did not use ion pair reagents, but instead adjusted the pH to 1.25 or 3. Recoveries for three dyes ranged between 4 and 25%. Although the concentration of dye used in this study was at least a factor of 200 higher than used in the Rafols study, the excellent recoveries suggest it to be a better approach than pH adjustment and more applicable to dyes with a higher degree of sulphonation.

2.6 ELECTROSPRAY LC-MS INTERFACE EVALUATION

2.6.1 Initial evaluation of electrospray (ESI) MS

Reactive Blue H4R, W435 (100 mg l^{-1}), was added by continuous infusion (5 µl min^{-1}) to an LC eluent comprising of 60% ammonium acetate 40% acetonitrile at a flow rate of 0.7 ml min^{-1}. The peak intensity of the singly and doubly charged molecular ions (*m/z* 731 and 365) were monitored while nebuliser (sheath) and auxiliary gases were optimised for maximum signal response and stability using the guide-stability tuning package of the TSQ700 data system. The effect of capillary temperature was then evaluated over the

range 260 - 320 °C using the optimised gas pressures and the same LC eluent composition. This exercise was repeated using a 100% aqueous LC eluent.

2.6.2 Effects of mobile phase modifiers

The effect of adding organic modifier to the LC mobile phase was evaluated using various water/acetonitrile eluent compositions to represent regular steps of the standard gradient system (Section 2.1). W435 (5 µl min^{-1}, 1000 mg l^{-1}), was added to the eluent by continuous infusion and the peak intensities of the singly and doubly charged molecular ions (*m/z* 731 and 365) recorded for eluent compositions of: 100, 90, 80, 70, 60, 50, 40 and 30% aqueous phase.

The effect of ammonium acetate buffer on mass spectrometer response was determined by continuous infusion of W435 (5 µl min^{-1}, 100 mg l^{-1}) in to an aqueous LC eluent containing 0, 2, 4, 6, 8, 10 or 50 mM of ammonium acetate buffer. The peak intensities of the singly and doubly charged molecular ions (*m/z* 731 and 365 respectively), were monitored.

This exercise was repeated with an LC eluent of 50/50 aqueous phase/acetonitrile in the presence of 0.5, 1, 2, 3, 4 or 5 mM ammonium acetate, to determine the effect of buffer concentration at the final mobile phase composition of the standard gradient system (Section 2.1). The peak intensities of the singly and doubly charged molecular ions (*m/z* 731 and 365 respectively), were monitored.

An evaluation of the combined effect of organic modifier and buffer was carried out using various ammonium acetate/acetonitrile eluent compositions to represent regular steps of the standard gradient system (Section 2.1). W435 (5 µl min^{-1}, 100 mg l^{-1}), was added to

the eluent by continuous infusion and the peak intensities of the singly and doubly charged molecular ions (*m/z* 731 and 365) recorded for eluent compositions ranging from 100% 0.01M NH_4Ac to 40% aqueous phase (equivalent to 0.004M NH_4Ac).

2.6.3 Calibration and limit of detection

The mass spectrometer was scanned over a mass range of 200 - 900 daltons in 1 second using a capillary temperature of 300 °C, sheath gas: 60 psi and auxiliary gas: 10 psi. The multiplier was set to 1000 V and the dynode to -15 kV. Full scan data were collected by a Dec 5000 data system.

Calibration standards of W433 and W435 were prepared by serial dilution of a mixed stock solution to give concentrations in the range 1 - 30 mg l^{-1}, equivalent to a nominal concentration range of 0.08 - 2 µg on-column for a 40 µl injection volume. LC conditions as given in 2.1 were used. Major ions for each dye were summed to generate selected mass chromatograms. The resulting peaks were integrated and the areas plotted against concentration to produce calibration graphs for each dye. The signal to noise ratio for the lowest concentration standard was used to estimate the limit of detection.

2.6.4 Results for the optimisation of electrospray LCMS

2.6.4.1 Initial evaluation of electrospray (ESI) MS

A detailed description of ESI operation and ionisation process is given in the introduction.

The optimisation of the electrospray interface was somewhat simpler than for Thermospray. Where the latter had several key parameters to be defined such as vaporiser

and source temperature, flow rate, filament current, discharge and repeller voltages, ESI had only LC flow rate, capillary temperature and nebulizer and auxiliary gas pressures to consider.

The accepted LC flow rate for ESI was reported to be 0.7 ml min^{-1} or below, (Harrison, personal com.). The standard LC separation of dyes used for LC-UV and thermospray analysis (Section 2.1), was modified to use 0.7 ml min^{-1} mobile phase, without any discernible loss of chromatographic integrity.

The ESI interface was supplied with a syringe pump which enabled the continuous infusion of a tuning solution into the LC eluent *via* a tee piece. Optimisation was carried out by infusion of W435 into a mobile phase of 60% 0.01M ammonium acetate, 40% acetonitrile (ie the approximate mobile phase composition at elution of most of the selected dyes under the standard gradient conditions). The sheath and auxiliary gas pressures are dependent on the eluent flow rate only and were optimised at 65 and 10 psi respectively using a flow rate of 0.7 ml min^{-1}. Therefore the only remaining ESI parameter to be investigated was capillary temperature. For this, the mass spectrometer was set to monitor *m/z* 365 and 731, the doubly and singly charged molecular ions for W435 respectively, while the capillary temperature was varied between 260 and 320°C. Instrument tuning (particularly tube and capillary lenses), was checked following each change of capillary temperature. The peak intensities of the two molecular ions are shown in Figure 2.20.

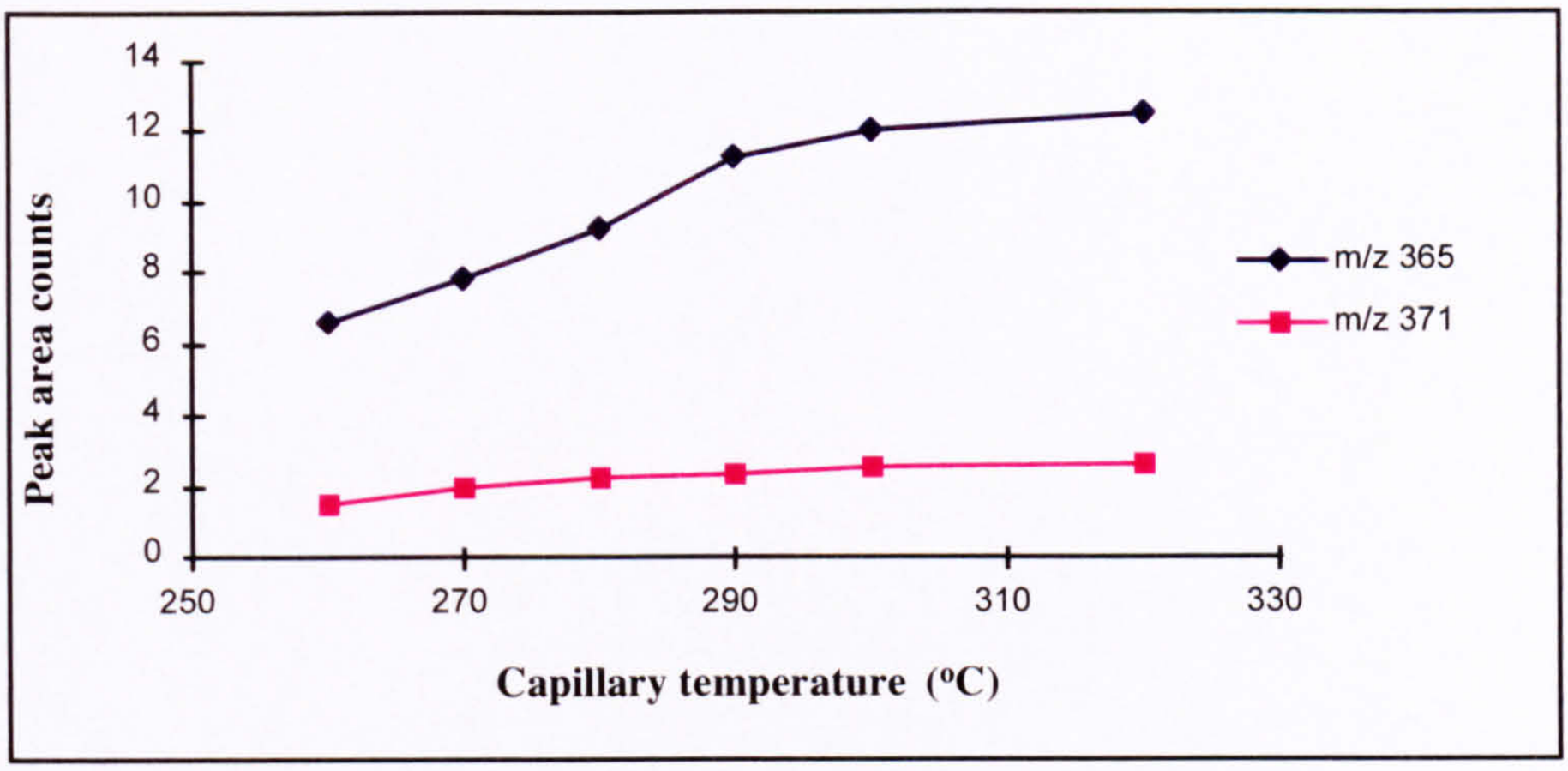

Figure 2.20. ESI capillary temperature optimisation

Interestingly, the capillary temperature appeared to have a greater effect on the doubly charged molecular ion. Also, ion intensities for both *m/z* 365 and 731 did not vary by more than 10% for a 30 °C change in capillary temperature between 290 and 320 °C, which suggests that ESI interface temperatures are not as critical as those observed for TSP. The capillary temperature was then checked for a 100% aqueous mobile phase, which also gave an optimum temperature of 300 °C. This temperature together with the optimised sheath and auxiliary gas pressures of 65 and 10 psi respectively, was used for all subsequent analysis.

Calibration solutions of W433 and W435 in the concentration range 1 - 35 mg l^{-1}, equivalent to a nominal concentration range of 0.04 - 1.4 µg on-column for 40 µl injection volumes, were analysed. The major ions for each dye were summed using selected mass chromatograms and the resulting peaks integrated and areas plotted against concentration to produce a calibration graphs for each dye, (Figures 2.21 and 2.22).

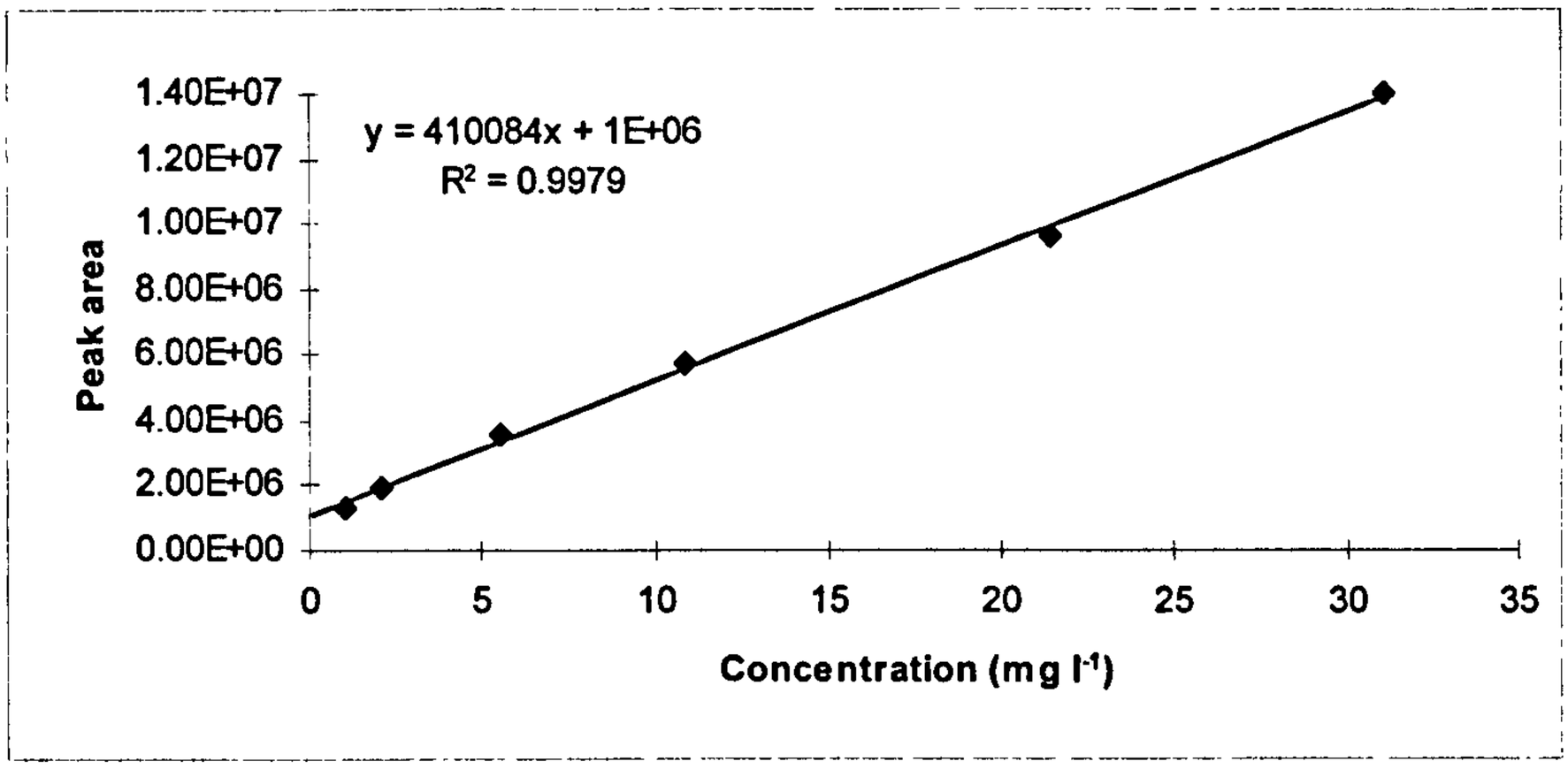

Figure 2.21. ESI LCMS calibration of W433

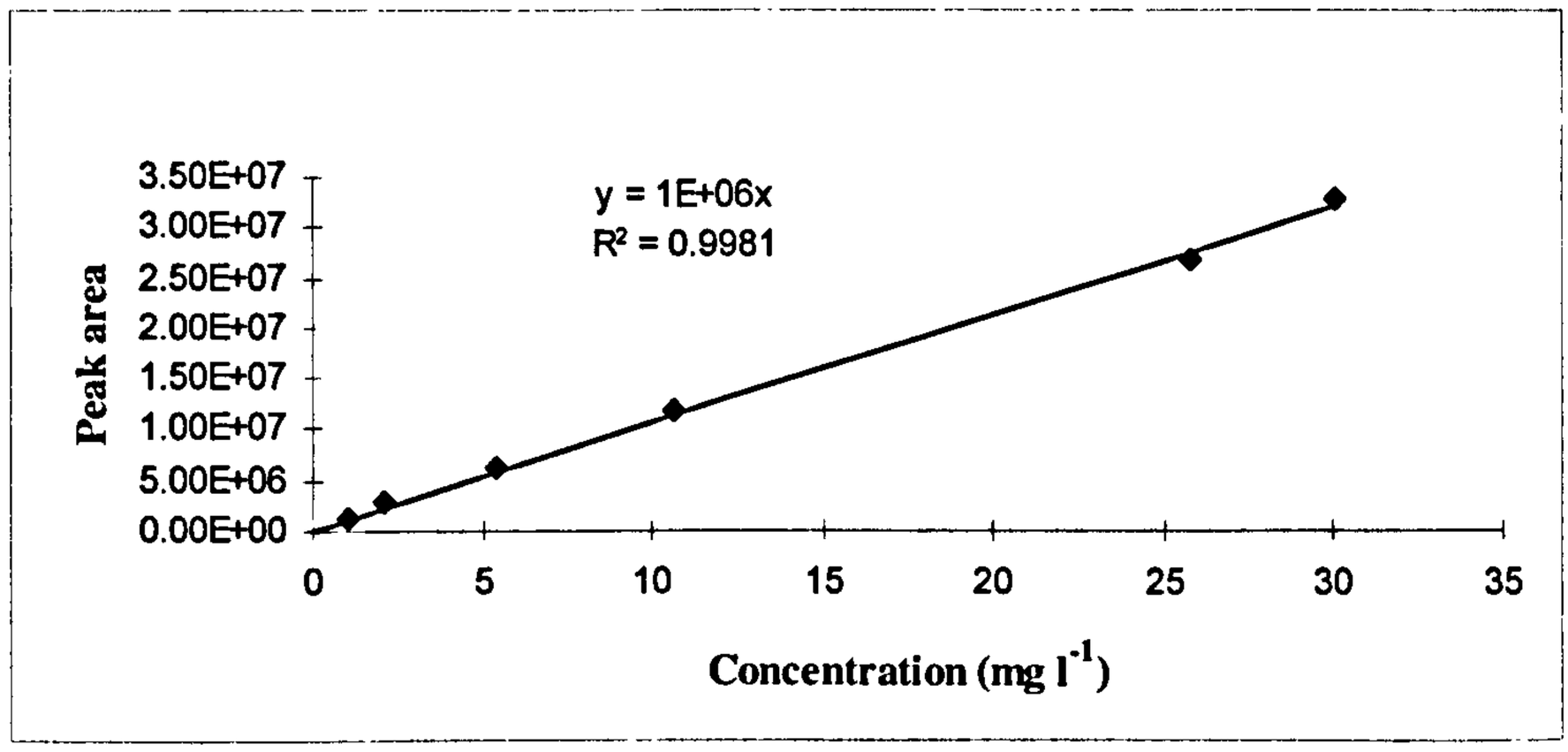

Figure 2.22. ESI LCMS calibration of W435

A comparison of ESI calibration with the previously described TSP data (Figures 2.14 and 2.15), show the latter to have a large positive Y-axis intercept, which was not so apparent for electrospray calibration graphs. It should also be noted that the ESI calibration was over a significantly lower concentration range, (1 - 30 mg l^{-1} compared to 25 - 300 mg l^{-1} for TSP).

An estimation of limit of detection for W433 and W435 using ESI was again calculated using a signal to noise ratio of >5:1. The S/N ratio for the lowest calibration standard (~60 ng on column), was greater than 20:1 for W433 and 40:1 for W435, suggesting an approximate LOD of 13 ng (W433) and 6 ng (W435) on column, in full scan mode.

Figure 2.23 shows a comparison of selected ion chromatograms (based on the summed area of all major ions for each dye, obtained using TSP (~25 mg l^{-1}) and ESI (~1 mg l^{-1}) LC-MS respectively. These clearly illustrate the better sensitivity provided by ESI for reactive dyes.

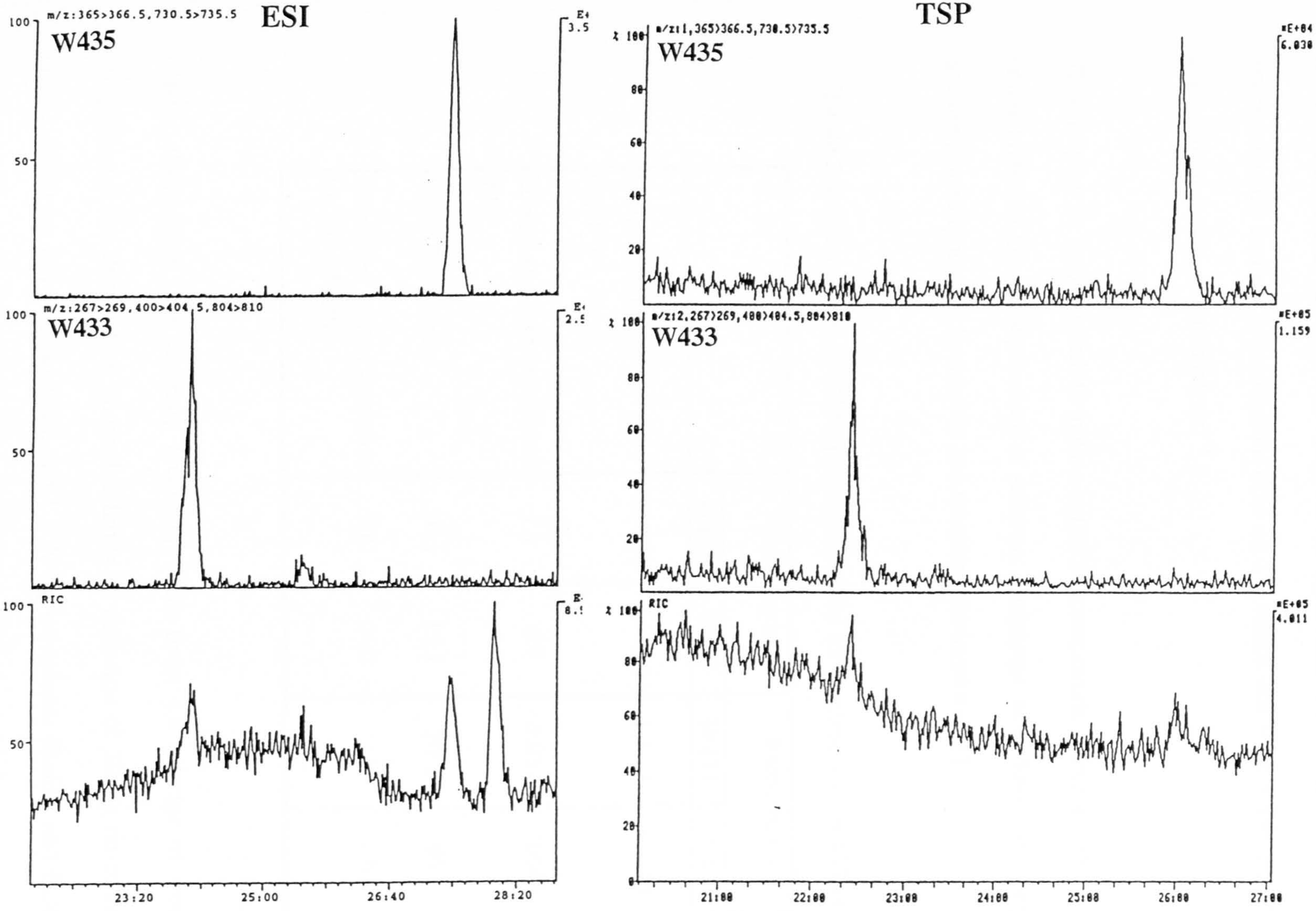

Figure 2.23 Comparison of selected mass chromatograms of W435 and W433 using electrospray (1 mg l^{-1}) and thermospray (5 mg l^{-1}) LC-MS interfaces

A comparison of TSP and ESI sensitivity under full scan acquisition, is provided in Table 2.6. ESI clearly provides far greater sensitivity than TSP. This was of particular significance because ESI could be used for analysis of dyes and their degradation products at environmentally realistic concentrations (low mg l^{-1}), which was not possible for TSP without a concentration step prior to analysis.

Thermospray is most suited to polar, ionisable compounds, whereas ESI is suited to compounds that are already ionised in solution. Sulphonic acids have extremely low pK_a and are generally ionised in solution and therefore favoured by ESI.

Table 2.6. Comparison of TSP and ESI sensitivity for reactive dyes W433 and W435

	Thermospray		Electrospray	
	W433	W435	W433	W435
Calibration range (mg l^{-1})	28-590	23-480	1.3-35	1.1-32
Lowest standard on-column (ug)	1.1	0.9	0.052	0.044
Signal/Noise ratio	20:1	15:1	20:1	40:1
Estimated limit of detection (ng on column)	300	300	13	6

These electrospray data compare favourably with those for a range of mono and di-sulphonated azo dyes which showed a limits of detection of 10 ng on-column (Straub *et al.*, 1992) for full scan analysis, and 1 - 70 ng on-column (Rafols and Barcelo, 1997) using selected ion monitoring.

2.6.4.2 Effect of buffer and mobile phase on ESI signal response

LC-MS requires a compromise between the conditions needed to provide an operable LC separation and those which enable reasonable mass spectrometer sensitivity. When ammonium acetate is used, the concentration has to be high enough to ensure ion pairing of the sulphonic acid groups of the dye. Failure to do this results in loss of chromatographic integrity. However, thermospray (TSP) analysis (Section 2.3), showed that mass spectrometer signal response is suppressed in the presence of buffer. It was, therefore, necessary to determine whether the buffer had the same effect on ESI signal response. Additionally, it was noted from the thermospray analysis that mobile phase composition, ie the % organic modifier in the eluent, had a significant effect on signal response. It was necessary to at least understand these phenomena, even though the gradient elution selected could not be significantly altered for dye analysis.

Using the standard gradient separation the mobile phase composition varies with time as follows:

Table 2.7 Mobile phase composition for analysis of W435

Time (minutes)	Aqueous (%)	Acetonitrile (%)
0	100	0
10	100	0
14	90	10
18	80	20
22	70	30
26	60	40
30	50	50

The mass spectrometer response at regular steps of the gradient was determined by infusion of W435 (5 µl min^{-1}) in to the mobile phase composition as outlined in Table 2.7. The peak intensity of the singly and doubly charged molecular ions (*m/z* 731 and 365

respectively), were monitored and their response plotted against mobile phase composition, (Figure 2.24).

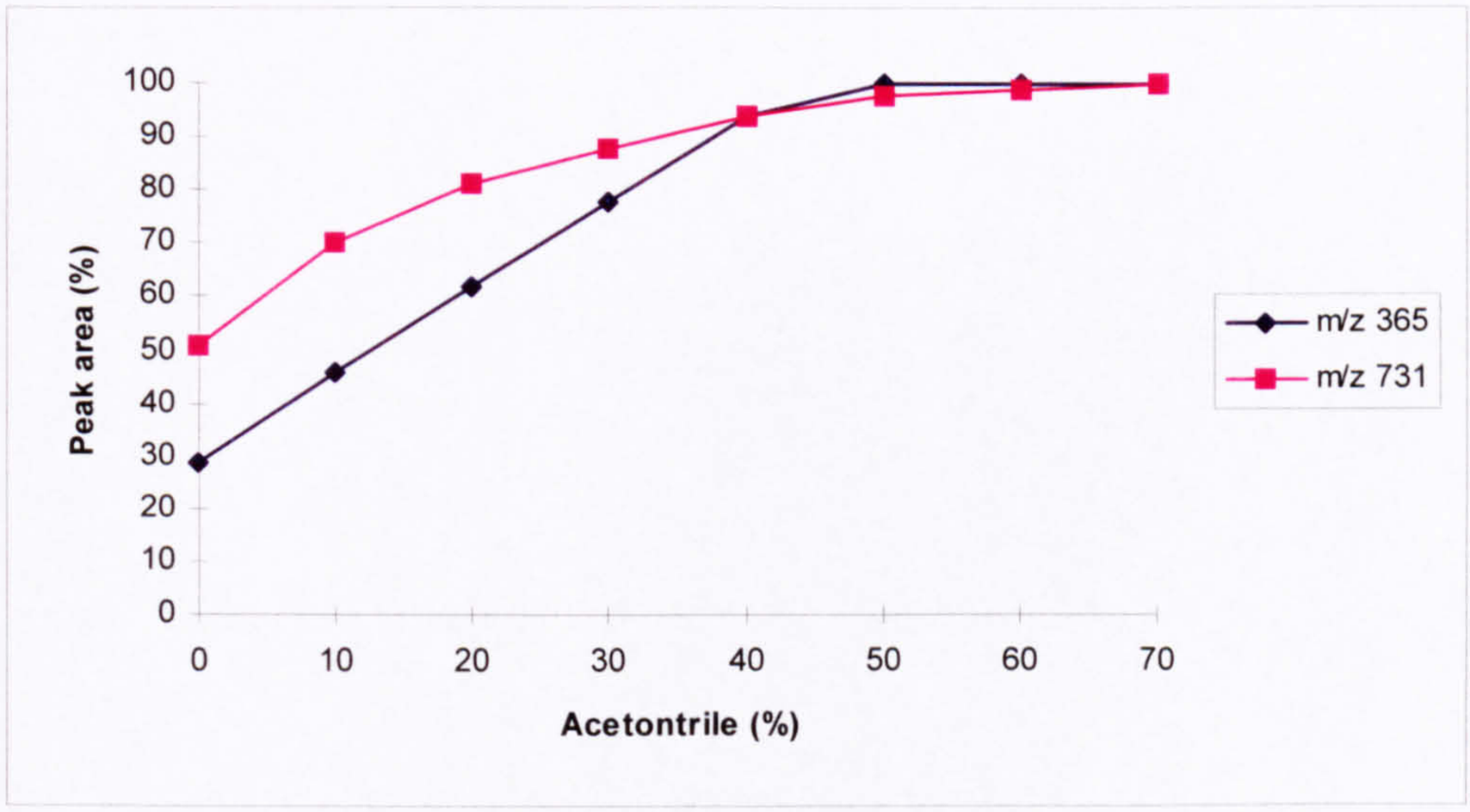

Figure 2.24 The effect of mobile phase composition on ESI signal response for W435

A significant increase in the mass spectrometer response for both singly and doubly charged molecular ions was observed with increasing percentage of organic modifier. A maximum response was observed for a composition containing approximately 40% acetonitrile, after which an increasing acetonitrile component had little effect on the mass spectrometer response. There was a greater effect for the doubly charged molecular ion which showed a greater than 3 fold increase in signal response between initial conditions and 40% acetonitrile composition, when compared to the singly charged species which doubled in response over the same range. This has implications for the overall sensitivity of the method - the earlier a peak elutes the poorer will be its response. All of the dyes used in this study elute with retention times between 20 and 30 minutes, equivalent to the mobile phase containing 30 - 50% organic modifier. Based solely on this criterion, the more polar dyes containing 3 or 4 sulphonic acid groups will show a response at least 30% below that of later eluting dyes. This may explain why W433 showed a higher limit of detection than W435 for the ESI calibration discussed earlier (Section 2.6).

The effect of organic modifier was repeated using 0.01M ammonium acetate in place of pure water in the LC eluent, to establish whether the same effect was observed in the presence of buffer. A very similar profile for both molecular ions of W435 was observed indicating the effect of organic modifier to be independent of buffer.

The effect of ammonium acetate buffer concentration on mass spectrometer response was determined by continuous infusion of W435 (5 µl min^{-1}) in to an aqueous LC eluent containing 0, 2, 4, 6, 8, 10 or 50 mM of ammonium acetate buffer. The peak intensities of the singly and doubly charged molecular ions (*m/z* 731 and 365 respectively), were monitored and their response plotted against buffer concentration, (Figure 2.25).

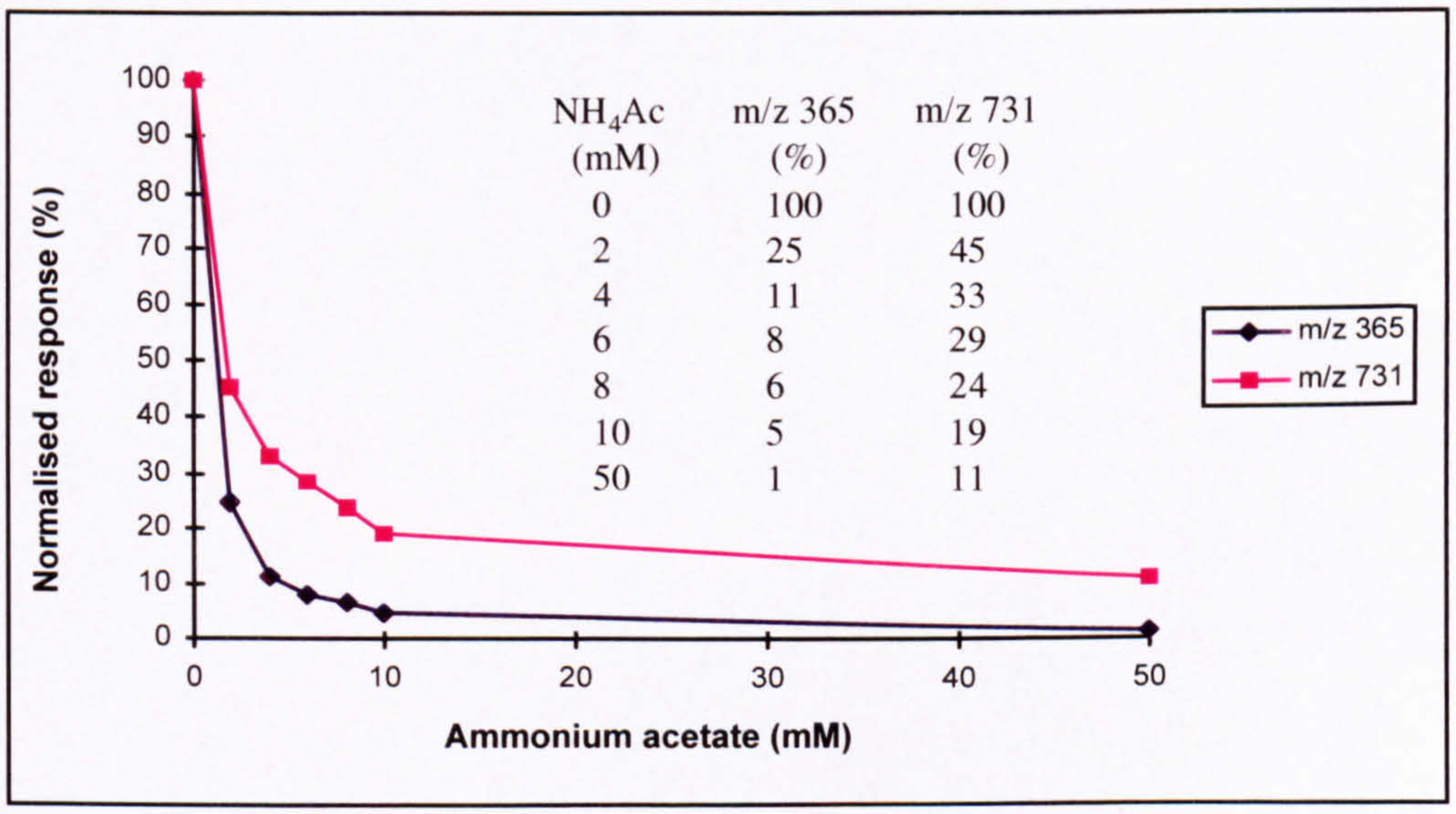

NH_4Ac (mM)	m/z 365 (%)	m/z 731 (%)
0	100	100
2	25	45
4	11	33
6	8	29
8	6	24
10	5	19
50	1	11

Figure 2.25. The effect of ammonium acetate buffer concentration on the response for singly (*m/z* 731) and doubly (*m/z* 365) charged molecular ions for reactive dye W435

Clearly the addition of even small amounts of buffer greatly diminishes the mass spectrometer response.

This exercise was repeated with an LC eluent of 50/50 aqueous phase/acetonitrile in the presence of 0.5, 1, 2, 3, 4 or 5 mM ammonium acetate, to explore the effect of buffer concentration at the final mobile phase composition of the standard gradient system. The

responses for singly and doubly charged molecular ions as a function of ammonium acetate concentration are shown in Figure 2.26.

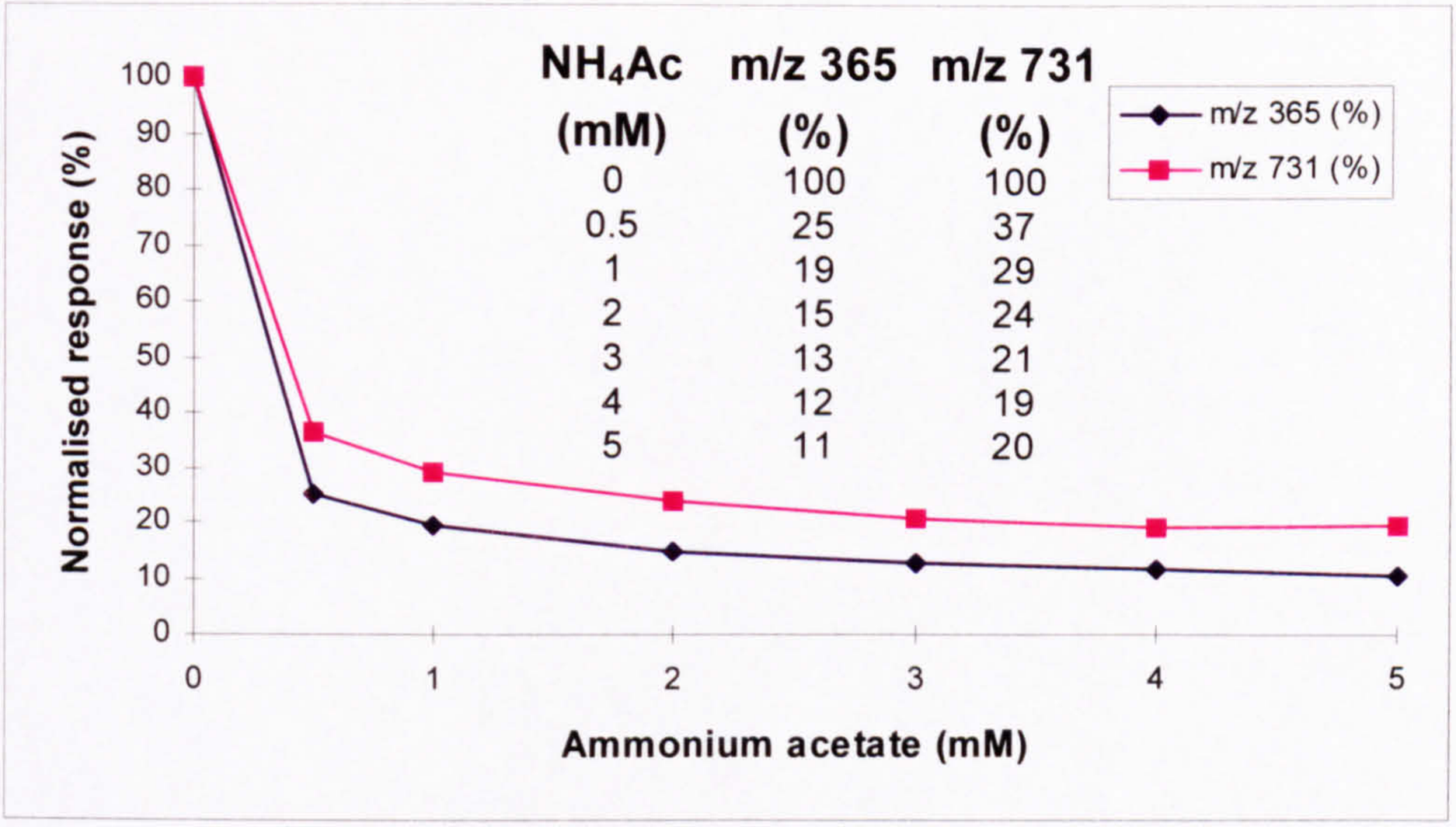

NH_4Ac (mM)	m/z 365 (%)	m/z 731 (%)
0	100	100
0.5	25	37
1	19	29
2	15	24
3	13	21
4	12	19
5	11	20

Figure 2.26 The effect of buffer concentration on ESI signal response for W435

Once again there was a rapid decrease in mass spectrometer response for both singly and doubly charged ions with increasing ammonium acetate concentration. However, it was noticeable that following the initial dramatic drop-off in signal response, the decline in response became quite shallow. The presence of organic modifier appeared to moderate the effect of buffer. These findings are consistent with previous reports (Flory *et al.*, 1987; Covey *et al.*, 1988; Rafols and Barcelo, 1997), which indicated that 1 mM ammonium acetate was a suitable buffer concentration for a mobile phase composition of 50/50 aqueous/organic phase.

The final part of the present evaluation was to determine the combined effect of organic modifier and buffer at the proportions used for the standard LC separation. Again W435 was added to the LC eluent by infusion (5 µl min^{-1}). On this occasion the mobile phase composition was changed in steps between 100% (0.01M NH_4Ac) and 40% (equivalent to 0.004M NH_4Ac), aqueous phase.

The response for singly and doubly charged molecular ions as a function of ammonium acetate concentration is shown in Figure 2.27.

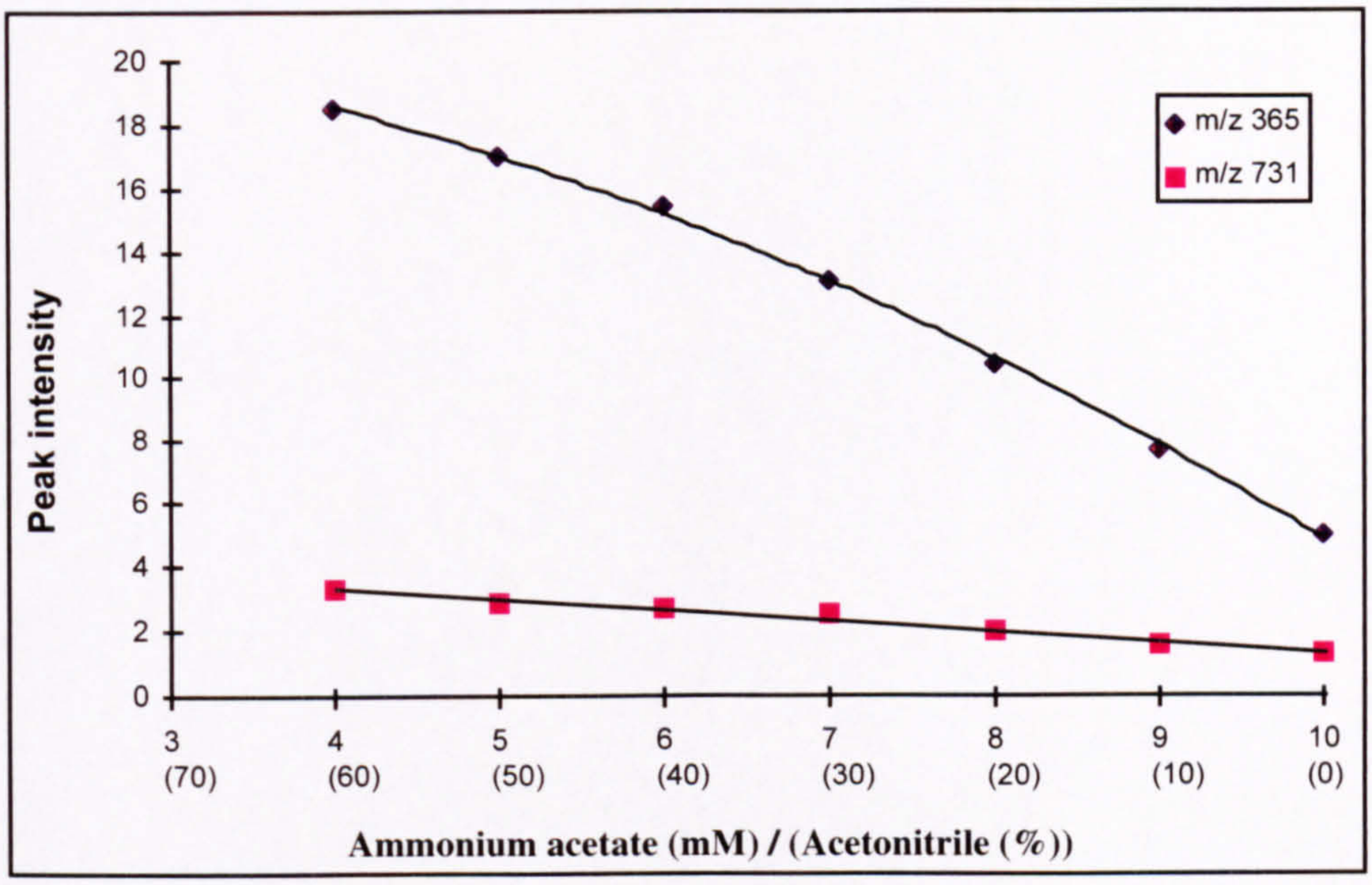

Figure 2.27 The effect of gradient elution on the ESI signal response for W435

This confirms the previous observations. A near linear increase in signal response for W435 was observed with increase in the organic modifier of the mobile phase, (and with concurrent dilution of the buffer). The biggest effect was observed for the doubly charged ion, which showed a 4 fold increase in sensitivity at 40% aqueous phase compared to the initial conditions.

In summary, the combination of buffer concentration and % organic modifier in the mobile phase, has an impact on the mass spectrometer response. In general, degradation products formed within this study are expected to be more polar than the parent dye they are derived from and therefore to elute earlier, so will be less responsive than parent dye under the standard LC-MS conditions. This needs to be considered when estimating the concentration of degradation products by reference to the parent dye response factor.

2.7 MSMS OPTIMISATION and INTERPRETATION

2.7.1 Experimental

W435 (100 mg l^{-1}), was added by continuous infusion (5 µl min^{-1}) to an LC eluent comprising of 50% water, 50% acetonitrile at a flow rate of 0.7 ml min^{-1}. The mass spectrometer was set to monitor the daughter ion spectra derived from *m/z* 731 and *m/z* 365 the singly and doubly charged molecular ions respectively, over a mass range of 200 - 900 daltons in 2 seconds, using a capillary temperature of 300°C, sheath gas 60 psi, auxiliary gas 10 psi and a spray voltage of 4.5 kV.

The collision gas (argon), was maintained at 1 mTorr while the collision energy (COFF) was adjusted in 5 eV steps from 10 to 60 eV for *m/z* 731 and 10 - 40 eV for *m/z* 365. This process was repeated for collision gas pressures of 2, 3 and 4 mTorr to achieve an optimum value.

This optimisation was then repeated for *m/z* 402.5 the doubly charged molecular ion of W433 (100 mg l^{-1}), using collision energies between 10 and 40 eV. W433 has three chlorine atoms which may be present as either ^{35}Cl or ^{37}Cl isotopes. The chlorine isotope ratio for the doubly deprotonated molecular ions *m/z* 401.5, 402.5, 403.5 and 404.5 is 27:27:9:1 respectively. Additionally, W433 has three sulphur atoms which will modify this isotope ratio to 27:30:12:2. Therefore, *m/z* 401.5 and 402.5 are the most prominent ions in the W433 mass spectrum.

Additionally, the daughter ion spectra of *m/z* 733 (the ^{37}Cl-isotope containing ion of the singly charged molecular ion of W435), and *m/z* 401.5 (the ^{35}Cl isotope of the doubly charged molecular ion of W433), were obtained using the same conditions but at 3 mTorr only. These spectra were obtained to aid the interpretation of MSMS data.

2.7.2 Results for collision offset optimisation

2.7.2.1 Introduction

The only MSMS experiments used in this study were in daughter ion mode. There were three stages to the analyses:

1 An ion, usually the molecular ion, formed in the source under electrospray conditions is selected using the first mass analyser (Q1). The single mass chosen is termed the parent ion.

2 This ion enters an octapole rod assembly (Q2), which acts as a collision cell. Q2 is an RF-only device which can efficiently transmit (>90%) ions of a wide range of mass to charge ratio (*m/z*). Ions entering the collision cell can be fragmented by interaction with an inert collision gas present in the cell at a pressure which is elevated relative to the surrounding environment, typically 1 to 4 mTorr. This process is termed collision activation because the parent ion gains energy from the collisions. When this leads to the formation of fragment ions (daughter ions), the process is known as collision induced dissociation (CID) or sometimes collision activated dissociation (CAD).

3. Fragment ions formed in the collision cell then enter the second mass analyser (Q3), which is scanned to produce a daughter ion mass spectrum of ions derived from the selected parent mass.

The whole process can be represented by the equation:

$$M_p^+ \xrightarrow{N} M_d^+ + M_n$$

where p and d are parent and daughter ions respectively, n represents a neutral loss and N is the inert (neutral) collision gas. The terms d and n suggest only one daughter ion or neutral loss take place, but these can in reality be the sum of several fragmentations. Also, the daughter ion itself may collide and dissociate to form further fragment ions which collectively produce a daughter ion mass spectrum.

For dissociation (fragmentation) of the parent ion to take place following collisional activation, the parent ion has to overcome an activation barrier. The mechanism of dissociation involves the conversion of translational kinetic energy (TKE) of the parent ion, into internal energy, raising the ion to an excited state. The internal energy may be stabilised within the ion but if it is sufficiently high, fragmentation occurs.

The efficiency of the fragmentation process depends on several factors: The more stable the ion, the less likely it is to fragment on collision. The more massive an ion the more likely it will be able to stabilise the vibrational energy imparted to it by the collision and, therefore, the less likely it will be to fragment. At very high collision gas pressures (ie above 4 mTorr), most ions will fragment due to the potential for multiple collisions. However, increasing collision gas pressure also increases the degree of scattering of ions and decreases the overall transmission of ions through Q2. The mass and molecular diameter of the collision gas also have an effect, the more massive the gas (or larger its diameter), the greater the probability of collision, therefore fragmentation increases. Argon is the most common choice of collision gas, but nitrogen and helium are also used.

One other variable which has a major impact on CID is the collision energy. This is the quadrapole offset voltage applied to Q2, which represents the potential difference between the ion source and Q2. An increase in the collision energy increases the TKE of the parent ion, thus increasing the energy of ion/molecule collisions in Q2, leading to increased fragmentation.

In summary, a useful analogy would be driving a car into a brick wall in order to break it up. The faster the car is travelling (increasing the collision energy, increases the TKE of the ion), the more fragmentation will occur. Similarly, the thicker the wall (collision gas pressure) the more fragmentation. The type of collision gas used is usually not changed, therefore, optimisation of CID information is a balance between collision energy and collision gas pressure, to produce the optimum degree of fragmentation.

2.7.2.2 MSMS optimisation

Two reactive dyes were selected for the determination of the effect of collision gas pressure and collision energy on daughter ion fragmentation. The disulphonated anthraquinone dye W435, using the singly (*m/z* 731) and doubly charged (*m/z* 365) molecular ions and the tri-sulphonated azo dye W433, using the doubly charged molecular ion (*m/z* 402.5) only, because the singly charged ion was too weak to provide useful daughter ion spectra. In each case the molecular ion was selected using Q1 and fragmented in the collision cell Q2, at a fixed collision gas pressure, whilst the collision energy was increased in regular steps. This process was repeated at collision gas pressures of 1, 2, 3 or 4 mTorr for each of the selected molecular ions.

Figure 2.28 shows a comparison of the effect of increasing COFF on transmission of the singly charged parent ion of W435 (*m/z* 731), at each of the four collision gas pressures.

Increasing collision energy increased fragmentation resulting in a decrease in the intensity of the parent ion. The parent ion was totally removed at collision energies above 35 eV for 2, 3 and 4 mTorr gas pressure, whilst significantly less fragmentation was observed at 1 mTorr pressure.

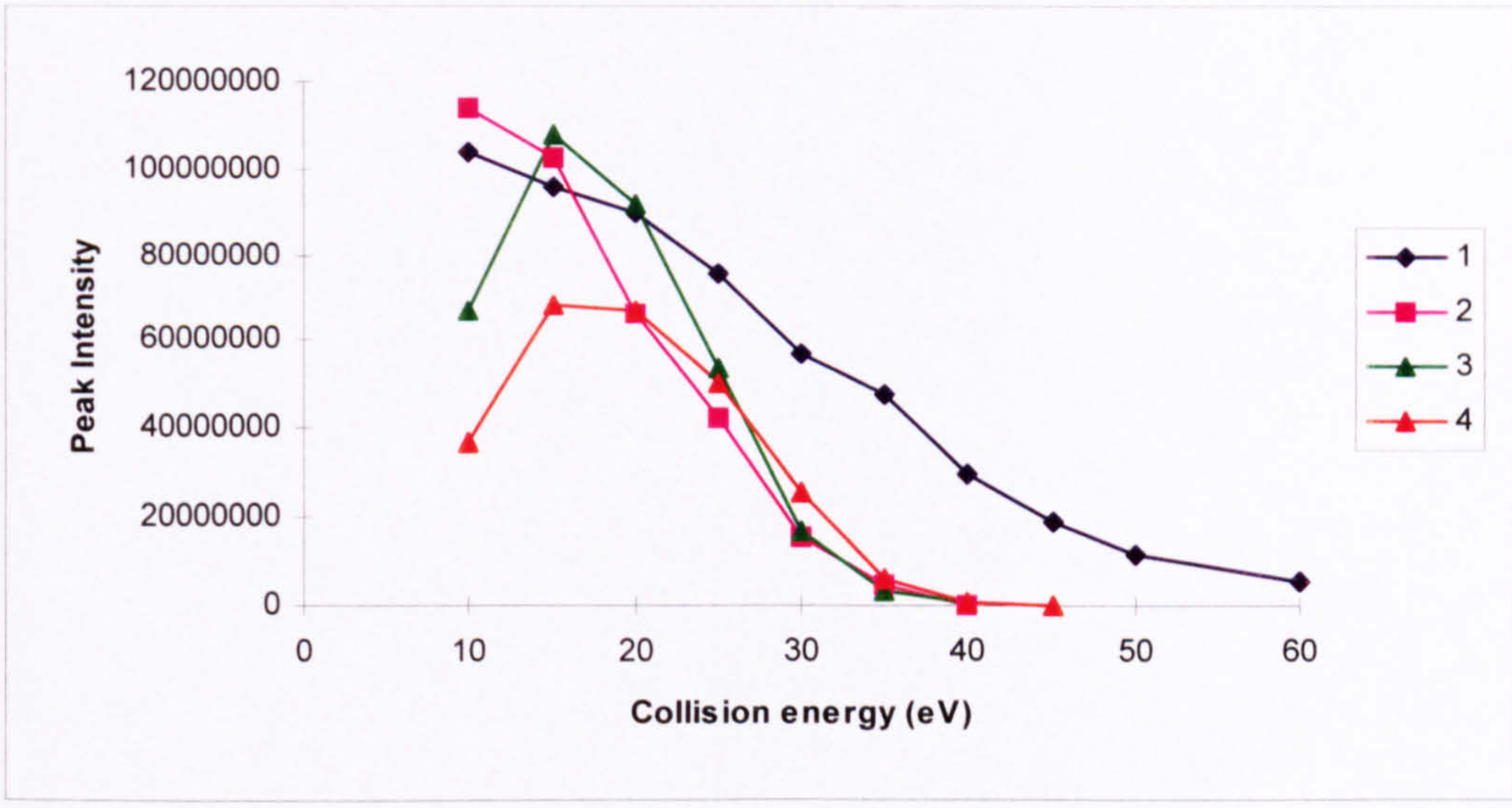

Figure 2.28. Effect of increasing collision energy on the parent ion in the daughter ion spectra of *m/z* 731 ($[M-H]^-$) for W435, at collision gas pressures of 1, 2, 3 and 4 mTorr

Figure 2.29 shows a comparison of total fragment ion current (ie all ions derived from dissociation of *m/z* 731, but not including the contribution made by this ion). A collision gas pressure of 1 mTorr produced significantly less fragmentation than the others. Pressures of 2 and 3 mTorr appeared to produce a quite similar response with maximum transmission of fragment ions occurring in the range 35 - 45 eV. A collision gas pressure of 4 mTorr showed a similar maximum at 35 eV, but also showed a rapid drop-off in response for collision energies above this maximum.

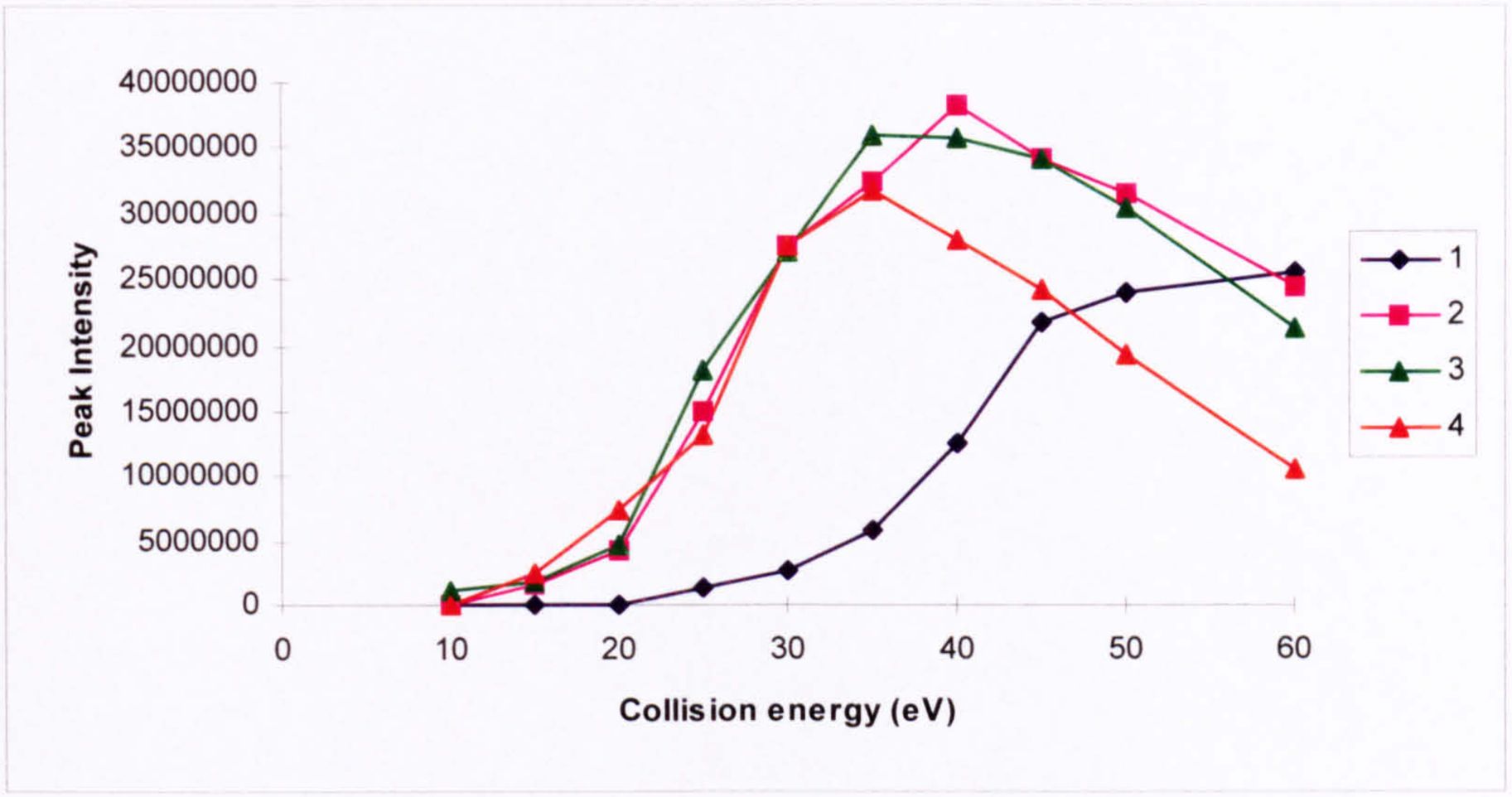

Figure 2.29. Effect of increasing collision energy on the sum of major fragment ions in the daughter ion spectra of *m/z* 731 ($[M-H]^-$) for W435, at collision gas pressures of 1, 2, 3 and 4 mTorr

Figure 2.30 shows profiles for the major fragment ions formed on dissociation of the W435 parent ion *m/z* 731. At higher collision gas pressures the onset of fragmentation occurs earlier and lower collision energies are required to induce fragmentation. Using *m/z* 580 as an example, the maximum response is observed for a COFF of 45 - 50 eV at 1 mTorr gas pressure, compared to 35 - 40, 35 and 30 - 35 eV for 2, 3 and 4 mTorr gas pressure respectively. This is generally consistent with the profiles obtained for the sum of fragment ions shown in Figure 2.29. The profiles observed for occurrence and disappearance of the major fragment ions were similar at each gas pressure, yet there was no one combination of collision energy and collision gas pressure that produced all of the major fragment ions. This is illustrated by the daughter ion *m/z* 652, which was almost completely removed before the appearance of *m/z* 500 and 475. This demonstrates the need to use a range of COFF setting for MSMS experiment. A COFF of 30 - 45 eV produced the most useful fragment ion spectrum from *m/z* 731.

It was noticeable that little fragmentation occurred at 1 mTorr gas pressure, indicating that this was not a suitable collision gas pressure for MSMS studies. Also, as shown in Figure 2.28, the parent ion was present at collision energies up to 35 eV for each gas

pressure. The presence of the parent ion in the mass spectra although not absolutely necessary, is useful for explanation of fragmentation pathways. Therefore, considering the lower ion transmission at 4 mTorr for collision energies above 30 eV and the relative lack of fragmentation at 1 mTorr, the optimum conditions for singly charged dyes was established as 2 - 3 mTorr collision gas pressure using a COFF of 30 - 45 eV.

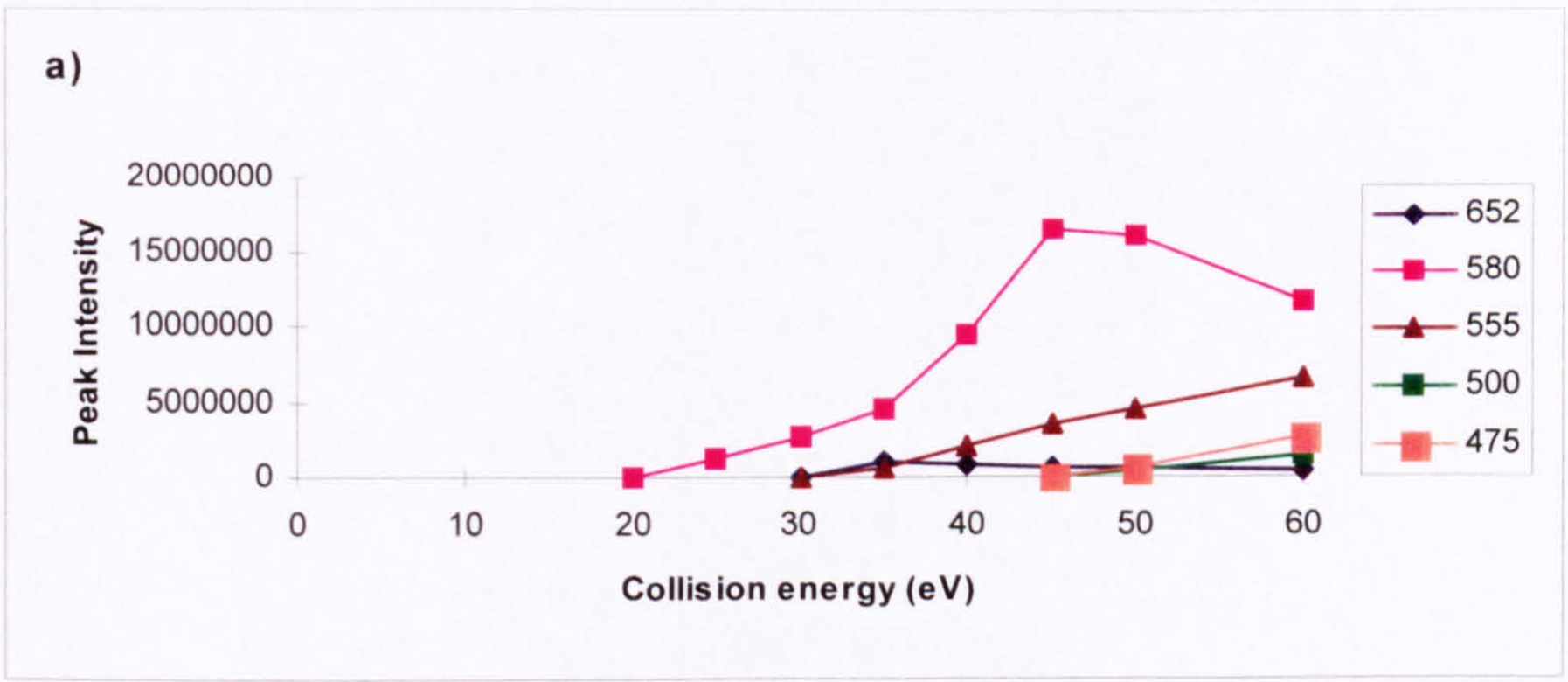

Figure 2.30. Effect of increasing collision energy on major fragment ions of *m/z* 731 ([M-H]$^-$) for W435, at a collision gas pressure of 1, 2, 3 and 4 mTorr, Figures a-d respectively

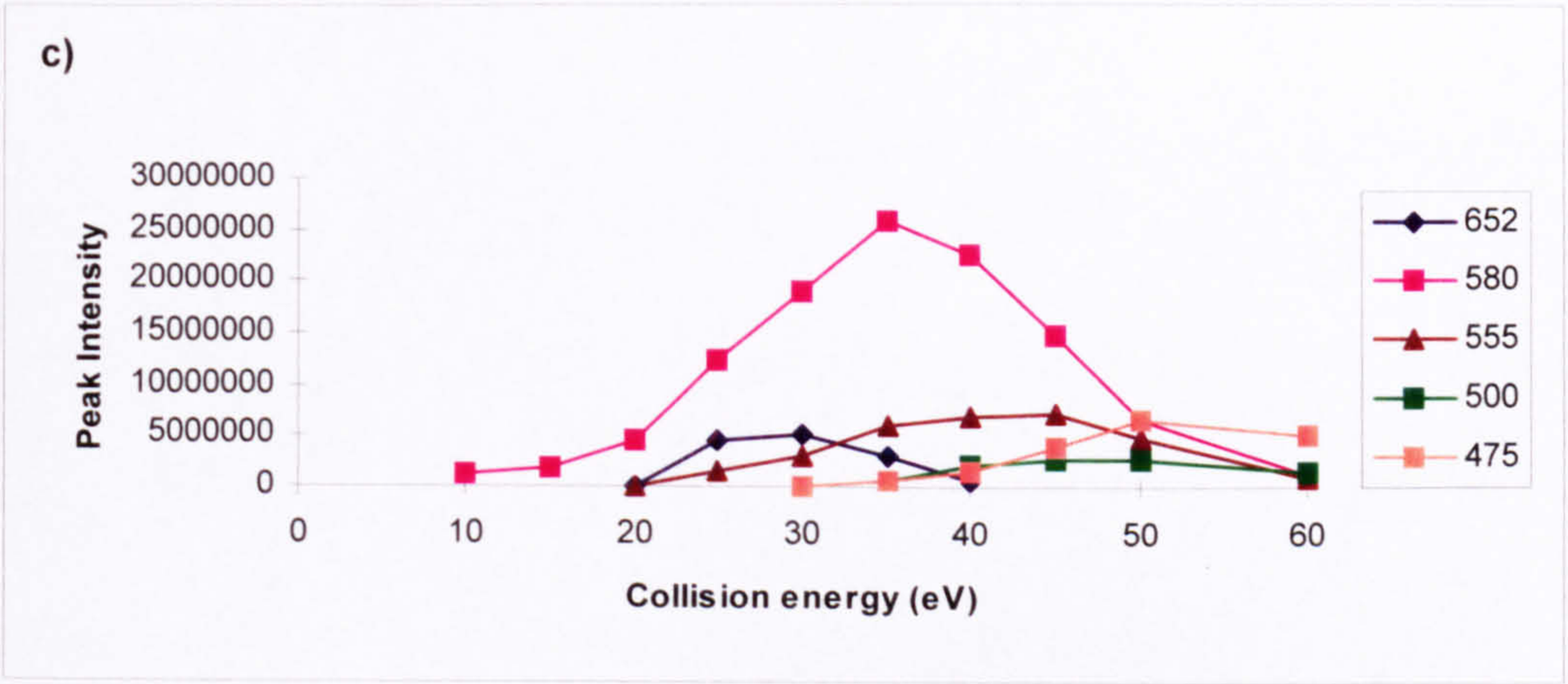

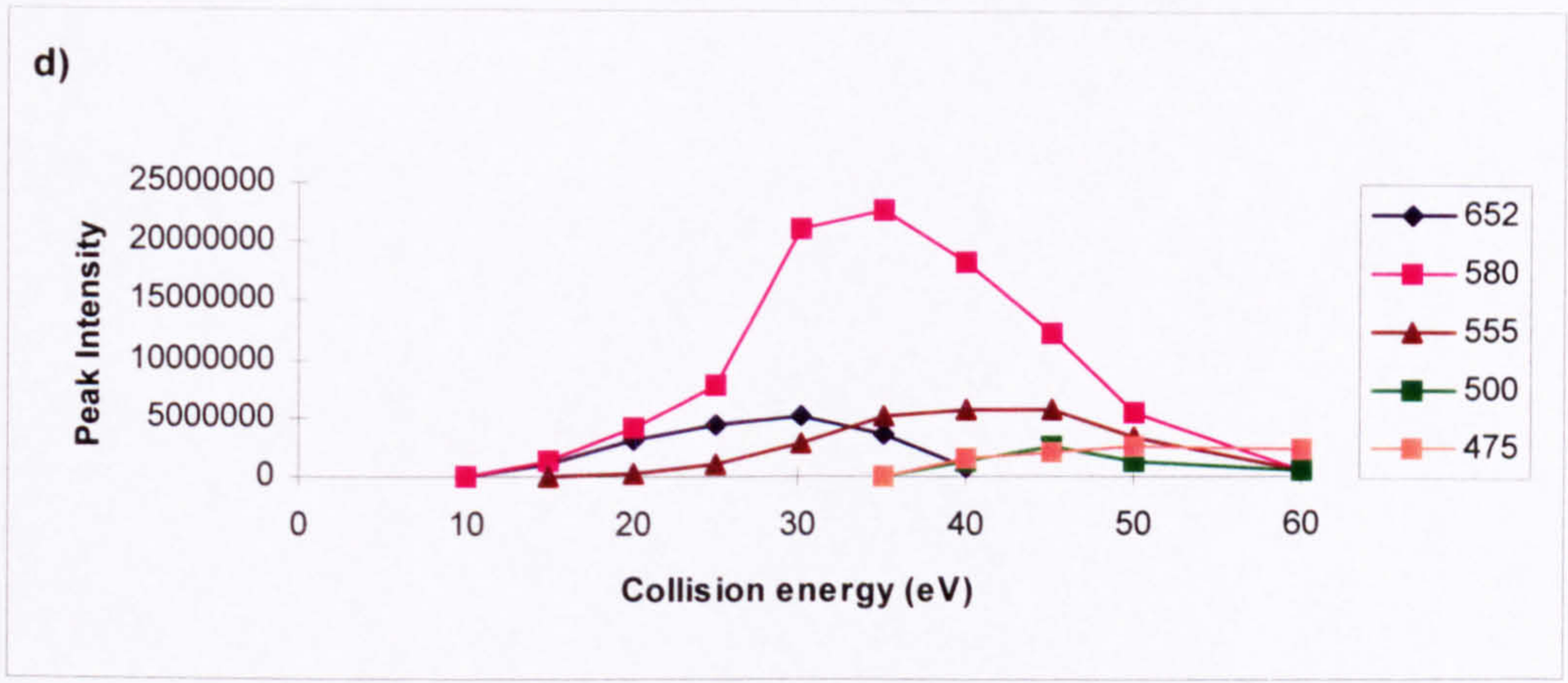

Figure 2.30 (contd). Effect of increasing collision energy on major fragment ions of *m/z* 731 ([M-H]$^-$) for W435, at a collision gas pressure of 1, 2, 3 and 4 mTorr, Figures a-d respectively

The effect of increasing collision energy on the doubly charged molecular ion of W435, *m/z* 365, is shown in Figure 2.31. When compared to the singly charged parent ion (Figure 2.28), complete dissociation of the parent ion was observed at a much lower collision energy, ie 20 - 25 eV for collision gas pressures of 2 - 4 mTorr. Once again the parent ion was less susceptible to fragmentation at 1 mTorr gas pressure.

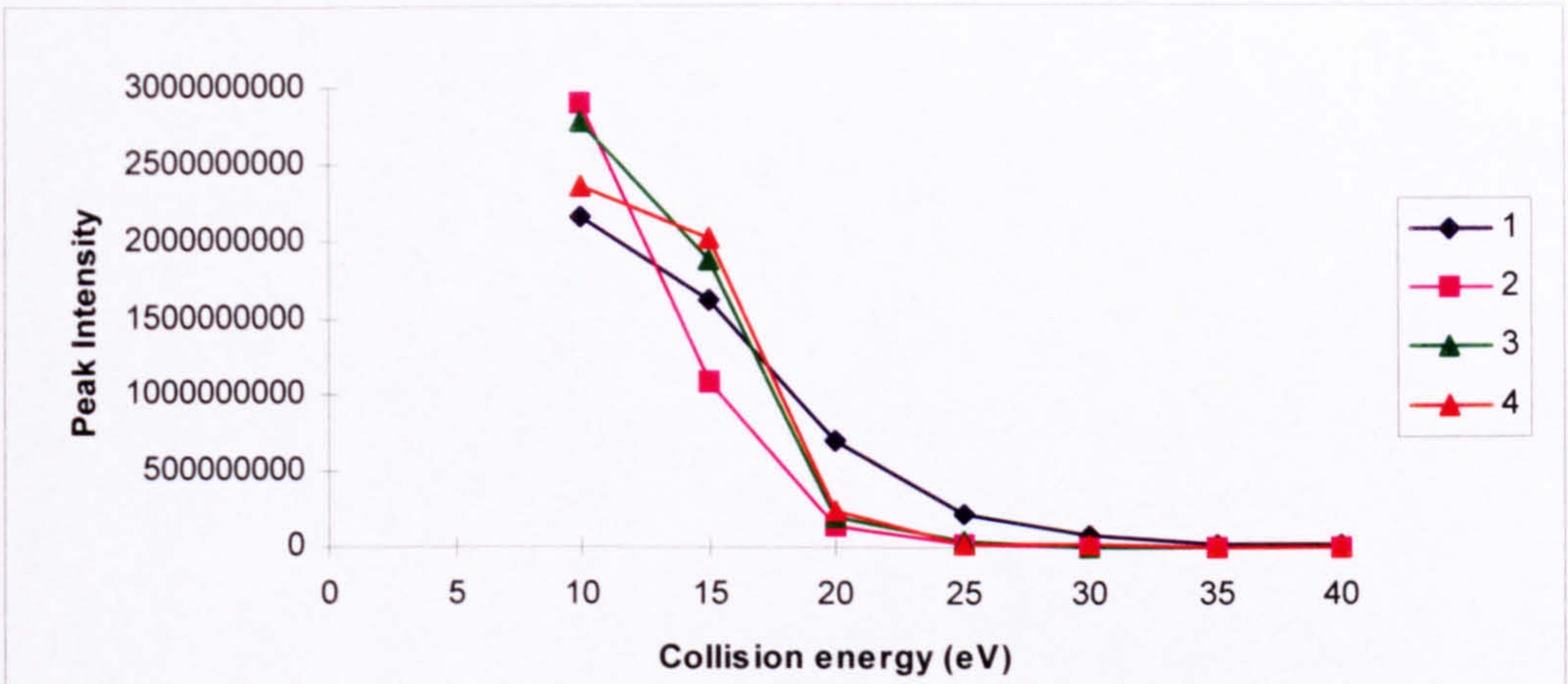

Figure 2.31. Effect of increasing collision energy on the parent ion in the daughter ion spectra of *m/z* 365 ($[M-2H]^{2-}$) for W435, at collision gas pressures of 1, 2, 3 and 4 mTorr

Figure 2.32 shows a comparison of total fragment ion current (ie all ions derived from dissociation of the parent but not including the contribution made by the parent ion). The total abundance of fragment ions increased with increasing collision gas pressure. There was little difference between the responses at 3 and 4 mTorr gas pressures, which both provided significantly more abundant fragmentation than at 1 and 2 mTorr gas pressure. Also, the optimum collision energy was not only the same for each collision gas pressure, (20 eV), it was considerably lower than the optimum for the corresponding singly charged parent ion (ca 35 - 40 eV; Figure 2.28), suggesting that the doubly charged parent ion is less stable than the corresponding singly charged species and therefore more prone to dissociation.

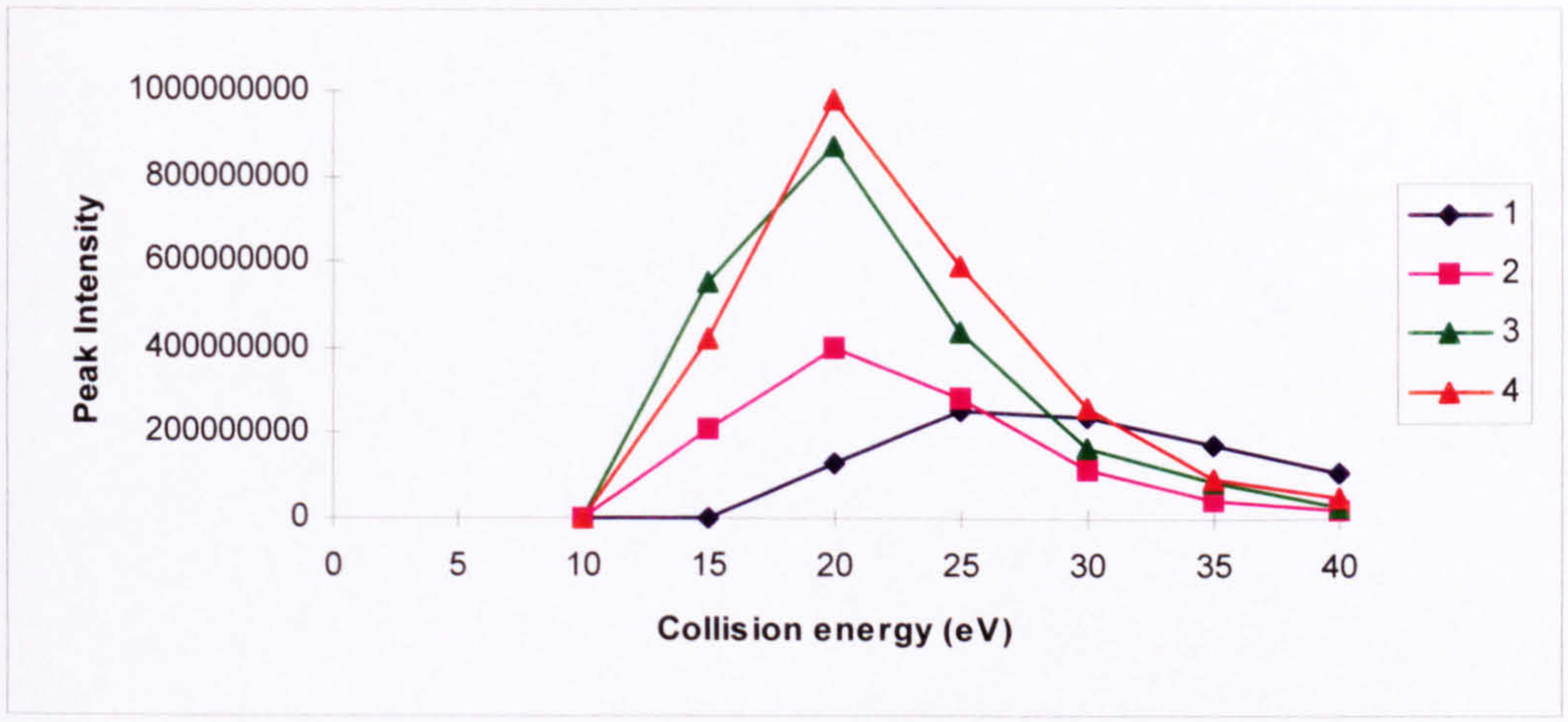

Figure 2.32. Effect of increasing collision energy on the sum of major fragment ions in the daughter ion spectra of *m/z* 365 ($[M-2H]^{2-}$) for W435, at collision gas pressures of 1, 2, 3 and 4 mTorr

The profiles for the formation of major fragment ions with increasing collision energy for each gas pressure are shown in Figure 2.33. With the notable exception of the 1 mTorr optimisation, the other three produced very similar profiles. It was also noticeable that a much narrower range of collision energies (20 - 25 eV), was required to produce all of the major fragment ions derived from the doubly charged species.

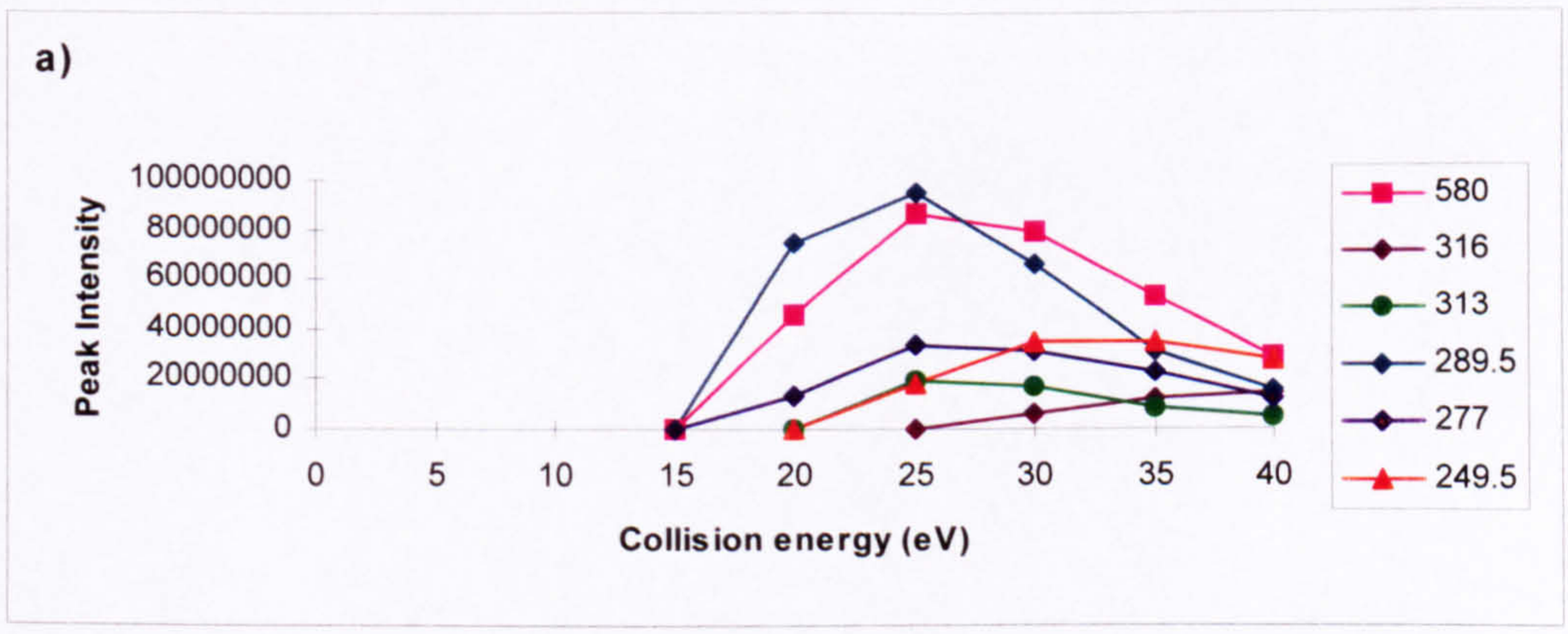

Figure 2.33. Effect of increasing collision energy on major fragment ions of *m/z* 365 ($[M-2H]^{2-}$) for W435, at collision gas pressures of 1, 2, 3 and 4 mTorr, a-d respectively

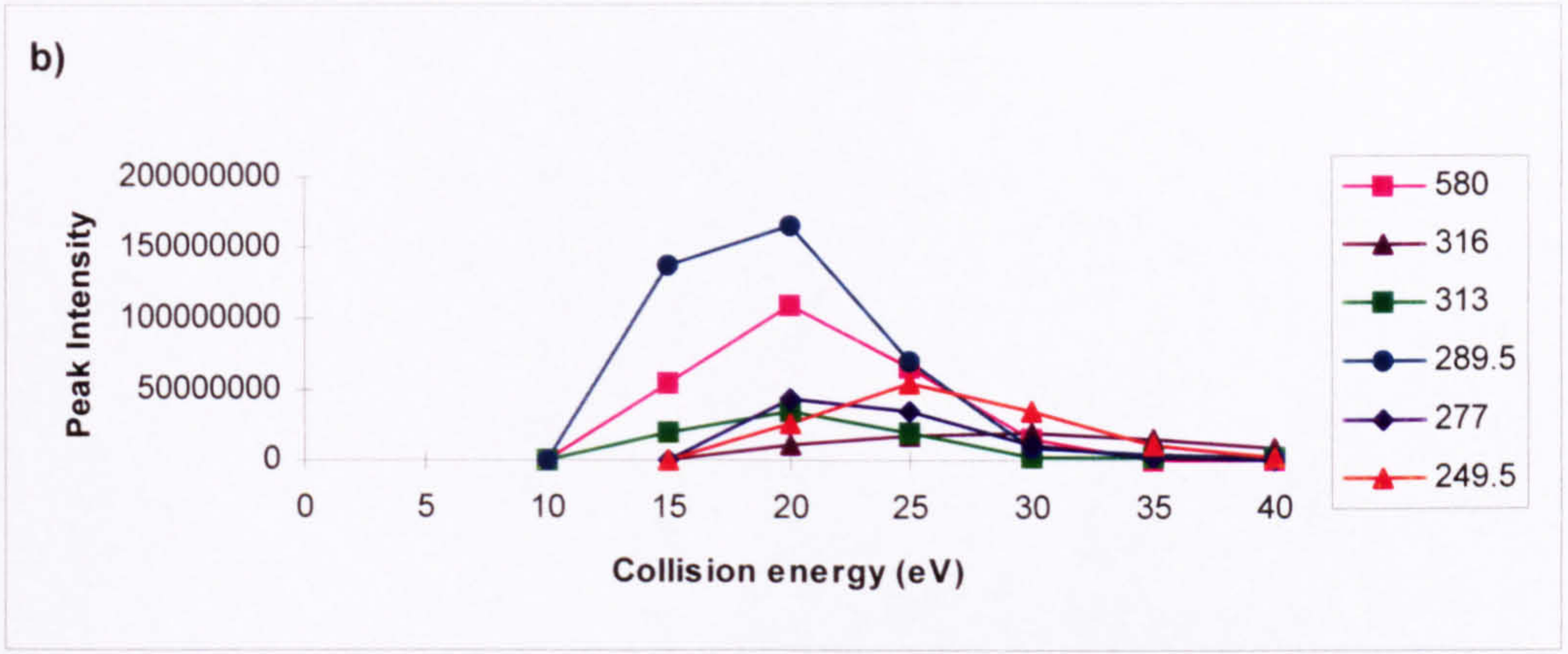

Figure 2.33 (contd). Effect of increasing collision energy on major fragment ions of *m/z* 365 ($[M-2H]^{2-}$) for W435, at collision gas pressures of 1, 2, 3 and 4 mTorr, a-d respectively

To determine whether these findings were consistent for other reactive dyes, the doubly charge molecular ion of W433 (Reactive yellow 2) was also subjected to similar profiling.

The effect of increasing collision energy on the doubly charged molecular ion of W433, *m/z* 402.5, is shown in Figure 2.34. The profiles were much the same as observed for the doubly charged ion of W435 (*m/z* 365, Fig 2.31). Once again complete dissociation of the parent ion was observed at a much lower collision energy than for singly charged ions, (20 eV) for collision gas pressures of 2 - 4 mTorr and again the parent ion was less susceptible to fragmentation at 1 mTorr gas pressure.

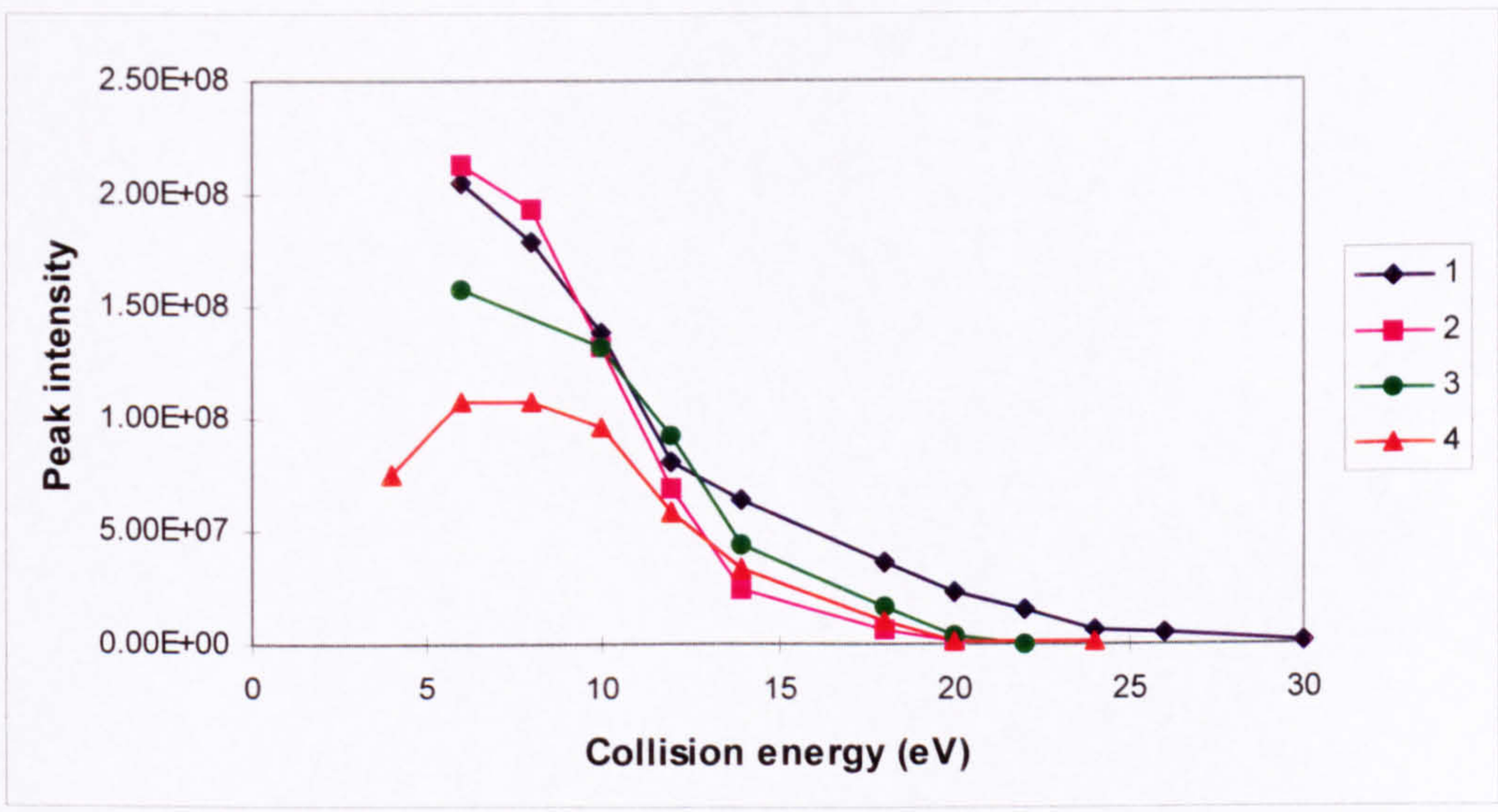

Figure 2.34. Effect of increasing collision energy on the parent ion in the daughter ion spectra of *m/z* 402.5 ($[M-2H]^{2-}$) for W433, at collision gas pressures of 1, 2, 3 and 4 mTorr

The effect of collision energy on the sum of fragment ions for *m/z* 402.5 is shown in Figure 2.35. This was similar to the profile for *m/z* 365 the doubly charged ion of W435 (Fig 2.32). The least degree of dissociation was shown at 1 mTorr pressure. The transmission of ions is slightly impaired by the high degree of collisions for the 4 mTorr gas pressure leading to a lower response than either of the 2 and 3 mTorr gas pressure, which gave a very similar response. However the onset of fragmentation and the position

of most fragmentation , (ca 6 and 18 eV respectively) were both lower than observed for *m/z* 365 of W435. As previously discussed, the degree of fragmentation is compound dependent and is affected by the ability of the ion to stabilise the internal energy gained through collision with the inert gas. This data suggests the anthraquinone dye W435 is more able to stabilise this energy gained in the MSMS process than the azo dye W433.

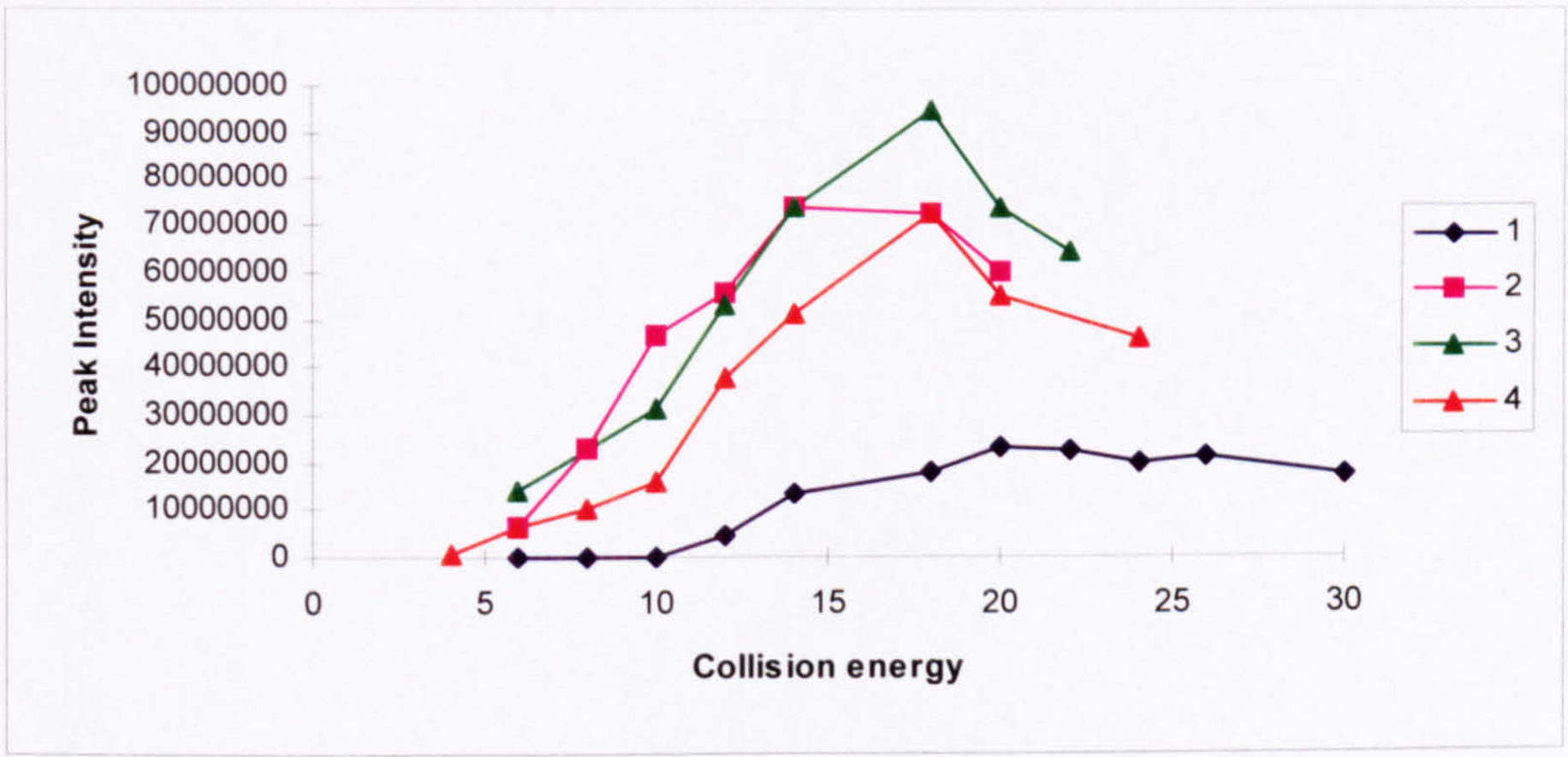

Figure 2.35. Effect of increasing collision energy on the sum of major fragment ions in the daughter ion spectra of *m/z* 402.5 ($[M-2H]^{2-}$) for W433, at collision gas pressures of 1, 2, 3 and 4 mTorr

The profiles for the formation of major fragment ions with increasing collision energy for each gas pressure are shown in Figures 2.36. Once again, with the exception of the 1 mTorr optimisation, the other three gas pressures produced very similar profiles. However, there appeared to be a broader spread of collision energies required to produce fragment ions than was observed for the equivalent *m/z* 365 parent ion of W435. This maybe because W433 contains three sulphonic acid groups and the doubly charged species could involve any two of the three possibilities, whereas W435 contains only two sulphonic acid groups both of which must be charge carrying in the doubly charged state. Further work would be needed to confirm this observation. The outcome is that, for W433, a wider range of collision energies could be used to obtain useful MSMS spectra. That is, COFF was not such a critical parameter for W433 as it was for W435 analysis.

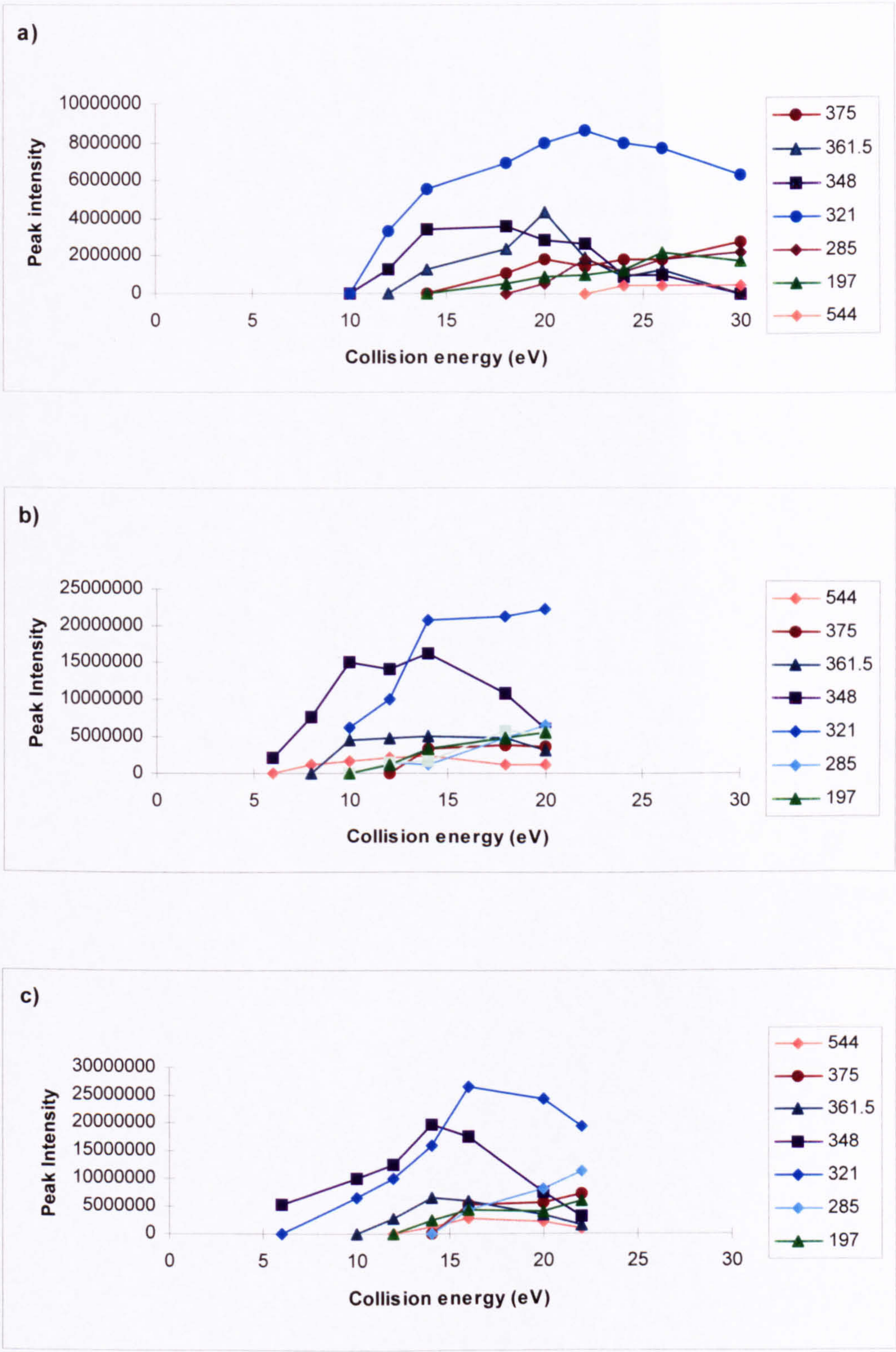

Figure 2.36. Effect of increasing collision energy on major fragment ions of *m/z* 402.5 ($[M-2H]^{2-}$) for W433, at collision gas pressures of 1, 2, 3 and 4 mTorr, a-d respectively

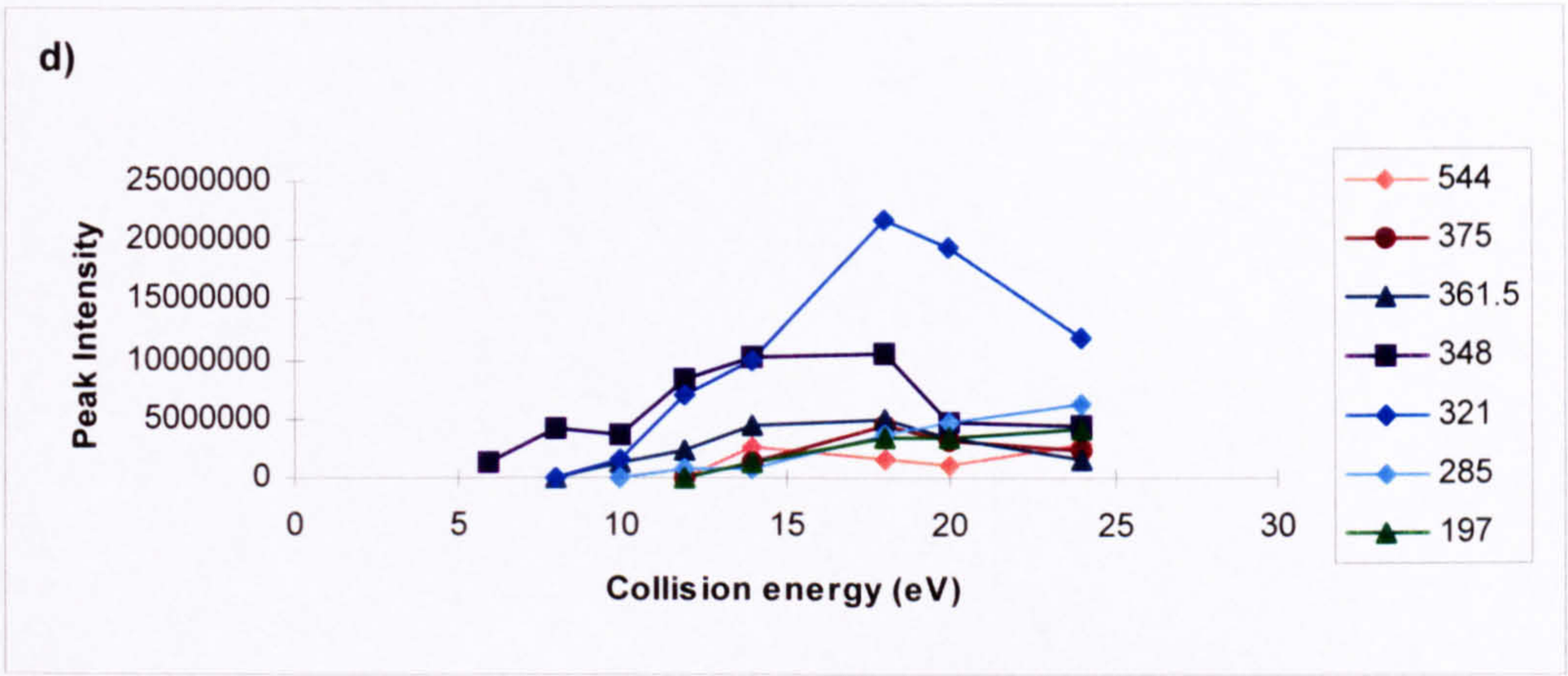

Figure 2.36 (contd). Effect of increasing collision energy on major fragment ions of *m/z* 402.5 ($[M-2H]^{2-}$) for W433, at collision gas pressures of 1, 2, 3 and 4 mTorr, a-d respectively

Another method of displaying the change in ion abundance with increasing collision energy is to use contour plots (Figure 2.37). These show that diversity as well as intensity of fragment ions was favoured by a collision gas pressure of 3 mTorr. They also confirm that no one collision energy can be used to produce a maximum for each of the fragment ions.

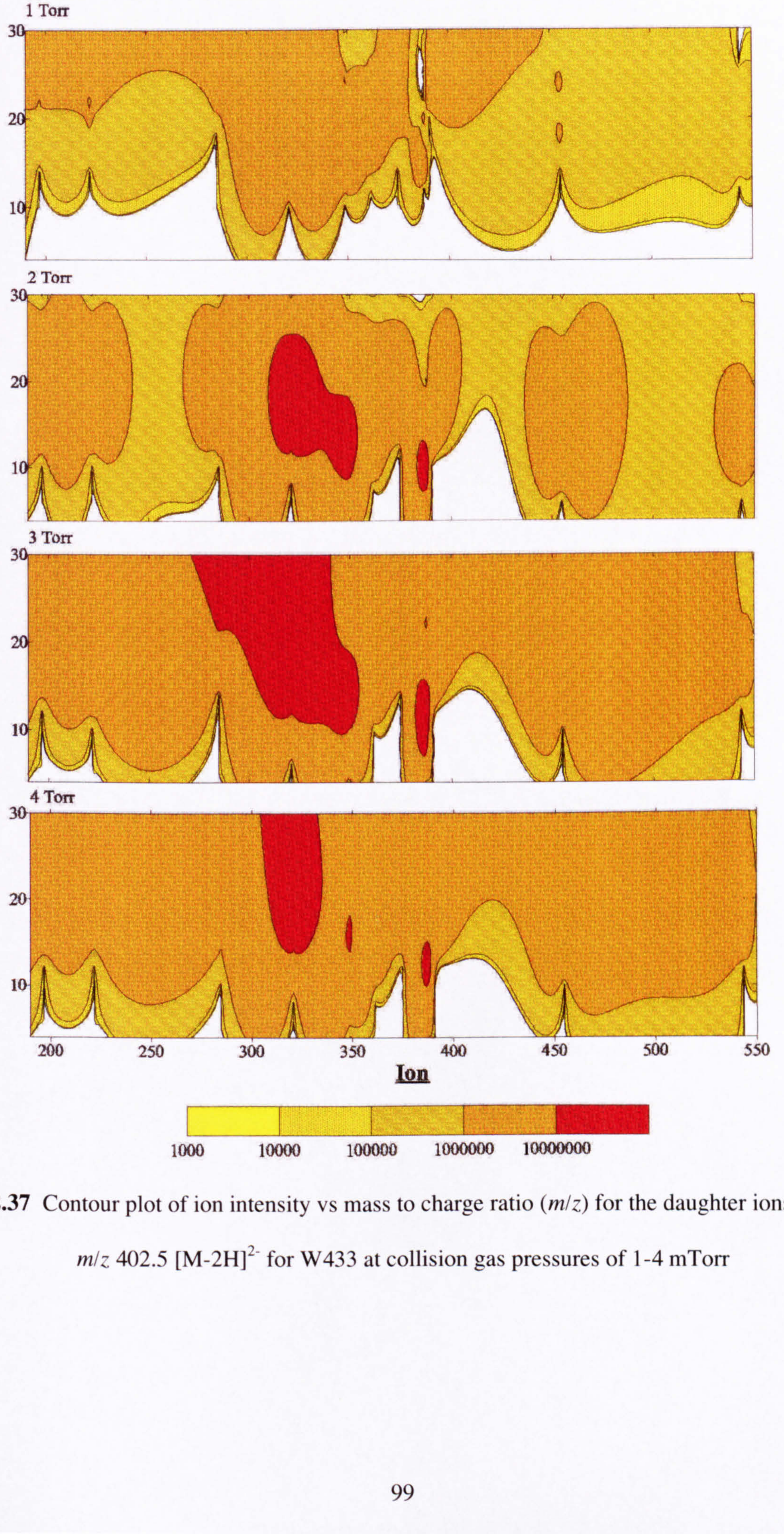

2.37 Contour plot of ion intensity vs mass to charge ratio (m/z) for the daughter ions of m/z 402.5 $[M-2H]^{2-}$ for W433 at collision gas pressures of 1-4 mTorr

2.7.2.3 Summary

Under LC-ESI-MSMS conditions increasing collision energy and or collision gas pressure increased the degree of dissociation (fragmentation) of parent ions of the dyestuffs under study. From the fragmentation patterns observed, 1 mTorr collision gas pressure is too low to provide abundant fragment ions for large molecules such as reactive dyes. Conversely, high gas pressures such as 4 mTorr have a tendency to produce too many collisions, reducing the overall transmission of ions leading in some cases to poor signal response. The collision energy (COFF) required to induce fragmentation was dependent on charge state. Energies of 30 - 40 eV were required for singly charged parent ions compared to about 20 eV for doubly charged ions. Also, MS-MS spectra were influenced by the collision energy, as observed for daughters of *m/z* 731, where additional fragment ions were observed with increasing collision energy. This did not appear to be the case with doubly charged ions. However, this phenomenon highlighted the need for use of a range of collision energies when attempting to obtain structural information from the MSMS analysis of unknowns.

Based on these observations it would be imprudent to select one collision gas pressure and one collision energy to analyse unknown dye degradation products. Instead, the detailed optimisation studies above suggest choice of a collision gas pressure in the upper part of a range from 2 - 3 mTorr with collision energies of 30 - 45 eV for singly charged ions and 15 - 25 eV for doubly charged ions are appropriate.

2.7.2.4 Interpretation of MSMS Spectra

W435 (Reactive Blue H4R)

Daughter ion spectra derived from singly charged parent ion *m/z* 731.

Figure 2.38 shows the daughter ion mass spectrum derived from the collision induced dissociation (CID) of parent ion *m/z* 731, the singly charged molecular ion of W435 (I).

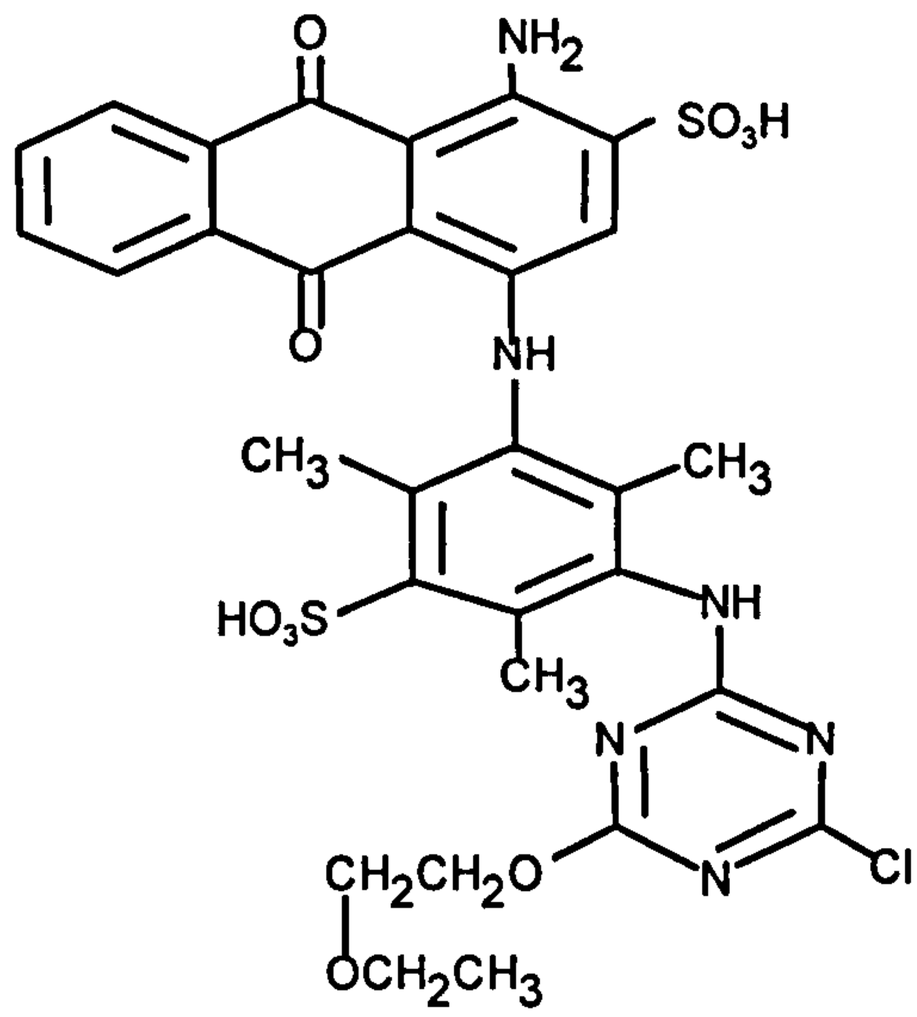

(I)

The first and most significant observation from this spectrum is the lack of low mass fragment ions (not shown in Figure 3.38 for clarity of high mass ions). Many of the more intense ions are associated with losses of neutral molecules from the ethoxy side chain and/or loss of HCl from the triazine ring.

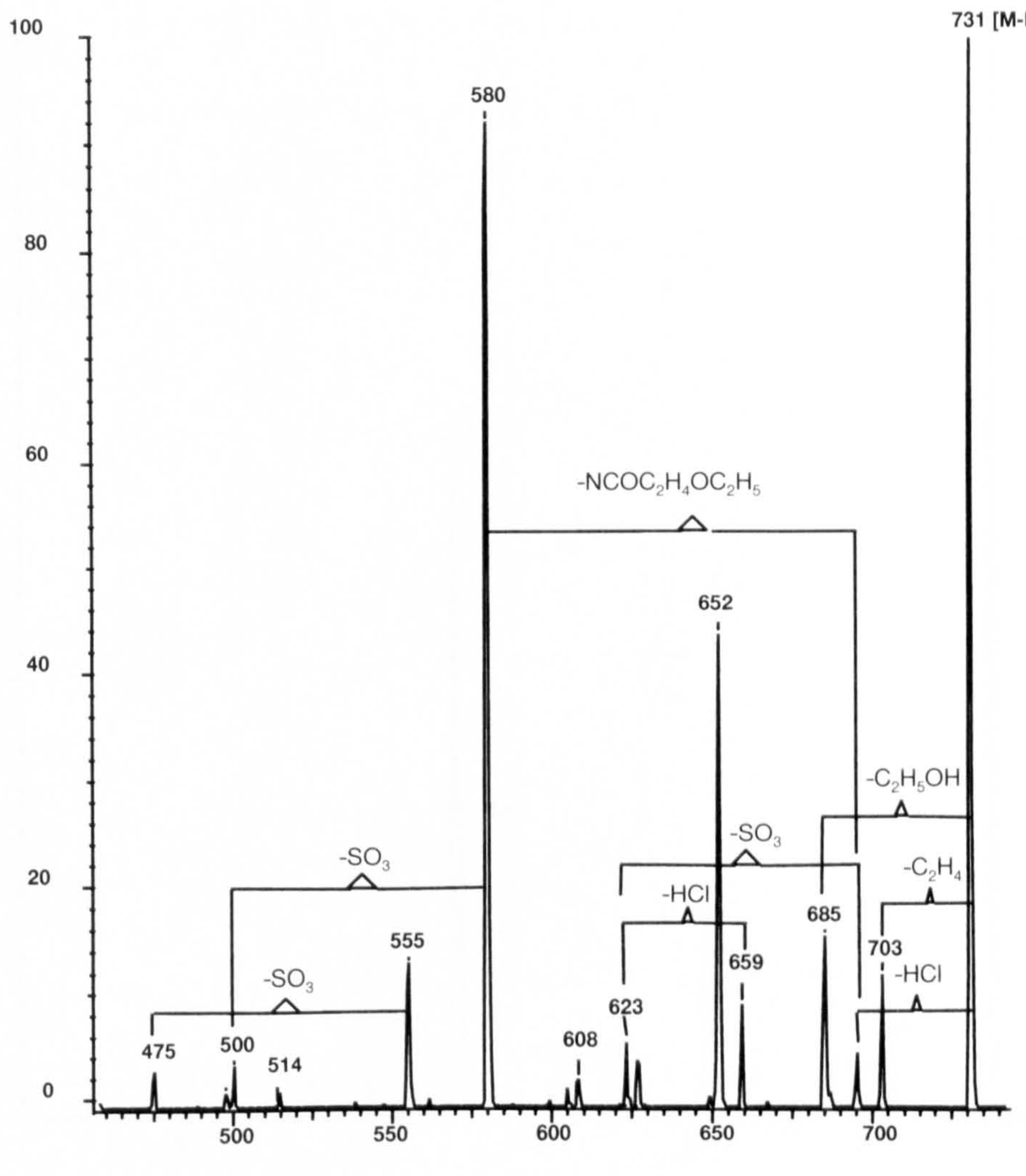

Figure 2.38. Daughter ion mass spectrum derived from *m/z* 731, $[M-H]^-$ for W435

When proposing structures for such fragmentation, it was useful to determine which fragment ions were chlorine-containing. This was achieved by examining the daughter ion spectrum of *m/z* 733 shown in Figure 2.39. This ion contains an A+2 isotope contribution from ^{37}Cl (32.5% of ^{35}Cl) and a second contribution from ^{35}Cl together with ^{34}S (8.4%), ^{16}O (2%) and a contribution from the 30 carbon atoms in W435 (5.4%). The ratio of ^{37}Cl to the contribution made by isotopes of the other elements was calculated to be approximately 2:1.

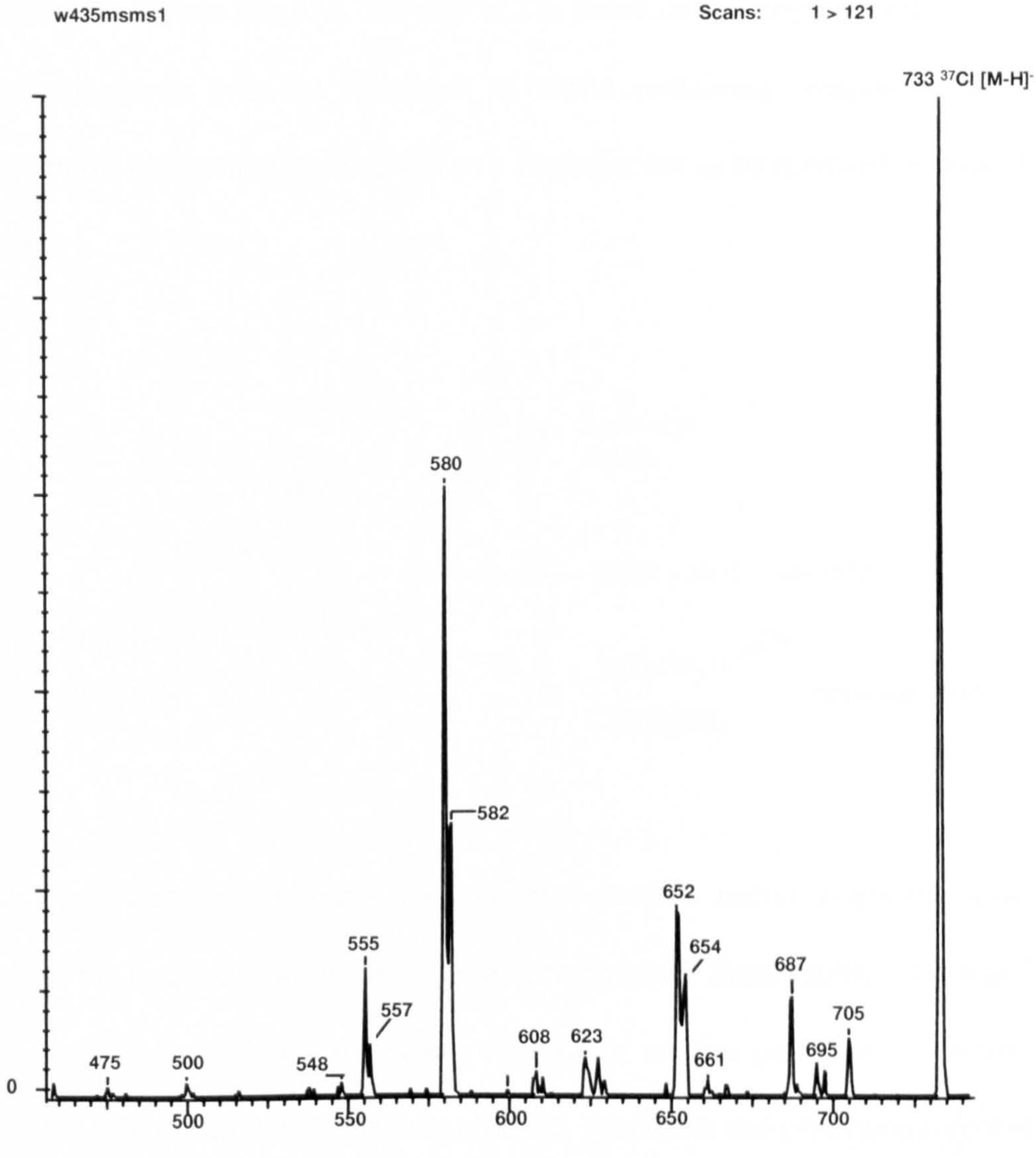

Figure 2.39 Daughter ion mass spectrum derived from *m/z* 733, $[M-H]^-$ for W435 (^{37}Cl)

A comparison of spectra derived from *m/z* 731 and 733, showed which fragment ions contained chlorine. Daughter ions of *m/z* 733 which contain chlorine were shown as a single peak two mass units higher than the equivalent ion derived from *m/z* 731, due to the presence of ^{37}Cl. Daughter ions which **did not** contain chlorine were seen as a doublet: loss of ^{37}Cl to give an ion of the same mass observed for *m/z* 731 and a peak 2 mass units higher due to loss of ^{35}Cl from the A+2 ion still containing ^{34}S ^{16}O isotopes and a contribution from carbon. The ratio of the two peaks was approximately 2:1. Clearly *m/z* 705, 687 and 661 contain chlorine, whereas *m/z* 695, 652, 580 and 555 do not.

The assignment of ions *m/z* 555, 580 and 652 is based on the ring opening of the reactive chlorotriazine group with the formation of nitrile containing compounds which could either retain the charge and be observed as a fragment ion or be removed by loss of neutral molecules:

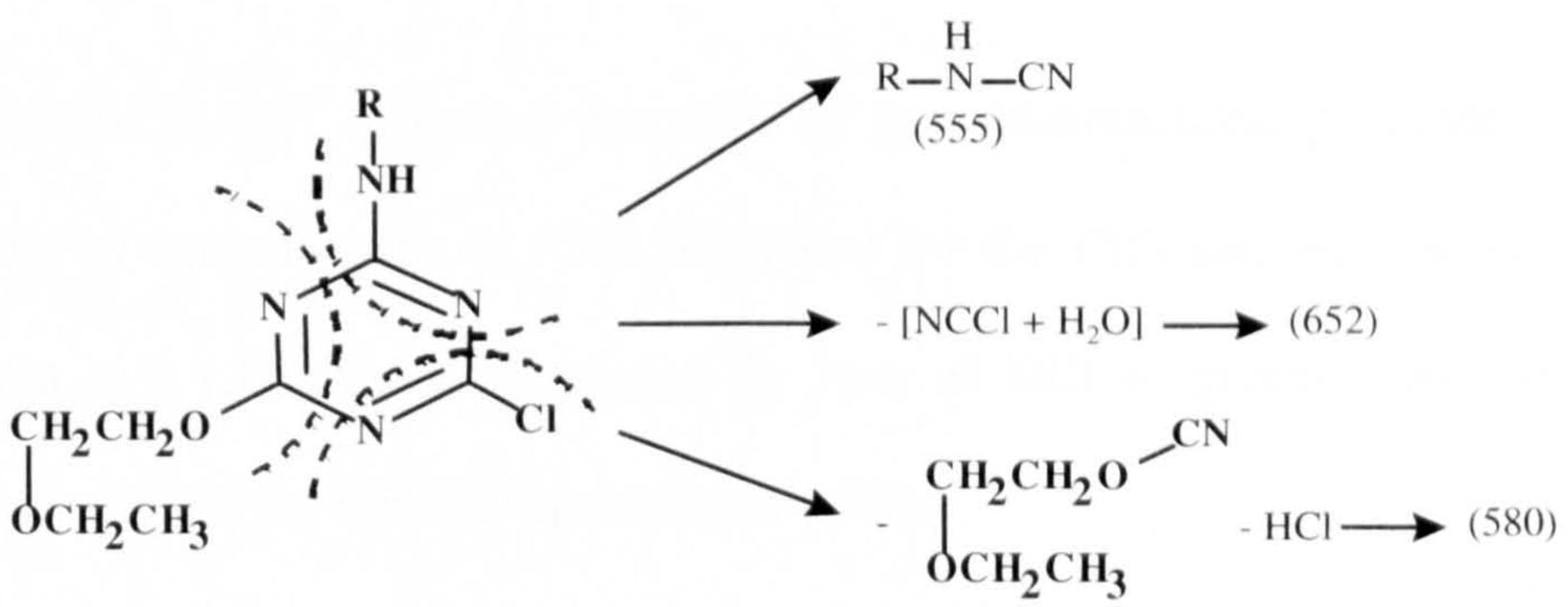

Fragment ions and neutral losses such as these provide useful diagnostic ions for the presence of the reactive chlorotriazine group. Support for these assignments was found in reported positive ionisation thermospray analysis of triazine pesticides (Voyksner *et al.*, 1987b). The chlorotriazines: cyprazine, atrazine, cyanazine and procyazine were shown to exhibit a characteristic ring opening reaction with the neutral loss of:

Where R= an alkyl side chain.

The fragmentation for atrazine for instance, is as follows:

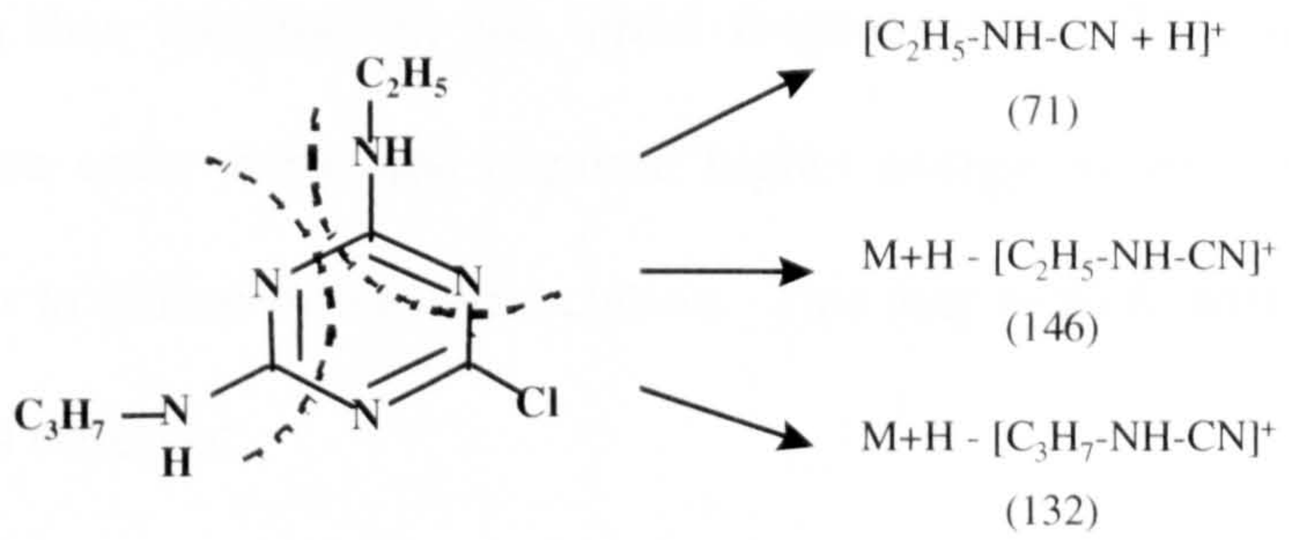

The ion $[RNH\text{-}CN+H]^+$, observed for each of the chlorotriazine pesticides (Voyksner, *et al.*, 1987b) is equivalent to *m/z* 555 described for the CID spectrum of *m/z* 731. The fragment ion *m/z* 132 was accompanied by loss of HCl to produce *m/z* 96, which is equivalent to *m/z* 580 for the CID spectrum *m/z* 731.

Voyksner *et al.*, (1987b) suggested the ring opening process to be 'diagnostic' for chlorotriazines. This fragmentation pathway could be used to provide useful structural information for the identification of unknowns observed in subsequent degradation studies. Interestingly, this ring opening reaction was not observed for triazine pesticides which did not contain chlorine. This has implications for degradation studies of reactive dyes where hydrolysis (replacement of reactive chlorine by an hydroxyl) may be observed.

The ion *m/z* 652 was difficult to explain. It does not contain chlorine (as shown by the daughter ion spectrum of *m/z* 733) and the elimination of NC-Cl would be predicted from the ring opening reaction previously discussed. However the associated loss of water could not be explained in terms of a simple elimination.

Returning to the proposed structures for fragment ions of *m/z* 731, Figure 2.38, several fragment ions showed a further dissociation to loose 80 mass units due to SO_3. These included 703 → 623, 580 → 500 and 555 → 475. It was noticeable from the collision offset optimisation for *m/z* 731 (Fig 2.30) that each of these transitions occurred at higher

collision energies than required for the initial fragmentation. This suggests the initial fragment ions were quite stable and required higher energy to overcome the activation energy (E_a) barrier to induce further dissociation. This may explain why so little low mass fragmentation was observed.

Daughter ion spectrum of *m/z* 365 the doubly charged molecular ion of W435

The fragmentation pattern observed for *m/z* 365 is shown in Figure 2.40. These ions were effectively the same or equivalent to those described for the singly charged parent ion, *m/z* 731 and did not provide additional structural information.

The CID spectra of multiply charged ions can produce fragment ions of higher mass as well as at a lower mass than the parent ion. For doubly charged parent ions, higher mass ions can be formed by loss of one of the charges. This can occur in two ways. One of the charge carrying groups (eg SO_3^-) can be lost. This is frequently observed as *m/z* 80 in the spectra of sulphonated compounds. Alternatively, one of the charge-carrying groups can be neutralised by collision with another dye molecule or with the collision gas. Several of the fragment ions formed by dissociation of *m/z* 365 the doubly charged parent ion of W435, (ie *m/z* 695, 580 and 652) showed this neutralisation reaction.

Molecules containing sulphonic acid groups often produce an ion *m/z* 80 under CID experiments in negative ionisation mode, due to SO_3^-, (Lee *et al.*, 1989; Bruins *et al.*, 1986; Straub *et al.*, 1992). Ions formed by such a loss were not prominent in the daughter ion spectra of either of the W435 molecular ions selected for these experiments.

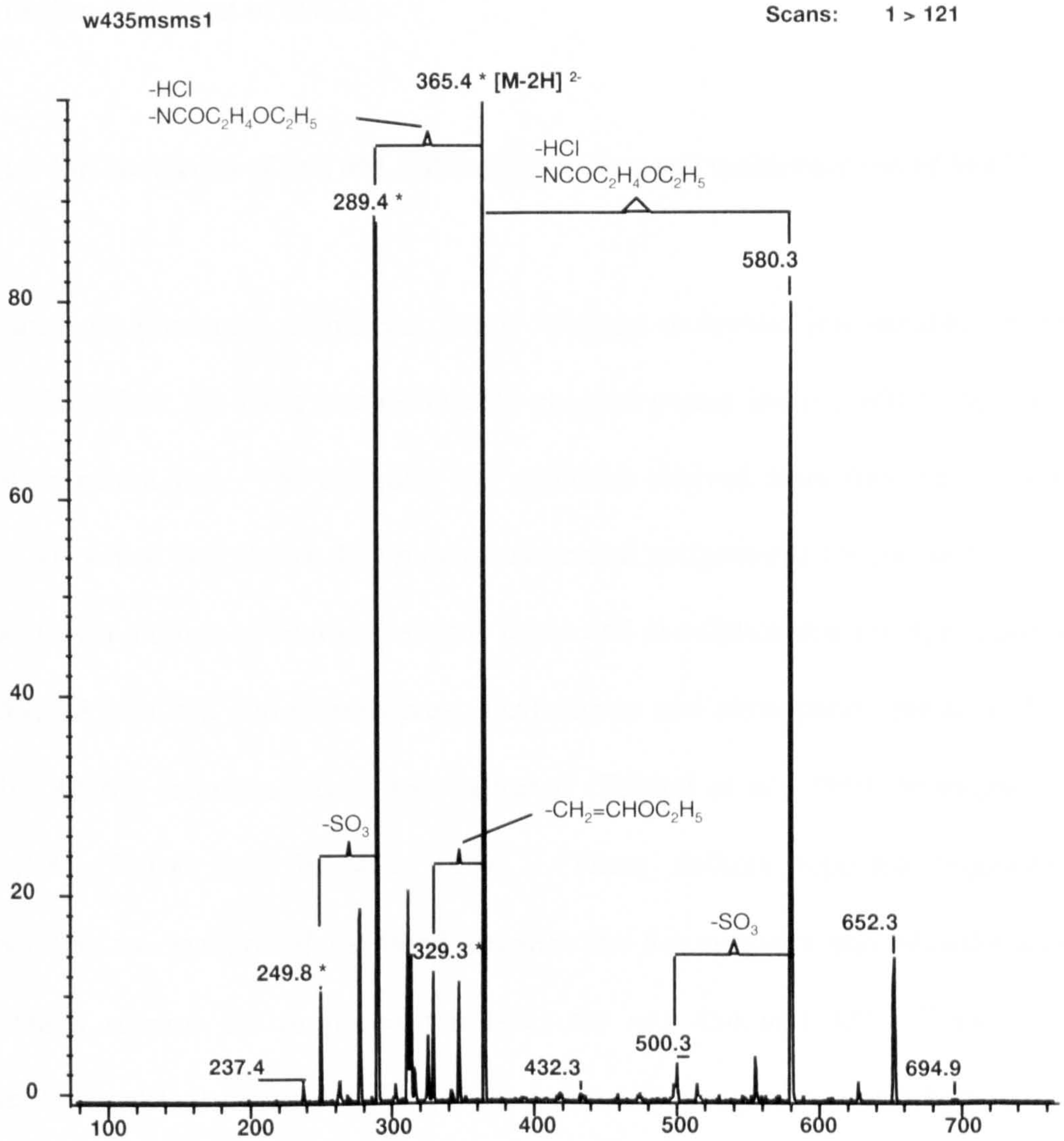

Figure 2.40 Daughter ion mass spectrum derived from *m/z* 365, $[M-2H]^{2-}$ for W435

Daughter ion spectrum of W433

Daughter ion spectrum of *m/z* 401.5 the doubly charged molecular ion of W433

W433 does not produce a significant singly charged molecular ion suitable for MSMS studies. Therefore, the more intense doubly charged parent ion *m/z* 401.5 $[M-2H]^{2-}$ was selected as parent ion. The daughter ion spectrum derived from this ion is shown in Figure 2.41, which also shows the proposed structural assignments for fragment ions. The CID spectra for a range of relatively simple mono and di-sulphonated azo dyes analysed by CZE-MS, FAB-LCMS and thermospray, electrospray and atmospheric pressure chemical ionisation LCMS interfaces have been reported (Edlund *et al.*, 1989; Monaghan *et al.*, 1982, 1983; Rafols and Barcelo, 1997). These authors reported fragment ions corresponding to cleavage of the bond between the azo nitrogen and adjacent aromatic rings, which support the proposed structures for *m/z* 454 and 321. These ions are particularly important because they provide information regarding each half of the dye molecule and can be used as diagnostic tools when considering structural changes to the dye in subsequent degradation studies. However another significant assignment, the fission of the azo bond to form either an imine or amine which was reported by several authors, was not observed for W433. Another observation for the reported data was that of a common fragment ion *m/z* 80, which corresponds to SO_3^-, the intensity of which varied considerably in the literature spectra and which appeared to be very much compound dependent. This was not a significant fragment ion in the daughter ion spectra derived from *m/z* 401.5 of W433 although loss of SO_3 from the parent ion was observed (401.5 → 361.5).

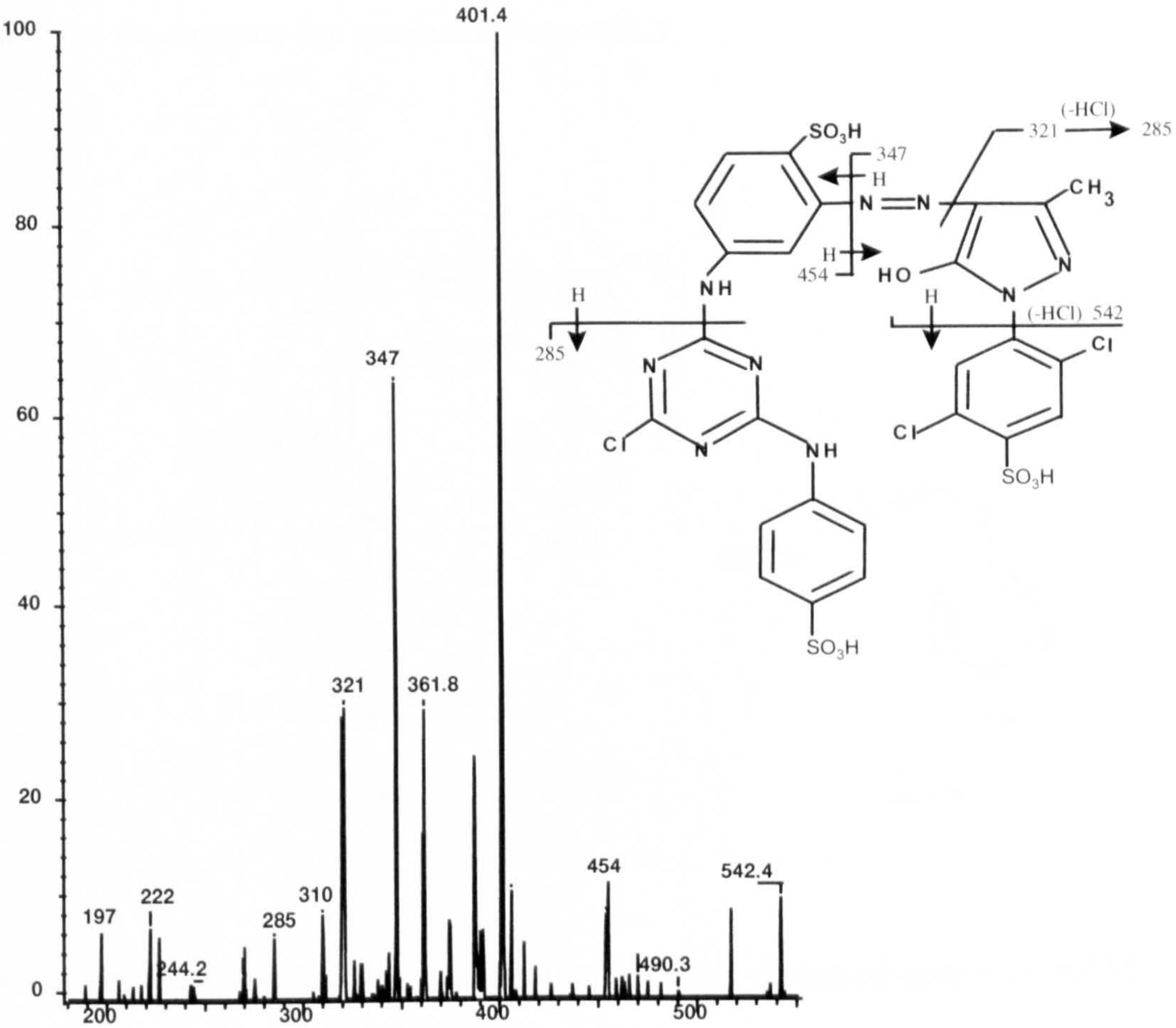

Figure 2.41 Daughter ion mass spectrum derived from *m/z* 401.5, $[M-2H]^{2-}$ for W433

The apparent loss of nitrogen (401.5 → 387.5 and possibly 361.5 → 347.5) in the daughter ion spectrum of W433 is a fragmentation pathway which should be a characteristic of azo compounds. However there was only one reported observation of this fragmentation (Richardson, 1990), suggesting it may not be a common loss. An alternative but less likely explanation is loss of carbon monoxide from the pyrazone ring adjacent to the azo bond, but this was not observed in the previously cited studies of azo-pyrazone dyes. A loss of 28 daltons (assumed to be from the hydroxyl of a naphthol group) was reported for Acid Orange 10 (Straub, 1992).

The previous discussion of the daughter ion fragmentation of W435, highlighted a ring opening of the chlorotriazine group to form three nitrile containing fragments which were

observed as ions or as loss of neutral molecules. This ring opening reaction was again observed in the daughter ion spectrum of *m/z* 401.5:

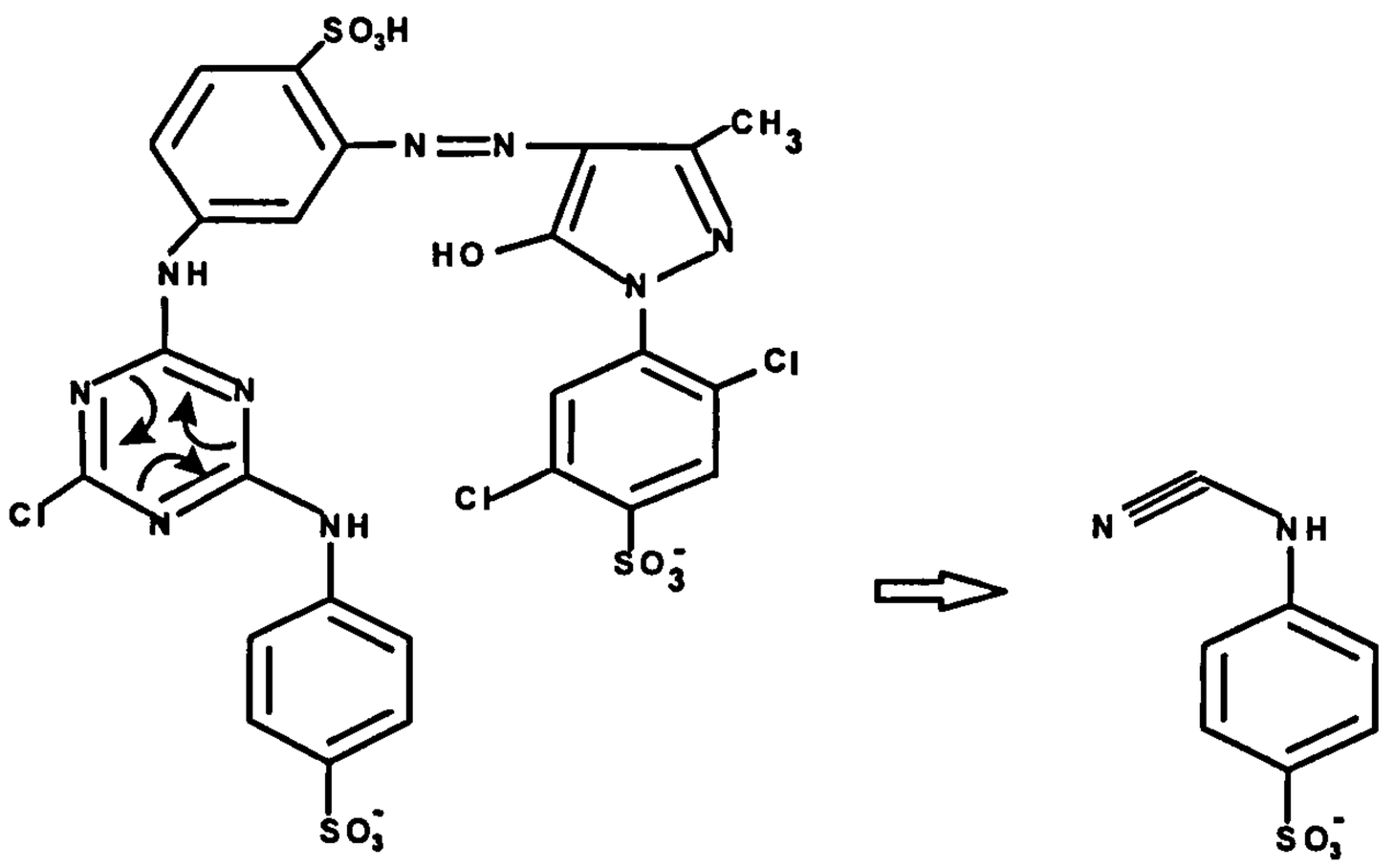

(m/z 401.5) (m/z 197)

This was very similar to the ring opening fragmentation discussed earlier for W435, except that in this case the dissociated nitrile fragment also had a charge-carrying sulphonic acid group, so was observed as a fragment ion (*m/z* 197) instead of a neutral loss. The other possible fragment ions derived from ring opening of the chlorotriazine were not observed, but the presence of at least one of these ring-opening products in a dye that has a very different structure to W435, suggests that this fragmentation may be a very useful indicator of the presence of a chlorotriazine reactive group.

One other fragmentation observed in the reported MSMS spectra of azo pyrazone dyes, was the formation of isocyanate and amine moieties from fission of the pyrazone ring (Monaghan *et al.*, 1984; Rafols and Barcelo, 1997):

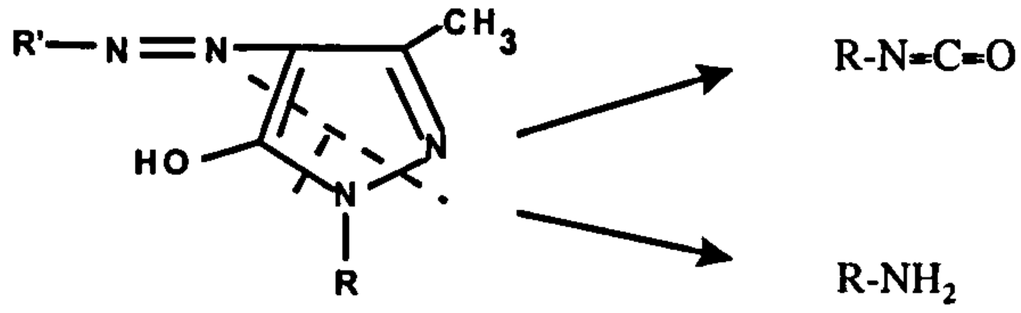

For W433, this would produce ions at *m/z* 266 and 240 for the isocyanate and amine respectively, however these ions were not observed.

Daughter ion spectrum of *m/z* 267 the triply charged molecular ion of W433

Additional useful information was not provided by the daughter ion spectrum derived from *m/z* 267 $[M-3H]^{3-}$. Most of the ions were the same (*m/z* 320 and 285) or equivalent to (226.5≡ 454) those discussed earlier for the doubly charged species. The exception was *m/z* 255 which corresponds to $[M-HCl]^{3-}$.

2.8. CONCLUSIONS

- Optimised conditions have been established for the LC-MS and LC-MSMS analysis of four reactive dyes.
- Conditions have been determined which allow the HPLC separation of the reactive dyes using ammonium acetate as an ion pairing reagent. At low buffer concentration this system is compatible with commonly available mass spectrometer interfaces such as thermospray and electrospray.
- Separation of dyes was achieved on the basis of polarity. The greater the number of sulphonic acid groups on the dye, the earlier they eluted.
- Mass spectrometer signal response increased with increasing organic modifier content in the mobile phase and decreased with increasing buffer concentration.

- The greater the number of sulphonic acid groups on the dye, the greater the number of potential charge states that could be formed and, generally, the less intense were the singly charged molecular ions.
- Reactive dyes could be extracted and concentrated using a similar system to that used for HPLC separation (ie C18 cartridges preconditioned with either tetrabutyl ammonium hydroxide or ammonium acetate).
- Of the two commercially available LCMS interfaces evaluated, electrospray provided the better sensitivity and linearity of response.
- MS-MS produced quite complex spectra, but several fragmentation pathways were seen to provide useful and diagnostic information for dyes containing chlorotriazine reactive groups. Additionally the loss of N_2 from the molecular ion was observed for azo dyes.
- The optimised conditions and mass spectral interpretations provide a sound basis for analysis of dyestuffs in laboratory and field degradation experiments.

CHAPTER 3

PHOTODEGRADATION OF REACTIVE DYES

3.1 INTRODUCTION

Factors which may determine the environmental fate of water soluble dyes in water include biotransformation, photolysis and partitioning onto suspended solids and sediments. Considerable research into the effects of aerobic and anaerobic microbial degradation on the environmental degradation of dyes has been made (Horitzu, 1977; Spadaro, 1992; Carlielli, 1995; Haug, 1991; Junqi, 1992; Chung, 1993). However the photochemical transformation of dyes under environmental conditions has received little attention (Baughman, 1988). One reason for this is that a high degree of photo-stability is a desired property of commercial fabric dyes and so photodegradation has been tacitly assumed to be of little significance. However it is known that temperature, humidity and the presence of oxygen can effect the photo-stability of dyes (Clarke, 1980). Therefore investigations of the effects of sunlight on the fate of reactive dyes, especially considering the extensive use of such materials in sub-tropical climates such as those found in India and South America are justified and indeed possibly overdue.

A study of the photo-stability of azo dyes (Porter, 1973) concluded that the half life for many synthetic azo dyes in sunlight was generally greater than 2000 hours. However the experiments were performed with concentrated solutions whereas test guidelines (EPA 1996), suggest that optically thin solutions (<0.5 absorbance units) are required to obtain meaningful degradation rates.

Haag and Mill (1987) reported studies of the direct and indirect photolysis of a range of azo dyes. The observed half lives varied between 2.6 hours, and 310 hours depending on

dye structure. These studies demonstrate that photodegradation is potentially a major route for transformation for some azo dyes in the environment.

Several studies have investigated the photostability of dyes on materials such as silk and cotton. Massafra *et al.*, (1999) compared the effect of photofading of two azo dyes Acid Red 1 and Acid Orange 8 on silk and in water at different pH values. Photodegradation in water was slow with half lives generally in excess of 100 hours, but appeared to be faster for dyes bound to silk. However no kinetic calculations were available to confirm this observation and no attempt to identify the degradation products was made.

The photostability of a range of azo reactive dyes on cellulose in the dry state, in the presence of water, or artificial perspiration, was studied by Bredereck and Schumacher (1993). They concluded that the rate of degradation was dependent on the nature of substituents adjacent to the azo group of azo dyes. Those containing a strong electron donating function tended to fade 8 - 10 times faster when wet compared to the dry state. The impact of water on fading decreased with increasing electron withdrawing power of the substituents. They concluded that azo dyes with strong electron donating substituents fade by an oxidative mechanism favoured by dissolved oxygen in water, whereas those with strong electron accepting functionality fade by a reductive process favoured by the absence of oxygenated water. Shastri and Ali (1992) also suggested that the light stability of simple anthraquinone dyes could be predicted from the nature of substituent groups in positions 1 - 4 (see Structure XII, Section 1.1). Photostability was increased by the presence of strong electron withdrawing groups.

The photostability of four azo pyridone disperse dyes on polyester fabric and films was investigated (Wang and Wang, 1992). The authors were able to characterise the degradation products by LC-UV and TLC retention time coincidence compared to

reference materials. The identification of aromatic amines led them to conclude that photoreduction was the characteristic degradation pathway for disperse dyes on a polyester substrate.

Aranyosi *et al.*, (1999), carried out a comparison of photodegradation of two sulphonated azo reactive dyes in distilled water and artificial perspiration. As part of this study they used dye standards in distilled water, in distilled water saturated with oxygen before or after light exposure and in distilled water de-aerated by argon purging. Photodegradation in water was rapid and followed first order kinetics. Half lives for the two dyes were determined to lie between 100 and 200 minutes depending on dye and interestingly, on the dissolved oxygen concentration. Distilled water alone and argon-purged water produced similar degradation rates, but the two aerated water samples showed a marked increase in rate of degradation. Conversely, the rate of degradation was decreased by an increase in oxygen concentration for both dyes in the presence of synthetic perspiration. This was assigned to the presence of reducing components, probably lactic acid. The authors concluded that for aqueous dye solutions (in the absence of reducing agents), photodecomposition is oxidative and therefore increased by dissolved oxygen and that a radical oxidation mechanism can be assumed. In the presence of reducing agents (such as lactic or maltic acid), photodegradation proceeds by a radical reduction mechanism and is slowed in the presence of dissolved oxygen.

From these studies it is clear that photodegradation of dyes may depend on the nature of substituents about their chromaphores, on the presence of additives within the test solution and on the dissolved oxygen concentration.

The potential of photodegradation for the treatment of industrial and domestic waste is reflected by an increasing number of publications describing the use of photosensitisers to

aid the degradation process. Pasin and Rickabaugh (1991) determined the effect of acetone on photodegradation of two sulphonated azo dyes, Acid Yellow 6 and Acid Red 40. Both showed 99% colour removal in 20 minutes compared to minimal degradation in 50 minutes in distilled water alone. Colonna *et al.*, (1999) showed the UV enhanced degradation of several acid and disperse dyes in the presence of hydrogen peroxide. However Shu and Huang (1995) found that a combination of UV light and ozone had no discernible effect on dye decolouration for the azo dyes tested. The use of TiO_2 as a photosensitiser has become very popular for effluent treatment. Tang *et al.*, (1997) reported the decolourisation of 11 mono-, di- and tri-azo acid, basic and direct dyes. Colour removal was observed and the mechanism proposed was oxidation involving hydroxyl radicals ($HO^{\cdot}$). Hu and Wang (1999) demonstrated the >90% decolouration of three reactive dyes within 1 hour of treatment. They also showed that decoloured water samples were subsequently more amenable to conventional biodegradation treatment systems and proposed sensitised photodegradation followed by aerobic degradation, as a suitable treatment system for dye waste waters and effluent.

Notably, with the exception of Wang and Wang (1992), studies reported colour removal by change in UV absorbance and there were no attempts to identify photodegradation products to confirm degradation mechanisms in any of the other cited literature.

A number of publications have suggested that humic substances have sensitising effects on photodegradation. Haag and Mill (1987) showed that photodegradation rate increased for a range of azo dyes in the presence of humic substances. Zepp *et al.*, (1985) compared the photosensitising effect of humic substances isolated from different origins and used the transformation of simple organic compounds to probe the mechanism and kinetics of this process. The authors concluded that absorption of sunlight by humic substances can lead to the rapid photosensitised reactions of certain pollutants. Moza (1995) observed an

increase in the rate of photodegradation for the fungicide Bayltin in the presence of both humic and fulvic acids. Contrary to these findings, Fukuda, (1988) and Hwang (1987) found humic substances to inhibit photodegradation of alkylnaphthalenes and chloroanilines, respectively.

The propensity for humic substances to encourage or interfere with photodegradation processes may depend on whether degradation is an oxidative or reductive process and also on the nature of the humic substance used (Aranyosi *et al.*, 1999). Humic substance is a generic term referring to humic acids, fulvic acids and the water insoluble fraction, humin. These terms are derived from their mode of isolation. Humic acids are insoluble in water at low pH (< 2) and can therefore be precipitated from solution and filtered. They form the major extractable component of soil humic substances. Fulvic acids are the fraction of humic substances that are soluble in water under all pH conditions. They remain in solution after removal of humic acid by acidification. Humin is the fraction of humic substances that is not soluble in water.

When considering the photochemical transformations within environmental water bodies it is necessary to first understand the spectral distribution and intensity of sun light impacting on the media. Solar spectral irradiation, transmission through the Earth's atmosphere and transmission of sunlight through the water body, will all have an impact on rates of degradation.

Solar Radiation

As sunlight passes through the Earth's atmosphere, its intensity is diminished or attenuated by scattering from water droplets, atmospheric particles and aerosols, and through absorption by atmospheric gases, in particular ozone. The transmitance of light decreases

with decreasing wavelength (UV and visible region). There is a rapid decrease between 280 and 320 nm such that there is little light transmitted below 300 nm. Low wavelength radiation such as UV-B is highly energetic and is responsible for the photodegradation of many chemicals (Zepp, 1977), which emphasises the need to use a light source that is closely related to natural sunlight when laboratory simulations of photodegradation are made.

The intensity of natural radiation will also vary according to the angular height of the sun such that it decreases from midday to sunset and from summer to winter and to a certain degree from the equator to higher latitudes. The latter has a more marked effect in winter months. Calculations to allow extrapolation from observed photodegradation rates to different seasons and latitudes are described later in this chapter.

The scattering of sunlight by water droplets and air-borne particulates also tend to increase for decreasing wavelengths (UV-B). This scattered light can also contribute to the total amount of light incident on the earth's surface and is termed diffuse light. Light impacting on a water body consists of a mixture of direct and diffuse or scattered radiation.

Transfer from air to water

When sunlight impacts on water surface, part is reflected at an angle equal to the angle of incidence and part passes into the water body and is reflected. The fraction reflected is on average approximately 10% (Leifer, 1988). The intensity of sunlight in water is attenuated by absorption and scattering. In "pure" water, such as oceans and lakes, absorption is primarily due to water itself and light can penetrate to great depths. In inland water bodies the presence of dissolved natural organics such as humic substances, result in light attenuation due to both absorption and scattering. Once again absorption is wavelength

dependent and tends to increase with decreasing wavelength from the visible to the UV region of the spectrum. Therefore, chemicals that only show absorbance in the UV-low visible region will be affected more than dyes which also show strong absorbance at higher wavelengths. The presence of humic materials can lead to increased photodegradation rates. Zepp (1985) concluded that absorption of sunlight by humic materials can lead to rapid, photosensitised reactions and that most polyaromatic chemicals were potentially susceptible. Equally Haag (1987) demonstrated increased rates of photodegradation for 15 azo dyes in the presence of humic material (indirect photolysis) when compared to pure water solutions (direct photolysis). However humic materials are light-absorbing which can slow the photodegradation rates for those compounds which undergo direct photolysis, (Mill, 1981). The attenuation of light due to the effect of scattering is in general less important than attenuation due to absorption in natural water bodies and is only of significance in particularly turbid lake and river waters.

Photodegradation rates in water are therefore dependent on the intensity of the light source, the attenuation by the water body and the absorption characteristics of the pollutant.

3.2 EXPERIMENTAL CONSIDERATIONS

A number of experimental conditions need to be considered for construction of appropriate laboratory-simulated photodegradation studies. It is important that the most appropriate light source and filter system be selected and that quartz glass sample tubes which allow maximum transmission of light at most wavelengths are used. The temperature of the sample vessels needs to be constant if kinetic data are to be obtained and losses of test chemical from the reaction vessels by processes other than photodegradation should be minimised. The loss of sample through volatilisation or biodegradation can be avoided through the use of minimum headspace in the vessel (Literathy, 1989) and use of sterile

conditions (Paalme, 1990), respectively. Losses due to hydrolysis are difficult to avoid but these can be evaluated by using dark controls (ie vessels containing test substances which are not exposed to light). Losses due to hydrolysis can then be corrected for in photodegradation rate calculations.

Light source

Natural sunlight comprises a broad range of wavelengths. However, as discussed earlier, light with wavelengths below 300 nm is largely absorbed by ozone in the upper atmosphere, so for photochemical reactions taking place at the Earth's surface, wavelengths greater than 300 nm are most important. The Grothus-Drapr law (the first law of photochemistry) states that *only light that is absorbed can be effective in producing a chemical transformation.* Therefore only chemicals showing UV-visible absorption in the 300 - 800 nm range can absorb energy and would be expected to be photodegraded. All dyes are designed to absorb light in the visible region. Typical UV-visible spectra for a range of dyes (Figure 2.3, Chapter 2), show that all of those in the present study meet this criterion.

Several light sources have been used previously for photodegradation experiments. These include low, medium and high pressure mercury lamps, fluorescent daylight lamps and xenon arc burners (reviewed by Gould, 1989). Most of these emit light at the low end of the UV-visible region (ie below 300 nm) which although more energetic is not available at the Earth's surface in natural daylight because of absorption by ozone. Artificial light sources therefore have to be filtered to simulate natural light. This is achieved through the use of borosilicate glass filters (EPA guidelines, 1996) or by the use of chemical filters (Leifer, 1988). A schematic representation of the spectra of several light sources and of natural light (Roof, 1982) is shown in Figure 3.1. A direct comparison of the spectrum of

natural daylight (midday, Spring) with that of filtered xenon arc source lamp over relevant UV-visible wavelengths (250 - 800 nm), is shown in Figure 3.2. Xenon lamp show particularly good agreement with natural light up to approximately 550 nm. Thereafter the correlation is somewhat poorer. However the lower wavelength radiation is most energetic and therefore most important and the xenon lamp probably represents the best available simulation of natural daylight for laboratory studies. A comparison of a filtered xenon lamp with natural daylight for aqueous photodegradation studies was reported by Yager (1988), who concluded the xenon lamp provided data comparable to those obtained with natural light. Zepp (1982), reported a comparison of xenon, medium pressure mercury and fluorescent lamps with natural sunlight for the photodegradation of three PAHs and showed that the degradation rates obtained using the xenon lamp were closest to natural sunlight.

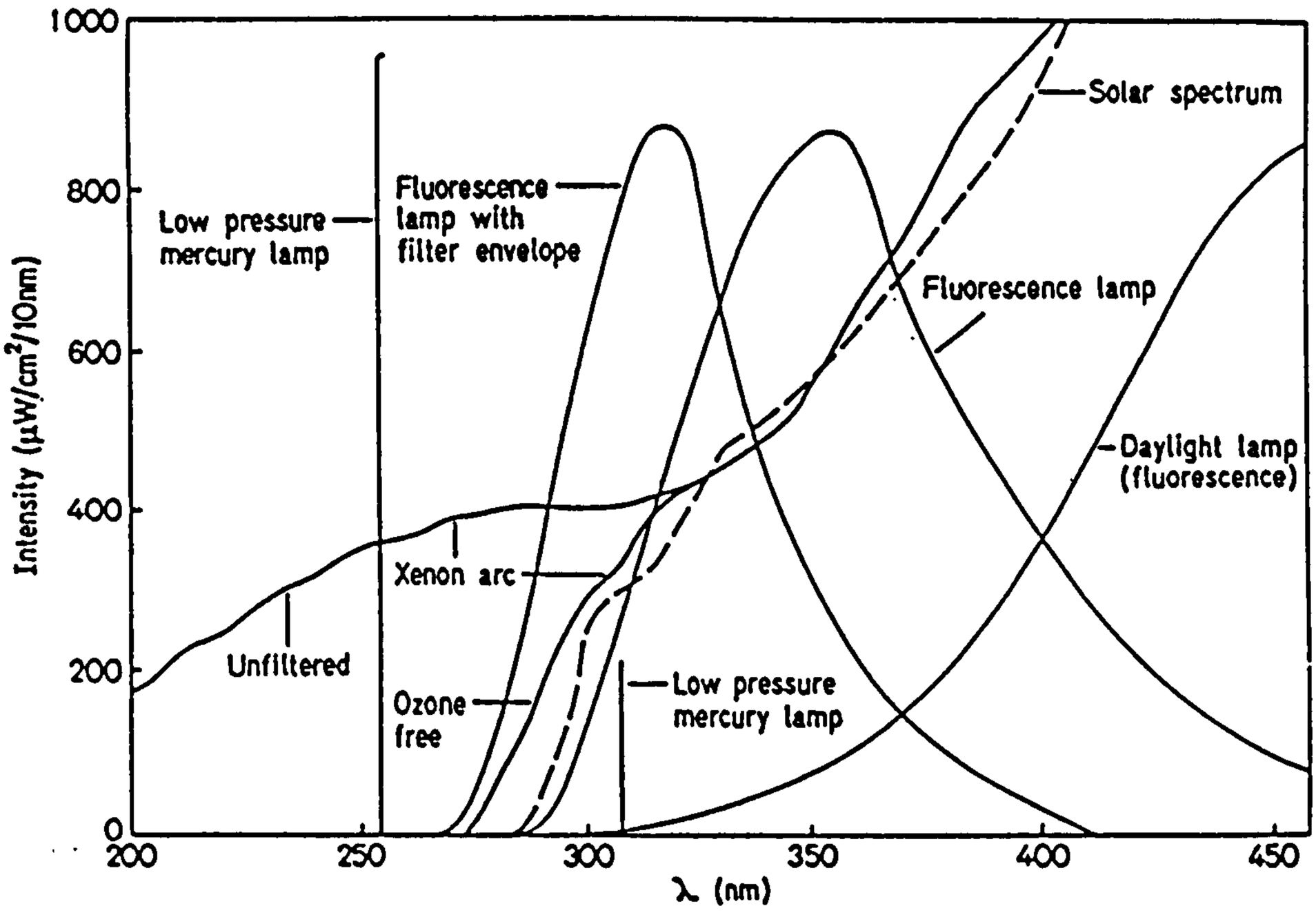

Figure 3.1 Comparison of the spectral intensities of different laboratory light sources with natural daylight

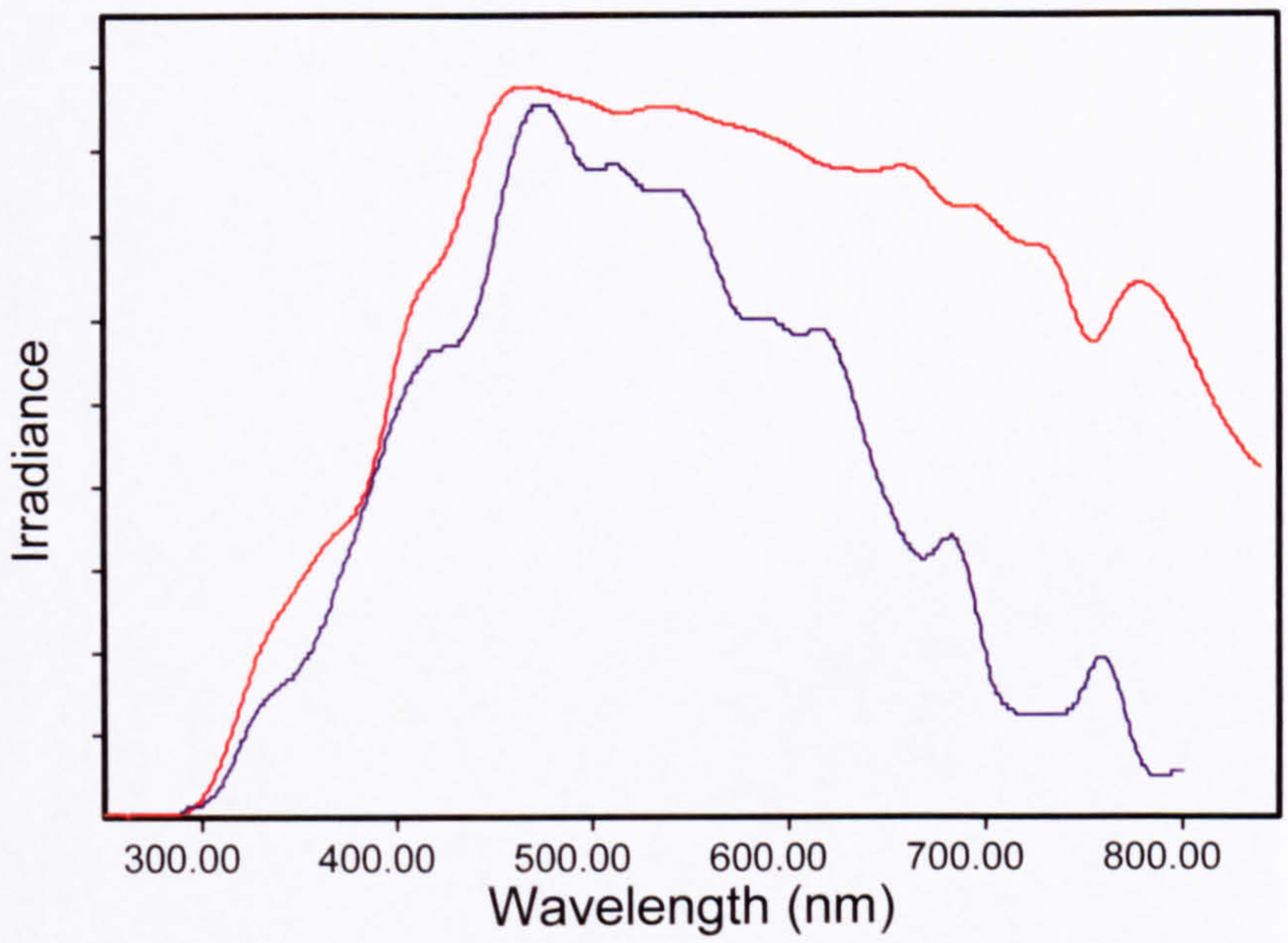

Figure 3.2 Comparison of UV-Visible spectra of a Xenon lamp — with natural daylight (Midday in March) —

Light intensity is one of the most critical factors in laboratory photodegradation studies. Therefore to obtain useful degradation rates and to extrapolate these to environmental conditions, it is particularly important to accurately measure the intensity of the light source. Two approaches are generally used for lamp calibration; chemical actinometers and radiometers. Both have advantages and disadvantages.

Chemical actinometers are photochemical reactions which have been calibrated with light sources of known flux and have well defined quantum yields at particular wavelengths. They are used to measure the integrated light intensity incident on a sample within a test vessel during irradiation with either natural or artificial light.

Chemical actinometers have the advantage that they undergo the same experimental regime as the test sample and can give an accurate measure of light intensity. Their photodegradation properties are well characterised and understood. The main disadvantage of chemical actinometers is that they may not absorb light at the same

wavelength as the chemical under test, particularly as most useful actinometers absorb light in the 290 - 400 nm region (Liefer, 1988).

Radiometers are easier and more convenient to use than chemical actinometers. They give a measure of total light incident on the sample vessels and can easily be used to compare light intensity of lamps with natural daylight for the estimation of environmentally relevant photodegradation rates (Parker and Leahey, 1988). However the equipment is relatively expensive and not particularly portable for use with field studies. Given that laboratory studies were to be made in the present programme, a spectro-radiometer was used in this study to calibrate the lamp source.

Temperature control

The photodegradation rate constant will be affected by temperature as described by the Arrhenius equation. Therefore it is necessary to maintain a constant temperature for experiments in order to obtain reliable kinetic data. Leifer (1988) suggested the sample temperature should be maintained to within 2°C of the chosen experimental temperature.

Other experimental considerations

Since contaminants may absorb light, laboratory photodegradation experiments should be carried out using homogenous solutions of pure test chemical at concentrations at least half the water solubility (EPA, 1996). Since pure dyes were to be used in the present study and since sulphonated reactive dyes are water soluble no solubility problems were expected and difficulties with photosensitisation by co-solvents, Pasin (1991) should be avoided.

The incorporation of dark controls in laboratory experiments is also essential since these show the degree of degradation not caused by irradiation (ie due to chemical hydrolysis or biodegradation in water). In practice this requires a sample tube to be bench-stored wrapped in foil to exclude light, for the duration of photolysis study. An initial evaluation can be used to determine whether hydrolysis makes a significant contribution to degradation over the exposure period of the experiment. If it does not, the dark control only requires confirmatory analysis at the end of the exposure period. For experiments where hydrolysis is an issue, analysis of the dark control for each irradiation time period is required and the measured concentration of sample chemical corrected to reflect photodegradation only.

3. 3 EXPERIMENTAL

Two dyes, Reactive yellow P5G (W433) and Reactive Blue H4R (W435) were supplied by ICI Colours Ltd, Blackley, Manchester UK. Aldrich Humic acid was obtained from Aldrich Chemical co. Milwaukee, USA. The humic materials used in this study were isolated from UK and Irish river waters using filtration, adsorption chromatography (XAD-8 and XAD-4 resin) and ion chromatography to purify and fractionate samples into humic, fulvic and hydrophilic acids. Humic substances are the major components of the organic surface coating on particles found in water. The structures of these substances are unknown, and they tend to be characterised by their elemental composition and aromatic content. The humics used in this study have been characterised previously in terms of carbon, nitrogen and oxygen content and degree of aromaticity (Zhou and Rowland, 1994). River Dodder, Dublin (Eire) and River Trent (UK) humic, fulvic and hydrophilic acids were provided by Dr M Hayes (University of Birmingham).

The Suntest CPS xenon lamp was manufactured by Heraeus instruments GmbH, Germany. The water cooled stainless steel sample vessel holder was manufactured and supplied by the engineering department of Zeneca Agrochemicals, Jealott's Hill, Bracknell, UK.

3.3.1 Exposure apparatus

A schematic diagram of the xenon lamp/filter system and the laboratory arrangement for suntest photolysis unit, water cooled sample tube holder and chiller unit, respectively are shown in Figures 3.3 and 3.4. Radiation from the xenon arc lamp or reflected from the UV mirror above the lamp, passes through a quartz glass filter which has a UV cut-off at approximately 290 nm. The parabolic reflector ensures even distribution of the filtered UV-Visible light over the whole sample tank.

Samples were placed in up to six 25 × 2 cm (od) quartz tubes, each with a sample volume of 50 ml. Samples were placed in the stainless steel tank (Parker and Leahey, 1988), partially filled with glycerol as coolant. Initially water was used as coolant but this tended to evaporate on prolonged irradiation and therefore offered inadequate temperature control. Samples were therefore maintained at constant temperature by circulating dilute ethylene glycol from the chiller unit through a reservoir at the bottom of the tank. A thermocouple attached to a digital thermometer was used to monitor the sample temperature at the centre of the tank at mid depth. The sample tank was held in position at the bottom of the Suntest unit, such that it made a light tight seal, using a lab jack.

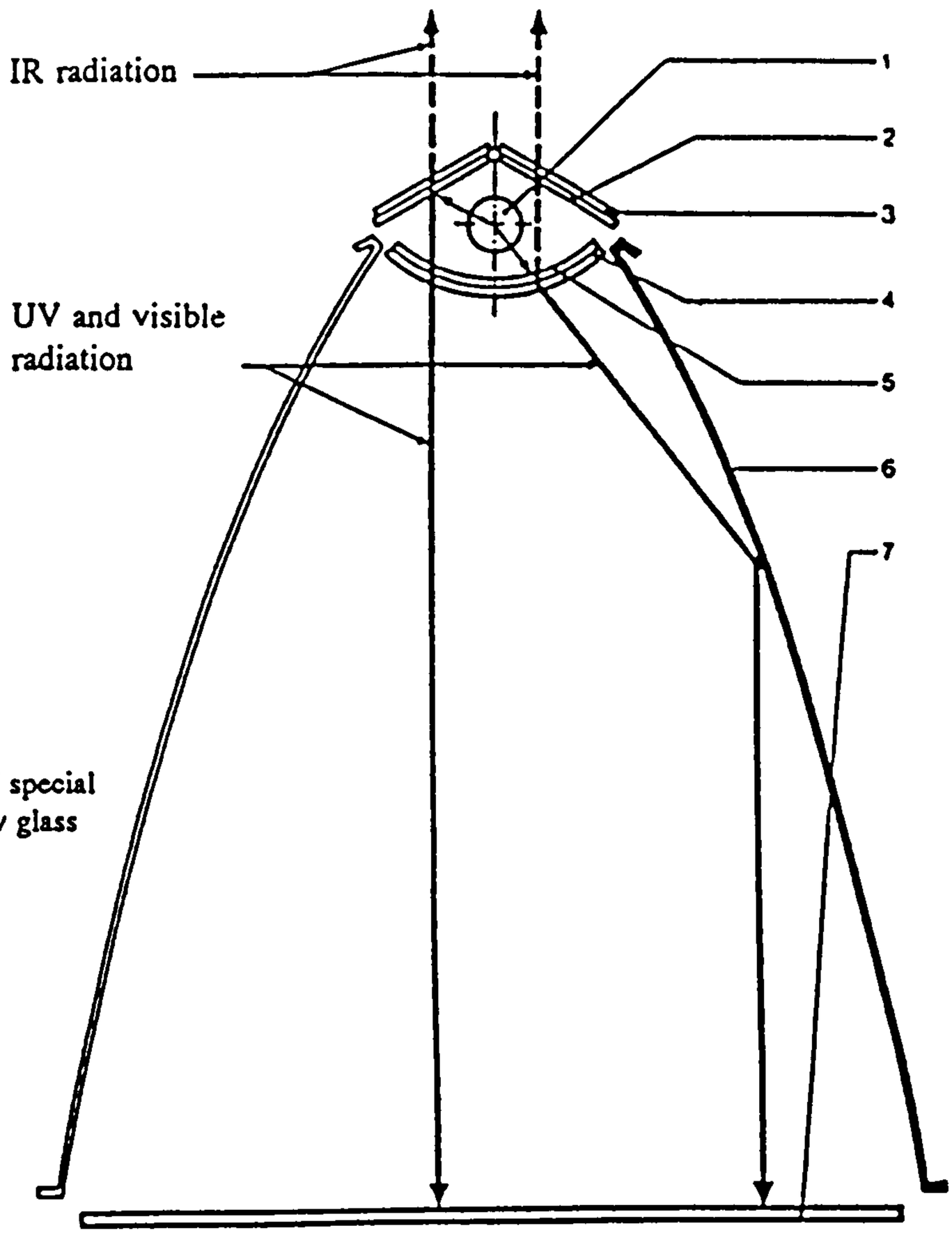

1 Xenon burner
2 UV mirror
3 Visible light mirror
4 Quartz-glass dish with reflecting coating
5 Additional filter in UV special glass or special window glass
6 Parabolic reflector
7 Sample level

Figure 3.3 Schematic diagram for the Xenon lamp/filter system

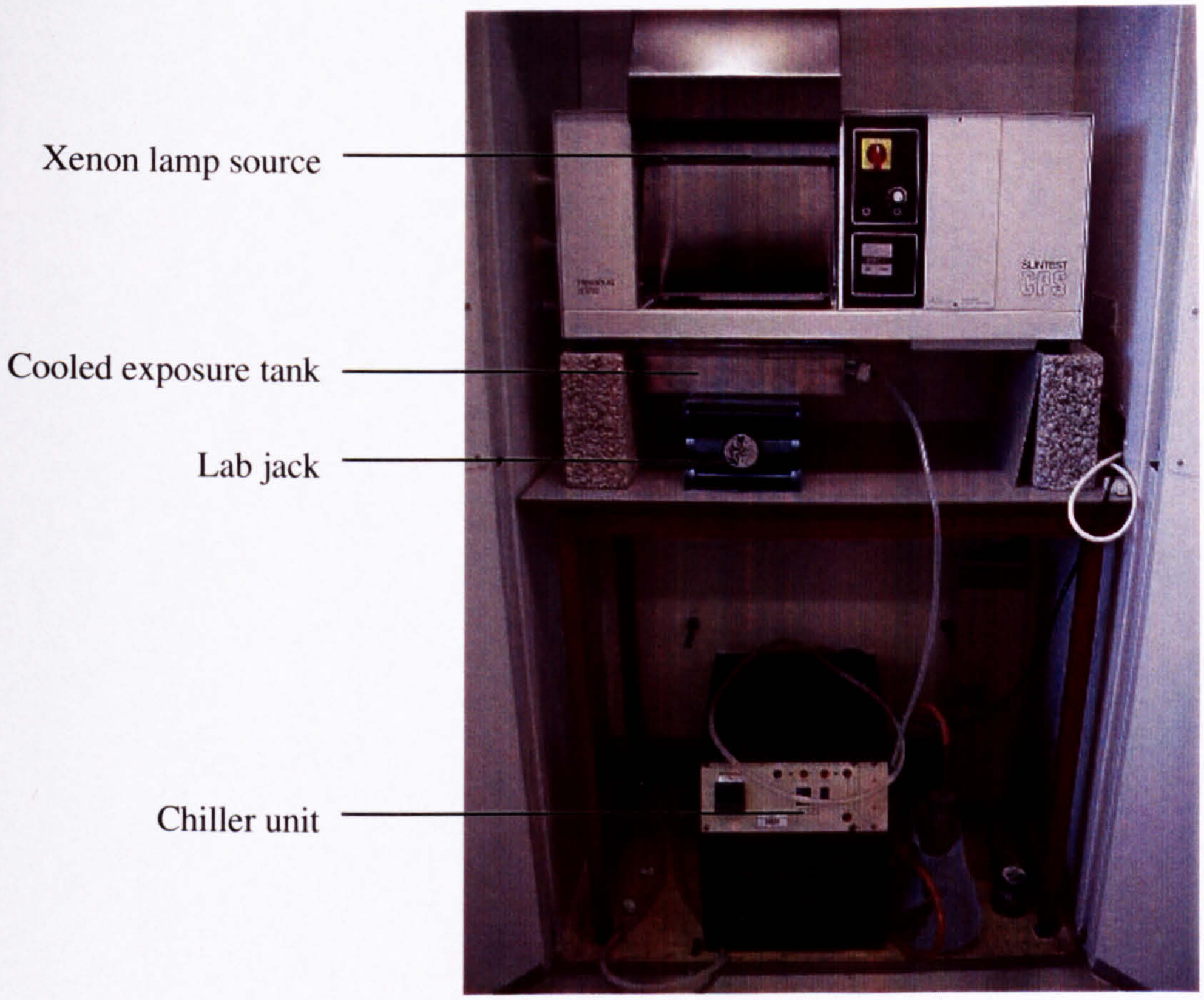

Figure 3.4 Experimental set-up for photolysis studies

The xenon lamp and cooling system for the stainless steel tank were operated for 1 hour prior to the start of photolysis experiments to allow both to equilibrate. The variation of radiation intensity at different parts of the sample tank has been evaluated previously (Ali, 1996). Less than 2% variation over 7 different points within the tank was found, indicating consistent incident light on each sample vessel.

Initial experiments were carried out at the University of Plymouth, with subsequent experiments at Brixham Environmental Laboratory. The photolysis equipment used at each site was effectively the same, but the xenon lamp intensity differed due to the age of each lamp. The radiation intensity of the Plymouth and Brixham systems were measured by radiometry (Ali, 1994) as 7.6 mE cm^{-2} day^{-1} and 14.1 mE cm^{-2} day^{-1} respectively.

Each photodegradation experiment used essentially the same apparatus and conditions, but differed by exposure time, temperature and substances added to the dye solutions, such as humic acids.

3.3.2 Photolysis of reactive dye W433 in the presence and absence of humic substances

Standard solutions of W433 were prepared in distilled water. Aliquots (40 ml) were added to quartz photolysis tubes, spiked with humic substances (1 mg l^{-1}, where appropriate), placed in a bath which was water cooled to a constant temperature and irradiated using the Heraeus Suntest CPS xenon lamp (Table 3.1). Control samples were stored wrapped in foil on the bench. The temperature of the ethylene glycol cooling bath was constantly monitored using a thermocouple linked to a temperature data logger (Ali, 1996).

Table 3.1 Experimental parameters for the photolysis of W433 using an Heraeus Suntest xenon lamp. Humic substances were present at 1 mg l^{-1} total.

Experiment	Dye concentration (mg l^{-1})	Sampling times (h)	Additives	Temp. (°C)
1	8	0.5, 1, 2, 4, 8, 12 and 18 [a] 1, 2, 4, 6, 8, 15 and 24[b]	None River Trent humic acid	26 +/- 3
2.	11	4, 8, 12, 18, 24 and 48 [a]	None	23 +/- 2
		4, 8, 12, 18, 28 and 40	River Dodder humic acid	22 +/- 2
		4, 8, 12, 18, 28, 40 and 70	River Dodder fulvic and hydrophilic acids	22 +/- 2
		6, 12, 18, 28 and 40	Aldrich humic acid	23 +/- 2

(a) Duplicate test vessels for each sampling time

(b) Sample concentrated ten-fold prior to LC-MS analysis (as per Section 2.3).

After irradiation, each sample was transferred to a volumetric flask, made up to 50 ml, covered with foil and stored refrigerated until required. Aliquots (1 ml) of each photolysed dye, the corresponding dark stored control and calibration standards (0.2 to 10 mg l^{-1}) were spiked with

internal standard (naphthalene sulphonic acid, 10 µl equivalent to 10 mg l^{-1}), and analysed by LC-$UV_{254\,nm}$ and LC-MS using the conditions described in Section 2.1.

3.3.3 Photolysis of reactive dye W435

Standard solutions of W435 were prepared in distilled water. Aliquots (40 ml) were added to quartz photolysis tubes and irradiated using the Heraeus Suntest CPS xenon lamp, using the method described in Section 3.1. Experimental variables are shown in Table 3.2.

Table 3.2 Experimental parameters for the photolysis of W435 using the Heraeus Suntest xenon lamp.

Experiment	Dye concentration (mg l^{-1})	Sampling times (h)	Additives	Temp. (°C)
1	10	0.5, 1, 2, 4[a], 8, 12 and 18 [b]	None	28 +/- 3
2	10	2, 4, 8, 12, 18, 24 and 40 [b]	None	28 +/- 3

(a) Sample concentrated ten-fold for LC-MS analysis (as per Section 2.3).

(b) Duplicate test vessels for each sampling time

3.4 RESULTS

Preliminary experiments with dyes W428, W430, W433 and W435 established that only W433 and W435 were photolabile following 8 hours irradiation. W430 did not photodegrade over the photolysis period. W428 degraded on storage in the dark to three major products (described in Section 2.4), plus the unchanged dye, therefore a thorough investigation of the effects of photolysis could not be made. The photolysed solution of W428 showed only two major components, one of which had a different retention time to all of the degradation products of the control stored standard. Solutions of known

concentration of W433 or W435 and the internal standard were examined by LC-UV_{254} and calibration graphs of response were drawn (Fig 3.5). These were used to determine the concentrations of dyes in various photolysed samples.

Calibration standards were analysed with each photodegradation experiment to accurately determine dye concentration and estimate degradation product concentration in degraded samples. A detector wavelength of 254 nm was chosen rather than a more selective one for the dyes (e.g. λ_{max} 590 nm W435; 400 nm W433), in order that degradation products with different λ_{max} might be detected.

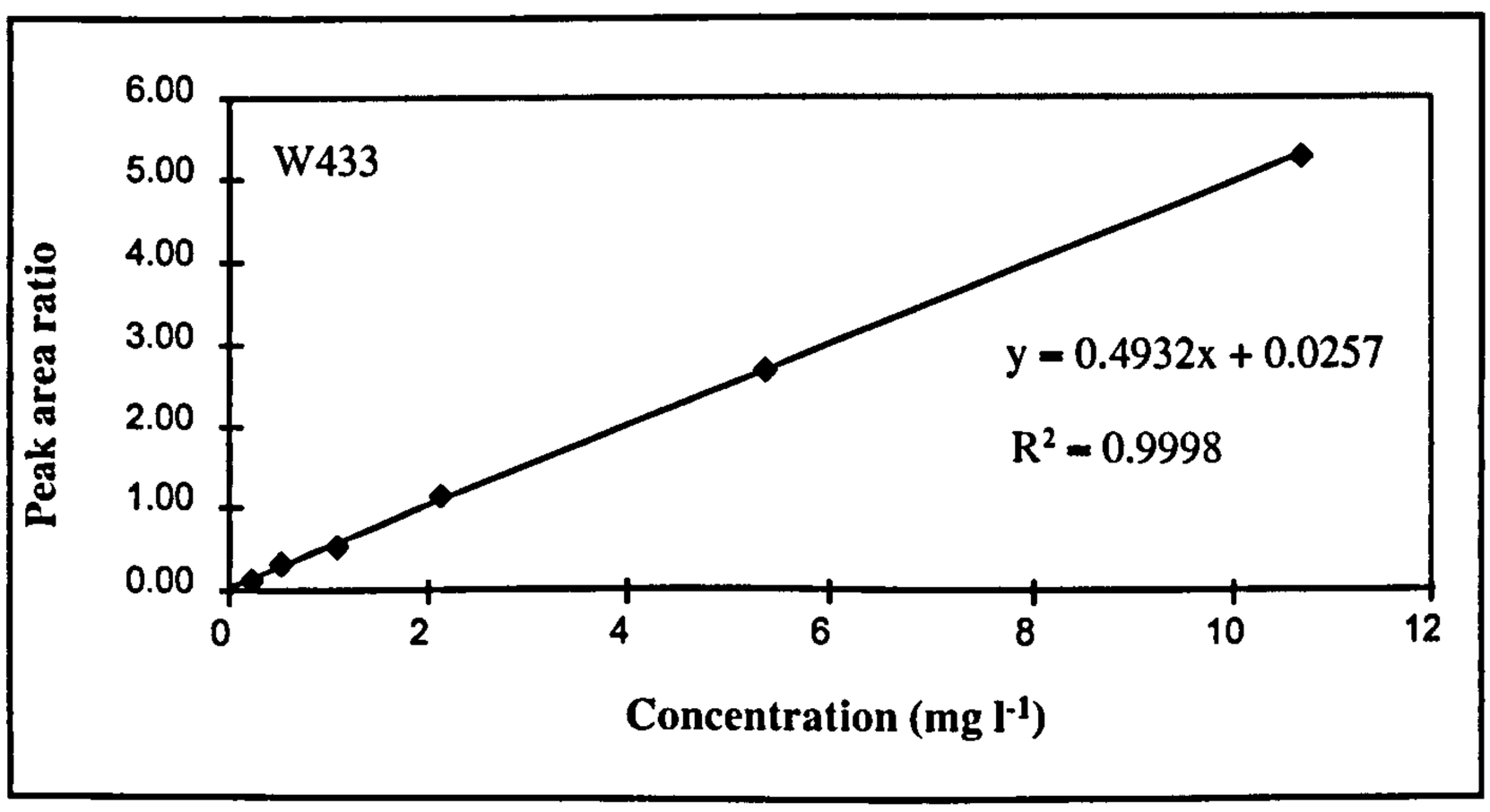

Figure 3.5 HPLC-UV (254 nm) calibration graphs for aqueous solutions of (0.2 to 11 mg l^{-1}) of W433 and W435. Peak area ratio is the ratio of peak areas of the dye to a known concentration of internal standard (naphthalene sulphonic acid).

3.4.1 Photolysis of W433 in the presence and absence of river Trent humic acids.

Degradation and half lives

The concentrations of W433 remaining after irradiation in two different experiments are shown in Table 3.3. River Trent humic acids (1 mg l^{-1}) were added to the W433 solutions in experiment 2. A number of publications have described humic acids as having either sensitising effects (Haag, 1986; Zepp, 1985), or inhibiting effects on photolysis (Fukuda, 1988). River Trent (north east UK) humic acids was chosen because many of the major UK dye processors discharge to rivers in this region. A concentration of humic acids of 1 mg l^{-1} is environmentally realistic for riverine waters (Thurman, 1985).

Table 3.3 Effects of irradiation time on photolysis of W433 in the absence and presence of 1 mg l^{-1} river Trent humic acids.

Time (h)	Experiment 1 (W433)		Experiment 2 (W433 + 1 mg l^{-1} Trent humic acids)	
	Conc. (mg l^{-1})	% of initial	Conc. (mg l^{-1})	% of initial
0.0	8.1	100	7.2	100
0.5	8.0	99	n.d	n.d
1.0	7.9	98	7.0	97
2.0	7.9	98	6.9	96
4.0	7.4	91	6.9	96
6.0	n.d	n.d	6.5	90
8.0	7.0	86	6.1	85
12.0	6.4	79	n.d	n.d
15.0	n.d	n.d	5.0	69
18.0	5.5	68	n.d	n.d
24.0	n.d	n.d	4.4	61

n.d = Not Determined

The dark control for each experiment was analysed at the end of each experiment and found to be equal to the starting concentration in both cases, indicating degradation was

due to photolysis only. The decline in W433 concentrations with increasing irradiation time for both experiments is shown graphically in Figures 3.6a and b. The decreases follow zero order kinetics whereby the photodegradation rate constant (k_p) is independent of concentration:

$$C_t = C_o\, k_p\, t$$

Where C_t is the concentration at time t and C_o is the initial concentration. k_p, determined from the slope of a plot of $[C_t/C_o]$ vs irradiation time t, was -0.0164 and -0.0166 hr^{-1} for experiments without and with humic acids respectively. The half life was determined from the equation of a straight line: $y = mx + C$, where $y = 0.5$ (concentration ratio at half the original concentration). This gave a $t_{1/2}$ value of 30.5 and 30.1 hours for W433 photodegradation in pure water and with river Trent humic acids, respectively. These half lives are essentially the same. Interestingly, this suggests that in the case of W433 river Trent humic acids had no observable effect on the photodegradation process.

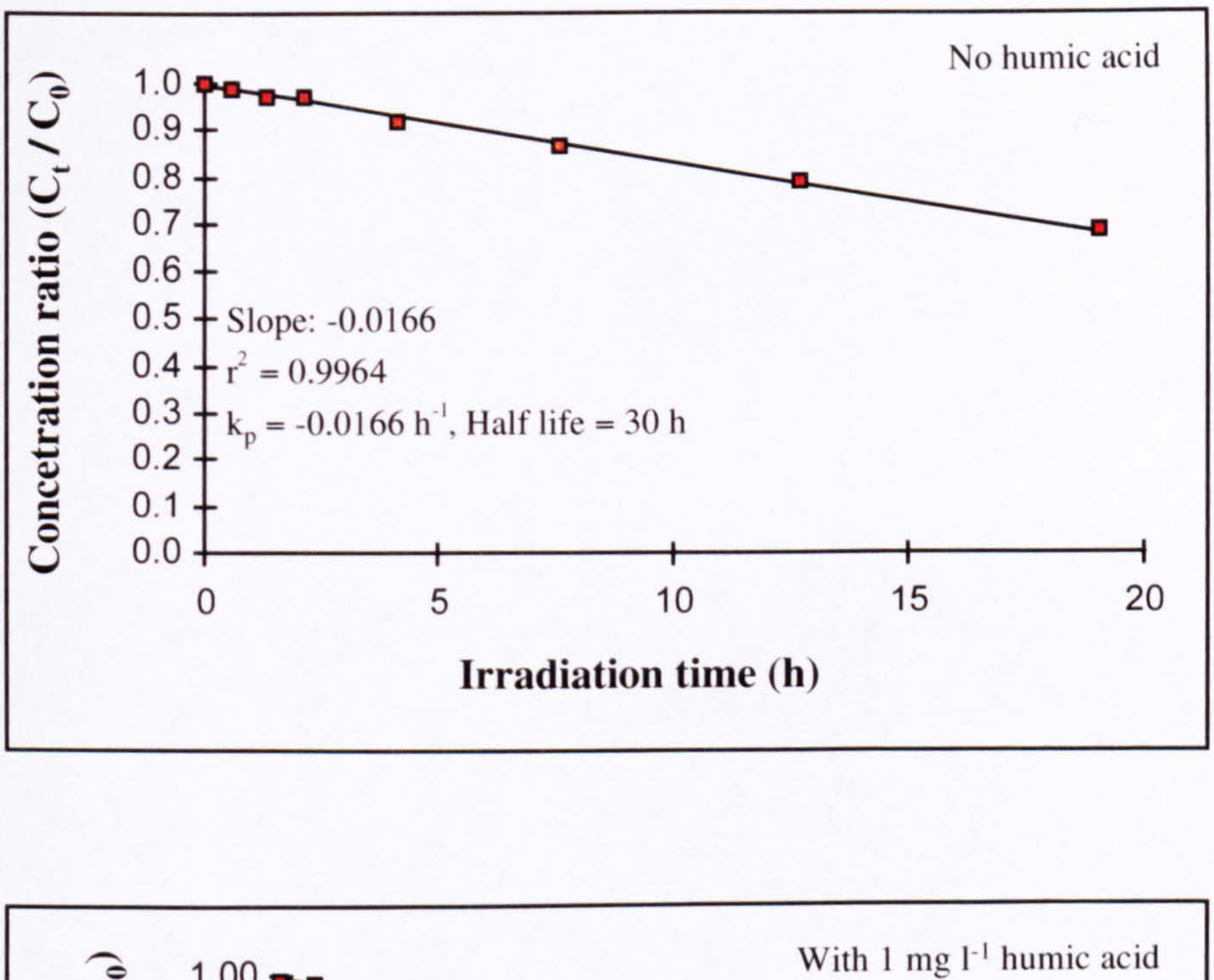

Figure 3.6 Change in concentration with time of dye W433 in pure water and in the presence of river Trent humic acids (1 mg l^{-1}).

Analysis of degradation products

Only one degradation product was observed in the LC-UV chromatograms of irradiated W433 solutions. The concentration of this product was measured by reference to the W433 calibration curve, Figure 3.7 shows the changes of concentration with irradiation time. The sum of the concentrations of unchanged W433 and the degradation product was approximately equal to the initial dye concentration, suggesting that no other degradation

pathways had occurred. A very similar pattern was observed for the dye exposed in the presence of river Trent humic acids.

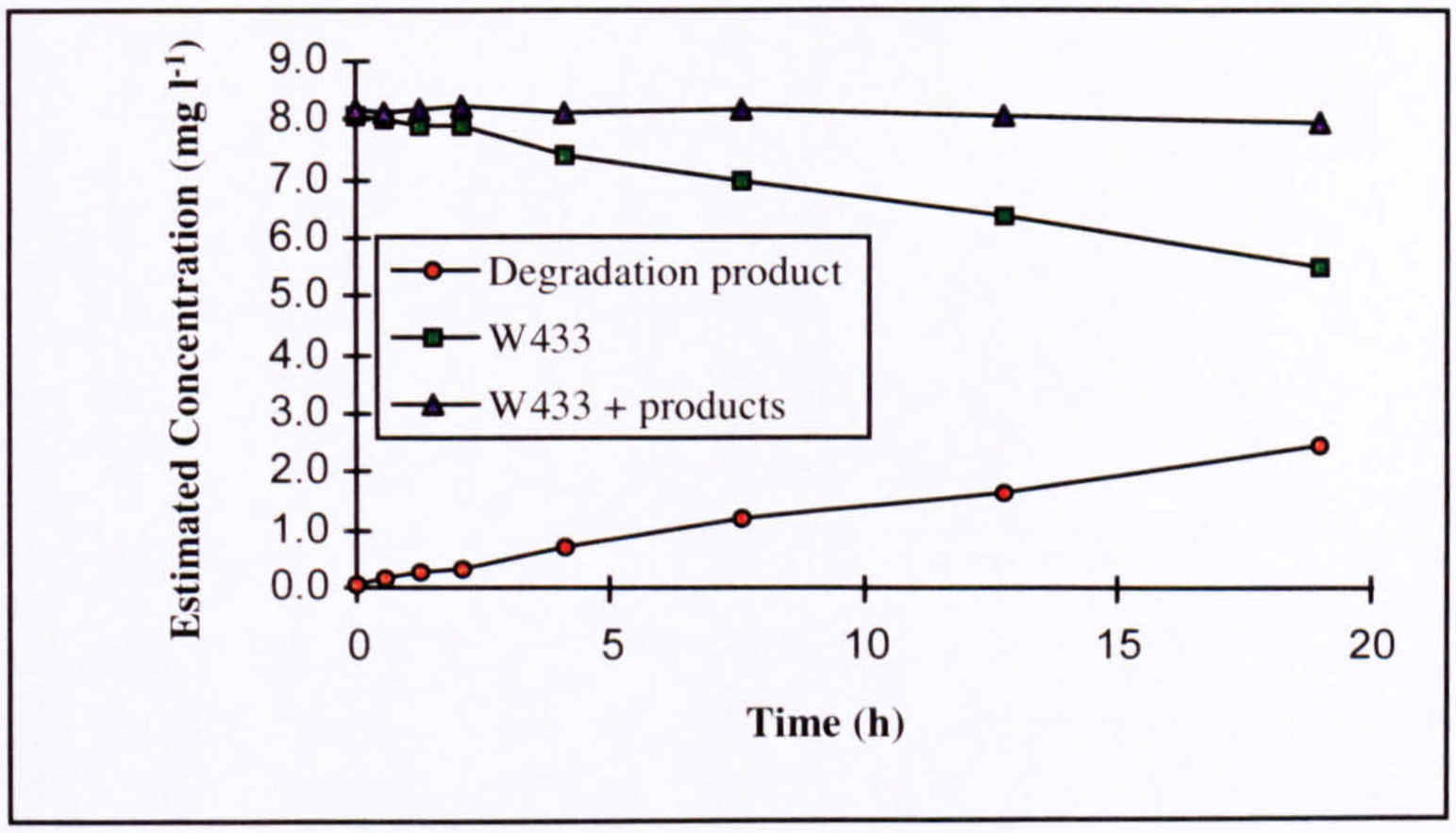

Figure 3.7 Change in concentration of parent dye (W433 in pure water) and single degradation product with increasing irradiation time.

In an attempt to identify the W433 degradation product, electrospray LC-MS was used to obtain mass spectra of an extract of W433 in pure water following irradiation for 18 hour. Figure 3.8 shows a comparison of LC-UV and LC-MS chromatograms, indicating the presence of two components.

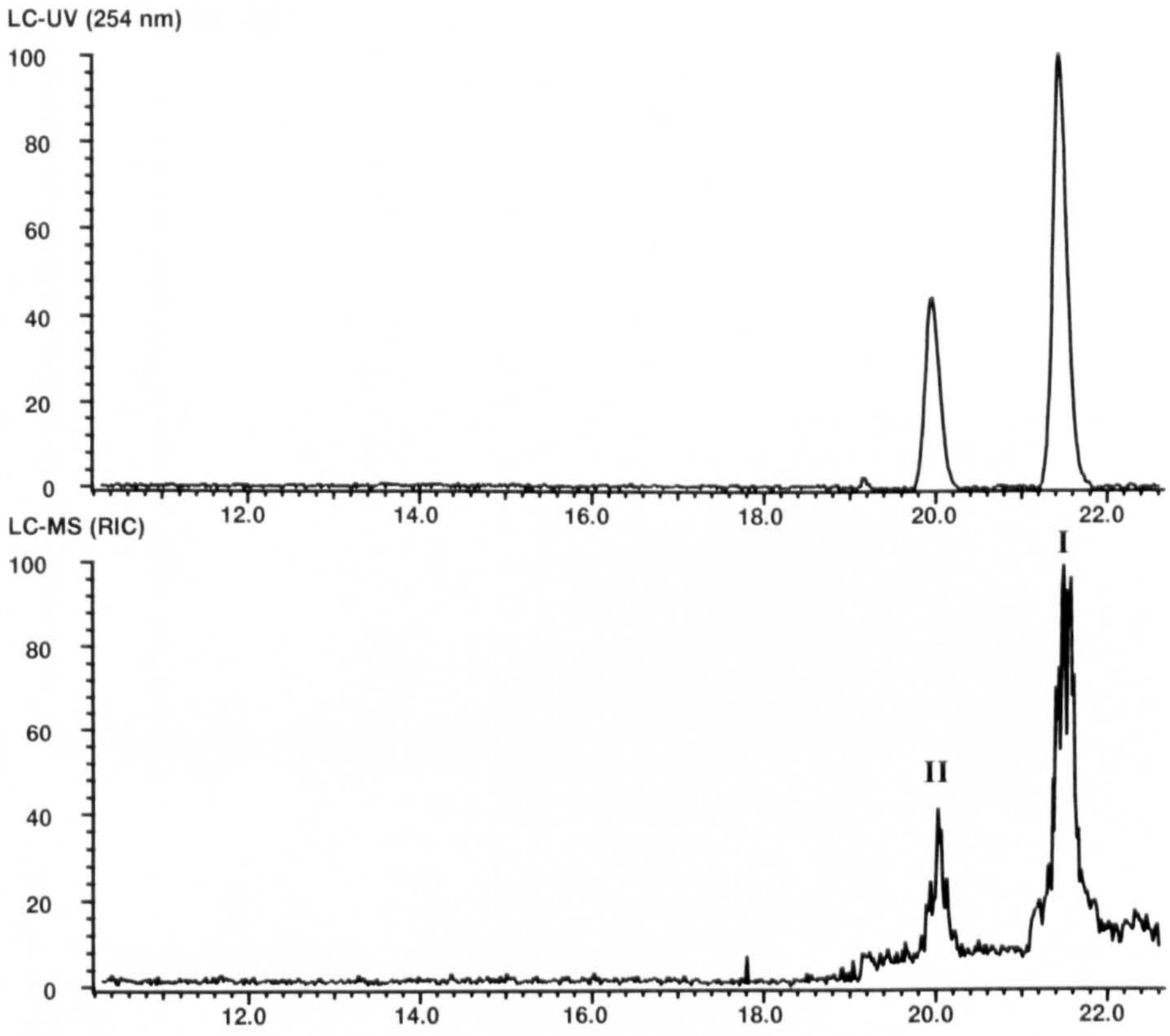

Figure 3.8 LC-UV and LC-MS chromatograms of W433 solutions following irradiation for 18 hours

Electrospray mass spectra of each of the two components are shown in Figure 3.9. The spectrum of peak I, (*m/z* 267.3 $[M-3H]^{3-}$, 401.5 $[M-2H]^{2-}$ and 804 $[M-H]^{-}$), is consistent with unchanged W433. The observed singly, doubly and triply charged molecular ions of the photodegradation product (peak II), indicated a molecular weight of 787. This is 18 mass units lower than W433 which is consistent with the displacement of -Cl by -OH and suggests product (II).

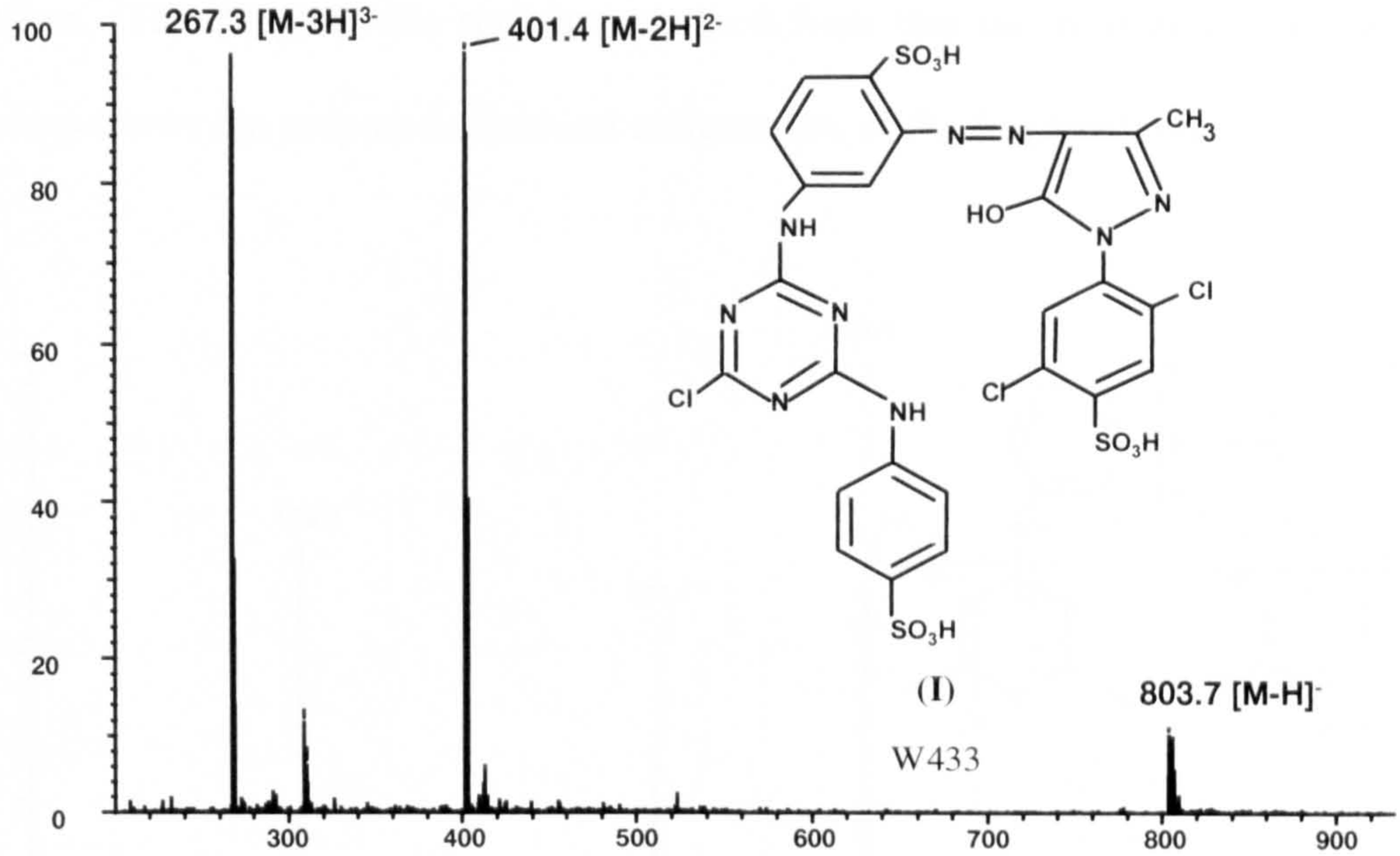

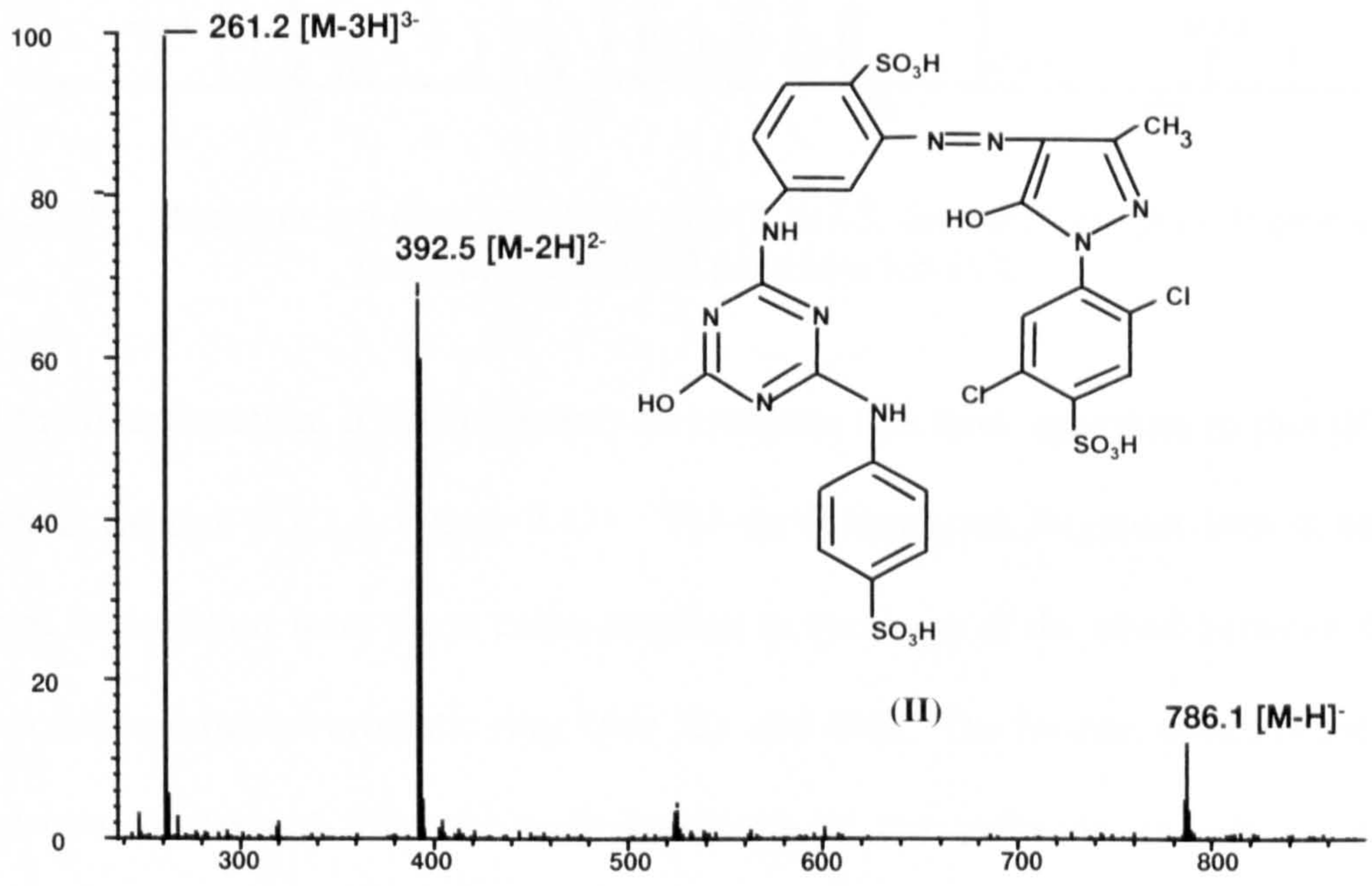

Figure 3.9 Mass spectra derived from peak I and peak II obtained from irradiation of W433 solutions for 18 h. The spectrum of peak I is consistent with W433

The mass spectrum of peak II although indicating the displacement of Cl, which one would expect to be the reactive chlorine of the triazine group, could not be used to assign which of the three chlorine atoms on W433 was removed, but this was achieved using daughter ion MSMS. The singly charged molecular ion (*m/z* 786) was too weak for MSMS studies. Therefore the more intense doubly charged parent ion *m/z* 392.5 $[M-2H]^{2-}$ was selected as

parent ion. The daughter ion spectrum derived from this ion is shown in Figure 3.10, which also shows the proposed structural assignments of the fragment ions.

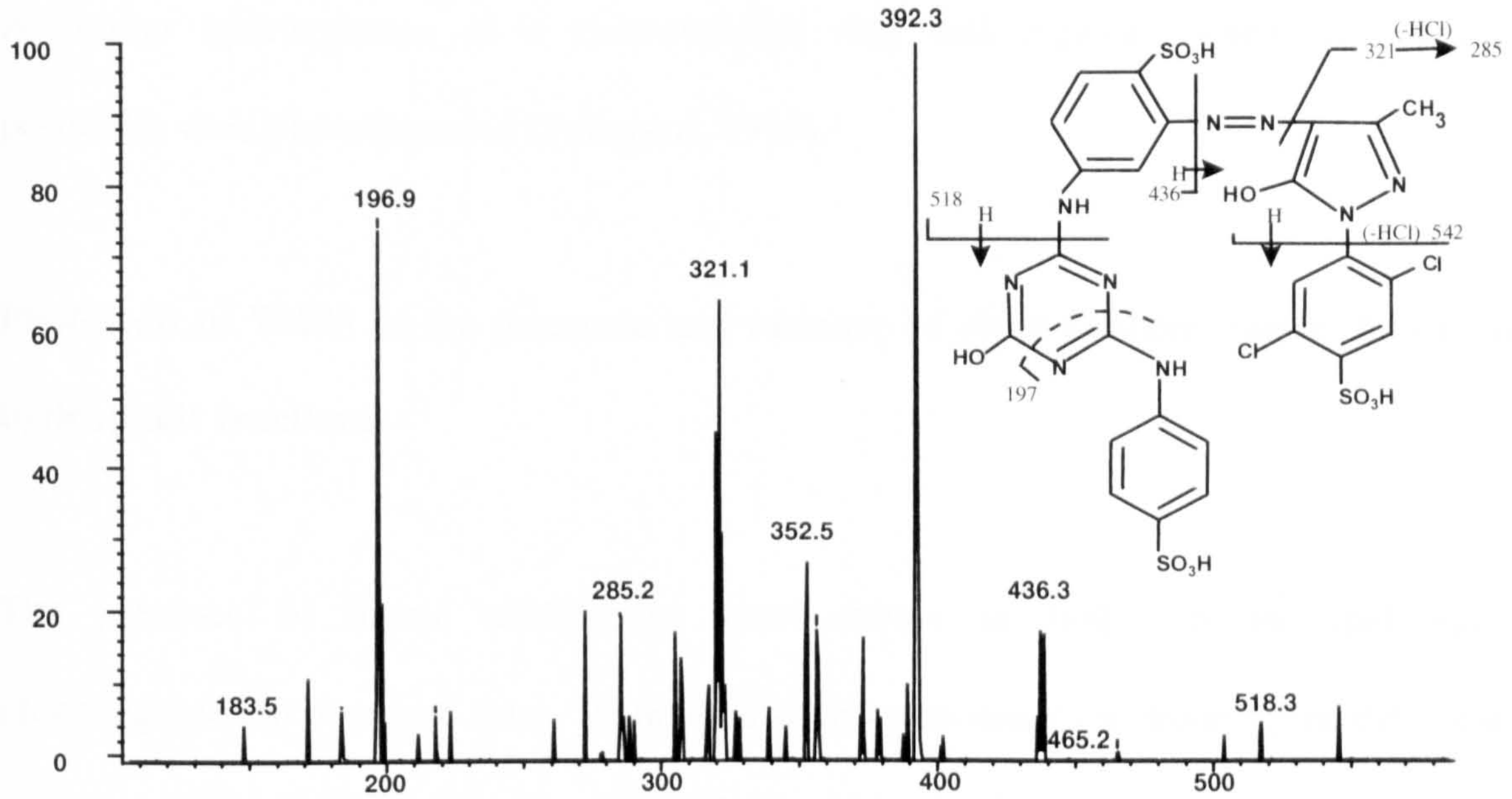

Figure 3.10 Daughter ion mass spectrum of *m/z* 392.5, derived from peak II produced by irradiation of W433 solutions for 18 h

To aid the interpretation, it was necessary to compare this mass spectrum to that of W433 (Chapter 2, Section 2.7.2.4, Figure 2.41). The most important fragment ions in terms of structural information were those corresponding to cleavage of the bond between the azo nitrogen and an adjacent aromatic ring, (*m/z* 321 and 436). The former, which is present in both spectra, is derived from the right hand side of the molecule and shows the two chlorine atoms to be present. However *m/z* 436 (Figure 3.10), is 18 mass units lower than the equivalent ion for W433 (*m/z* 454), confirming the structural change has occurred on the left hand side of the molecule. The weak fragment ion *m/z* 518, is derived from cleavage at the secondary amino group adjacent to the triazine ring, this was also observed for W433 and again supports the proposed hydroxy-triazine assignment.

Interestingly, the ring opening reaction proposed for W433 to produce the fragment ion *m/z* 197, was again observed. This fragmentation was not observed for hydroxy-triazine

pesticides, (Voyksner, 1987), but appears to be a useful characteristic fragment for the triazine group within dyes.

A similar hydroxylation of a chlorotriazine ring was reported when chlorotriazine pesticides were photodegraded (Pelizzetti, 1990).

Photolysis of W433 in the presence and absence of river Dodder humic, fulvic and hydrophilic fractions.

The presence of humic acids have been shown to both sensitise and inhibit photodegradation reactions rates. Humic substances in water are made up of three main components referred to as humic acids, fulvic acids and a hydrophilic acids (Section 3.3). River Dodder, Dublin, (Eire), humic substances and a commercially available humic acid (Aldrich), were each added to W433 at concentrations of 1 mg l^{-1} and the mixtures irradiated for up to 72 hours. W433 was chosen because a rather slow photodegradation rate was observed in pure water. Figure 3.11 shows a graphical representation of the changes in concentration vs time for each mixture, for duplicate analyses.

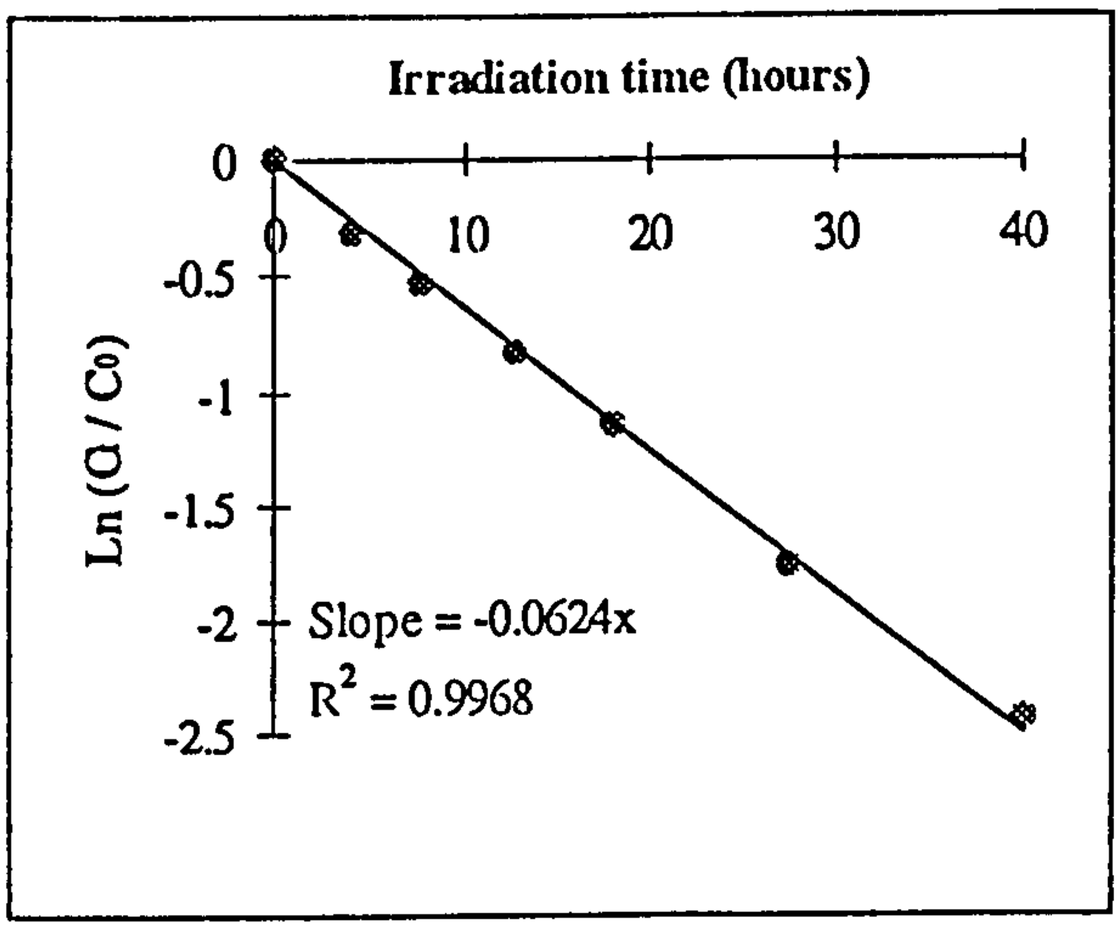

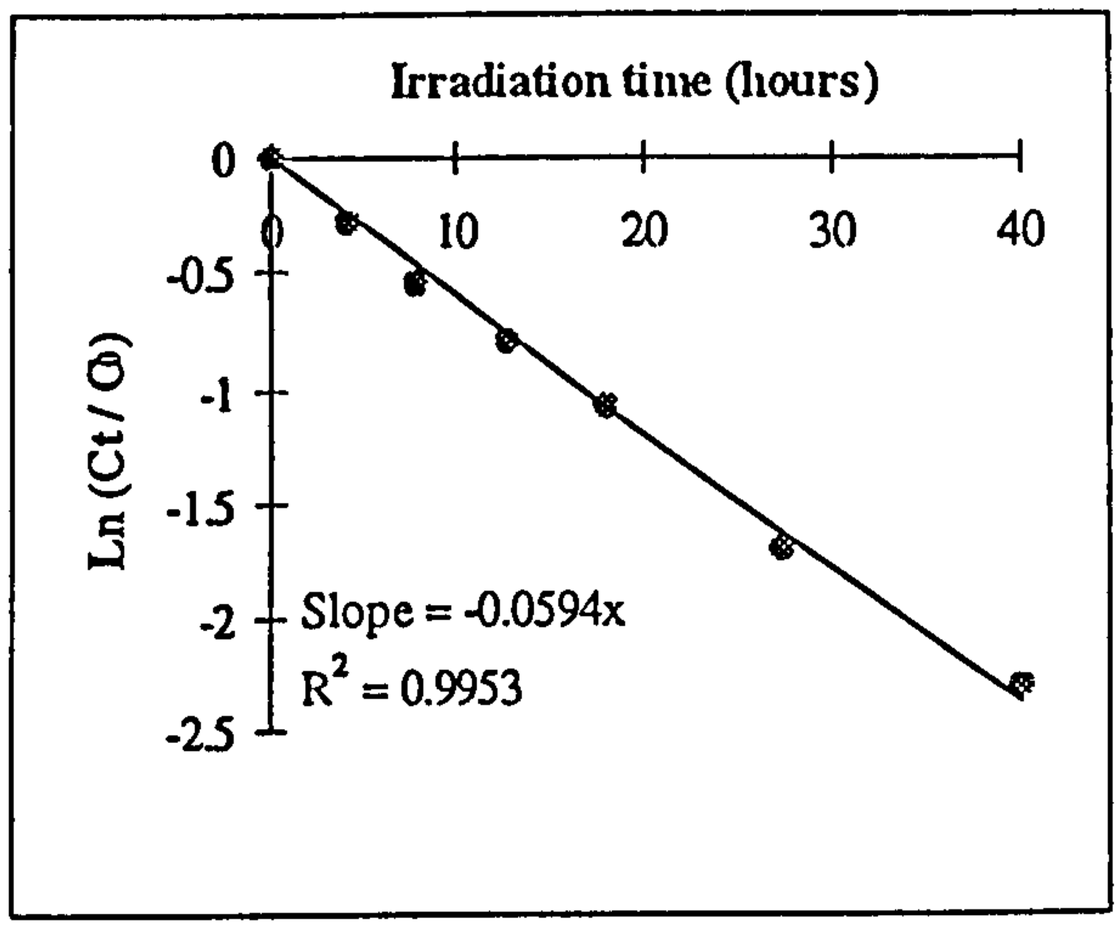

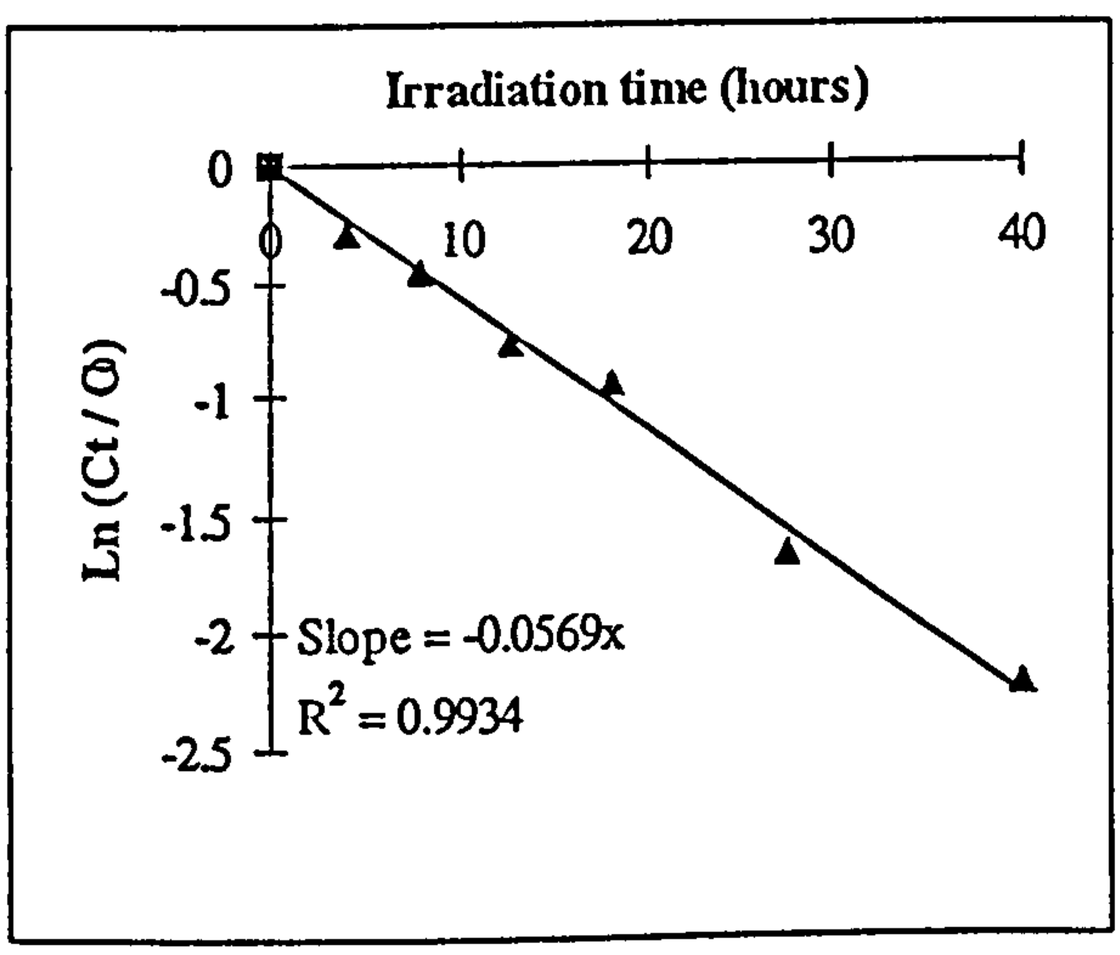

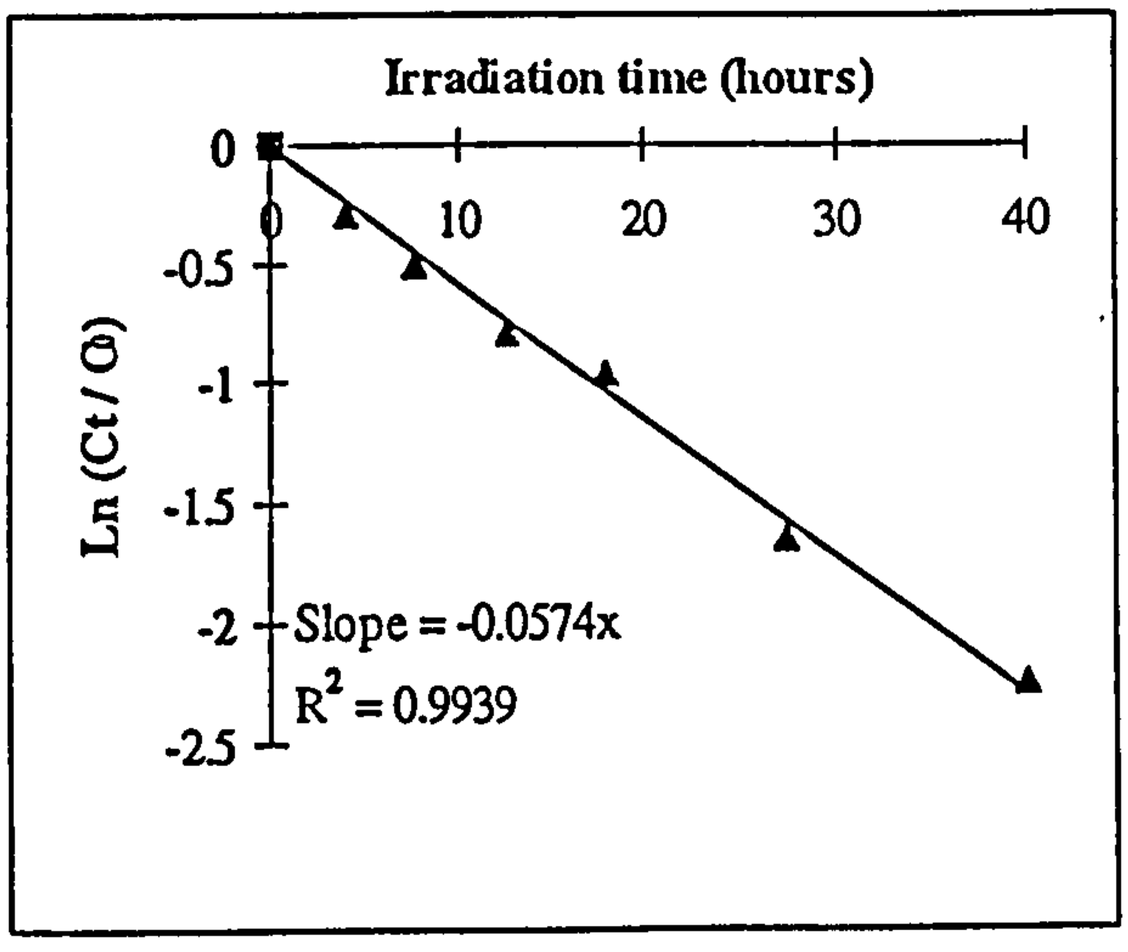

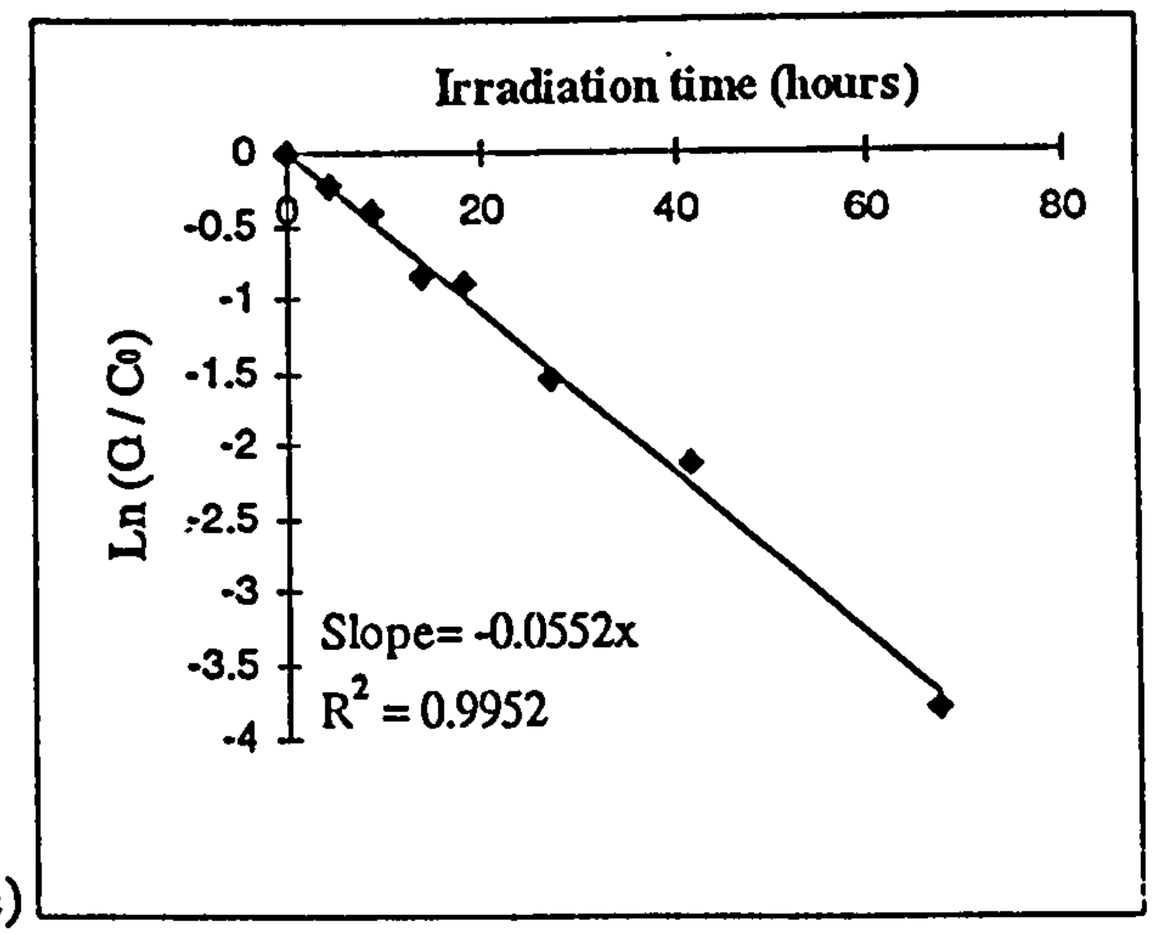

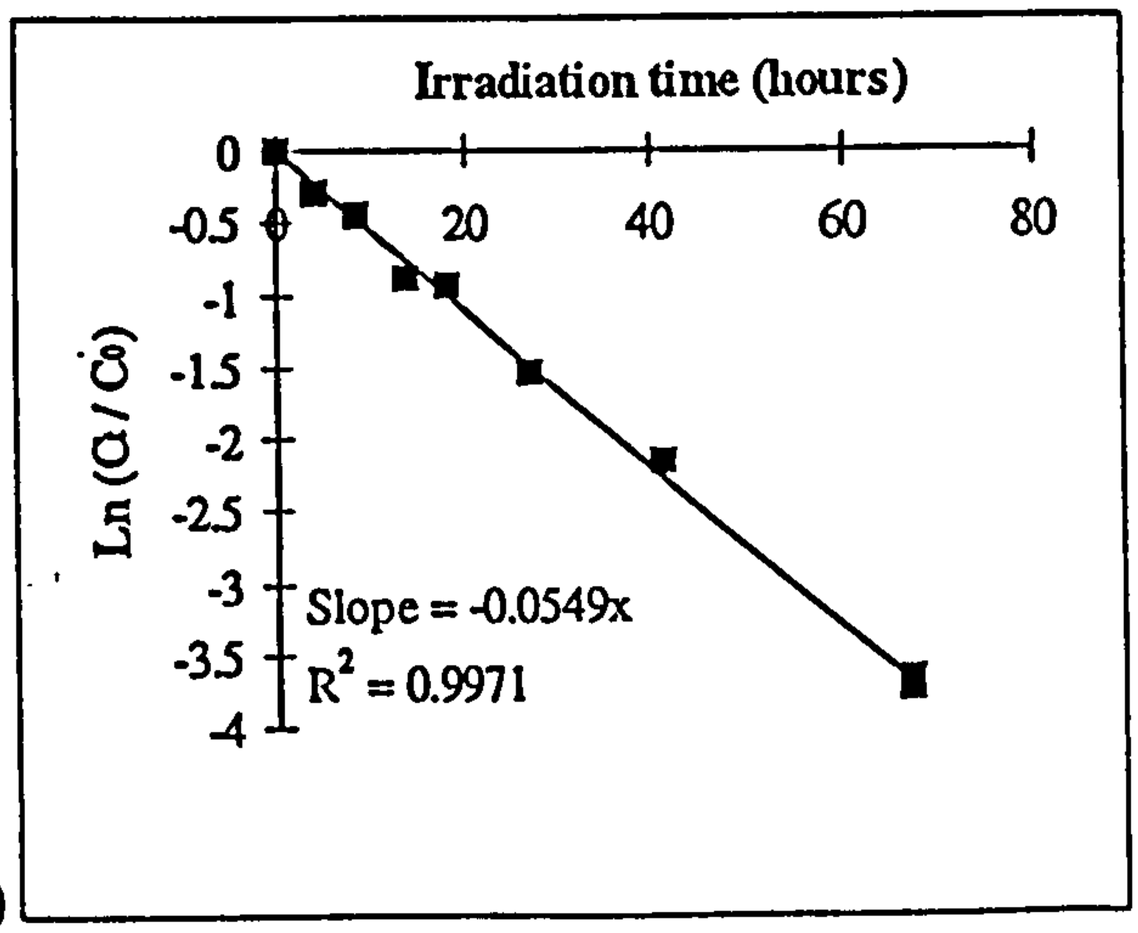

Figure 3.11 Changes in concentration of W433 with increasing irradiation time in (a-b) pure water, (c-d) river Dodder humic acid and (e-f) river Dodder fulvic acid

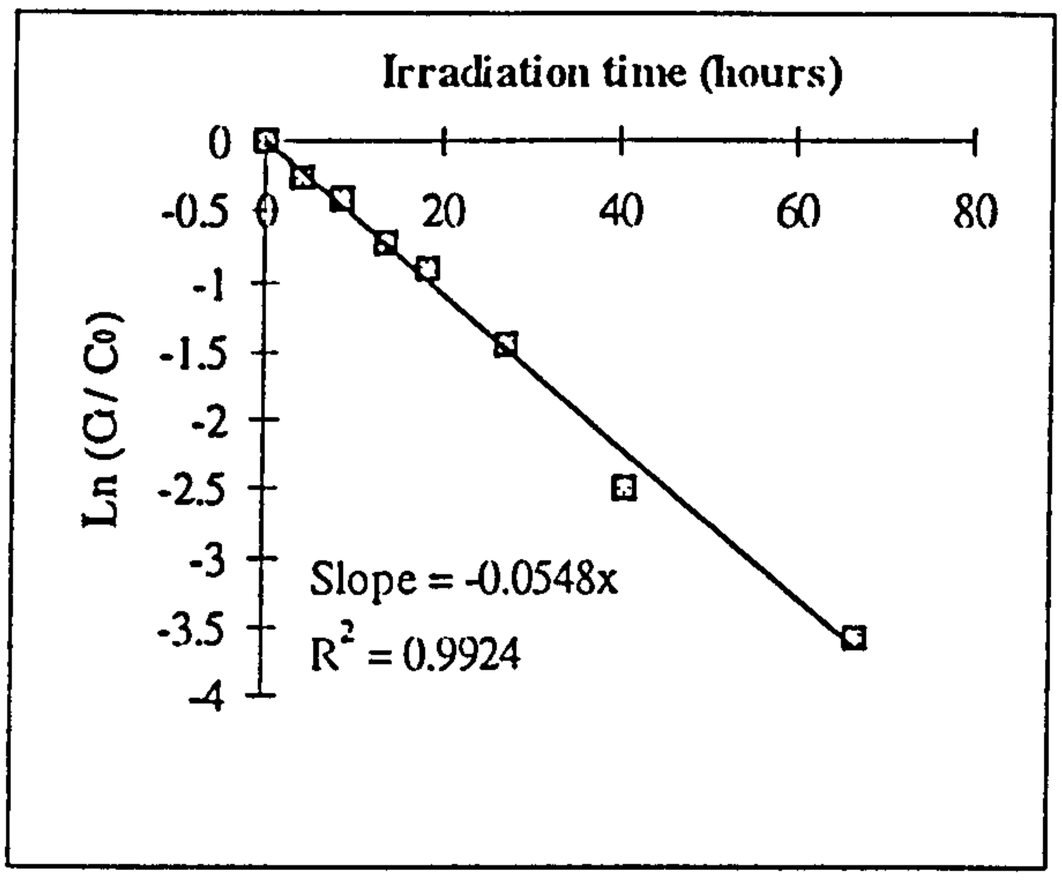

g)

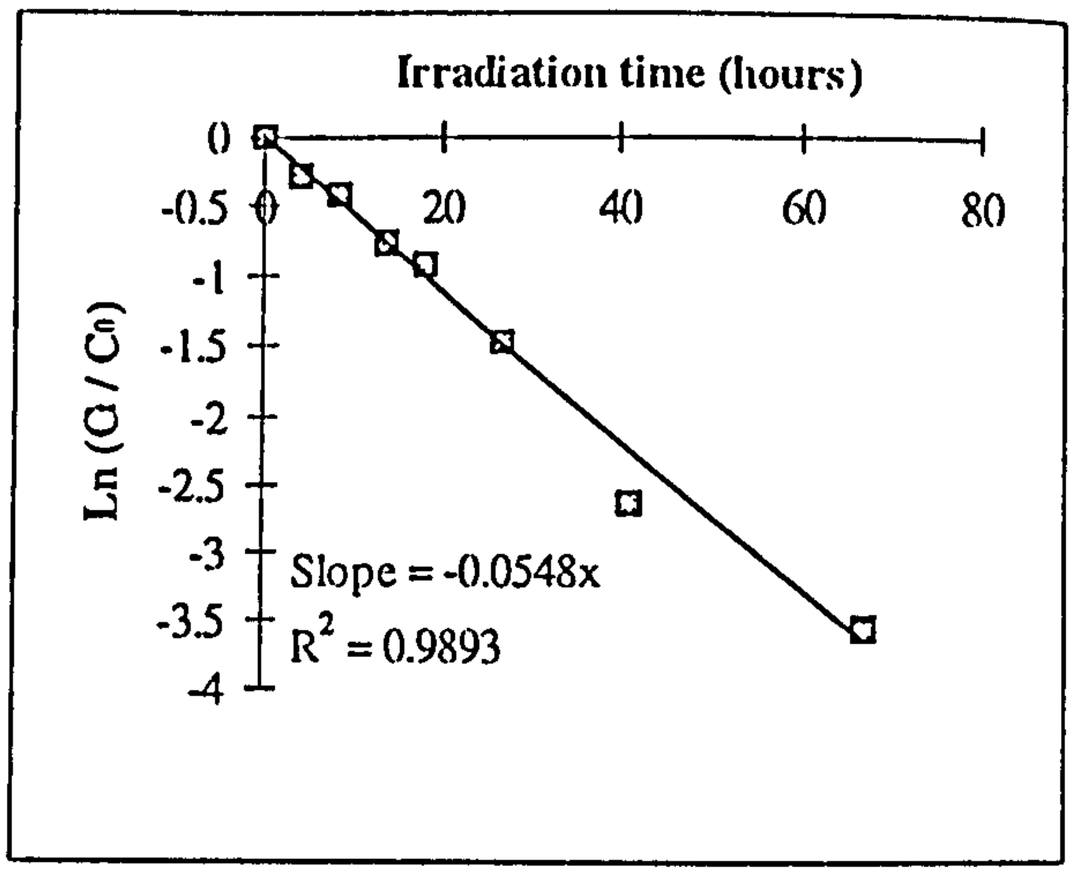

h)

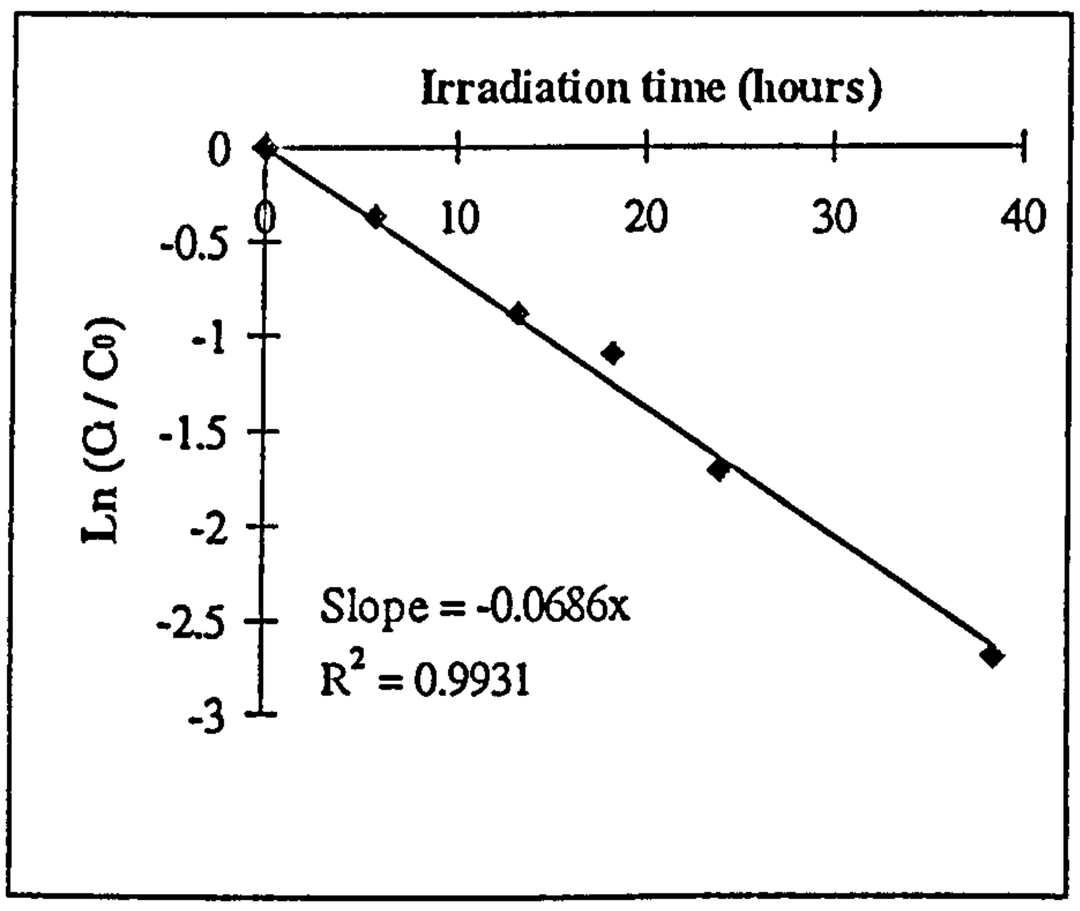

i)

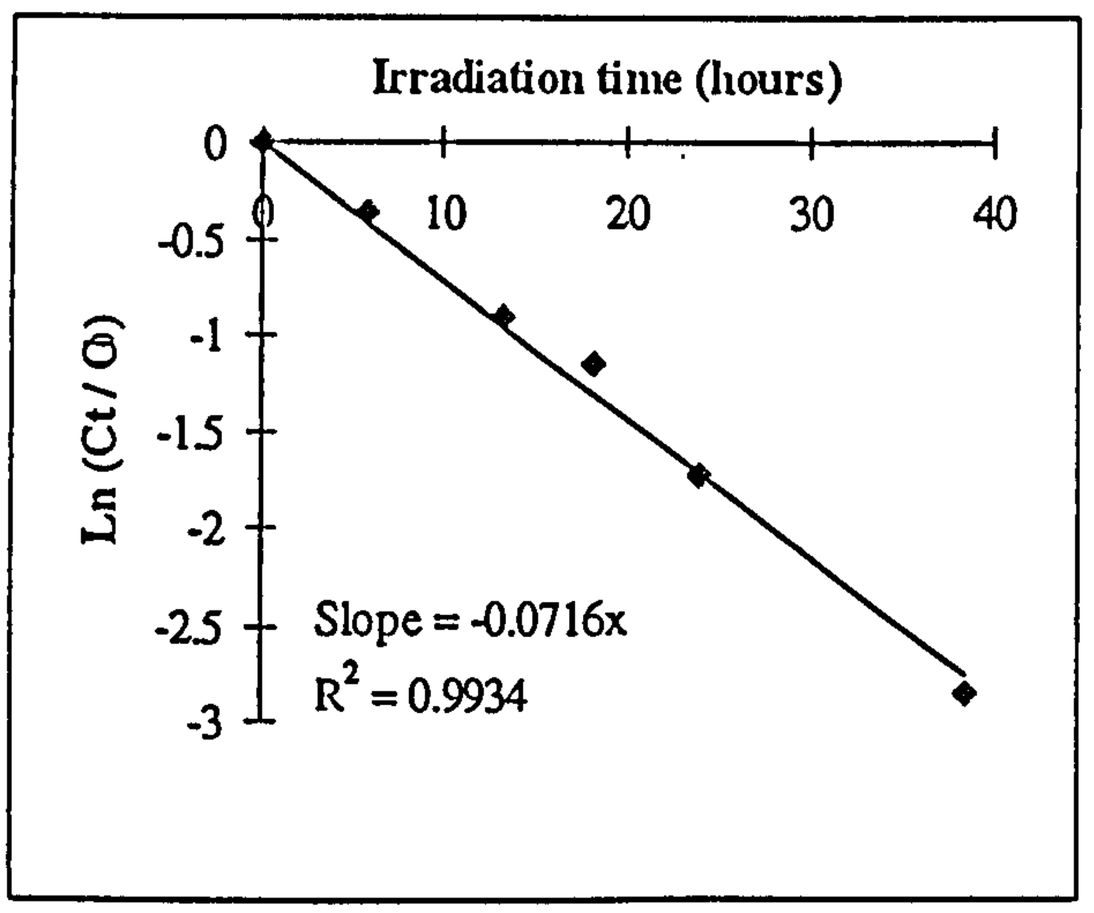

j)

Figure 3.11 (contd) Changes in concentration of W433 with increasing irradiation time in (g-h) river Dodder hydrophilic acid and (i-j) Aldrich humic acid

The slope of each graph is equal to the photodegradation rate constant and from this the half lives of each mixture were calculated (Table 3.4).

Table 3.4 Photodegradation rate constants and half lives for the photolysis of W433 in the presence of humic materials.

Humic substance	k_p (h^{-1})		$t_{1/2}$ (h)		Mean $t_{1/2}$ (h)
	1	2	1	2	
None	-0.0624	-0.0594	11.1	11.7	11.4
Dodder humic acid	-0.0569	-0.0574	12.2	12.1	12.1
Dodder fulvic acid	-0.0552	-0.0549	12.6	12.6	12.6
Dodder hydrophilic	-0.0548	-0.0548	12.6	12.6	12.6
Aldrich humic acid	-0.0686	-0.0716	10.1	9.8	9.9

From these limited data it appears that the river Dodder humic substances tend to slow the rate of photolytic degradation, whilst the commercial humic mixture slightly enhanced the photodegradation process. However it should be noted that commercial Aldrich humic acid is derived from German lignite and is not necessarily representative of humic acids typically found in rivers and estuaries. This is apparent from a comparison of reported elemental analyses and aromatic carbon contents of humic acids isolated from the river Dodder (Zhou and Rowland, 1994) and river Suwannee, USA (Murphey *et al.*, 1990).

None of the humic substances made a dramatic change to reaction rate at the concentrations used. Haag (1988) showed how the presence of humic substances sensitised the photolysis of a range of simple azo dyes, often shortening their half lives by factors of 2 - 10. The concentration of humic acid used by Haag (1988) was 5 mg l^{-1}, five times higher than that used in this study. A further experiment would be needed to evaluate the impact of increased humic substances concentrations on the photodegradation of W433.

Profiles of reaction products from irradiated samples are very similar regardless of which humic substance is present. A typical chromatogram of W433 plus river Dodder fulvic acid following 72 hour irradiation is shown in Figure 3.12. The major peak (retention time 22 min) was hydroxylated W433 (II). There are at least 10 minor components which elute before this which are therefore probably more polar degradation products. The change in concentration of W433 and its photodegradation products in the presence of the same fulvic acid solution is shown in Figure 3.13. Quantification of the reaction products was carried out by reference to the W433 calibration.

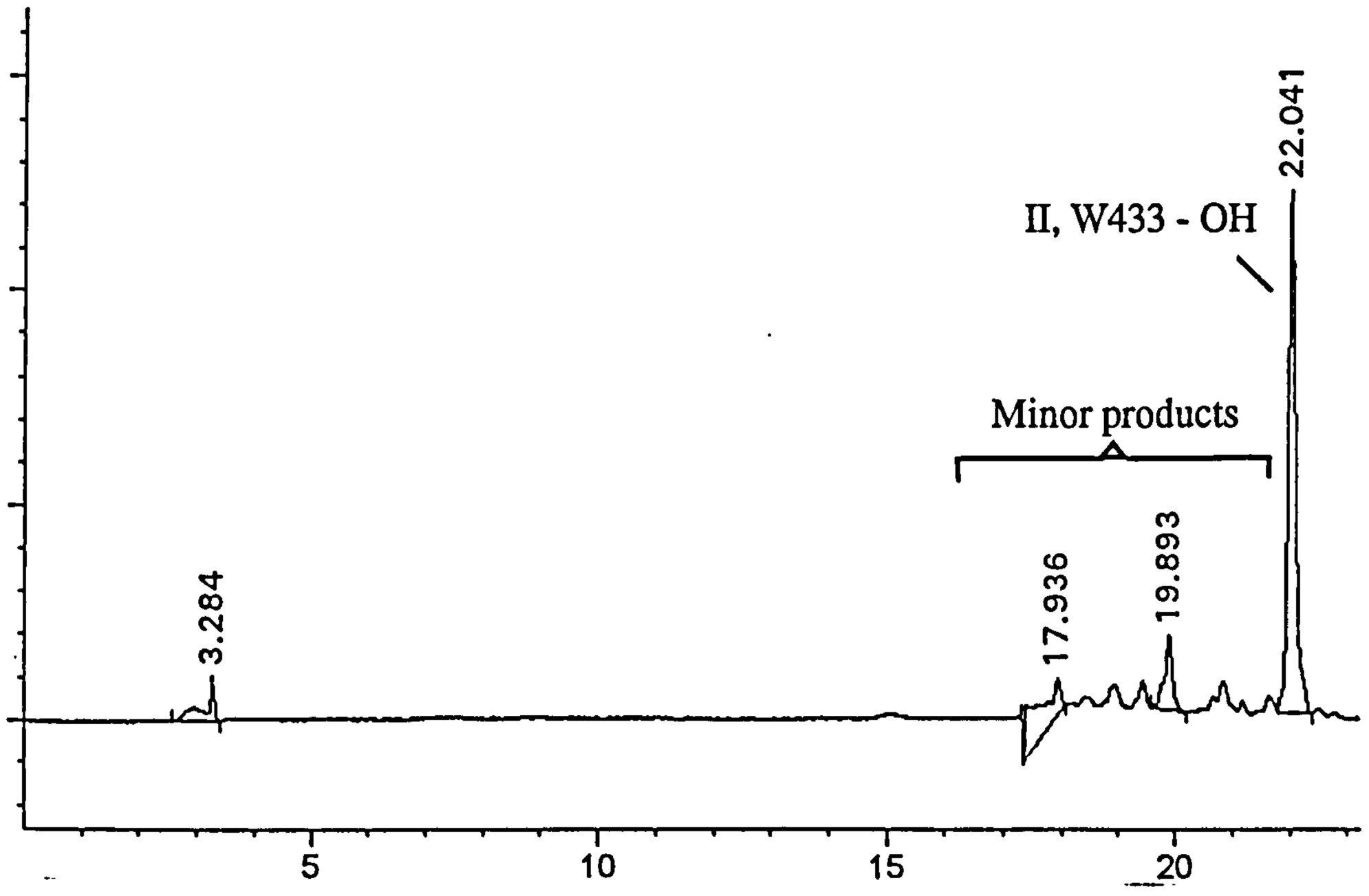

Figure 3.12 HPLC-UV chromatogram for W433 following 72 h photolysis in the presence of river Dodder fulvic acid

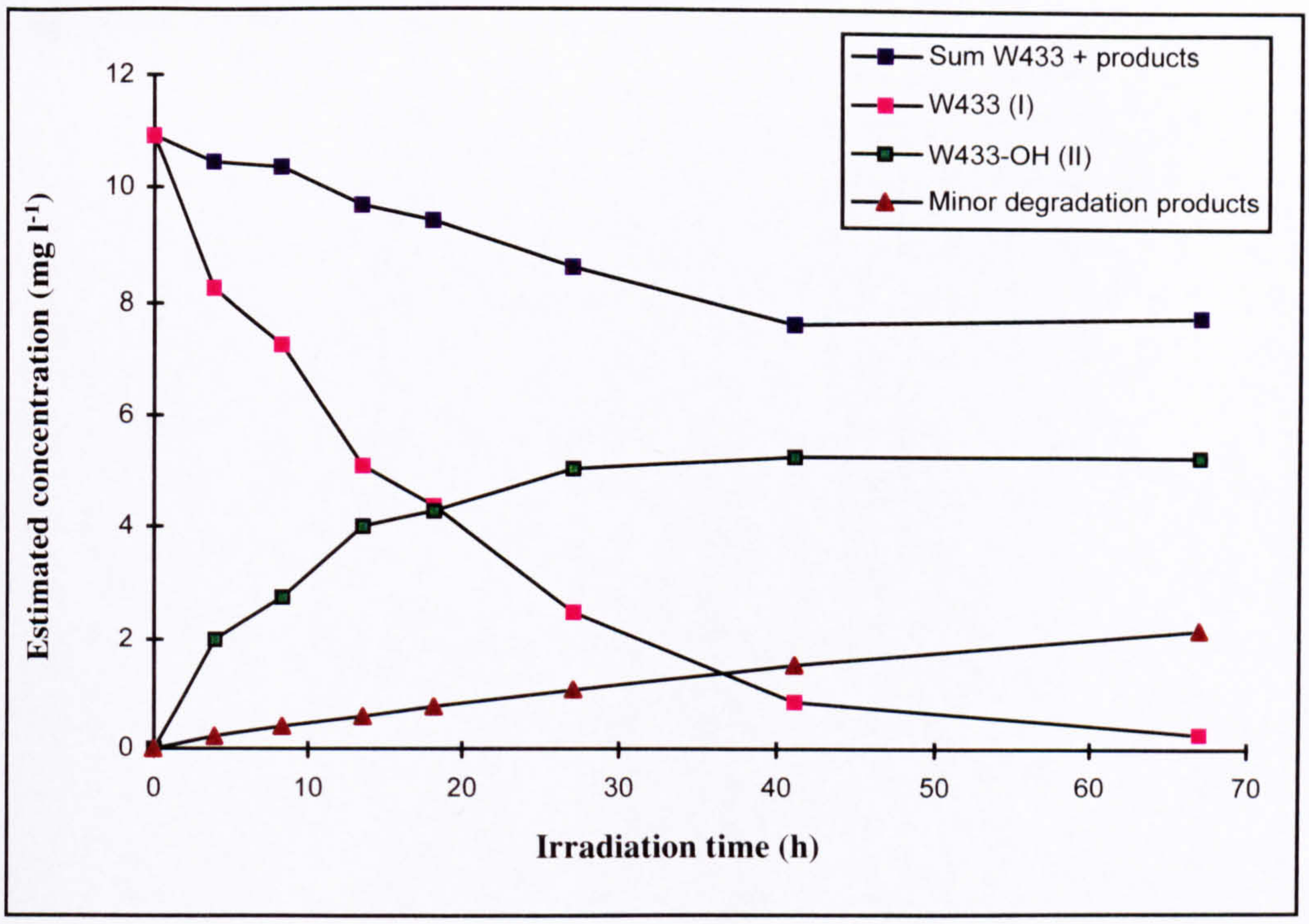

Figure 3.13 Change in concentration of photodegradation products of W433 in the presence of river Dodder fulvic acid, with increasing irradiation time

This approach assumes the degradation products have similar UV absorption properties to parent dye which may not be the case for all products, therefore the results provide only an estimate of product concentrations. The sum of W433 and photodegradation products accounted for greater than 80% of the initial dye concentration, the majority of which was due to the stable hydroxylated product (II). It should be noted that the minor component (Fig 3.13) consists of the sum of up to 10 different compounds, separated on the LC system (Fig 3.12) and quantified by reference to the W433 calibration curve. It was not possible to identify these relatively weak components by LC-MS. Further work would be needed, including either photolysis of a more concentrated solution or for a longer period of time, to produce a more concentrated sample for LC-MS and MSMS identification. However these data indicate that azo reactive dyes do photodegrade partially in 72 hours irradiation time.

3.4.2 Photolysis of W435 in pure water.

The effects of irradiation on solutions of W435 are shown in Table 3.5 for duplicate experiments.

Table 3.5 Effects of irradiation time on photolysis of W435

Time (h)	W435		W435 (repeat)	
	Conc. (mg l^{-1})	% of initial	Conc. (mg l^{-1})	% of initial
0.0	8.1	100	8.4	100
0.5	6.5	80	6.4	76
1.0	4.2	52	4.7	56
2.0	2.8	35	2.9	35
4.0	1.3	16	1.4	17
8.0	0.3	4	0.3	4
12.0	0.0	0	0.0	0
19.0	0.0	0	0.0	0

Data from both W435 experiments were very similar. The decline in W435 concentration with increasing irradiation time is exponential i.e. can be represented by the equation:

$$C_t = C_o\, e^{-Kp,t}$$

Where C_t is the concentration at time t and C_o is the initial concentration. Therefore W435 photodegradation kinetics can be described as first order:

$$\text{Ln}\,[C_t/C_o] = -k_p,t$$

and the first order photodegradation rate constant k_p can be determined from the slope of a graph of Ln $[C_t/C_o]$ vs irradiation time (Figure 3.14).

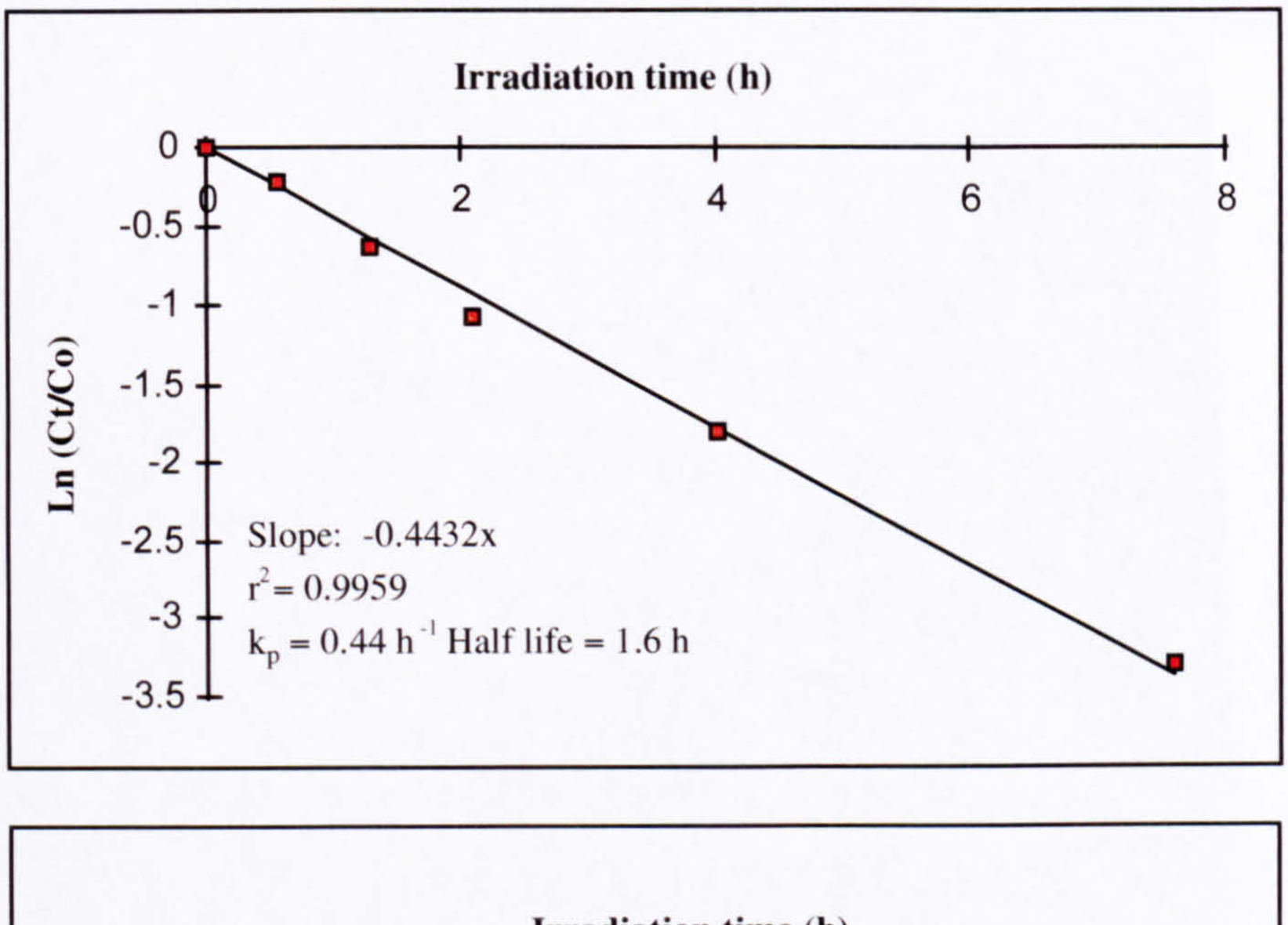

Figure 3.14 Change of concentration with time for duplicate W435 photodegradation experiments

The first order photodegradation rate constants (k_p); were -0.43 and -0.44 h^{-1}. The half lives were 1.7 and 1.6 hours respectively.

The close correlation between calculated results demonstrates the reproducibility of experiments under controlled laboratory conditions. LC-UV (254 nm) analysis of the photodegraded samples indicated that one major and four minor products were formed which persisted on further irradiation. These had LC retention times between 19 and 25 minutes and were labelled II - VI. Undergraded W435 (I) was also present. A further product (VII) was barely retained on the LC column and a small transient peak with a

variable retention time (VIII) was also observed. Quantification of these products was measured by reference to the W435 calibration graph. Figures 3.15 and 3.16 show the change of concentrations of each component with increasing irradiation time. Since peaks III and IV were of similar intensity and overlapped, they could not be reproducibly integrated as individual peaks and their areas were combined.

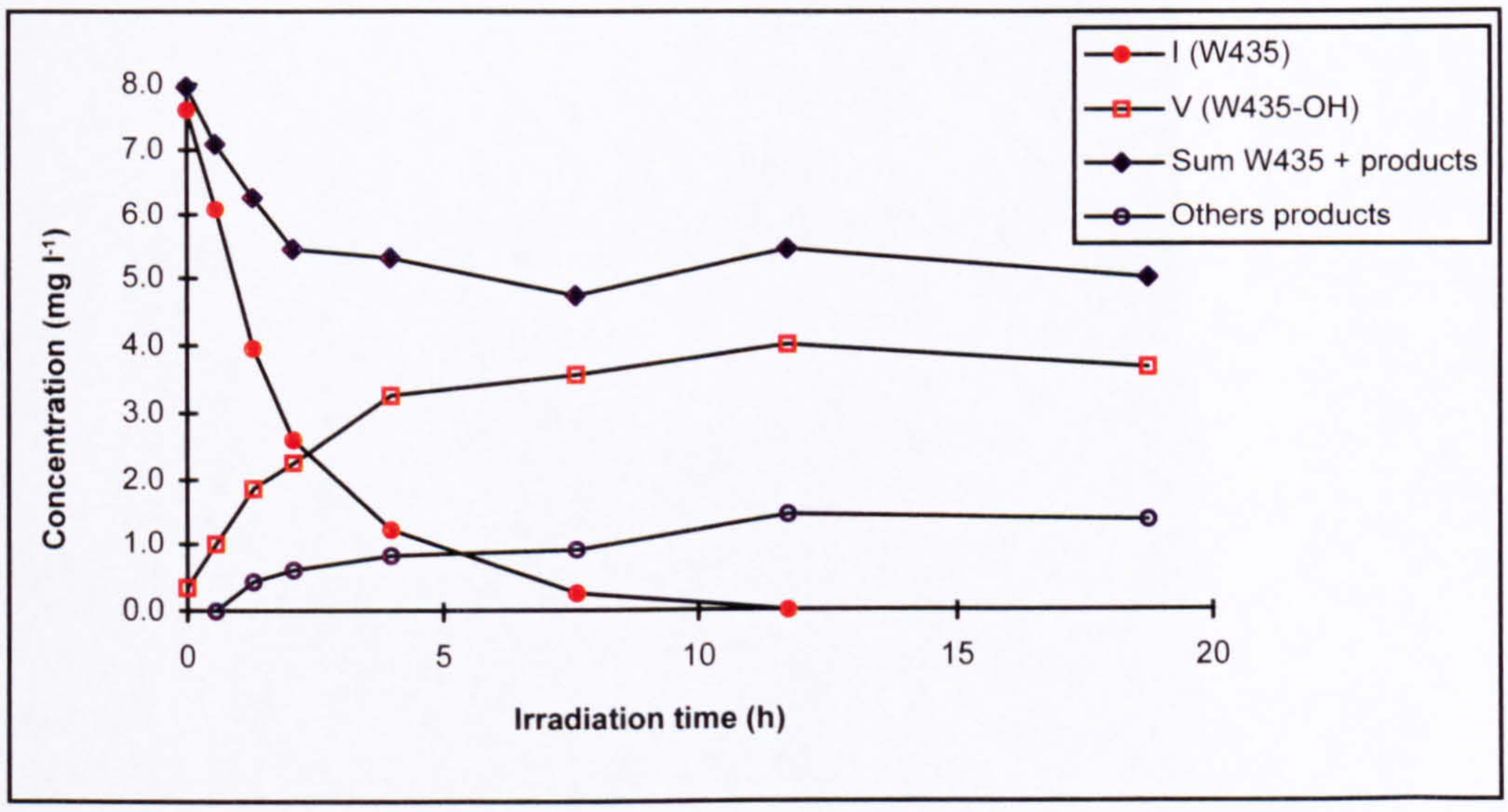

Figure 3.15 Change in concentration of W435 (I), the major photodegradation product (V) and the sum of degradation products, with increasing irradiation time

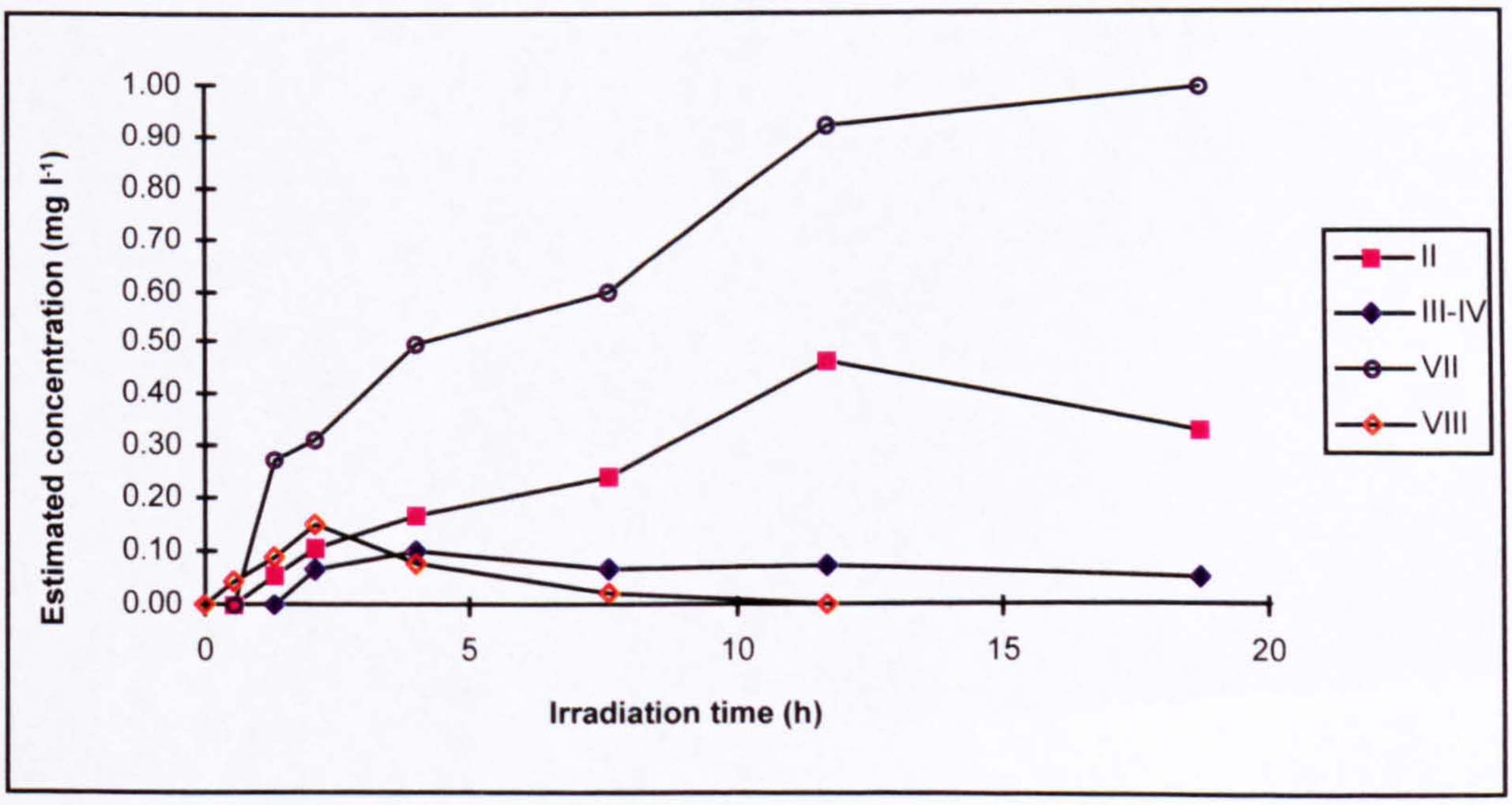

Figure 3.16 Change in concentration of the minor photodegradation products of W435 with increasing irradiation time

This approach assumes the degradation products have similar UV absorption properties to parent dye which may not be the case for products not containing the anthraquinone chromophore. Therefore these results provide only an estimate of product concentration. The sum of W435 and photodegradation products accounted for only 60 - 69% of the initial dye concentration following >1 hour irradiation. This suggests that either some of the degradation products of W435 have much weaker UV absorptions than W435 at 254 nm, or that some products are not amenable to analysis by LC-UV.

In an attempt to identify the W435 degradation products, electrospray mass spectra were obtained for an extract derived from W435 irradiated for 4 hours. Figure 3.17 shows a comparison of LC-UV (254 nm) and LC-MS chromatograms, which show the presence of two major and four minor components. The poorly retained product, VII, was not observed in either the UV or MS chromatograms and appears not to have been retained on the extraction cartridge. Also, there was no evidence for product VIII in either chromatogram. However this was a very minor and short lived component (Fig 3.16) and may have further degraded before LC-MS analysis.

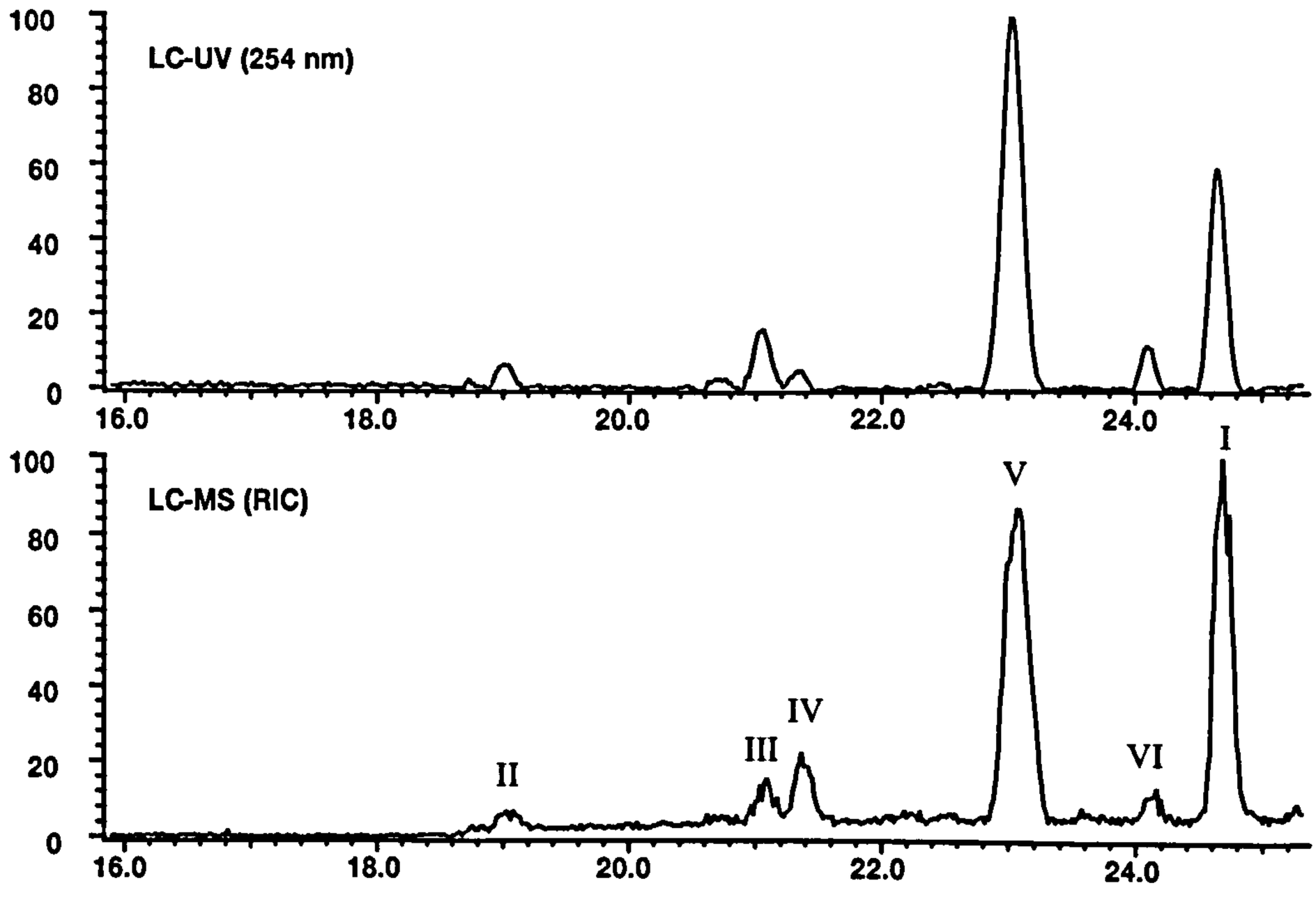

Figure 3.17 Comparison of LC-UV (254 nm) and LC-MS (RIC) chromatograms for an extract of dyestuff W435 following photodegradation for 4 h

Based on molecular weight and molecular ion isotope contribution information, structures were postulated for each of the observed degradation products. These were supported by MSMS daughter ion analysis of the molecular ions derived from each of these products.

Interpretation of MSMS spectra of degradation products was aided by reference to the fragmentation pattern of W435, (Chapter 2, Section 2.15, Figure 2.38), where certain fragment ions provided particularly useful structural information. Prominent among these were *m/z* 555 due to cleavage of the triazine ring and losses of 115 and 72 mass units due to neutral loss of $CH_3CH_2OCH_2CH_2OCN$ and $CH_3CH_2OCH{=}CH_2$ from the ethoxylate side chain (Fig 3.18).

The LC retention time and molecular ions observed in the mass spectrum derived from component I, *m/z* 731 and 365 (Figure 3.18) were consistent with unchanged parent dye W435. The proposed structures of fragment ions observed in the MSMS spectrum of W435 are shown in Figure 3.18 to aid interpretation of subsequent data.

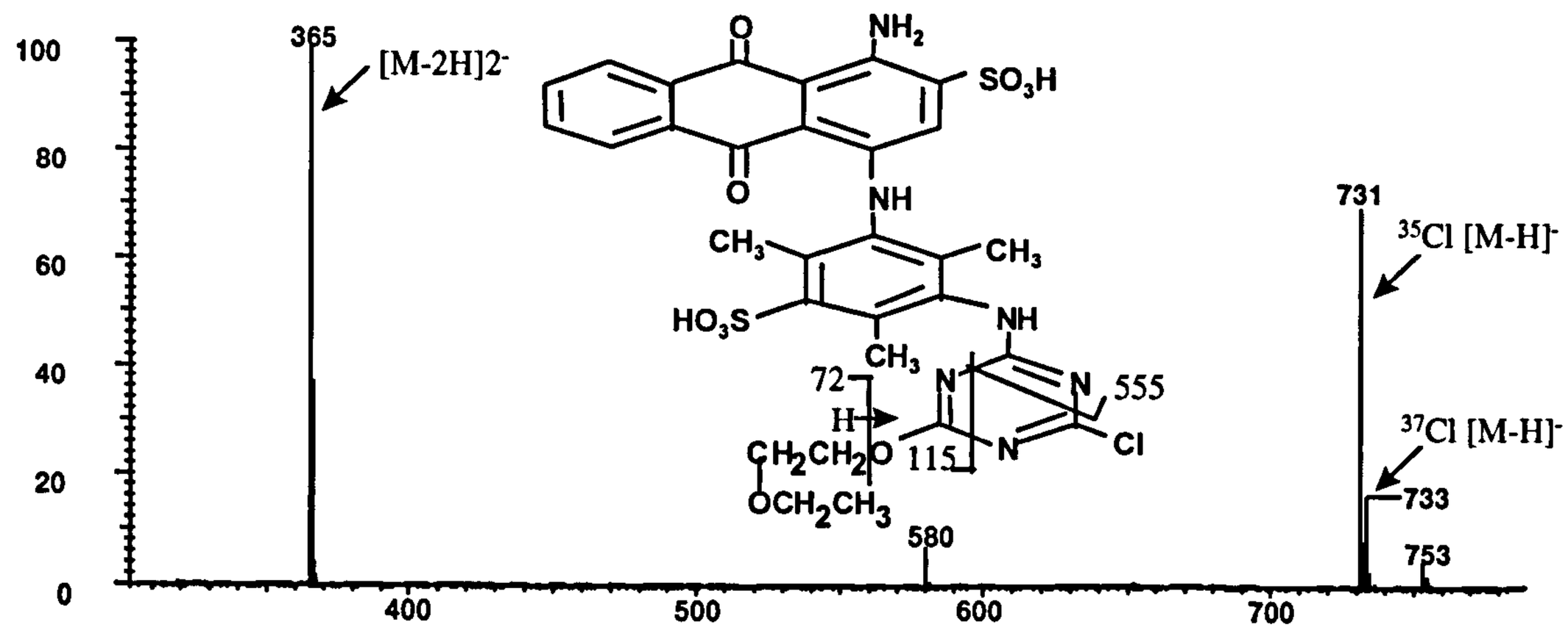

Figure 3.18 Mass spectrum derived from component I (Figure 3.17)

Based on a comparison with photodegradation data for W433, component V, the most intense and persistent of the photodegradation products was assigned to the hydroxylated form of W435 in which the reactive chlorine is replaced by a hydroxyl group. The mass

spectrum of this component, Figure 3.19, showed singly and doubly charged molecular ions at *m/z* 713 and 356 which were consistent with this proposal.

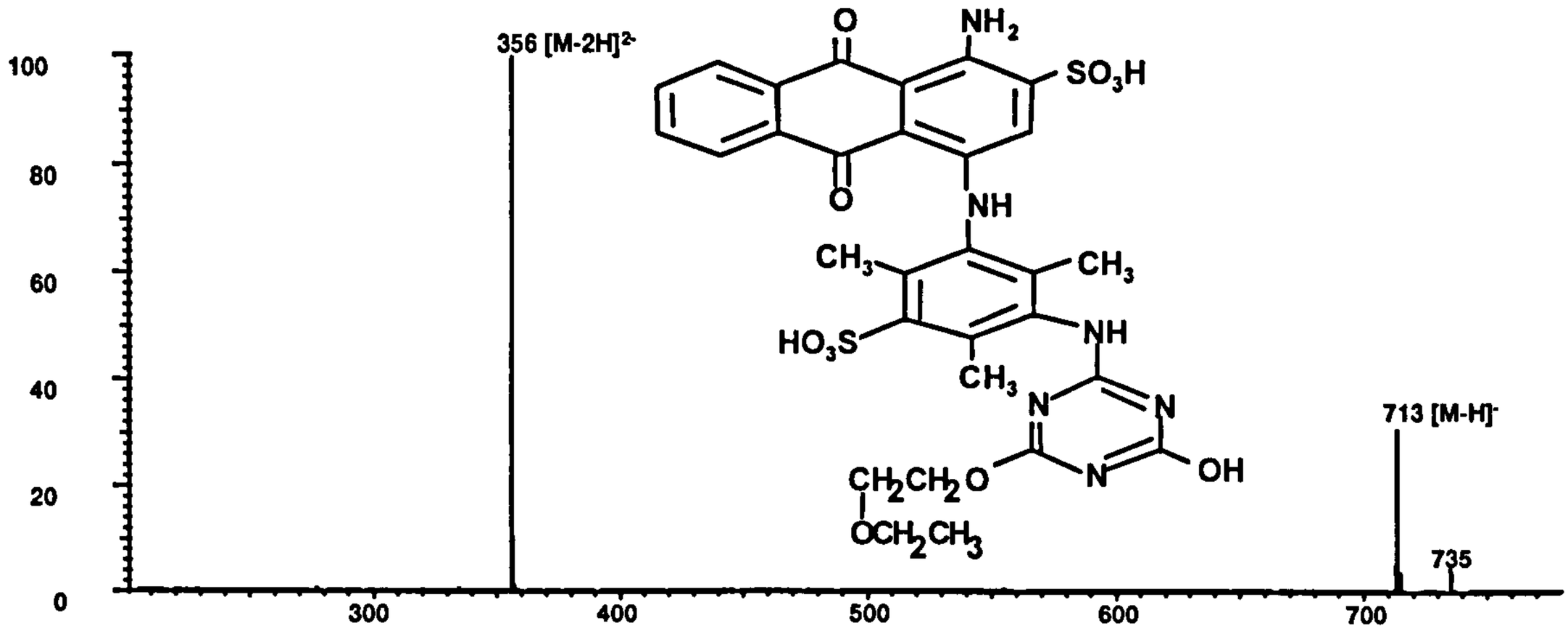

Figure 3.19 Mass spectrum of component V (Figure 3.17) formed by photolysis of W435 for 4 h

Figure 3.20 shows the daughter ion spectrum derived from ion *m/z* 713. The characteristic ion at *m/z* 555 was indicative of cleavage of the triazine ring and losses of 115 and 72 confirmed that no change had occurred to the ethoxylated side chain of the triazine ring (cf Fig 3.17). Additionally, losses of H_2O (*m/z* 695) and HO-CN (*m/z* 670), eliminated from the triazine ring, confirmed the proposed structure.

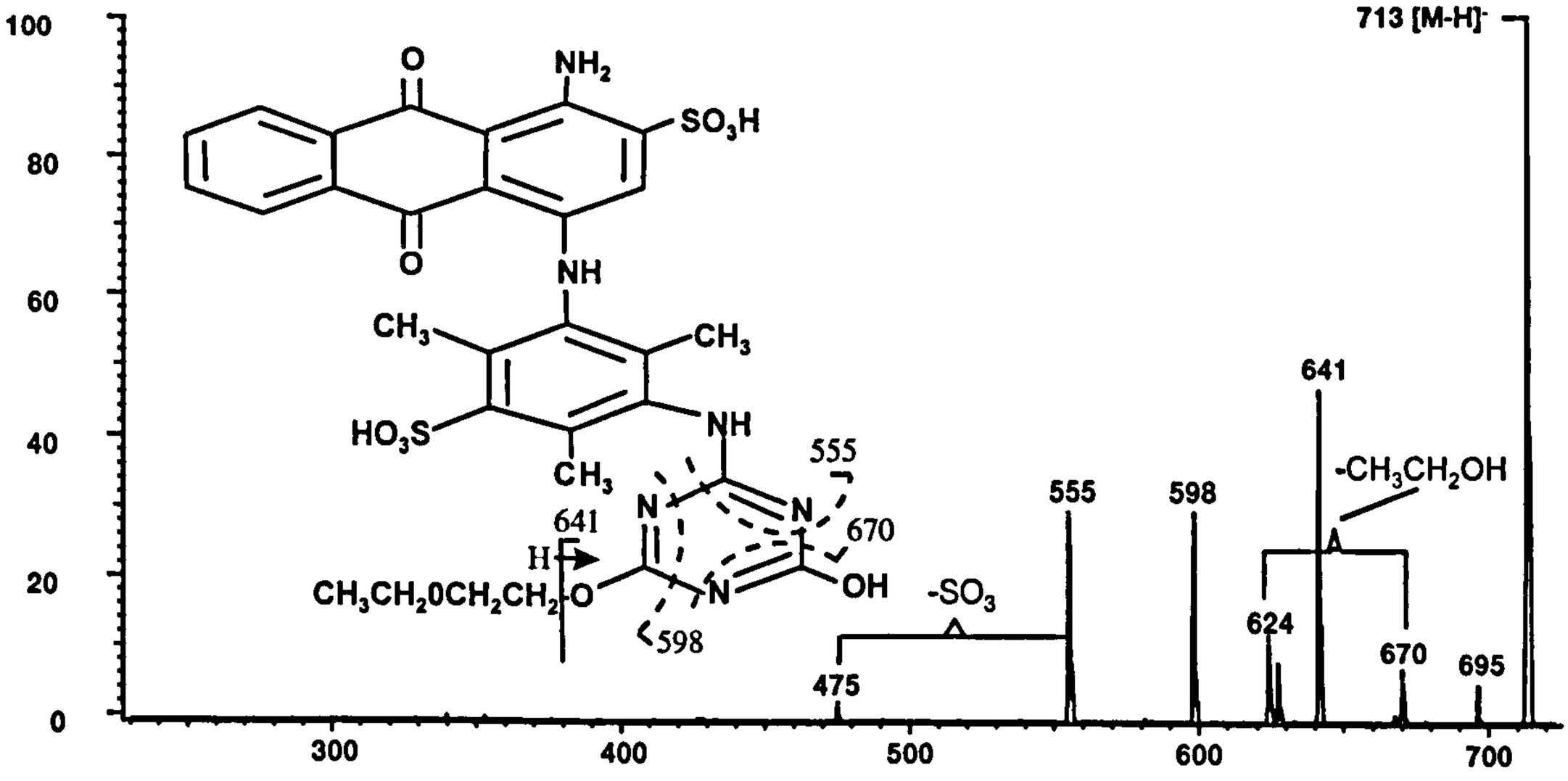

Figure 3.20 Daughter ion spectrum of *m/z* 713 $[M-H]^-$ (Peak V) formed by photolysis of W435 for 4 h

Initial inspection of the mass spectrum derived from component VI, (Fig 3.21), suggested that it may be an isomer of W435 because it showed the same molecular ions, but inspection of the molecular ion isotope cluster indicated the absence of chlorine (cf Fig 3.18).

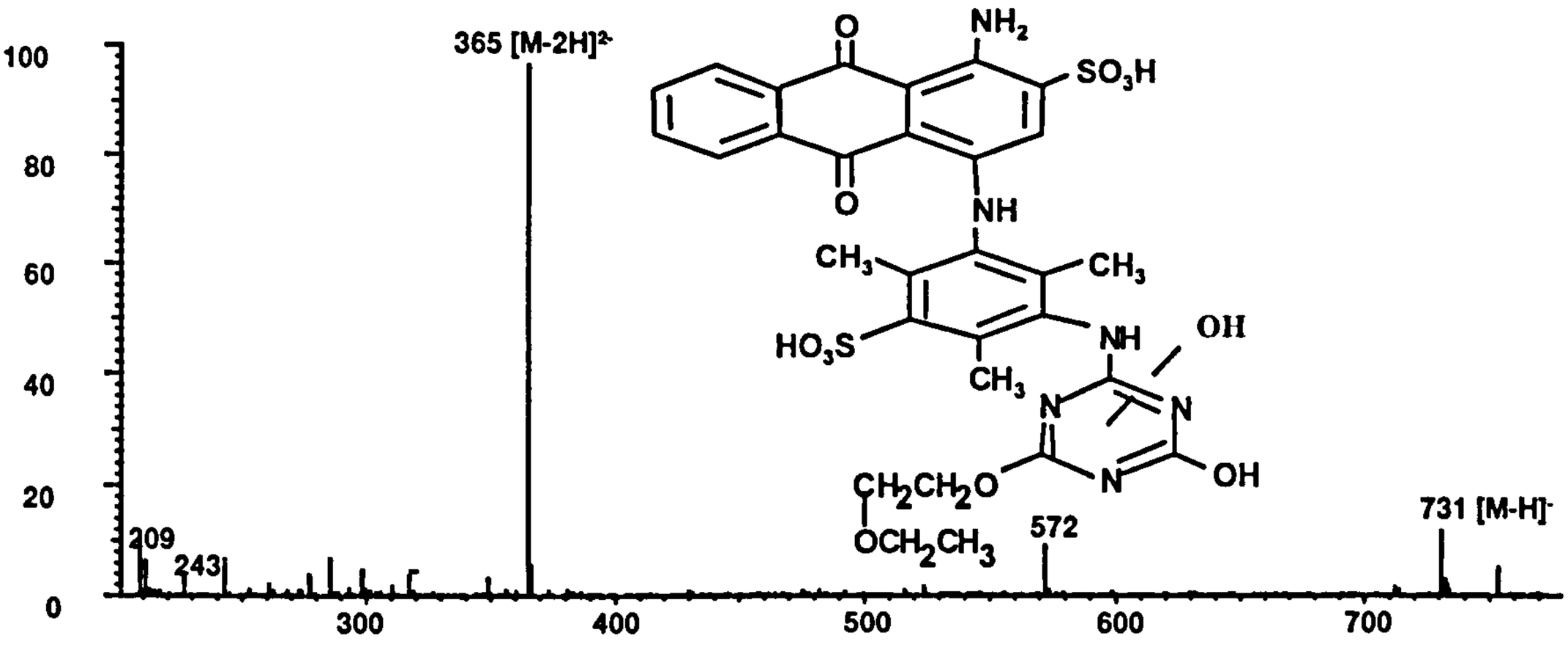

Figure 3.21 Mass spectrum derived from Peak VI (Figure 3.17)

The daughter ion spectrum derived from *m/z* 731 is shown in Figure 3.22. It is quite different from that observed for W435 (Chapter 2, Figure 2.38) and the hydrolysis product, Figure 3.20. The absence of chlorine implies this has been removed by hydrolysis. This leaves a mass difference of 18, suggesting a molecule of water has been added and since the presence of the characteristic *m/z* 555 ion indicates the anthraquinone and attached substituted benzene ring part of the molecule must be unchanged, hydration must have occurred on the triazine ring. The ion *m/z* 598, [M-H-133] is probably equivalent to the characteristic loss of $CH_3CH_2OCH_2CH_2OCN$ observed in the mass spectra of components I and V. This would indicate addition of water across the -C=N group attached to the ethoxylate side chain.

The key to the identification of this degradation product was *m/z* 572, the base peak in the daughter ion spectrum. This may be rationalised by the following elimination:

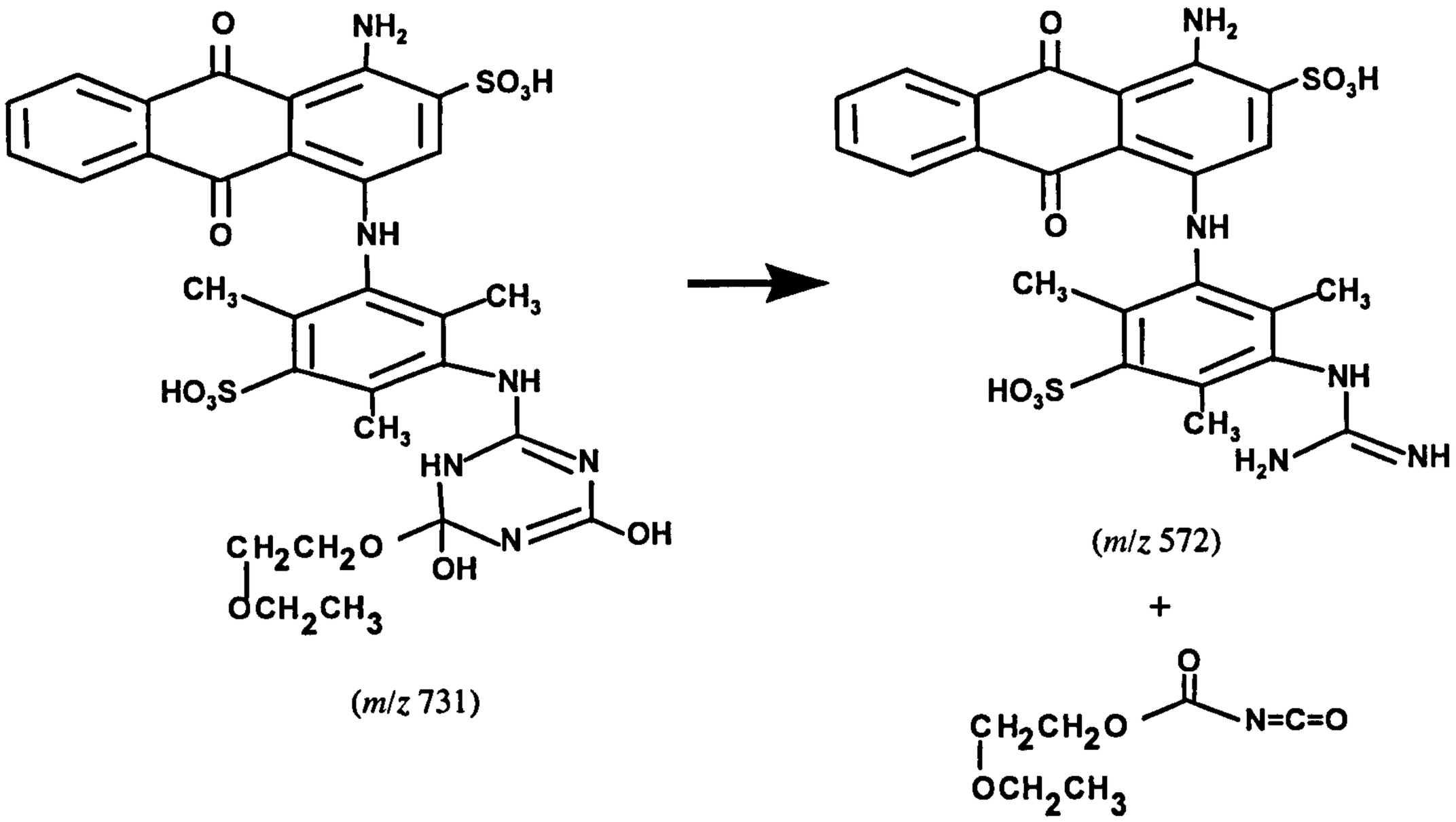

but this assignment should be treated as speculative.

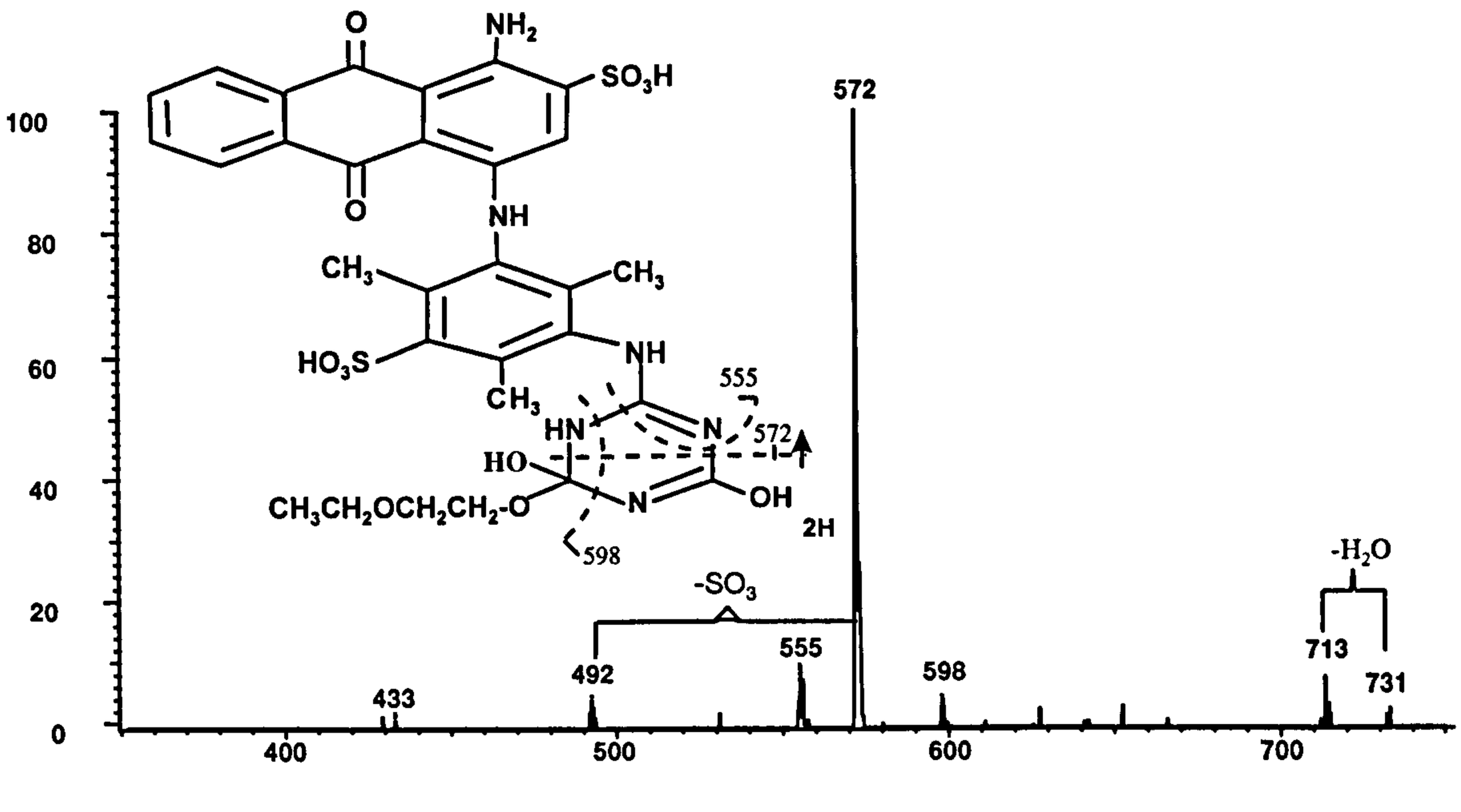

Figure 3.22 Daughter ion spectrum of *m/z* 731 $[M-H]^-$ (component VI)

Components II and IV appear to be related (Figs 3.23 and 3.24). Mass spectra of both exhibited only singly charged molecular ions (*m/z* 412 and *m/z* 430 respectively), indicating they possessed only one sulphonic acid group. The isotope pattern for component IV showed it to be chlorine containing and as component II has a molecular

weight 18 mass units lower and no chlorine isotope, it is likely to be the hydroxylated version of component IV.

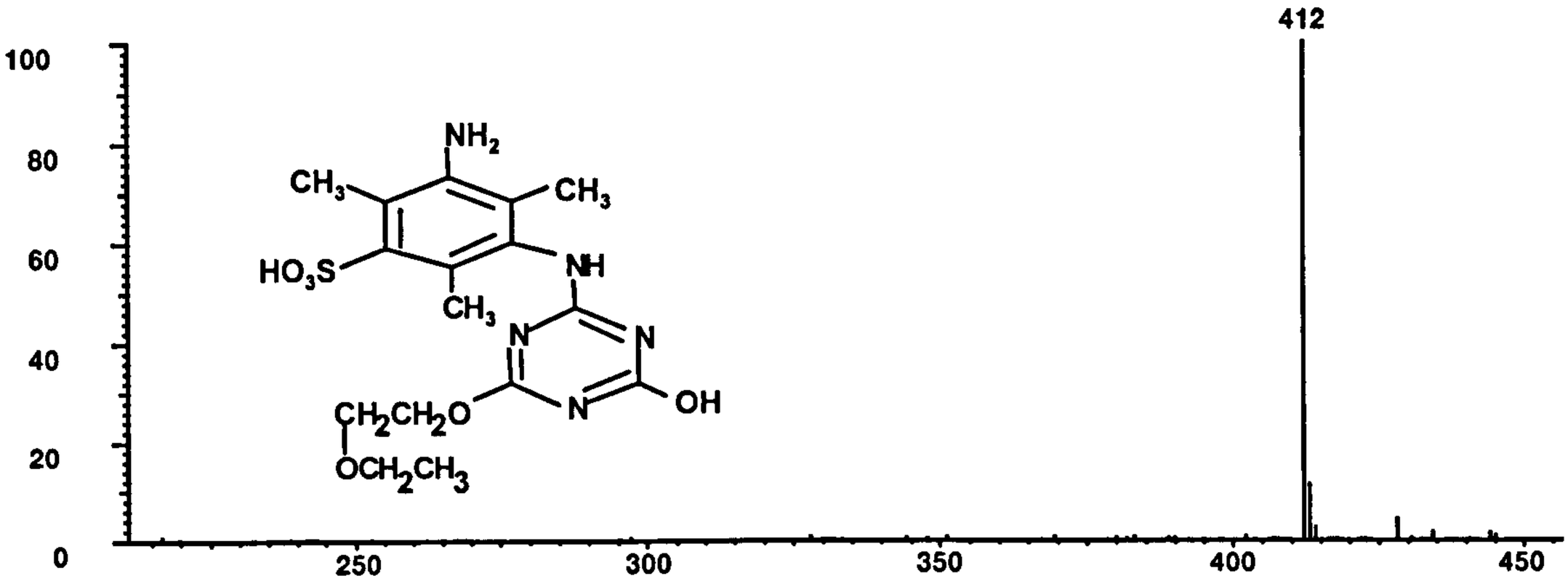

Figure 3.23 Mass spectrum of component II (Figure 3.17) derived from photolysis of W435 for 4 h

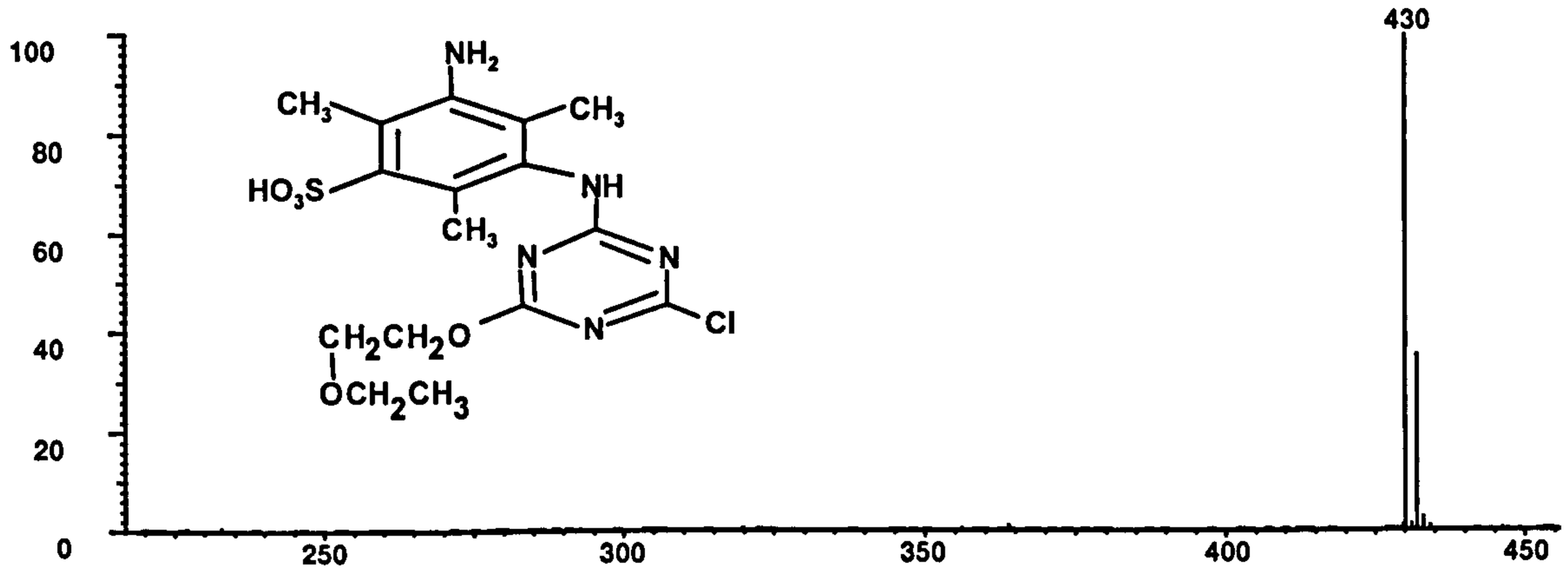

Figure 3.24 Mass spectrum of component IV (Figure 3.17) derived from photolysis of W435 for 4 h

The daughter ion spectra derived from *m/z* 412 and 430 are shown in Figures 3.25 and 3.26.

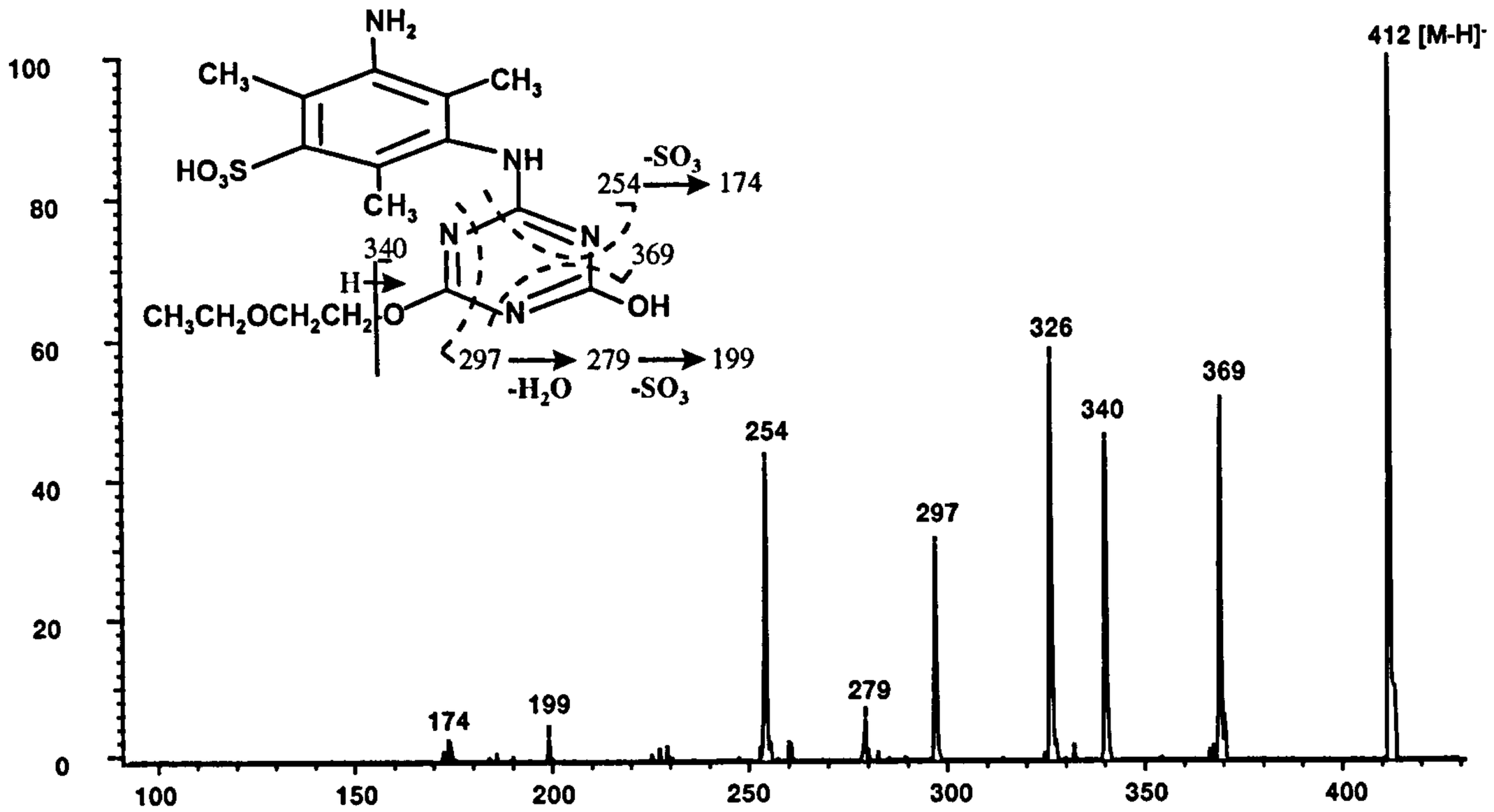

Figure 3.25 Daughter ion spectrum of *m/z* 412 $[M-H]^-$ (component II) derived from photolysis of W435 for 4 h

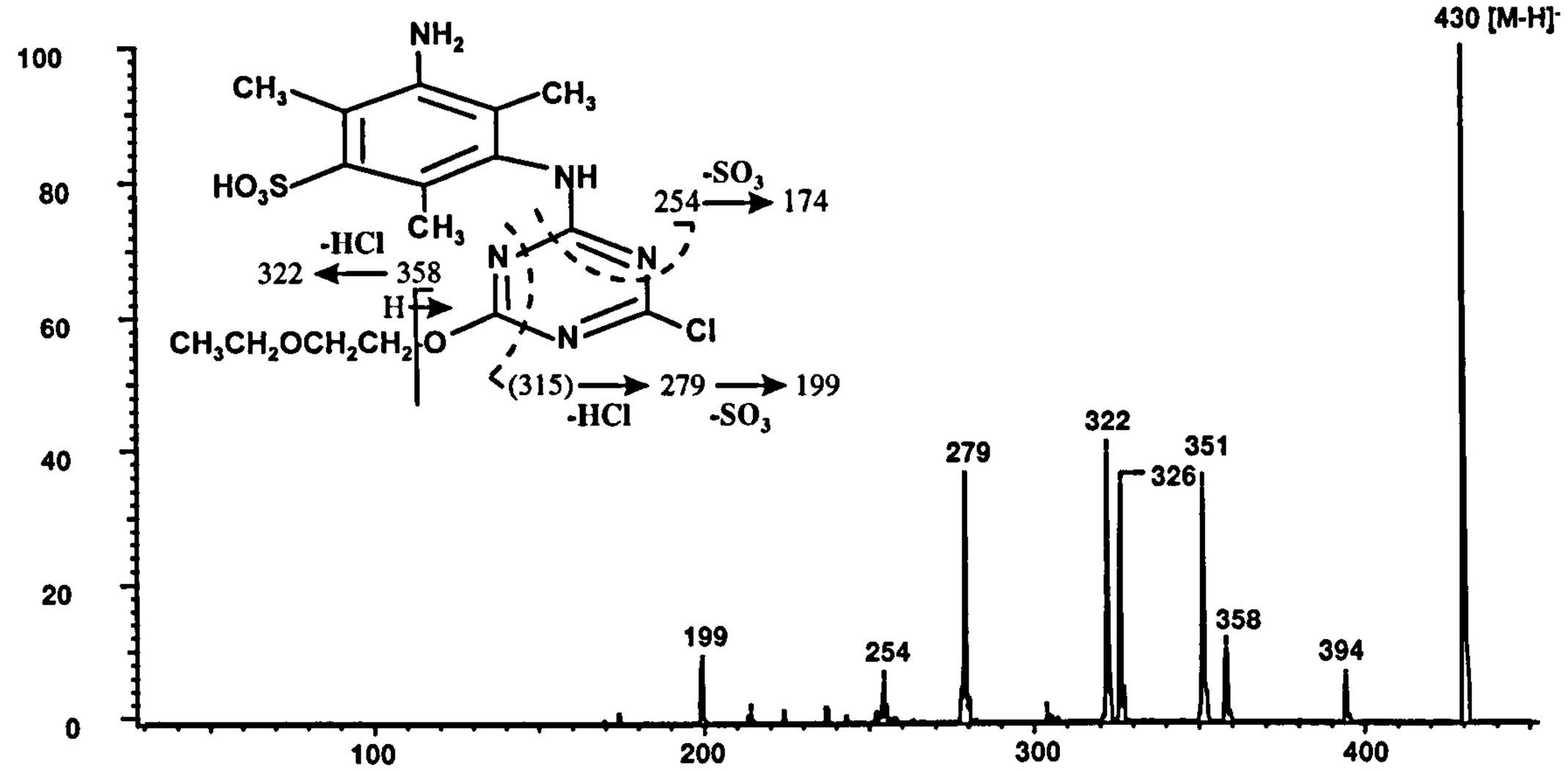

Figure 3.26 Daughter ion spectrum of *m/z* 430 $[M-H]^-$ (component IV) derived from photolysis of W435 for 4 h

It was noticeable that the chlorine present in the latter changed the nature of fragmentation. However losses of 115 and 72 were evident in both spectra, indicating the presence of the ethoxylated side chain. Additionally, both contained a fragment ion at *m/z* 254 which was consistent with:

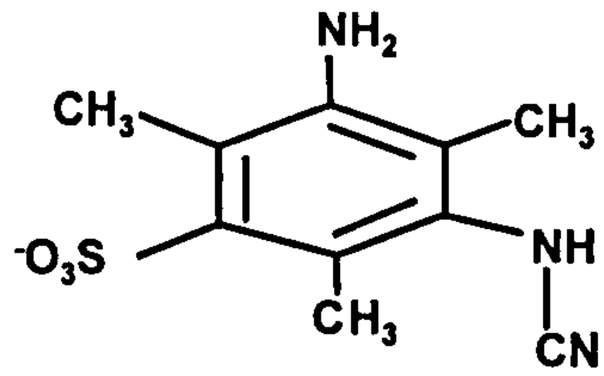

which is the equivalent of the ion *m/z* 555 for compounds I, V and VI. Both of these compounds therefore are derived from loss of the anthraquinone chromophore. This would probably reduce their UV response compared to W435 and may in part account for the "missing" (*viz* under assessed) 30 - 40% of products in the mass balance observed for this experiment.

The mass spectrum derived from the remaining photodegradation product (III; Figure 3.27) contained a base peak at *m/z* 320, with a very weak ion at *m/z* 641. It was difficult to determine whether the former was a singly or doubly charged ion.

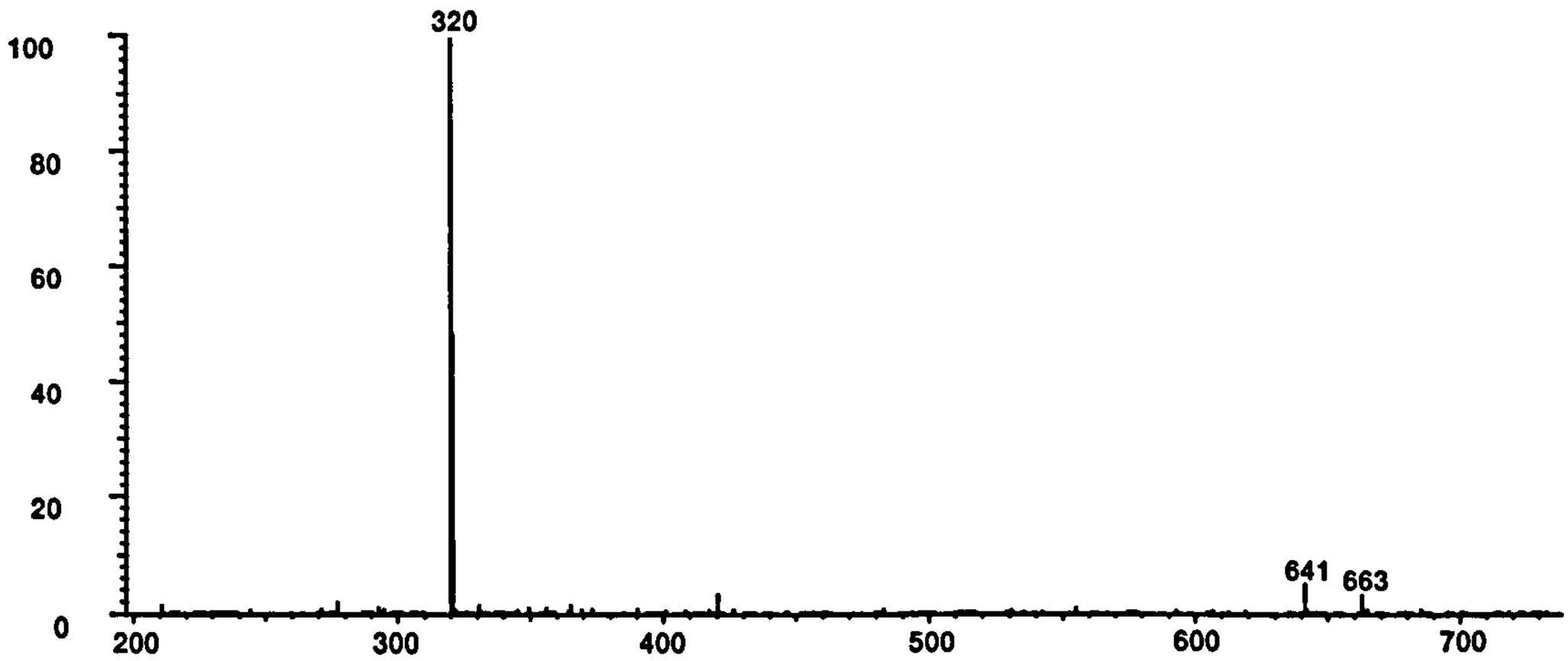

Figure 3.27 Mass spectrum derived from component III (Figure 3.17) derived from photolysis of W435 for 4 h

However, the daughter ion spectrum derived from *m/z* 320 (Fig 3.28) gave fragment ions of higher mass indicating that the parent ion was doubly charged.

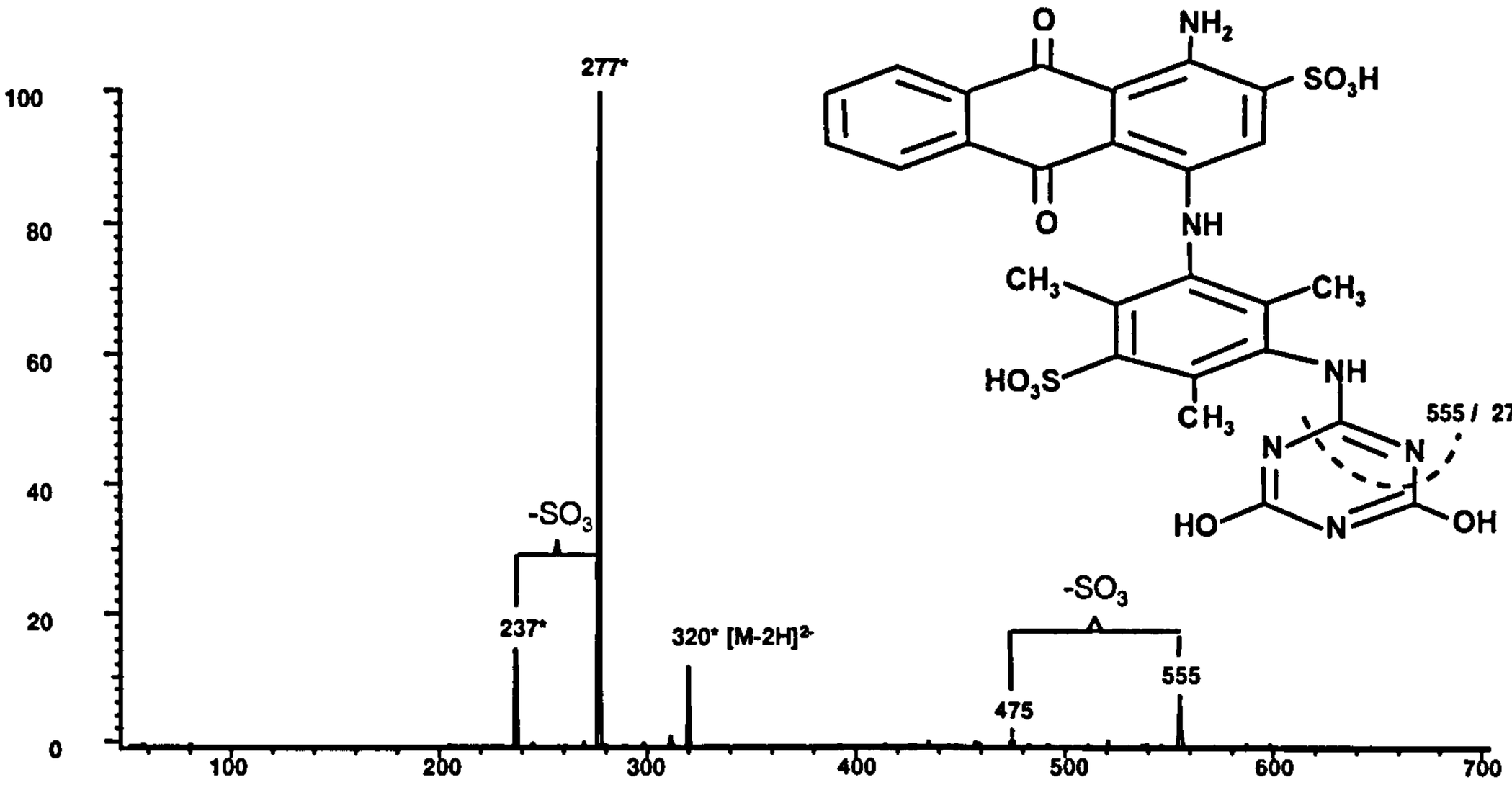

Figure 3.28 Daughter ion spectrum of *m/z* 320 $[M-H]^{2-}$ (component III) derived from photolysis of W435 for 4 h. Note, * denotes doubly charged ions

Once again the characteristic ion *m/z* 555 was observed, indicating the presence of the anthraquinone to triazine group of the molecule. The ion *m/z* 277 was the doubly charged version of the same fragment. There was no evidence for the ethoxylated side chain. A di-hydroxy structure was therefore proposed (Fig 3.28).

Based on the assignments presented, the proposed photodegradation pathway of W435 is shown below:

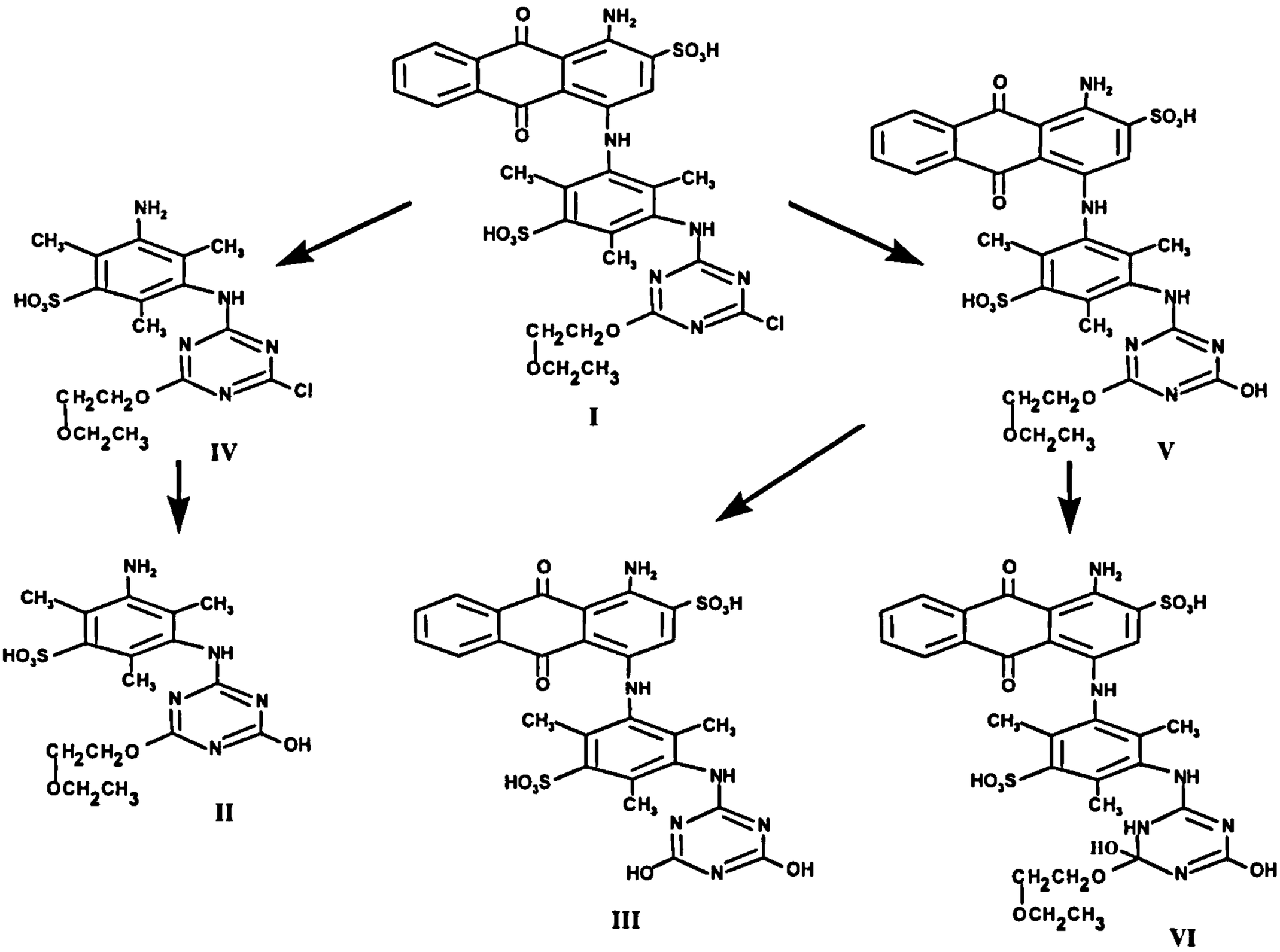

An experiment involving the irradiation of W435 over a prolonged period of time was carried out in order to determine whether the initial photodegradation products identified would degrade further. Figure 3.29 shows the estimated degradation product concentration with increasing irradiation time. The parent dye was rapidly removed and is not shown on this graph.

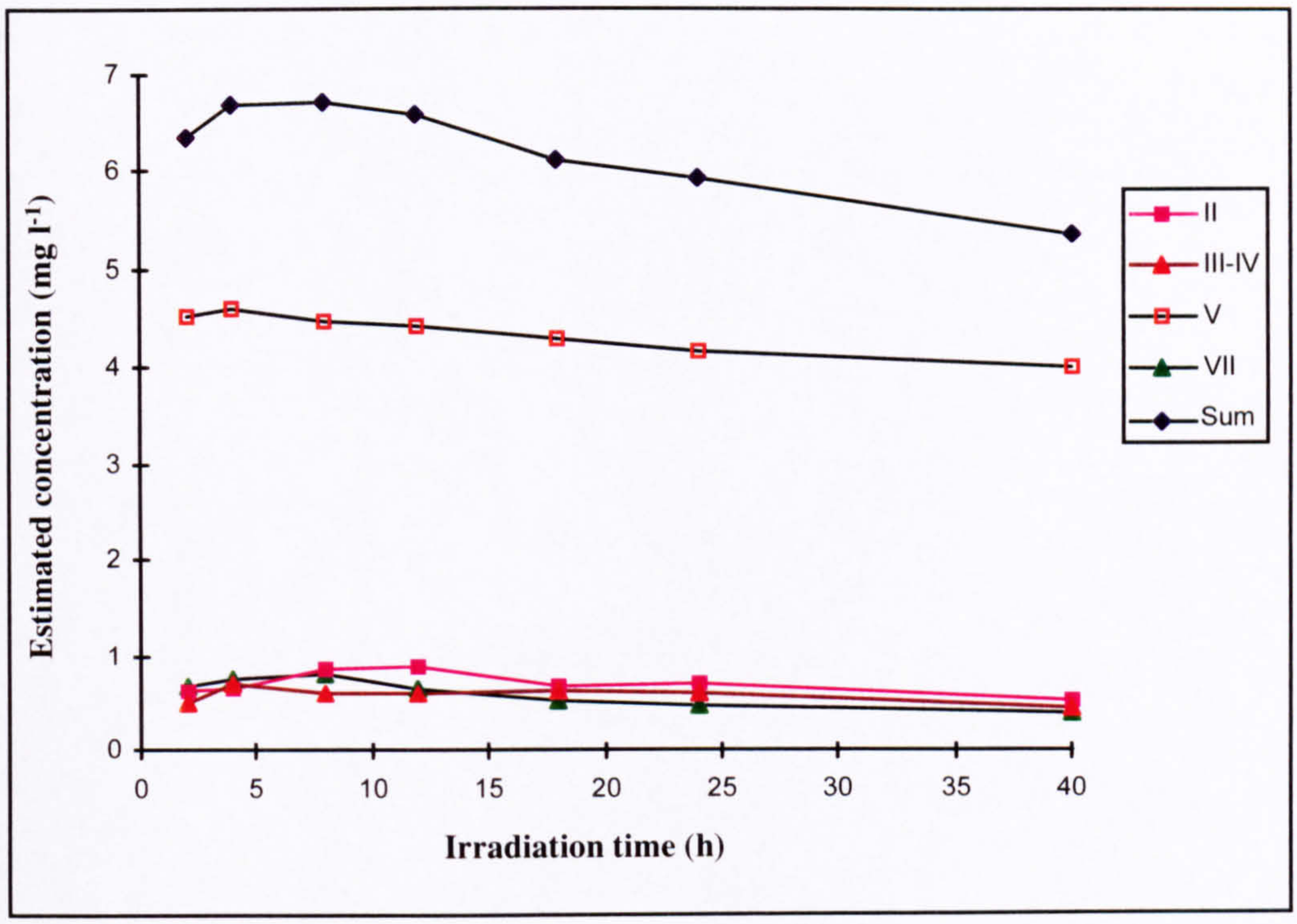

Figure 3.29 Change in concentration of photodegradation products of W435 with increasing irradiation time

Surprisingly the data suggest that following the rapid formation of the initial photodegradation products, further degradation proceeded at a very slow rate. For instance, one might expect product IV, which is chlorinated, to rapidly hydrolyse to product II, but this was not observed. It appears likely that the concentration of oxygen is the limiting factor. Mill (1981) studied the effect of reduced levels of dissolved oxygen in aqueous solution for the photodegradation of benzo[a]anthracene, whereby photodegradation was inhibited when the test sample was nitrogen purged. Sigman (1991) also demonstrated the level of dissolved oxygen to effect both the products and product yield for the photolysis of anthracene. More relevant was a recent study by Aranyosi (1999) which showed the rate of photodegradation of two azo reactive dyes to be accelerated by increasing the concentration of dissolved oxygen.

Relating laboratory xenon lamp to natural sunlight

Whilst the photodegradation rates of two reactive dyes have been determined herein using laboratory simulation experiments with an artificial light source. In order for the data to be used to model environmental scenarios the data need to be compared to those for natural sunlight conditions.

Parker and Leahey (1988), describe how a controlled laboratory experiment for the photolysis of pesticides using the same xenon lamp used herein, could be compared to natural sunlight conditions and how the calculated photodegradation rates could subsequently be used to predict rates at different latitudes and seasons.

In order to establish this relationship it is first necessary to compare the radiation intensity of the xenon lamp to that of midday sunlight at a known latitude (L) and season (S). For instance, UK (approximately 50° North), spring sunlight. These were determined herein using a spectroradiometer, which was able to measure radiation intensity, over the bandwidths of 300 - 800 nm. The ratio (A) of incident xenon light to natural light can then be described by the expression:

$$A = \frac{\text{Measured incident light intensity of xenon burner}}{\text{Measured daylight intensity at latitude (L) for season (S).}}$$

Therefore 12 hours of midday sunlight at latitude L and for season S is equivalent to 12/A hours under a xenon lamp. This ratio is effectively a simple calibration of the xenon lamp against natural light. Referring to Figure 3.30, it is beneficial to carry out this procedure at a season where irradiation is most intense (ie summer or spring) to minimise errors in subsequent calculations.

Parker and Leahey (1988) also reported that based on information from the UK meteorological office, Bracknell, the average radiation for a 12 hour day is approximately equivalent to ¾ of the intensity at midday. Therefore 12 hours of midday sunlight at latitude L and for season S is equivalent to 0.75 x 12/A hours under a xenon lamp, or conversely:

1 h xenon lamp = A/0.75 hours of natural sunlight at specified latitude and season

Parker and Leahey (1988) also described how data published by Mill (1986) and Leifer (1988), and subsequently updated within EPA guidelines (1996), could be used to convert data obtained for the xenon burner to predict photodegradation rates at other latitudes and seasons. These data, first published by Mill (1986) involve the term L_λ, the solar radiance in water, which is proportional to the day averaged radiation from sunlight available to cause photolysis over a 24 hour day at a specific latitude and for each of the four seasons. Calculation of L_λ is based on one specific day in each season as defined by the declination of the sun: -20° (winter), -10° (autumn), +10° (Spring) and +20° (Summer). Values for each season are given in 10° intervals for latitudes from 0 to 70° North. An example of how the values for the sum of L_λ vary from season to season at different latitudes is shown in Figure 3.30. For summer sunlight the intensity of incident radiation does not change significantly from equator to northern latitudes. However a marked difference is observed for autumn and winter seasons.

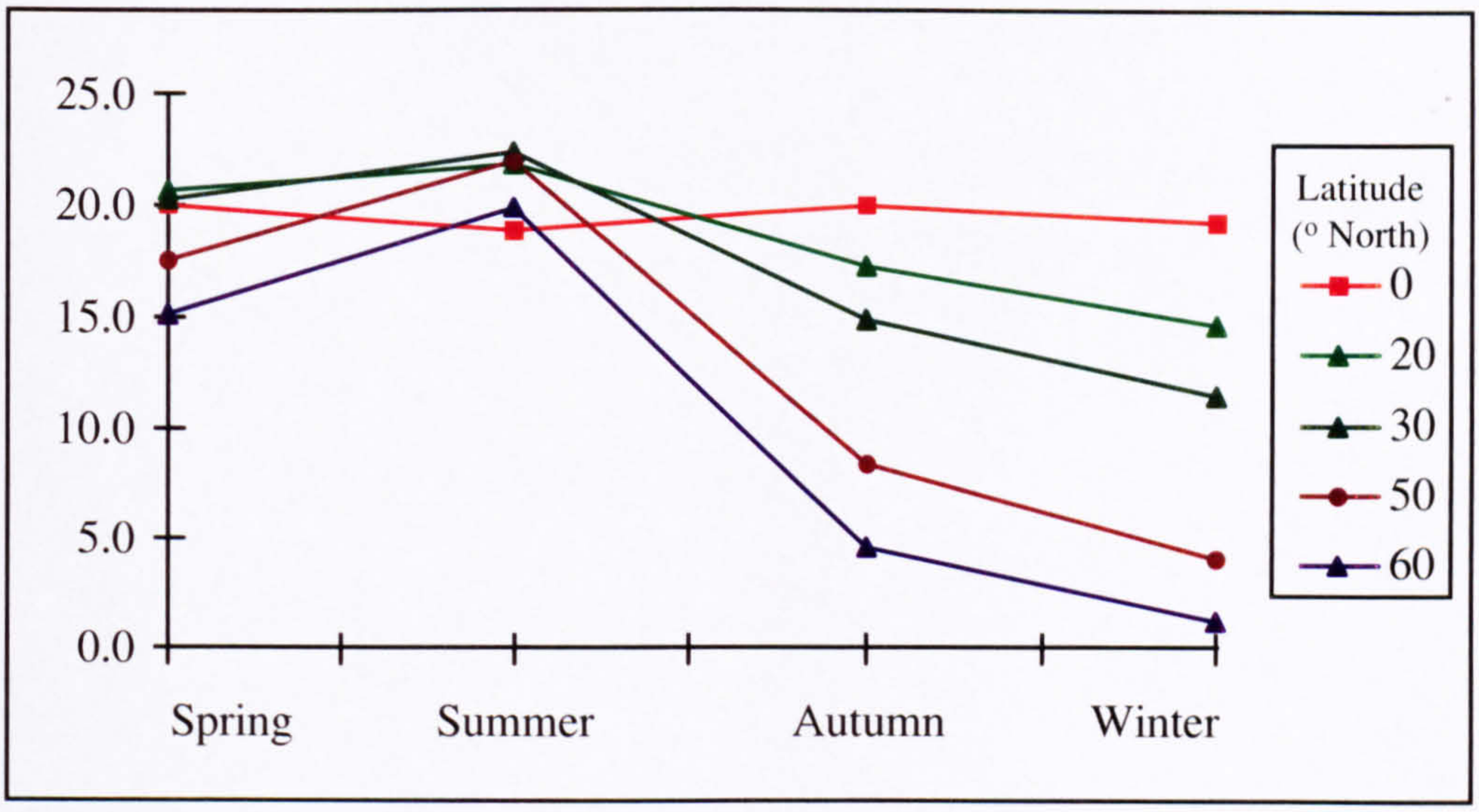

Figure 3.30 Change in $\sum L_\lambda$ for northern latitudes at different seasons

In order to convert measured photodegradation rates expressed for latitudes (L) and for season (S) into rates at another latitudes (L_X) and season (S_X), it is necessary to ratio the sum of calculated L_λ values over the wavelength range of interest:

$$\text{Ratio (R)} = \frac{\Sigma L_{\lambda\,(300\text{-}800\ nm)} \text{ for latitude (L) and season (S)}}{\Sigma L_{\lambda\,(300\text{-}800\ nm)} \text{ for latitude } (L_X) \text{ and season } (S_X)}$$

Therefore one day of sunlight (assumed to be 12 hours) at latitude (L_X) and season (S_X) is equal to:

(12/A x 0.75 x 1/R) hours of irradiation under the xenon lamp, or

1 hour xenon lamp = (A/0.75 x R) hours natural daylight

Example calculation

The intensity of incident xenon burner light for the initial experiments herein was measured as 7.57 mE cm^{-2} day^{-1}, and natural light measured at midday (spring) at Brixham (approximately 50° North), as 14.2 mE cm^{-2} day^{-1}, giving a ratio (A) = 0.533, ie the xenon lamp was less intense than spring midday sunlight.

1 hour xenon burner is equivalent to A/0.75 hours of natural sunlight at specified latitude and season:

0.533 / 0.75 = 0.711 hours Brixham (UK) spring daylight.

The calculated half life for W435 derived from the initial experiment was 1.6 hours, which gives an estimated environmental half life of 1.1 hours for UK spring daylight.

In order to relate this data to other locations around the world it is necessary to ratio the sum of calculated L_λ values over the wavelength range of interest (Leifer, 1988). Typical values are shown in Table 3.6 below.

Table 3.6 Lλ values for 50° North (UK) and 30° North (USA)

λ	Spring 50° North	Summer 50° North	Summer 30° North
297.5	3.61E-06	2.86E-05	1.09E-04
300	3.05E-05	1.50E-04	4.11E-04
302.5	1.54E-04	5.33E-04	1.14E-03
305	5.24E-04	1.39E-03	2.46E-03
307.5	1.32E-03	2.89E-03	4.45E-03
310	2.66E-03	5.05E-03	7.02E-03
312.5	4.53E-03	7.75E-03	1.00E-02
315	6.82E-03	1.08E-02	1.32E-02
317.5	9.34E-03	1.40E-02	1.64E-02
320	1.19E-02	1.71E-02	1.95E-02
323.1	2.25E-02	3.12E-02	3.46E-02
330	8.26E-02	1.10E-01	1.18E-01
340	1.08E-01	1.40E-01	1.48E-01
350	1.22E-01	1.57E-01	1.63E-01
360	1.36E-01	1.74E-01	1.80E-01
370	1.47E-01	1.86E-01	1.91E-01
380	1.57E-01	1.99E-01	2.04E-01
390	1.48E-01	1.87E-01	1.93E-01
400	2.12E-01	2.69E-01	2.77E-01
410	2.80E-01	3.55E-01	3.64E-01
420	2.89E-01	3.65E-01	3.74E-01
430	2.79E-01	3.52E-01	3.61E-01
440	3.31E-01	4.17E-01	4.26E-01
450	3.73E-01	4.69E-01	4.79E-01
460	3.78E-01	4.75E-01	4.85E-01
470	3.90E-01	4.91E-01	5.01E-01
480	4.00E-01	5.03E-01	5.13E-01
490	3.78E-01	4.76E-01	4.85E-01
500	3.86E-01	4.85E-01	4.95E-01
525	1.10E+00	1.28E+00	1.31E+00
550	1.05E+00	1.33E+00	1.36E+00
575	1.05E+00	1.34E+00	1.37E+00
600	1.06E+00	1.35E+00	1.38E+00
625	1.08E+00	1.37E+00	1.39E+00
650	1.10E+00	1.38E+00	1.40E+00
675	1.11E+00	1.39E+00	1.40E+00
700	1.11E+00	1.38E+00	1.39E+00
750	2.15E+00	2.66E+00	2.67E+00
800	2.08E+00	2.57E+00	2.57E+00
$\sum L_{\lambda\,(300\text{-}800)}$	17.5	22.0	22.3

Therefore for a comparison of UK spring daylight (50° North) to Florida daylight (30° North), for instance, the ratio R = 17.5 / 22.3 = 0.78

1 hour xenon lamp = (A/0.75) x R = (0.533 / 0.75) x 0.78 = 0.55 hours natural Florida daylight, which gives a half life for W435 in Florida of 0.89 hour.

Using the same procedure it was possible to estimate the half lives for W433 and W435 for the UK and other countries where azo and anthraquinone dyes are manufactured. Currently these include India, South and Central America, for different seasons of the year.

Two xenon lamp systems were used in the current studies. The lamp for initial studies at Plymouth University had a measured intensity of 7.6 mE cm^{-2} day^{-1}. The system at Brixham laboratory had a newer lamp and was measured at 14.1 mE cm^{-2} day^{-1} which, coincidentally, was very similar to the value measured for natural midday sunlight recorded outside of the laboratory (20^{th} March 2000) as 14.2 mE cm^{-2} day^{-1}. Ideally this measurement should have been taken on the same day as those used to calculate Ll values to enable a more accurate comparison with other latitudes, but this was not possible due to the requirement of having a clear (cloudless) midday sky on the days for which the spectra-radiometer was available to take measurements.

Using the ratio of xenon lamp to natural sunlight, 1 hour of xenon light was equivalent to 0.711 and 1.32 hours of UK spring daylight for the Plymouth and Brixham lamps respectively.

The table below shows the sum of L_λ values (Leifer, 1988) for different latitudes and seasons of the year which have been used in the calculation.

Latitude (°N)	Spring	Summer	Autumn	Winter
50	17.5	22.0	8.4	4.0
40	19.2	22.4	12.0	7.8
30	20.2	22.3	14.9	11.4
20	20.7	21.9	17.2	14.6
10	20.7	20.7	18.8	17.1
0	20.0	18.9	20.0	19.2

The estimated half lives for W433 and W435 are shown in Table 3.7 below:

Table 3.7 Calculated half lives (h) for W433 and W435 for different locations: UK=50° N, Florida=30° N, India 20° N and South America (Brazil) 0°

	Additive	Xenon	UK Spring	UK Summer	UK Winter	Florida Summer	India Summer	India Winter	South America Summer	South America Winter
W433-1		30	21.3	17.0	93	16.8	17.1	25.7	19.8	19.5
		30	21.3	17.0	93	16.8	17.1	25.7	19.8	19.5
W433-2		11.4	15.1	12.1	66	11.9	12.1	18.2	14.0	13.8
	HA	12.1	16.0	12.8	70	12.6	12.8	19.3	14.9	14.7
	FA	12.6	16.7	13.3	73	13.1	13.4	20.1	15.5	15.3
	HA	12.6	16.7	13.3	73	13.1	13.4	20.1	15.5	15.3
	AHA	9.9	13.1	10.5	57	10.3	10.5	15.8	12.2	12.0
W435		1.6	1.1	0.91	5.0	0.89	0.91	1.4	1.06	1.04
		1.7	1.2	0.97	5.3	0.95	0.97	1.5	1.12	1.11

Key: HA River Dodder humic acid, FA River Dodder fulvic acid, Hy River Dodder hydrophilic acid and AHA Aldrich humic acid. W433-1 and W433-2 refer to experiments 1 and 2 respectively.

From these data it is clear that the short half life of W435 indicates that photolysis is a major route of degradation for this dye in the aquatic environment, particularly in summer time for northern Europe and in countries at lower latitudes which have intense sunlight for most of the year. It is important to note that while European and American manufacturing has moved towards azo dyes, anthraquinone dyes such as W435 remain the second most

important class of reactive dyes world wide and they are still widely used in India and South America.

By contrast, W433 is degraded at a much slower rate and it seems less likely from these results that photolysis would be a major route of degradation for such reactive azo dyes. Although Haag (1988) reported a significant increase in degradation rate in the presence of high concentrations of humic substances this did not seem to be the case with the nearly riverine humic substances used herein. Further experiments are required to better understand the relationship between humic substances on photodegradation rates.

3.4.3 Conclusions

A laboratory xenon lamp was successfully used for simulated aqueous photolysis studies of two reactive dyes. The main benefits of the laboratory system were shorter exposure times (unlike sunlight a xenon lamp can be used for 24 hours each day), which is particularly important where test chemicals could undergo non-photolytic degradation in aqueous solution. Studies can be performed at any time of year, which is particularly important for northern latitudes. Unlike natural daylight, the xenon lamp provides a constant exposure and sample temperatures can be closely monitored and regulated, both of which lead to reproducible kinetic data. The correlation coefficients for graphs of change in concentration against irradiation time (Ln (C_t/C_0) vs t) were generally better than 0.99, particularly for the experiments where a laboratory chiller unit was used to carefully control the test vessel temperature. This allowed a reliable comparison between different photodegradation experiments.

Following comparison of the laboratory xenon lamp with natural daylight (Brixham, springtime) it was possible to estimate half lives for both dyes in different parts of the

world and for each season. This rather simple extrapolation relies on several assumptions. The measurements of natural daylight on one day over a very limited time are extrapolated *via* L_λ tables (Leifer, 1988) to a global situation. Hazy conditions, high cloud cover etc could introduce errors in the calculation. Also, the calculations assume the xenon lamp is closely matched to natural light at the wavelengths that excite the target chemical. The spectral comparison shown earlier, (Fig 3.2), clearly shows a good correlation for wavelengths up to approximately 600 nm, but is relatively poor thereafter. Dyes of all colour show absorption over the whole spectrum 300 - 800 nm and therefore could be 'energised' at a wavelength that is not well correlated with natural daylight.

These limitations accepted, this study found that 1 hour irradiation with a xenon lamp was equivalent to 1.04 hours of Southern USA natural sunlight. Data published by Yager (1988) describing a direct comparison of natural sunlight with a xenon source, calculated 9.06 hours of xenon lamp to equate to 12 hours Florida sunlight or 1 hour = 1.3 hours Florida sunlight, which is in very good agreement with the estimates of this study.

Photodegradation was very rapid for the anthraquinone dye W435 for which a $t_{1/2}$ of 1.5 h was determined. The observed degradation pathway indicated cleavage at several parts of the dye structure some of which retained the reactive chlorine. It was interesting that following initial rapid degradation, continued irradiation did not appear to significantly effect the concentration of products.

Further experiments comparing a continuously aerated sample with a nitrogen purged solution may clarify the involvement of oxygen in the degradation process. Photodegradation of the azo dye W433 was significantly slower ($t_{1/2}$ 30 hours) and dechlorination and hydroxylation was the only initial transformation reaction. Extended periods of irradiation (up to 72 hours), produced at least 10 degradation products which

collectively accounted for an estimated 15% of the initial dye concentration. However each component was relatively minor and could not be identified by LC-MS. A further experiment over an extended irradiation time would undoubtedly produce a higher yield of degradation products which could be concentrated by solid phase extraction for MSMS identification.

The addition of humic substances (1 mg l^{-1}) isolated from the River Dodder, Eire, appeared to have either no effect or slightly reduce the rate of photodegradation of W433. Conversely Aldrich humic acid increased the rate of photodegradation. From the limited work reported here and that of Haag (1988), humic acids may have an effect on the rate of photodegradation, either by absorbing energy which otherwise might energise dye material to cause degradation, or by sensitising the photodegradation reaction to encourage a faster rate. Further work, including a broader range of origins and concentration of characterised humic substances is required to better understand their role in photolysis of reactive dyes.

The optimised analytical conditions described in Section 2, LC-UV and LC-MS, were successfully used for the separation concentration and tentative identification of degradation products derived form the photolysis of two reactive dyes.

The proposed structural fragmentation pattern obtained using optimised LC-MSMS parameters were then successfully applied to confirm the structures of proposed degradation products. The triazine ring opening reaction postulated in Section 2, was also observed for degradation products of both W433 and W435 and mass spectra were found to contain useful diagnostic fragment ions for the structural elucidation of this type of reactive dye.

CHAPTER 4.

ANAEROBIC DEGRADATION AND AUTOXIDATION OF AZO DYES

4.1 INTRODUCTION

Decolourisation of azo dyes has attracted considerable attention over the last 20 years. The dyes are generally regarded as being resistant to oxidation by most bacteria under aerobic conditions as used in conventional sewage treatment systems. However, some cleavage of the azo bond of simple azo dyes has been reported under aerobic conditions; this is normally a reductive cleavage (eg Horitsu *et al.*, 1977; Idaka *et al.*, 1978). Aerobic decolourisation by white rot fungi and by lignolytic *Streptomycetes* spp. has been widely reported (eg Paszczynski *et al.*, 1991; Pasti-Grigsby *et al.*, 1992) and mechanisms have been proposed (Goszczynski *et al.*, 1994). These are discussed in more detail in Chapter 5.

Anaerobic reduction of azo dyes is well known. Weber (1995) compared the rate of chemical reduction of a mono azo dye, Disperse Blue 79, with reduction of the dye by the bacteria present in an anaerobic sediment. He concluded that azo disperse dyes are rapidly reduced to their corresponding aromatic amines in anoxic bottom sediments. The reduction of many dyes of commercial importance was reported by Brown and Laboureur (1983). These included Mordant Black 9, Acid Yellow 151, Acid Red 14, Acid Blue 14 and the reactive dyes, Blue 19 and Acid Black. A review (Chung *et al.*, 1992) highlighted the ability of many different bacterial species to reduce azo bonds under anaerobic conditions. These included five species of *Bacillus*, four of *Salmonella* and six *Pseudomonads* amongst several others. The anaerobic reduction of azo dyes using isolates from environmental matrices including soil, polluted river bed, sewage and activated sludge (Wuhrmann, 1980), and from the drainage ditches of a dyestuffs manufacturing factory (Idaka, 1978) was also reported. Nigram (1996) described the isolation of mixed

bacteria cultures from prolonged anaerobic enrichment cultures of dye effluent samples. Complete decolourisation of 5 of 9 azo dyes, including 2 reactive dyes, was reported. Kulla (1984) reported the adaptation of a *Pseudomonas* culture capable of utilising the carboxylated azo dye Orange II (1-(4'-carboxyphenylazo)-2-naphthol), as a sole carbon and nitrogen source. Similarly, an isomer, Orange I (1-(4'-carboxyphenylazo)-4-naphthol) was also reduced by a different *Pseudomonas* culture. However, when the dyes were substituted with their 4'-sulphonic acid analogues, reduction occurred but neither dye could be used as a sole carbon source (ie sulphonation appeared to stop further metabolism). It was unclear as to whether this was due to an inability of the cells to uptake the sulphonilic acid reduction product, or the suspected antibacterial properties of this material. The mode of action of azo reduction was attributed to intracellular azo-reductase enzymes. The enzyme from each *Pseudomonas* strain was isolated and characterised, and found to be highly selective such that each had no cross-reactivity with the others substrate.

Wuhrmann (1980) reported the decolourisation of several sulphonated azo dyes including Acid Orange 7, 29 and 52 and Acid Red 66 using both anaerobic bacteria and aerobic bacteria under temporary anoxic conditions. He determined that dyes that were adsorbed onto the cell walls of bacteria were generally reduced at a much slower rate than those able to permeate into the cell. However, these same adsorbed dyes were readily reduced by extracts of the same bacteria. These data were interpreted by Wuhrmann to indicate that the reduction process was intracellular, non-enzymatic and also that the rate limiting step in azo reduction was the transport of the dye through the cell membrane. Additionally, the presence of sulphonic acid groups on the dye (such as found in acid and reactive dyes) tended to impair permeation of the cell wall which therefore inhibited reduction. Yatome (1991) also concluded that the rate of azo reduction was limited by the degree of sulphonation of the dye and that azo reduction must be intracellular and that permeation

through the cell membrane was the principal rate determining factor. Carliell *et al.*, (1995) reported the use of acclimated anaerobic digester sludge to reduce Reactive Red 141, a high molecular weight diazo dye possessing eight sulphonic acid groups. The rate of reduction was, however, very slow ($K = 0.44\ h^{-1}$) but was greatly increased ($0.012\ h^{-1}$) by the presence of glucose as a supplemental carbon source, an observation also noted by Haug *et al.*, (1991). Carliell *et al.*, suggested this was due to increased production of reduced flavin nucleotides within bacterial cells and this was the rate limiting step for the reduction of dyes and not transport across the cell membrane as previously suggested by Wuhrmann (1980) and Yatome (1991).

Haug *et al.*, (1991) demonstrated the mineralisation of the sulphonated azo dye Mordant Yellow 3. A bacterial consortium capable of mineralising a range of substituted naphthalene sulphonic acids was first pre-adapted to aerobic growth on 6-aminonaphthalene-2-sulphonic acid (the predicted reduction product of Mordant Yellow 3). Mordant Yellow 3 was then successfully reduced by this consortium under anaerobic conditions. The aromatic amine reduction products were then metabolised following the re-aeration of the culture. This provided an anaerobic-aerobic system capable of the complete mineralisation of azo dyes. The ability of the consortia to reduce the azo dye was correlated with the presence of bacterial strain BN6. Nortman, (1994) examined a range of amino and hydroxy substituted naphthalene sulphonic acid compounds (the building blocks of many azo dyes) to establish that most were amenable to aerobic mineralisation by BN6 and similar consortia. More recently, work by Keck *et al.*, (1997) and Kudlich *et al.*, (1997) using the same BN6 strain, has suggested an alternative mechanism for the anaerobic reduction of azo dyes. They have demonstrated that an intermediate formed in the aerobic degradation of naphthalene sulphonic acids can act as a redox mediator which can 'shuttle reduction equivalents' from the cell to the extracellular dye so that it is not always necessary for the dye to penetrate the cell membrane. This may

explain how highly sulphonated poly-azo dyes that cannot penetrate the cell wall may still be reduced by anaerobic bacteria.

As demonstrated by Haag *et al.*, (1991) alternating anaerobic and aerobic conditions may allow an azo bond to be cleaved anaerobically and the resultant aromatic amines to be mineralised aerobically. Seshadri *et al.*, (1994) examined the potential of this approach in a simulated treatment process for the de-colourisation of azo dyes. He used an anaerobic fluidised-bed reactor, followed by a bench scale activated sludge system for subsequent aerobic treatment. Four rather simple sulphonated azo dyes were studied: Acid Orange 7, 8 and 10 and Acid Red 14. All four dyes were reduced using hydraulic retention times (HRT) up to 24 hours. Aerobic treatment then appeared to remove the majority of the primary degradation products but this was only monitored in terms of COD removal and appeared to be inconclusive. A similar approach was adopted by Fitzgerald and Bishop (1995) for the treatment of three simple sulphonated azo dyes: Acid Orange 10, Acid Red 14 and 18. Not only were the dyes reduced in the anaerobic digestor (65 - 90% removal), but so too were the aromatic amine metabolites (>99% removal). This is rather surprising considering most previous work has indicated that aromatic amines do not show significant degradation under anaerobic conditions.

Knapp and Newby (1995) described the successful decolourisation (>85%) of a highly coloured industrial effluent discharge by anaerobic treatment with mixed bacterial consortia derived from a variety of sources. Interestingly, when the decolourised effluent (pale yellow) was exposed to air, it developed a different, much deeper colour which showed a stronger absorbance in the visible region. This suggests the substituted aromatic amines produced by the reduction of azo dyes may then autoxidise to products that are more highly coloured than the starting material.

It is not only in the environment that azo reduction has been reported. Walker (1970) reviewed the mammalian metabolism of azo dyes. He concluded that intestinal azo reduction was considerably more effective and non-specific than the hepatic system. The latter showing negligible azo reductive ability in most animals studied. Metabolism in the intestine was believed to be, at least in part, due to bacteria present in the gut microflora. Similar findings were made by Watabe (1979) in a study of the decolourisation of four sulphonated dyes including Amaranth, Sunset Yellow and Tartrazine, by cultures derived from human faeces. Chung (1978) concluded that because the reduction of azo dyes occurs anaerobically, it is likely to take place in the colon, which is the most anaerobic part of the body. Interestingly, he also suggested that reduction takes place outside of the cell and involves an extracellular shuttle for this to occur. This is consistent with the findings of Keck (1997) and Kudlich (1997), as discussed earlier. In a further study Chung (1992), described the azoreductase(s) catalysed reduction of 27 mono and diazo dyes, many of them sulphonated, using bacteria derived from intestinal microflora.

Most azo dyes are relatively non-toxic. However, on reduction of the azo bond, aromatic amines are released which may be toxic, carcinogenic or teratogenic (Brown and De Vito, 1993). The release of azo dyes into the environment where they can be readily reduced, or the release of their aromatic amine metabolites into the environment is therefore a cause for concern. It is therefore desirable that a means of biological treatment be devised so that potential problems caused by their uncontrolled reduction in the wider environment can be obviated.

4.2 AUTOXIDATION OF AMARANTH, SUNSET YELLOW AND NAPHTHOL BLUE-BLACK

The reduction of dyes has been widely studied as discussed above, and it has been demonstrated that azo-dyes undergo microbial reduction under anaerobic conditions yielding the corresponding aromatic amines. Most industrially applied azo-dyes contain at least one aromatic ring system that carries a hydroxy group in the *ortho*-position to the azo bond to stabilise the compound by the formation of hydrogen bonds (eg Fig 4.1). The corresponding reduction products carry an amino group *ortho* to this hydroxy group on the aromatic ring. It has been suggested that these compounds can undergo autoxidation in the presence of oxygen, although little is known of the constitution and stability of the autoxidation products. The biological and chemical reduction of three model dyes, Amaranth, Sunset Yellow and Naphthol Blue-Black, (Fig 4.1) and the stability and kinetics of autoxidation of their associated reduction products has been investigated recently (Kudlich, 1998), but the identity of these products is unknown.

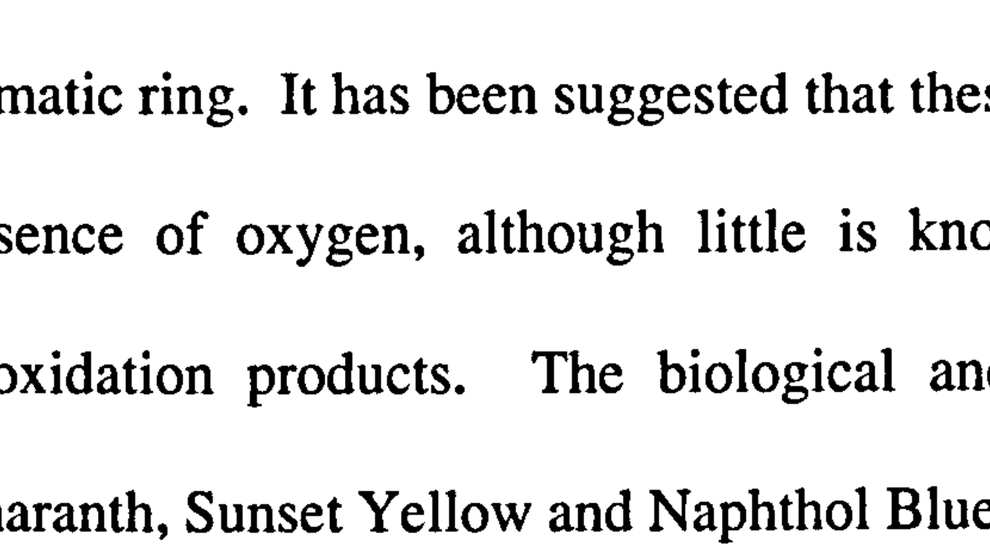

I

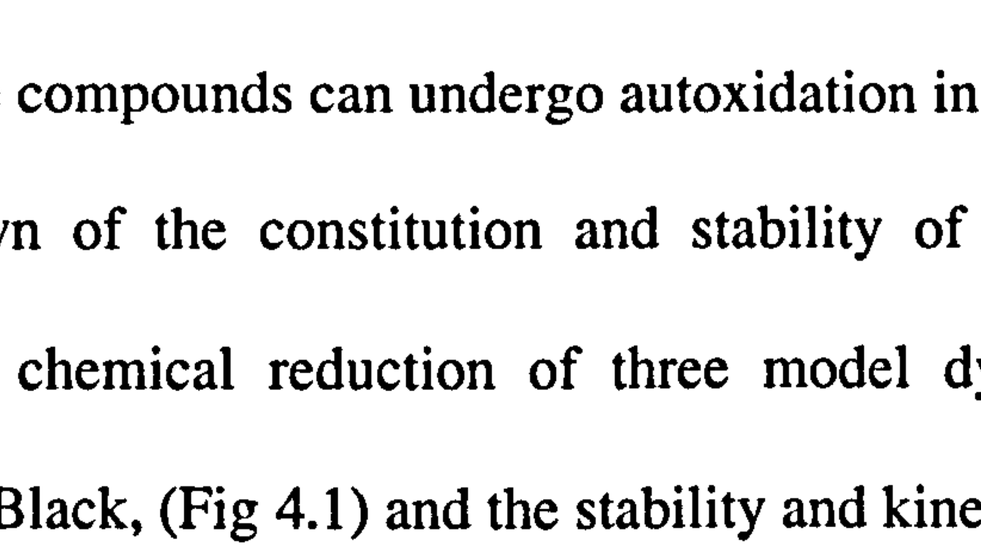

II

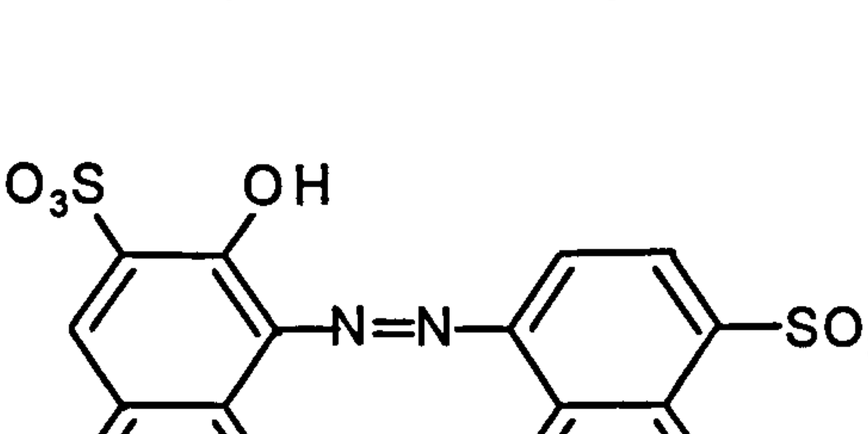

III

Figure 4.1. Structures of (I) Amaranth, (II) Sunset Yellow and (III) Naphthol Blue-Black

Dr Kudlich kindly agreed to supply the same three dyes in their reduced form such that the LCMS methods developed within this project could be used to better understand the autoxidation process.

4.3 METHODS

4.3.1 Reduction of azo-dyes

Reduced dyes (Amaranth, Sunset Yellow and Naphthol Blue-Black) were supplied by kind permission of Dr Michael Kudlich of the University of Stuttgart. These were prepared at the university by catalytic reduction according to the following method:

Stock solutions of each dye (50 ml, 20 mM) were incubated in a hydrogen atmosphere in the presence of palladium on barium sulphate (200 mg). After complete loss of colour, the solution was transferred anaerobically to a rubber-stoppered serum bottle and stored, protected from light, in a nitrogen atmosphere. There was a pressure of 1.5 atm in the bottles to prevent the introduction of air when taking samples. Reduced dyes were then transported to Brixham for analysis.

4.3.2 Autoxidation of reduced dyes

Sub-samples were taken from the stock of reduced Amaranth dye, using a gas tight syringe and spiked into control water (8 ml) to give solutions of approximately 0.5 mM reduced dye in a 10 ml test tube. A stirring bar was used to help aeration of the solution. Aliquots (approximately 1.2 ml) were taken at regular intervals (0, 30, 55, 85 and 105 min) and analysed by LC-Photodiode Array (PDA) and LC-MS. The autoxidation process was

repeated for Sunset Yellow with samples taken at 0, 10 minutes, 1, 4 and 6 hours, and Naphthalene Blue-Black which was sampled following 0 and 45 minutes oxidation only.

4.3.3 Analytical methods

Two liquid chromatography systems were used coupled to photodiode array and mass spectrometer detectors (LC-PDA, LC-MS). Where possible these were used in parallel to allow a direct correlation of UV-visible and mass spectra. Where this was not possible, oxidation experiments were repeated with samples taken at the same time points, and analysed using the same LC column.

The High Performance Liquid Chromatography (LC) system used consisted of a Hewlett Packard 1090 gradient elution pump equipped with a 1100 autosampler (10 µl injection volumes) and photo diode array (PDA) detector. The analytical column used was a 250 × 4 mm, 5 µm, C-18 (Hichrom), operated at 0.7 ml min^{-1}. Separation was achieved by isocratic elution using 100% ammonium acetate (10 mM) as the mobile phase.

The LC-MS system comprised a Waters 600 ms pump with Jasco 851AS autosampler (10 µl injection volume), with a Jasco 875 UV detector operated at 210 nm placed in-line for comparison of UV and MS data. The analytical column and mobile phase were the same as for LC-PDA to allow direct comparison. Mass spectra were obtained using a Finnigan MAT TSQ-700 mass spectrometer fitted with electrospray ionisation (ESI) source operated in negative ionisation mode. The source was operated at a spray voltage of 4.5 kV, with nitrogen sheath and auxiliary gas at 60 psi and 10 psi respectively, and a capillary temperature of 260°C.

The molecular ions observed for the reduction and autoxidation products derived from Amaranth were subjected to MSMS analysis. In each case the singly and/or doubly charged molecular ion was subjected to daughter ion fragmentation using an argon collision gas at 3 mTorr, and collision offset voltages of 15 - 25 eV. The third quadrupole was scanned over the range 30 to 350 mass units at 2 seconds per scan. All other parameters were as stated above.

4.4 RESULTS AND DISCUSSION

4.4.1 Amaranth

LC-PDA Analysis

Amaranth (I) when reduced by hydrogen in the presence of palladium on barium sulphate, produced two products with retention times of 4.1 and 9.3 min respectively when examined by LC-PDA (Fig 4.2).

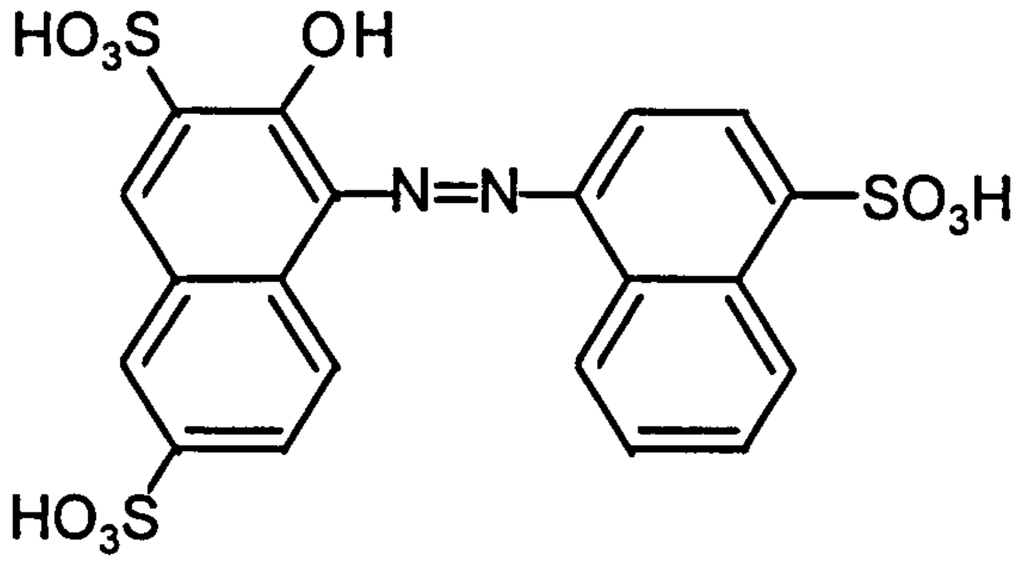

I

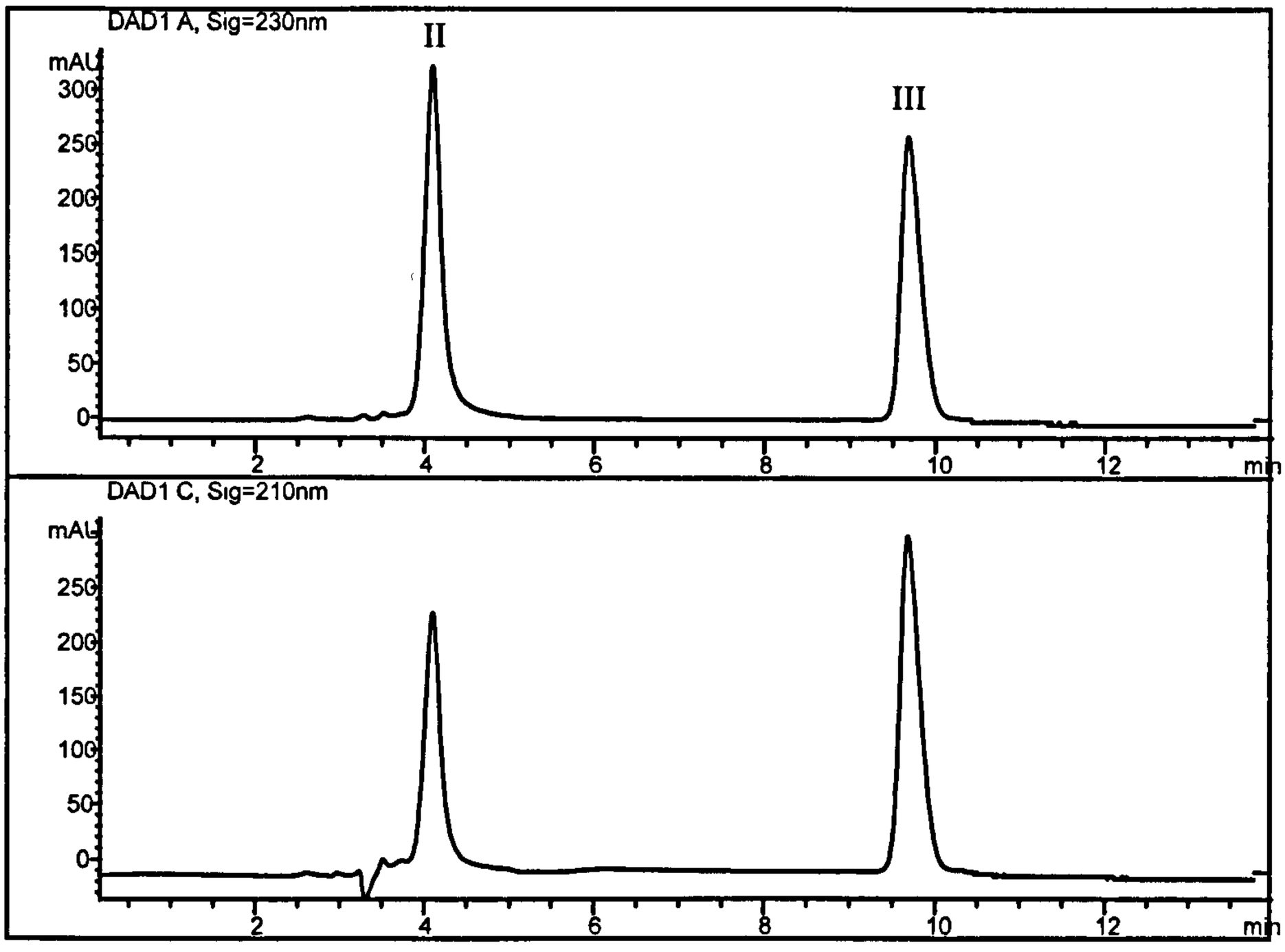

Figure 4.2. LC-UV (230 and 210 nm) chromatogram for reduced Amaranth at time zero (t0)

The reduced Amaranth sample was also analysed using Electrospray (ESI) LC-MS operated in negative ionisation mode. This ionisation mode tends to produce de-protonated molecular ions such that compounds with more than one sulphonic acid group may exhibit both single and doubly charged molecular ions, $[M-H]^-$ and $[M-2H]^{2-}$, depending on whether one or both acid groups are de-protonated. Generally no fragmentation is observed.

The mass spectra of components producing peaks II and III are shown in Figure 4.3. These were consistent with the expected reduction products of Amaranth. The spectra derived from II shows both singly and doubly charged molecular ions at *m/z* 318 and 158.5 indicating two sulphonic acid groups and a molecular weight of 319 which indicates the presence of an odd number of nitrogen atoms and is consistent with 1-amino-2-hydroxynaphthalene-3,6-disulphonic acid (II). The mass spectrum of III shows only one

major ion, *m/z* 222, indicating only one sulphonic acid group and a molecular weight of 223, consistent with 4-aminonaphthalene-1-sulphonic acid (III).

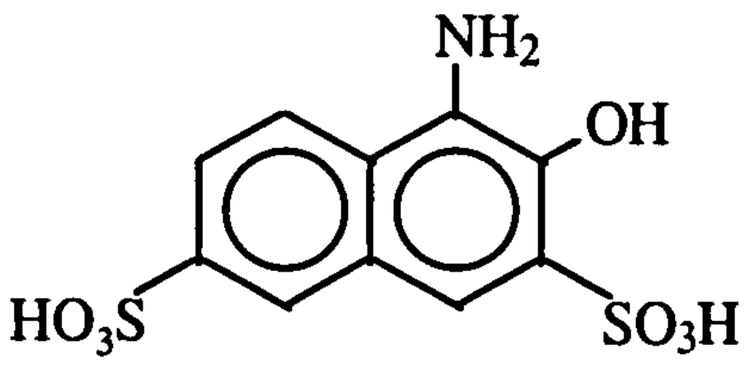

(II)

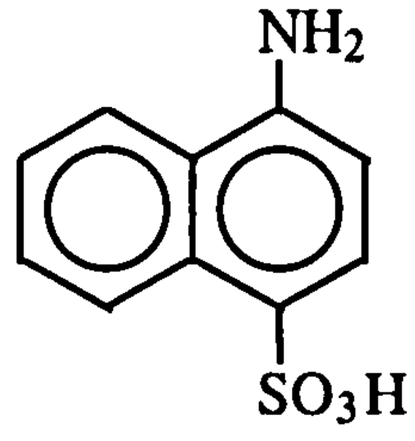

(III)

Useful though the molecular weight information provided by LC-MS is, the data are insufficient for firm identification of analytes. Thus LC-MSMS was employed to provide further structural information. The daughter ion spectra of the singly charged molecular ions for compounds II and III, (*m/z* 318 and *m/z* 222 respectively) were selected. Additionally, the doubly charged ion for peak II (*m/z* 158.5) was also examined to provide further structural information. Daughter ion spectra are shown together with an interpretation of fragmentation patterns in Figures 4.4 and 4.5.

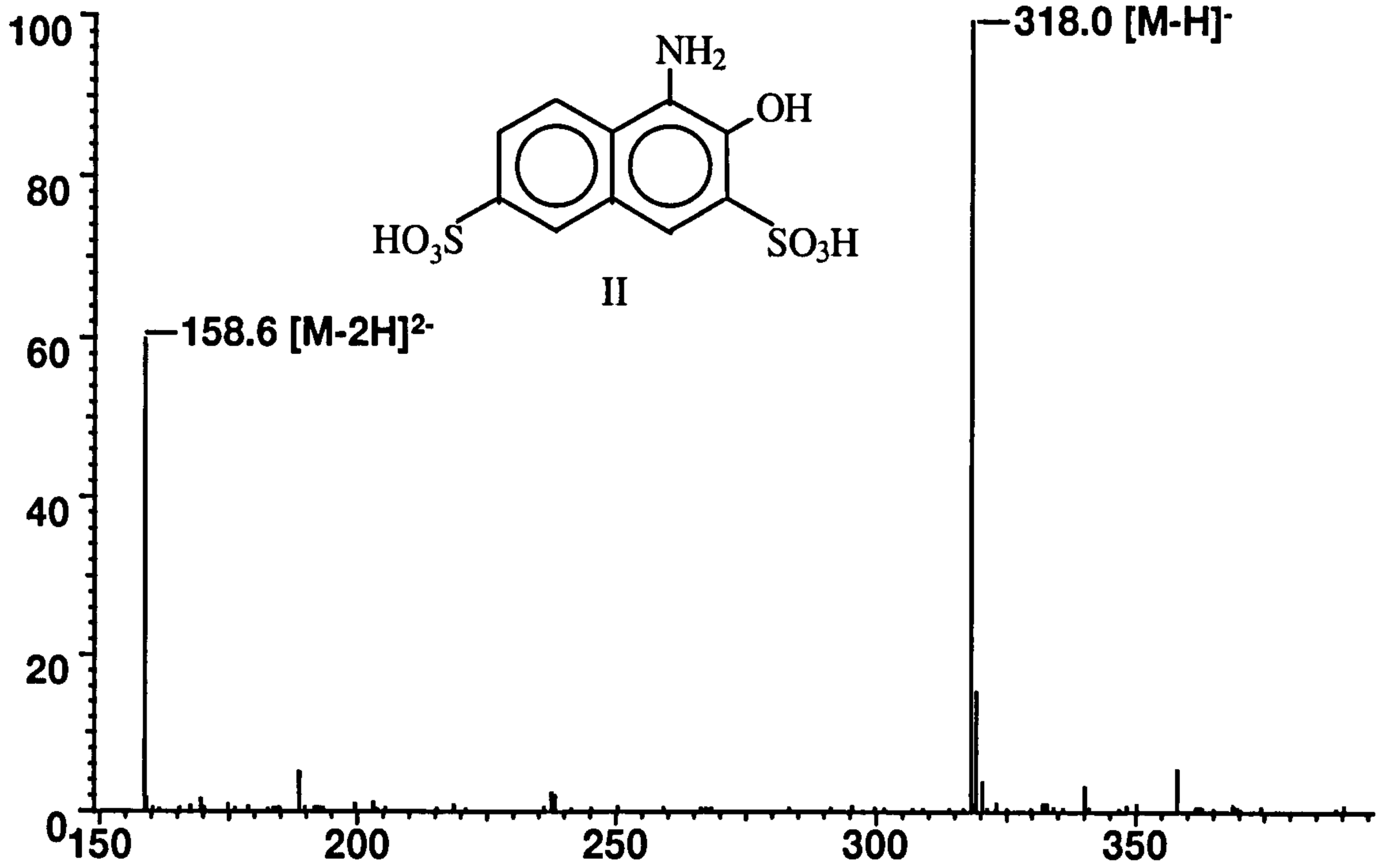

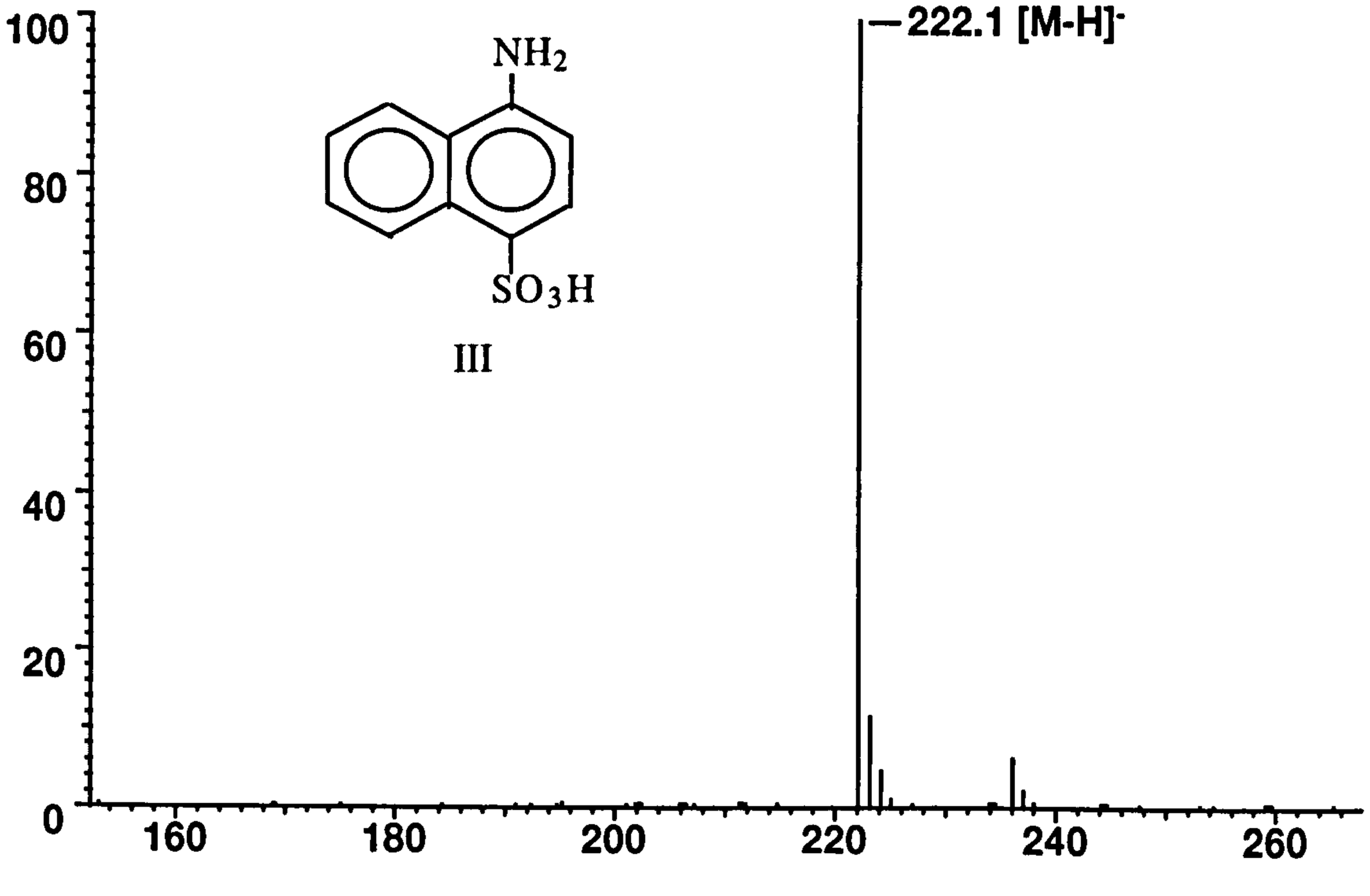

Figure 4.3 Mass spectra derived from peaks II and III for the LC-MS analysis of reduced Amaranth at time zero (t_0)

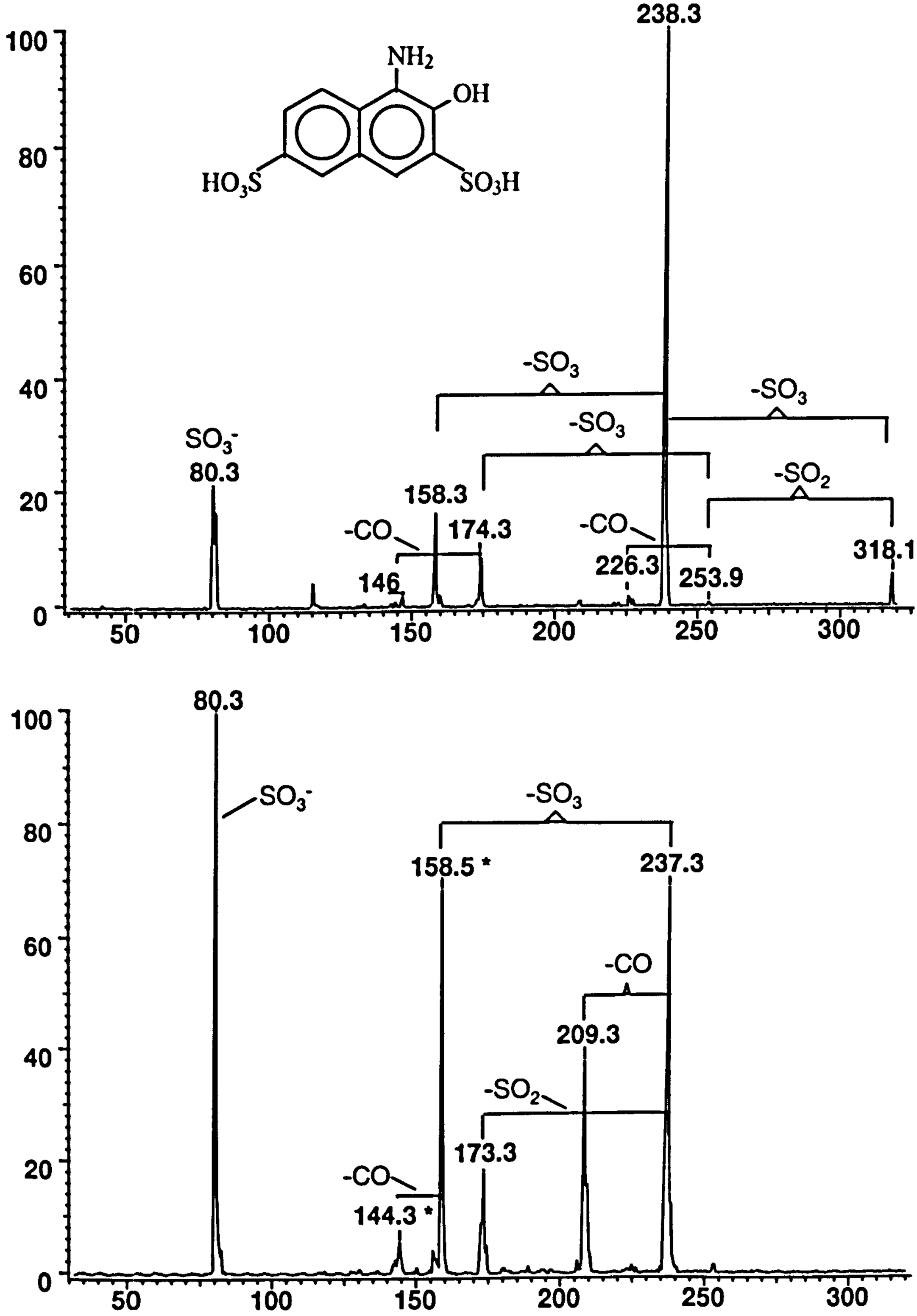

Figure 4.4 Daughter ion spectra for peak II derived from *m/z* 318 ($[M-H]^-$, top) and *m/z* 158.5 ($[M-2H]^{2-}$, bottom. Note * denotes doubly charged ions

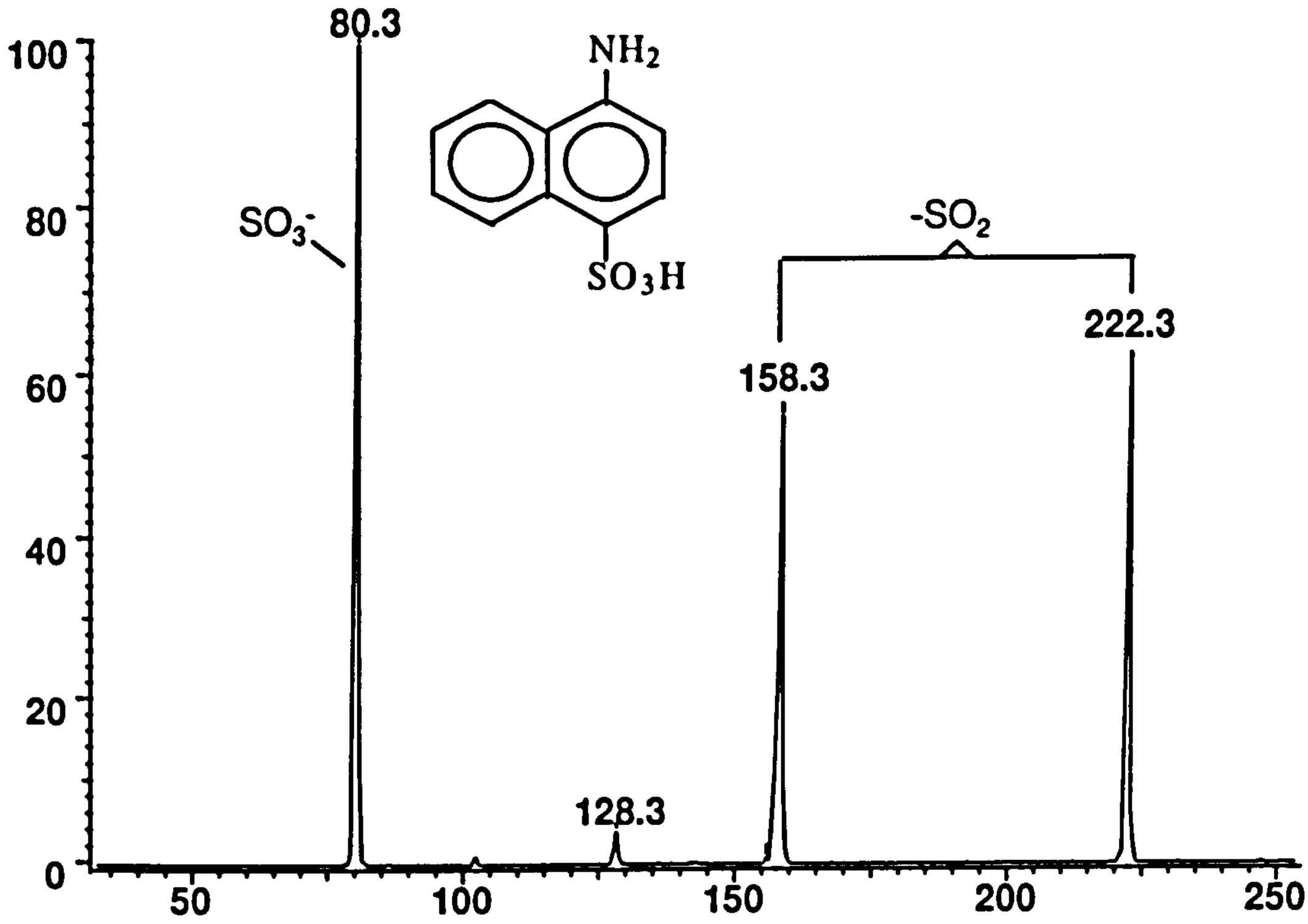

Figure 4.5 Daughter ion spectra derived from *m/z* 222 ($[M-H]^-$) for peak III

The first observation was that all of the MSMS spectra were dominated by ions associated with sulphonate groups. These were generally observed as ions at *m/z* 80 $[SO_3]^-$, and losses of $[SO_3]$ (80), and $[SO_2]$ (64). The latter was formed by a re-arrangement resulting in formation of a phenolate anion:

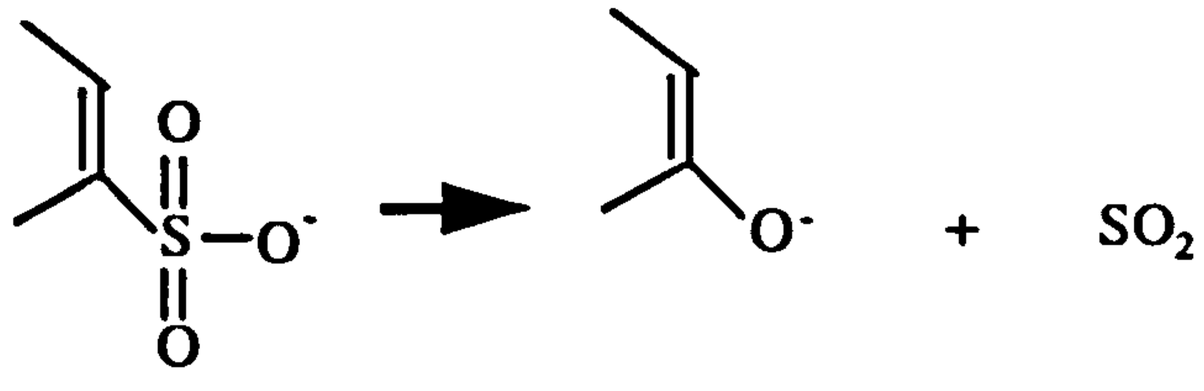

This was generally followed by loss of 28 mass units due to expulsion of carbon monoxide.

Unfortunately, the suspected nitrogen containing amines II and III did not produce any significant fragment ions derived from loss of a nitrogen containing molecule, which would have provided a useful diagnostic tool for MSMS interpretation of amines. MSMS

fragmentation generally produces loss of a neutral molecule, which for a singly charged ion would be of odd mass if the loss contained nitrogen. However, these were not observed. The mass spectra, Figures 4.4 (peak II) and 4.5 (peak III), contained fragment ions associated with the sulphonate groups only.

Additional structural information can sometimes be provided by daughter ion spectra derived from the doubly charged molecular ion species. The daughter ion spectrum derived from *m/z* 158.5 together with assignments for the associated fragmentation is shown in Figure 4.4. It should be noted that for MSMS of a doubly charged species, loss of a charge carrying fragment ion such as SO_3^-, changes the charge state of the remaining ions from two to one. Fragment ions, because they become singly charged appear at higher mass to charge ratio than the parent ion. Thus in the MSMS spectrum of *m/z* 158.5, Figure 4.4, loss of SO_3^- (80 mass units) from the parent ion (*m/z* 158.5) produces an ion of mass 237 (2*158.5-80). Interestingly and unlike the equivalent fragmentation pattern derived from the singly charged molecular ion, loss of CO from the phenolic -OH is observed, (158.5 → 144 (doubly charged) and 237 → 209).

A comparison of LC-PDA chromatograms for each of the reduced Amaranth samples exposed to air over a period of 0 to 105 minutes, are shown in Figure 4.6. The measured peak area of 4-aminonaphthalene-1-sulphonic acid, peak III, (not shown in figure to allow an expanded view of the reaction products of interest), remained constant over the duration of the experiment, indicating that it was not oxidised. At time 0, only the two proposed reduction products, II, (RT 4.1 min) and III, (RT 9.7 min) were observed. Little change was seen in the sample following 30 minutes oxidation. Two small peaks (IV, 3.3 min and V, 3.55 min) were observed after 55 minutes oxidation. These became more prominent in the sample oxidised for 85 minutes and were joined by two further peaks (VI and VII, RT 2.9 min and RT 3.8 min respectively). Here, Peak II had noticeably degraded, now

being approximately 20% of its original intensity. Following 105 minutes of oxidation the original reduction product was totally transformed and one major autoxidation product remained (VI, RT 2.9 min), together with an additional minor product (VIII, RT 2.6 min). These data suggest the initial reduction product 1-amino,-2-hydroxynaphthalene disulphonic acid, II, is rapidly oxidised, *via* a collection of at least four transient intermediates, to one major, relatively stable, product.

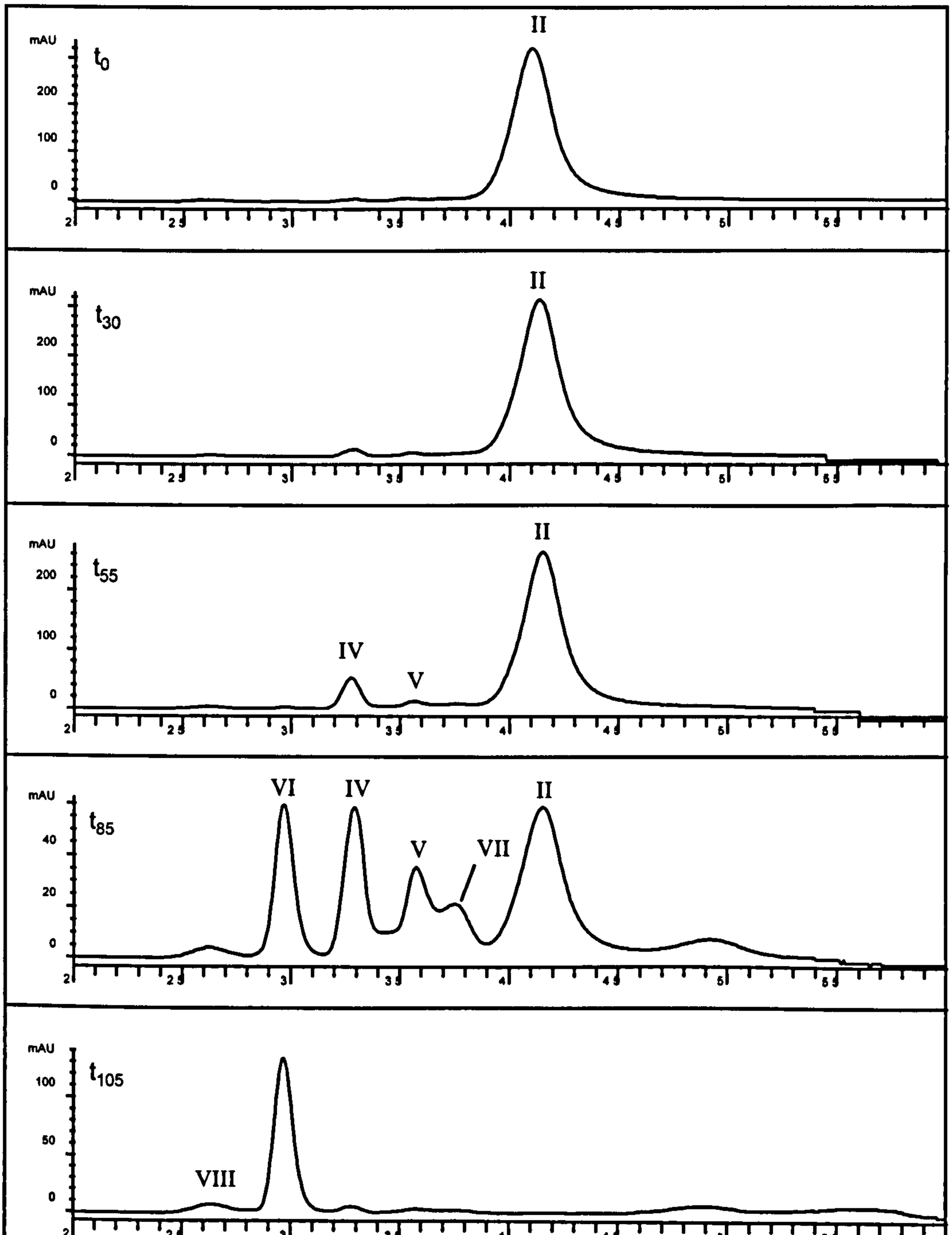

Figure 4.6. HPLC-UV chromatogram (230 nm) of reduced Amaranth following exposure to air for 0, 30, 55, 85 and 105 minutes

A graphical representation is shown in Figure 4.7. This clearly shows the removal of the initial reduction product II, and formation of intermediates IV, V and VII, which in turn are degraded to a final, relatively stable compound VI. The formation of a further product, VIII, is interesting but the experiment was not continued beyond 105 minutes. Kudlich (personal com.) suggested compound VI is the only prominent degradation product after the initial transformations and that this is stable for greater than 11 hours.

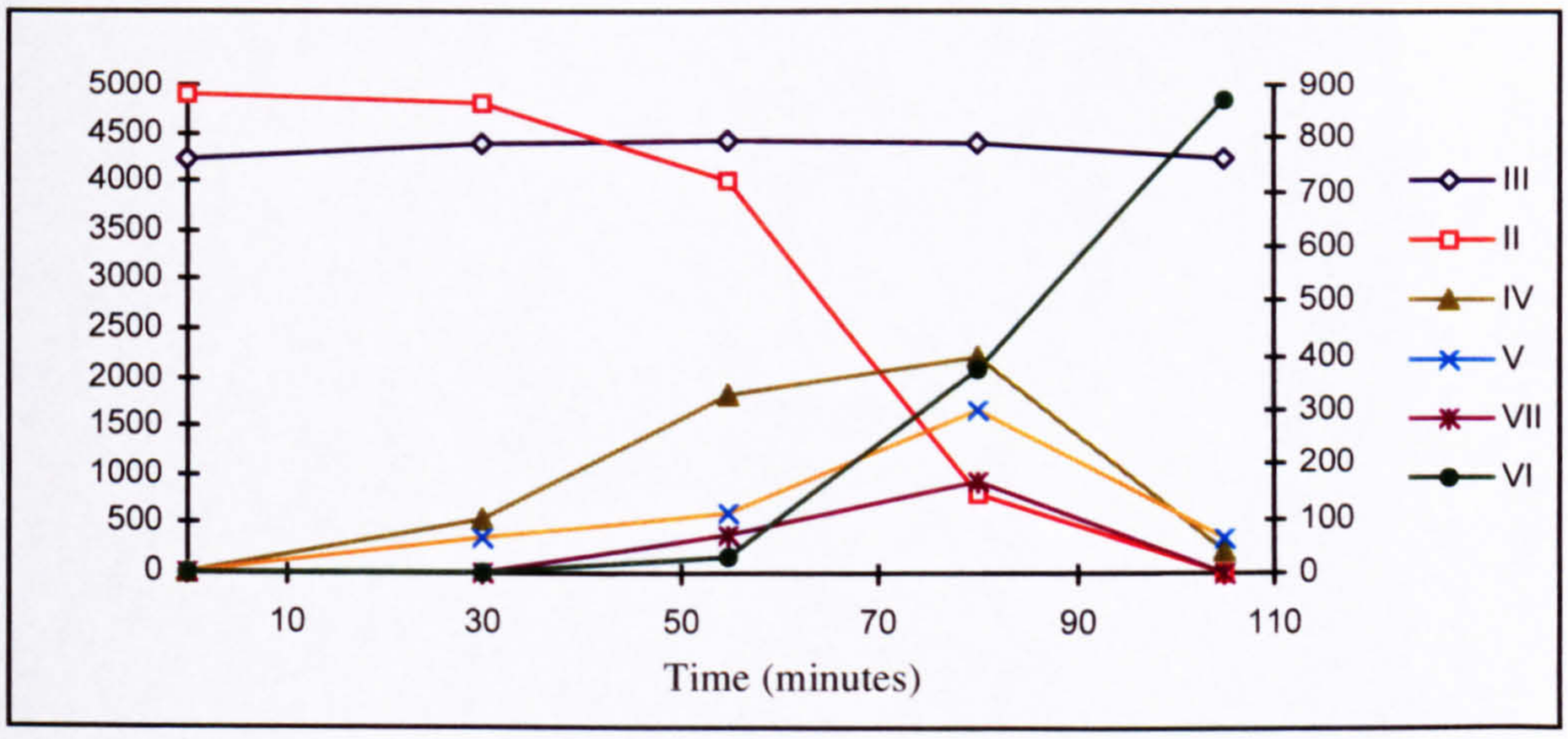

Figure 4.7. LC-UV(230 nm) Peak areas for each component found in the autoxidation of Amaranth

One of the major benefits of photodiode array is the ability to acquire UV spectra of the components separated by HPLC. The wavelength maxima derived from the UV-visible spectra obtained for the two reduction products and major autoxidation products are summarised in Table 4.1.

The main aim of this experiment was to identify the transition and stable degradation products (I - VIII) produced from the autoxidation of the reduction products of Amaranth and through this to better understand the processes that may occur with more complex dyes. Therefore LC-MS was used in parallel with the LC-PDA analysis to provide molecular weight information for each of the oxidised samples. In-line UV (230 nm) was used with LC-MS to provide a real time comparison of UV and MS data. Reconstructed

ion current (RIC) and selected mass chromatograms ($[M-H]^-$ molecular ions) for major components in the Amaranth sample oxidised for 85 minutes, were compared to the in-line UV signal in Figure 4.8. Care has to taken here, because several of the observed molecular ions are of similar mass (ie *m/z* 316, 317, 318 and 319). Each of these will exhibit an ion 1 mass unit higher than the molecular ion because of the naturally occurring ^{13}C isotope (1.1 times number of carbon atoms, expressed as % of ^{12}C isotope), and 2 mass units higher due to sulphur isotopes (4.4 times number of sulphurs, expressed as % of ^{12}C isotope). Thus isotopes associated with the component producing the molecular ion at *m/z* 316 will also have a contribution to the *m/z* 317 (approximately 11%) and *m/z* 318 (approximately 9%) mass chromatograms.

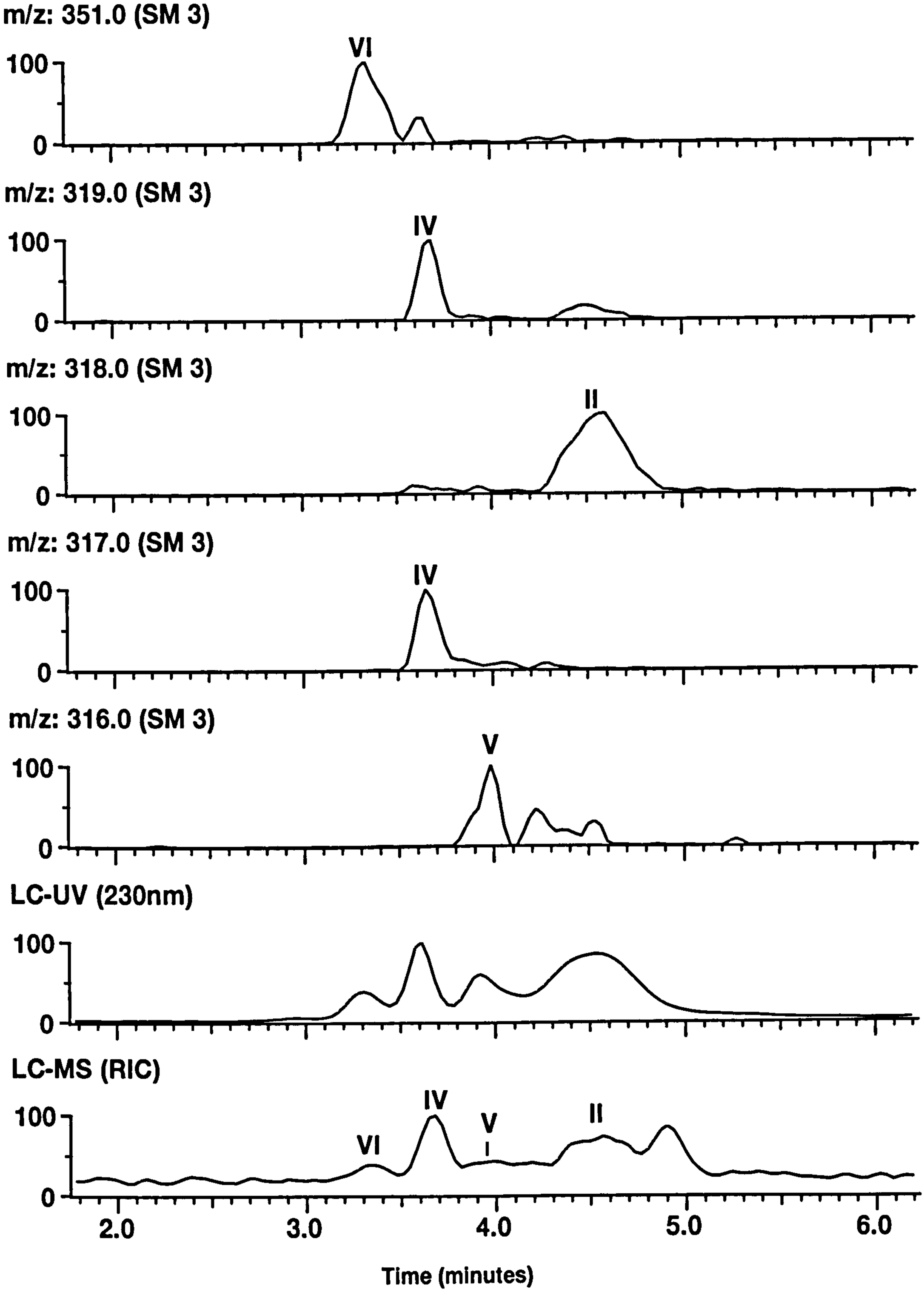

Figure 4.8. LC-MS chromatograms for reduced Amaranth following exposure to air for 85 minutes, (Peak III, RT 9.7 min, not shown to clarify region of interest)

Comparison of the LC-MS in-line UV chromatogram to that obtained by LC-PDA, (Figs 4.8 and 4.6 respectively), shows that the chromatographic resolution was significantly worse for the LC-MS analysis. Peaks IV and VI, for instance, were not base

line resolved. However, one of the advantages of mass spectrometry is the ability to use selected mass chromatograms to differentiate the molecular ions of interest from co-eluting components. Thus it was possible, using mass chromatography, to measure the peak area of each of the identified components in each of the oxidised samples. The results are shown graphically in Figure 4.9. Interestingly, peak IV was found to consist of two components, which could not be perceived from LC-PDA analysis.

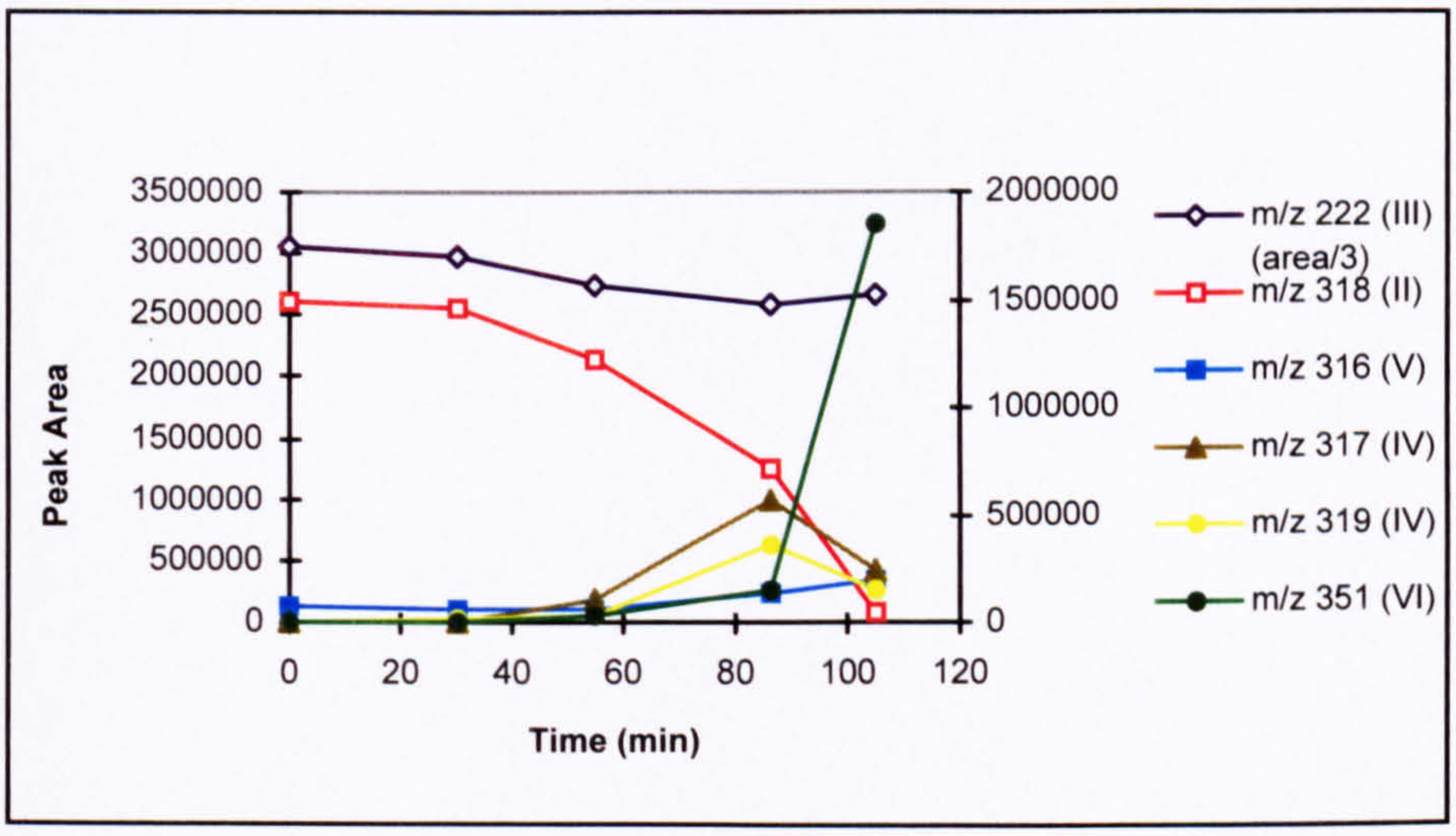

Figure 4.9. LC-MS Peak areas for the major components found for reduced Amaranth following exposure to air for up to 105 minutes

From these data it was possible to correlate LC-PDA peaks to those observed in LC-MS data. These have been summarised in Table 4.1.

Table 4.1. Summary of LC-UV and HPLC-MS data for each peak produced by oxidation of the reduction products of Amaranth.

Peak	Retention time (min)		Peak Information		
	LC-PDA	LC-MS	UV/vis λmax (nm)	MS $[M-H]^-$	$[M-2H]^{2-}$
II	**4.1**	**4.3**	**220/250/300-380**	**318**	**158.5**
III	**9.8**	**10.5**	**220/240/320**	**222**	
IV	**3.3**	**3.6**	**210/260/310-380**	**317** **319**	**158** **159**
V	**3.6**	**3.8**	**210/260/320-420**	**316**	**157.5**
VI	**2.9**	**3.3**	**215/260/300**	**351**	**175**
VII	**3.7**	**not observed**	**215/260/320-420**	**n/a**	

The initial autoxidation product (peak IV in Figure 4.3, RT: 3.27 min) had a UV/VIS-spectrum typical of quinones, ie with a broad λmax in the range of 300 - 400 nm. The corresponding mass spectrum, Figure 4.10, indicated the presence of two compounds. The first showed molecular ions at *m/z* 158 $[M-2H]^{2-}$and 317 $[M-H]^-$ suggesting a molecular weight 318 with two sulphonic acid groups and the even molecular weight indicating no nitrogen. This was consistent with 1,2-naphthoquinone-3,6-disulfonic acid (IVa). Co-eluting with this peak in the LC-MS chromatogram was a compound with molecular ions at *m/z* 159 and 319, molecular weight 320. These data were consistent with 1,2-dihydroxynaphthalene-3,6-disulfonic acid (IVb), the reduced form of 1,2-naphthoquinone-3,6-disulfonic acid (IVa). Since quinones are known to readily interconvert to hydroquinones (Morrison and Boyd, 1977), often acting as reducing agents and quinones in general act as redox-mediators, it seems probable these exist in equilibrium as the reduced (hydroquinone) and oxidized (quinone) form in aqueous solution.

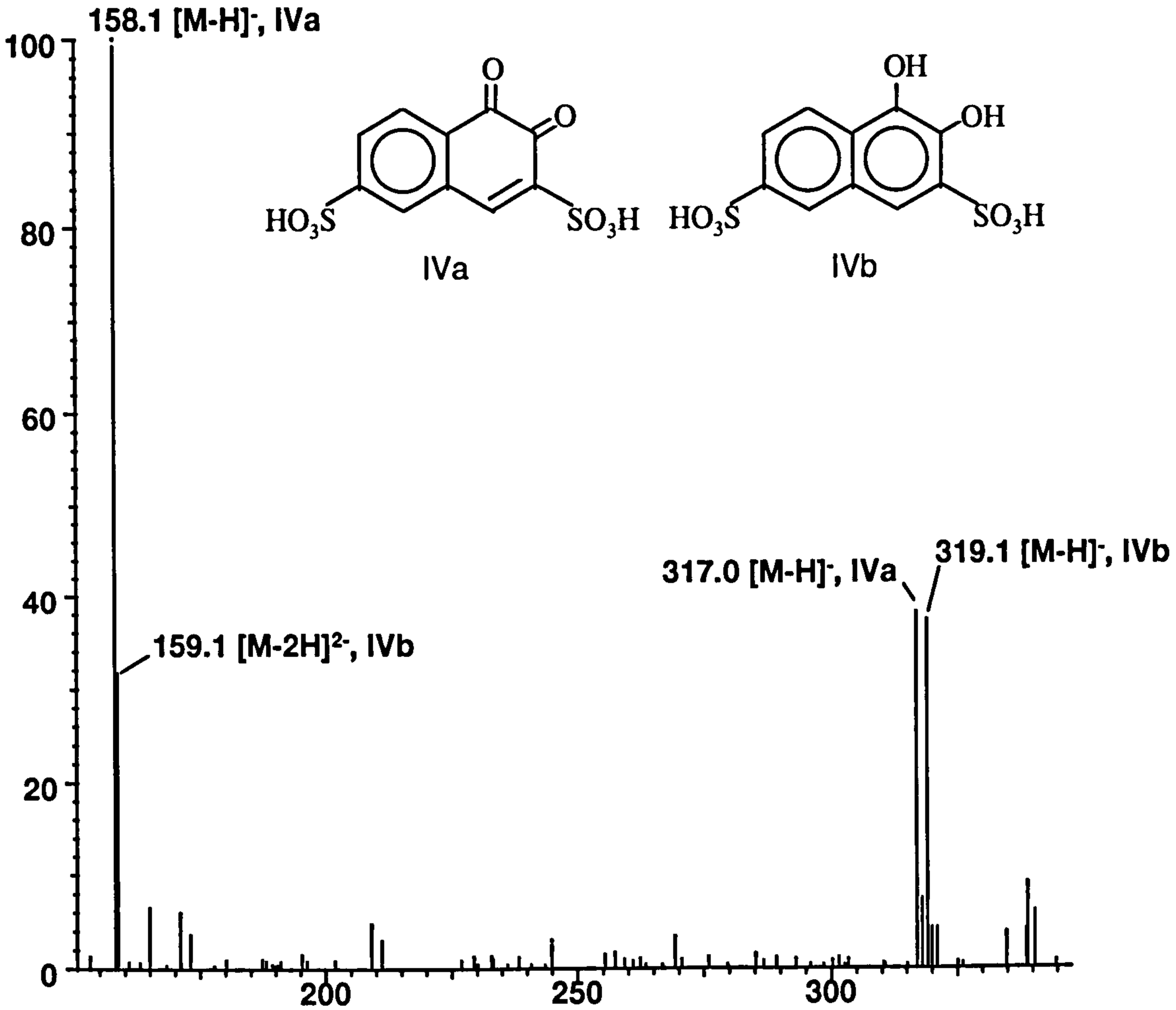

Figure 4.10 Mass spectrum derived from peak IV in reduced Amaranth sample following exposure to air for 85 minutes

The daughter ion spectrum derived from the molecular ion *m/z* 317 is shown in Figure 4.11 together with proposed fragmentation which supports the proposed structure. The observed characteristic loss of carbon monoxide from the molecular ion (317 → 289) is important. This direct loss is an important diagnostic marker for compounds containing a carbonyl group and phenols, and is in agreement with the proposed structure (IVa).

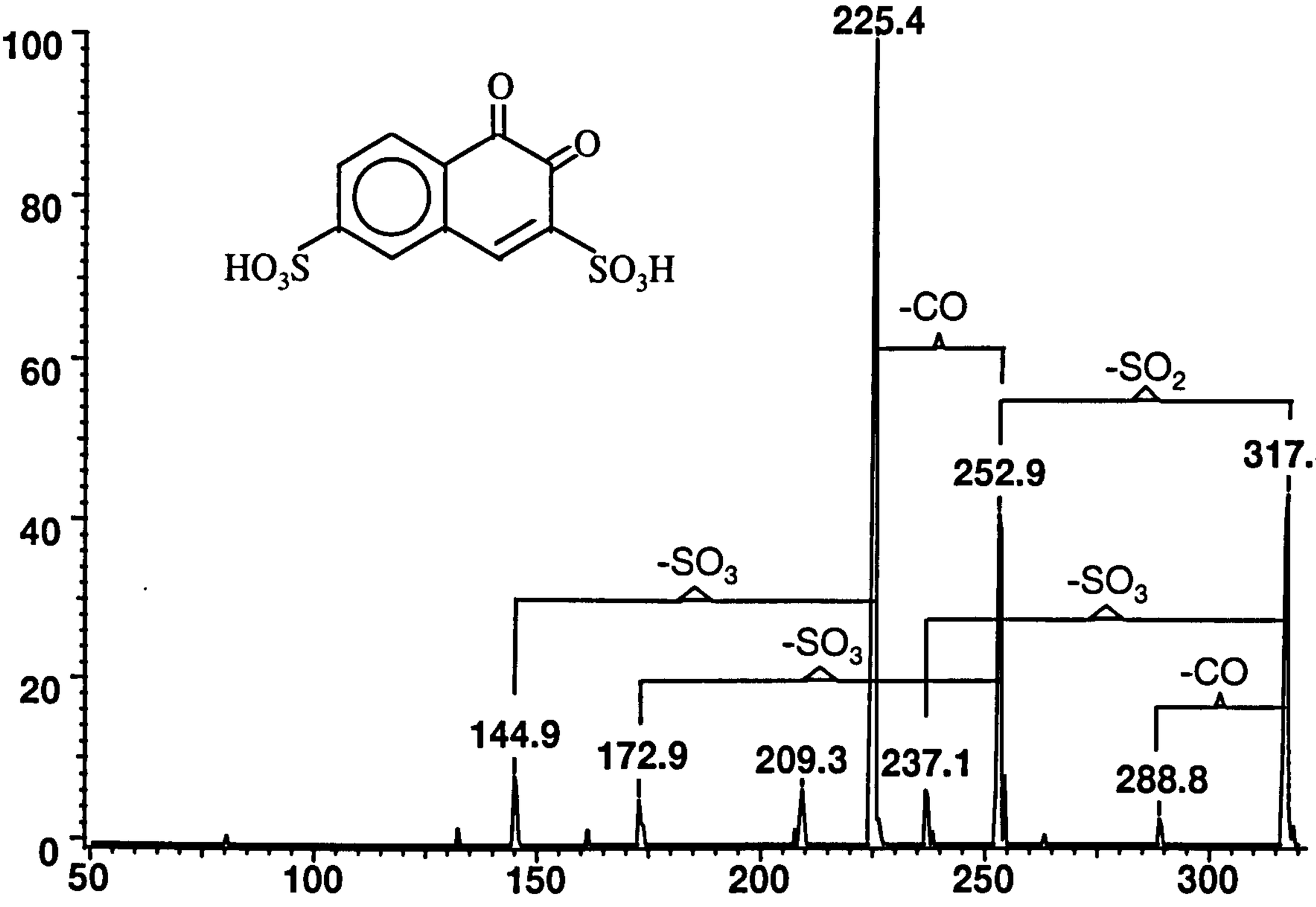

Figure 4.11 Daughter ion spectra derived from *m/z* 317 ([M-H]$^-$) for peak IVa

The daughter ion spectrum derived from the proposed hydroquinone compound (IVb, Figure 4.12) was very weak and showed only fragment ions associated with the loss of sulphonic acid groups. Presumably a hydrogen atom was not available for transfer to the hydroxyl group to allow the elimination of water.

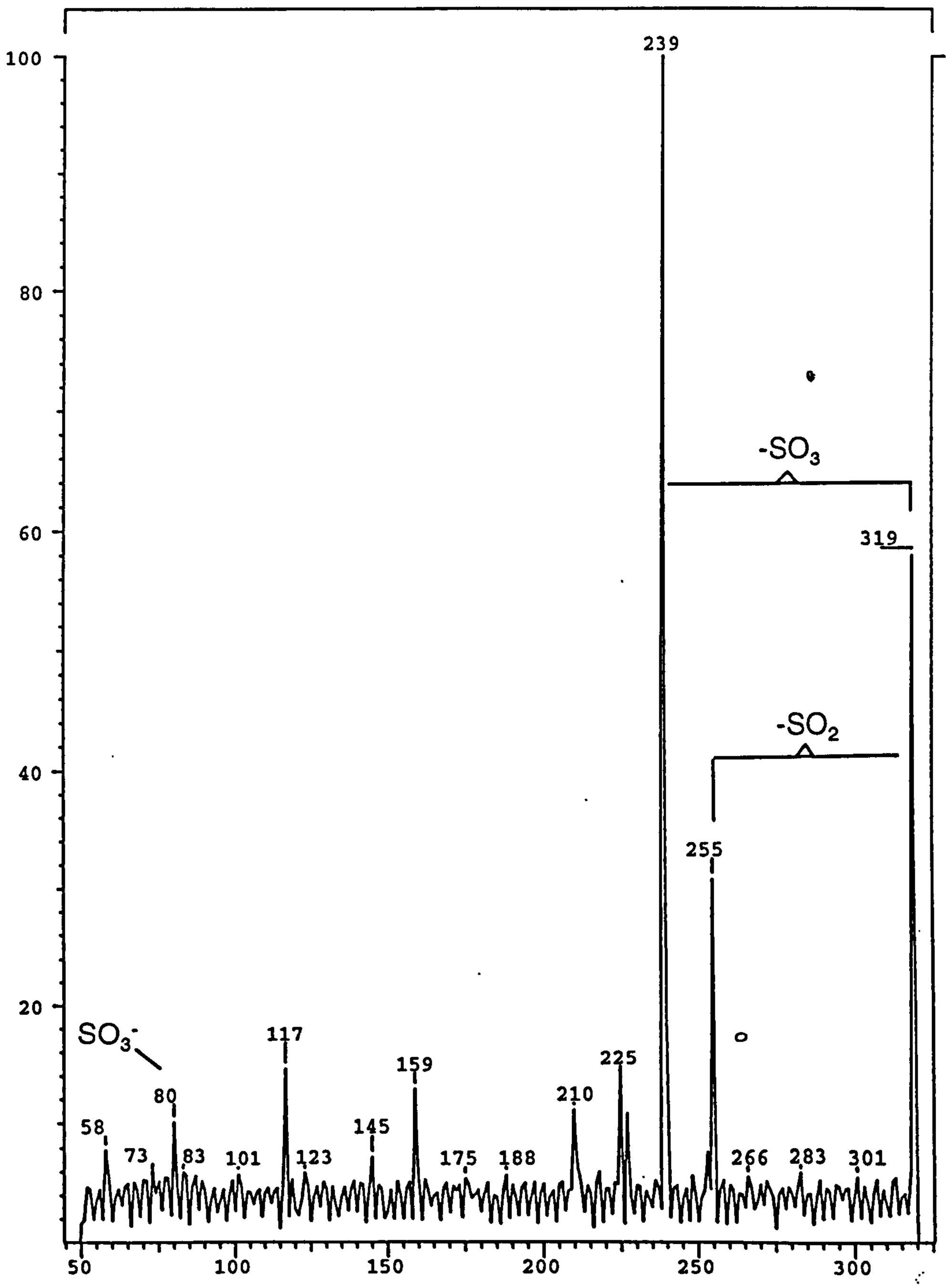

Figure 4.12 Daughter ion spectra derived from m/z 319 ($[M-H]^-$) for peak IVb

From these data the structures of compounds IVa and IVb were proposed as:

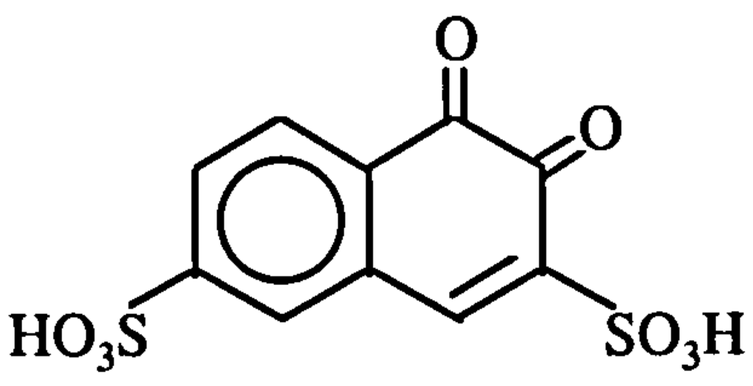

(IVa)

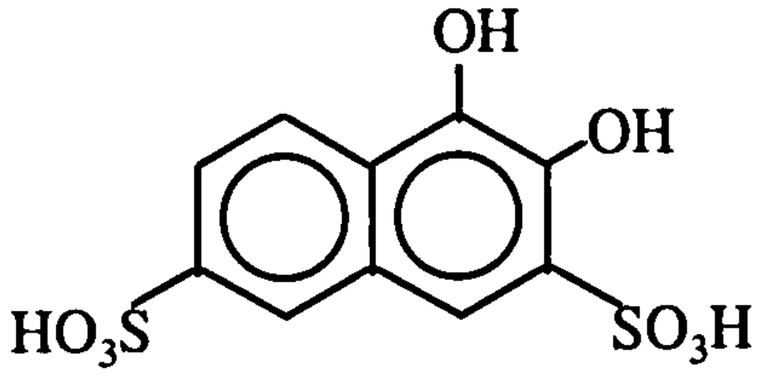

(IVb)

The peak observed in the LC-MS chromatogram (Fig 4.8) corresponding to V, showed molecular ions at *m/z* 157.6 $[M-2H]^{2-}$and 316 $[M-H]^{-}$ (Fig 4.13), indicating a molecular weight of 317, one nitrogen, and two sulphonic acid groups.

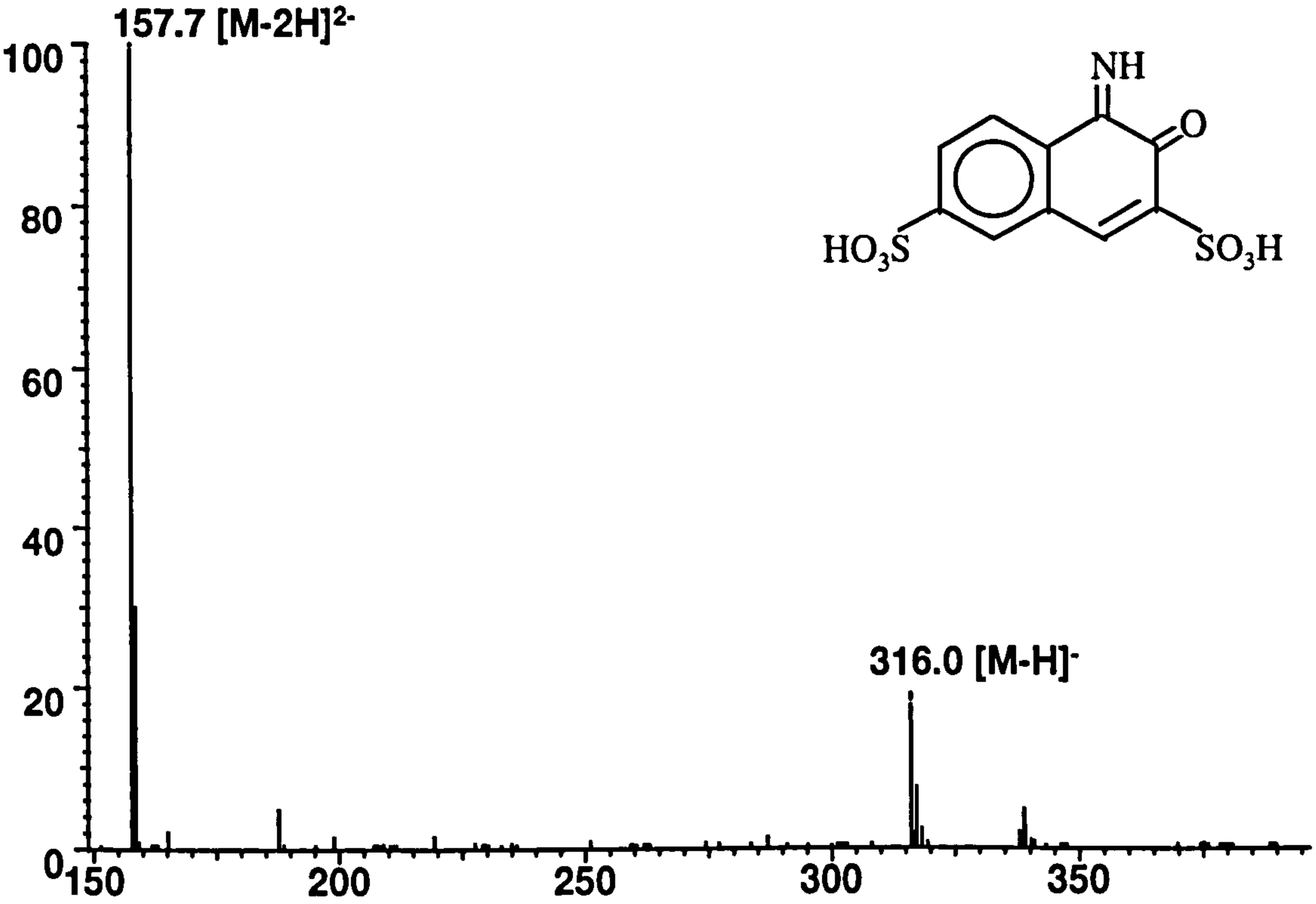

Figure 4.13 Mass spectrum derived from peak V in reduced Amaranth sample following exposure to air for 85 minutes

The molecular ion of this compound was two mass units lower than that of the starting material II, consistent with 2-naphthoquinone-1-imine-3,6-disulphonic acid (V). The UV

spectrum showed a broad maximum in the 300 - 400 nm region again confirming extended conjugation consistent with the proposed structure (V).

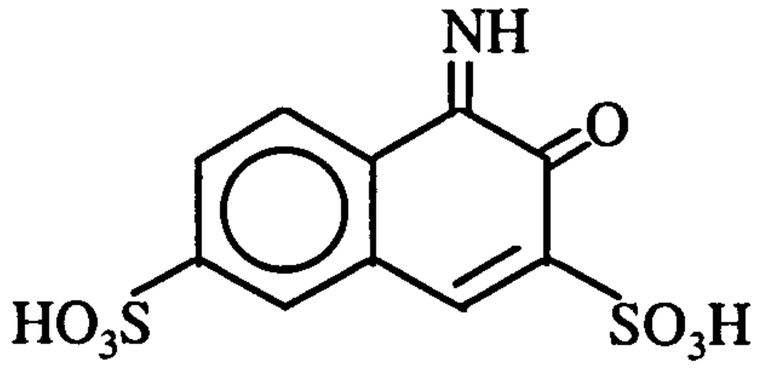

(V)

The most persistent of the autoxidation products, component VI, produced a UV-spectrum which differed quite markedly from the other products in that it showed no UV absorbance in the visible region (300 - 400 nm), suggesting an absence of the naphthoquinone type structure, consistent with ring opening. MS data (Figure 4.14) showed molecular ions at *m/z* 175 $[M-2H]^{2-}$and 351 $[M-H]^{-}$ indicating a molecular weight of 352.

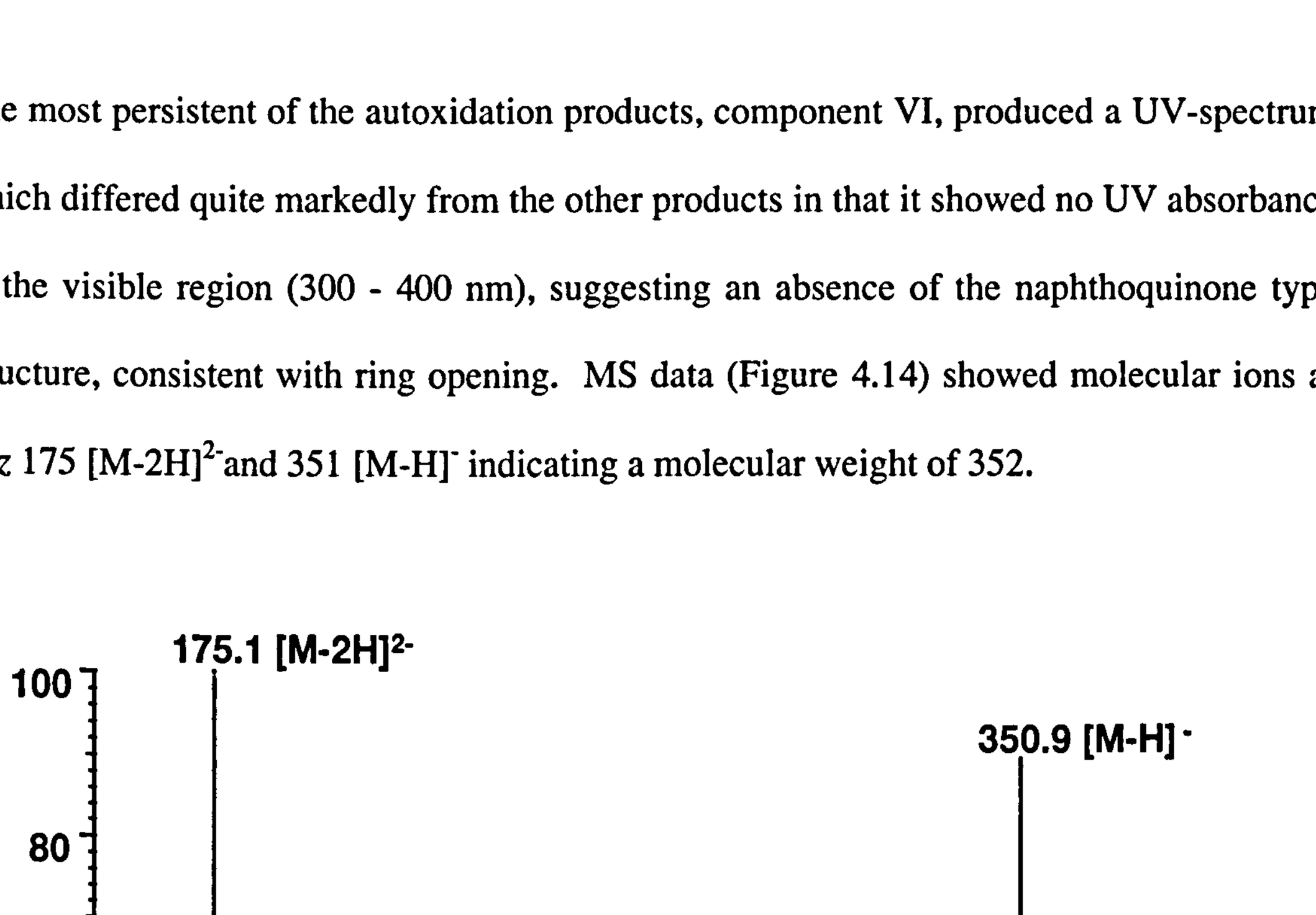

Figure 4.14 Mass spectrum derived from peak VI in reduced Amaranth sample following exposure to air for 85 minutes

This suggests a compound containing zero or an even number of nitrogen atoms, with two sulphonic acid groups and is consistent with a molecule two oxygen atoms higher than the naphthoquinone structure IVa. Considering the proposed structures for the intermediates and the UV data, it seems quite likely that ring opening would occur around the existing hydroxyl groups. Several structures are consistent with these data: eg a *bis* hydroxylated naphthoquinone:

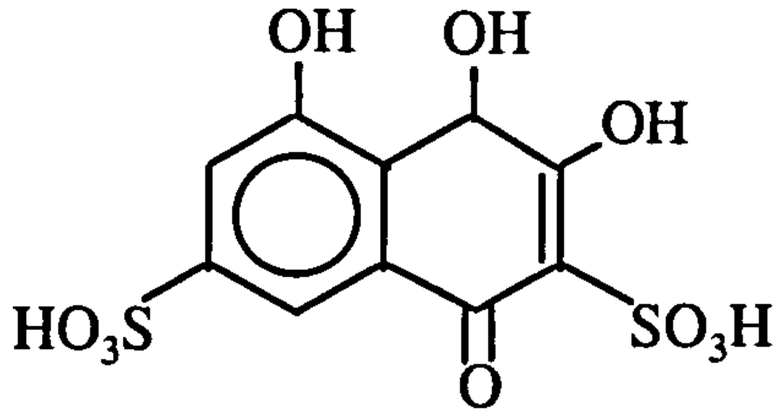

(VIa)

However, this seems unlikely and can be discounted because absorbance in the visible region of the UV/Vis spectrum would be expected for this type of conjugated system.

A second alternative is a *bis* carboxylic acid, 3-carboxy-4 (2-sulfonyl-vinyl)-benzene-1-sulfonic acid, formed through a hydrolytic intradiol cleavage of the naphthoquinone.

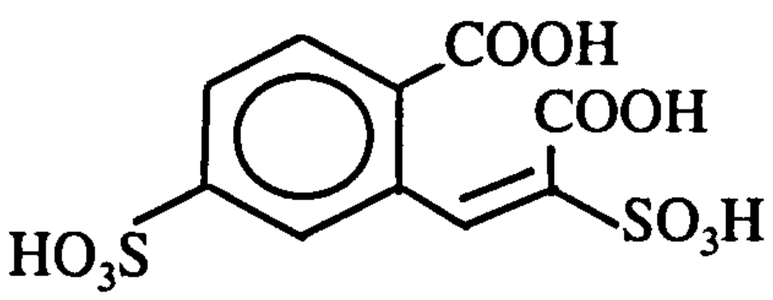

(VIb)

An analogous compound has been proposed by Boeseken (1911) as a product of the peroxide oxidation of 1,2-naphthaquinone:

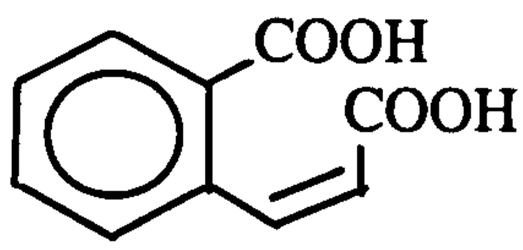

However this is an extremely polar molecule and it would be surprising to find its retention to be so long on the analytical system employed. However without suitable reference standards this structure cannot be entirely ruled out.

Two further possibilities appear more appropriate. Both would be formed by ring opening to form a carboxylic acid group, but they differ in the position of this ring opening.

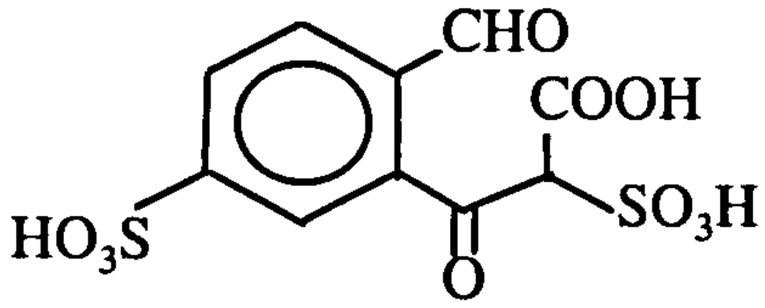

(VIc)

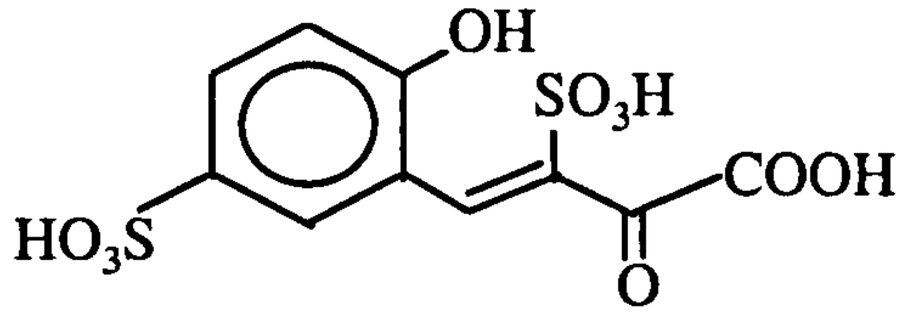

(VId)

There is evidence in published literature for structure (VId). Wittich (1988), proposed an analogous compound for the bacterial (*Moraxella* strain ASL4), degradation of naphthalene-1,6 and 2,6-disulphonic acids. The initial stages of this degradation involved oxidation, followed by elimination of sulphate to form a 1,2-dihydroxy-6-sulphonic acid which was then further oxidised to an intermediate analogous to structure (VId) above:

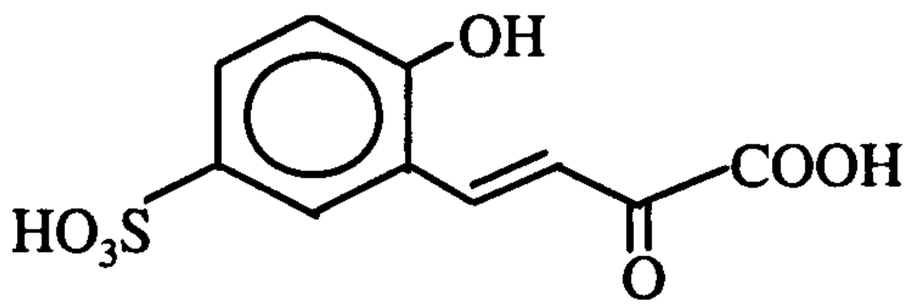

Similarly Haug *et al.*, (1991), referred to an intermediate formed in the mixed culture bacterial mineralisation of Mordant Yellow 3. In this case the initial reduction product, 6-aminonaphthalene-2-sulphonic acid was oxidised to 6-amino-1,2-dihydroxy naphthalene, which was further oxidised to a structure again analogous to (VId):

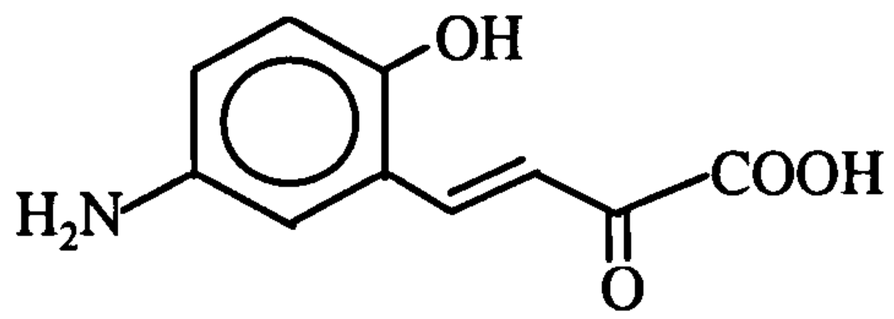

A further, very similar degradation pathway was also proposed by Kuhm *et al.*, (1991), although care has to be taken when comparing biological degradation with autoxidation. In all three cited articles the degradation continued with the elimination of the side chain to produce substituted 5-hydroxy benzoic acid compounds, where the substituents were 3-hydroxy or 3-amino, depending on starting material. These products are likely to be formed through biological breakdown rather than an autoxidation process, which explains why further degradation was not observed for Amaranth.

From these data it seems likely that structure (VId) is most appropriate. However it was decided to obtain MSMS data to gain supporting evidence for this and the other proposed autoxidation products, especially given the relevance to the understanding of more complicated systems such as the biological treatment of dye effluent.

By comparison to the spectra of the other reduction and autoxidation transition products, the daughter ion spectrum of the stable oxidation product, (VI), showed extensive fragmentation, (Fig 4.15). The initial loss of water (351 $\rightarrow$ 333) indicated that unlike the hydroxyl groups of the proposed hydroquinone (IVa), this molecule had a hydrogen atom available for transfer with subsequent elimination of water. This may be explained by a ring opened structure. Additionally, this loss coupled with the subsequent elimination of carbon monoxide (333 $\rightarrow$ 305), suggests the presence of a carboxylic acid. The remaining fragment ions provide little additional structural information and in particular show no further losses of H_2O and CO or CO_2 which might be expected from a *bis*-carboxylic acid compound. These data indicate structure VIb to be unlikely.

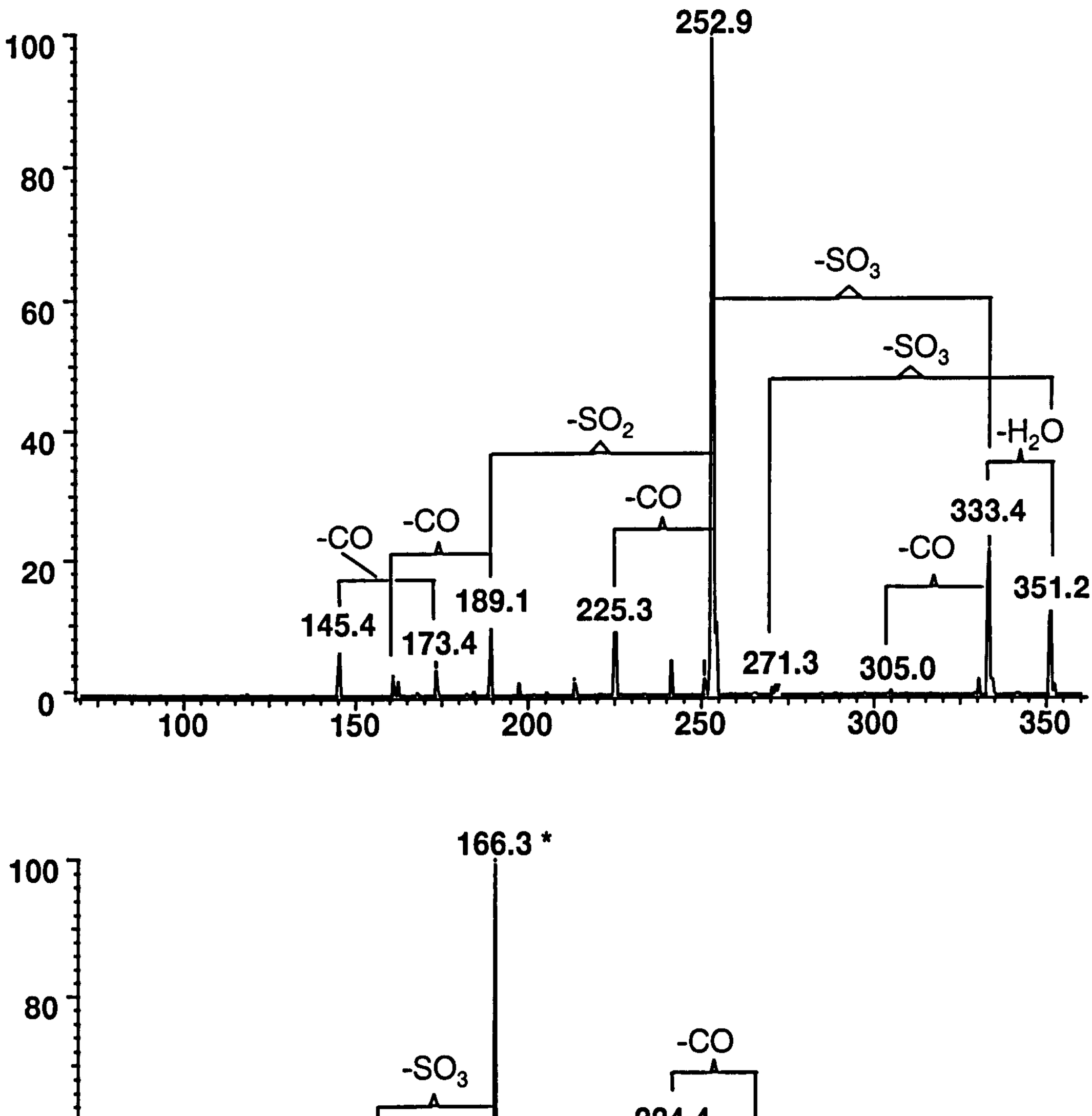

Figure 4.15 Daughter ion spectra for peak VI derived from *m/z* 351 ($[M-H]^-$, top) and *m/z* 175 ($[M-2H]^{2-}$, bottom. Note * denotes doubly charged ions

The daughter ion spectrum for the doubly charged molecular ion derived from peak VI, Figure 4.15, appears quite different from that of the singly charged species. Notably, loss of water (270 → 252) and successive losses of CO (252 → 224 → 196) are significant, as well as the primary loss of CO (175 → 161). These suggest a carbonyl (derived from a ketone, phenol or aldehyde), in addition to a carboxylic acid group, is readily available for expulsion. This again sheds doubt on the second of the proposed structures (VIb), because this structure contains two carboxylic acid groups and one would expect to see multiple losses of H_2O and CO and/or CO_2 from this structure, which was not observed. Suggested structures (VIc) and (VId) can both lose water, followed by two carbonyls (one from the carboxylic acid and one from either the aldehyde or phenol group). This tends to suggest either VIc or VId, both of which are consistent with the MSMS data, should provide the most likely structure, although it was not possible from these data to determine which of them is most likely.

Both the present study and that of Kudlich (1999) suggest the final autoxidation product VI, is relatively stable to further oxidation. However the ring opened structure, although resistant to autoxidation, would be expected to be highly susceptible to decarboxylation and further degradation under aerobic biological treatment. Such reactivity, if confirmed would indicate good potential for the removal of azo dyes by sewage treatment systems.

From the present reduction/autoxidation experiment we can postulate a degradation pathway for Amaranth, as detailed in Figure 4.16 below.

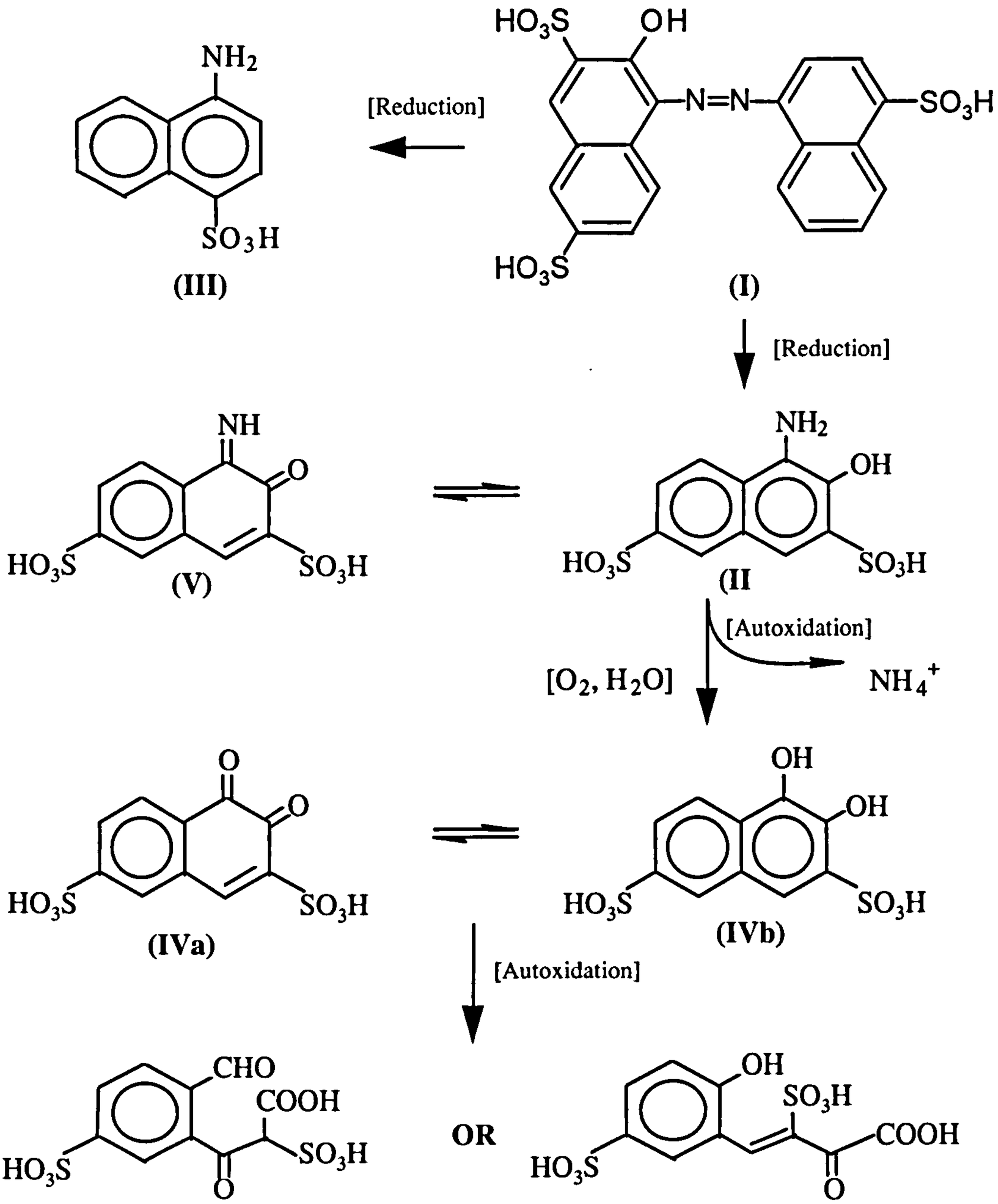

Figure 4.16 Proposed autoxidation pathway for the reduction products of Amaranth

4.4.2 Autoxidation of reduced Sunset Yellow

A different approach was taken for the determination of autoxidation products of reduced Sunset Yellow. Here the kinetics of autoxidation had already been assessed (Kudlich personal com), which indicated that unlike Amaranth, only one autoxidation product was formed within the first 5 hours of oxidation. Therefore the approach taken was to use the limited material available to concentrate on the identification of autoxidation products and to compare these to the degradation pathway of Amaranth (Section 4.3.1) as these two compounds differ only by the presence or absence of a sulphonic acid group in the 3-position.

Sunset Yellow (I) when reduced by hydrogen in the presence of palladium on barium sulphate, produced two products with retention times of 3.6 and 10.8 minutes, respectively when examined by LC-PDA and by LC-MS, (Fig 4.17).

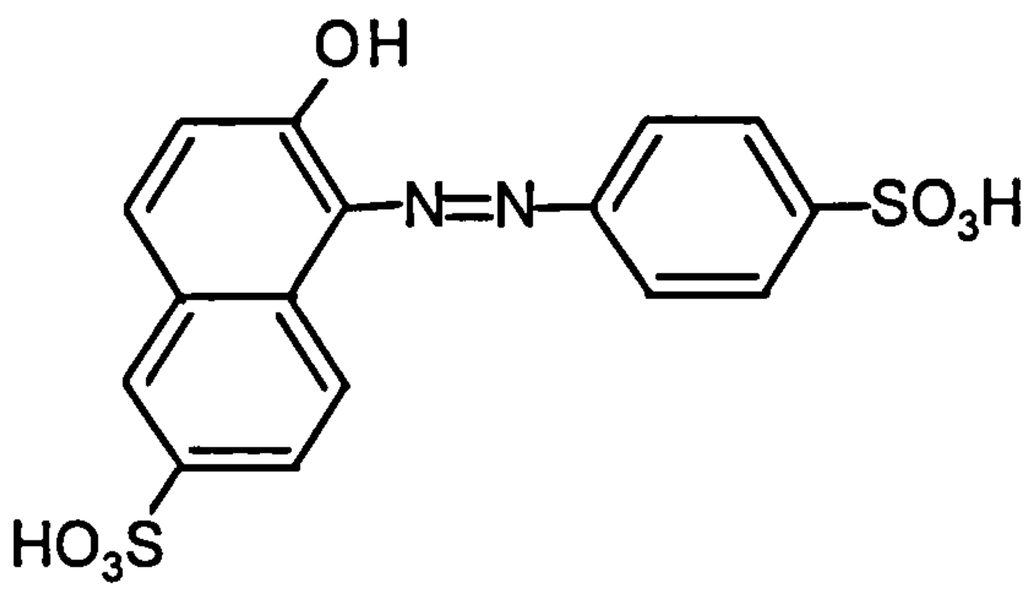

(I)

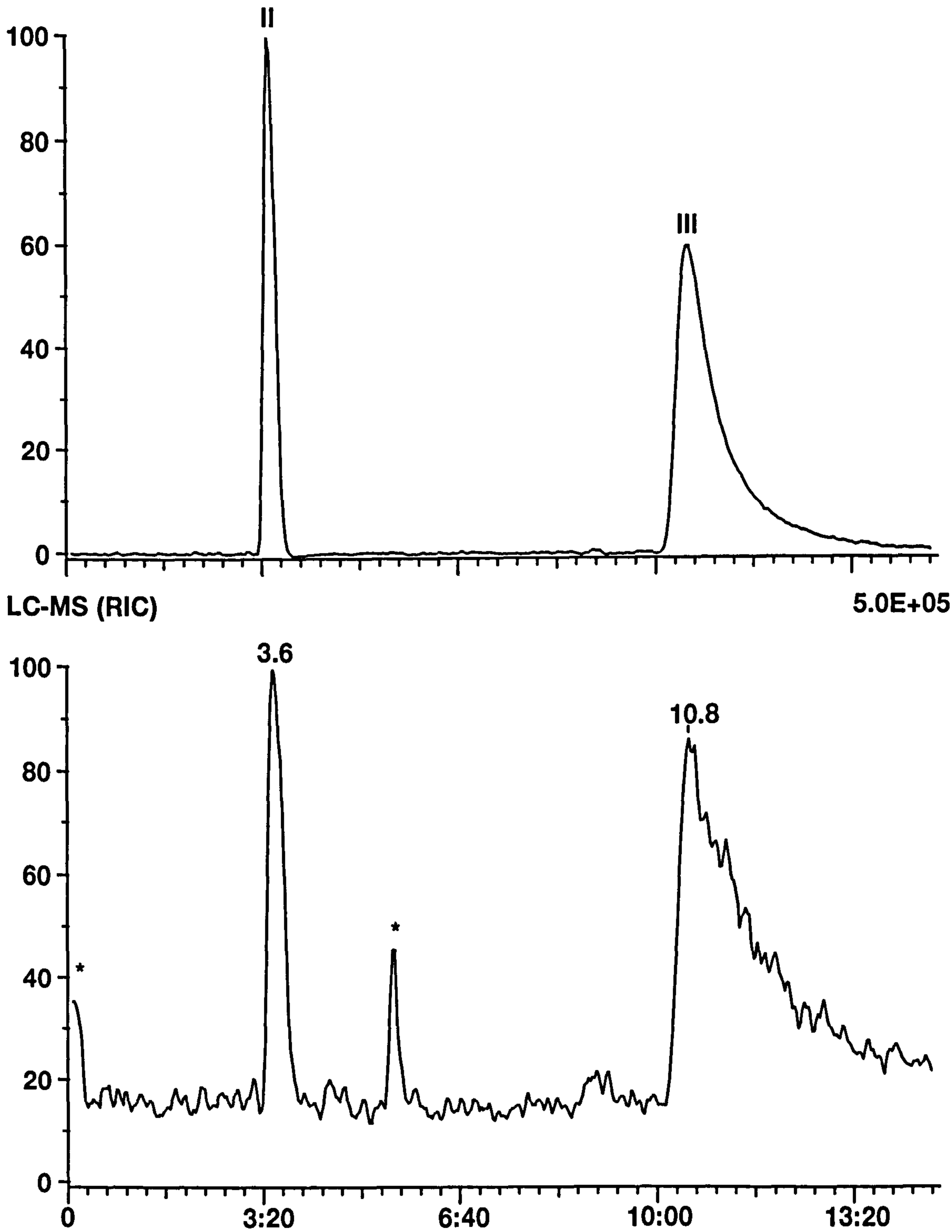

Figure 4.17 LC-MS chromatogram for reduced Sunset Yellow (* denotes background peaks also in control)

The negative ionisation mass spectra suggested molecular weights of 173 ($[M-H]^-$, *m/z* 172) and 239 ($[M-H]^-$, *m/z* 238) for peaks II and III respectively, consistent with the

expected reduction products 4-aminobenzene-1-sulphonic acid (sulphanilic acid, II) and 1-amino-2-hydroxynaphthalene-6-sulphonic acid (III, Fig 4.18).

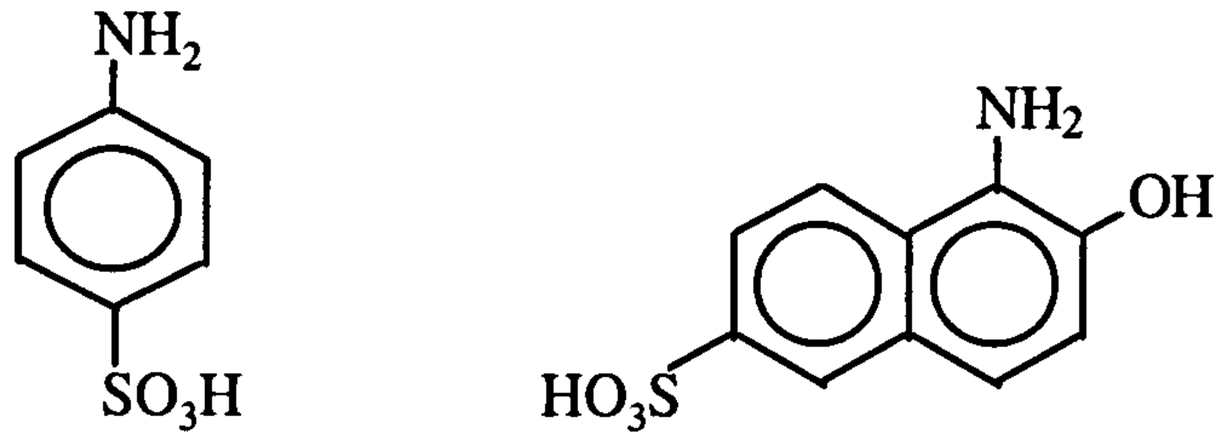

(II) (III)

However the mass spectrum of (III) (Fig 4.18) also revealed the presence of a second component with a molecular weight of 237 ($[M-H]^-$, *m/z* 236). The presence of this component would not have been suspected from the LC-PDA analysis alone. Because the molecular weight of compound (IV) differed by only 2 mass units from the initial reduction product (III), 2-napthoquinone-1-imine-6- sulphonic acid was proposed. This assignment was supported by the observation of the equivalent compound in the autoxidation of Amaranth (Compound V, Fig 4.16)

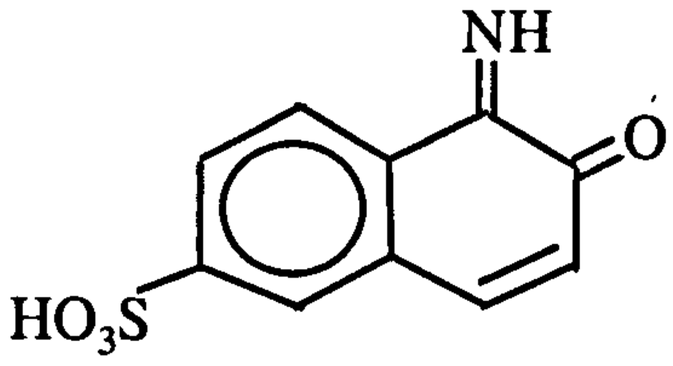

(IV)

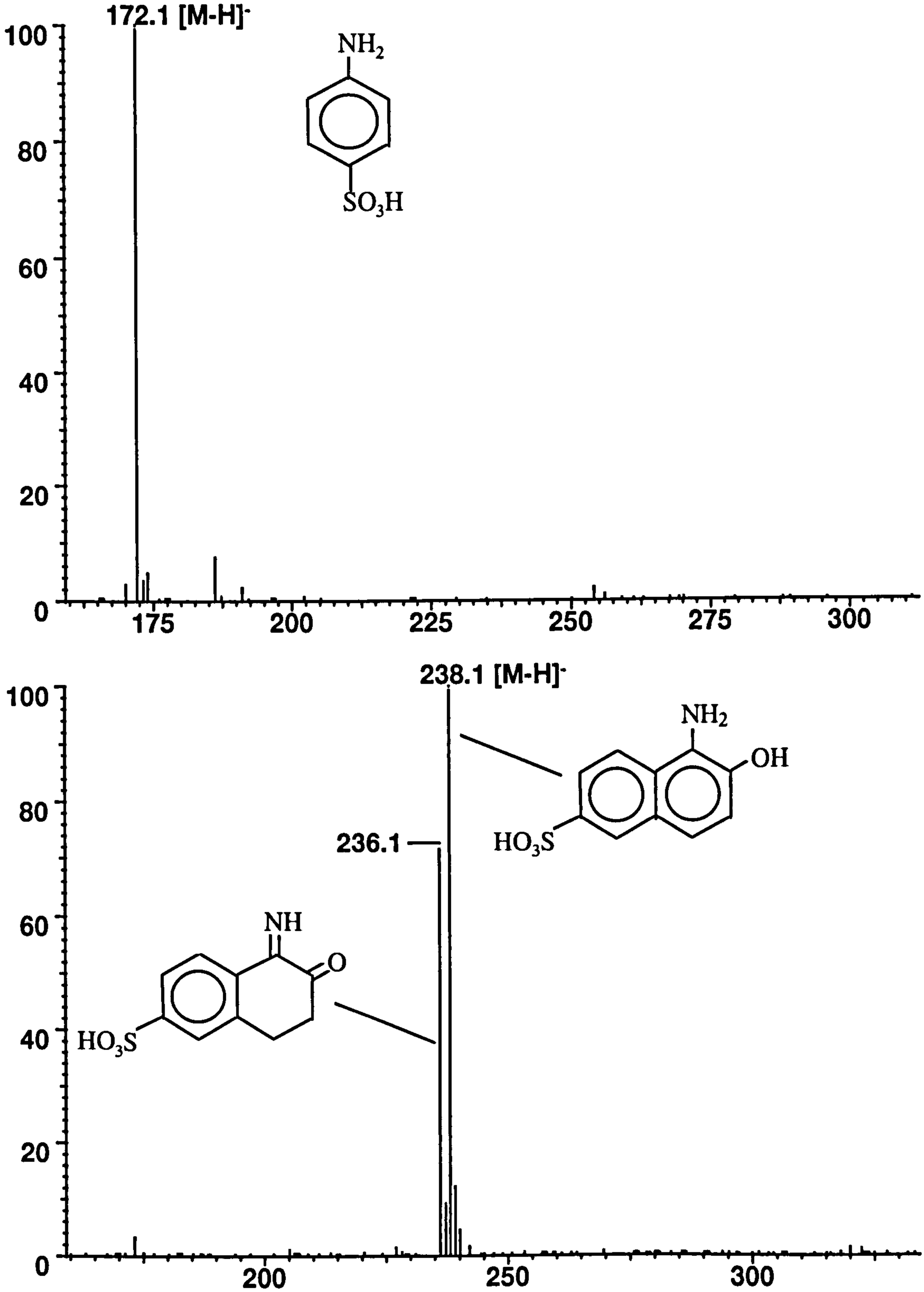

Figure 4.18 Mass spectra derived from peaks II (top) and III (bottom) for the LC-MS analysis of reduced Sunset Yellow at time zero (t_0)

This sample was re-analysed following aeration for 10 and 60 minutes to examine the ratio of III to IV (*m/z* 318 to *m/z* 316). This was to determine whether compound III, the initial reduction product, degraded to compound IV or whether the two compounds were in

equilibrium. The measured ratio remained constant over the 1 hour duration, suggesting the two compounds to be in equilibrium.

Figure 4.19 shows a comparison of LC-MS and LC-$UV_{230\ nm}$ chromatograms of a sample of reduced Sunset Yellow, oxidised for 1 hour. Peaks annotated (II), (III) and (IV) were confirmed as sulphanilic acid and 1-amino-2-hydroxynaphthalene-6-sulphonic acid, the reduction products of Sunset Yellow and 2-napthoquinone-1-imine-6- sulphonic acid respectively. The remaining component (V) was obviously the result of autoxidation. The mass spectrum of this major autoxidation product contained ions at *m/z* 236.5 and 474, suggesting a molecular weight of 475 (Fig 4.20). The presence of a doubly charged ion (236.5 $[M-2H]^{2-}$) is indicative of two sulphonic acid groups and because the initial reduction products II and III contained only one, suggests dimerization. The odd molecular weight suggests this dimer must contain only one nitrogen.

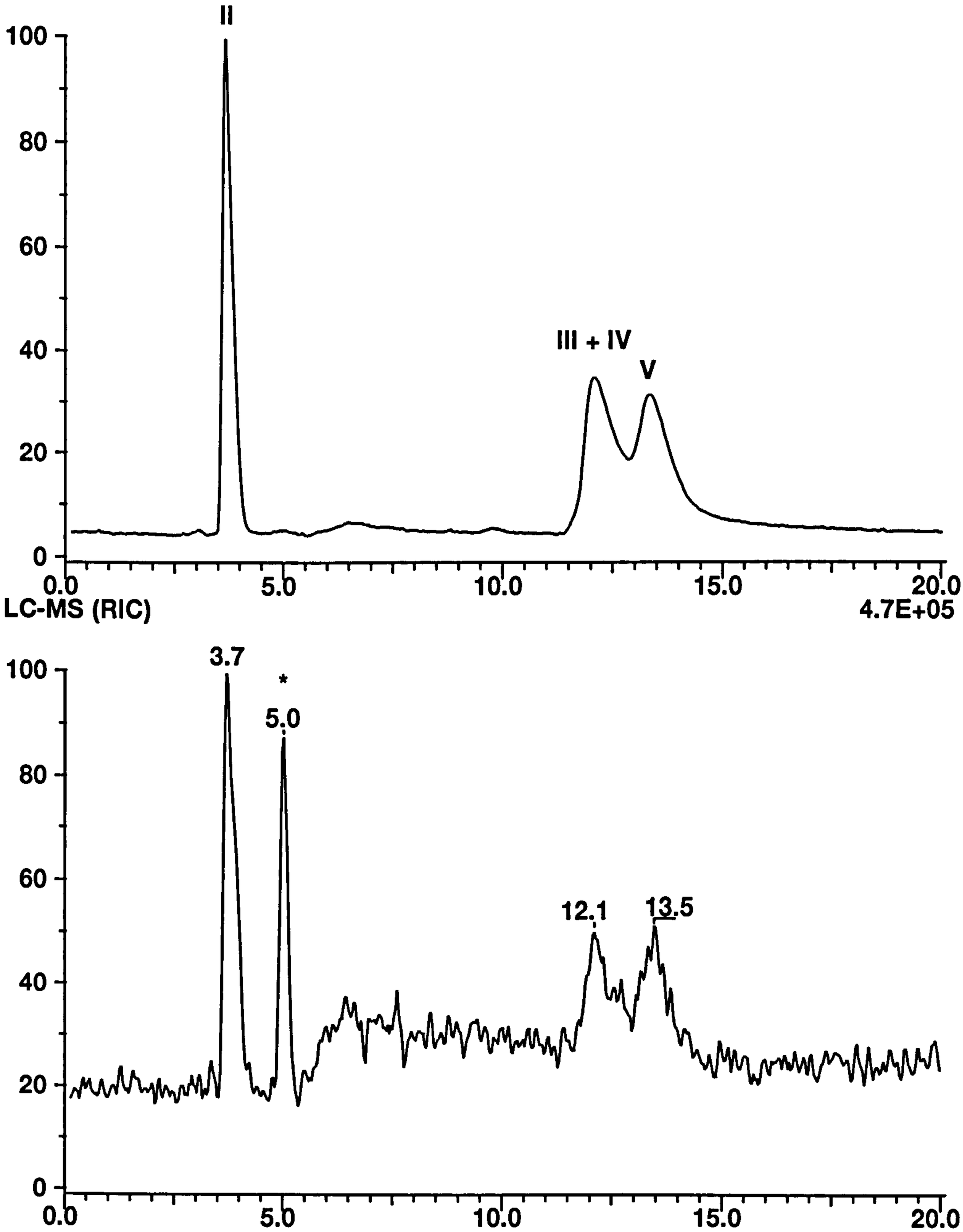

Figure 4.19 LC-MS chromatogram for reduced Sunset Yellow following exposure to air for 1 hour, (* denotes background peaks also in control)

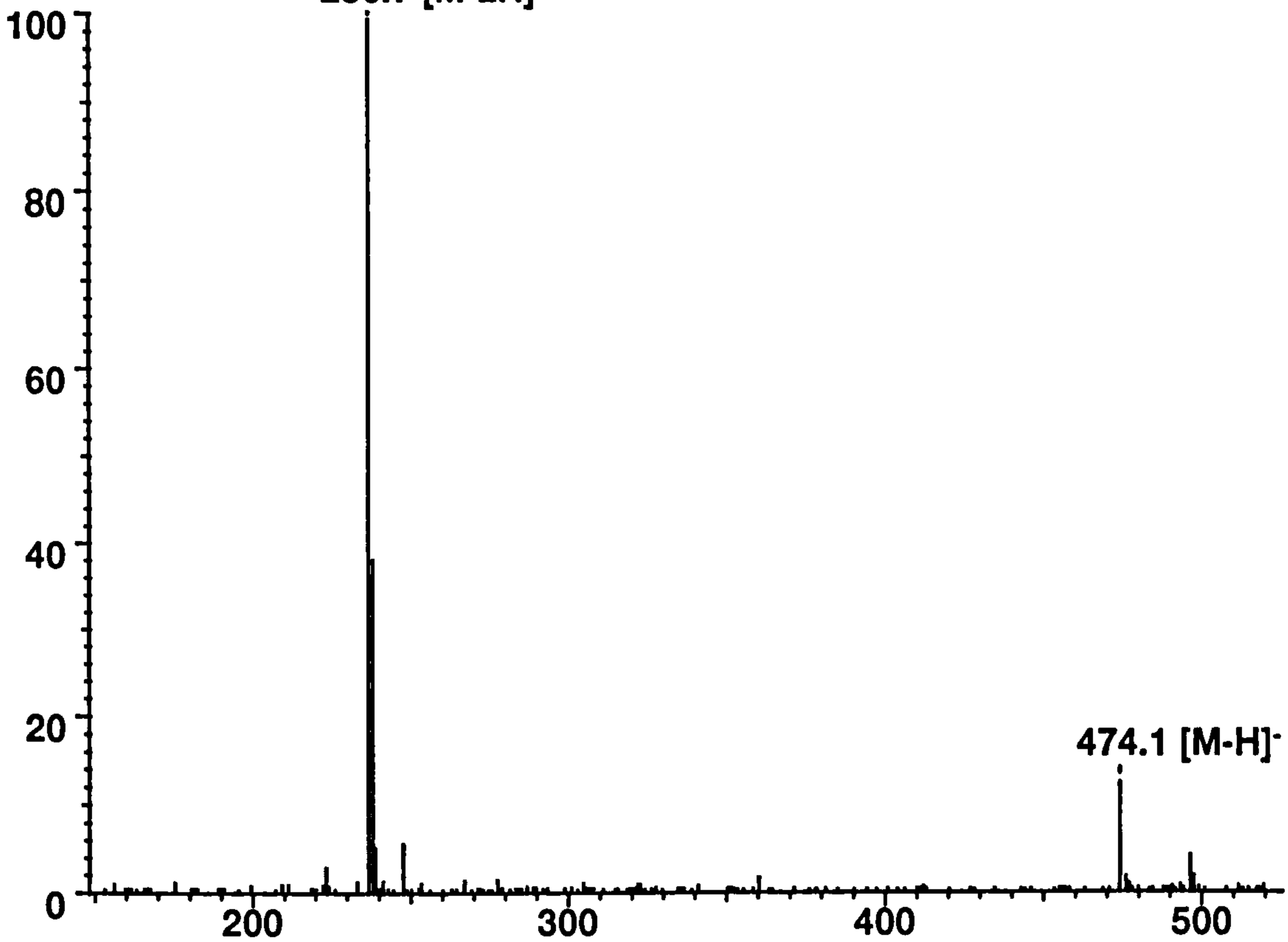

Figure 4.20 Mass spectrum derived from peak V for the LC-MS analysis of reduced Sunset Yellow following exposure to air for 1 hour (t_{60})

By comparison with the closely related disulphonic acid (Amaranth), autoxidation may have been expected to produce 1-2-naphthoquinone-6-sulphonate, (equivalent to structure IV, Fig 4.16) as an intermediate. However no evidence for this compound was observed. It seems possible that 1-2-naphthoquinone-6-sulphonate could be removed by reaction with the amine (primary reduction product III) to form a dimer. The following reaction scheme is envisaged:

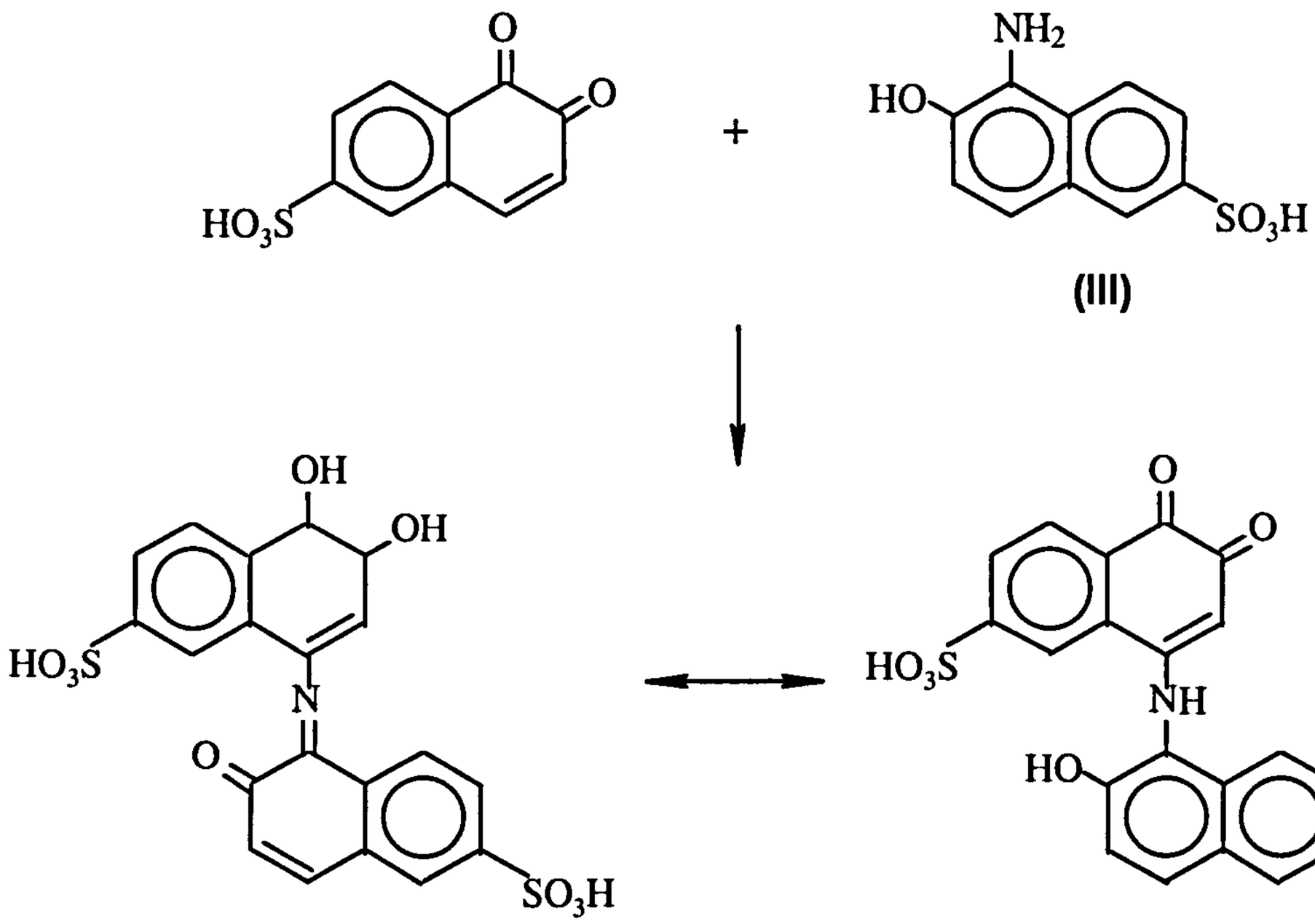

(III)

(V)

In order to confirm that the proposed dimeric structure of the autoxidation product, the charge state of the observed molecular ions was investigated. This should eliminate the possibility that a higher polymer produces the same ions. A mass spectrometer separates ions on the basis of mass (*m*) to charge (*z*) ratio (*m*/*z*). The charge state of an ion can therefore be determined by the mass difference between ions containing ^{12}C and ^{13}C isotopes. A 1 mass unit difference will be observed for a singly charged ion (m/1), 0.5 mass units for a doubly charged species, 0.33 for a triply charged species and so on. Figure 4.21 shows the singly and doubly charged molecular ions for peak V, obtained under enhanced MS resolution conditions. The results clearly show unit resolution for the *m*/*z* 474 molecular ion and 0.5 mass units difference between isotopes at *m*/*z* 236.5. This confirms the molecular weight of 475 for the main autoxidation product.

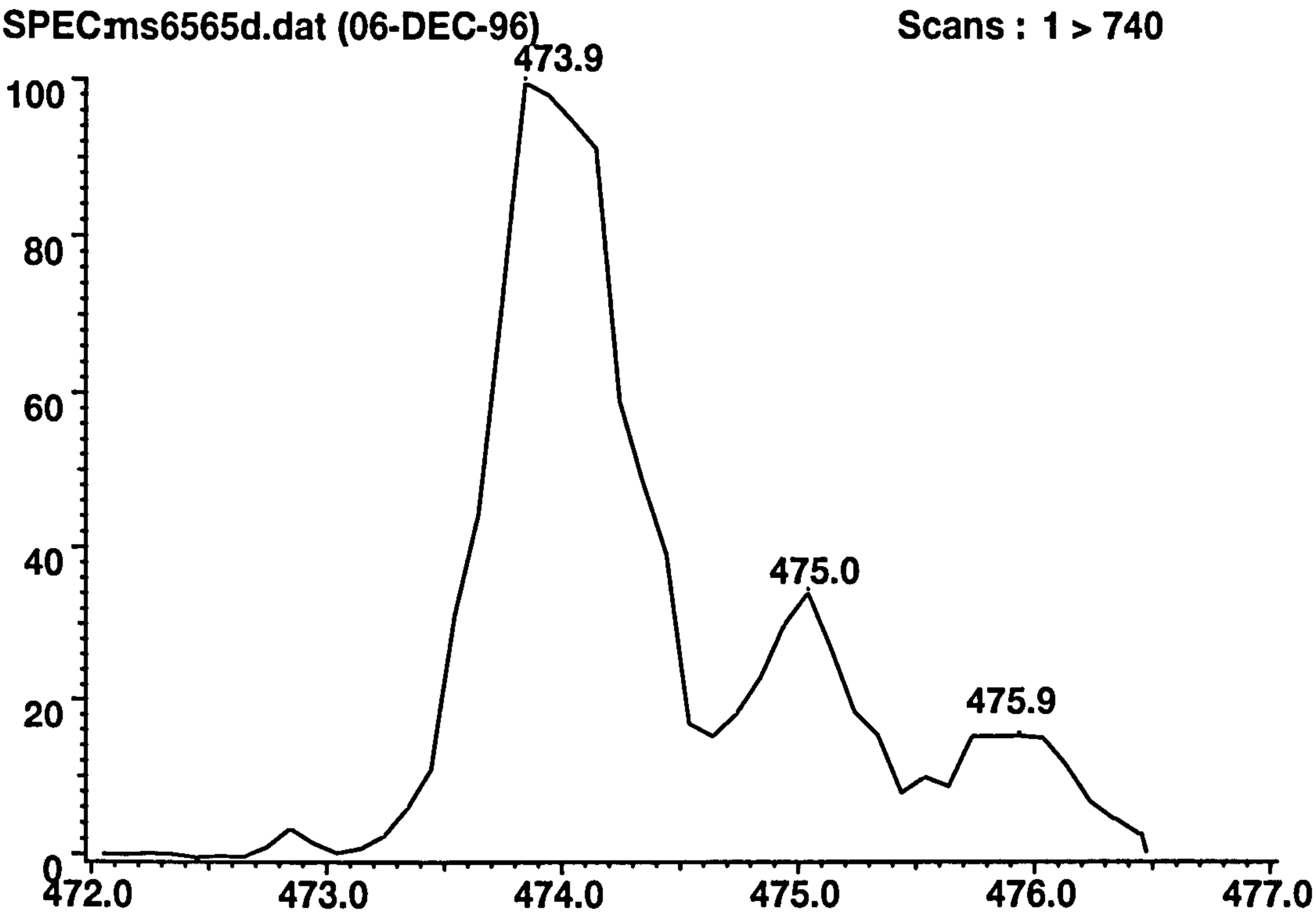

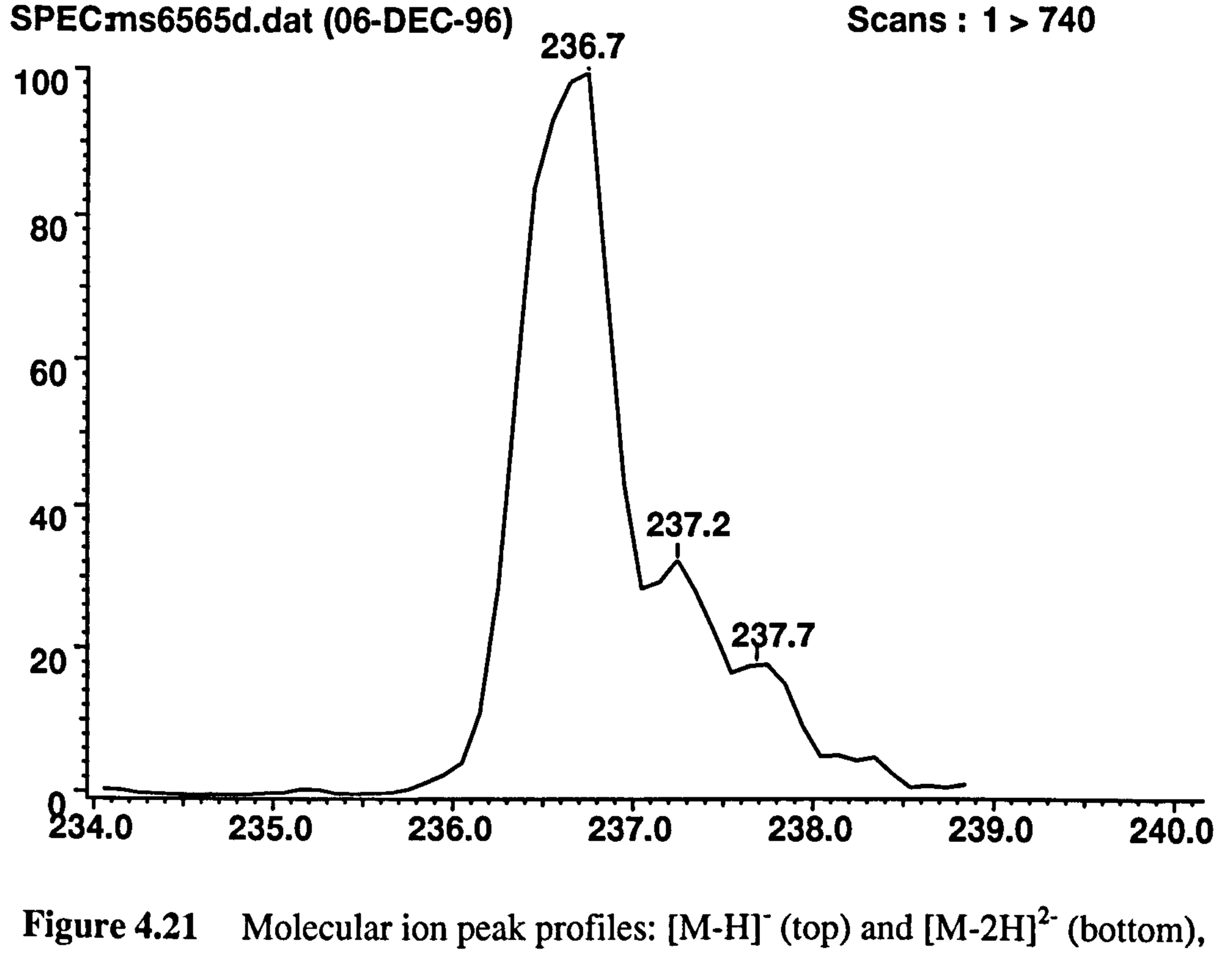

Figure 4.21 Molecular ion peak profiles: $[M-H]^-$ (top) and $[M-2H]^{2-}$ (bottom), for compound V for the LC-MS analysis of reduced Sunset Yellow following exposure to air for 1 hour (t_{60})

LC-MS analysis of the samples of reduced Sunset Yellow oxidised for 4 and 6 hours showed complete removal of the initial reduction product (III), whilst sulphanilic acid (II) and the major autoxidation product (V) proved to be stable. One other minor peak was observed in these two samples, as illustrated by peak VI in Figure 4.22. Although of similar retention time to a background peak observed in earlier chromatograms, the mass spectra derived from this (Fig 4.23) showed additional molecular ions for three compounds at *m/z* 225, 253 and 271, suggesting molecular weights of 226 (VIi), 254 (VIii) and 272 (VIiii) respectively. Also, a small peak was observed in the LC-$UV_{210\,nm}$ chromatogram at the same retention time as LC-MS which was not present in the earlier samples.

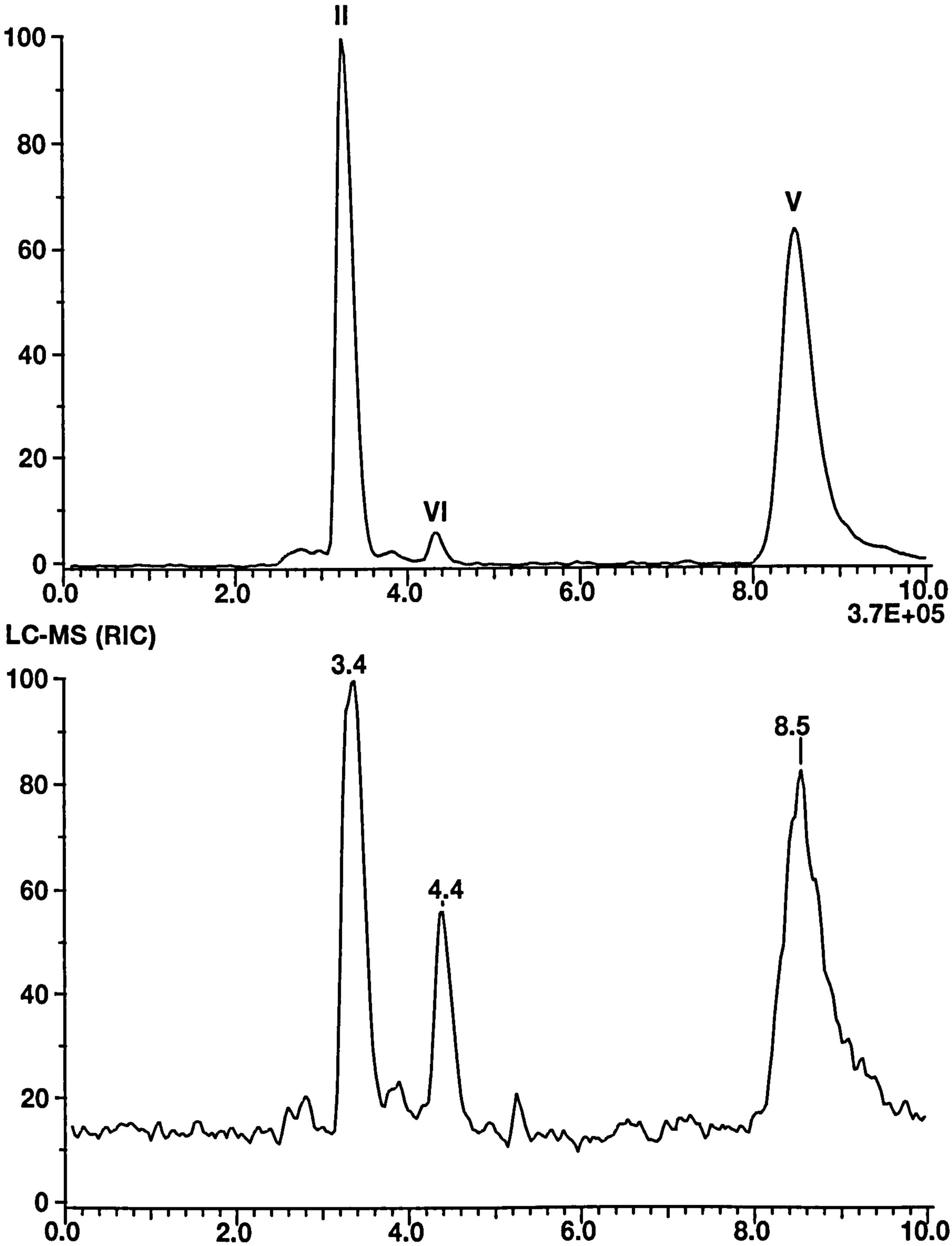

Figure 4.22 LC-MS chromatogram for reduced Sunset Yellow following exposure to air for 4 hours

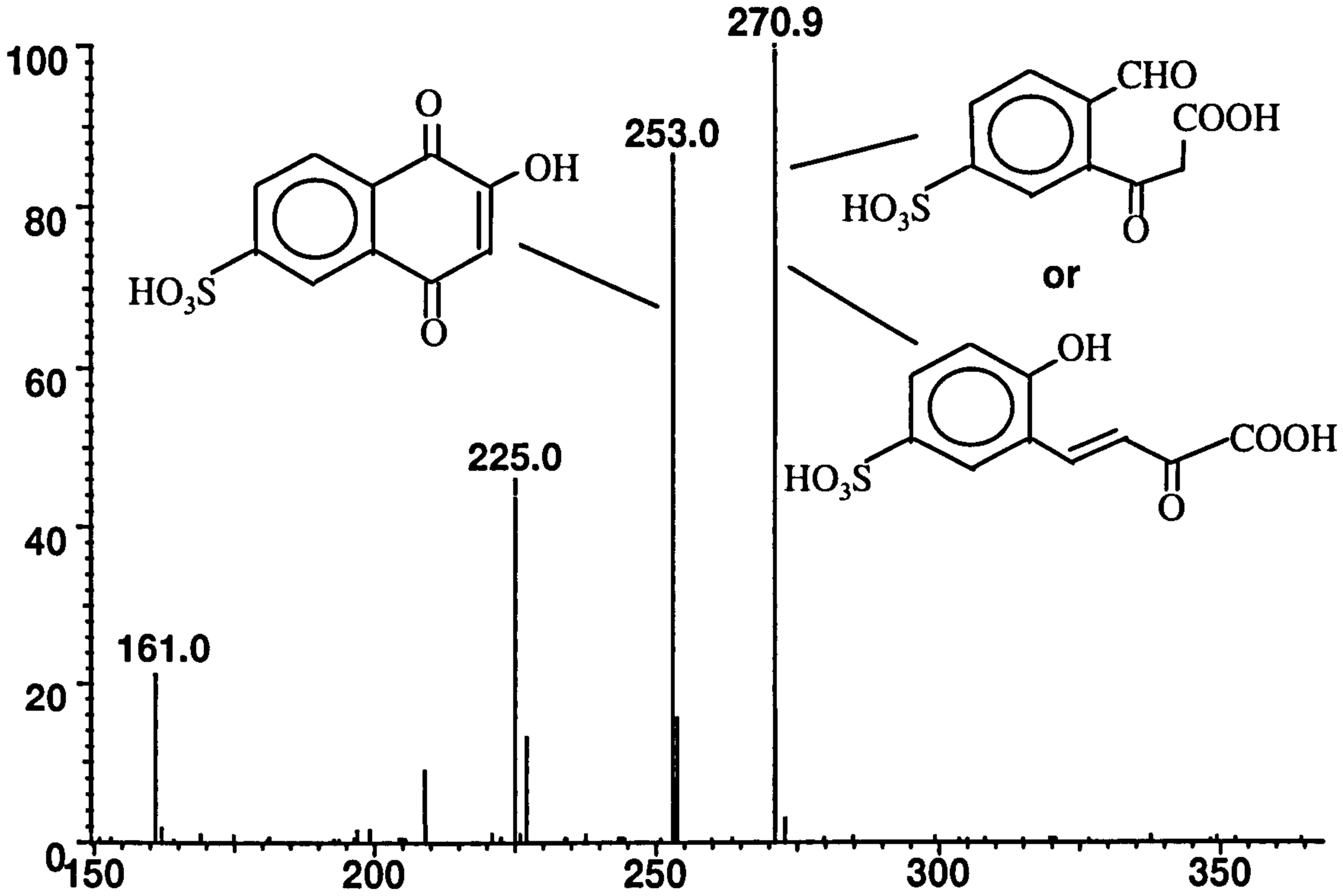

Figure 4.23 Mass spectra derived from peak VI for the LC-MS analysis of reduced Sunset Yellow following exposure to air for 4 hours (t_{4h})

Based purely on molecular weight information, the following structure was suggested for (VIii):

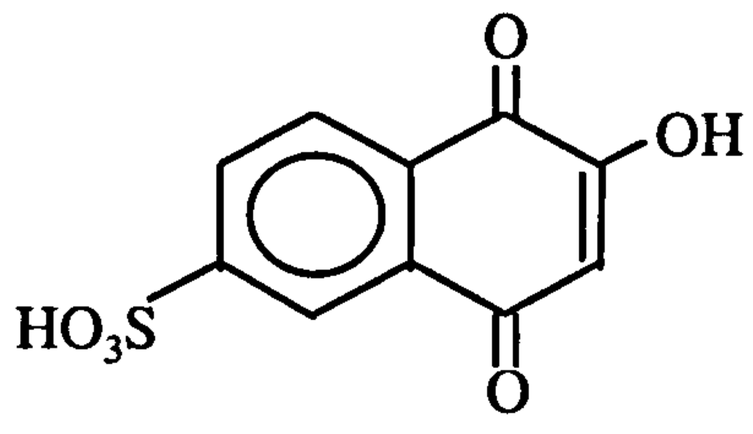

(VIii)

This is not entirely unexpected, it being a further oxidised form of naphthaquinone sulphonic acid, an expected autoxidation product for the reduced starting material. The second compound (VIiii), being 18 mass units higher could be a further oxidised product derived from (VIii), being formed by the addition of water presumably with ring opening:

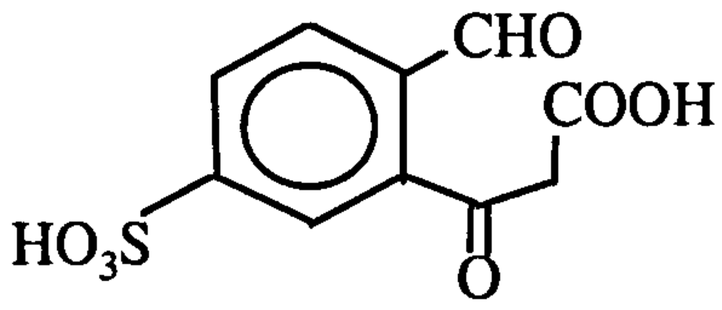

This is equivalent to peak 'VIb' observed for Amaranth, (Fig 4.14).

However another alternative is possible:

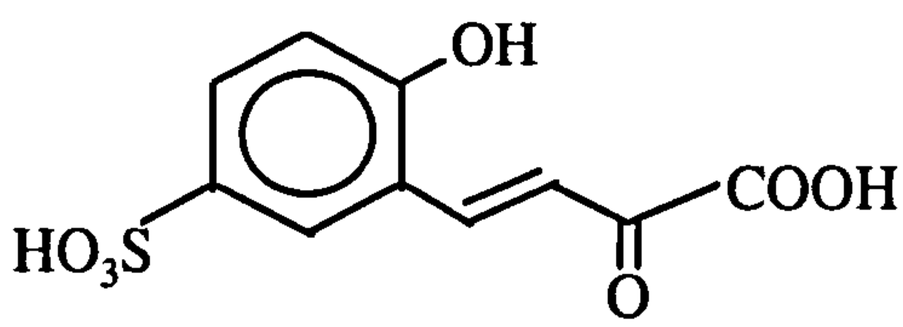

This structure has already been identified by Wittich *et al.*, as an intermediate for the bacterial degradation of 1,6- and 2,6-naphthalene disulphonic acids. These were oxidised in the degradation process to the 1,3-dihydroxy-6-sulphonic acid, followed by further oxidation with ring opening to the structure above. However, it seems unlikely this structure could be derived from further oxidation of proposed structure VIii. More likely it is formed directly from ring opening of the naphthoquinone structure.

From these data it would appear that 1-amino-2-hydroxynaphthalene-6-sulphonic acid, a reduction product of Sunset Yellow, is highly unstable. It is oxidised to the naphthoquinone which is highly susceptible to either rapid addition of the parent (reduced) material to form a dimer, or hydroxylation. The former is stable and shows no sign of further degradation, whilst the latter appears to undergo further oxidation with ring opening. The postulated degradation pathway is shown in Figure 4.24:

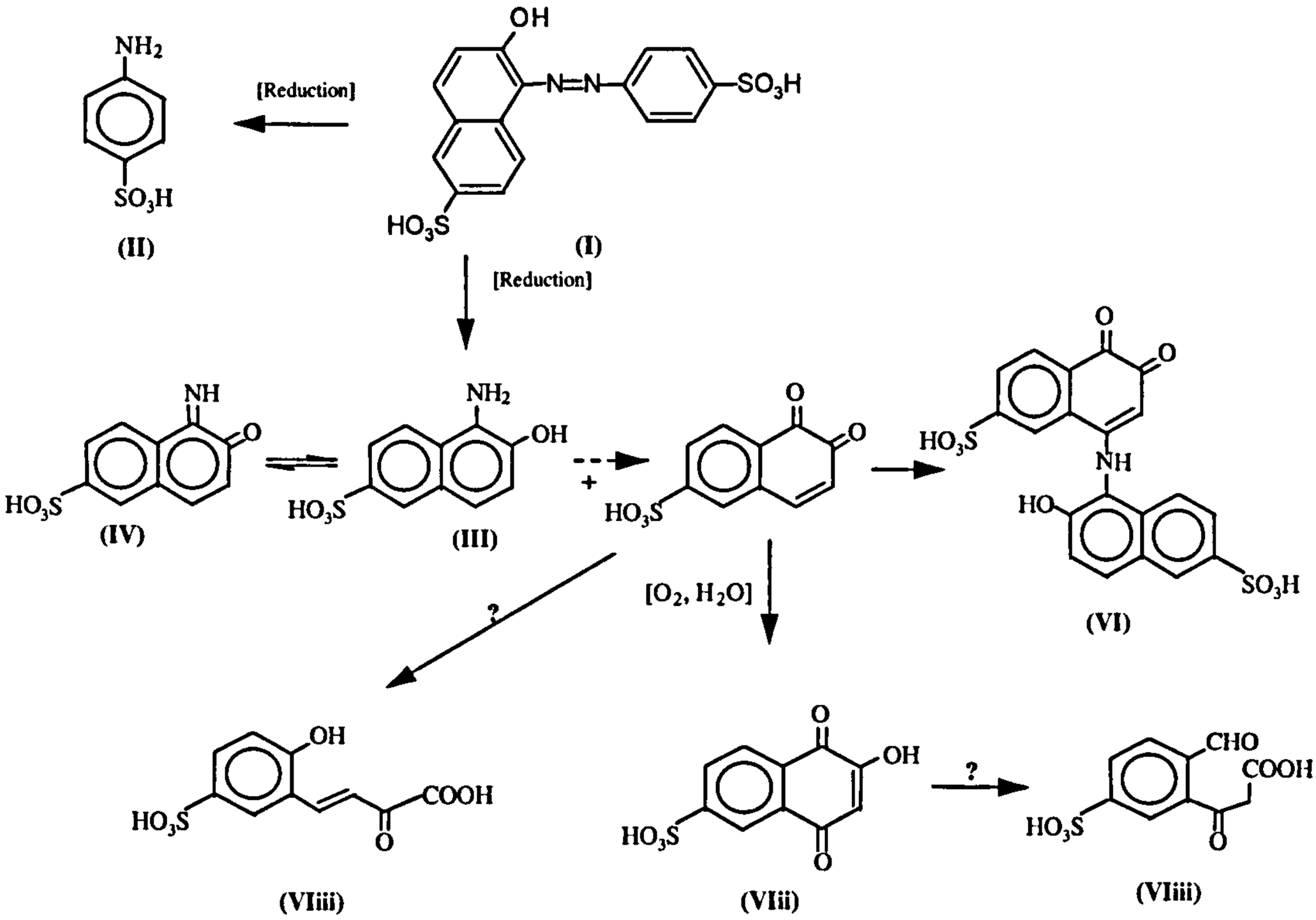

Figure 4.24 Proposed autoxidation degradation pathway for Sunset Yellow

4.4.3 Autoxidation of Napthol Blue Black

Based on the reduction of Sunset Yellow and Amaranth, Naphthol Blue Black (I) when reduced by hydrogen in the presence of palladium on barium sulphate was expected to produce three aromatic amines: 1-hydroxy-2,7,8-triamino-naphthalene-3,6-disulfonic acid (II) aniline (III) and 1-amino-4-nitrobenzene (IV).

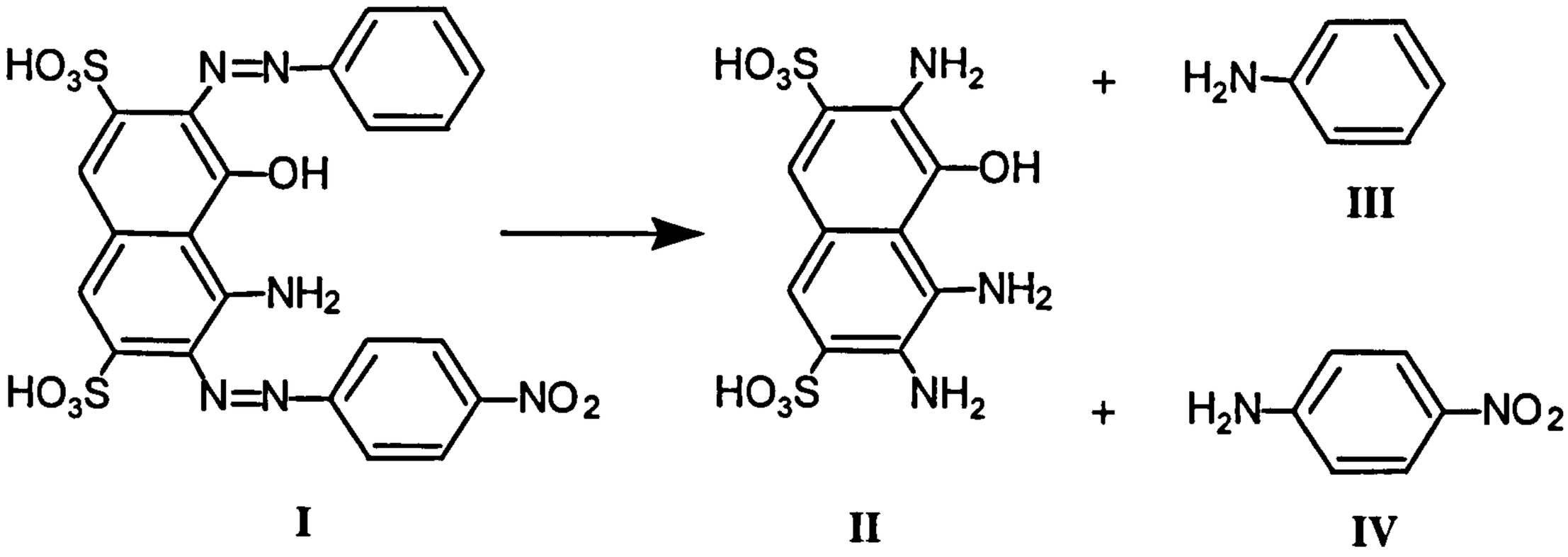

Aniline and 1-amino-4-nitrobenzene would not be observed under the analytical regime used herein.

The first observation on transfer of the reduced material from serum bottle to test tube was the change in colour. In fact, it was not possible to transfer the transparent or slightly green reduced dye solution without a dramatic change of colour- the solution quickly turned dark blue. This rapid reaction is not totally unexpected considering the proposed reduction product (II) which has three amino groups, one of which is *ortho* to a hydroxy substituent. By reference to reduced samples of Amaranth and Sunset Yellow, this would be prone to autoxidation.

The structure of the initial reduction product could not be deduced. Instead, efforts were concentrated on the identification of the two major autoxidation products. The LC separation obtained for a reduced Naphthol Blue-Black sample analysed following 4 hours storage in water with no stirring, is shown in Figure 4.25. Two major peaks were observed which had retention times of 2.5 and 3.5 minutes respectively. The UV spectrum derived from peak VI, showed a strong absorption above 500 nm, suggesting it was responsible for the blue colour change observed in the autoxidation process. A further two minor peaks were also observed at retention times of 4.2 and 5.6 minutes respectively.

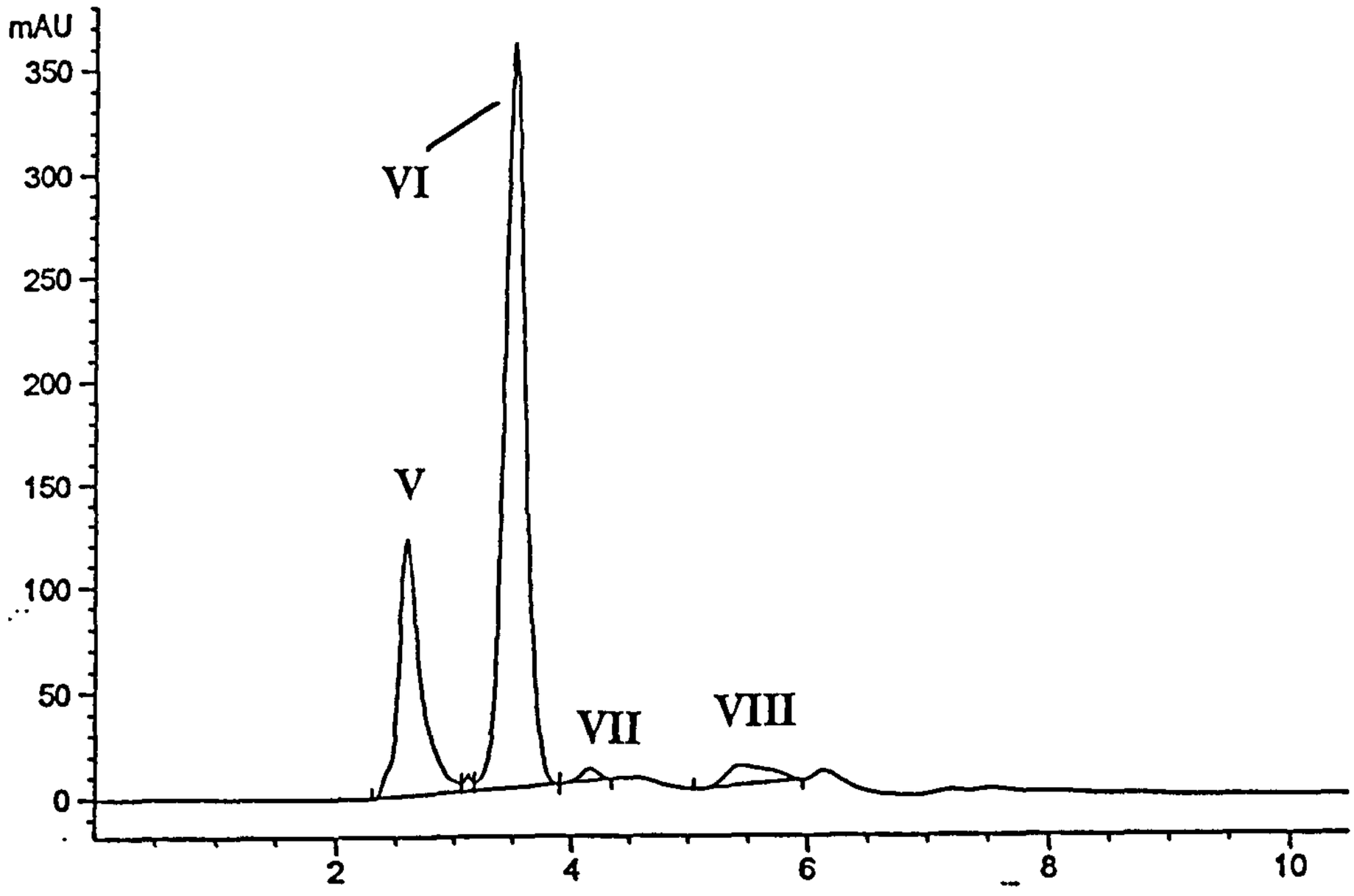

Figure 4.25 HPLC-UV (230 nm) chromatogram of reduced Naphthol Blue-Black following aeration for 4 h.

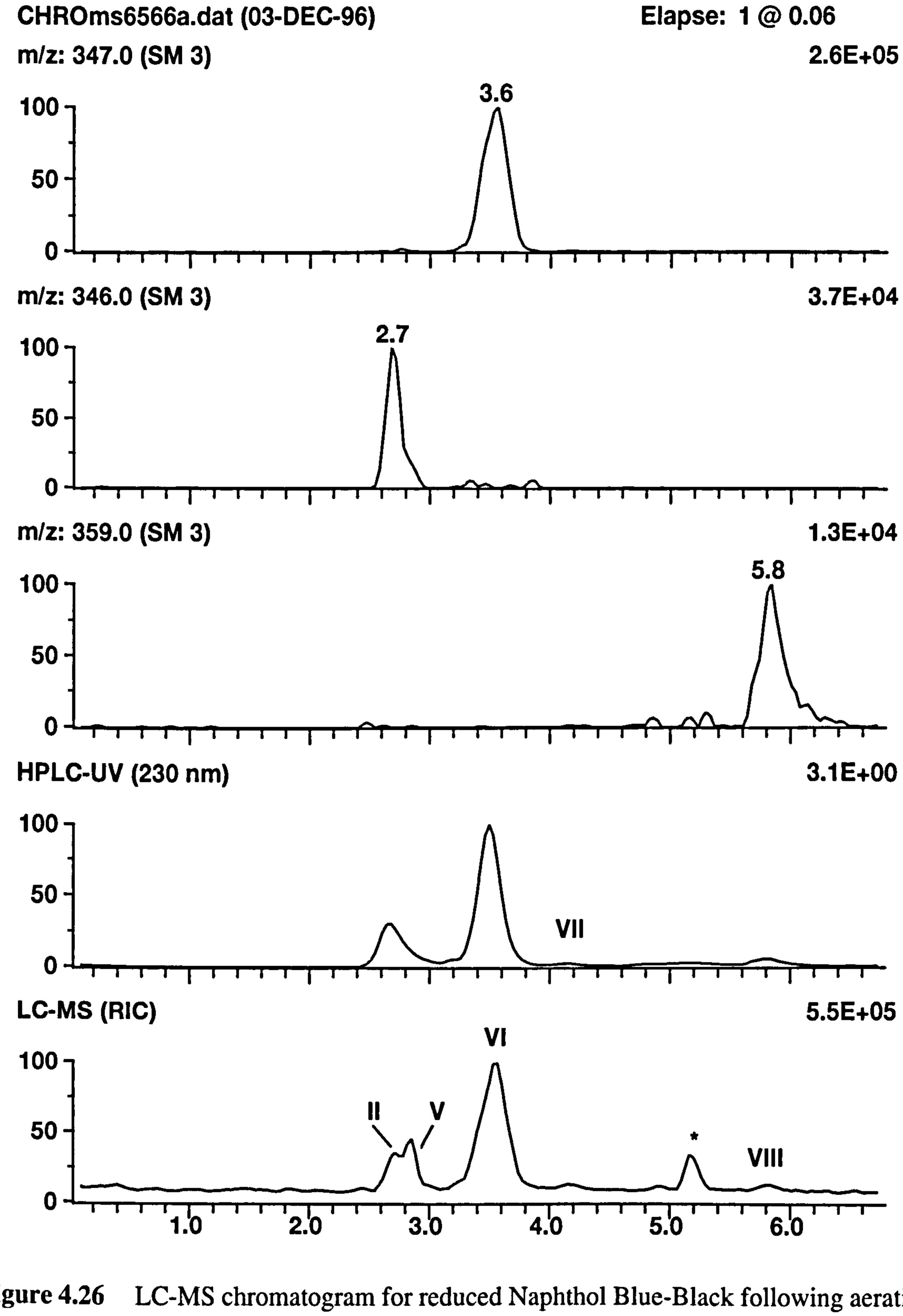

Figure 4.26 LC-MS chromatogram for reduced Naphthol Blue-Black following aeration for 4 hours (* denotes background peaks also in control)

Two major and one minor peaks were observed in the LC-MS analysis of the 4 hour oxidised sample (Fig 4.26). Peak VII in the LC-UV analysis (Fig 4.25) did not produce a useful mass spectrum under the conditions used. The observed molecular ions $[M-H]^-$ for the two major peaks (346 and 347), are illustrated by selected ion mass chromatograms, which suggest molecular weights of 347 and 348 respectively. The minor component peak VIII, showed an ion of mass 359, equivalent to a molecular weight of 360. These molecular weights did not support the initial assumptions of Kudlich (1997 personal Communication) who postulated that autoxidation proceeded through the formation of high molecular weight polymers. All three compounds produced doubly charged ions indicating that each possessed two sulphonic acid groups. LC-MS analysis of a sample oxidised for 6 hours indicated a reduction in the amount of peak V present, with a corresponding increase in peak VI. This indicates the former to be the relatively unstable transition product in the formation of the more stable peak VI. Taking into account the odd molecular weight of peak V, that its mass is only two mass units lower than that of the predicted initial reduction product, that it contains two sulphonates and is a relatively unstable intermediate, the imine of the initial reduction product is suggested:

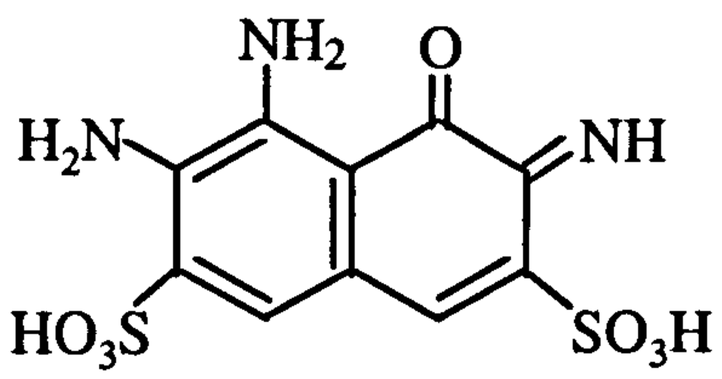

V

On close inspection of the mass spectrum of peak V, it was noticeable that the [M+2] isotope (mainly due to ^{34}S) was larger than would be predicted. A comparison of selected ion chromatograms for peaks V and VI showed the latter to give a close to predicted [M+2] isotope contribution, whilst that for peak V, was significantly higher. These measurements are quite crude and one has to be careful when dealing with an unstable

starting reactant and intermediate. Also, the accuracy of such measurements in LC-MS mode when scanning a large mass range, is not precise. However, assuming the observation is correct, this would suggest the imine to be in equilibrium with the parent reduction product, II, (much in favour of the former), in much the same way as observed for both Sunset Yellow and Amaranth.

On consideration of peak VI, the deep blue colour suggested a large conjugate system, yet the prediction of a dimer proved to be inconsistent with the molecular weight and the number of charges (sulphonic acid groups) present. The observed even molecular weight suggests arrest of autoxidation after the initial loss of one or all three nitrogens. Since the compound is deeply coloured, the probability that all three nitrogens are lost by autoxidation seems quite low. Therefore, one might expect the formation of a naphthaquinone type of structure, similar to that observed for Amaranth and Sunset Yellow:

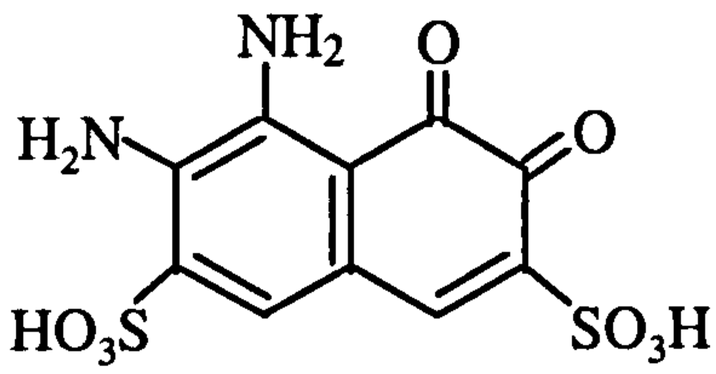

VI

Against this, in the case of Amaranth and Sunset Yellow, the naphthaquinone was unstable and continued to oxidise with ring opening. This was not observed for Naphthol Blue-Black, so perhaps the stable autoxidation product is an isomer of that suggested above.

The third component observed in the LC-MS analysis (peak VIII) showed a molecular weight of 360 but a structure could not be proposed for this minor component.

From the results discussed above it was possible to propose the following autoxidation pathway:

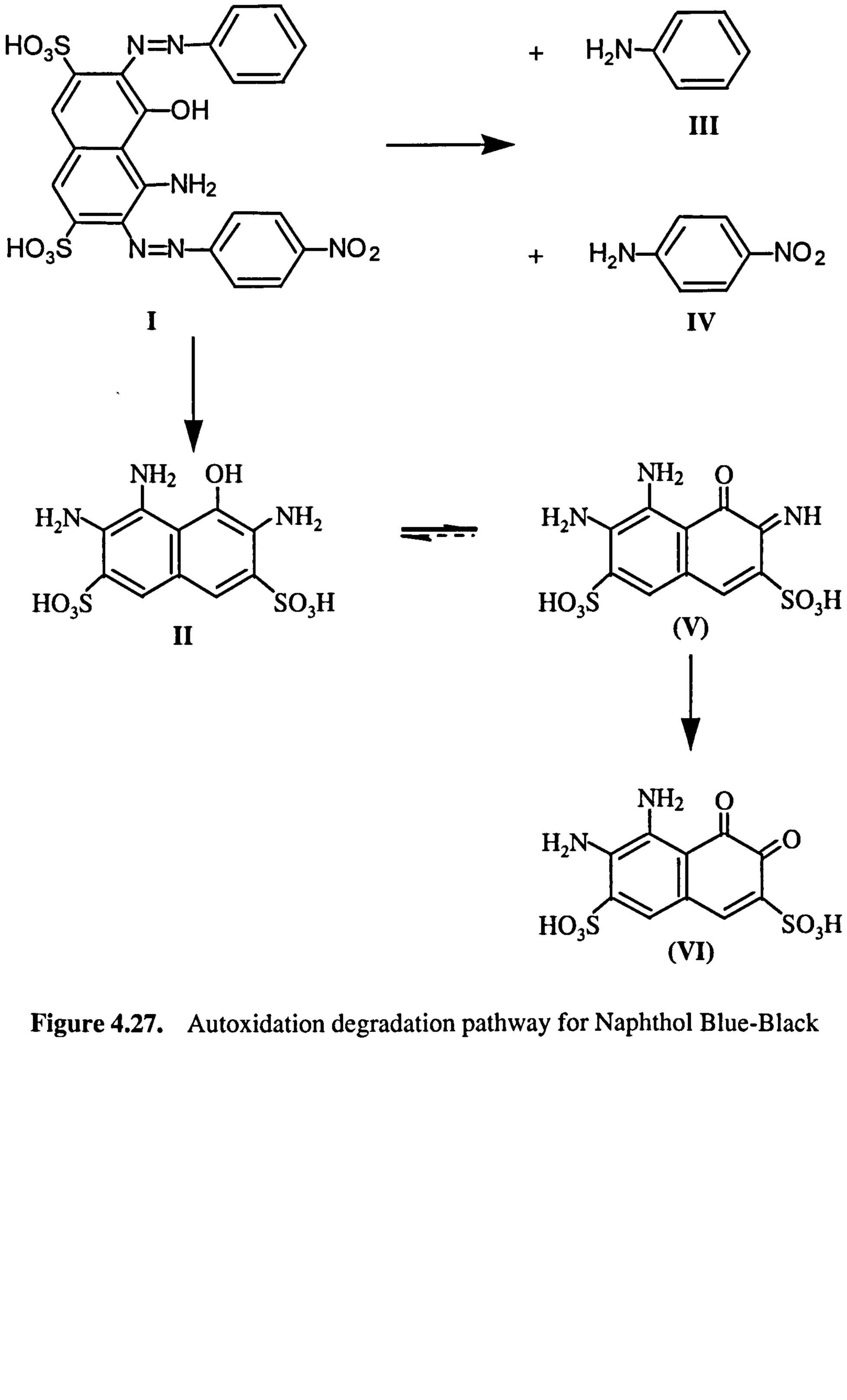

Figure 4.27. Autoxidation degradation pathway for Naphthol Blue-Black

4.5 CONCLUSIONS FROM AUTOXIDATION STUDIES

The primary reduction products of Amaranth, Sunset Yellow and Naphthol Blue-Black, contain a hydroxy-group in a position *ortho* to an amino-group, and in each case these were found to be unstable in the presence of air (ie prone to rapid oxidation). The autoxidation process was affected by the type and degree of substitution on the naphthalene ring. Reduction products of Amaranth and Sunset Yellow were oxidised *via* a naphthoquinone intermediate to stable ring-opened structures. However, oxidation of reduction products of Naphthol Blue-Black (which has additional amino substituents in the 7- and 8-positions of the naphthalene ring) stopped at the formation of a naphthoquinone structure. Additionally, Sunset Yellow was able to form dimers, which were not observed for the reduction products of the other two dyes. The primary reduction products of both Amaranth and Naphthol Blue-Black have a sulphonic acid group in the 3-position, which may hinder addition at the 4-position. This would suggest dimerisation would take place by addition at the 4-position of Sunset Yellow.

4.6 REDUCTION AND AUTOXIDATION OF AZO DYE REACTIVE RED 3.1 (RR3.1).

4.6.1 Introduction

The rather simple dye structures of Amaranth, Sunset Yellow and Naphthol blue/black, proved very useful probes for the investigation of reduction/ autoxidation degradation pathways. The similarities in degradation products of each dye (ie the formation of naphthoquinone-imine, leading to naphthoquinone-type intermediates, which may then undergo further hydroxylation and ring opening) gave some confidence in the ability to predict degradation products for more complex dye structures. An opportunity arose for

collaboration with researchers at the University of Leeds who were attempting to optimise the degradation of azo dyes for the treatment of industrial waste (Knapp and Newby, 1995, Bromley-Challenor *et al.*, 2000). The aim of this part of the present research was to determine whether the initial autoxidation products derived from a complex dye could be predicted from the information gained from the study of simpler structures (eg Amaranth, Sunset Yellow and Naphthol Blue Black). Structural information regarding degradation products was needed to enable optimisation of the treatment process. The dye chosen for this study was Reactive Red 3.1, (RR3.1, I)

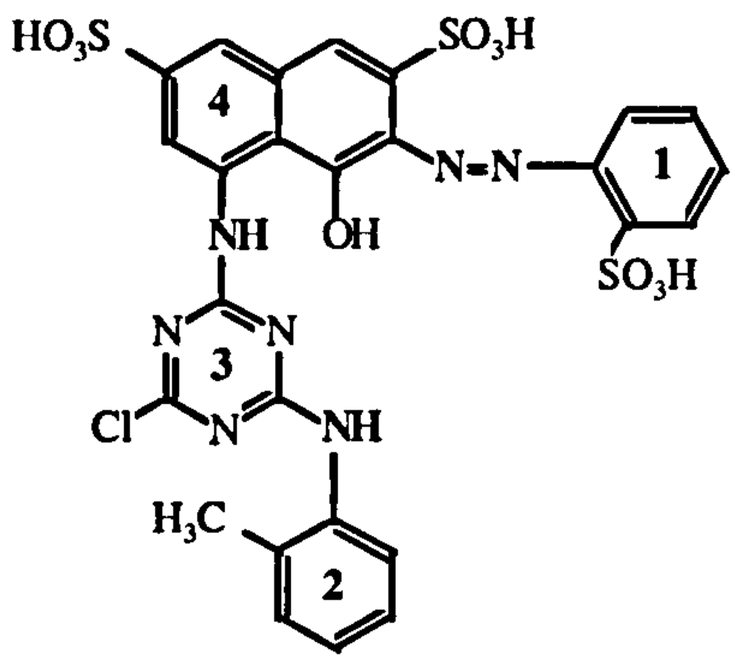

I

The structure of RR 3.1 shows component parts which include the N=N azo bond, secondary amino groups: aniline-2-sulphonic acid (1) and toluidine (2), the chlorotriazine reactive group (3) and a 1-hydroxy-naphthalene-2,8-diamino-3,6-disulphonic acid group (4; H-Acid).

4.6.2 Experimental procedures

All samples of reduced RR3.1 were prepared at the University of Leeds and immediately transferred to Brixham Laboratory for subsequent analysis. The experimental detail and results are given in the following text.

Synthetic sewage

Synthetic sewage mineral salts (SSMS) medium was used throughout the study and contained the following (mg l^{-1}); NH_4Cl (380), KH_2PO_4 (4000), $CaCl_2.2H_2O$ (22), $MgSO_4.7H_2O$ (40), $FeCl_3.6H_2O$ (7.5), $Na_2MoO_4.2H_2O$ (1.1), $ZnSO_4.7H_2O$ (0.7), $MnSO_4.4H_2O$ (0.6), $CuSO_4.5H_2O$ (0.6), $CoCl_2.6H_2O$ (0.6).

Enrichment cultures

Enrichment cultures were grown using an inoculum made from the following components (ml):- Oil field produced water (200); marine mud (100); acid peat bog water (100); acidic peat soil (from 2 sources) (2 x 100); acidic iron water from an iron-bearing moorland stream (100); river water and mud from the river Aire at Beal Weir (100 of each); and activated sludge from a laboratory reactor (porous pot). After thorough mixing, the inoculum was divided into two and pH adjusted as described for individual experiments. Prior to use, oxygen was removed from the inoculum by evacuation using a vacuum pump for 2 hours and then sparged with oxygen-free nitrogen overnight. Dye reduction experiments were carried out in glass serum bottles (160 ml total volume), which were sealed with Neoprene rubber septa and secured in place with aluminium seals. Experiments were performed at 27°C. To maintain anaerobic conditions during sampling, bottles were stored in a constant temperature cabinet flushed with nitrogen. A 10% ($^{v}/_{v}$) inoculum was used per serum bottle and serum bottles were not mixed during incubation..

Experiment 1. Initial evaluation of reduction/ autoxidation

Reactive Red 3.1 was added to serum bottles to give a concentration of either 60 or 480 mg l^{-1}, and the pH adjusted to either 5 or 7. Three bottles contained heat sterilised inoculum to act as controls. Details of each bottle are listed in Table 4.3.

Table 4.2 Summary of conditions of bottles incubated in experiment 1 containing Reactive Red 3.1 dye (RR 3.1) and a mixed bacterial culture at 27°C

Flask	pH	Salinity (%)	Concentration RR 3.1 (mg l^{-1})	Comments
A	**5**	**0.2**	**480**	
B	**7**	**0.2**	**480**	
C	**5**	**0.2**	**480**	**Sterile biomass control**
D	**7**	**0.2**	**60**	
E	**5**	**0.2**	**60**	
F	**7**	**0.2**	**60**	**Sterile biomass control**
G	**5**	**0.2**	**60**	**Sterile biomass control**

Each bottle was incubated until maximum colour loss was observed, (approx 9 days). Samples were taken using a hypodermic syringe and were centrifuged at 13,500 rpm in an MSE Micro Centaur centrifuge for 5 minutes to remove suspended particles prior to transfer to Brixham Laboratory for analysis by LC-MS.

Experiment 2. Evaluation of stored reduced samples.

The experiment described in the previous section was repeated using only a 480 mg l^{-1} RR3.1 solution, 0.2% NaCl and at pH 7. Samples were incubated for a time which produced maximum colour loss in the dye (ie a change from red to pale straw coloration)

this being about 9 days. Samples (Bottle A; reduced dye, B; Dye, mineral salts but no inoculum and C; Dye, mineral salt and sterile inoculum) were transferred to Brixham Laboratory in gas tight bottles. This was to allow analysis without the possibility of autoxidation of the samples during manipulation at Leeds or in transit. Samples of all three bottles were taken through the rubber septum by syringe and analysed directly by LC-MS. No sample preparation was used.

Experiment 3. Reduction in the presence of activated sludge

Serum bottles containing activated sludge from Knostrop or Owlwood (UK) sewage treatment works, were provided with fresh sludge within 6 - 8 hours of collection. Each bottle contained 80 ml of mineral medium/activated sludge mixture and had a headspace of 80 ml and was incubated at 27°C. Prior to use, activated sludge was washed and centrifuged (4,000 rpm, *ca.* 2600 g). The sludge concentration was then adjusted to 6 g l^{-1} (dry weight) with mineral media (pH 7, 0.2% NaCl). After the sludge had been mixed thoroughly, it was sparged with oxygen-free nitrogen overnight to ensure the development of anaerobic conditions, then oxygen was removed under a vacuum. Reactive Red 3.1 was used at a concentration of 120 mg l^{-1} and the biomass was constantly stirred during incubation. Four samples were taken per activated sludge type. In each case, 200 ml of reaction volume was centrifuged at 2600 g for 10 minutes. The sludge was discarded and a subsample of the supernatant was transferred to autosampler vials for LC-MS analysis. Samples were taken immediately after the addition of the dye (untreated dye, t = 0 hours) and immediately after decolorization (decolorized dye, t = 0 hours). After decolorization, samples were incubated aerobically for 48 hours (decolorized dye, t = 48 hours) and 7 days (decolorized dye, t = 7 days). Samples were also taken for analysis using the *activated sludge respiration inhibition test* (ASRIT) which was adapted from a standard method

(HMSO, 1982). Samples were cooled in ice during transit to Brixham Laboratory, where they were analysed by LC-MS on the day of arrival.

LC and LC-MS Methods

All samples from the above degradation studies were first screened using HPLC with Photodiode array (PDA) detection to determine effects of the treatment on Reactive Red 3.1. Separation was achieved using a 250 mm × 4.6 mm 5 µm C18 column operated under gradient conditions with a mobile phase of 100% ammonium acetate (10 mM) for 10 minutes, to 50/50 with acetonitrile at 30 minutes and using a flow rate of 0.7 ml min^{-1}. Samples were subsequently analysed by LC-MS using a TSQ-700 mass spectrometer fitted with an electrospray (ESI) interface operated in negative ionisation mode with a spray voltage of 3.5 kV, at a capillary temperature of 255°C, sheath gas at 65 psi and auxiliary gas at 10 psi. The system also had an in-line UV/Vis detector operated at 254 nm, for comparison with LC-PDA data. The analytical column and mobile phase were the same as that used in the LC-PDA system.

4.6.3 Results

LC-PDA Analysis of initial batch study

Attempts were made to develop, through enrichment, cultures which were capable of the decolorization of Reactive Red 3.1 (RR3.1) under anaerobic conditions. Attempts were made to simulate the conditions of different sewage treatment conditions using variations in pH, NaCl concentration and dye concentration. The inoculum used in all experiments was a mixed inoculum obtained from a variety of diverse environmental sources which included sites with low pH and elevated NaCl. Samples of the mixed anaerobic cultures

plus dye (60 and 480 mg l^{-1}) were taken at time zero and after dye decolorization. These were centrifuged to remove suspended particles and the supernatants were transferred to Brixham for analysis. This analysis showed that control bottles; those without inoculum or heat sterilised, showed no change in the concentration of Reactive Red 3.1, demonstrating the stability of the compound under the experimental conditions used. On the other hand, decolorization of RR3.1 occurred in all serum bottles receiving a live inoculum under all experimental conditions. A colour change from red to a very pale yellow was reported by the University of Leeds. However a further change had occurred in three of the reduced samples arriving at Brixham: A (yellow/orange), B and D (yellow/green), indicating the onset of autoxidation during the time taken for transportation. All four degraded samples were analysed and a total of eighteen significant peaks were observed, together with numerous smaller and less well defined components contributing to an elevated baseline signal. Chromatograms from these samples were similar in constitution, although differing in the relative intensity of individual components. This is demonstrated by a comparison of the two most concentrated samples (A and B, initial RR3.1 concentration of 480 mg l^{-1}), with the corresponding uninoculated control (C), (Fig 4.28; expanded to show the most complex part of the chromatogram in Fig 4.29). Peak XVII was by far the most abundant peak in each sample, with peaks IX and XVI also prominent in the less concentrated samples D and E (60 mg l^{-1}).

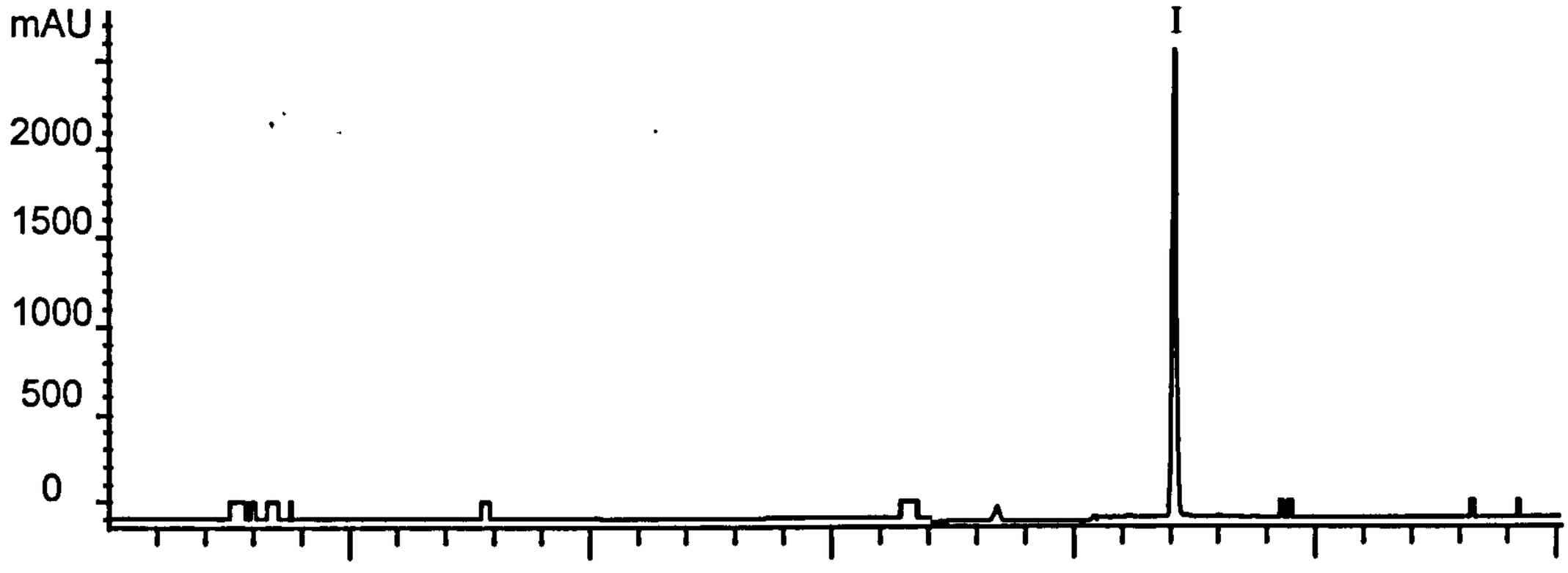

Figure 4.28 LC-PDA (254 nm) chromatograms for reduced samples of RR 3.1 control sample (top), sample A, following anaerobic incubation at pH 5 (middle) and sample B, following anaerobic incubation at pH 7 (bottom), Peak I is RR 3.1.

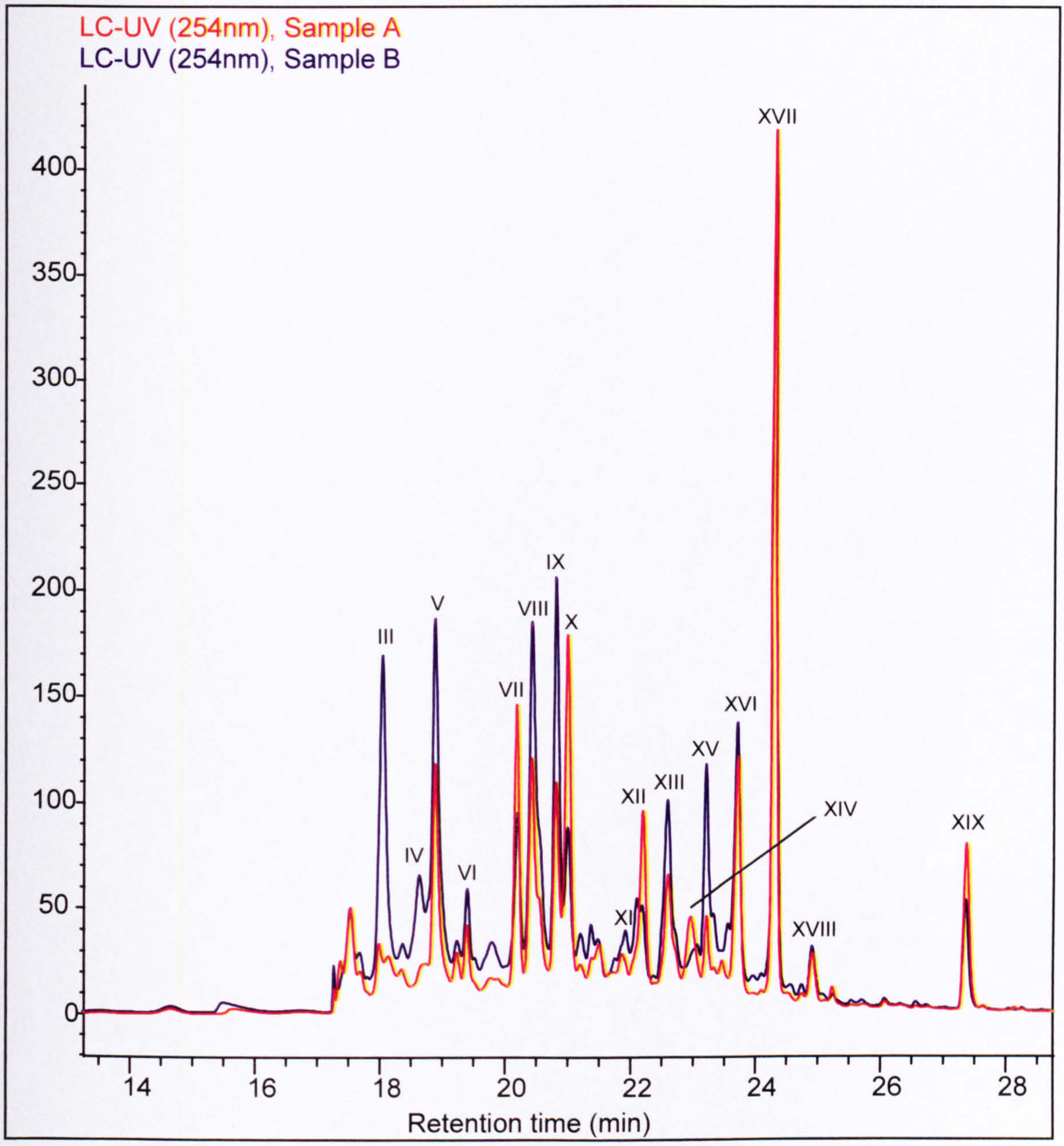

Figure 4.29 Comparison of LC-PDA (254 nm) chromatograms for reduced samples of RR 3.1. A, RR3.1 following anaerobic incubation at pH 5 (top) B, following anaerobic incubation at pH 7 (bottom)

The peak height of the eighteen most significant peaks in sample A and B are shown plotted against peak number and retention time in Figure 4.30. This provided a useful guide for subsequent LC-MS identification because it showed the relative importance of each component.

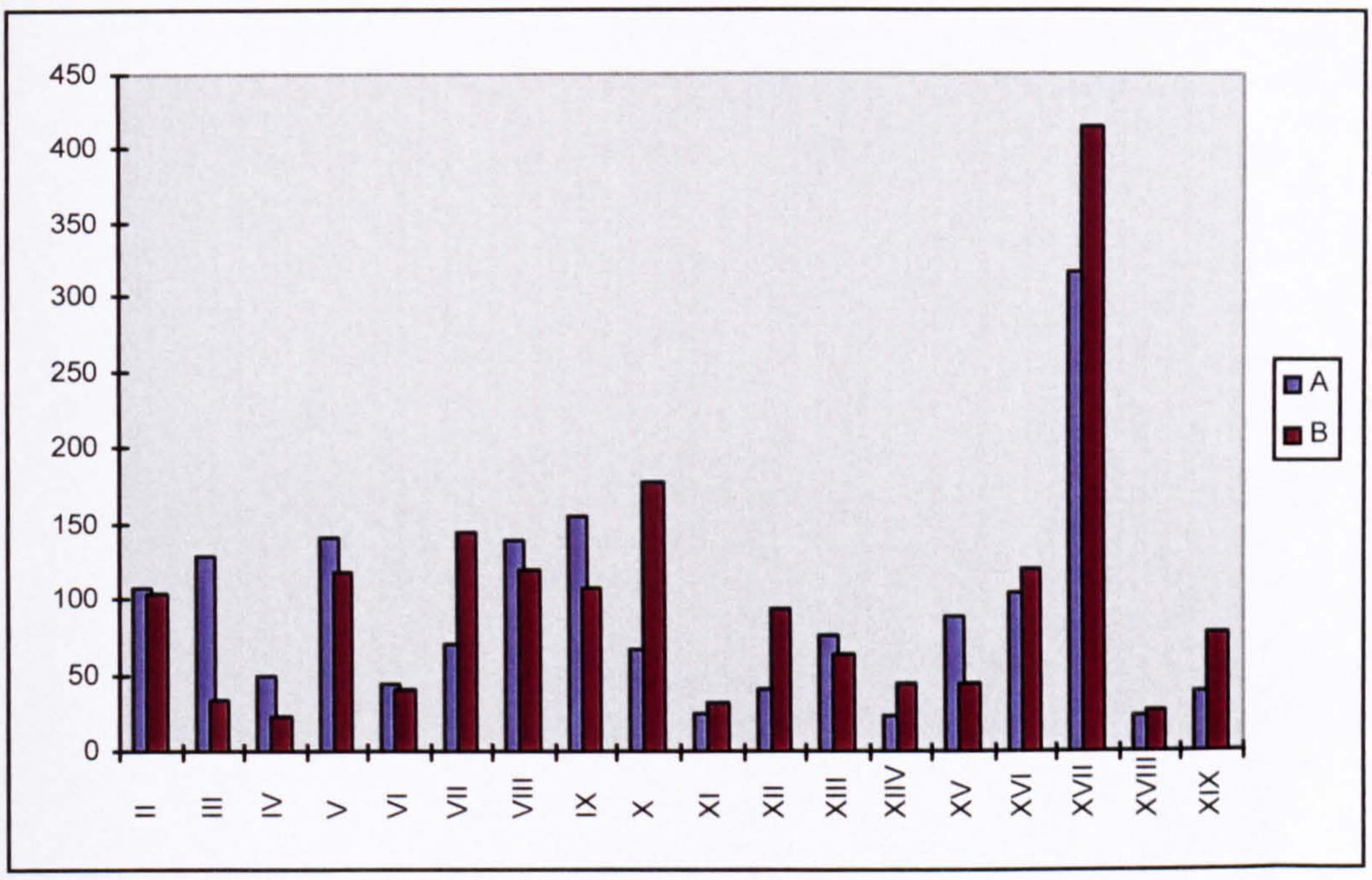

Figure 4.30. Comparison of peak height data for major peaks in samples A (pH 5) and B (pH 7) for autoxidised samples of reduced Reactive Red 3.1

LC - MS Studies

The LC-MS data confirmed the complete removal of Reactive Red 3.1 and furthermore allowed the identification of several degradation products. All of the peaks observed in the LC-UV analysis were also observed by LC-MS, although in some cases only weak mass spectra were obtained. The retention times observed for each peak were generally 2 - 3 minutes less than LC-PDA, but use of in-line UV spectroscopy allowed correlation between the two systems. The LC-MS analysis in fact showed the autoxidised samples to be even more complex than suggested by the LC-PDA data. Many of the peaks observed in LC-UV were shown to consist of mixtures of two or more components. Chromatograms from all four samples showed they were similar in constitution, although differing in the

relative intensity of individual components. A typical chromatogram for sample A showing both MS and in-line UV (230 nm) data, is shown in Figure 4.31 and an expanded section showing the most complex part of the chromatogram in Figure 4.32.

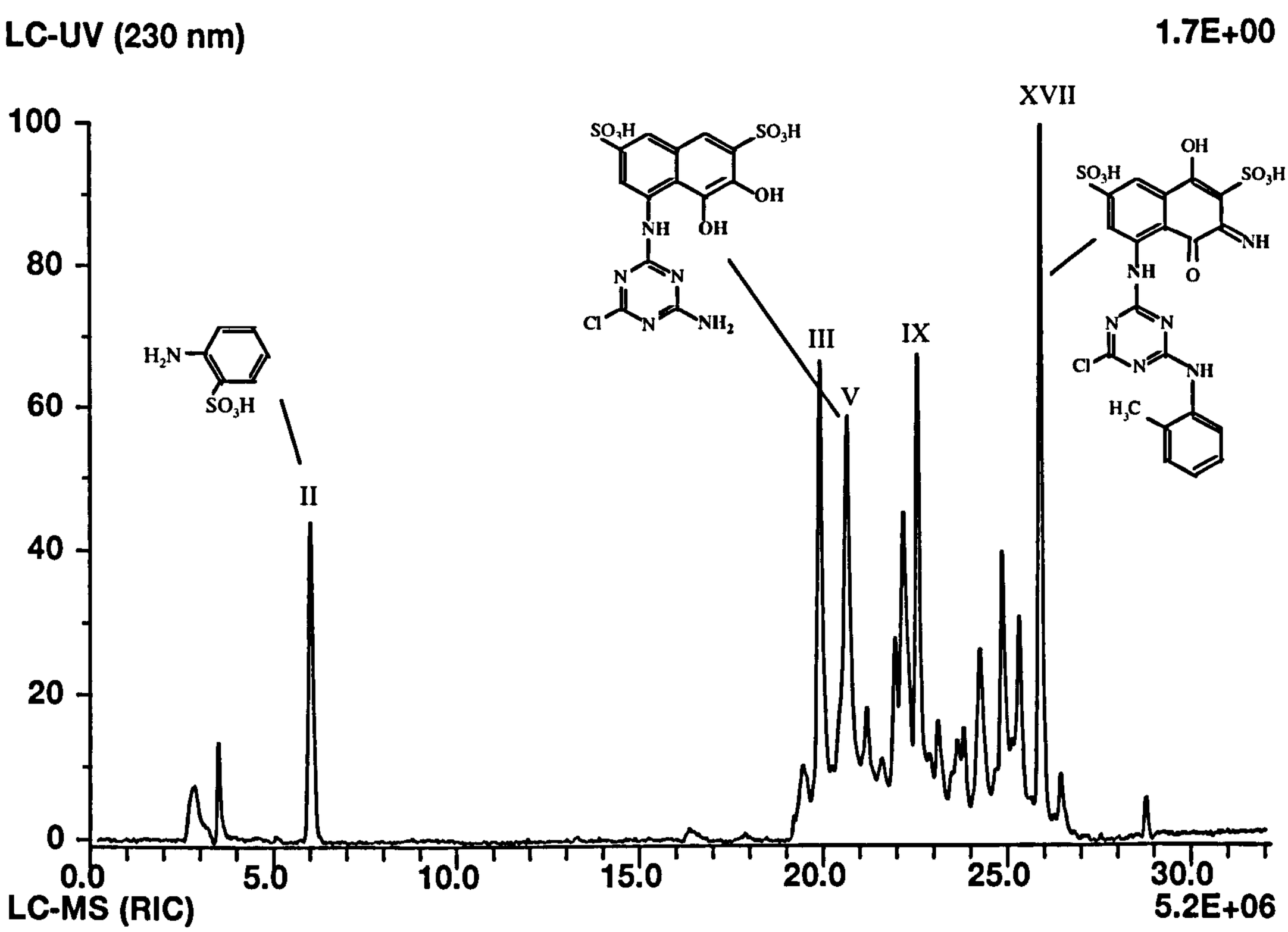

Figure 4.31 LC-MS and LC-UV (230 nm) chromatograms of reduced RR 3.1 sample A, following autoxidation.

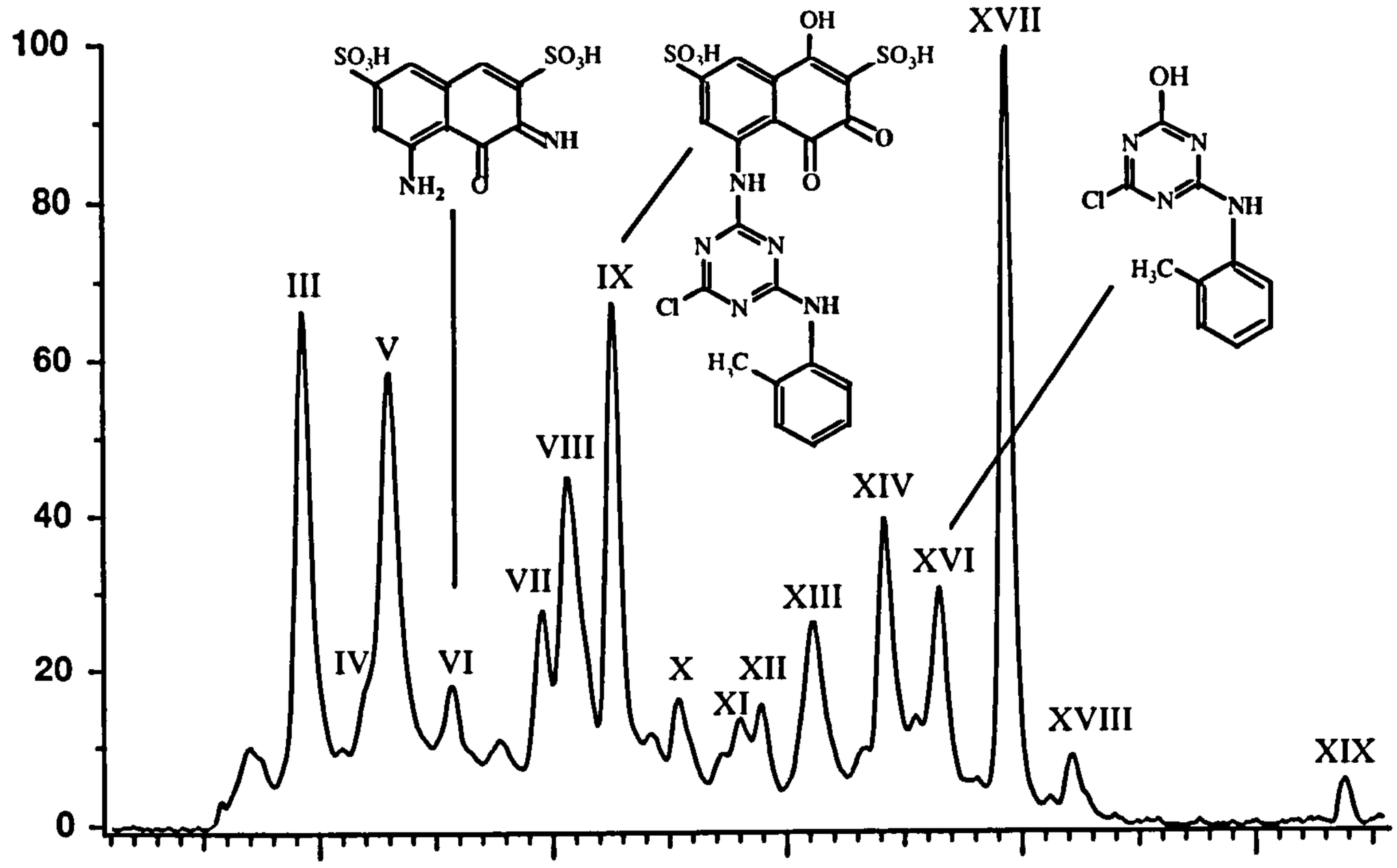

Figure 4.32 LC-MS and LC-UV (230 nm) chromatograms of reduced RR 3.1 following autoxidation

The study of the autoxidation processes of reduced Amaranth, Sunset Yellow and Naphthol Blue Black (Section 4.4) showed a range of common and characteristic degradation products. These processes suggest likely degradation products of the more

complex dye RR3.1 would include products of reduction of the azo linkage such as primary amines (a) and 1-aminobenzene-2-sulphonic acid, (b) below, which would have molecular weights of 552 and 173 respectively.

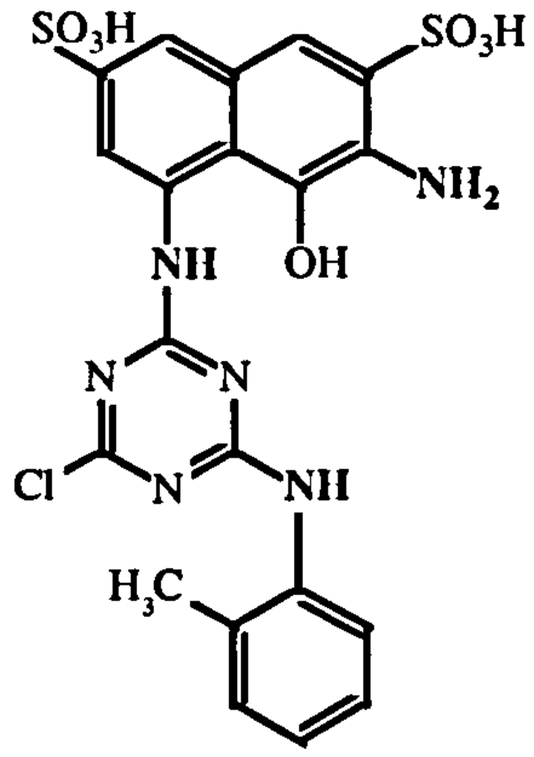

(a)

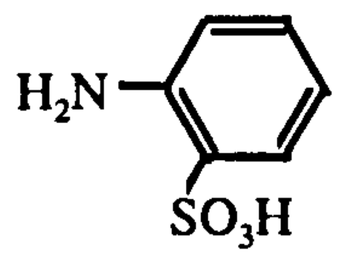

(b)

The research described in the previous section showed that 1-aminobenzene-2-sulphonic acid was stable. However, a naphthalene ring with an amino and hydroxyl group *ortho* to one another as in amine (a), would be expected to oxidise rapidly to naphtho-imine and naphthoquinone type structures:

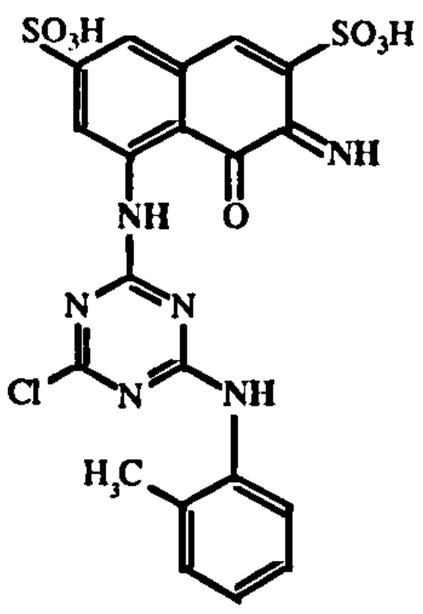

(c)

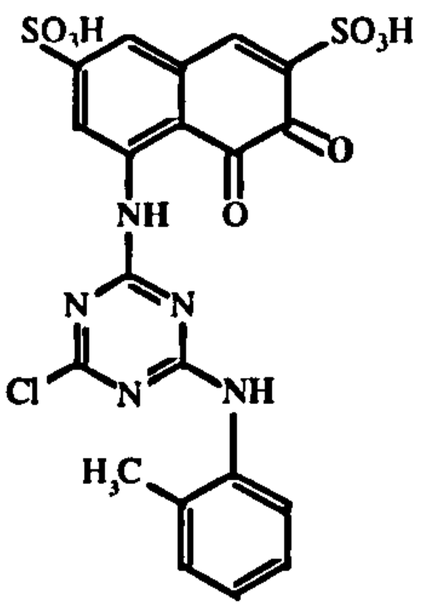

(d)

RR3.1 has two sulphonic acid groups on the main naphthalene ring in the 3 and 6 positions. By analogy to Amaranth and Naphthol Blue Black, these groups would be expected to hinder formation of dimers through a 1 - 4 addition and subsequent

degradation would be predicted to continue by hydroxylation of the aromatic ring with the possibility of ring opening:

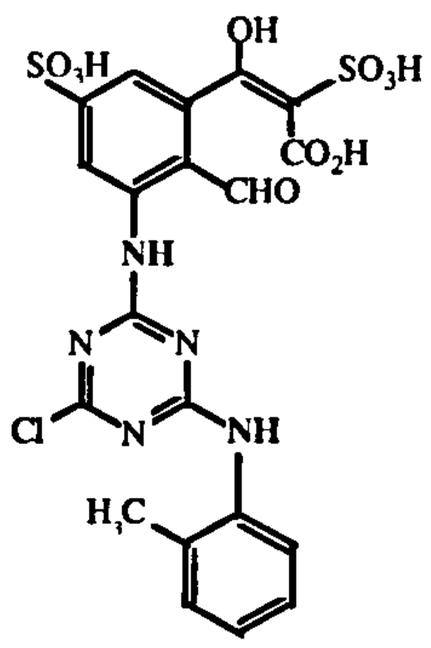

(e)

Alternatively the nitrogen-containing intermediates might be stabilised and persist as observed for Naphthol Blue-Black. Potentially, the secondary amines present in RR 3.1 can also be reduced, which on subsequent autoxidation may form another group of products:

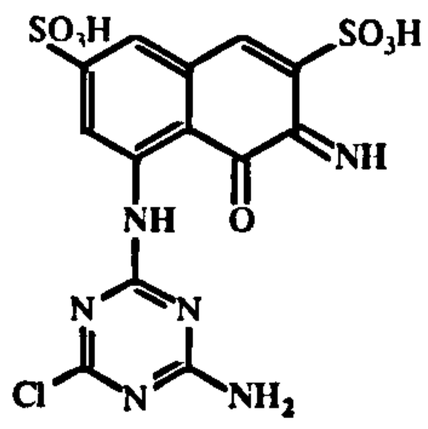

(f)

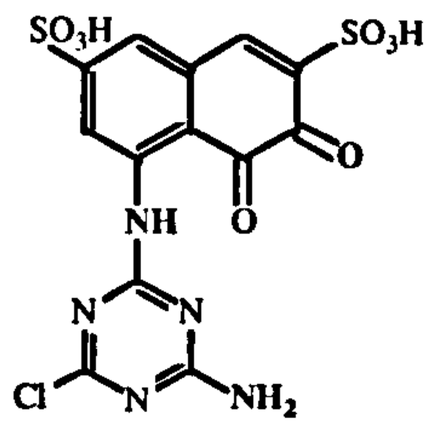

(g)

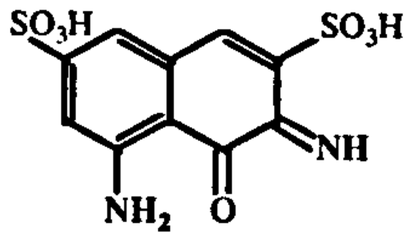

(h)

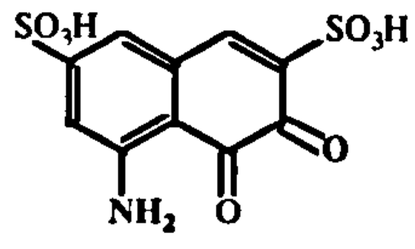

(i)

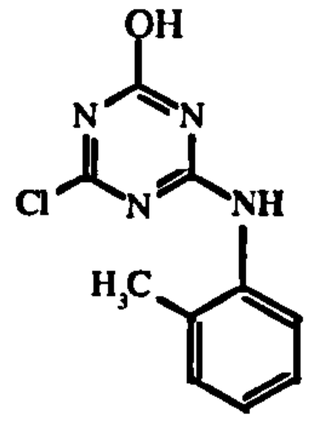

(j)

Additionally, the process may be further complicated by the presence of the reactive group, the chlorine of which is quite labile and may be hydrolysed in the autoxidation process. This would produce most of the above structures (a-f plus i) with a hydroxyl group (-OH) in place of the reactive chlorine (-Cl), a net change of 18 Daltons (+17 - 35) in the predicted molecular weight. Clearly once one moves to a more complex substrate such as RR3.1, there are numerous possibilities for degradation products. To aid interpretation and to test the predictions described above, all of these proposals were summarised in a check list (Table 4.3) which was subsequently used to aid interpretation of the LC-MS data obtained for the samples derived from anaerobic degradation studies:

Table 4.3. Molecular weight information for possible degradation products of Reactive Red 3.1.

Proposed structure	Comment	Number of SO_3H	Chlorine (y/n)	Molecular weight	Molecular ions
a	Amine	2	y	552	551, 275
b	Amino sulphonic acid	1	n	173	172
c	Naphthoquinone-Imine	2	y	550	549, 274
d	Naphthoquinone	2	y	551	550, 274.5
e	Hydroxy acid	2	y	585	584, 291.5
f	(c) - toluidine	2	y	460	459, 229
g	(d) - toluidine	2	y	461	460, 229.5
h		2	n	332	331, 165
i		2	n	333	332, 165.5
j		0	y	236	235
Structures produced by hydroxylation of the naphthalene ring					
a1	Hydroxylated a	2	y	568	567, 283
c1	Hydroxylated c	2	y	566	565, 282
d1	Hydroxylated d	2	y	567	566, 282.5
f1	Hydroxylated f	2	y	476	475, 237
g1	Hydroxylated g	2	y	477	476, 237.5
h1	Hydroxylated h	2	y	348	347, 173
i1	Hydroxylated i	2	y	349	348, 173.5
Structures produced by substitution of reactive chlorine by hydroxyl					
a2	a-Cl +OH	2	n	534	533, 266
c2	c-Cl +OH	2	n	532	531, 265
d2	d-Cl +OH	2	n	533	532, 265.5
e2	e-Cl + OH	2	n	567	566, 282.5
f2	f-Cl +OH	2	n	442	441, 220
g2	g-Cl +OH	2	n	443	442, 220.5
j2	j-Cl +OH	0	n	218	217
Structures produced by hydroxylation of naphthalene ring and exchange of chlorine with hydroxyl					
a3	Hydroxylated a2	2	n	550	549, 274
c3	Hydroxylated c2	2	n	548	547, 273
d3	Hydroxylated d2	2	n	549	548, 273.5
e3	Hydroxylated e2	2	n	458	457, 228
f3	Hydroxylated f2	2	n	459	458, 228.5

In the light of the known structure of RR3.1, the mass of each component, the presence or absence of chlorine, the number of nitrogen atoms, the presence and/or number of sulphonic acid groups and the predictions derived from earlier experiments, it was possible to suggest structures for several components in the degraded mixtures. A summary of

mass spectral information is given in Table 4.4, which also highlights those peaks which match predicted structures. Additionally, representative mass spectra for some of the major components are shown in Figure 4.33.

Table 4.4. LC-MS data for autoxidation products of reduced RR3.1

Peak Number (Figures 4.33 and 4.34)	Retention time	Number of SO_3H	Chlorine (y/n)	Molecular weight	Molecular ions	Predicted Structure
II	6:00	1	n	173	172	b
III (i)		4	?	1032	515/343/257	
(ii)		4	?	1112	555/369/277	
(iii)		2		537	536/267.5	
IV		2	y	585	584/291.5	e
V (i)		2	y	507	506/252.5	
(ii)		2	y	463	462/230.5	g-dihydro
VI (i)		?	n	332	331	h
(ii)				317	316	
VII (i)	22.6	2	y	633	632/315.5	
(ii)			y	478	477	
VIII		2		507	506/252.5	
IX		2	y	567	566/282.5	d1
X		4	?	1032	515/343/257	
XI				292	291	
XII (i)					536	
(ii)					287.5	
XIII	24.3	2		722	721/360	
XIV		2	y	566	565/282	c1 isomer
XV (i)	24.9			463	462 (b only)	
XVI (i)	25.3	0	y	236	235	j
(ii)			y	551	550/274.5	d
(iii)			y	662	661/330	
XVII	25.9		y	566	565/282	c1 isomer
XVIII (i)	26.4	2		615	614/306.5	
(ii)				617	616/307.5	
XIX			y	509	508	

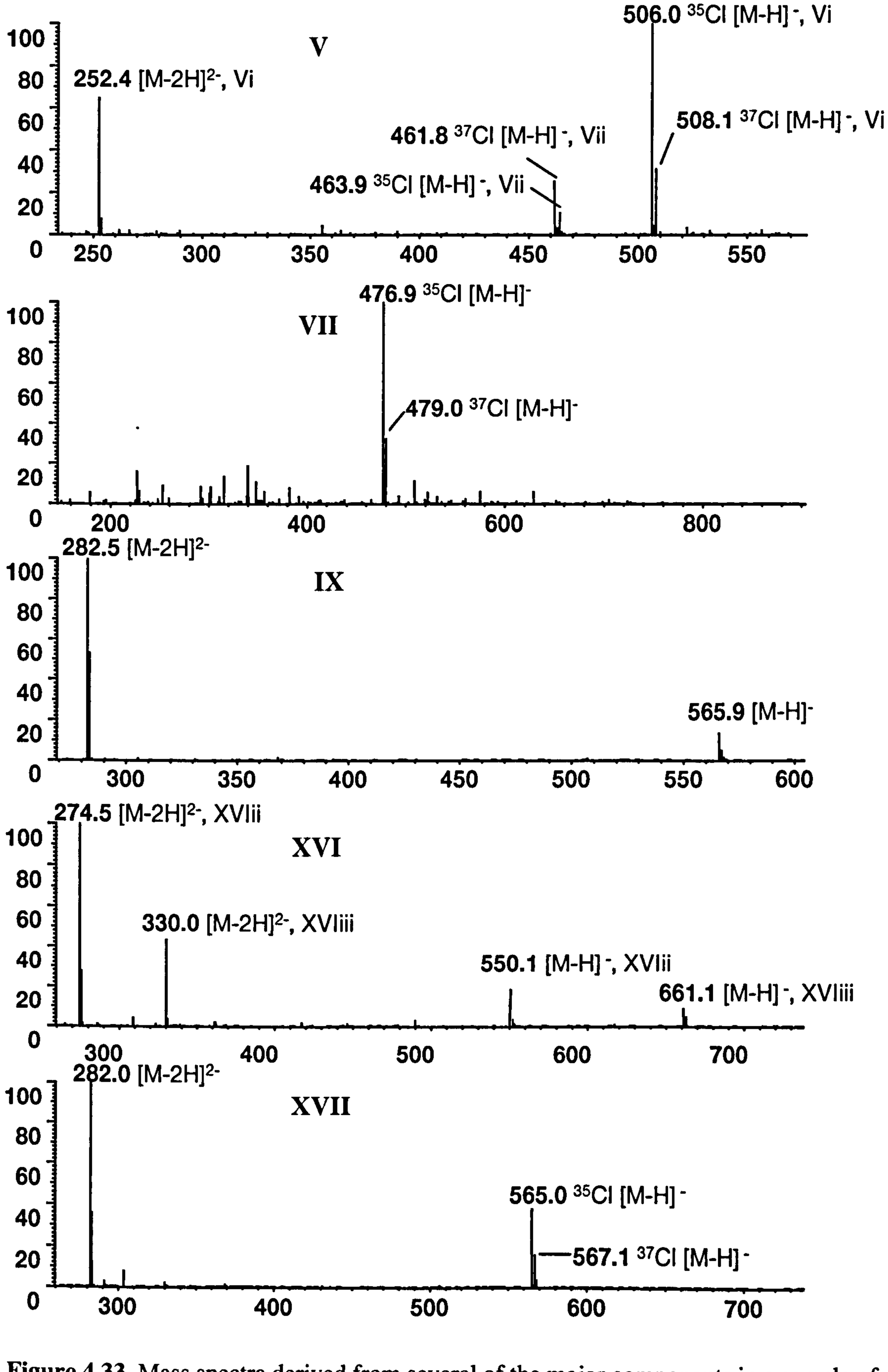

Figure 4.33 Mass spectra derived from several of the major components in a sample of reduced RR 3.1, following autoxidation.

Peak II was confirmed as 1-amino-2-sulphonic acid. This gave strong evidence for the reductive cleavage of the azo bond of Reactive Red 3.1, with the production of aniline-2-sulphonic acid and an amine based on the reduced amino-naphthalene disulphonic acid moiety linked to the reactive chlorotriazine group:

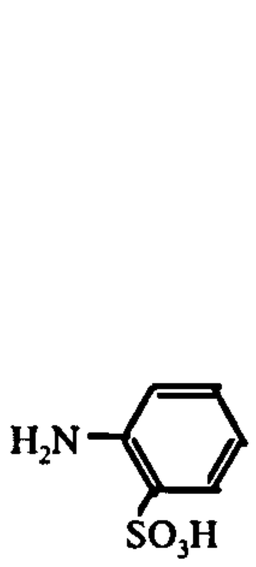

(II)

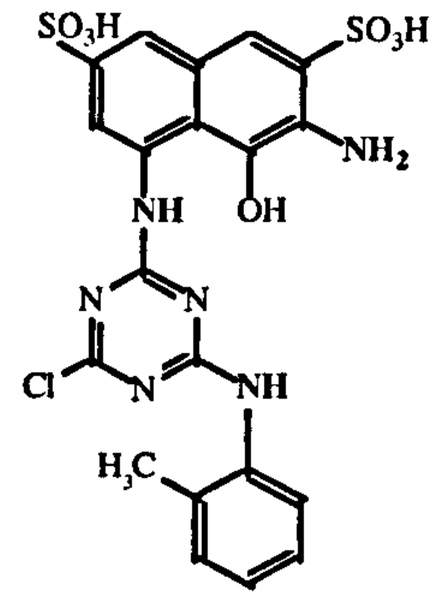

(a)

A mass spectrum for the latter was not observed, but this was not surprising bearing in mind the highly reactive nature of these compounds. Previous work with Amaranth and Sunset Yellow had suggested the primary 1-hydroxy-2-amino-naphthalene based reduction product of azo dyes was stable for only 2 - 3 hours in the presence of air. These samples had been stored under aerobic conditions for *ca* 8 hours prior to analysis, although they were obviously not stirred so care is needed when making a direct comparison with Amaranth or Sunset Yellow reduction product stability. There was also no evidence for the proposed naphthoquinone-imine (c, Table 4.3) or naphtho-hydroquinone based structure. However one of the components of major peak XVI produced a molecular ion corresponding to the proposed naphthaquinone structure, (d):

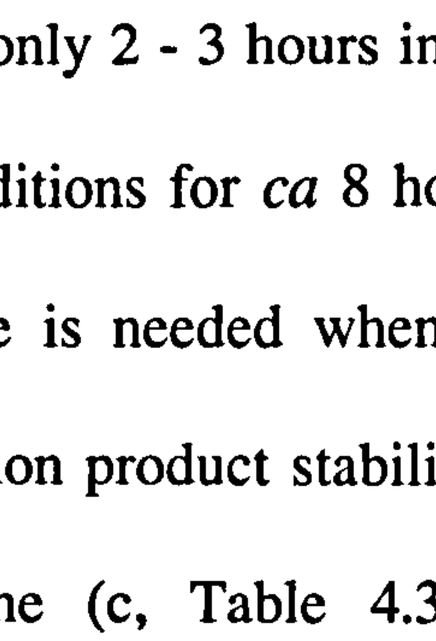

(XVIii)

This was not particularly surprising when considering the relatively high stability of naphthoquinoic structures compared to their corresponding imines and hydroquinones, as discussed in the previous studies. Of particular interest were three other significant peaks; IX, XIV and the most prominent peak in both the UV and MS chromatograms, XVII. The first of these showed a molecular ion 16 mass units higher than observed for the aforementioned naphthaquinone peak XVIii. This suggested the addition of a hydroxyl group, which by comparison to Sunset Yellow would be predicted in the 4 position and equates to proposed structure d1:

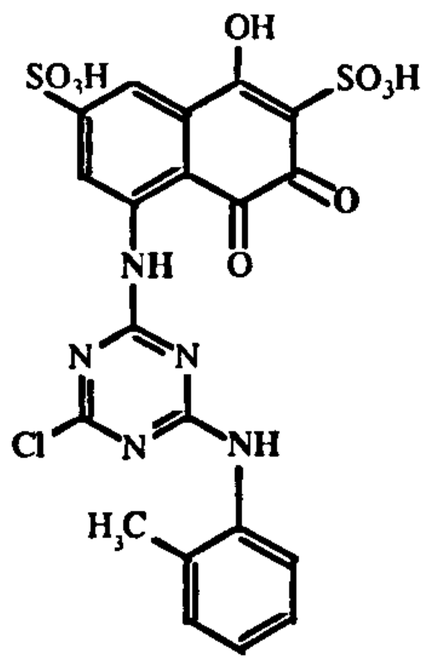

(IX)

The mass spectra obtained for peaks XIV and XVII suggest they are isomers and these spectra are consistent with addition of an hydroxyl group to a napthaquinone-imine structure (predicted c1). Again one would predict addition at the 4- position to be most likely, although hydroxylation of the toluidine ring attached to the reactive group is also possible and may explain the presence of two isomers:

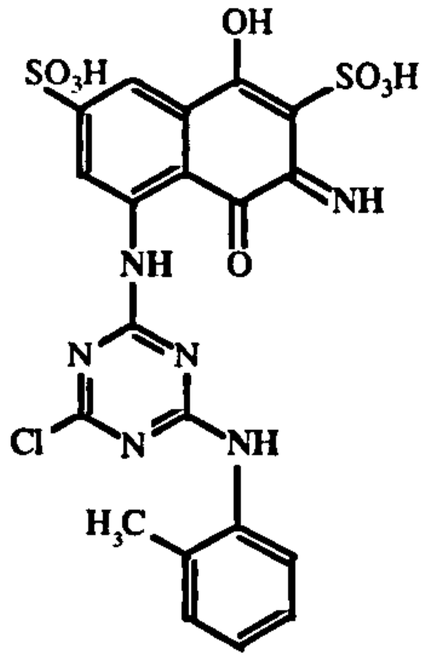

(XVII)

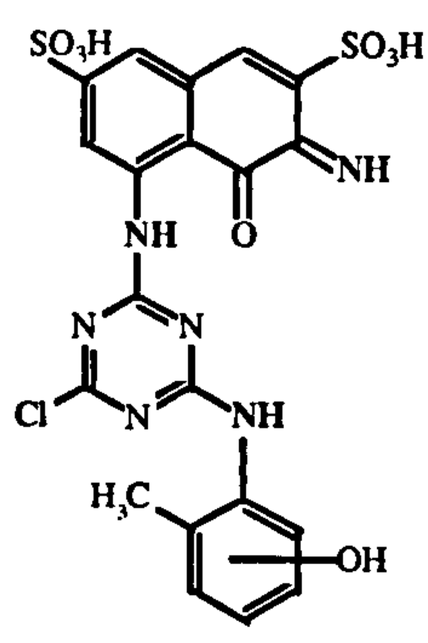

(XIV)

The retention times of these four structures are in the range 23:30 - 27 minutes, similar to that of RR3.1, 24:10 minutes. These structures might be expected to have a similar polarity to RR3.1 because although they have one less sulphonic acid group, making them less polar, this was compensated by the extra functionality (formation of the quinone and/or hydroxylation etc) in the remaining structure.

Peak IV, is of particular significance. This peak had one of the shortest retention times of the observed components, indicating a higher polarity than other degradation products. The observed molecular ion is consistent with the proposed ring opened carboxylate (e), which by analogy to the discussion of the equivalent compounds identified in the autoxidation of Amaranth and Sunset Yellow, suggest one of the following structures:

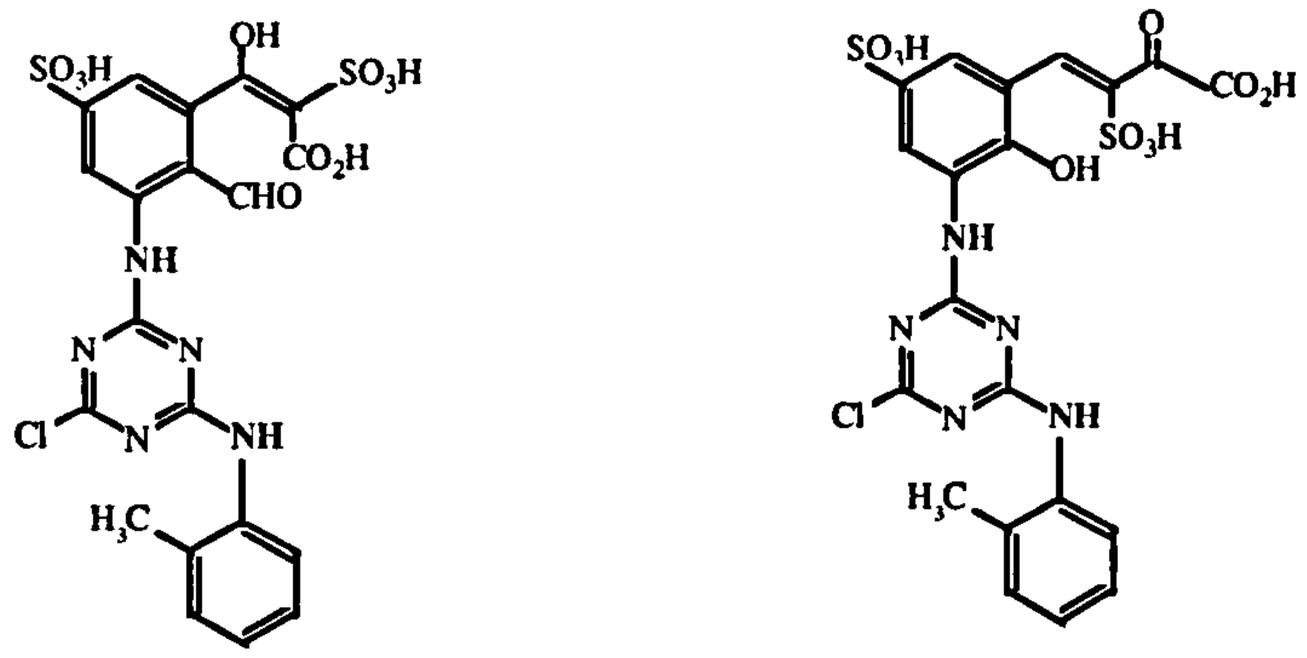

(IV)

The low retention time of this compound is consistent with a polar constituent and with both of the proposed structures, each of which contains a carboxylic acid function in addition to two sulphonate groups. Also, the UV spectrum showed no characteristic adsorption in the 350 - 450 nm range as observed for other autoxidation products of RR3.1, Amaranth and Sunset Yellow, indicating a loss of conjugation of the ring structure consistent with ring opening which supports this identification. It was not possible to determine which of the two structures proposed is correct, but the second is in agreement with proposals for analogous, though much simpler, structures made by Wittich (1988), Haug *et al.*, (1991) and Kuhm *et al.*, (1991), for the degradation of substituted naphthalenes. This tends to suggest the second of these proposed structures is most likely.

The observation of this structure is of particular significance to the treatment of azo dyes, because it indicates two desired effects. Firstly, the highly oxidised state of this intermediate and the effect of ring opening, leave it susceptible to further aerobic degradation including the potential for complete mineralisation of the dye, which is the ultimate desired outcome of any treatment process. Secondly, ring opening reduces the degree of conjugation within the molecule reducing its light absorption in the visible region and therefore helping to remove the colour- another desirable outcome of a treatment process.

The structures proposed for Peaks V and VII suggest that cleavage of the secondary amine bond between the *o*-toluidine group and the reactive chlorotriazine (between sub-structures 2 and 3, compound I) has occurred. Peak V is a little surprising as it indicates the formation of the hydroquinone structure, which one might expect to be in equilibrium with a naphthaquinone equivalent. However there was no evidence for the latter.

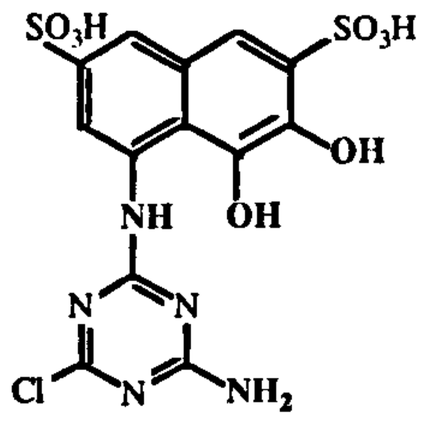

(Vii)

Since it has an even molecular weight, peak VII may contain 4 or 6 nitrogen atoms. The presence of the chlorine isotope pattern confirms the inclusion of three nitrogen atoms of the triazine ring. Two structures can be proposed :

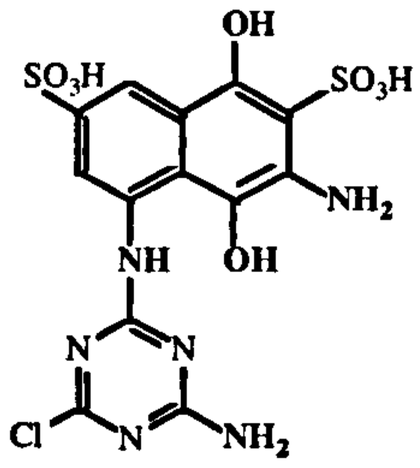

(VIIa)

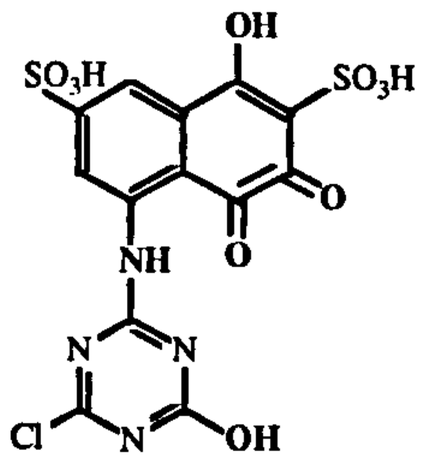

(VIIb)

The second of these compounds (VIIb) features a naphthoquinone sub-structure which by analogy to the products of the Amaranth and Sunset Yellow autoxidation experiments is a favoured autoxidation pathway and tends to support (VIIb) as the most likely structure.

o-Toluidine or *o*-cresol, compounds that might be expected to be released upon scission of the toluidine/chlorotriazine-secondary amine bond were unlikely to be detected using the analytical protocol used.

Further evidence for the reduction of the secondary amines within RR3.1 was given by peaks VI and XVI. The mass spectra derived from these indicate scission of the secondary amine between the naphthalene ring and chlorotriazine ring (between substructures 3 and 4, compound I), resulting in proposed structures (h) and (j):

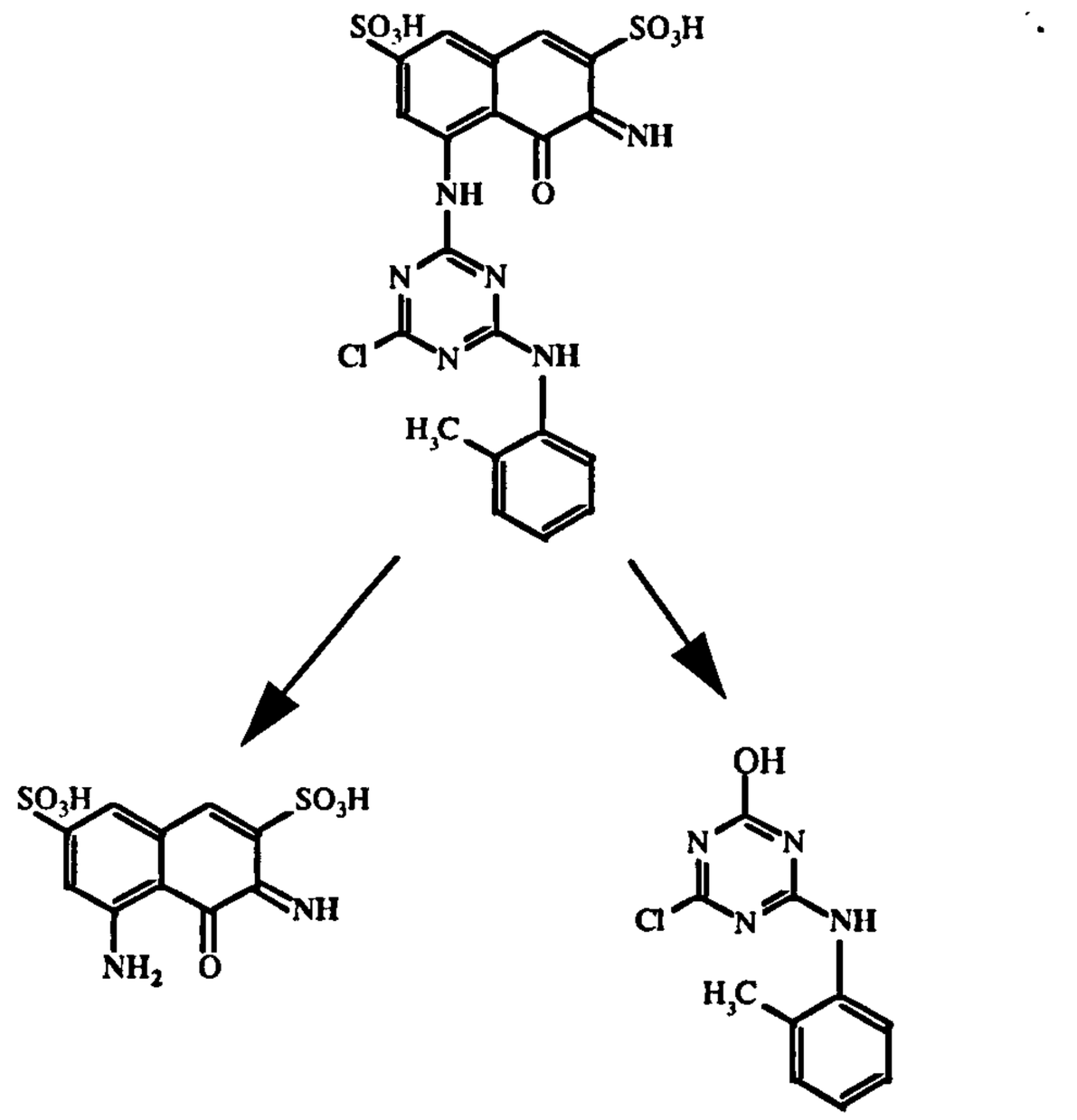

(VIi) (XVIi)

One might expect this naphthaquinone-imine type of compound (VI) to be in equilibrium with a naphthaquinone as observed for Amaranth, which by analogy would hydroxylate and further oxidise with potential for ring opening. No evidence was found for these

autoxidation products. Perhaps the extended conjugation of this system stabilises the structure and restricts further oxidation (discussed later).

The components derived from cleavage of the secondary amine bonds form only a small contribution to the overall complexity of the oxidised samples, which suggests such mechanisms are a relatively minor part of the degradation pathway. The presence of these products does however, support the observations of Carleill *et al.*, (1995), who proposed the cleavage of azo and secondary amine bonds for the anaerobic degradation of Reactive Red 141. Such cleavage is encouraging when considering the whole treatment process, because it indicates the bulky naphthalene/chlorotriazine moiety is capable of further degradation.

The presence of proposed imines is interesting because the comparable compounds for the autoxidation of both Amaranth and Sunset Yellow were unstable. Yet most of the identified peaks for RR3.1 autoxidation appear to contain either a quinoic or an imine function. A more significant comparison maybe Naphthol Blue/Black which showed the initial reduction/autoxidation products to be stabilised by extended conjugation. By analogy the quinones and imines of RR3.1 autoxidation products can be similarly stabilised through extended conjugation with the secondary amine in the 8-position:

and similarly for the quinone structures.

Likewise the addition of a hydroxyl group at the 4-position can also extend conjugation and stabilise the hydroxylated autoxidation products, which again would explain why several of these compounds appear to be stable:

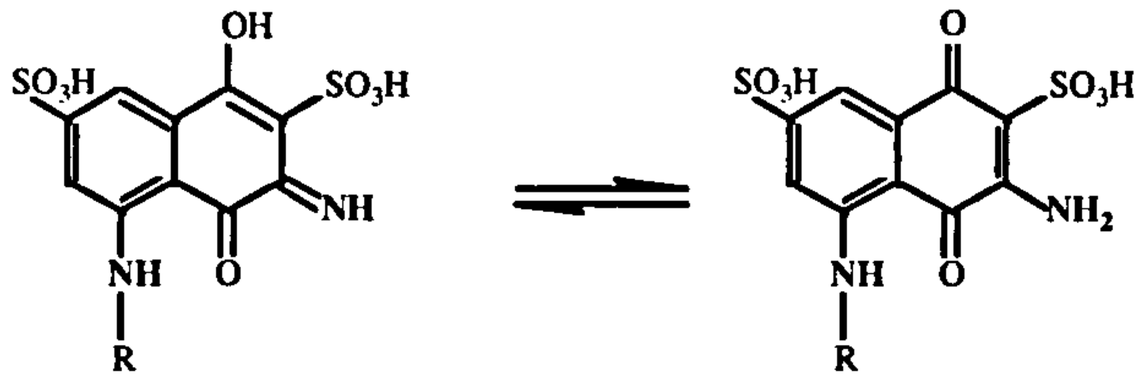

and similarly for the quinone structures.

So it can be seen how quinones and imines- and in particular their 4-hydroxy- analogues may be stabilised through conjugation and may therefore become preferred autoxidation products.

Associated with peak (XVIi) was the mass spectrum derived from a very minor peak observed at a retention time of ~26 minutes, which indicated the formation of a dimer of this degradation product:

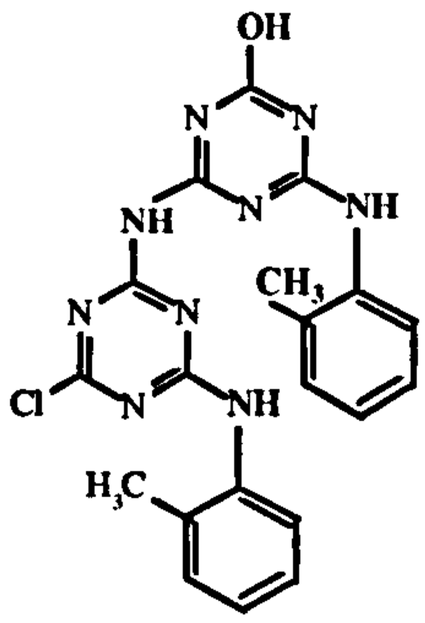

This clearly illustrates the propensity of the reactive triazine group to react with breakdown intermediates present in the test media.

It is probable this reactive triazine group reacts with other breakdown products in similar fashion, possibly accounting for the dimers observed in peak III, but no supporting data were obtained to confirm this theory.

One other component within major peak V, has been tentatively assigned as follows:

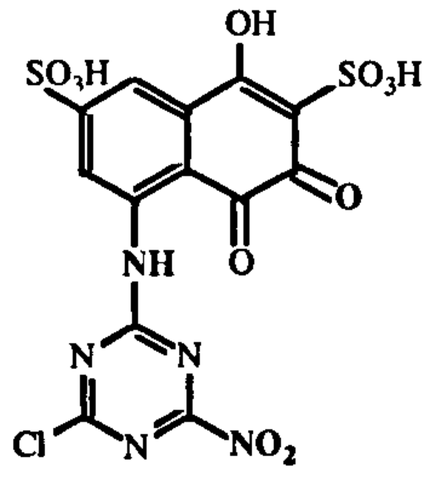

(Vi)

This was based on the odd molecular weight, 2 sulphonates and presence of chlorine, but should be considered a tentative assignment.

Several dimers were observed in the LC-MS analysis. In particular, peak III contained two compounds and peak X another, with molecular weight above 1000 mass units. These are recognisable from the observed multiple charge states ie $[M-4H]^{4-}$, Figure 4.34, indicating four sulphonic acid groups. The potential of Amaranth and Sunset Yellow to form dimers has been discussed previously (Sections 4.4 and 4.5). Amaranth did not produce dimers because of steric hindrance caused by the bulky sulphonic acid groups adjacent to the 4-position of the naphthalene ring. Sunset Yellow, on the other hand, does not have this adjacent group and did form dimers by 1,4 addition. Based on this information it seems likely that dimers formed in the autoxidation of RR3.1 occur *via* an interaction between the amine or hydroxyl of one product with the chlorine of the reactive triazine of another. No structural assignments were possible based on the molecular weight information obtained. Unfortunately compounds capable of adopting multiple charge states, particularly those greater than two, tend not to form singly charged molecular ion species.

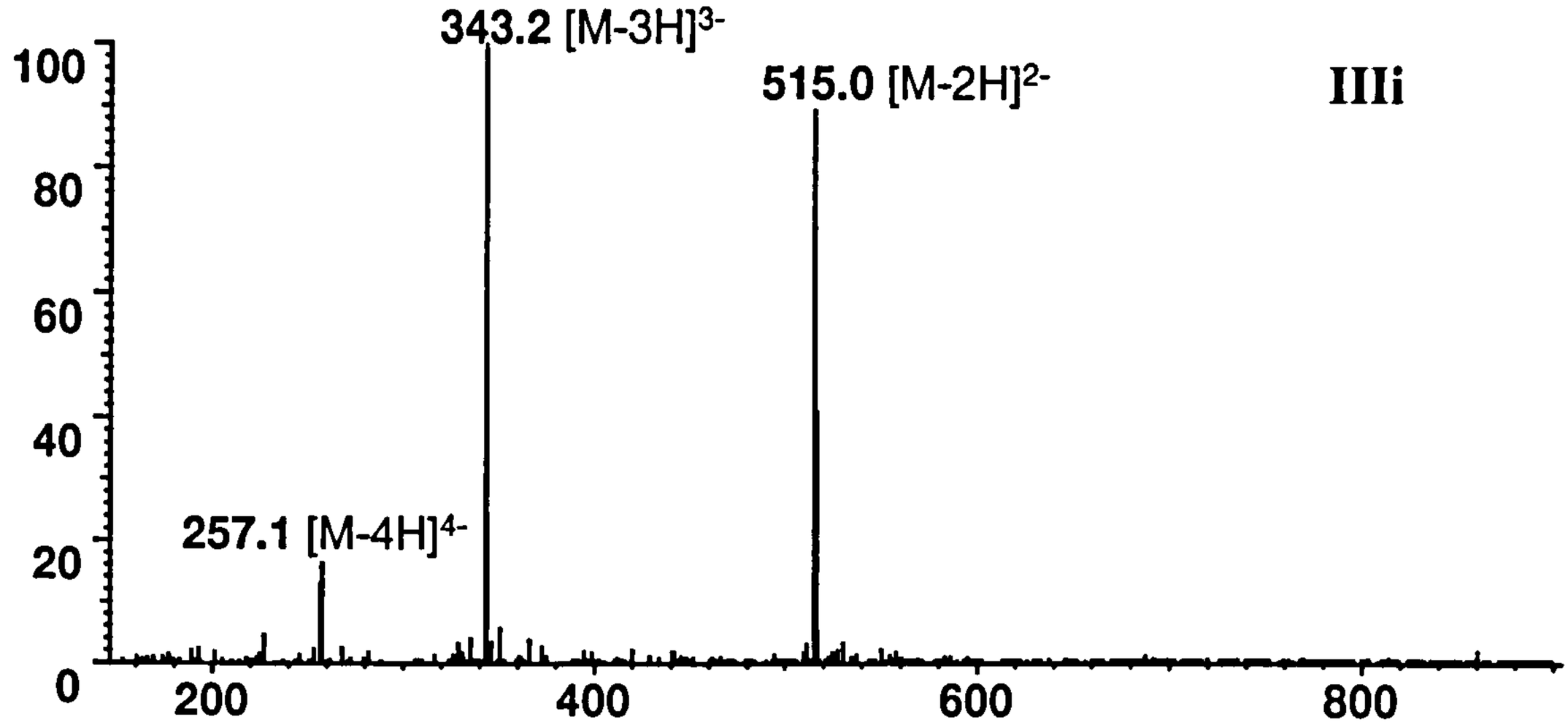

Figure 4.34 Mass spectrum of suspected dimer derived from peak IIIi for a sample of reduced RR 3.1 following autoxidation.

Conventional quadrupole mass spectrometers provide no energy focusing of the ions, therefore multiply charged ions are poorly resolved and accurate isotope contributions are difficult to determine. In the case of the proposed dimers it was not possible to determine whether the dimer contained 0, 1 or 2 chlorine atoms. This information would have provided an extremely useful guide to how the dimers were formed. Using the 'zoom scan' facility of an ion-trap mass spectrometer (*cf* McCormack *et al.*, 2001), would have been extremely useful to determine the isotope ratios of the observed multiply charged ions, but unfortunately this was not available at the time of this experimentation. The observation of dimers is of particular relevance to treatment studies, where the aim is to formulate a process that will mineralise azo dyes. Dimers derived from dyes or their breakdown products tend to be large, highly conjugated therefore coloured, and very stable molecules which may be recalcitrant in conventional treatment processes. Some attempts to mineralise azo dyes actually form substances that are more stable and coloured than the original dyestuff (Knapp and Newby, 1995).

Also observed were several components with molecular weights in the region of 600 - 650 mass units (examples shown in Fig 4.35). Structures could not be assigned to these based on observations from previous studies. It seems likely that these have been formed by reaction between degradation products, once again possibly involving the reactive triazine group. The chlorine of this reactive group is extremely labile and designed to react with amino and hydroxyl groups of the intended target material. It seems likely that as many of the autoxidation products contain either or both of these functionalities, that reaction between degradation products is inevitable. This would also contribute to the complexity of the observed chromatograms. Interestingly, this suggests that for the autoxidation process there are competitive reactions between dye degradation with removal of colour, and the formation of new highly conjugated and stable adducts, which in some cases may be larger molecules than the original dye. The successful treatment of azo dyes using the recognised best approach of anaerobic reduction of the dye followed by aerobic removal of the reduced products, will depend on the ability of the aerobic treatment to remove autoxidation products before they have the opportunity to form adducts which may be recalcitrant and coloured.

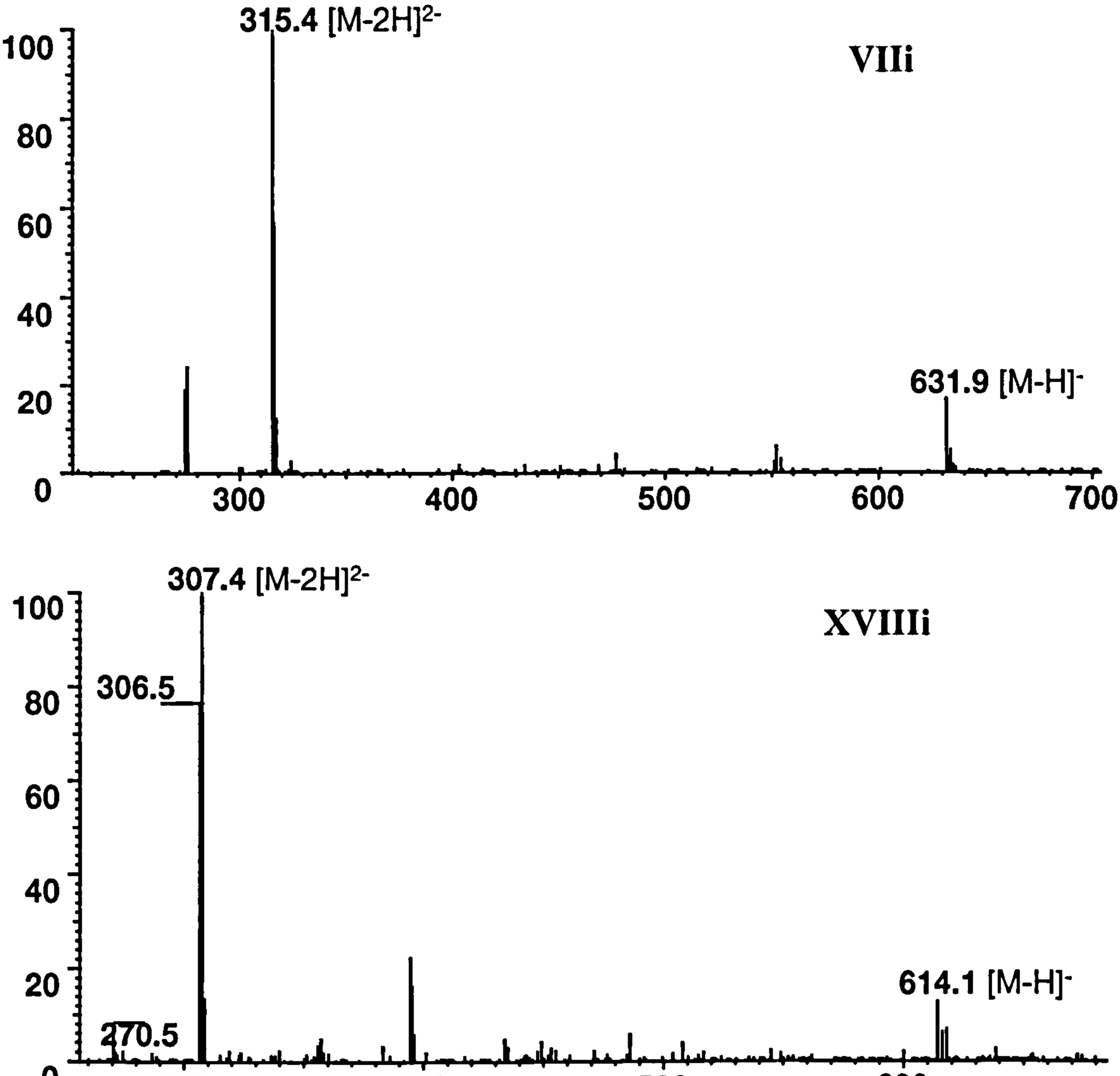

Figure 4.35 Mass spectra of two unidentified components present in a sample of reduced RR 3.1 following autoxidation

Although the LC-UV chromatograms for the dilute samples, D and E, were similar to those of higher concentration, because of the large number of products formed in the reduction/autoxidation process, and the high background, it was difficult to obtain useful mass spectra of many of the components. However, the major peaks observed were confirmed as the hydroxylated napthaquinone-imine (XIV), hydroxylated naphthaquinone (IX) and naphthaquinone (XVI). There was also some evidence for the presence of dimers/adducts, (ie molecular weights greater than 1000 mass units) which suggests this

process is not a consequence of high dye concentration, but may also occur at lower dye concentrations. However, once again they do not appear to be products of the major autoxidation pathway.

4.7 ANALYSIS OF REDUCED RR 3.1 SAMPLES STORED UNDER ANAEROBIC CONDITIONS

Three samples were provided by the University of Leeds, consisting of two controls and one biologically reduced Reactive Red 3.1 sample. Samples were prepared and shipped in septum sealed vials in a nitrogen atmosphere to prevent oxidation. On arrival at Brixham, all three vessels were sub-sampled and analysed by LC-MS. The colour changes of the reduced dye over an extended period of storage were observed. The initial colour on delivery to Brixham was pale yellow, but on subsequent multiple sampling and storage over several weeks, the colour deepened to a much darker, more intense yellow. Apparently contact with even small amounts of oxygen admitted to the sealed vessel during sampling was sufficient to induce an autoxidation process.

LC-MS analysis of the sterile and non-inoculated controls showed two major peaks, the largest being due to RR3.1. The smaller peak (~10%) was identified as the hydrolysed form of the dye, suggesting a slight deterioration in the starting material. It is well known that on standing, aqueous solutions of some reactive dyes can hydrolyse, with replacement of the reactive chlorine by hydroxyl.

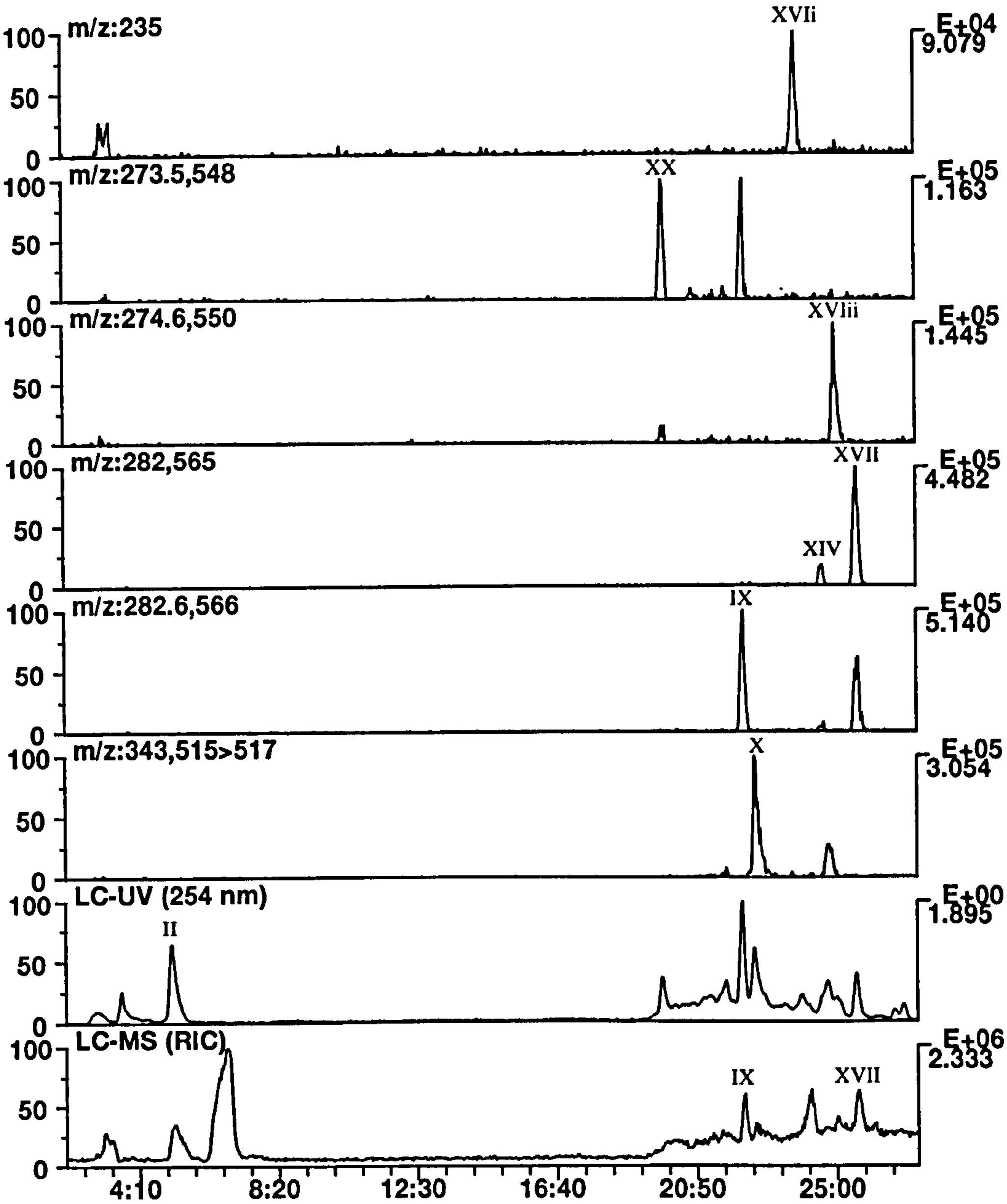

Figure 4.36. LC-MS selected ion chromatograms of reduced Reactive Red 3.1 (480 mg l^{-1}, 0.2% NaCl at pH 7), stored under a nitrogen atmosphere to limit autoxidation.

A comparison of LC-UV (254 nm), reconstructed ion current (RIC) and selected ion LC-MS chromatograms of the reduced RR3.1 dye sample is shown in Figure 4.36. Seven peaks have been annotated and these have been identified from their molecular weights and by reference to the interpretation of MS data from the previous section. There was no evidence for the presence of the parent dye (I) and the presence of amino benzene sulphonic acid (II) gave a strong indication for the successful reduction of RR3.1. Once

again there was no evidence for the proposed primary amine reduction product (proposed structure 'a'), which suggests the amine is unstable and reacts on sampling and standing in the autosampler vial, or that with trace amounts of oxygen present in the incubation vessel. The major products of the reduction were similar to those observed for the initial experiment. The most significant peak observed in the LC-UV chromatogram, IX (mwt 567), was identified as the hydroxy naphthaquinone, equivalent to proposed structure d1. Peaks XIV and XVII (mwt 566), were identified as two isomers of the hydroxylated imine. Peak XVIi, (mwt 236), provided evidence for the breaking of the secondary amine bond between the reactive triazine and naphthalene ring. This was also observed for the analysis discussed earlier, where formation from an imine intermediate was proposed. However its presence in the preserved anaerobic sample suggests that it is formed in the initial reductive process rather than from the imine intermediate. This provides evidence for the ability of an anaerobic degradation process to metabolise secondary amines in addition to azo compounds. Peak XVIii, (mwt 551) is consistent with a naphthoquinone structure. Peak IIIi appears to be due to a dimer, *m/z* 257, 343 and 515 are consistent with 4^-, 3^- and 2^- ions respectively, indicating a molecular weight of 1032. These ions were also observed in the initial sample (Figure 4.34) but at a shorter retention time, (*ca* 22 minutes compared to 20 minutes for initial sample). A structure was not proposed for this dimer. Two additional peaks observed in the *m/z* 273.5, 548 selected ion chromatogram (XX, Fig 4.36) are consistent with isomers of the hydrolysed form of the major hydroxylated naphthaquinone component IX. These were probably formed from the 10% hydrolysed dye present in the starting material used for this experiment, a mass spectrum is shown in Figure 4.37.

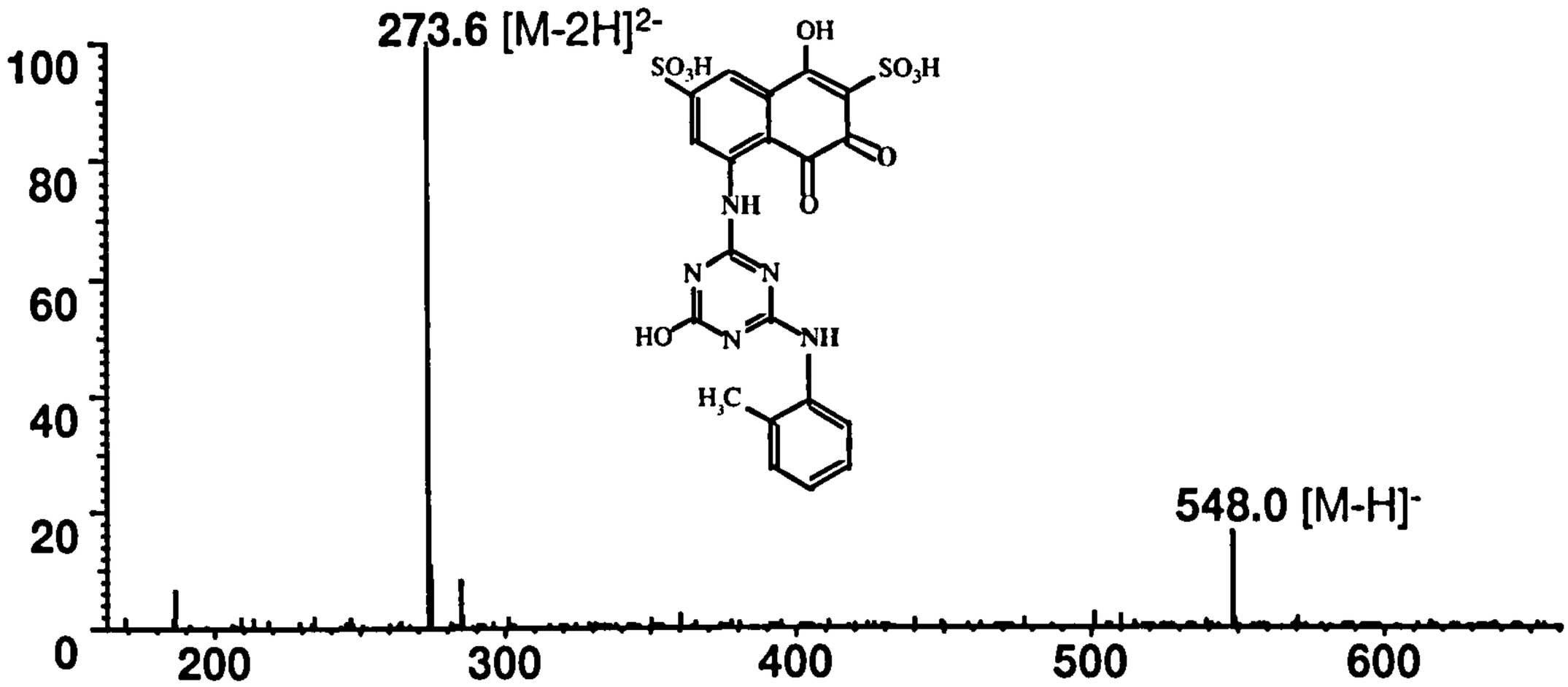

Figure 4.37 mass spectrum of peak XX in a sample of reduced Reactive Red 3.1 (480 mg l^{-1}, 0.2% NaCl at pH 7), stored under a nitrogen atmosphere to limit autoxidation.

The other significant peaks observed in the 'initial' samples such as the early eluting dimers (peak IIIii-iii), the ring opened acid (peak IV) and in particular the unidentified compounds with molecular weights above 600 mass units, were not observed in this sample.

The data obtained from the two experiments suggest the initial amine reduction product quickly oxidises, either with trace amounts of dissolved oxygen, or more likely once exposed to air in the autosampler vial, to form a range of naphthoquinoic and naphthoquinone-imine structures. These are themselves hydroxylated to more stable products. Then as observed with the 'initial' sample, over a longer period of time, further oxidation is observed with ring opening, and at the same time there is interaction between some of the degradation products, possibly through the reactive chlorine group, to form a range of aducts and dimers. Support for this theory was obtained from the re-analysis of the reduced reactive red dye taken from the sealed vessel and allowed to stand open to the atmosphere for 24 hours. This sample showed a marked change to the original sample. The most prominent peak in the UV chromatogram was derived from the hydroxylated naphthoquinone-imine (proposed structure c1). Also significant was the much reduced

intensity of the hydroxylated naphthoquinone, IX, although the ring opened acid (mwt 585, IV) derived from the naphthoquinone, was very prominent. Also present were many small peaks which appeared to be due to dimers or adducts the structures of which have not been identified.

From the interpretation of LC-MS data, it has been possible to postulate a degradation pathway for the autoxidation of RR3.1 (Fig 4.38). This is based on the major components only and does not account for the minor contributions in what is a highly complex mixture. However the observations here are important considering the limited information on autoxidation available in the published literature.

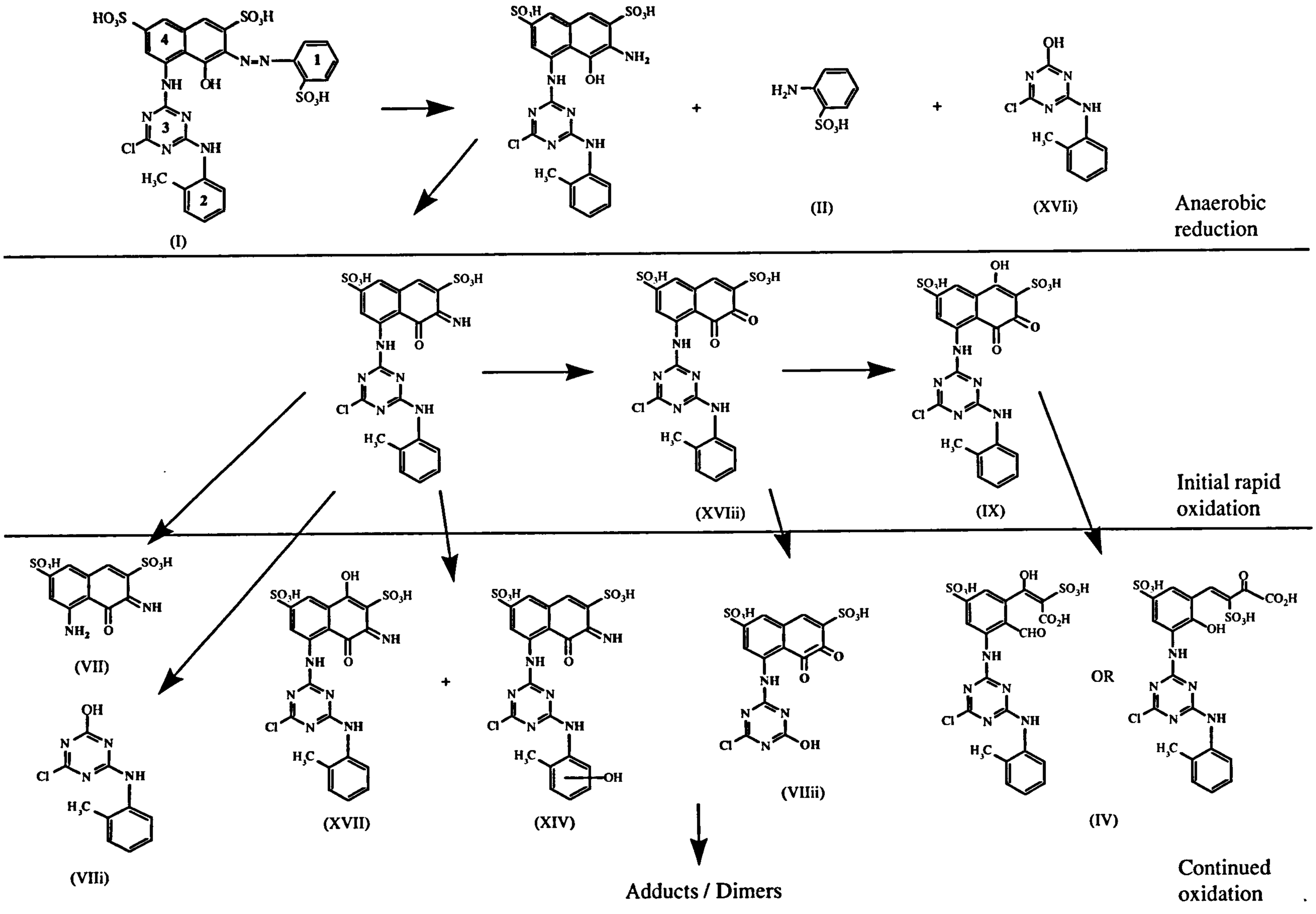

Figure 4.38. Degradation pathway for the reduction / autoxidation of Reactive Red 3.1

4.8 ANALYSIS OF REDUCED REACTIVE RED 3.1, FOLLOWING AEROBIC TREATMENT

Reactive Red 3.1 was reduced under anaerobic conditions in sewage treatment works sludge from two different works, Knostrop and Owlwood (initial dye concentration of 120 mg l^{-1}). Samples were taken at the start of experimentation, (sample t_0-red), and immediately following dye decolourization (ie on change from red to pale yellow coloration; sample t_0-yellow), and stored prior to analysis. Following anaerobic treatment, reduced dye samples from each sewage source were subjected to aerobic incubation. Samples were taken after 2 and 7 days, then all samples were transported to Brixham for analysis by LC-UV. A comparison of chromatograms for all four time points derived from each sludge, together with 100 mg l^{-1} RR3.1, are shown in Figures 4.39 and 4.40. The first observation from these is that the initial dye solution (t_0-red), hydrolysed over the course of the experiment. It was not possible to determine whether this was prior to the start of the study, or during storage of the samples. This is unfortunate but should not detract from some useful information that can still be obtained from the study. The second observation is that all of the dye has been removed in the reduced Knostrop and >98% in the reduced Owlswood (t_0-yellow) samples. These clearly show the removal of RR3.1 following anaerobic treatment with the formation of one major component. A minor degradation product was also observed in the Owlwood sample. In both sludge types the intensity of the major degradation product did not diminish during the aerobic incubation period of 7 days.

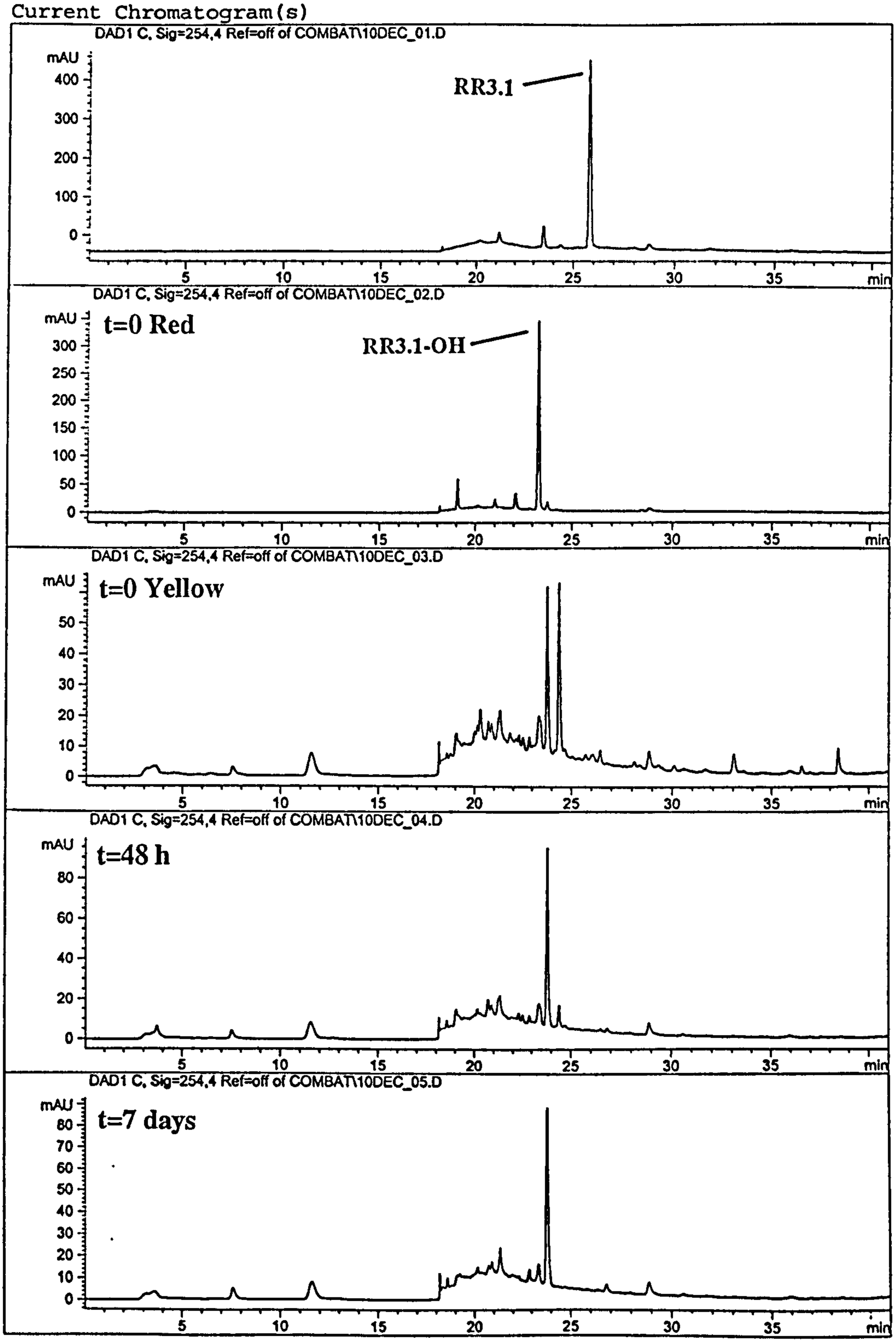

Figure 4.39 LC-UV (254 nm) chromatograms of samples containing Reactive Red 3.1 before and after anaerobic degradation and following aerobic treatment with inocula derived from Knostrop sewage works.

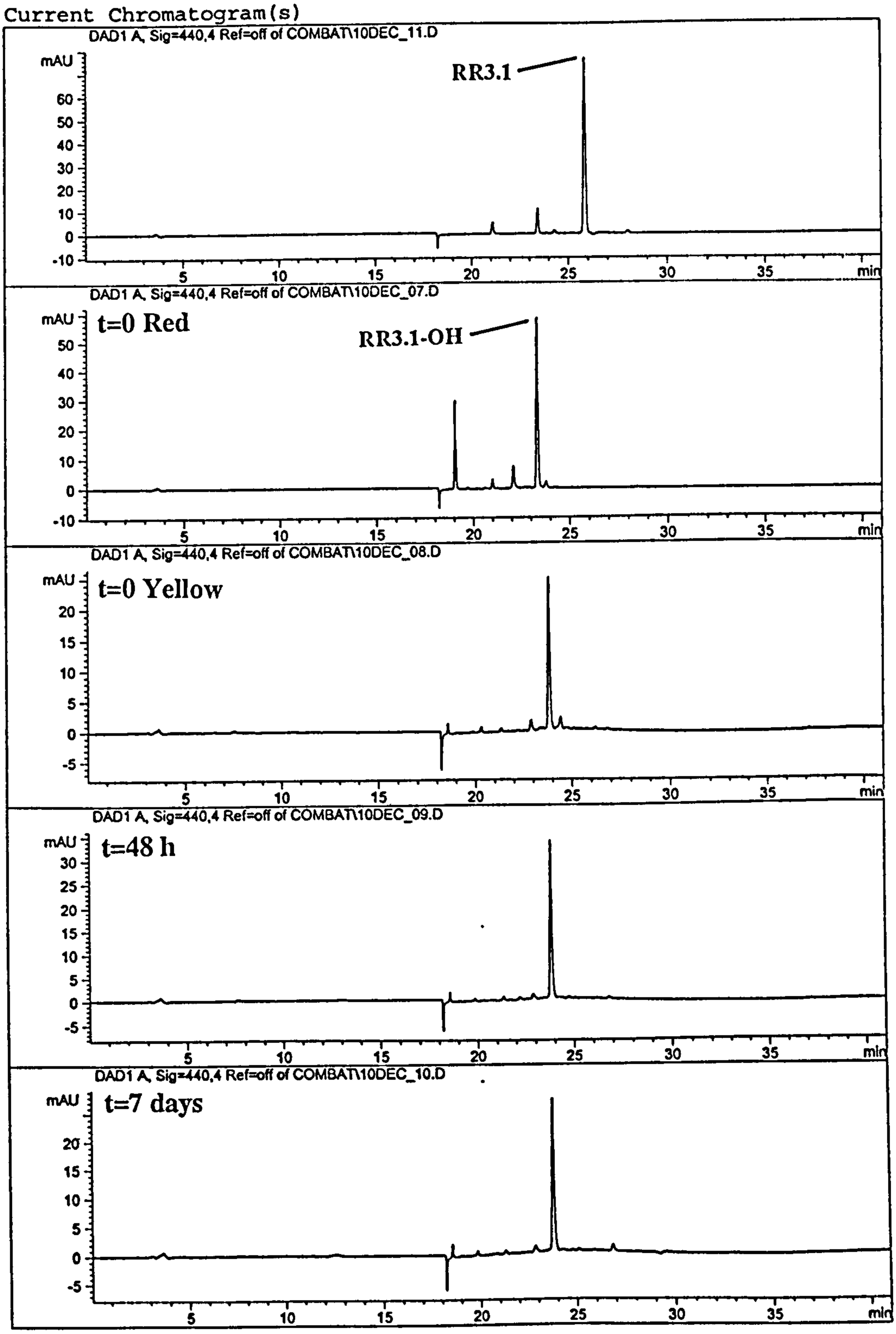

Figure 4.40 LC-UV (440 nm) chromatograms of samples containing Reactive Red 3.1 before and after anaerobic degradation and following aerobic treatment with inocula derived from Owlwood sewage works.

LC-MS analysis of the initial Owlwood dye solution (t_0-red), is shown in Figure 4.41. The mass spectrum derived from the major dye component (XXI) confirmed RR3.1 was in the hydrolysed form (ie the reactive chlorine had been replaced by -OH).

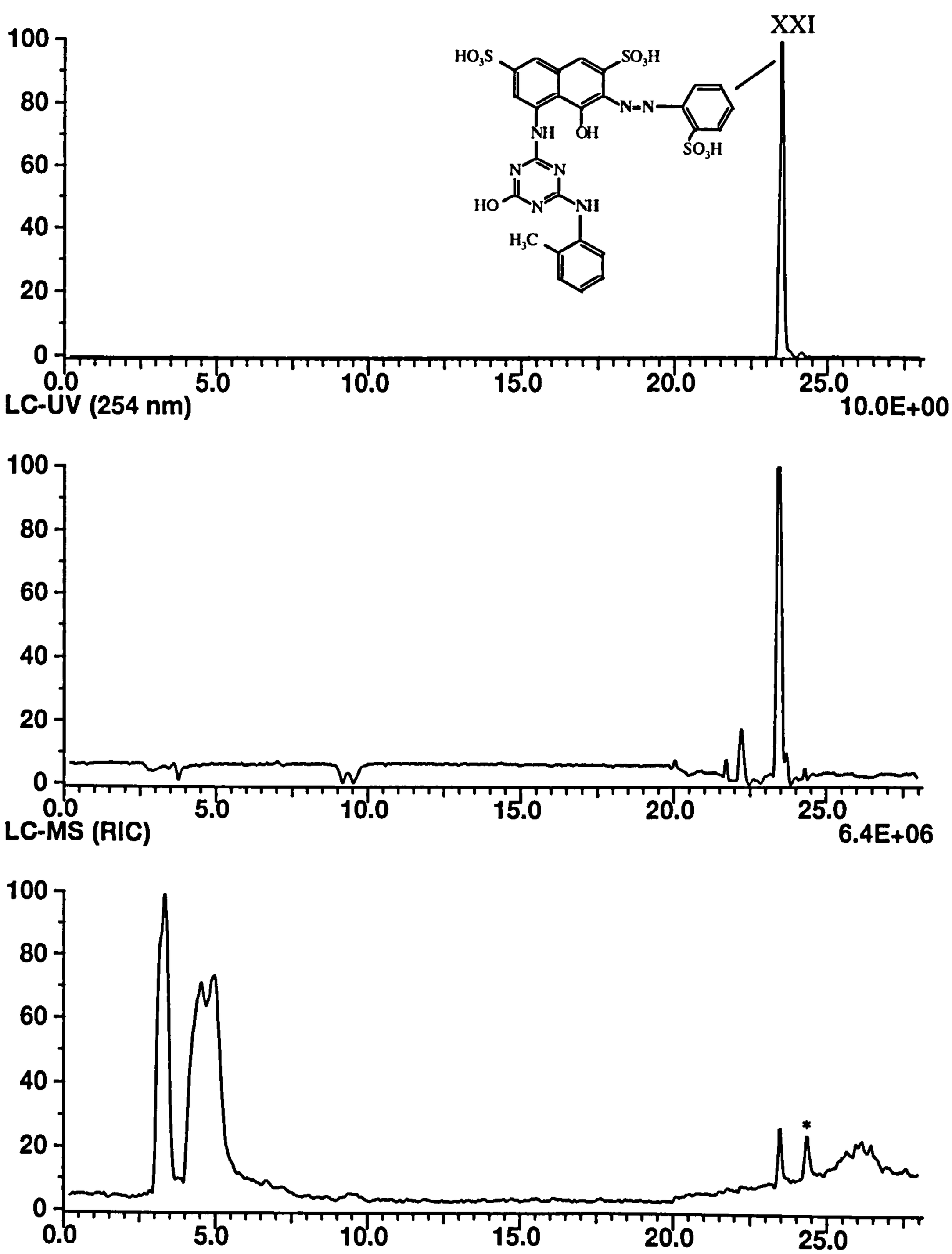

Figure 4.41 LC-MS selected ion chromatogram for reduced Owlwood sample t_0-red (* denotes background peaks also in control)

Early eluting peaks (RT <8 minutes) gave weak UV absorption and were therefore unlikely to be dye related but were possibly artefacts of the biological test media.

LC-MS analysis of the Owlwood (t_0-yellow) decolorised dye sample (Fig 4.42), showed one major dye related peak, (XXII). The mass spectrum of this (Fig 4.43) showed molecular ions at mass *m/z* 273 and 547 indicating a molecular weight of 548 mass units, an even number of nitrogen atoms and two sulphonic acid groups. This was consistent with the hydrolysed form of hydroxy naphthoquinone-imine (XIV and XVII) in which the chlorine of the chlorotriazine group was replaced by a hydroxyl (-OH) group).

Peak II, highlighted by the selected ion mass chromatogram (*m/z* 172), confirms the presence of aminobenzene-2-sulphonic acid, the initial reduction product. Additional small peaks observed in the LC-UV chromatogram did not produce useful mass spectra for identification.

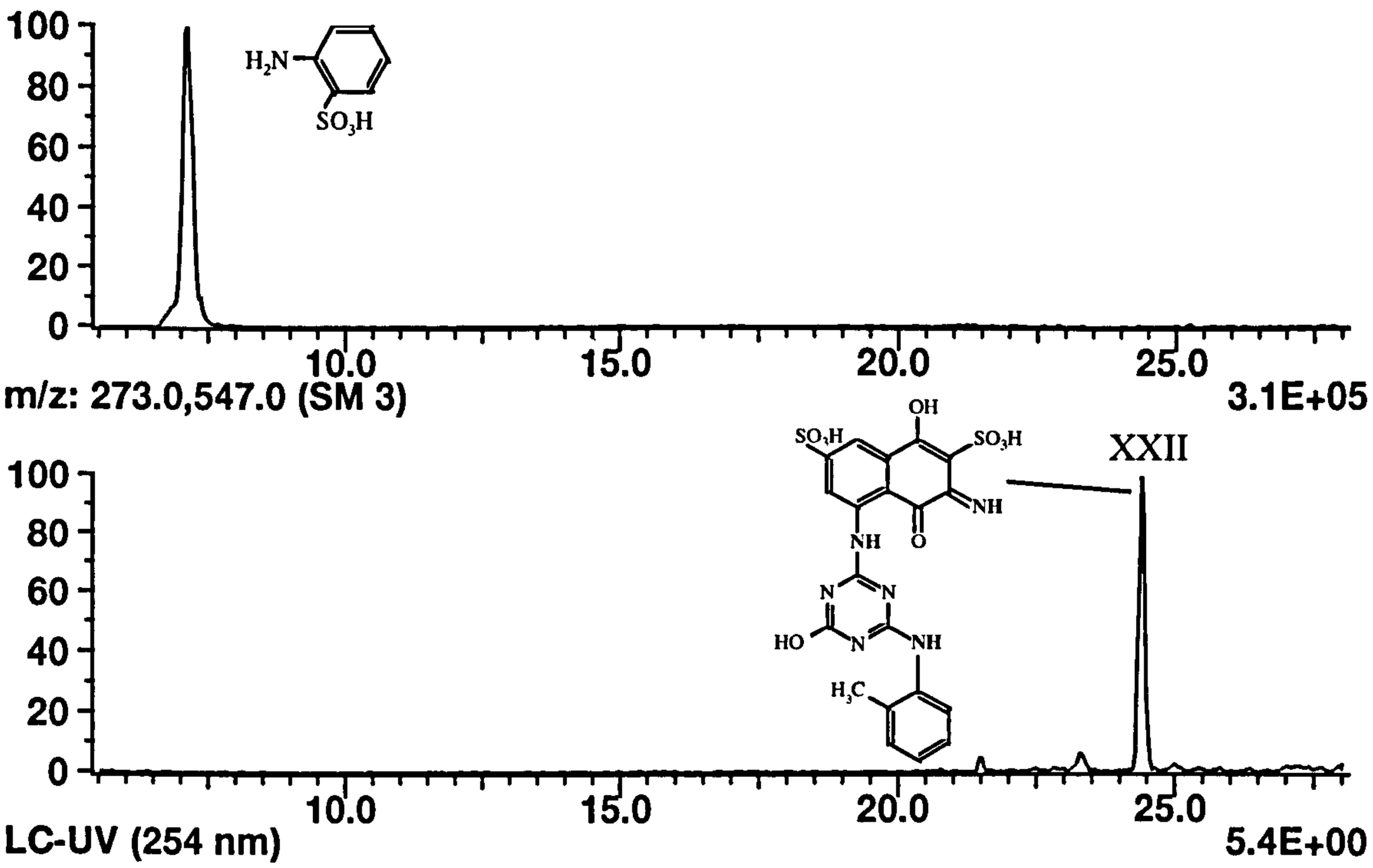

Figure 4.42 LC-MS selected ion chromatograms for reduced Owlwood sample t_0-yellow (* denotes background peaks also in control)

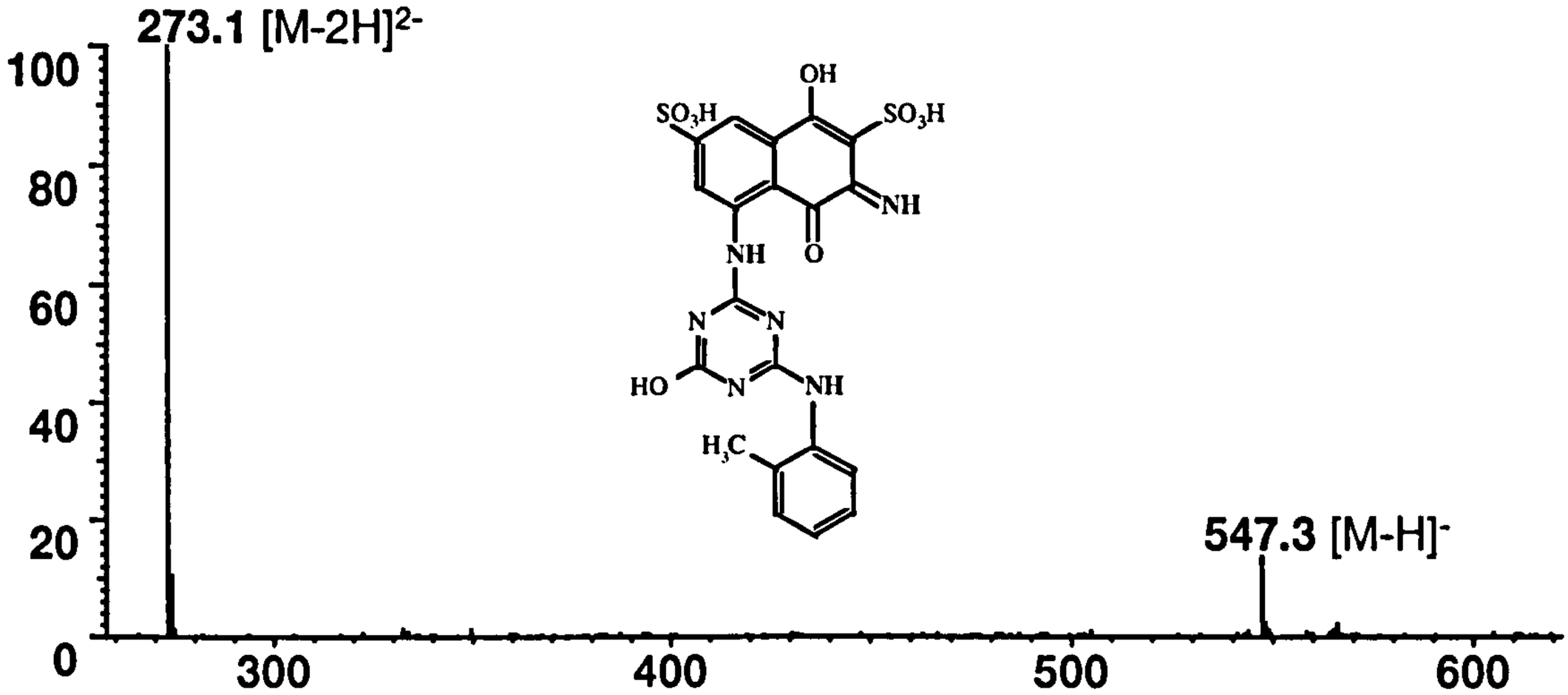

Figure 4.43 Mass spectrum of peak XXII in a sample of reduced Owlwood t_0-yellow

LC-MS analysis of the aerobic degradation samples showed the presence of two peaks only, these being due to aminobenzene-2-sulphonic acid (II) and hydrolysed naphthoquinone-imine (XXII), as described earlier. It appears that once formed these compounds are relatively stable to aerobic degradation, at least under the laboratory conditions used for this study. There was no evidence for the dimers and high mass (>600 daltons) compounds observed in the previous reduced samples. This indicates that they were formed by interaction between the reactive groups of various degradation products and therefore could not be formed in this sample which appears to have started with the hydrolysed dye (ie effectively with no reactive group). Also, there was no evidence for any of the degradation products previously identified. However, the majority of these compounds contained chlorine, which increases MS sensitivity and the previous tests were run at a higher initial dye concentration, which may explain why the few peaks observed in the UV did not provide an equivalent mass spectrum. Also of concern was the relative simplicity of the chromatograms for the initial reduction samples (t_0-yellow) for both sludges. Numerous intermediates were observed in previous studies. This tends to suggest that the mode of storage (unknown) over the remaining 7 days of the study was inappropriate, leading to continued oxidation and possibly aerobic activity over this period.

This does not detract from the fact that one compound persists over the whole degradation test.

The lack of degradation in the aerobic experiment may have been explained by toxicity of the dye to the inoculum. Using activated sludge from two sources (Owlwood and Knostrop), samples were taken during both the anaerobic dye decolourization phase and during a period of aerobic incubation after the decolourization phase. After removing the biomass, the samples were analysed using the *activated sludge respiration inhibition test* (ASRIT). Of the four Knostrop samples tested using ASRIT (at a concentration of 10% $^{v}/_{v}$), only the *untreated* dye (ie sampled immediately after the dye was added) inhibited the respiration of un-acclimatised activated sludge (24.6%) and this inhibition was not observed for subsequent samples (i.e. following dye decolourization). None of the Owlwood samples (at a concentration of 10% $^{v}/_{v}$) inhibited respiration. Therefore toxicity of the dye to inoculum does not appear to have been an issue.

4.9 CONCLUSIONS FOR ANAEROBIC DEGRADATION WORK

The LC-MS and MSMS techniques optimised in this study (Chapter 2), were successfully used to elucidate the effects of autoxidation on the reduction products of three relatively simple azo dyes. Additionally, several autoxidation products that were not apparent in the LC-UV analysis were identified by LC-MS.

The substituted aromatic amine products of the reduction process were found to be highly susceptible to oxidation once air was allowed into the reaction media and some of the resulting products were highly conjugated and therefore coloured. Many of the autoxidation products of a complex azo dye, Reactive Red 3.1 were predicted from the study of relatively simple azo dyes, Amaranth and Sunset Yellow.

The analysis of a reduced sample of Reactive Red 3.1, indicated the fission of several secondary amine groups had occurred in the reduction process. This is particularly relevant since the reduction products of azo dyes are often thought to be recalcitrant. Additionally, ring opened autoxidation products of Amaranth, Sunset Yellow and Reactive Red 3.1 were observed. These are believed to be readily degraded by aerobic degradation and highlight the potential to mineralise azo dyes through a mixed anaerobic-aerobic treatment process. Ring opened structures were not observed in samples derived from a subsequent mixed treatment process for Reactive Red 3.1. However, one persistent degradation product was identified which was stable over the 7 day aerobic degradation period of the study and was therefore resistant to aerobic degradation.

CHAPTER 5

AEROBIC DEGRADATION

5.1 INTRODUCTION

Although reactive dyes are generally regarded as being resistant to oxidative attack by bacteria under aerobic conditions and indeed Hobbs, (1988) and Pagga and Brown (1986), concluded that static biodegradation tests on 87 dyestuffs, including reactive dyes were negative, closer inspection of their data indicates that this conclusion may not be entirely valid. The findings of Pagga and Brown were based on observations of >80% biodegradation (ie loss of colour). About 50% of the dyes did show signs of degradation to some extent. In fact of 19 reactive dyes used in the study, 12 showed greater than 30% removal over the 28 - 42 day test period.

Likewise Shaul (1991) found that three of fifteen acid azo dyes were biodegraded within 24 hours following spiking into a pilot scale treatment plant. A review of biological treatment (Dubrow, 1996) concluded that aerobic degradation was very much dependent on dye structure. Where biodegradation did occur, it tended to be at too slow a rate to be of use in a treatment process for removal of colour from effluent such as dye house waste. However these studies did show that some water soluble dyes are degraded under aerobic conditions. Also, some cleavage of the azo bond of simple azo dyes has been reported under aerobic conditions by *Pseudomonas cepacia*; (Idaka, 1987).

Reactive dyes are very water soluble and do not tend to be absorbed onto solids. It is believed that anaerobic degradation which is responsible for colour removal in azo dyes (azo reduction) takes place on the surface of the solids rather than in the liquid phase which, although important for potential treatment processes, may be less important in the

environment. Therefore, although aerobic degradation tends to be relatively slow, it may have an important role in environmental situations where the residence times will be much longer.

Aminobenzene sulphonates and amino- and hydroxy- substituted naphthalene disulphonates are important structural units of many anthraquinone and azo dyes, including those used in this study. The biodegradation of these types of compound has been reported by several researchers. A range of amino, nitro, methyl and nitro-benzene sulphonates were degraded by different single strain cultures of *Pseudomonas,* which used the benzene sulphonates as a sole carbon source (Locher, 1989). However, each culture had a very narrow substrate range, each being able to degrade only two or three of the nine compounds tested. Other similar examples were included in a review of biodegradation (Hooper, 1996). Thurnheer (1988), mixed five different cultures to degrade a range of substituted sulphonated benzenes in a reactor. Not only did the degradative capacity of the mixed-culture increase, but the new 'evolved' consortium were also capable of degrading new compounds that were exposed to the culture for the first time.

The aerobic biodegradation of substituted amino- and hydroxy- naphthalene sulphonic acids by single strains of bacteria, has been widely reported (Ohe, 1986; 1990; Kuhm, 1991; Nortemann, 1994). Ohe (1986) used two different strains of *Pseudomonas* isolated from soil. Interestingly a degradation pathway for 2-aminonaphthalene-1-sulphonic acid *via* 2-hydroxynaphthalene-sulphonic acid to 1,2-dihydroxynaphthalene, then ring opening to produce salicylic acid, was proposed. This entails removal of the sulphonic acid function that is believed to cause resistance to biodegradation (Hooper, 1996). Kuhm (1990), proposed a similar pathway for hydroxynaphthalene sulphonic acid and demonstrated using various strains of *Pseudomonas*, that degradative pathways for naphthalene sulphonic acids were analogous to those of substituted naphthalene.

An extension of this work saw the aerobic degradation of naphthalene disulphonic acids by bacterial strains of *Pseudomonas* (Ohe, 1988) and *Moraxella sp.* (Wittich, 1988). The latter proposed a degradation pathway similar to that of the monosulphonic acids previously described, but also proposed removal of both sulphonic acid groups.

These data clearly indicate that both single strain and mixed strains of bacteria can successfully degrade sulphonated aromatic materials similar to those present in many reactive dyes. The key to degradation appears to be the removal of the sulphonic acid groups which subsequently render the material susceptible to further degradation.

The aerobic decolorization of azo dyes by the white rot fungi *Phanaerochaete chrysosporium* was first reported by Cripps (1990) for Orange II, Trapeolin O and Congo Red. Lignin peroxidase was expected to be involved in this degradation, but this was not the case for Congo Red. Spadaro (1992) used a ^{14}C labelled azo dye to demonstrate complete mineralisation by *Phanaerochaete chrysosporium*. Further degradation studies (eg Paszczynski, 1992; Pasti-Grigsby, 1992) have also demonstrated mineralisation of several structurally related sulphonated azo dyes, where structure did not appear to significantly influence susceptibility to degradation. In a continuation of these studies Goszczynski (1994) proposed mechanisms for the peroxidase-catalysed degradation pathways of several azo dyes. Recent studies (Heinfling, 1998), demonstrated the degradation of six reactive azo and phthalocyanine dyes using the ligninolytic peroxidases derived from white rot fungi.

The majority of studies cited above involved the use of simple azo dyes. None of them examined the effects on anthraquinone dyes and only Heinflung (1998) examined the effects on more complex reactive dyes. The studies reported herein used both reactive anthraquinone and azo dyes to determine the effects of single strain bacteria and activated

sludge on aerobic degradation. The single strain cultures were three species of *Pseudomonas*, because these had previously been demonstrated to degrade azo dyes.

Two approaches were used for evaluation of aerobic biodegradation in this study. The semi-continuous activated sludge (SCAS) method was based on the inherent biodegradability OECD test guideline 302 (1981) and because of the reported success of aerobic degradation using *Pseudomonas* (discussed above), three single strain cultures were also evaluated in this study.

5.2 METHODS

5.2.1 Evaluation of Semi-Continuous Activated Sludge (SCAS) aerobic degradation

A schematic diagram of a typical unit is shown in Figure 5.1. The unit consists of a cylindrical glass vessel calibrated to 0.5 and 1 litre. A drain tap at approximately the 350 ml level was used to decant off supernatant and the vessel was aerated using compressed air *via* a sintered glass disc in the base of the vessel. The air supply has a duel role in that it oxygenates the test mixture and provides mixing of the test solution and keeps the sludge solids in suspension.

The SCAS units are charged with sewage containing approximately 1000 mg l^{-1} solids and require a period of equilibration before the test substance is added. At regular intervals over this period, aeration is stopped, solids allowed to settle and 500 ml (50%) of supernatant decanted. This is replaced by fresh sewage liquor (no solids) which will contain fresh bacteria and nutrients. The cycle is repeated until the dissolved organic carbon (DOC) in the decanted supernatant shows greater than 80% removal when compared to fresh sludge; usually 10 - 14 days. This shows that carbonaceous material in

the sewage feed is extensively oxidised. Test guidelines (ISO/DIS 9887, 1990), suggest this is normally completed within 8 hours of the onset of aeration. Thereafter, bacteria in the sludge respire endogenously for the remainder of the aeration period where the only food source is the test compound. This process, with the regular introduction of relatively high concentrations of fresh inoculum and nutrients to the test system (every 2 days), provides highly favourable conditions for the selection and adaptation of bacteria for the test compound and therefore maximises the potential for extensive biodegradation. As such the test is meant to provide an indication of the biodegradability of the test substance rather than a simulation of a sewage treatment plant.

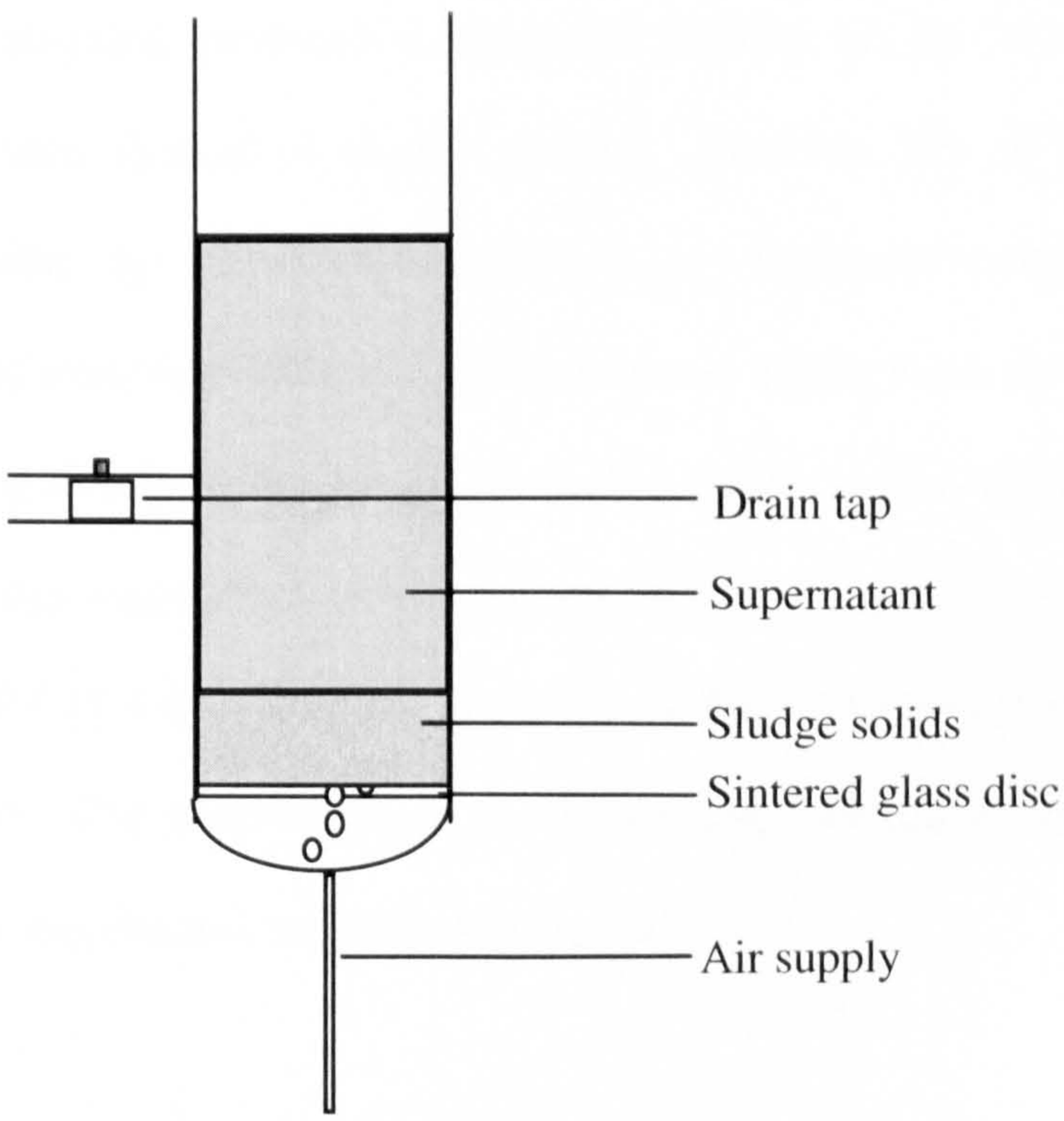

Figure 5.1 Schematic diagram of a Semi-Continuous Activated Sludge (SCAS) system

The test guidelines recommended a test substance concentration providing a DOC level of 20 - 50 mg carbon l^{-1}. The mass fraction of carbon in the three test dyes used (expressed as the number of carbon atom x 12/molecular weight), was 0.49, 0.37 and 0.43, giving approximate test concentrations of 40, 54 and 46 mg l^{-1} for W435, W433 and Reactive Red 3.1 respectively. However the SCAS units were initially charged with half of this

concentration, then increased over approximately a one week period to the required DOC, in order to allow the inoculum a better opportunity to acclimate.

Activated sludge (192 ml) was added to each of four SCAS units to give a concentration of 1000 mg l^{-1} of solids. Each unit was topped up with deionised water and the mixture aerated. On every-other day over a two week period, the aeration was stopped and the solids allowed to settle for approximately 1 hour and 500 ml of supernatant decanted and replaced by fresh settled sewage liquor. After this time each SCAS unit was ready for the addition of the test dyes and these were added along with the fresh sewage liquor at an initial concentration of 20 mg l^{-1} (W435), 25 mg l^{-1} (W433) and 25 mg l^{-1} (RR3.1), which on subsequent charging produced a maximum loading of 40, 50 and 50 mg l^{-1}, as determined for their theoretical oxygen demand. Because 50% of the liquid phase is removed every-other day, the system is said to have a hydraulic residence time of 4 days. This procedure of removing 500 ml of supernatant and adding fresh sewage liquor and dye, was continued on alternate days for 27 days, after which it was sampled once every three days to save on dye usage (Hydraulic residence time (HRT) of 6 days). However this was returned to a HRT of 4 days after a period of 9 weeks, which was then maintained to the end of the study. The temperature of the SCAS units was maintained at 22°C ± 2°C. Additionally pH was checked on each sampling day.

The samples of supernatant removed from each SCAS unit were stored refrigerated and analysed by LC using the conditions described in Section 2.1.

5.2.2 Single strain bacterial cultures

5.2.2.1 Initial evaluation of single strain degradation

Cultures of *Pseudomonas dacunhae*, *P. fluoriscens 9046* and *P. texaco* were each prepared in sterile tryptone soy broth consisting of casein digest (17 g l^{-1}), soy peptone (3 g l^{-1}), sodium chloride (5 g l^{-1}), dipotassium phosphate (2.5 g l^{-1}) and dextrose (2.5 g l^{-1}), at pH 7.3. Each culture was sealed within a conical flask and allowed to grow for 72 hours.

Eight test vessels (25 ml) were set-up, four containing W433 and four W435 dyes, (100 µl; 1000 mg l^{-1}). To each vessel were added media salts (9 ml) and glucose (500 µl, 1M). One vessel of each dye was sealed for use as a control, while 200 µl of each prepared culture broth was added to each remaining vessel. Each vessel was then sealed and incubated in a water bath at 19°C.

Samples were taken from each vessel at regular intervals up to 7 days. Samples (1 ml) were taken using sterile pipettes and centrifuged in Eppendorf tubes using a micro-centrifuge (MSE), at 13,000 rpm for 5 minutes. Supernatant was transferred to sample vials and chloroform (100 µl) added to destroy bacterial activity. Each sample was then spiked with naphthalene sulphonic acid as internal standard and analysed by LC-UV using the conditions described in Section 2.1.

5.2.2.2 Extended evaluation of single strain culture biodegradation

Ten conical flasks were prepared for each of three dyes: W433, W435 and Reactive Red 3.1 (RR3.1), each at a nominal concentration of 50 mg l^{-1}. To each conical flask was added: deionised water (70 ml), growth media (4 ml) which contained a mixture of dipotassium hydrogen phosphate, potassium dihydrogen phosphate, trisodium citrate dihydrate, ammonium sulphate and magnesium sulphate heptahydrate, and one inoculum (2 ml) as detailed in Table 5.1. Glucose (4 ml; 6 g l^{-1}), was added to each of flasks 1 - 6, flasks 7 - 9 were used as glucose free controls to determine whether the bacteria would utilise the dye as a sole carbon source and flask 10 was a negative control.

Table 5.1 Distribution of inoculum, growth media and glucose for each batch of test vessels.

Contents	Vessel Number									
	1	2	3	4	5	6	7	8	9	10
P.dacunhae	X	X					X			
P.9046			X	X				X		
P.texaco					X	X			X	
Media	X	X	X	X	X	X	X	X	X	X
Glucose	X	X	X	X	X	X				X

All flasks were incubated at 24°C in the dark, using an incubator shaker at 150 rpm for a period of up to 4 weeks. Samples were taken at regular intervals using sterile pipettes (1 ml), transferred to glass Reacti-vials and stored frozen until required. It was assumed that the freeze-thaw process would not only preserve the sample, but would also disrupt the bacteria cell walls to stop subsequent degradation. Samples were thawed at room temperature and an aliquot (approximately 100 µl) transferred to an Eppendorf micro-

centrifuge container and centrifuged at 13,000 rpm for ten minutes. The supernatant was then transferred to low volume autosampler vials for analysis by LC-UV using the method described in Section 2.1.

5.3 RESULTS

5.3.1 Evaluation of Semi-Continuous Activated Sludge (SCAS) aerobic degradation of W435

The SCAS units were initially run with an HRT of 4 days (half of the liquid content (500 ml) was decanted off every two days and replaced by a fresh solution of dye made up with the liquid supernatant from sewage liquor). The initial concentration of W435 was 23 mg l^{-1} which was supplemented by the addition of 23 mg at the start of each cycle. The concentration of dye in the SCAS unit therefore increased on each cycle: 50% of initial solution (11.5 mg) plus 23 mg fresh dye equal to 34.5 mg l^{-1}, up to a maximum of approximately 46 mg l^{-1} after 9 cycles (i.e. 18 days). This is shown by the theoretical SCAS dye concentration in Figure 5.2.

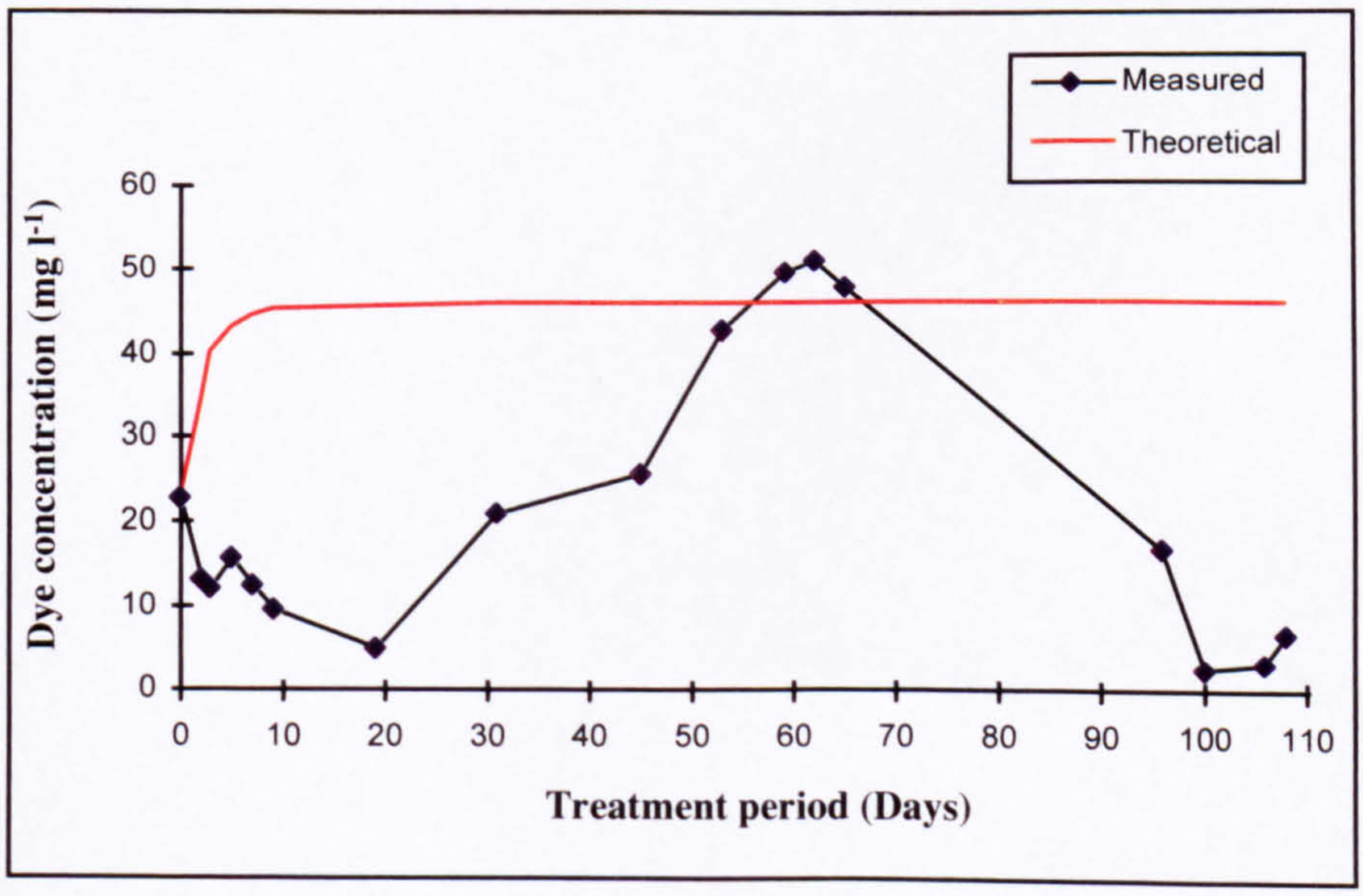

Figure 5.2 105 day aerobic incubation of W435 using Semi-Continuous Activated Sludge system (SCAS)

Clearly W435 was rapidly biodegraded in the test system. The bacteria present, although from domestic sewage and therefore not previously exposed to high concentrations of dyestuffs, were able to degrade the dye without the need for extensive acclimation. During this early part of the study, the maximum extent of degradation was observed on day 19, where the measured concentration of parent dye was 5 mg l^{-1} compared to a theoretical concentration of 46 mg l^{-1}. This represents 89% degradation, which according to OECD guidelines, indicates extensive biodegradation. Interestingly, the observed concentration of W435 then continually increased, eventually reaching the theoretical concentration at approximately day 50. This coincided with a change in HRT from 4 to 6 days (ie fresh nutrient added every three days) and implies that either degradation only occurs when W435 was not the sole carbon source (ie co-metabolism was required for degradation), or that a metabolite was formed which inhibited degradation on prolonged treatment where the dye became the sole carbon source. Additionally, because the measured concentration of dye reached the theoretical level, it can be assumed that W435 was not extensively adsorbed onto the solids within the SCAS unit. On reverting to the original HRT of 4 days (on day 64), extensive degradation was again observed (>80%), confirming the original observation for the need for nutrients in the sewage liqour as a co-substrate. It was quite surprising that a small change in HRT could have such a marked effect on degradation. However this is not significant in terms of a sewage treatment works environment which has a constant replenishment of nutrients. Aerobic biodegradation would therefore appear to be a major route for elimination of anthraquinone dyes.

The extent of degradation may be seen in the LC-UV (254 nm) chromatograms of W435 samples taken up to day 19 during the initial stages of the study (Fig 5.3). These clearly demonstrate the diversity of degradation products formed, where at least ten products, none of which were present in the control sample, were observed during this initial period.

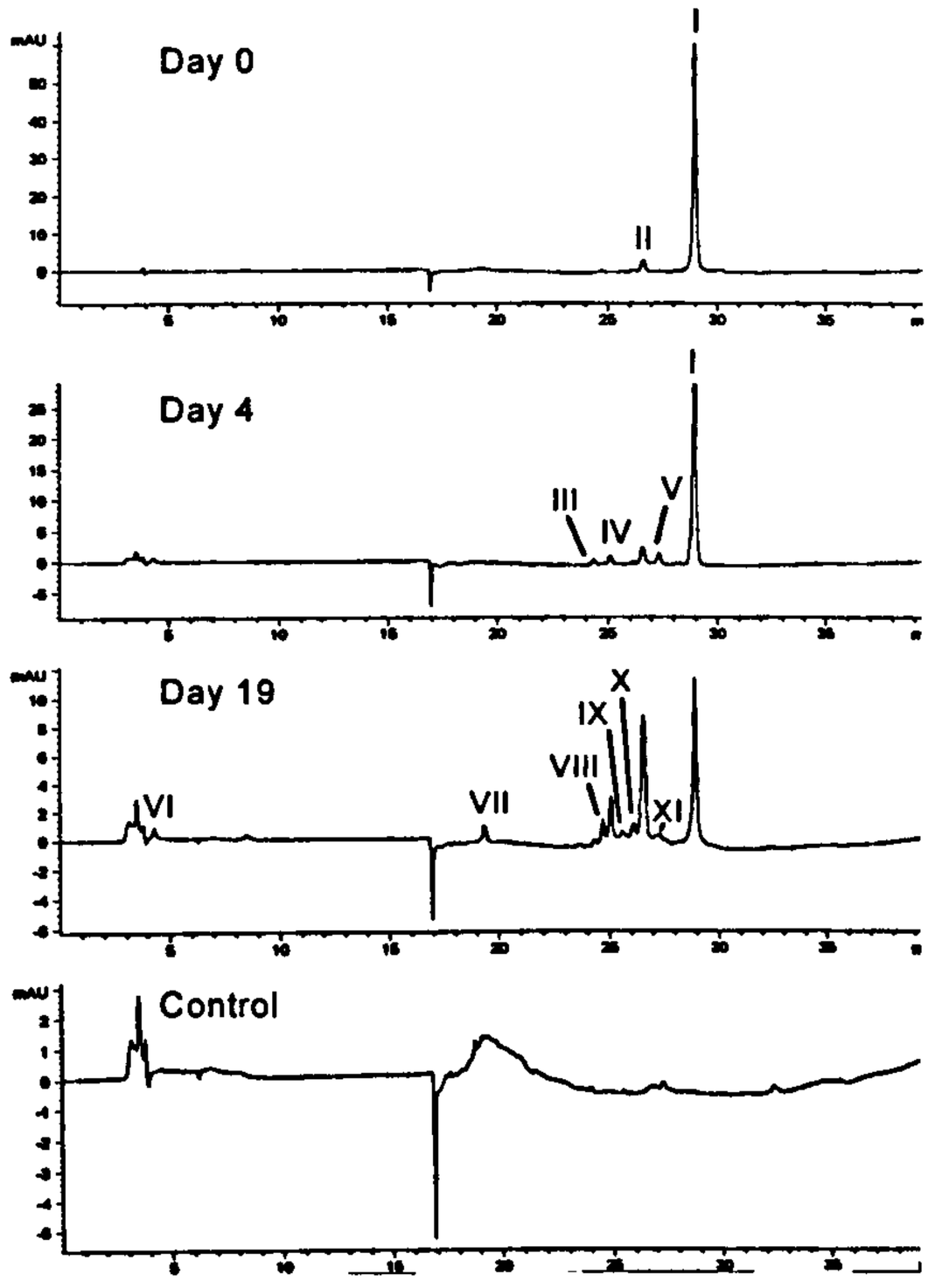

Figure 5.3 LC-UV (254 nm) chromatogram of samples taken for a sample of dyestuff W435 degraded for zero, 4 and 19 days by a consortium of aerobic bacteria (SCAS unit)

The identification of the degradation products was attempted using LC-MS. A comparison of reconstructed ion current (RIC) and UV (254 nm) traces for the day 19 sample is shown in Figures 5.4 and 5.5. A comparison of these chromatograms with the HPLC-UV chromatogram of the same sample analysed on the corresponding day, (Figure 5.3c), suggests that degradation had continued despite refrigerated storage (4°C) of the sample prior to LC-MS analysis. In particular, the intensity of peak VIII decreased whilst peak IV increased. Despite this, it was possible to correlate the major peaks in each chromatogram by calculating retention times relative to the parent dye, peak XI.

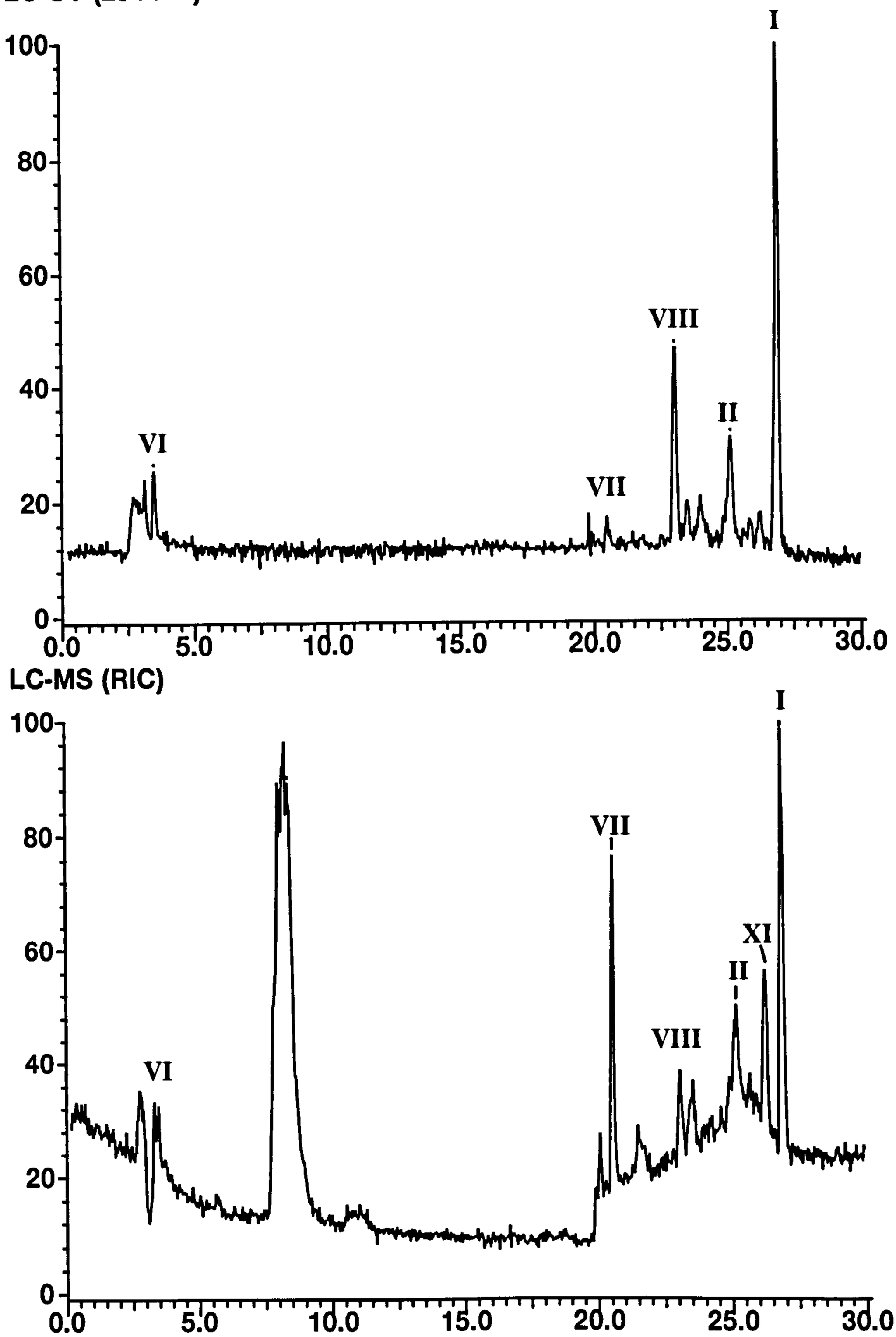

Figure 5.4 Comparison of LC-UV(254 nm) and LC-MS (RIC) chromatograms for a sample of dye W435 degraded for 19 days in a SCAS system.

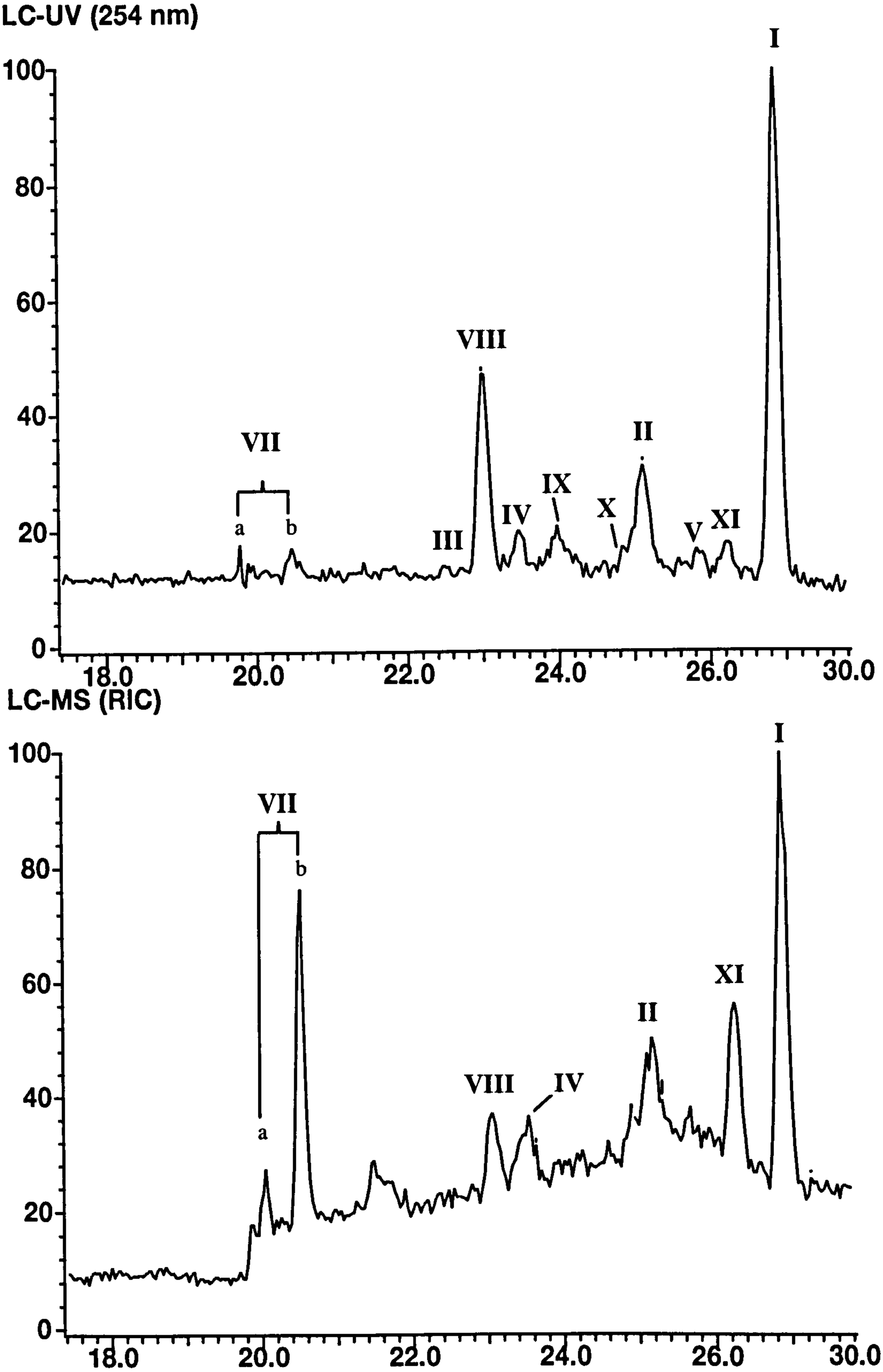

Figure 5.5 Comparison of LC-UV(upper) and LC-MS (lower) chromatograms (17.5 to 30 minutes) for a sample of dyestuff W435 degraded for 19 days by a consortium of aerobic bacteria (SCAS unit)

The identification of products was based on several criteria, including the molecular weight (odd or even number of nitrogen atoms), number of sulphonic acid groups (determined by number of charge states present) and presence or absence of chlorine isotopes. The mass spectra for some of the products, including the parent dye (I), an hydrolysis product (II) and two further products with molecular ions at *m/z* 320 / 641 (IV) and *m/z* 430 (IX), were previously identified by analysis of samples from the photolysis study, (Section 3.4.2).

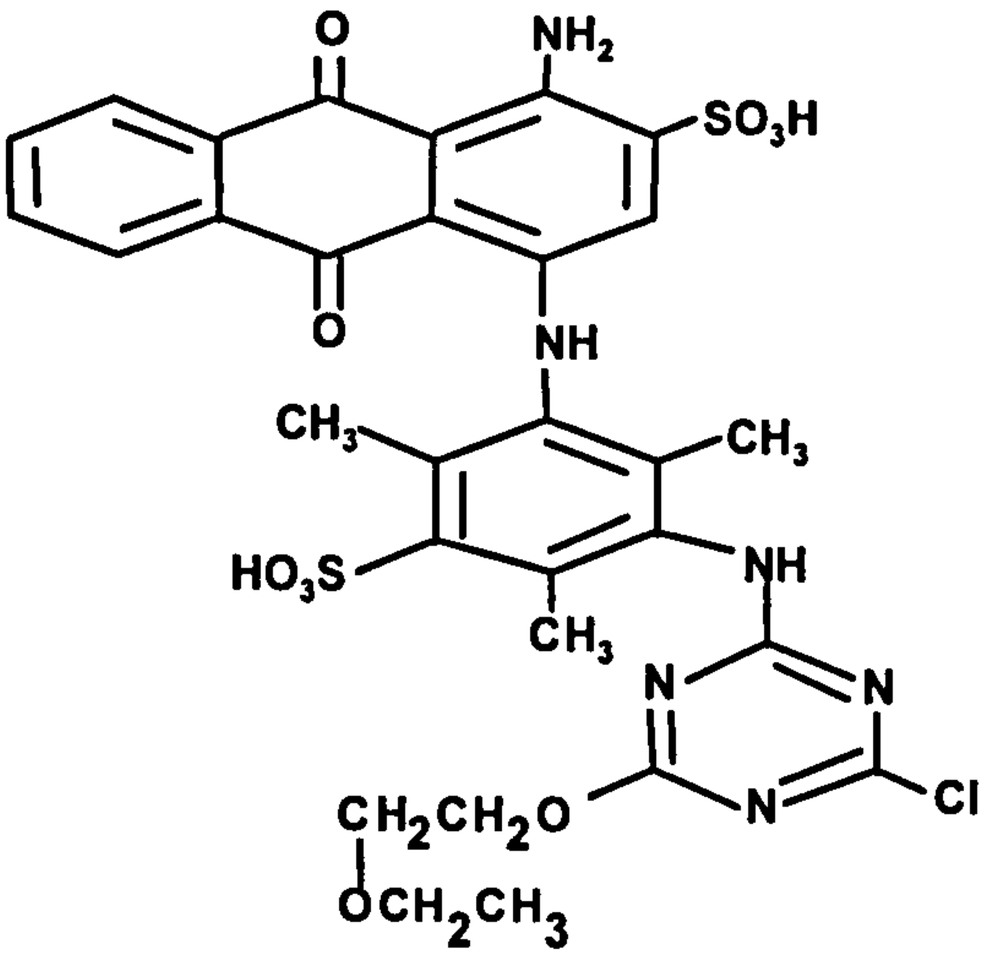

I

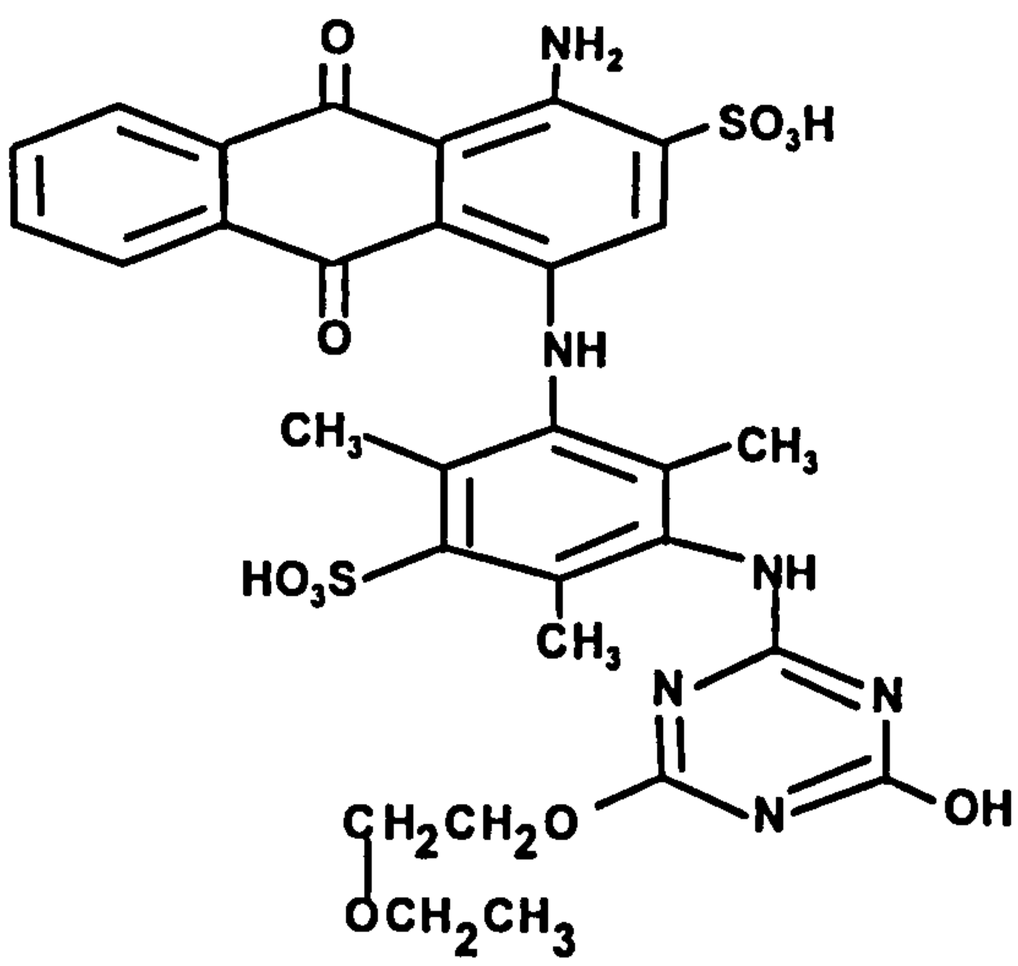

II

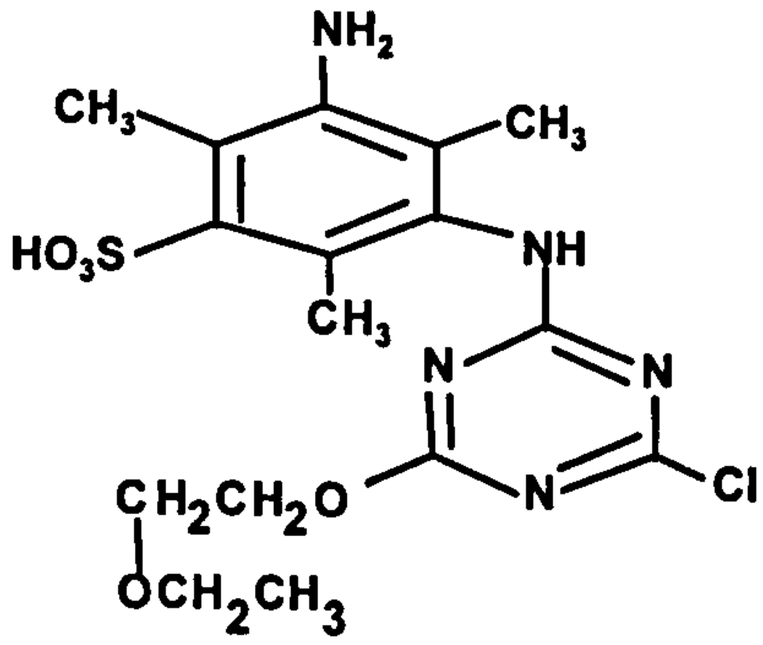

IX

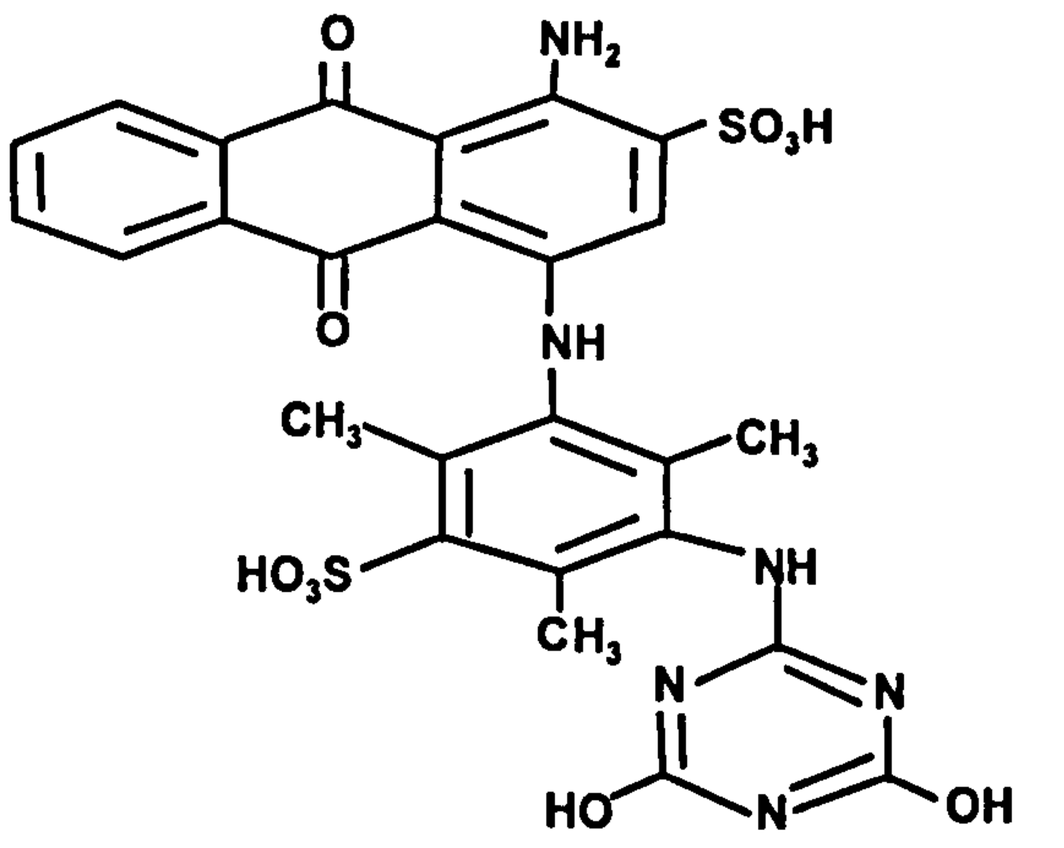

IV

The mass spectrum observed for component VIIb, (Fig 5.6), shows a molecular ion $[M-H]^-$ *m/z* 218 which indicates an odd molecular weight and therefore an odd number of nitrogen

atoms and appeared to be singly charged, therefore possessing no more than one sulphonic acid group. A characteristic chlorine isotope pattern was present. This was consistent with a hydroxylated compound derived from the chlorotriazine reactive group function of the dye W435.

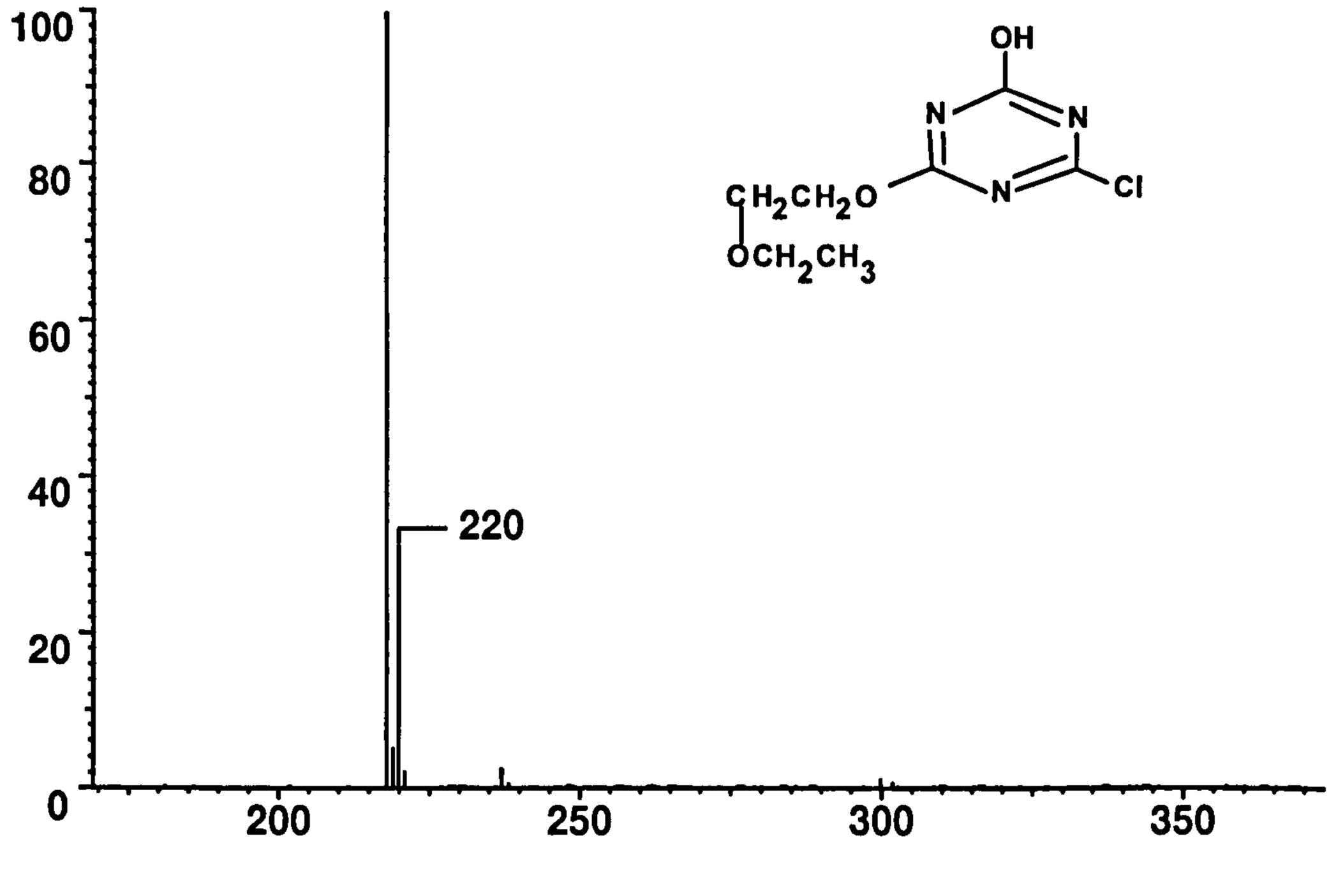

Figure 5.6 Mass spectrum derived from component VIIb (Figure 5.5) for a sample of dyestuff W435 degraded for 19 days by a consortium of aerobic bacteria (SCAS unit)

A much smaller component, (VIIa) was not observed in the original LC-UV chromatogram, (Fig 5.3). The molecular ion of this component (*m/z* 200; Fig 5.7), differed by 18 mass units from that observed for peak VIIb and no chlorine isotope pattern was present. This is consistent with de-chlorination and concurrent hydroxylation of compound VIIb:

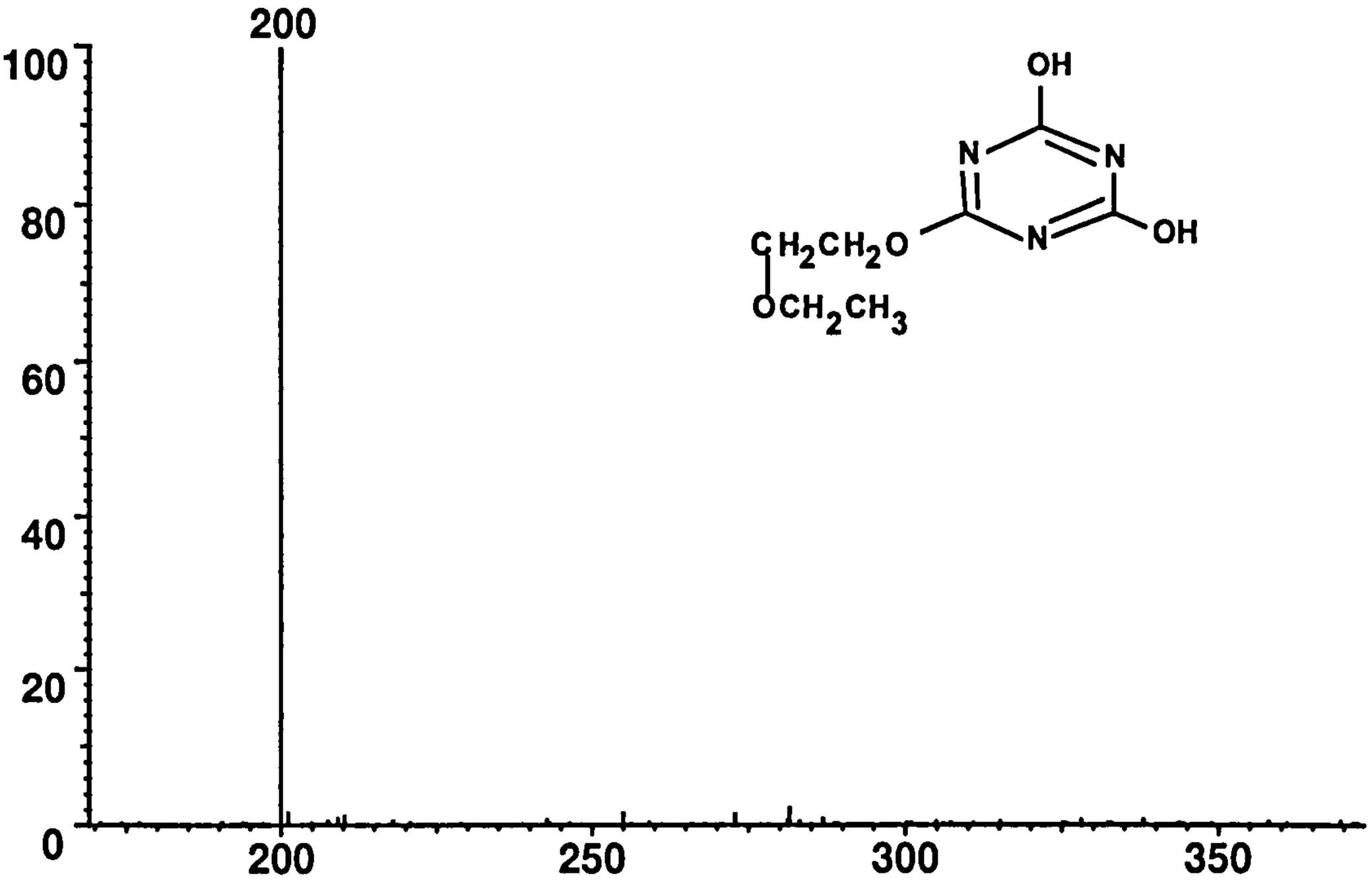

Figure 5.7 Mass spectrum of component VIIa (Figure 5.5) for a sample of dyestuff W435 degraded for 19 days by a consortium of aerobic bacteria (SCAS unit)

The mass spectrum of component V, (Fig 5.8), produced molecular ions at *m/z* 351 and 703 indicating a molecular weight of 704 and the presence of two sulphonic acid groups. The even molecular weight is indicative of an even number of nitrogen atoms in the molecule. The presence of chlorine was confirmed by the isotope pattern of the singly charged molecular ion. The mass difference between the molecular weight of component VI and the parent dye W435 (equal to 28 mass units) is most likely to be due to the net loss of C_2H_4 which can be rationalised by the hydrolytic fission of the ethoxylate side chain to produce an alcohol, with the elimination of ethanol:

$$\text{R-OCH}_2\text{CH}_2\text{-O-CH}_2\text{CH}_3 \longrightarrow \text{R-OCH}_2\text{CH}_2\text{-OH} + \text{HO-CH}_2\text{CH}_3$$

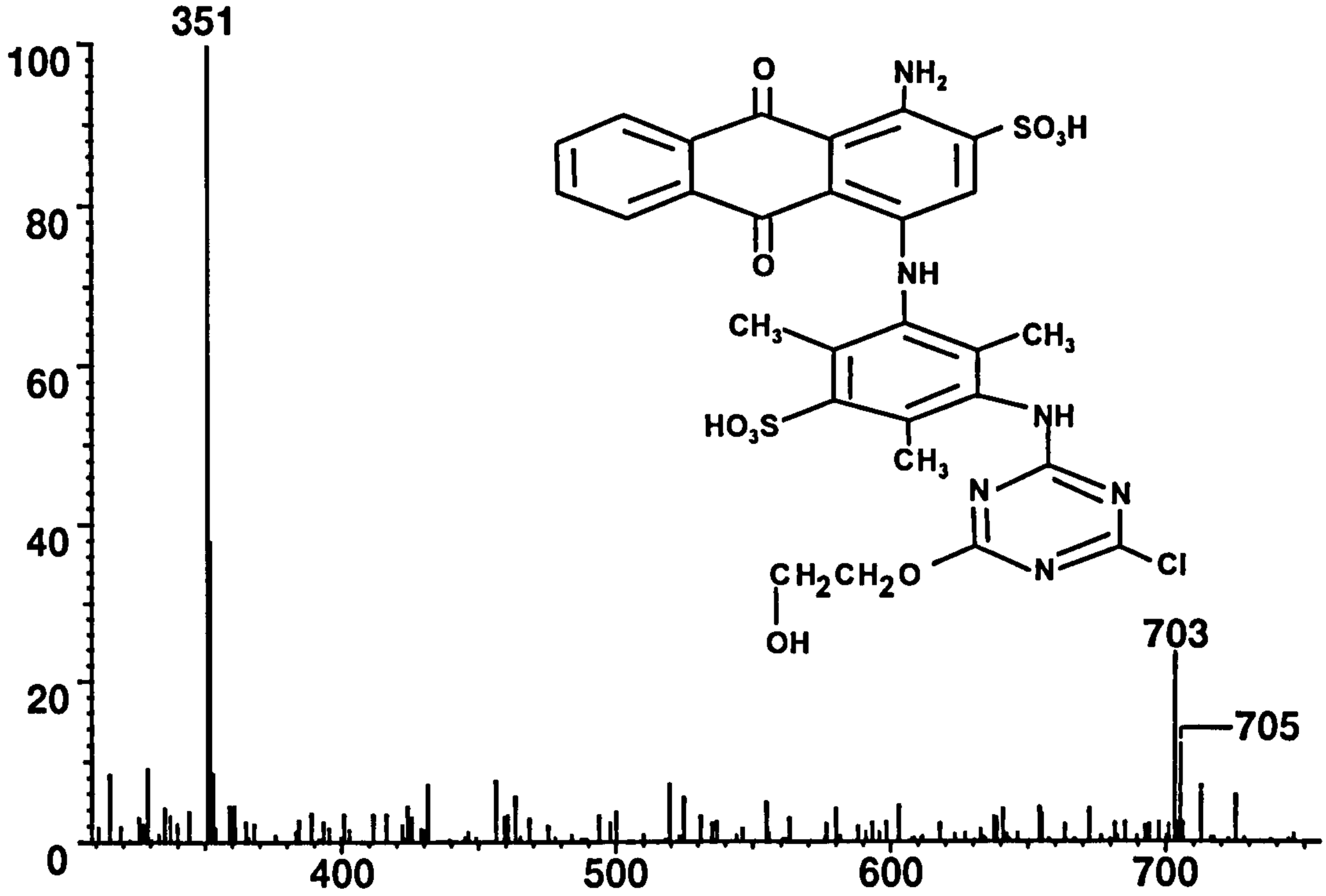

Figure 5.8 Mass spectrum of component V (Figure 5.5) for a sample of dyestuff W435 degraded for 19 days by a consortium of aerobic bacteria (SCAS unit)

The mass spectrum of component VIII, (Fig 5.9), contained molecular ions at *m/z* 717 and 358 (ie two sulphonic acid groups) an even number of nitrogen atoms and a characteristic chlorine isotope pattern. Interestingly the molecular weight of this compound (718) was only 14 mass units less than that of the parent dye W435, yet its retention time was nearly 4 minutes less than the parent, suggesting it was significantly more polar. These data can be explained by the further oxidation of component V to form a carboxylic acid, which would result in a net change in molecular weight of 14 mass units compared to the parent dye:

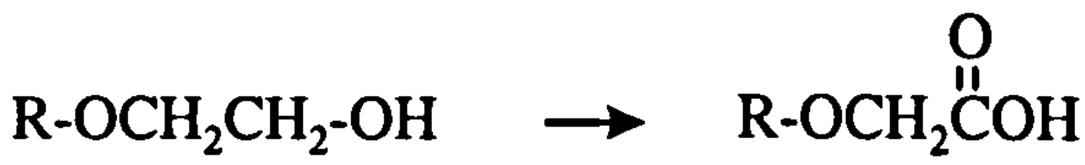

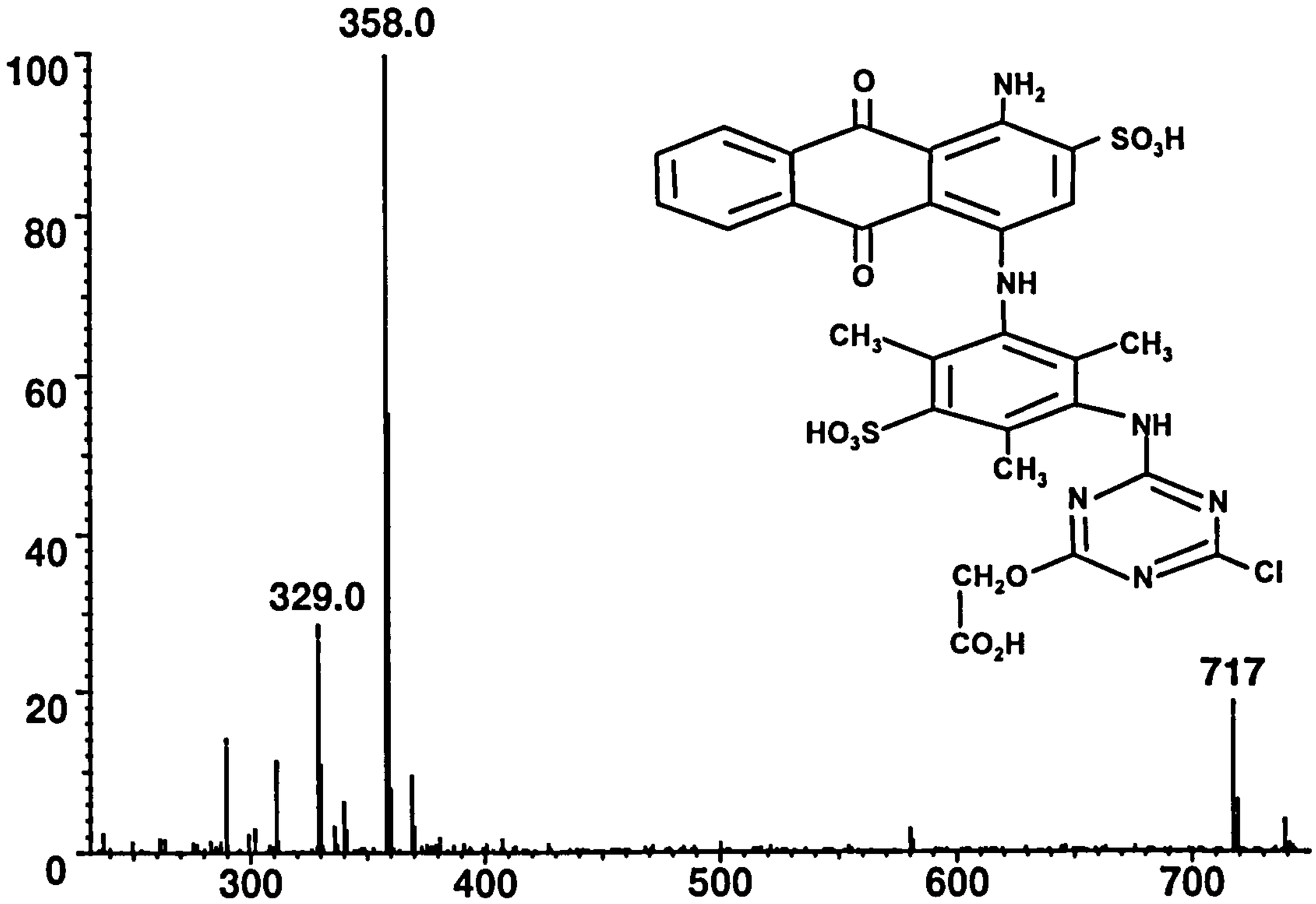

Figure 5.9 Mass spectrum of component VIII (Figure 5.5) for a sample of dyestuff W435 degraded for 19 days by a consortium of aerobic bacteria (SCAS unit)

The mass spectrum for component XI (Fig 5.10) was not observed in the initial LC-UV (254 nm) analysis, (Fig 5.3). The observed molecular ion *m/z* 302, indicated an odd number of nitrogen atoms and showed no chlorine isotope pattern. The presence of only one charge state suggested no more than one sulphonic acid group. This was consistent with 1-amino-anthraquinone-2-sulphonic acid.

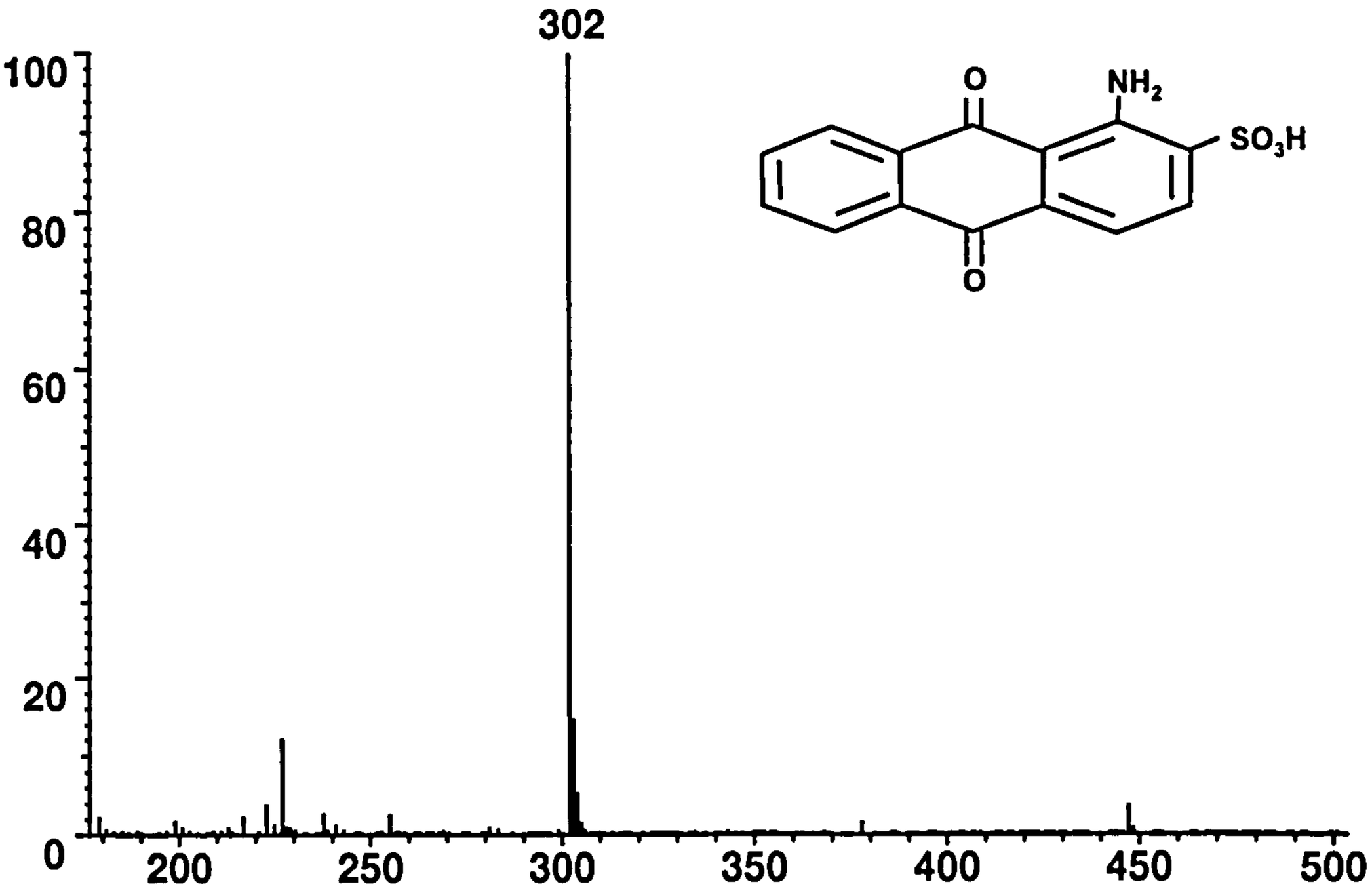

Figure 5.10 Mass spectrum of component XI (Figure 5.5) for a sample of dyestuff W435 degraded for 19 days by a consortium of aerobic bacteria (SCAS unit)

Peaks III, VI and X did not produce mass spectra under the conditions used for this analysis. The proposed aerobic biodegradation pathway for W435 is summarised in Figure 5.11.

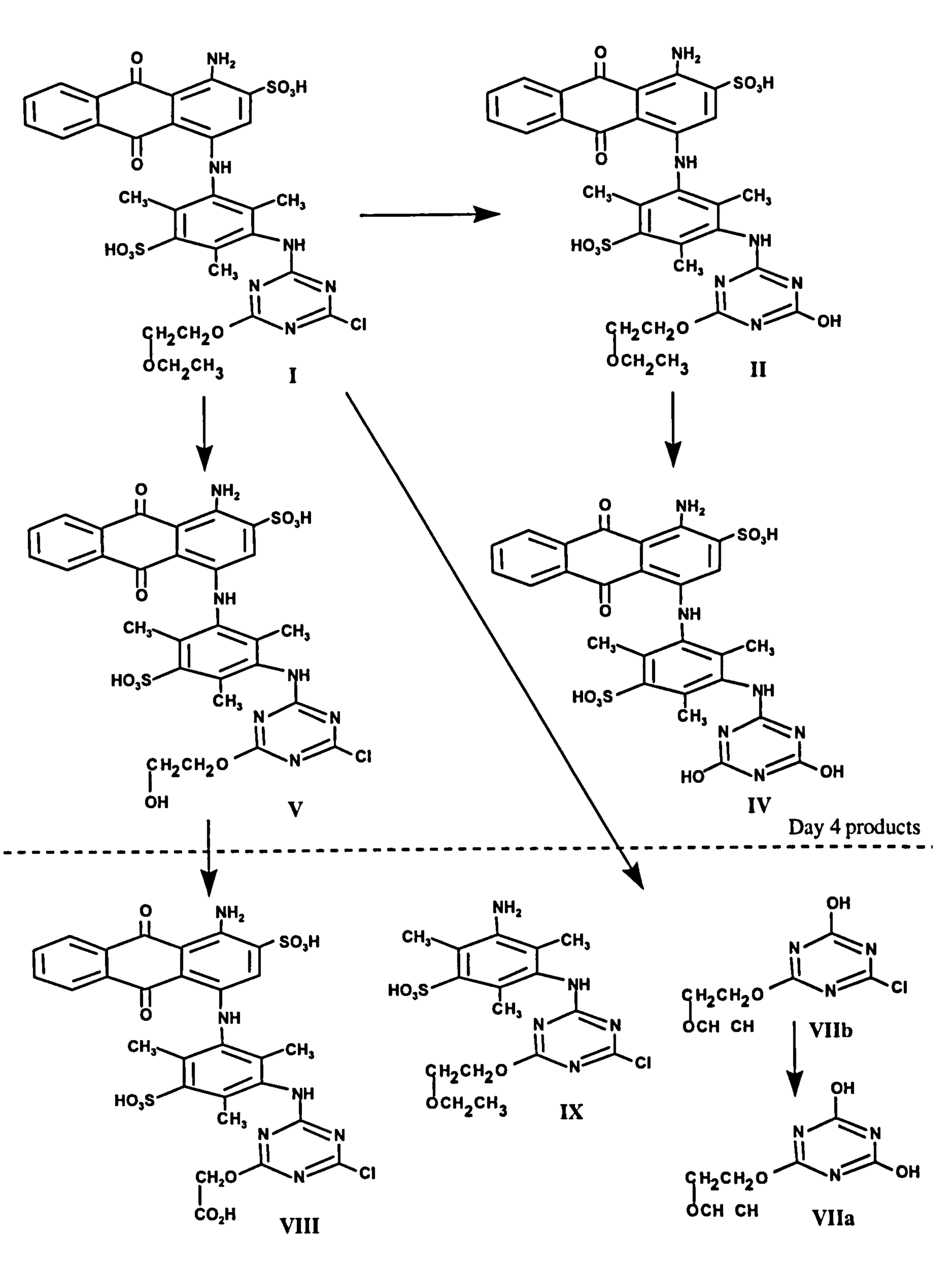

Figure 5.11 Proposed aerobic degradation pathway for dyestuff W435 following degradation for 19 days by a consortium of aerobic bacteria (SCAS unit)

It was noticeable that at the end of the experiment the sludge residue was blue, indicating that unlike the parent dye, at least some of the degradation products were absorbed onto the sludge. A sample of filtered sludge was stored frozen for future analysis.

5.3.2 Products of incubation of dyestuff W435 with single strain cultures of bacteria

The concentrations of W435 determined for samples incubated with three different single strain cultures of bacteria, are shown in Table 5.2. It was noticeable that the control sample (no culture) showed 100% degradation of parent dye on day 7, indicating that it had become non-sterile. Also, re-analysis of samples showed that chloroform added to each sample to terminate biological activity was ineffective and degradation within samples had continued. The data below should therefore be treated with care, although rapid degradation by *P. 9046* and *P. texaco* was observed.

Table 5.2 Concentration of W435 incubated with three different single strain cultures of bacteria

Day	Relative amount of dye (%)			
	Control	*P. docunhae*	*P. fluoriscens* - 9046	*P. texaco*
1	100	94	92	87
2	92	97	60	24
3	94	96	21	9
4	95	63	13	6
7	0	0	0	0

The second single strain culture experiment was carried out in a more controlled environment. Each test vessel not only had a sterilised foam bung, but was sealed with aluminium foil, to prevent cross contamination of the cultures. This enabled the experiment to be extended to 24 days. Additionally, it was possible to have a control for each dye (no culture) and a glucose free test vessel for each dye with each culture to determine the potential of each dye as the sole carbon source for degradation.

Figures 5.12a-c show the measured concentration for duplicate test vessels of W435 incubated with *P. docunhae*, *P. 9046* and *P. texaco* respectively. There was no loss of W435 in the dye only control, confirming the observation in the SCAS experiment that

W435 does not adsorb to bacterial cultures or solids. Also, there was no loss of W435 in the glucose-free vessels, again confirming the SCAS observation that W435 does not degrade when it is the sole carbon source.

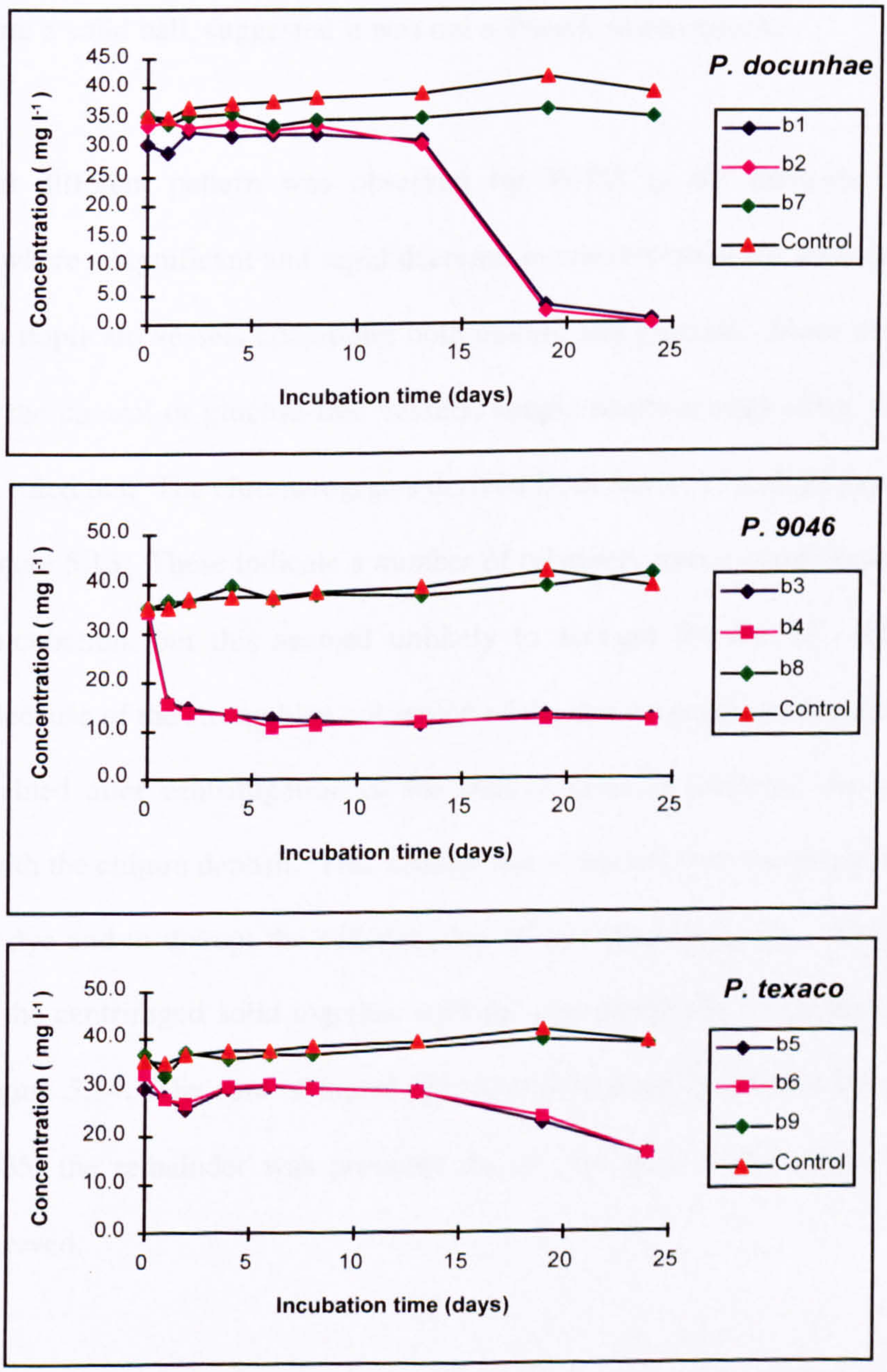

Figure 5.12 Incubation of replicate test vessels of W435 with single strain cultures of a) *P. docunhae* (b1, b2), b) *P. 9046* (b3, b4) and c) *P. texaco*(b5,b6). The control vessels contained W435 but no glucose or culture and b7, b8 and b9 contained culture but no glucose

Removal of W435 was observed in samples taken after day 13 from the *P. docunhae* test vessels, (Fig 5.12a) but there was no evidence for major degradation products in the LC-UV chromatograms of day 19 or day 24 samples. Growth was observed in both

P. docunhae duplicate test vessels, which was not observed in the controls or any of the other test vessels. This growth started on day 13 and effectively removed the dye leaving a colourless solution by day 24. The origins of the growth were not investigated, but its physical form; a solid ball, suggested it was not a *Pseudomonas* species.

A somewhat different pattern was observed for W435 in the presence of *P. 9046*, (Fig 5.12b) where a significant and rapid decrease in concentration (to 46% on day 1) was observed for duplicate vessels containing both culture and glucose. Since no losses were observed in the control or glucose-free vessels, simple sorption onto either the culture or glucose was ruled out. The chromatograms derived from day 1, 13 and 24 experiments are shown in Figure 5.13. These indicate a number of relatively minor components formed on prolonged incubation, but this seemed unlikely to account for the 54 - 60% removal observed. Because of the strong blue coloration of the dye it became noticeable that a blue residue remained after centrifugation of the sample prior to analysis, the colour being associated with the culture deposit. This residue was extracted with methanol, used both to dissolve the dye and to disrupt the cell structure of associated bacteria. The recovery of W435 from the centrifuged solid together with the concentrations in the liquid phase are shown in Figure 5.14. The sum of liquid plus sorbed material accounted for greater than 70% of W435, the remainder was probably due to the sum of the minor degradation products observed.

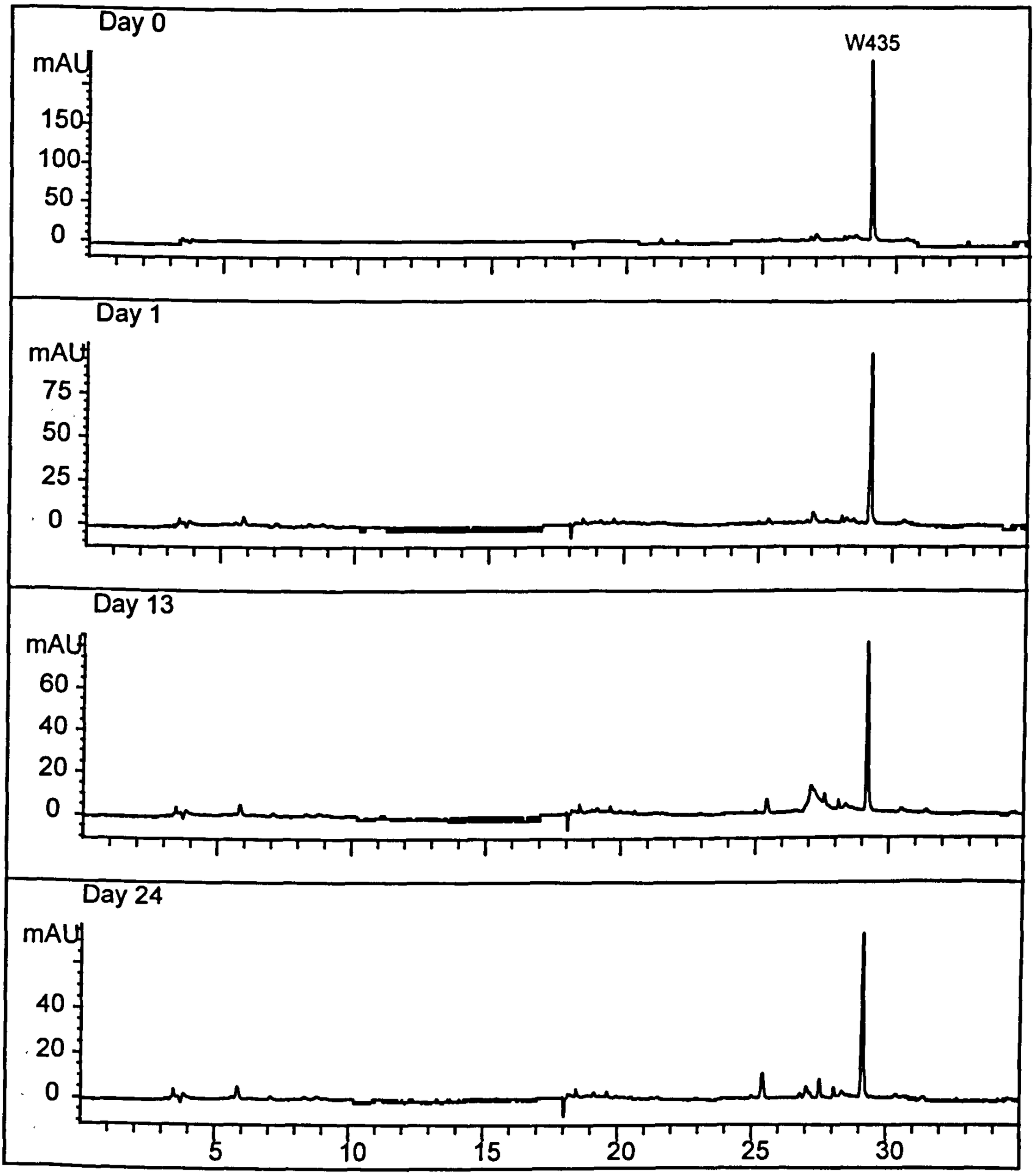

Figure 5.13 LC-UV (254 nm) chromatograms of samples taken during the 24 day aerobic incubation of W435 with *Pseudomonas 9046*

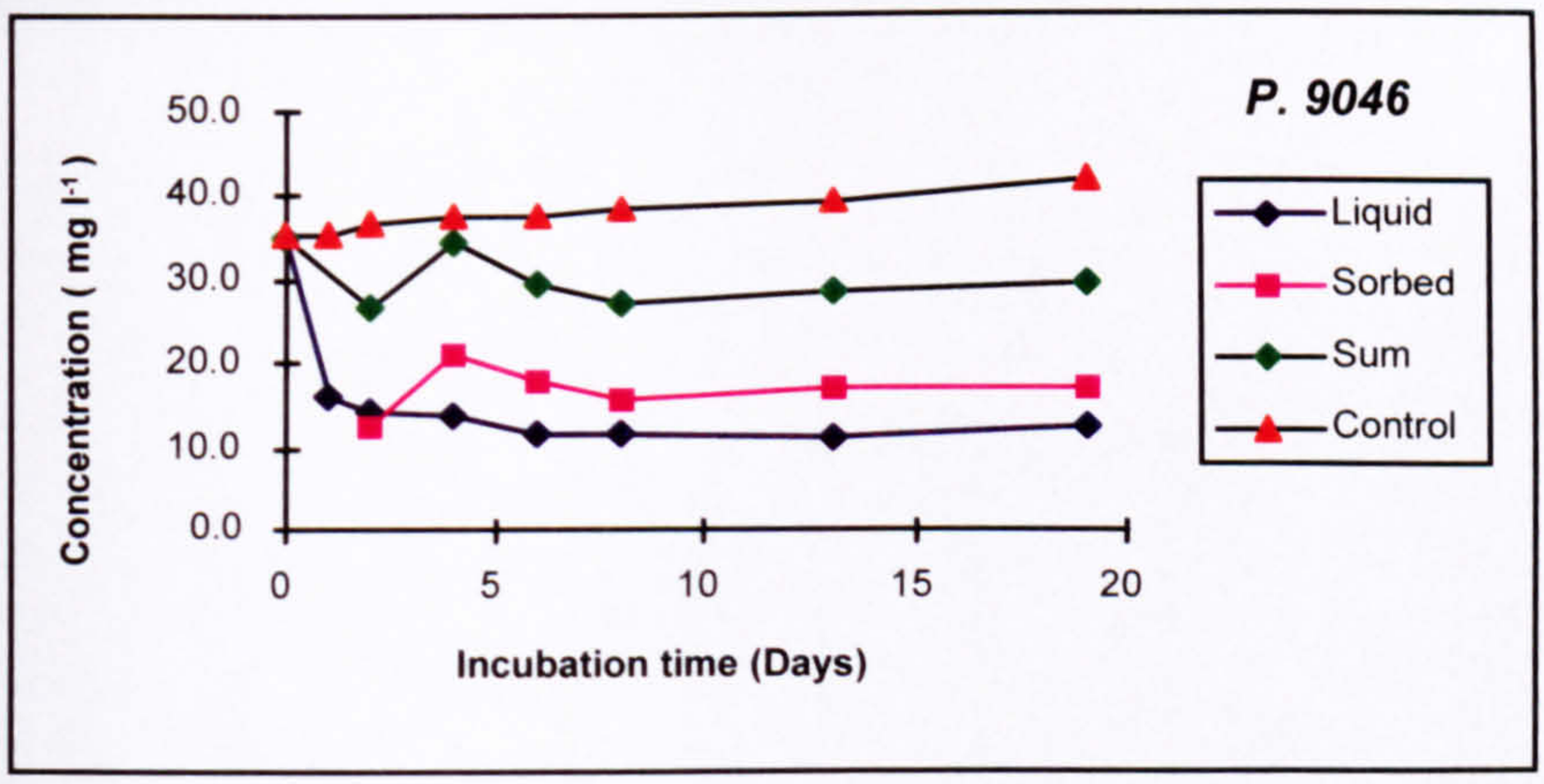

Figure 5.14 Comparison of W435 concentration in liquid (mean of b3 and b4) and methanol extracts from solid residue (sorbed), derived from the incubation of W435 with single strain culture of *P. 9046*. The control vessel contained W435 but no glucose or culture

It was interesting that adsorption occurred only when glucose was also present. Sorption may have been associated with the rapid growth of the culture in the presence of glucose as a carbon source, or possibly due to dual uptake of dye and glucose by the bacteria.

The effect of incubation of W435 with *P. texaco* is shown in Figure 5.12c. Significant biodegradation was observed after 19 days incubation, with numerous degradation products observed in the LC chromatograms of samples taken at days 19 and 24, (Fig 5.15). These data suggest that a period of acclimation was required before the dye could be digested by *P. texaco*. The LC retention times of the degradation products could not be related to any observed in previous studies. Samples were not identified further, but stored frozen for future analysis.

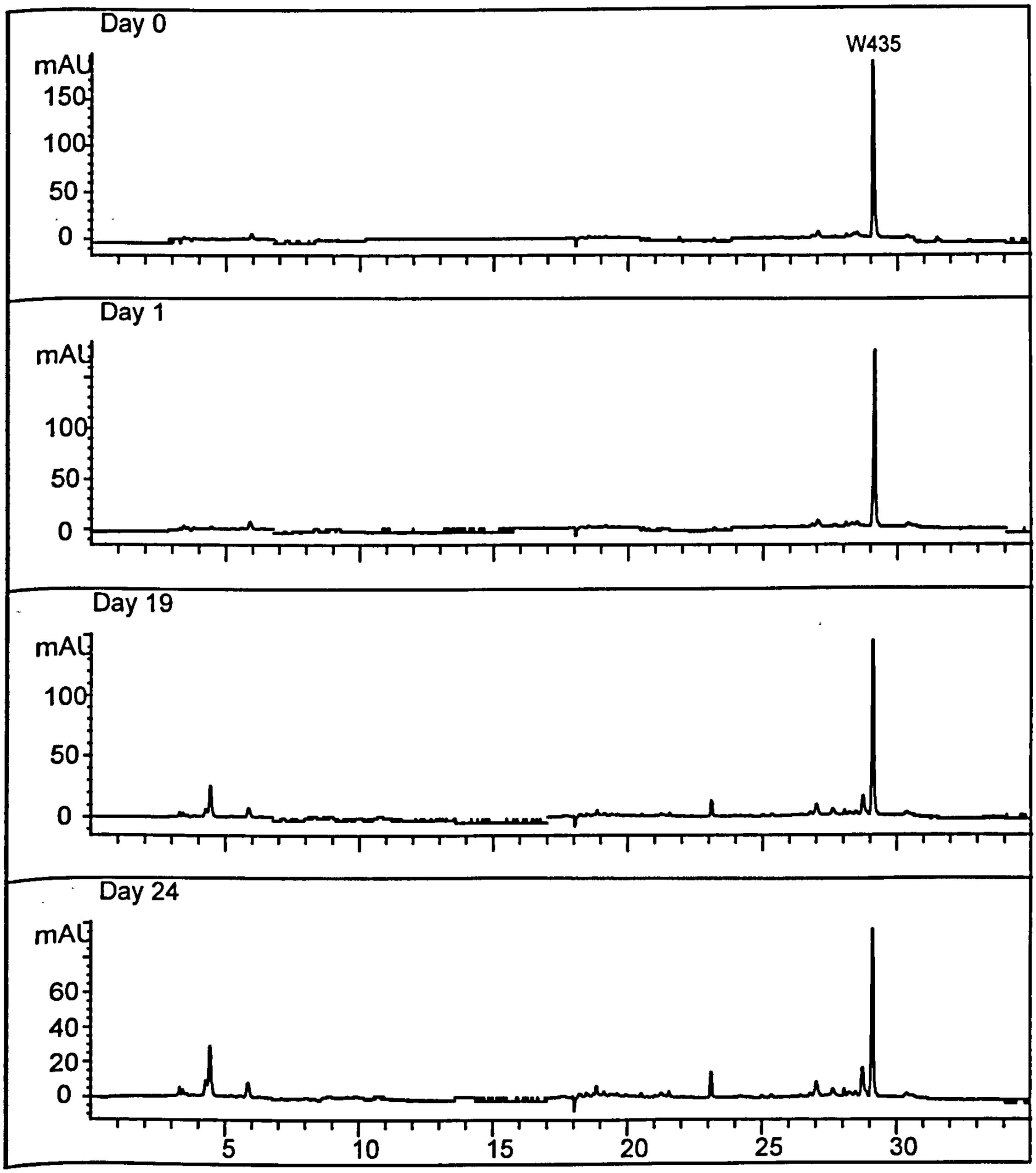

Figure 5.15 LC-UV (254 nm) chromatograms of samples taken during the 24 day aerobic incubation of W435 with *Pseudomonas texaco*

In summary, some evidence for partial aerobic degradation of dye W435 by *P. texaco* and to a lesser extent *P. 9046*, was observed. Based on LC-UV retention times, the products formed were different from those observed in the SCAS study, suggesting a different metabolic pathway. Additionally, a substantial amount of dye was removed by sorption to *P. 9046* in the presence of glucose. There was no evidence of degradation by *P. Docunhae*.

5.3.3 Evaluation of Semi-Continuous Activated Sludge (SCAS) aerobic degradation of W433

The changes in measured concentrations with incubation time for the SCAS biodegradation of W433 are shown in Figure 5.16. The observed and theoretical concentrations were very similar, indicating no significant aerobic degradation or sorption of the dye. There were no additional peaks observed in the LC-UV (254 nm) chromatograms of extracts following incubation, confirming that W433 was not degraded under the test regime used. The dip in measured and theoretical concentrations from day 38 was due to a change in added stock solution concentration.

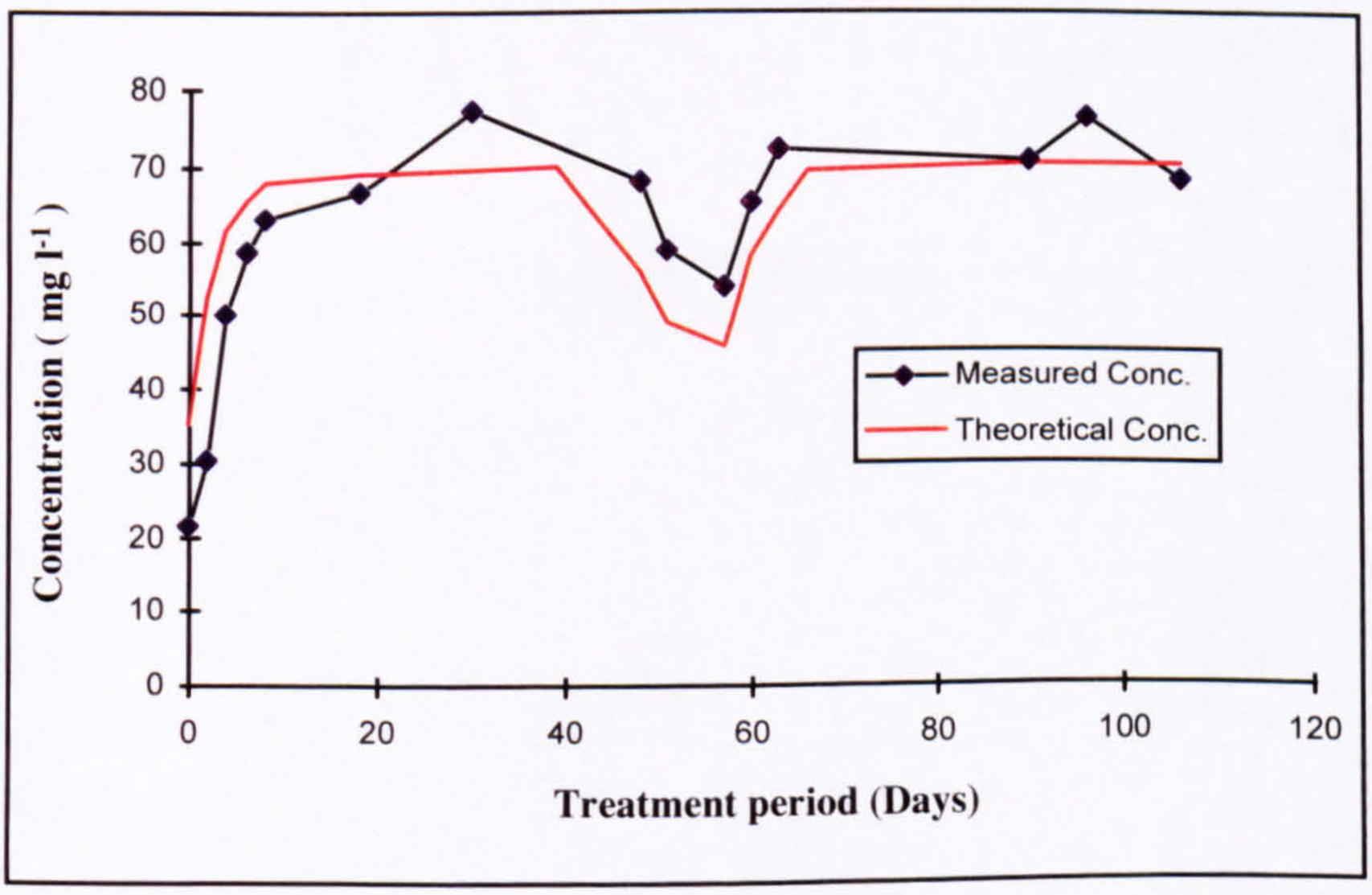

Figure 5.16 105 day aerobic incubation of W433 using Semi-Continuous Activated Sludge system (SCAS)

5.3.4 Incubation of dye W433 with single strain cultures of bacteria

The concentrations of W433 determined in samples of dye W433 inoculated with three different single strain cultures of bacteria, are shown in Table 5.3. As previously discussed for W435, re-analysis of samples showed that chloroform added to each sample to terminate biological activity was ineffective and that degradation within samples had continued after extraction. However the data suggest rapid degradation of W433 by *P. 9046* and *P. texaco*. This was particularly interesting considering there was no degradation of W433 in the SCAS experiment (Section 5.3.3).

Table 5.3.

Day	Relative amount of dye (% of starting concentration)			
	Control	*P. docunhae*	*P. 9046*	*P. texaco*
1	103	98	91	99
2	102	103	65	57
3	99	82	23	49
4	95	80	14	45
7	101	62	0	35

Figure 5.17 shows the measured concentrations in duplicate test vessels of dye W433 incubated with *P. docunhae* for 24 days. There was no loss of W433 in the control but a significant decrease in dye concentration was observed after 3 days incubation in the presence of glucose and after 12 days in the absence of glucose.

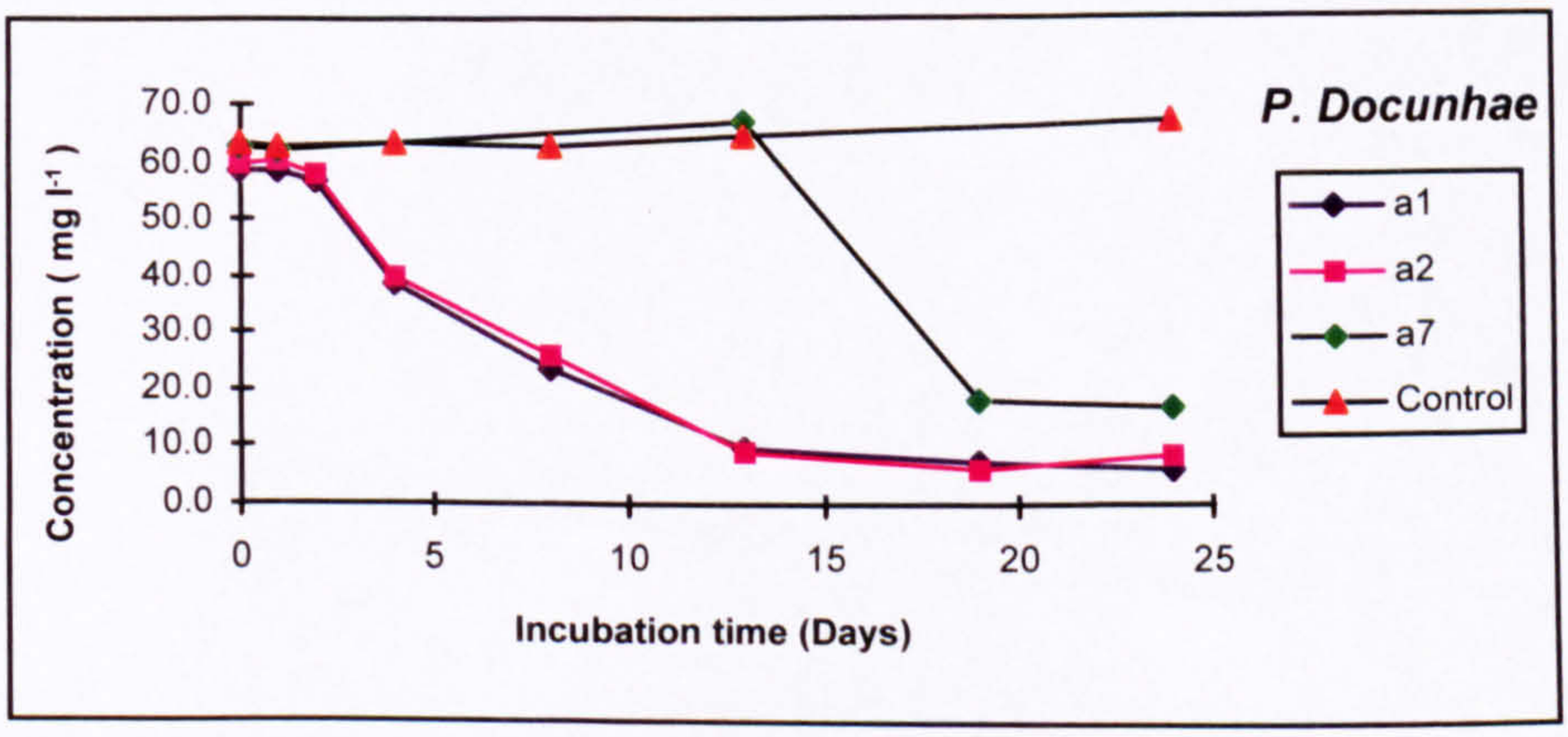

Figure 5.17 Incubation of replicate test vessels of W433 (a1, a2, with glucose and a7, no glucose) with *P. docunhae*. The control vessel contained W433 but no glucose or culture.

The concentration of dye in the duplicate samples containing both culture and glucose remained constant for the first 3 days (indicating no sorption), but then decreased rapidly from day 4 onwards. This suggests a short acclimation period was required before the culture was able to degrade the dye. LC-UV analysis of extracts from these samples (Fig 5.18) revealed a range of degradation products in samples incubated for 19 and 24 days, confirming the extensive degradation of dye by *P. docunhae*.

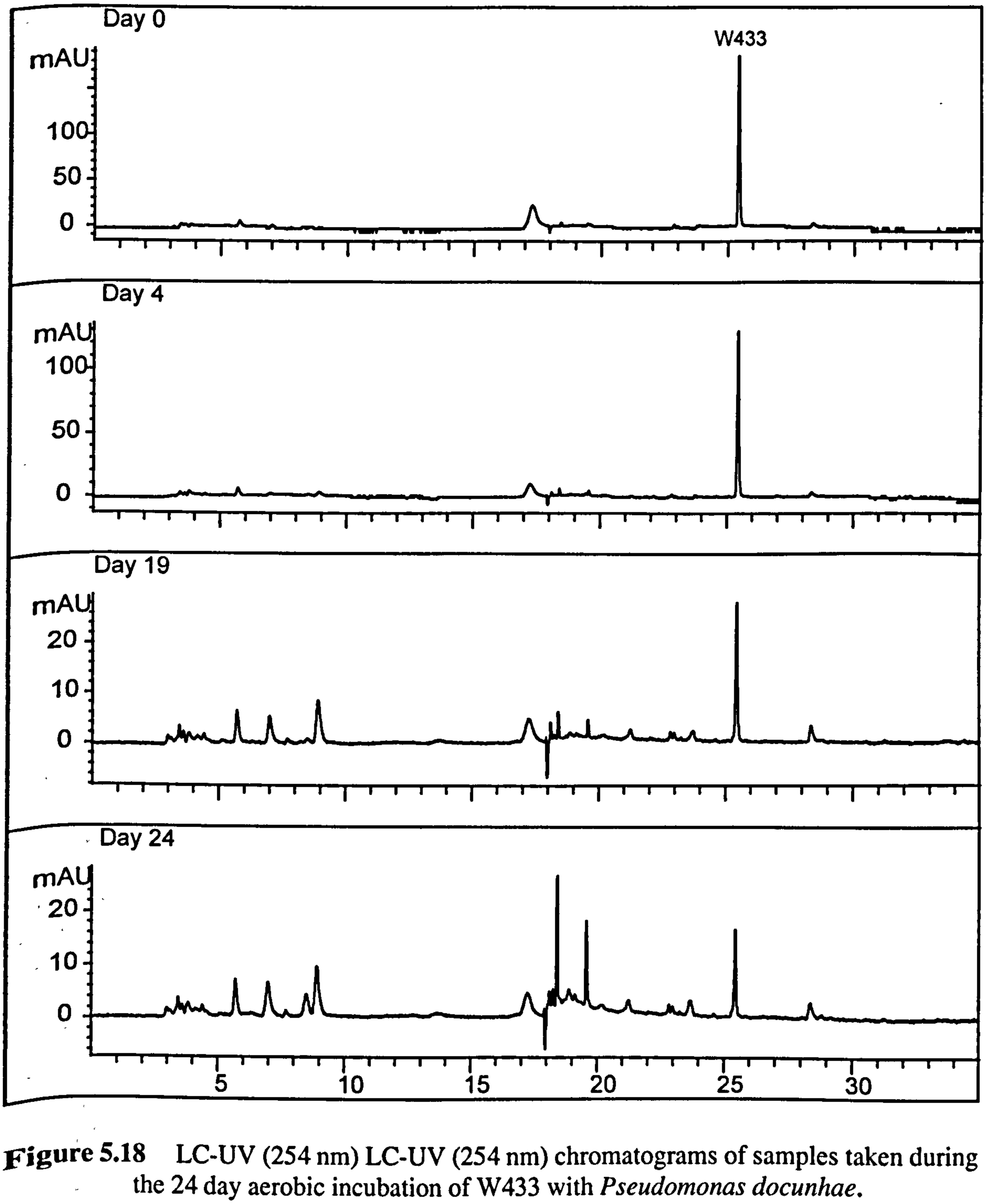

Figure 5.18 LC-UV (254 nm) LC-UV (254 nm) chromatograms of samples taken during the 24 day aerobic incubation of W433 with *Pseudomonas docunhae*.

Figure 5.19 shows the change in concentration of W433 following incubation with *P. 9046*. The dye was rapidly and extensively removed from solution over the incubation period suggesting significant degradation. However LC-UV chromatography of extracts showed no evidence for the presence of degradation products. The data for the test system with no glucose (a8) demonstrates that W433 does not simply adsorb onto the culture, indicating that an interaction between the dye, glucose and culture led to the adsorption of the dye. This effect was also observed for W435 in the presence of *P. 9046*.

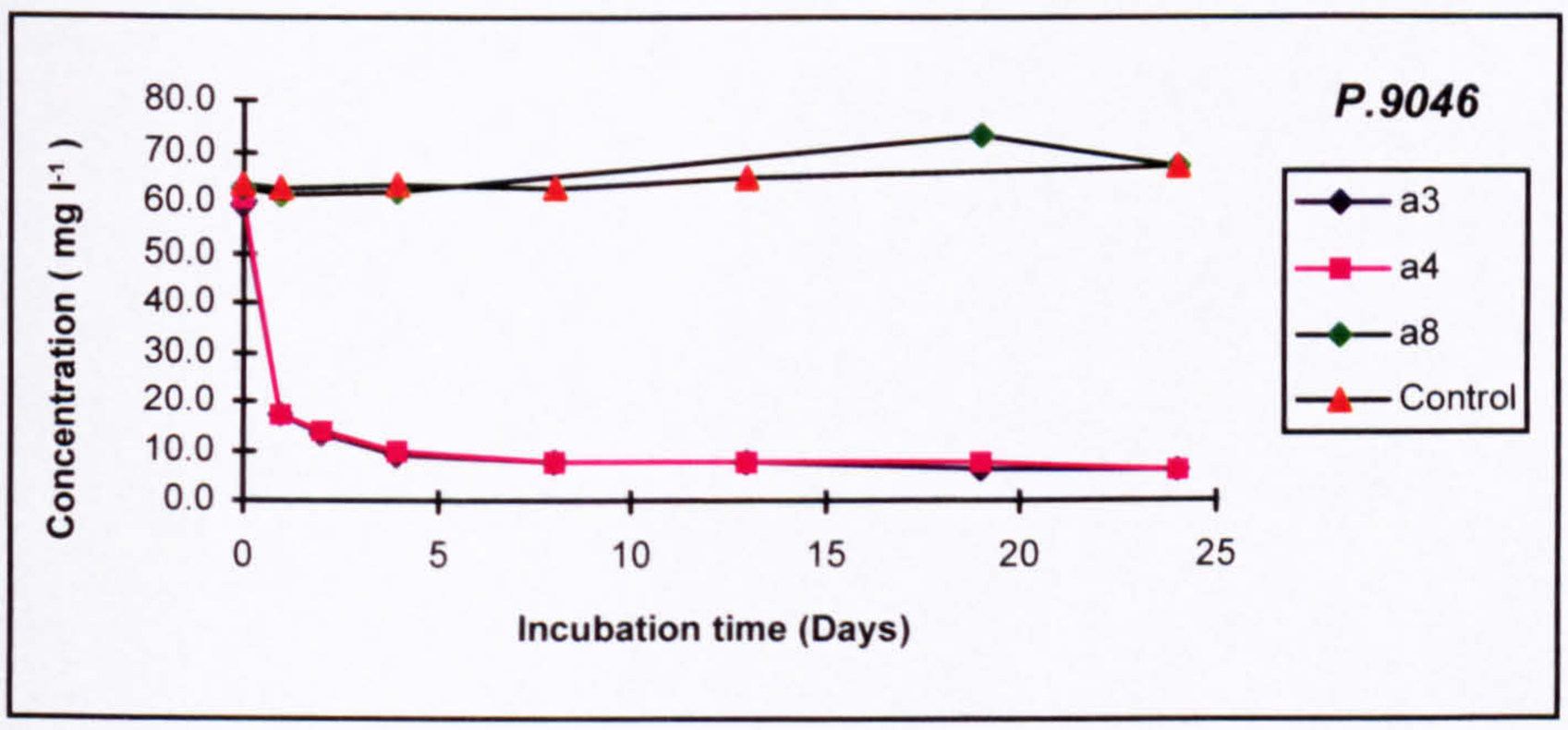

Figure 5.19 Incubation of replicate test vessels of W433 (a3, a4, with glucose and a8, no glucose) with single strain culture of *P. 9046*. The control vessel contained W433 but no glucose or culture.

Figure 5.20 shows the measured concentration for duplicate test vessels of W433 incubated with *P. texaco* for up to 24 days. There was no loss of dye in the control or with culture in the absence of glucose (a9). The initial concentration of dye decreased by 50% on day 1, but then remained at this concentration for the remainder of the incubation period. LC-UV analysis of extracts showed a few minor degradation products in the day 1 sample, but this would not account for the large decrease in W433 concentration and suggests the dye was removed by a process other than degradation. Only one degradation product was observed following 24 days incubation, Interestingly, this had a very short retention time indicating high polarity.

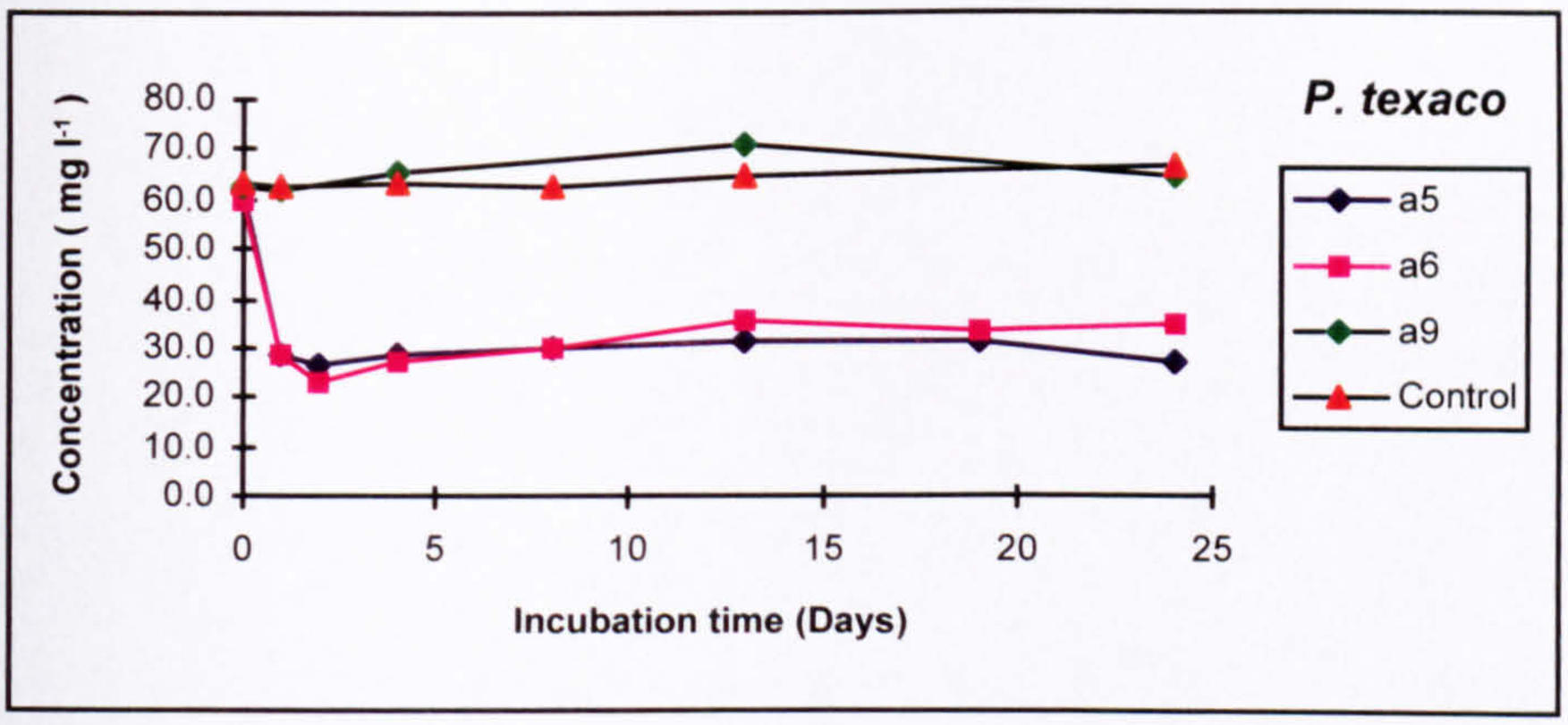

Figure 5.20 Incubation of replicate test vessels of W433 (a5, a6, with glucose and a9, no glucose) with single strain culture of *P. texaco*. The control vessel contained W433 but no glucose or culture

In summary, extensive degradation of W433 was observed in the presence of *P. docunhae*. Removal of dye by *P. 9046* and *texaco* appeared to be due to adsorption with little evidence of biodegradation.

5.3.5 Evaluation of Semi-Continuous Activated Sludge (SCAS) aerobic degradation of Reactive Red 3.1

The change in measured concentration with incubation time for the SCAS biodegradation of RR3.1 is shown in Figure 5.21. The observed and theoretical concentrations were very similar, indicating no significant aerobic degradation or sorption of the dye. There were no significant degradation product peaks observed in the LC-UV (254 nm) chromatograms confirming that RR3.1 was not degraded under the test regime used. The feed concentration of dye to the SCAS unit was reduced after day 48 to observe the effect of biodegradation on lower concentrations of dye. However, this change in concentration did not induce degradation of the dye. A further reduction in concentration at day 91 was caused by exhaustion of available dye stock solution leading to dilution of the dye on each addition of fresh nutrients.

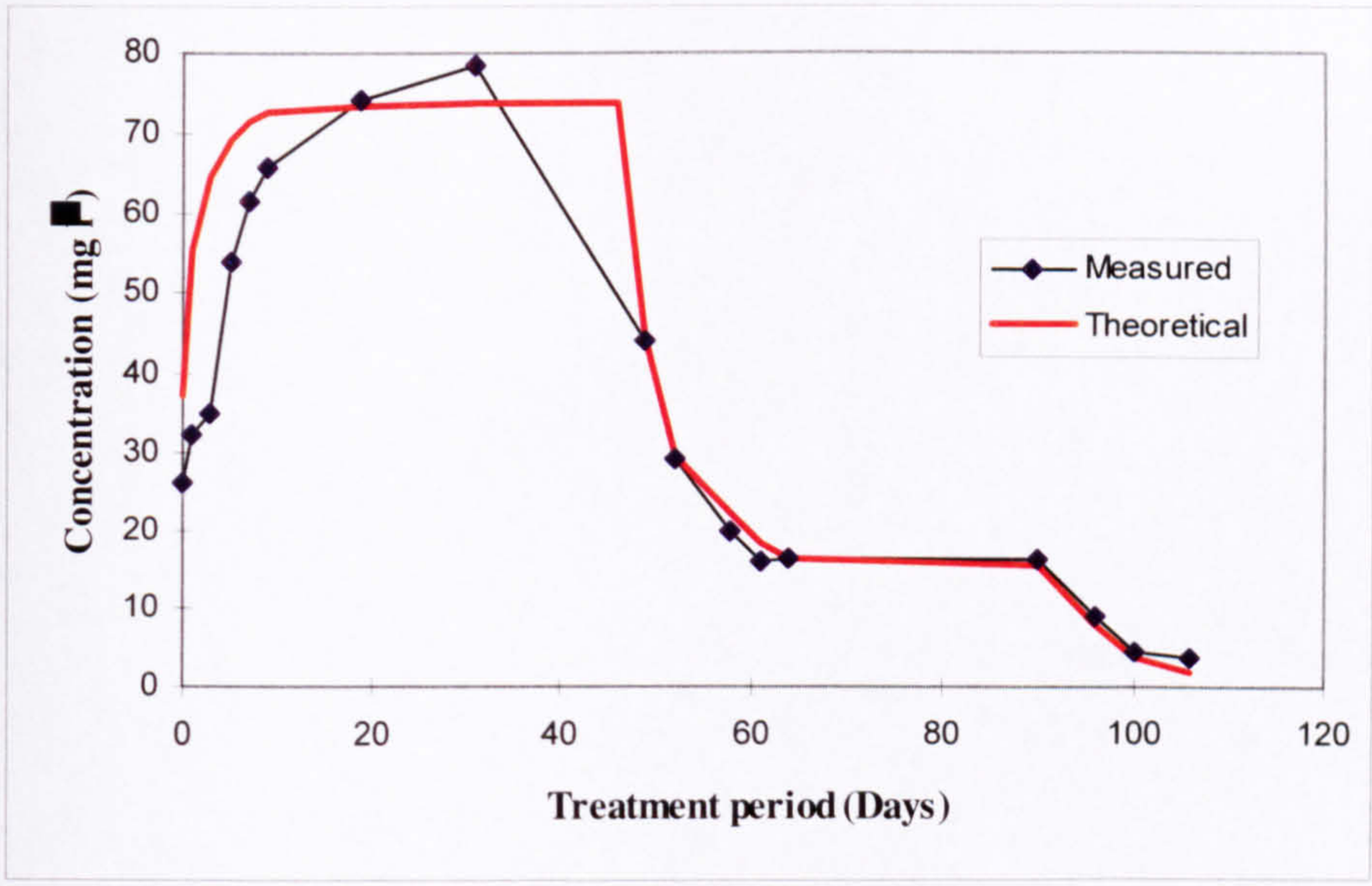

Figure 5.21 105 day aerobic incubation of W435 using Semi-Continuous Activated Sludge system (SCAS)

5.3.6 Incubation of Reactive Red 3.1 dye with single strain cultures of bacteria

Figure 5.22 shows the measured concentration for RR3.1 incubated with *P. docunhae* for 24 days. There was no loss of RR3.1 in the control. The onset of degradation for the test system containing both culture and glucose (c1) was observed on day 2. The number and concentration of products increased over the duration of the study (Fig 5.23). LC-UV chromatograms of samples taken on and beyond day 19 indicated extensive metabolism of the dye. A substantial decrease in dye concentration was observed for test system c7 (no glucose), suggesting the culture could use RR3.1 as a sole carbon source. However the LC-UV analysis showed a quite different pattern of degradation products to those observed in the presence of glucose suggesting that degradation occurred by a different pathway in the absence of glucose.

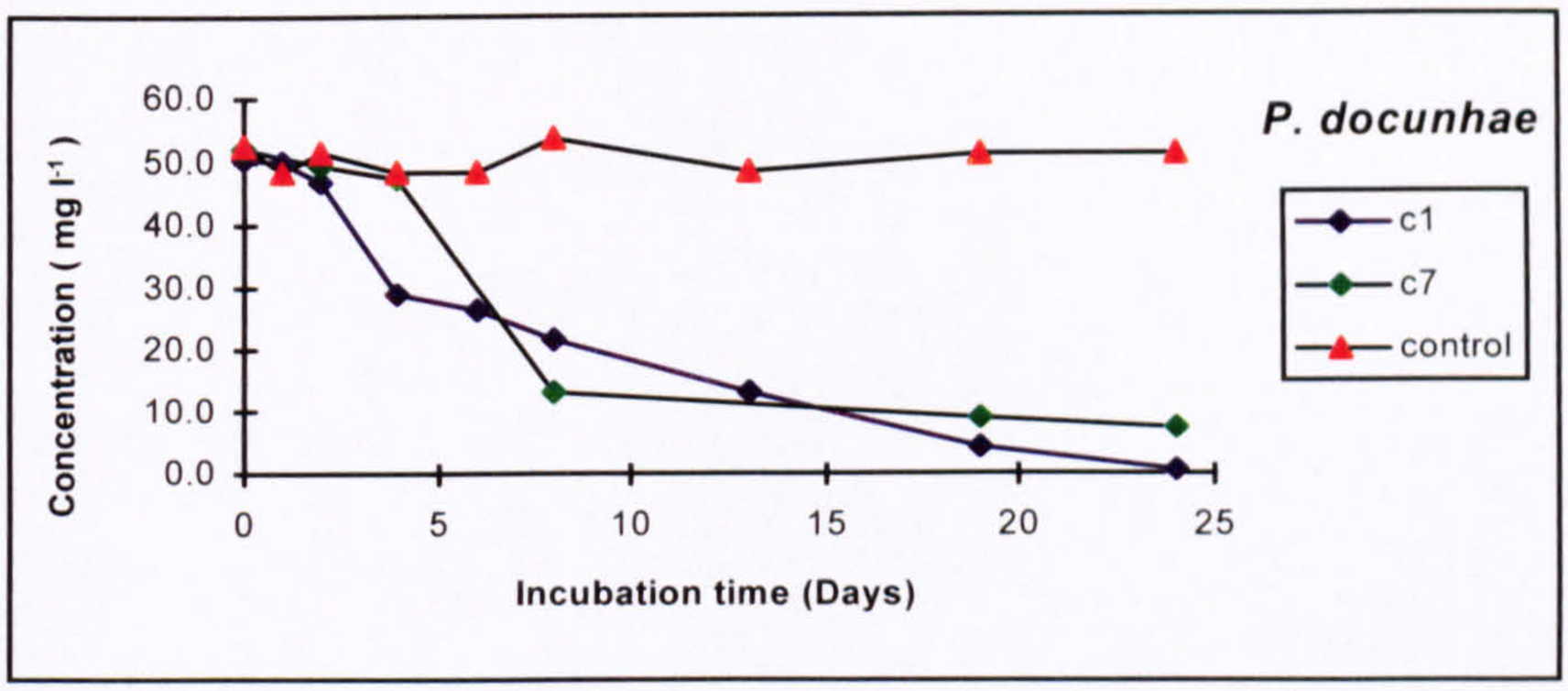

Figure 5.22 Incubation of replicate test vessels of RR3.1 (c1, with glucose and c7, no glucose) with single strain culture of *P. docunhae*. The control vessel contained RR3.1 but no glucose or culture

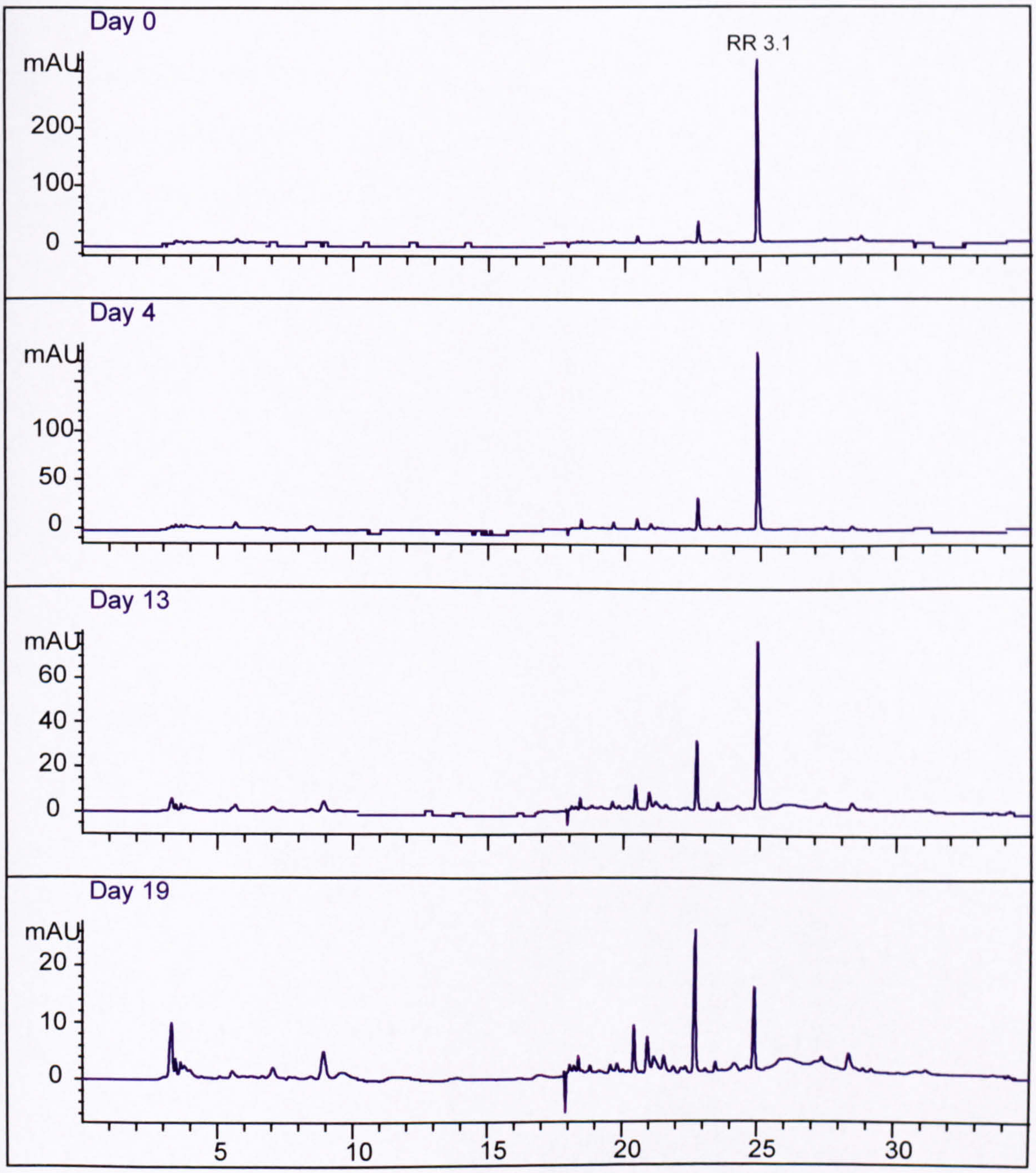

Figure 5.23 LC-UV (254 nm) chromatograms of samples taken during the 24 day aerobic incubation of W435 with *Pseudomonas docunhae* (c1, with glucose).

Figure 5.24 shows the measured concentration for RR3.1 incubated with *P. 9046* for 24 days. There was no loss of RR3.1 in the control or the glucose free test system indicating that RR3.1 was not degraded when present as the sole carbon source and was not adsorbed by the culture. The onset of degradation in the test vessel containing both culture and glucose was rapid, several products being observed on day 1. Additional products were observed following increasing incubation time, (Fig 5.25) including one with a later HPLC retention time than the parent dye (ie a less polar compound than RR3.1). However, although the range of products increased over the duration of the study, the measured concentration of parent dye showed only a slight decline up to day 24 of incubation. This suggests the degradation products formed on the first day were further transformed to new metabolites, but degradation of the parent dye ceased.

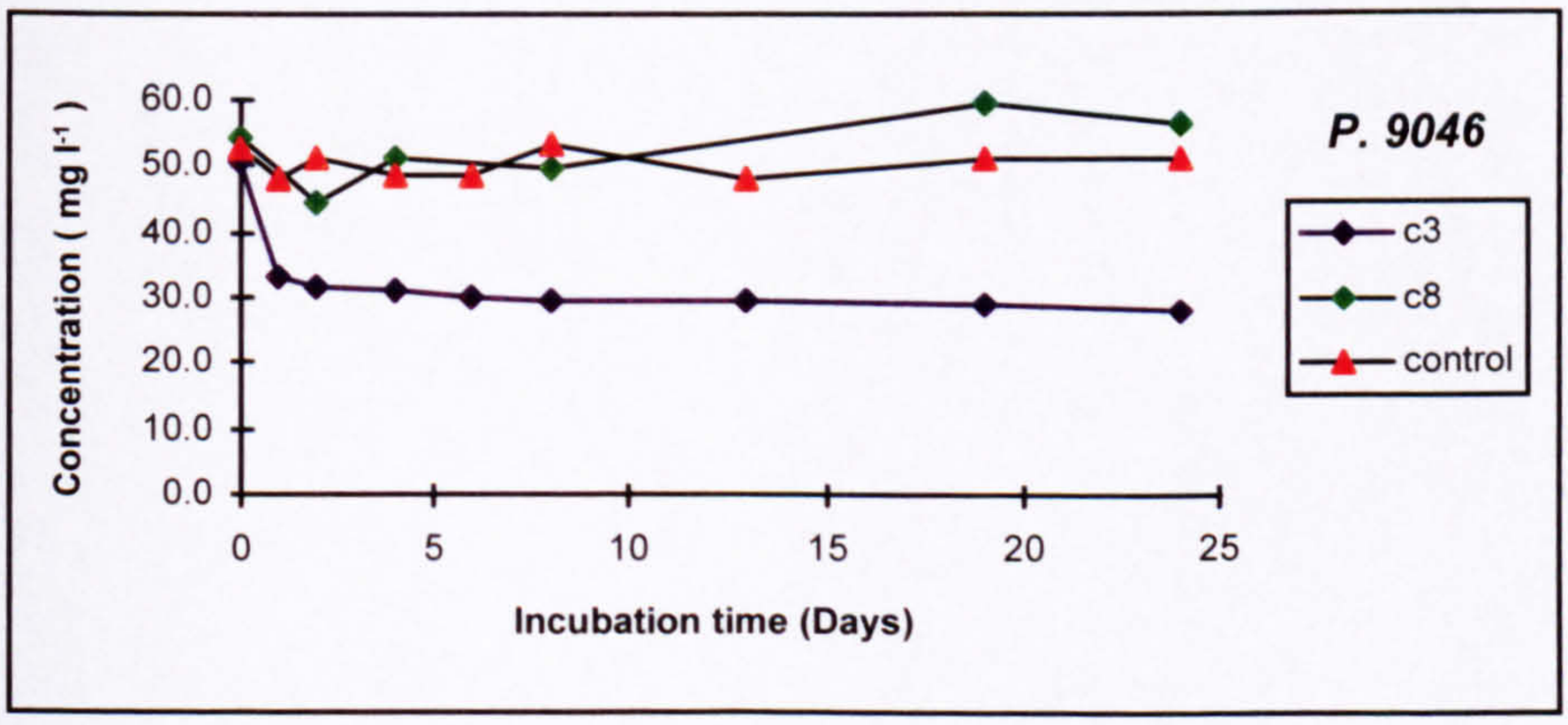

Figure 5.24 Incubation of replicate test vessels of RR3.1 (c3, with glucose and c8, no glucose) with single strain culture of *P. 9046*. The control vessel contained RR3.1 but no glucose or culture

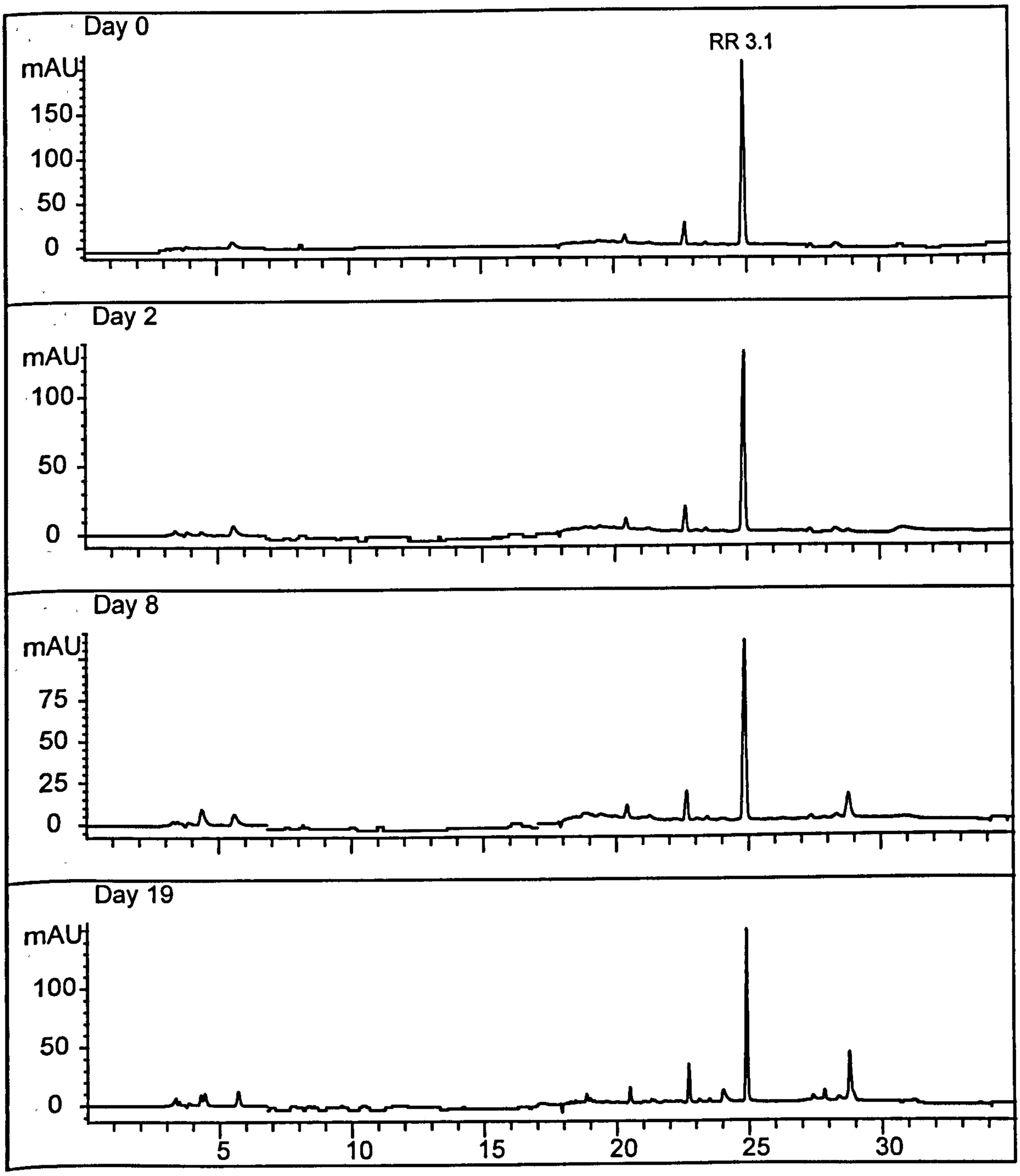

Figure 5.25 LC-UV (254 nm) chromatograms of samples taken during the 24 day aerobic incubation of W435 with *Pseudomonas 9046* (c3, with glucose).

Figure 5.26 shows the measured concentration for RR3.1 incubated with *P. texaco* for 24 days. There was no loss of RR3.1 in the control or the glucose free test system indicating that RR3.1 is not degraded when present as the sole carbon source and is not adsorbed by the culture.

One major metabolite was observed. This was confirmed by LC-UV retention time as the hydrolysis product of the parent dye:

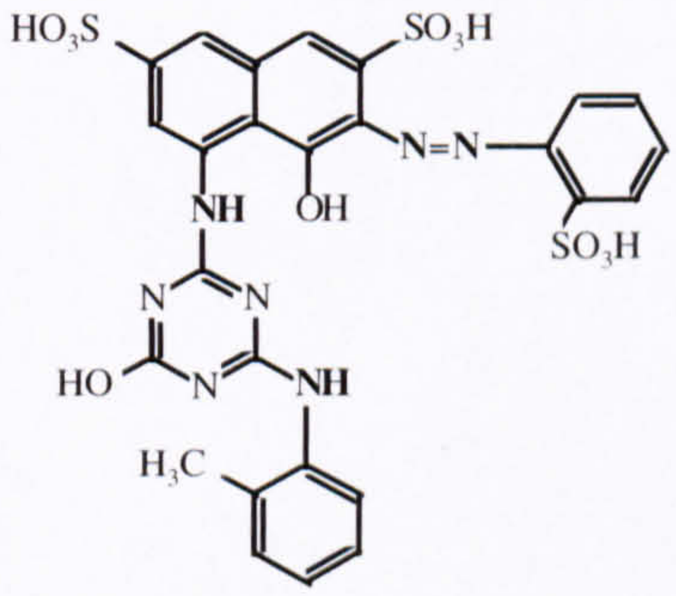

This suggests a simple oxidative process rather than extensive metabolism of RR3.1. The hydrolysis product was quantified using the parent dye calibration (since it had the same UV response factor), which confirmed the formation of the hydrolysis product as the only significant process.

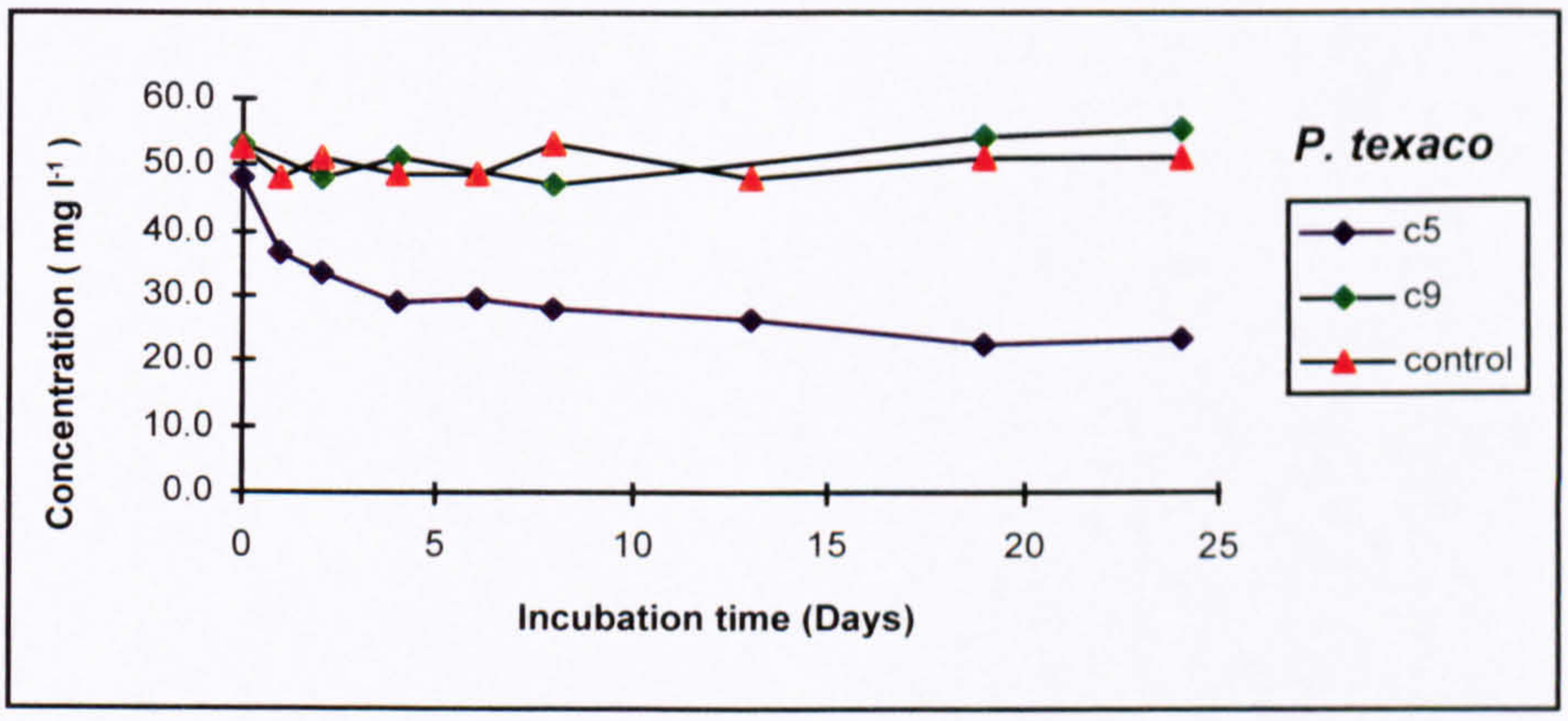

Figure 5.26 Incubation of replicate test vessels of RR3.1 (c5, with glucose and c9, no glucose) with single strain culture of *P. texaco*. The control vessel contained RR3.1 but no glucose or culture

5.4 CONCLUSIONS

Given suitable conditions of temperature, co-substrates, nutrients and time, bacterial aerobic degradation of dyes is likely to be a major pathway for the removal of anthraquinone dyes within sewage treatment works and in the environment. Many of the degradation products are formed from the fission of bonds attached to the anthraquinone

moiety and these do not have the same intense blue colour of the parent. Additionally, many of the degradation products can be removed by adsorption onto solids, whereas the parent dyes are highly water soluble.

Two azo dyes did not degrade under the SCAS biodegradation conditions suggesting this type of dye are not susceptible to aerobic degradation. However there was evidence of degradation by pure cultures of *Pseudomonas*, which suggest degradation may be possible given suitable conditions.

CHAPTER 6

CONCLUSIONS

The first aim of this project was to establish a robust LC separation that was compatible with mass spectrometer interfaces, for the identification of reactive dyes and their degradation products. This was achieved through the adaptation of an existing ion pairing method through the use of dilute ammonium acetate buffer. The method was capable of the reproducible separation of a range of di-, tri and tetra-sulphonated azo and anthraquinone reactive dyes and formed the basis of the analysis method used thereafter in this project. The same ion pair approach was also used to demonstrate the effective extraction and concentration of reactive dyes from aqueous solution, using either tetrabutyl ammonium hydroxide or ammonium acetate as buffers. The MSMS spectra of reactive dyes are quite complex. However, the optimisation of collision gas pressure and collision energy, and interpretation of the MSMS spectra of known azo and anthraquinone reactive dyes, provided novel fragment ions characteristic of reactive dyes. These optimised conditions and mass spectral interpretations provided a sound basis for the analysis of dyestuffs in subsequent fate studies.

The most likely routes of transformation of reactive dyes in the aqueous environment (eg rivers) are photodegradation, aerobic and anaerobic biodegradation. Aspects of all three of these processes were researched within this study.

Fibre reactive dyes are designed to have a degree of photostability and therefore their photodegradation behaviour has not been widely investigated. Little is known of their stability to light over prolonged periods of irradiation in dilute aqueous solutions and in the presence of humic substances.

In this study, a xenon lamp was successfully used for laboratory-simulated aqueous photolysis studies of two reactive dyes. In order to relate laboratory kinetic data to that of environmental situations around the world, it was necessary to compare the light intensity of natural sunlight to that of the laboratory system. In this study a spectro-radiometer was used to provide a direct comparison of UK midday sunlight (Brixham) with that of the xenon lamp of the laboratory system. It was then possible to predict the half lives for two reactive dyes in other parts of the world such as USA, Brazil and India.

Photodegradation was very rapid for the anthraquinone dye W435 for which a $t_{1/2}$ of 1.5 hours was determined. The solid phase extraction, LC-MS and LC-MSMS methods developed in the initial part of this study were utilised for the concentration and identification of photodegradation products respectively. The observed degradation pathway indicated cleavage at several parts of the dye structure some of which retained the reactive chlorine moiety. It was interesting that following initial rapid degradation, continued irradiation did not appear to significantly effect the concentration of products which suggests the process may have been limited by dissolved oxygen concentration.

Photodegradation of the azo dye W433 was significantly slower ($t_{1/2}$ 30 hours) than that of W435. LC-MS and LC-MSMS confirmed the only initial transformation reaction to be dechlorination with accompanying hydroxylation. Extended periods of irradiation (up to 72 hours), produced at least 10 degradation products which collectively accounted for an estimated 15% of the initial dye concentration. However each component was relatively minor and these were not identified by LC-MS.

The addition of humic substances (1 mg l^{-1}) isolated from the river Dodder, Eire, to dyestuffs in water appeared either to have no effect or to slightly reduce the rate of photodegradation of W433. Conversely, Aldrich humic acids slightly increased the rate of

photodegradation. From the limited work reported here humic acids may have an effect on the rate of photodegradation, either by absorbing energy which otherwise might energise dye material to cause degradation, or by sensitising the photodegradation reaction to encourage a faster rate. However, further work, including a broader range of origins and concentration of characterised humic substances is required to better understand their role in photolysis of reactive dyes.

The reduction of azo dyes under anaerobic treatment has been extensively studied, but most studies have made use of relatively simple model compounds rather than real dyes. Additionally, the subsequent fate of the initial reduction products in the presence of air (as may be expected for a mixed anaerobic-aerobic treatment system), is not understood. In this study, three dyes: Amaranth, Sunset Yellow and Naphthol Blue-Black, were reduced and the effect of aeration on the reduction products examined. The substituted 1-amino-2-hydroxynapthalene products of the reduction process were found to be highly susceptible to oxidation, and some of the resulting products were highly conjugated and therefore coloured. Optimised LC-MS and LC-MSMS conditions were used to identify and monitor autoxidation products as they changed with increasing time, and autoxidation pathways for each dye were proposed. Interestingly the formation of ring-opened structures was observed. These, although resistant to autoxidation, would be expected to be highly susceptible to decarboxylation and further degradation under aerobic biological treatment. Such reactivity, if confirmed by further studies, might indicate good potential for the removal of azo dyes by sewage treatment systems employing aerobic treatment. The primary reduction product of the more complex Naphthol Blue-Black dye proved to be very unstable; indeed few degradation products were observed by LC-MS. One major autoxidation product which produced a blue colouration was found to be stable and was identified by LC-MS.

The autoxidation products identified for Amaranth and Sunset Yellow were used to successfully predict the autoxidation products of the more complex azo dye, Reactive Red 3.1. This dye underwent rapid autoxidation to form more than nineteen major products. Several of these indicated that fission of secondary amine groups had occurred in the reduction process. This is particularly relevant since the reduction products of azo dyes are often thought to be recalcitrant.

Additionally, the ring-opened autoxidation products observed for Amaranth and Sunset Yellow were also observed for Reactive Red 3.1. These are believed to be readily degraded by aerobic degradation and highlight the potential to mineralise azo dyes through a mixed anaerobic-aerobic treatment process. Indeed, ring-opened structures were not observed in samples derived from a subsequent mixed treatment process for Reactive Red 3.1. However, in this anaerobic-aerobic treatment system, one persistent degradation product was identified which was stable over the 7 day aerobic period of the study and was therefore resistant to aerobic degradation. This suggests the need for optimisation of the degradation process to enhance the ring-opening process.

Three reactive dyes: W435, W433 and RR3.1 were subjected to aerobic biodegradation using both mixed culture (SCAS) and single strain inocula. Given suitable conditions of temperature, co-substrates, nutrients and time, bacterial aerobic degradation is likely to be a major pathway for the removal of anthraquinone dyes within sewage treatment works and in the environment. The major degradation products of the mixed culture (SCAS) experiment were identified by LC-MS and an aerobic biodegradation pathway proposed. This was quite different from the pathway described for photodegradation. Many of the degradation products were formed from the fission of bonds attached to the anthraquinone moiety and these do not have the same intense blue colour of the parent. Additionally, many of the degradation products were removed by adsorption onto solids within the

SCAS system, whereas the parent dyes are highly water soluble. For the single strain cultures, there was some evidence for partial aerobic degradation of W435 by *Pseudomonas texaco* and to a lesser extent by *Pseudomonas 9046*. Based on LC-UV retention times, the products formed were different from those observed in the semi-continuous activated sludge (SCAS) study, suggesting a different metabolic pathway. Additionally, a substantial amount of dye was removed by sorption to *Pseudomonas 9046* in the presence of glucose. Two azo dyes did not degrade under the SCAS biodegradation conditions suggesting this type of dye is generally not susceptible to aerobic degradation. However there was evidence of extensive degradation by pure cultures of *Pseudomonas docunhae*, which suggests that degradation of azo dyes may be possible given suitable conditions.

References

APCI systems Operators and service manual, Rev A, (1993), Finnigan Mat:.

Colour chemistry; 2nd ed, 1991: Synthesis properties and Applications of Organic Dyes and Pigments.. (Zollinger H, Ed). J.Wiley

Colour Index 3erd ed. The Society of Dyers and Colouists

Direct photolysis rate in water by sunlight (1996) EPA Guideline Fate transport and transformation test guidelines: OPPTS 835.2210.

Encyclopedia of Chemical technology, 1993: Dyes, application and Evaluation..

Environmental Chemistry of Dyes and Pigments, 1996, (Reife A and Freeman H S, Ed). J Wiley.

Organic Chemistry 3erd ed, Morison and Boyd (1977). Allyn and Bacon.

The kinetics of environmental aquatic photochemistry theory and practice, 1988. (Leifer A, Ed). ACS Professional Reference Books

The Chemistry and application of dyes, 1990: Classification of dyes by chemical structure (Waring and Hallis, Ed)

BIBLIOGRAPHY

1. Alexander A J and Kebale P (1986) Thermospray mass spectrometry. Use of gas-phase ion/molecule reactions to explain features of thermospray mass spectra. Anal. Chem. 58, 471-478

2. Ali L N (1994) The Dissolution and Photodegradation of Kuwait Crude Oil in Seawater. Ph.D Thesis, Department of Environmental Sciences, University of Plymouth.

3. Anliker R and Clarke E A (1980). The ecology and toxicology of synthetic organic pigments. Chemosphere 9, 595-609

4. Anliker R and Clarke E A (1981). Recent developments concerning the ecotoxicology of dyestuffs. Proc. 12th Congress of the International Federation of Associations of Textile Chemists and Colourists.

5. Anliker R, Moser P and Poppinger D (1988). Bioaccumulation of dyestuffs and organic pigments in fish. Relationships to hydrophobicity and steric factors. Chemospere

6. Aranyosi P, Czilik M, Remi E, Parlagh G, Vig A and Rusznak I (1999). The light stability of azo dyes and azo dyeings IV. Kinetic studies on the role of dissolved oxygen in the photofading of two heterobifunctional azo reactive dyes in aqueous solution. Dyes and Pigments, 43, 173-182

7. Barcelo D, Garcia J.F (1993). An overview of LC-MS interfacing systems with selected applications. J. High Res. Chrom. 16, 633-641.

8. Baughman G and Perenich T A (1988) Investigating the fate of dyes in the environment. American Dyestuff Reporter 19-48

9. Berzas J J, Guiberteau-Cabanillas C and Contento-Salcedo A M (1997) Separation and determination of dyes by ion-pair chromatography. J. Liq. Chrom. & Rel. Technol. 20, 3073-3088.

10. Betowski L.S, Ballard J.M (1984). Identification of dyes by Thermospray ionisation and mass spectrometry/mass spectrometry. J. Anal. Chem. 56, 2604-2607.

11. Ballard J.M and Betowski L.D (1986). Thermospray ionisation and tandem mass spectrometry of dyes. Org. Mass Spectrum. 21, 575-588.

12. Betowski L.S, Pyle S M, Ballard J.M and Shaul G M (1987). Thermospray LC/MS/MS analysis of wastewater for disperse azo dyes. Biomed. And Env. Mass Spectrometry 14, 343-354

13. Blakley C.R, Vestal M.L (1983). Thermospray interface for liquid chromatography/mass spectrometry. Anal Chem. 55, 750-754.

14. Böeseken, M. J. (1911). Quelques observations sur l'action du perhydrol sur les dicetones. *Recl. Trav. Chim. Pays-Bas.* 30, 142-144.

15. Bredereck K and Schumacher (1993) Structure reactivity correlations of azo reactive dyes based on H-acid. IV. Investigations into the light fastness in the dry state, in the wet state, and in the presence of perspiration. Dyes and Pigments, 23, 135-147.

16. K C A Bromley-Challenor, J S Knapp, Z Zhang, N C C Gray, M J Hetheridge and M R Evans (2000). Decolourisation of an azo dye by unacclimated activated sludge under anaerobic conditions Wat. Res. Vol.. 34, 18, 4410-4418.

17. Brown D (1987) Effects of colorants in the aquatic environment (1987). Ecotoxicology and Environmental Safety 13, 139-147

18. Brown, M. A. and De Vito, S. C. (1993) Predicting azo dye toxicity. Critical Reviews in Environmental Science and Technology, 23, 249-324.

19. Brown D and Labourer (1983) The degradation of dyestuffs: Part 1- Primary biodegradation under anaerobic conditions. Chemosphere 12, 397-404.

20. Bruins A P (1998) Mechanistic aspects of electrospray ionisation. J. Chrom. 794, 345-357.

21. Byrom D (1995). Biological decolourisation of textile dyehouse effluents. Proposal for environmental best practice award

22. Cairns T, Siegmund E G and Stamp J J (1987) Thermospray mass spectrometry of aldicarb and its metabolites. Rapid communication in mass spectrometry, 6, 89-90

23. Carliell,C. M., Barclay, S. J., Naidoo, N., Buckley, C. A., Mullholland, D. A. and Senior, E. (1995) Microbial decolourisation of a reactive azo dye under anaerobic conditions. Water SA, 21, 61-69.

24. Chung K, Fulk G E and Egan M (1978). Reduction of azo dyes by intestinal anaerobes. Appl.Env. Microbiol. 35, 558-562.

25. Chung K, Stevens E, Cerniglia C.E (1992). The reduction of azo dyes by the intestinal microflora. Crit. Rev. Microbiol. 18, 175-190.

26. Chung K and Stevens E, (1993). Degradation of azo dyes by environmental microorganisms and helminths. Environ. Toxicol. Chem. 12, 2121-2132.

27. Chung K, Cerniglia C.E (1992). Mutagenicity of azo dyes: Structure-activity relationships. Mutat. Res. 277, 201-220

28. Clarke E A and Anliker R (1980) organic dyes and pigments, in Handbook of environmental Chemistry 3A, 181-215.

29. Colonna G M, Caronna T and Marcandalli B (1999). Oxidative degradation of dyes by ultraviolet radiation in the presence of hydrogen peroxide. Dyes and Pigments 41, 211-220.

30. Collier S W, Storm J E and Bronaugh R L (1993). Reduction of azo dyes during *in vitro* percutaneous absorption. Toxicol. Appl. Pharmacol 118, 73-79

31. Conboy J.J, Henion J.D, Martin M.W, Zweigenbaum J.A (1990). Ion chromatography / mass spectrometry for the determination of organic ammonium and sulphate compounds. Anal. Chem. 62, 800-807.

32. Cooper, P. (1993) Removing colour from dyehouse wastewaters – a critical review of technology available. Journal of the Society of Dyers and Colourists, 109, 97-100.

33. Covey T R, Bruins A P and Henion J D (1988) Comparison of thermospray and ion spray mass spectrometry in an atmospheric pressure ion source. Organic Mass Spec. 23, 178-186

34. Cripps C, Bumpus JA and Aust S D (1990). Biodegradation of azo and hetrocyclic dyes by Phanerochaete crysosporium. App. Environ. Microbiol. 56, 1114-1118.

35. Cross and Bevan (1895)

36. Dickel, O., Haug, W. and Knackmuss, H-J. (1993) Biodegradation of nitrobenzene by a sequential anaerobic-aerobic process. Biodegradation, **4**, 187-194.

37. Dole M, Mack L L and Hines R L (1968) Molecular beams of macroions. J. Chem. Phys. 49, 2240-2249

38. Donlon, B., Razo-Flores, E., Luijten, M., Swarts, H., Lettinga, G. and Field, J. (1997) Detoxification, and partial mineralization of the azo dye mordant orange 1 in a continuous upflow anaerobic sludge-blanket reactor. Applied Microbiology and Biotechnology, 47, 83-90.

39. ENDS (1992). Dyeing industry put on notice to end colour pollution. The ENDS Report 207, 7.

40. ENDS (1993). Textile industry threads its way through the effluent challenge. Industry Report 58, TheENDS Report 225, 15-16.

41. Edlund P O, Lee E D and Henion J D (1989) The determination of sulphonated azo dyes in municipal wastewater by ionspray liquid chromatography tandem mass spectrometry. Biomedical and Environmental Mass spec. 18, 233-240

42. Fenn J B, Mann M, Meng C K and Wong S F (1990) Electrospray ionisation-principles and practice. Mass spectrometry Reviews 9, 37-70.

43. Fitzgerald, S. W. and Bishop. P. L. (1995) Two stage anaerobic/aerobic treatment of sulphonated azo dyes. Journal of Environmental Science and Health, A, 30, 1251-1276.

44. Flory D.A, McLean M.M, Vestal M.L (1987). Environmental applications of Thermospray LCMS: Qualitative analysis of sulphonated azo dyes. Rapid Commun. Mass Spectrum. 1, 48-50.

45. Fukuda K, Inagaki Y, Maruyama T (1988). On the photolysis of alkylated naphthalenes in aquatic systems. Chemosphere 17, 651-659.

46. Garteiz D A and Vestal M L (1985) Thermospray LC/MS interface: Principles and applications. J. Liquid Chromatography 3, 334-346

47. Gould, I.R. (1989). Conventional light sources. In: CRC Handbook of Organic Photochemistry, Volume 1, (Scaiano, J. A., Ed.), CRC Press, Inc. Florida, pp. 155-196

48. Goszczynski S., Paszczynski A., Pasti-Grigsby M. B., Crawford R. L. and Crawford D. L. (1994) New pathway for degradation of sulfonated azo dyes by microbial peroxidases of Phanerochaete chrysosporium and Streptomyces chromofuscus. Journal of Bacteriology, 176, 1339-1347.

49. Gregory, P. (1993) Dyes and dye intermediates. pp 542- 602 In: Encyclopedia of Chemical Technology, 4th Edition, volume 4, (Kirk-Othmer, Ed), John Wiley and Sons, New York.

50. Haag W.R, Mill T (1987). Direct and indirect photolysis of water soluble azodyes: Kinetic measurements and structure-activity relationships. Environ. Toxicol. Chem. 6, 359-369.

51. Haug W, Schmidt A, Nörtemann B, Hempel D C, Stolz A and Knackmuss H-J (1991) Mineralisation of the sulfonated azo dye mordant yellow 3 by a 6-aminonaphthalene-2-sulfonate-degrading bacterial consortium. Applied and Environmental Microbiology, 57, 3144-3149.

52. Heinfling A, Martinez M J, Martinez A T, Bergbauer M and Szewzyk U (1998) Transformation of industrial dyes by manganese peroxidases from *Bjerkandera adusta* and *Pleurotus eryngii* in a manganese-independent reaction. Applied and Environmental Microbiology, 64, 2788-2793.

53. Hinks D, Lewis D.M (1993). Capillary electrophoesis of dyes. Chromatography and analysis. August, 9-11.

54. Hobbs S J (1989) Acquisition and use of data for assessment of the environmental impact of colourants. JSDC 105, 355-362

55. Hitz H R, Huber W and Reed R H (1978). The adsorption of dyes on activated sludge. JSDC, 71-76

56. Holme, I. and Thornton, A. (1994) Reactive dyes pose main problem in colour clean-up. International Dyer January 1994, 19-21.

57. Horitsu H., Tateda M., Idaka E., Tomoyda M. and Ogawa T. (1977) Degradation of p-aminoazobenzene by Bacillus subtilis. European Journal of Applied Microbiology and Biotechnology, 4, 217-224.

58. Howe (1993). In: The Encyclopedia of Chemical technology.

59. Hu C and Wang Y (1999). Decolourisation and biodegradability of photocatalytic treated azo dyes and wool textile wastewater. Chemosphere 39, 2107-2115.

60. Hwang H-M, Hodson R E and Lee R F (1986) Degradation of aniline and chloroanilines by sunlight and mirobes in esturine water. Wat. Res 21, 309-316

61. Idaka, E., Ogawa T., Horitsu H. and Tomoyeda M. (1987) Degradation of azo compounds by Aeromonas hydrophila var 24B. Journal of the Society of Dyers and Colourists., 94, 91-94.

62. Iribarne J V and Thomson B A (1976) On the evaporation of small ions from charged droplets. J. Chem. Phys. 64, 2287-2294.

63. Jingi L and Houtian L (1992) Degradation of azo dyes by algae. Environmental pollution, 75, 273-278.

64. Kamat P V, Das S, Padmaja S and Madison S A (1999) Photochemical behavoir of anthraquinone based textile dye (Uniblue-A) bound to cellulose powder and cotton fabric. Res. Chem. Intermed. 25, 915-924.

65. Kebarle P and Tang L (1993). From ions in solution to ions in the gas phase. Anal. Chem 65, 972-986.

66. Kech A, Klein J, Kudlich, H.-J Stolz A, M, Knackmuss and Mattes R. (1997) Reduction of azo dyes by redox mediators originating in the naphthalenesulphonic acid degradation pathway of Sphingomonas sp. Strain BN6. *Appl. Microbiol. Biotechnol.* 63, 3684-3690

67. Khanna S K and Mukul D (1991) Toxicity, carcinogenic potential and clinico-epidemiological studies on dyes and dye intermediates. J. Scientific and Industrial Research, 50, 965-974

68. Knapp, J. S. and Newby, P. S. (1995) The microbiological decolourisation of an industrial effluent containing a diazo-linked chromophore. Water Research, 29, 1807-1809.

69. Kudlich, M.; Bishop, P.L.; Knackmuss, H.-J.; Stolz (1996) A. *Appl. Microbiol. Biotechnol.* 46, 597-603.

70. Kudlich, M.; Keck A; Klein J and Stolz A (1997) Localisation of the enzyme system involved in anaerobic reduction of azo dyes by Sphingomonas sp. Strain BN6 and effect of artificial redox mediators on the rate of azo dye reduction. Appl. Environ. Microbiology 63, 3691-3694

71. Kudlich, M., Hetheridge, M. J., Knackmuss, H-J, and Stolz, A. (1999) Autoxidation reactions of different aromatic ortho-aminohydroxynaphthalenes which are formed during the anaerobic reduction of sulphonated azo dyes. Environmental Science and Technology, 33, 896-901

72. Kuhm, A.E.; Stolz, A.; Ngai, K.-L.; Knackmuss, H.-J. (1991) Purification and characterisation of a 1,2-dihydroxynaphthalene dioxygenase from a bacterium that degrades naphthalene sulphonic acids. *J. Bacteriol*, 173, 3795-3802.

73. Kulla H G, Klausener E, Meyer U, Ludeke B and Leisinger T (1983). Interference of aromatic sulpho groups in the microbial degradation of azo dyes orange I and Orange II. Arch. Microbiol. 134, 37-43.

74. Lin H-Y and Voyksner R D (1993) Determination of environmental contaminants using an electrospray interface combined with an ion trap mass spectrometer. Anal. Chem. 65, 451-456.

75. Literathy, P., Haider, S., Samhan, O., and Morel, G., (1989). Experimental studies on biological and chemical oxidation of dispersed oil in seawater. Wat. Sci. Technol., 21, 845-856.

76. Lee E D, Muck W, Henion J D and Covey T R (1989) Liquid junction coupling for capillary zone electrophoresis/ion spray mass spectrometry. Biomedical and Environmental Mass Spectrometry 18, 844-850.

77. Long, J. L., Stensel, H. D., Ferguson, J. F., Strand, S. E. and Ongerth, J. E. (1993) Anaerobic and aerobic treatment of chlorinated aliphatic compounds. Journal of Environmental Engineering, **119 (2)**, 300-320.

78. Locher, H.H.; Thurnheer, T.; Leisinger, T.; Cook, A.M (1989). 3-Nitrobenzene sulphonate, 3-aminobenzene sulphonate and 4-aminobenzene sulphonate as sole carbon sources for bacteria. *Appl. Environ. Microbiol* 492-494.

79. Logan M S P, Newman L M, Schanke C A and Wackett L P (1993) Cosubstrate effects in reductive dehalogenation by *Pseudomonas putida* G786 expressing cytochrome P-450$_{CAM.}$ Biodegradation 4, 39-50.

80. Maguire R J and Tkacz R J (1991) Occurrence of dyes in the Yamaska river, Quebec. Water Poll. Res. 26, 145-161

81. Maguire R J (1992) Occurrence and persistence of dyes in a canadian river. Wat. Sci. Tech. 25, 265-270

82. Massafra M R, Selli E, Salsa S and Marcandalli B (1999) Kinetic study on the sunlight-induced degradation of acid azo dyes on silk. Dyes and Pigments 40, 171-180

83. Meyer U (1981) Biodegradation of synthetic organic colorants. In Microbial degradation of xenobiotics and recalcitrant compounds, London academic press, 371-385.

84. McFadden W H and Lammert S A (1987) Techniques for increased use of thermospray liquid chromatography mass spectrometry. J. Chrom. 385, 201-211.

85. McLean M.A, Freas R.B (1989). Enhanced analysis of sulphonated azo dyes using liquid chromatography/thermospray mass spectrometry. Anal. Chem. 61, 2054-2058.

86. Monaghan J J, Barber M, Bordolli R S, Sedgwick D and Tyler A N (1983) Fast atom bombardment mass spectra of involatile monophosphonated and mixed sulphonated/ monophosphonated azo dyestuffs. Org. Mass spec. 18, 75-82

87. Monaghan J J, Barber M, Bordolli R S, Sedgwick D and Tyler A N (1982) Fast atom bombardment mass spectra of involatile sulphonated azo dyestuffs. Org. Mass spec. 17, 569-574

88. Moza P N, Hustert K, Feicht E and Kettrup A. (1995) Comparative rate of photolysis of triadimefon in aqueous solution in the presence of humic and fulvic acid. *Chemosphere*, 30, 605-610

89. Murphy E M, Zachara J M and Smith S C (1990) Influence of mineral-bound humic substances on the sorption of hydrophobic organic compounds. Environ. Sci. Technol. 24, 1507-1516

90. Nigam, P. Banat, I. M., Singh, D. and Marchant, R. (1996) Microbial process for the decolorization of textile effluent containing azo, diazo and reactive dyes. Process. Biochem., 31, 435-442.

91. Nortemann B., Baumgarten J., Rast H G and Knackmuss H-J. (1986) Bacterial communities degrading amino- and hydroxynaphthalene- 2-sulfonates. Applied and Environmental Microbiology, 52, 1195-1202

92. Nortemann B., Kuhn, A. E., Knackmuss H-J. and Stolz A. (1994) Conversion of substituted naphthalene sulphonates by Pseudomonas sp. BN6. Archives in Microbiology, 161, 320-327

93. Ohe T. and Watanabe Y. (1986) Degradation of 2-naphthylamine-1-sulfonic acid by Pseudomonas strain TA-1. Agricultural and Biological Chemistry, 50, 1419-1426.

94. Ohe T. and Watanabe Y. (1988) Microbial degradation of 1,6- and 2,6-naphthalenedisulfonic acid by Pseudomonas sp. DS-1. Agricultural and Biological Chemistry 52, 2409-2414.

95. Ohe T., Ohmoto T., Kobayashi Y., Sato A. and Watanabe Y. (1990) Metabolism of naphthalenesulfonic acids by Pseudomonas sp. TA-2. Agricultural and Biological Chemistry 54, 669-675.

96. Pagga, U.; Brown, D (1986) The degradation of dyestuffs part II: Behaviour of dyestuffs in aerobic biodegradation tests. *Chemosphere* 15, 479-491.

97. Pagga, U and Taeger K (1994). Development of a method for adsorption of dyestuffs on activated sludge. Wat. Res. 28,1051-1057

98. Paalme, L., Irha, N., Urbas, E., Tsyban, A., Kirso, U. (1990). Model studies of photochemical oxidation of carcinogenic polyaromatic hydrocarbons. Mar. Chem., 30, 105-111.

99. Parker S and Leahey J P (1988) Development of a method to investigate the photodegradation of pesticides. Proceedings of the Brighton crop protection conference, (7-2), 663-668

100. Pasti-Grigsby M. B., Paszczynski A., Goszczynski S., Crawford D. L. and Crawford R. L. (1992) Influence of aromatic substitution patterns on azo dye degradability by Streptomyces spp. and Phanerochaete chrysosporium. Appied and Environmental Microbiology, 58, 3605-3613.

101. Pasin B and Rickabaugh J (1991) Destruction of azo dyes by sensitised photolysis. Proc. 23erd Mid-Atlantic Industrial waste conference, 23, 359-367

102. Paszczynski A., Pasti M. B., Goszczynski S., Crawford D. L., and Crawford R. L. (1991) New approach to improve degradation of recalcitrant azo dyes by Streptomyces spp. and Phanerochaete chrysosporium. Enzyme Microbiology. Technology, 13, 378-384

103. Pelizzetti E, Maurino V, Minero C, Carlin V, Pramauro E, Zerbinati O and Tosato M (1990) Photocatalytic degradation of atrazine and other triazine herbicides. Environmental Science and Technology, 24, 1559-1565.

104. Porter J J (1973) A study of the photodegradation of commercial dyes. EPA Report R2-73-058.

105. Rafols C and Barcelo D (1997) Determination of mono- and disulphonated azo dyes by liquid chromatography-atmospheric pressure ionisation mass spectrometry. J. chrom 777, 177-192.

106. Rattee and Stephen (1956). JSDC 72, 588

107. Richardson S D, McGuire J M, Thruston A D and Baughman G L (1990). Aapplication of liquid sims ms/ms to the analysis of sulphonated azo dyes. Proc. 30th ASMS conference 785-786.

108. Roof, A.A.M. (1982). Aquatic photochemistry. In: The Handbook of Environmental Chemistry, Reaction and Processes, Volume 2 Part B, (Hutzinger, O., Ed.), Springer-Verlag, Berlin, 43-72.

109. Seshadri, S., Bishop, P. L. and Agha, A. M. (1994) Anaerobic/aerobic treatment of selected azo dyes in wastewater. Waste Management, 14, 127-137

110. Shakra S and Ali N F (1992) Effect of chemical structure on colour/ lightfastness/ sublimation for some disperse anthraquinone dyes. American Dyestuff Reporter 28-30.

111. Shaul, G.M.; Holdsworth, T.J.; Dempsey, C.R.; Dostal, K.A. (1991) Fate of water soluble azo dyes in the activated sludge process. *Chemosphere* 1991, 22, 107-119.

112. Shu H-Y and Huang C-R (1995). Degradation of commercvial azo dyes in water using ozonation and UV enhanced ozonation process. Chemosphere 31, 3813-3825

113. Spadaro J T, Gold M H and Renganathan V (1992) Degradation of azo dyes by lignin-degrading fungus Phenerochaete chrysosporium. Applied and Environmental Microbiology, 2397-2401.

114. Speers S J, Little B H and Roy M (1994) Separation of acid, base and dispersed dyes by a single gradient elution reversed phase high-performance liquid chromatography system. J. Chrom. 674, 263-270

115. Straub R, Voyksner R D and Keever J T (1992) Thermospray, particle beam and electrospray liquid chromatography-mass spectrometry of azo dyes. J. Chrom. 627, 173-186.

116. Tang W Z, Zhang Z, An H, Quintana M o and Torres D F (1997). TiO2/UV Photodegradation of azo dyes in aqueous solution. Env. Technology 18, 1-12

117. Thurman, E.M (1985). Classification of Dissolved Organic Carbon. Organic Geochemistry of Natural Waters. Chapter 4, 103-110.

118. Thurnheer, T., Kohler, T., Cook, A.M. and Leisinger, T. (1986) Orthanilic acid and analogues as carbon sources for bacteria: growth, physiology and enzymic desulphonation. Journal of General Microbiology, 132, 1215-1220.

119. Tratnyek P G, Elovitz M S and Colverson P (1994) Photoeffects of textile dye wastewaters: sensitisation of singlet oxygen formation, oxidation of phenols and toxicity to bacteria. Environmental Toxicology and Chemistry, 13, 27-33

120. Truslove *et al* (1990). Environmental fate of a reactive dye. Zeneca Specialties Research, internal report.

121. Truslove *et al* (1992). Pathway to the environment : a study of the fate of Procion Red MX-5b from a dyehouse effluent. Zeneca Specialties Research, internal report.

122. Vestal M L (1983) Studies of ionisation mechanisms involved in Thermospray Lc-MS. International J. of Mass Spectrometry and Ion Physics 46, 193-196.

123. Vestal M L (1986) Mass Spectrometers as detectors for liquid chromatography. In The importance of chemical 'separation' in environmental processes. Ed Bernhard F E and Sadler P J. 613-629

124. Voyksner R D (1985). Charaterisation of dyes in environmental samples by thermospray high performance liquid chromatography / mass spectrometry. Anal. Chem 57, 2600-2605.

125. Voyksner R D (1985). Optimisation and applications of thermospray high performance liquid chromatography / mass spectrometry. Anal. Chem 57, 991-996

126. Voyksner R D (1987). Characteristics of ion evaporation ionisation in thermospray high performance liquid chromatography/mass spectrometry. Organic Mass Spectrometry 22, 513-518.

127. Voyksner R D, McFadden W H and Lammert S A (1987). Applications of thermospray HPLC/MS/MS for determination of triazine herbicides. In Applications of new mass spectrometry techniques in pesticide chemistry 91, Chapter 17, 247-258

128. Voyksner R D (1994). Atmospheric pressure ionisation LC/MS. Environ. Sci. Technol 28, 118-127.

129. Walker R (1970) The metabolism of azo compounds: A review of the literature. *Food. Cosmet. Toxicol.* 8, 659-676.

130. Wang P Y and Wang I J (1992) Photolytic behavior of some azo pyridone disperse dyes on polyester substrates. Textile Res. 62, 15-20

131. Watabe T, Ozawa N, Kobayashi F and Kurata H (1979) Reduction of sulphonated water-soluble azo dyes by micro-organisms from human faeces. *Food. Cosmet. Toxicol.* 18, 349-352

132. Weber E J, Adams R L (1885) Chemical- and sediment-mediated reduction of the azo dye Disperse Blue 79. Environmental Science and Technology, 29, 1163-1170.

133. Weatherall I L (1991) The analysis of some sulphonated azo dyes by mixed mode HPLC. J. Liq. Chrom. 14, 1903-1912.

134. Wittich R M., Rast H G. and Knackmuss H-J. (1988) Degradation of naphthalene-2-6- and naththalene-1-6-disulfonic acid by a Moraxella sp. Applied and Environmental Microbiology, 54, 1842-1847.

135. Wuhrmann K, Mechsner K and Kappeler T (1980) Investigation on rate-determining factors in the microbial reduction of azo dyes. European J. Appl. Microbiol, 9, 325-338.

136. Yagor J E and Yue C D (1988) Evaluation of the Xenon arc lamp as a light source for aquatic photodegradation studies: comparison with natural sunlight. Environ. Toxicol. Chem. 7, 1003-1011.

137. Yinon J, Jones T.L, Betowski L.D (1989). High sensitivity Thermosporay ionisation dyes. Biomed. Environ. Mass Spectrom. 18, 445-449.

138. Yinon J, Jones T.L, Betowski L.D (1989). Particle beam liquid chromatography-electron impact mass spectrometry of dyes. Chrom. 482, 75-85.

139. Yinon J, Jones T.L, Betowski L.D (1989). Enhanced sensitivity in liquid chromatography/Thermosporay mass spectrometry of dyes using a wire repeller. Rapid Commun. Mass Spectrom. 3, 38-41.

140. Zepp R.G and Cline (1977). Rates of photolysis in aquatic environment. Environ. Sci. Technol. 11, 359-366.

141. Zepp et al (1981). Chemosphere 10, 109-117

142. Zepp R.G, (1982). Experimental approaches to environmental photochemistry. In Experimental methods in photochemistry and photophysics. Wiley 19-14

143. Zepp R.G, Schlotzhauer P.F, Sink R.M (1985). Photosensitized transformations involving electronic energy transfer in natural waters: Role of humic substances. Environ. Sci. Technol. 19, 74-82

144. Zhou J L, Rowland S, Mantoura F C and Braven J (1994) The formation of humic coatings on mineral particles under simulated esturine conditions-A mechanistic study. Wat. Res. 28, 571-579.

APPENDIX 1

Dyes used in degradation studies

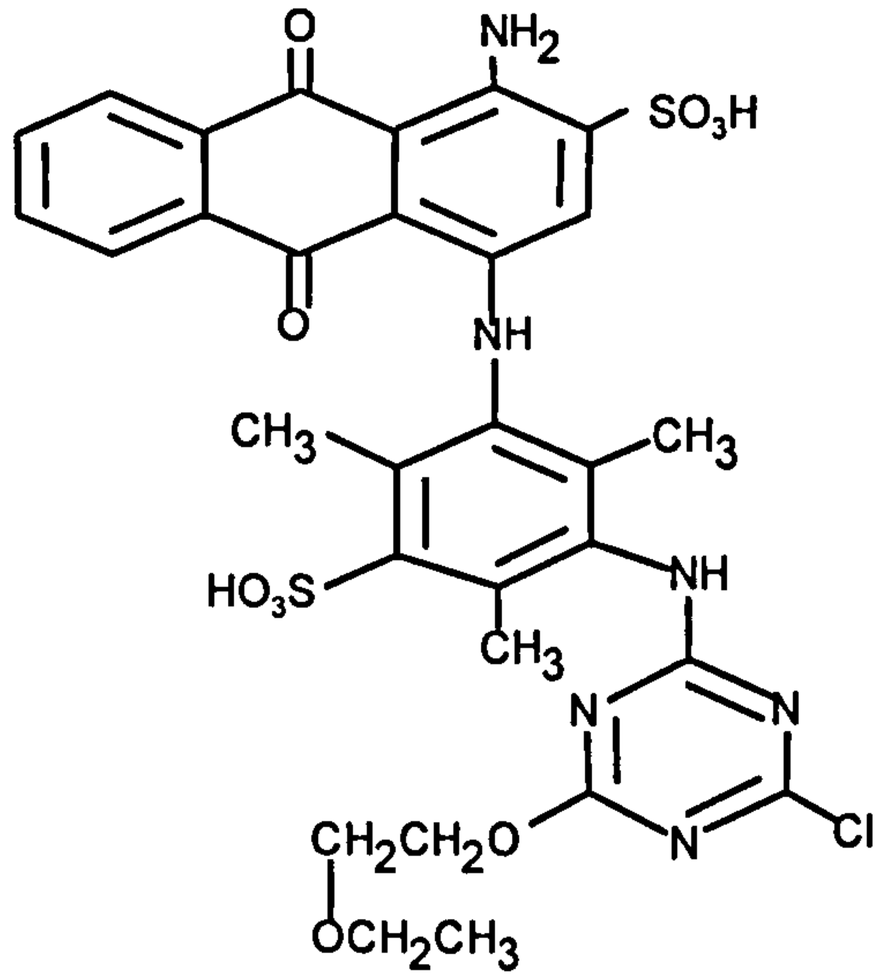

W435, Reactive Blue H4R (Chapters 2, 3, and 5)

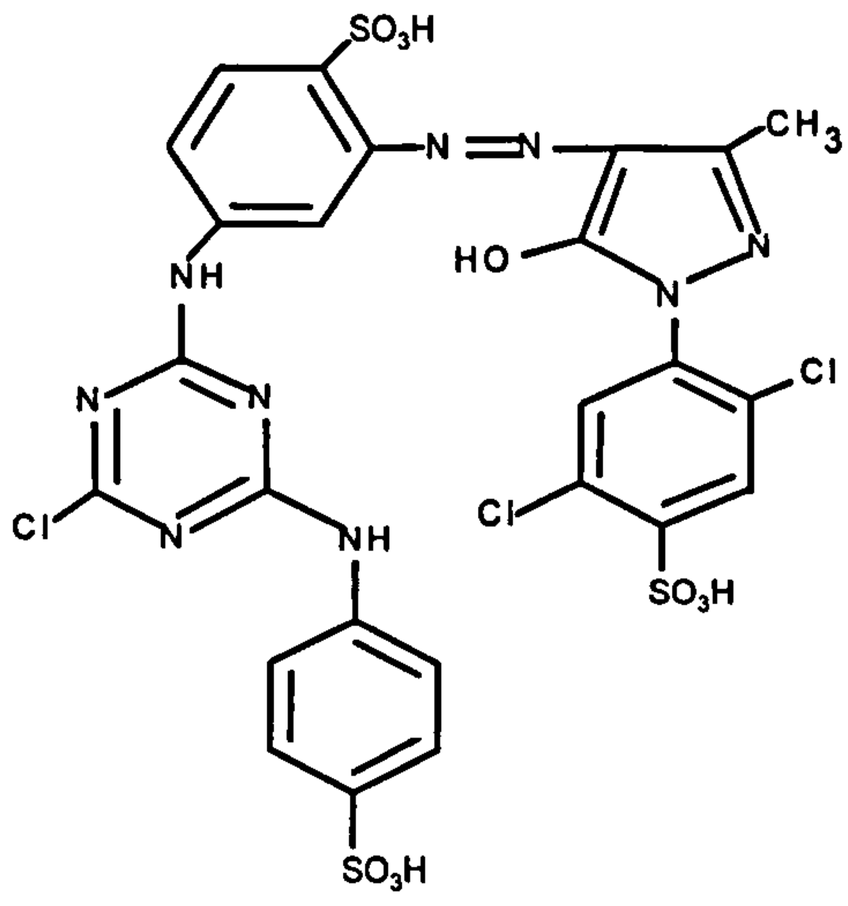

W433, Reactive Yellow 2 (Chapters 2, 3, and 5)

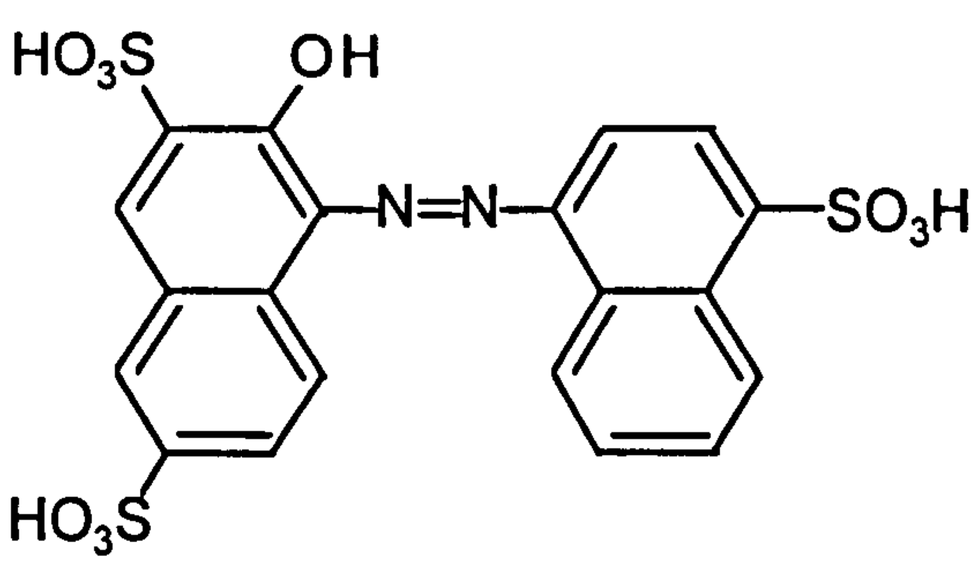

Amaranth (Chapter 4)

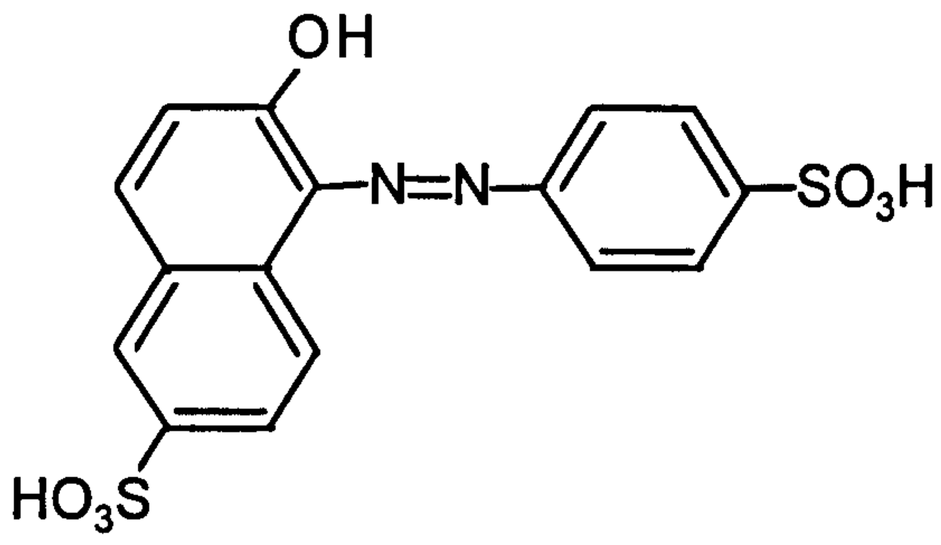

Sunset Yellow (Chapter 4)

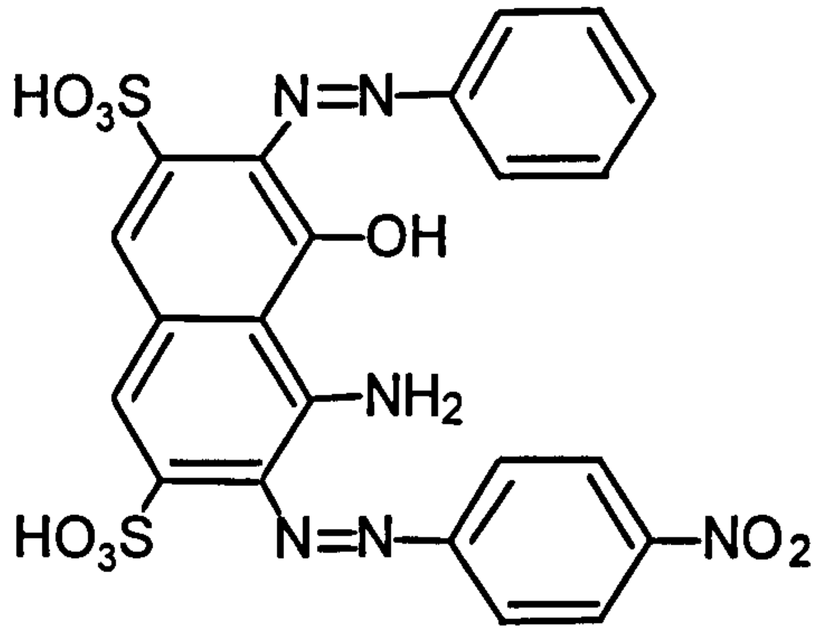

Naphthol Blue-Black (Chapter 4)

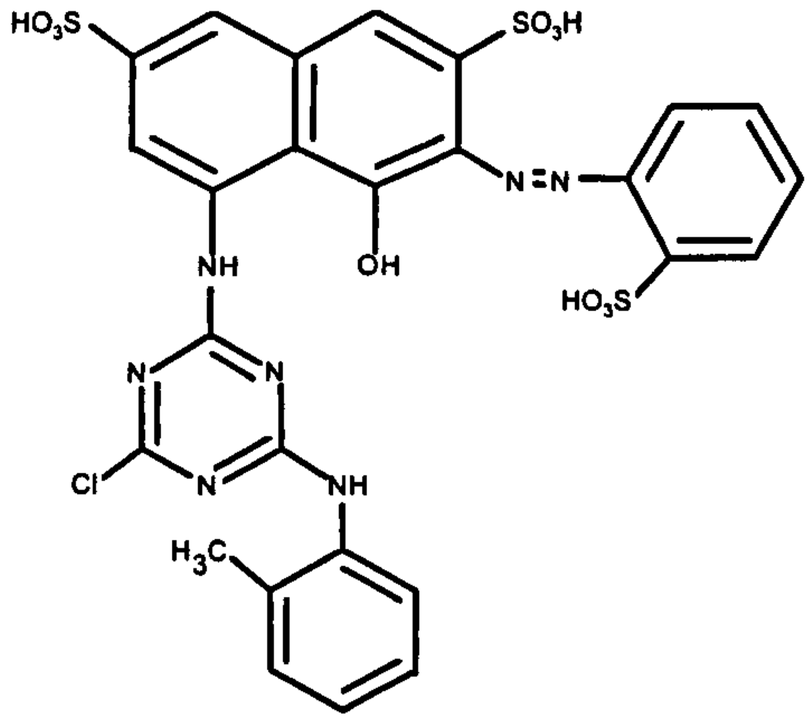

RR3.1, Reactive Red 3.1 (Chapters 4 and 5)

Reactive dyes used in LC optimisation only (Chapter 2)

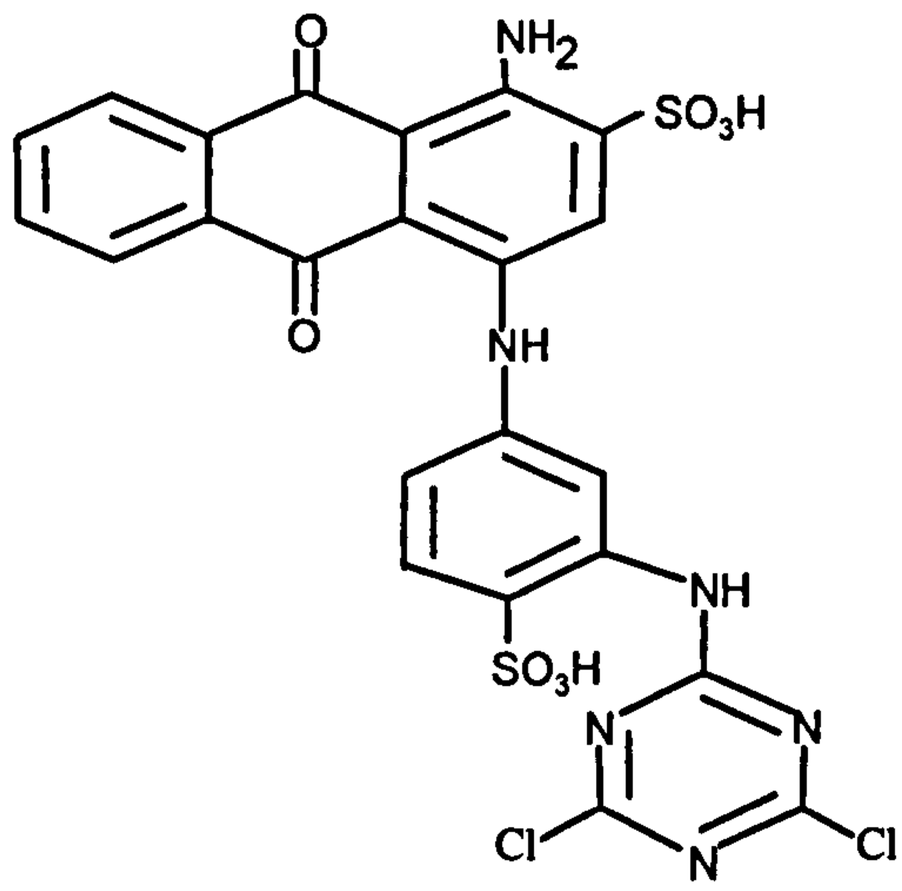

W428 Reactive Blue 4 Blue MX-R

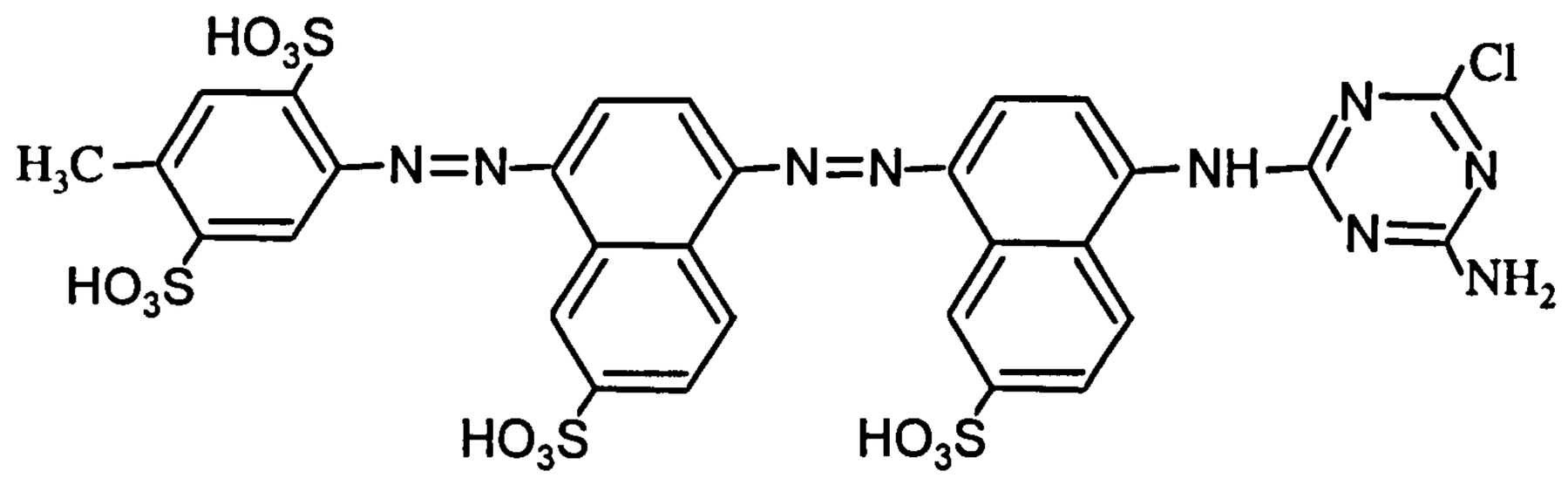

W429 Reactive Red-Brown HEXL

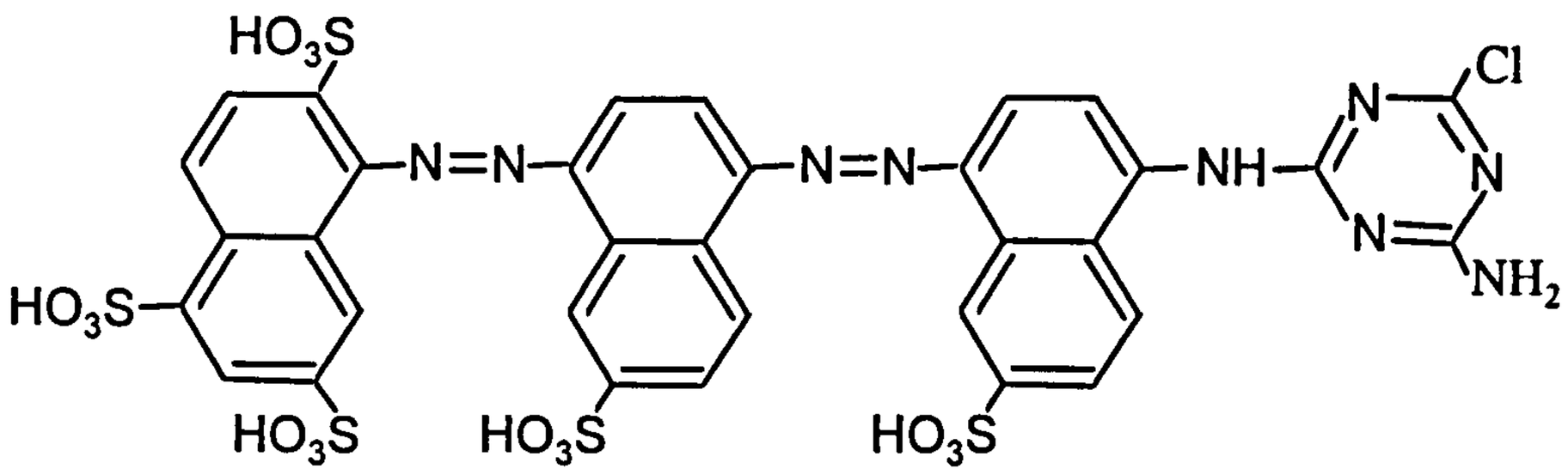

W430 Reactive Brown 7, Brown H3R